August 1993

Proceedings: EPRI-NSF Workshop on Anomalous Effects in Deuterided Metals

October 16-18, 1989
Washington, D.C.

REPORT SUMMARY

Proceedings: Workshop on Anomalous Effects in Deuterided Metals

Attempts to confirm Fleischmann and Pons's observations of cold fusion phenomena have met with inconsistent results. This second workshop on this topic brought together skeptics and advocates to facilitate communication, to examine closely the experimental results, and to identify research issues.

BACKGROUND The majority of attempts to confirm cold fusion phenomena have been unsuccessful. Although some researchers have confirmed portions of the Fleischmann and Pons experiment, these results have been sporadic and difficult to reproduce. The first workshop on this topic, sponsored by the Department of Energy, was held in May 1989 in Santa Fe, New Mexico.

OBJECTIVES
- To facilitate communication and collaboration among researchers from different laboratories/disciplines

- To evaluate data gathered since the Santa Fe Workshop

- To consider possible theoretical explanations of the anomalous effects and the implication of these explanations for future research

APPROACH As a follow-up to the Santa Fe Meeting, the National Science Foundation and EPRI cosponsored a workshop October 16-18, 1989, in Washington, D.C. Thirty presentations by workshop participants addressed issues of nuclear byproducts, excess heat, and possible theoretical mechanisms for cold fusion.

Three subgroups met separately to consider these issues and make recommendations for future experiments and other research in these areas.

KEY POINTS
- The scientific and/or technological significance of cold fusion ultimately will be determined experimentally.

- Procedures must be developed to facilitate reproducibility of an individual laboratory's results by other laboratories.

- Collaboration among researchers from laboratories reporting positive results and those reporting negative results is critical to efforts to evaluate the anomalous effects.

- A convincing set of experimental data should include positive, nonsporadic, simultaneous measurements of excess heat and nuclear byproducts.

Proceedings: EPRI-NSF Workshop on Anomalous Effects in Deuterided Metals

October 16-18, 1989
Washington, D.C.

August 1993

Editorial Committee

John Appleby, Texas A&M Univ.   Nate Hoffman, Rockwell ETEC

Thomas R. Schneider, EPRI   Harold Szu, NSWC-White Oak

Paul Werbos, NSF

Managing Editor

Thomas R. Schneider

Technical Editing

Henry Aeroeste

John Appleby

Production Editing

Carolee DeWitt, Wm. Nesbit & Associates

Note: This document has been prepared for workshop attendees and is not intended for wide distribution.

ABSTRACT

The Workshop on Anamalous Effects in Deuterated Metals was held October 16-18, 1989 in Washington, D.C. The workshop was cosponsored by the Electric Power Research Institute and the National Science Foundation.

The objectives of the workshop were to bring together skeptics and advocates to examine closely the anomalous effects reported by researchers who have attempted to confirm the cold fusion phenomena observed by Fleischmann and Pons and to consider possible theoretical explanations of the anomalous effects and their implications for future research. Key steps required to remove the ambiguities surrounding cold fusion were identified and proposed, including the establishment of procedures to facilitate the replication of one individual laboratory's results by other laboratories and collaboration among researchers through the exchange of personnel and experiments.

Presentations addressed issues of nuclear byproducts, excess heat, and possible theoretical mechanisms. Following the formal presentations a series of shorter presentations were given on more recent results. Subsequently three subgroups met to consider these topics and made recommendations for future experiments and other research in these areas.

These Proceedings contain papers submitted by authors of 30 presentations made at the workshop, the discussions that followed each presentation, and summaries prepared by the session chairs.

EDITORIAL PERSPECTIVE

This _Proceedings_ is an outcome of a workshop cosponsored by EPRI and the National Science Foundation (NSF) on the controversial topic of "cold fusion" research. This workshop, held October 16-18, 1989, was the first forum that succeeded in achieving a frank and open scientific discussion on the controversial findings reported by Pons and Fleischman and the various attempts to explain them. In addition, considerable insight was gained about how the experimental efforts could be improved. This aspect of the meeting's success is documented in this _Proceedings_, especially in the discussions and reports of the breakout sessions.

The assembly of this _Proceedings_ has been the result of considerable effort by several members of the editorial committee. We were ably assisted by Henry Aeroeste and Carolee DeWitt, who provided scientific and production editing support, respectively. Raw transcripts of the discussions were provided by AAA Capital; these were edited by John Appleby with support from Henry Aeroeste.

Credits and thanks for the sponsorship of this workshop go to the management of NSF and EPRI who were willing to make the session possible even in the face of considerable controversy. The success of the meeting, however, was the result of the participants. A very high degree of professionalism was exhibited by all in attendance, and both skeptics and advocates engaged in constructive discussions.

The passage of time between the workshop and publication of this _Proceedings_ has provided some additional perspective on this subject. Some of the measurements reported herein appear to be artifacts, unreproducible results, or mistakes. At this time, no clear evidence exists that "excess heat" is a result of a nuclear process. In general, the search for the kernels of real data has been difficult, and the relationships between all the anomalous effects are not yet understood. The final chapter of this saga is still to be written. My hope is that this _Proceedings_ will help those interested in the history of this controversial subject better understand both the degree of scientific uncertainty and the chaotic state of knowledge that existed at the time this workshop was held.

Thomas R. Schneider
Managing Editor

Subsequent Cold Fusion Conferences

1st Annual Conference on Cold Fusion: Conference Proceedings, March 28-31, 1990, Salt Lake City, Utah, National Cold Fusion Institute.

Anomalous Nuclear Effects in Deuterium/Solid Systems: AIP Conference Proceedings 228, 1990, Provo, Utah, Ed: Steven E. Jones, Franco Scaramuzzi, and David Worledge.

The Science of Cold Fusion: Proceedings of the 2nd Annual Conference on Cold Fusion, June 29-July 4, 1991, Como, Italy, Ed: T. Bressani, E. Del Giudici, and G. Preparata.

Frontiers of Cold Fusion: Proceedings of the 3rd Annual Conference on Cold Fusion, October 21-25, 1992, Nagoya, Japan, Ed: H. Ikegami.

CONTENTS

Part 1

OVERVIEW

Section 1

REMARKS OF DR. EDWARD TELLER:
ANOMALOUS EFFECTS ON DEUTERIDED METAL

REMARKS OF DR. EDWARD TELLER:
ANOMALOUS EFFECTS ON DEUTERIDED METAL

We are further than ever from a real agreement on cold fusion. What has been seen has a wide divergence in results. I do not remember any case in my lifetime in science when so many experts have differed for such a long time on such relatively simple and inexpensive experiments. We are seeing a great deal of variability in the results -- whether due to surface effects or cracks or small changes in some unknown parameter. The experiments differ in many more ways than a simple theorist can explain.

I feel like the visitor looking at the giraffe and concluding, "there ain't no such animal." According to nuclear theory -- from the point of view of the Gamow factor -- there cannot be such an effect. The Gamow factor is not as simple as it is normally considered. Indeed, one must consider the temperature average over the Gamow factors. But before the hydrogen nuclei really have a chance of interacting with each other, they must be within a fraction of an angstrom and at that point the Gamow factor has a value of about 10^{-50}. On that basis alone, what we are seeing must be a series of mistakes.

But this is not the end of the controversy. Some of the good experiments show that something is really wrong with the branching of $D+D \rightarrow T + H$ and $D+D \rightarrow He^3 + n$. While I will not exclude a small variation in the ratio, the actual value reported is 10^8! Proton producing reactions (the Tritium branch) being 10^8 times more likely than neutron producing reactions. This is simply out of the question if D-D fusion is what is happening.

However, the history of science and experimental physics is full of examples of predictions that things are impossible and yet they have happened. I remember what Ernest Lawrence once said about me: "When Teller says it is impossible, he is frequently wrong. When he says it can be done, he is always right."

But what if we are presented with the fact that the results are correct? Then we will have to ask ourselves what are the minimum changes which we need to make in nuclear physics to explain the facts. If the giraffe exists, how does his heart pump blood into his brain? If the results are correct, then you must assume that nucleons can interact not just when they touch. We need to be able to explain how the nucleons interact at distances as great as 1/10 of an angstrom.

I think it would help if we postulated that the nuclei can interact at 10^4 nuclear radii and that the interaction is not through tunnelling but some exchange of "particles" which can extend outside of the nucleus. It will be remarkable but not impossible that "quarks" could exchange or interact at 10^{-9} cm with very low

probability. This would be a low probability but still much greater than the Gamow factor. The probability that this could result in cold fusion is possible even if it is unlikely. If there is such an effect, we will then learn something very important. This would be a scientific discovery of the first order, the kind for which we are willing to spend 5×10^9 dollars (SSC).

I therefore applaud the National Science Foundation and the Electric Power Research Institute for maintaining enough interest and enough support so that a real clarification of the apparent contradictions can be pursued. If that clarification would lead to something on which we can agree and to a reaction probability which is small, but much bigger than the Gamow factor would allow, this would be a great discovery. Perhaps a neutral particle of small mass and marginal stability is catalyzing the reaction.

You will have not modified any strong nuclear reactions, but you may have opened up an interesting new field (i.e., the very improbable actions of nucleii on each other. So, I am arguing for a continuation of an effort, primarily for the sake of pure science. And, of course, where there is pure science, sometimes, at an unknown point, applications may also follow.

But, according to my hunch, this is a very unclear and low probability road into a thoroughly new area. The low probability has to be balanced against the great novelty. But to think beyond that and ask what is the practical application, what this very unknown area of nuclear physics may produce, that I claim, is completely premature.

Thank you very much.

Section 2

ELECTROCHEMISTRY OF THE PALLADIUM D$_2$O SYSTEM

Nathan Lewis

Department of Chemistry

California Institute of Technology

ELECTROCHEMISTRY OF THE PALLADIUM D$_2$O SYSTEM

Nathan Lewis
Department of Chemistry, California Institute of Technology

First, I would like to express my thanks to the organizers of the workshop for allowing me to describe my viewpoint concerning the electrochemistry of the palladium-D$_2$O system. My task is to describe it without taking a stand for or against the alleged phenomena which we are here to discuss. I was told by the organizers that my role was not to present negative data but to point out some of the key concepts and possible problems in electrochemistry as it applies to cold fusion. Therefore, my presentation is intended be of a pedagogical character, but it will not educate the electrochemists in the audience. However, I hope that it will provide some background to the physicists and others who may not be very familiar with the electrochemical details. I hope to demonstrate what has been measured, what has not been measured, what controls are needed, and what other issues exist, particularly in respect to the electrochemical charging of palladium cathodes with deuterium, to measuring the heat flux, and to measuring separation factors for the isotopes of hydrogen.

A substantial amount of hearsay and rumors have been heard concerning what might occur at this meeting and also concerning the citing of positive confirming results based on the work of laboratories whose results have not been discussed in scientific meetings or written up in peer-reviewed journals. I believe that we must avoid any of these pitfalls. Since I must be objective, I will discuss only those things which I feel that I definitely know, and which will therefore be from my own direct experience in my laboratory. I hope that the same philosophy will be adopted in other contributions to this workshop.

The electrolysis of water requires the application of a current and a voltage across two electrodes. A constant current, a constant voltage, or indeed a constant power, may be applied, depending on the source. The application of alternative parameters will require different measurements and measuring instruments. In addition, since different losses occur in different parts of the electrical circuit, the potential drops in the various circuit elements should be simultaneously measured. While electrochemists know the crucial role which the potential of an electrode plays, it has nevertheless been rare when the researchers working in this area have reported the values of the individual electrical potentials in their circuit elements. Usually, only the total applied cell voltage has been measured. This can be a great source of uncertainty in comparing experiments. Hence, the individual potential differences should be carefully documented by all workers in this field in the future. Measurement of the electrical power delivered to the cell does not appear to be too

complicated. However, if one is searching for small differences between the input power and the heat output, it turns out to be not quite so straightforward. Because of the experimental difficulties which are invariably involved in the calorimetric measurements, the facts as promoted by the popular press are certainly different from the real-time experimental data.

Accordingly, I will present some of the published experimental data on this subject, which will give a good impression of the magnitude of the effects we may be considering. The amounts of excess heat claimed vary from factors of 10% to factors of 400% or 100%. The size of such factors makes a large difference in the design of the experiments and in the equipment used. In short, we must appreciate what we are looking for in terms of heat detection.

The so-called isotope separation factors are also important. When water is electrolyzed to hydrogen isotopes and oxygen, it becomes enriched in the heavier isotope. This results from kinetic effects resulting from the different reaction activation energies, which depend on the zero-point energies, hence on the vibration frequencies, of the different isotopes, and on the complementary effects of nuclear tunnelling. These inevitably lead to a concentration of the heaviest isotope in the residue. This effect may therefore lead to the detection of tritium. If tritium is detected in large amounts, this cannot be explained by these kinetic effects alone. If very large effects occur, amounting to factors of a million or more, these cannot be obtained as a result of electrolytic enrichment. However, enrichment factors on the order of 2 to 3 certainly are within what one might expect from this mechanism. These facts will not be new for the electrochemists, or for those who routinely assay tritium.

In characteristic experiments, one can either apply a known voltage across the two electrodes and measure the corresponding current, or vice versa. In all cases, there will be an electrical lead resistance, and a resistance in the palladium cathode, which varies depending on its hydrogen or deuterium content. There will be a solution resistance, as shown. There will be an interfacial resistance at both electrodes, which derives from the existence of an electrochemical reaction, which is faradaic, rather than ohmic. In other words, unlike those of the other elements, its resistance varies with the applied current or voltage. However, for convenience the interfacial resistances can be expressed as an ohmic resistance at any given current density. As one would expect, all the above resistances will be in series, so that the largest values will dominate in the overall voltage drop. Thus, the component which contributes to the largest value must be determined. In a typical cell of Fleischmann-Pons type, the resistance in the leads and in the palladium itself will generally be unimportant. The most important factors contributing to the voltage drop in the cell will be the solution resistance, and probably more important, the interfacial resistance at

each of the two electrodes. Measurement of the interfacial component of the voltage drop is often measured by current interruption.

Voltage drop resulting from ohmic resistance decays immediately, whereas that from faradaic and diffusion processes decays more slowly. One needs to know the potential of the working cathode (or anode) relative to some reference potential, which is typically zero on the standard hydrogen electrode scale, i.e, the reversible hydrogen electrode at a pH equal to zero. It is difficult to give an absolute indication of this potential, but the best values lie between +4.5 V and +4.7 V versus the vacuum level. One can also measure the electrode potential versus a standard electrode whose value is pH independent, or on the normal hydrogen scale, which is measured at the same pH as the experiment. This scale is the most convenient for general use with hydrogen or oxygen electrode systems, and it will be used in any subsequent discussions. It is important to establish the interfacial potential of the electrodes relative to this value. In practical cell designs, it is also important to determine the solution resistance.

Equipment and experiments may differ, but in a typical case the lead resistances are small, generally less than 1 Ω. The palladium electrode resistance is 9.9 x 10^{-6} Ω-cm for the pure metal and 1.7 x 10^{-5} Ω-cm for the composition $PdD_{0.8}$. Thus, the resistance of a 0.2 cm diameter, 10 cm long rod will lie between 3 x 10^{-3} and 6 x 10^{-3} Ω, depending on its loading. This change in resistance may be used to measure the loading, but I believe that it is better to remove the palladium from the cell and desorb the deuterium at high temperature to obtain a reliable value of the composition.

Therefore, as is the case of the leads, the palladium cathode resistance is small. In constrast, the interfacial resistance, which varies with the current density, can lie between about 1 and perhaps 100 Ω. With typical electrodes and current densities, the interfacial voltage drop may be between 1.0 and 1.5 V. Electrochemists call this voltage drop the kinetic overpotential, and it represents the irreversible work which is necessary to pass a given current to produce deuterium and oxygen from D_2O at a given rate. The reaction is catalytic, with the result that the ease of reaction, which is to say the overpotential at a given current density, varies with the electrode material. Palladium and platinum surfaces are particularly effective for hydrogen or deuterium evolution. Platinum is one of the best surfaces for oxygen evolution, but this reaction occurs at higher overpotentials than the corresponding hydrogen process.

The solution resistance will generally also be quite high. That for 0.0858 M LiOH is 49 Ω-cm. The corresponding value for LiOD has been measured by Dr. Martin at Texas A&M University, and it is about 50% higher than that of LiOH over a wide concentration range. Thus, a typical value for 0.0858 M solution is 74 Ω-cm,

and in a typical cell with 0.5 cm^2 electrodes separated by a distance of 0.2 cm, the solution resistance would be about 60 Ω, which would increase if the interelectrode separation increased. Hence, the solution resistance will predominate at low current density, whereas the Faradaic resistance should predominate at high current density. Another important point is that if experiments in LiOH and LiOD solutions are to be compared, we should remember that the Joule heating will be 50% greater in the latter at the same concentration. This is important in the design of blank experiments.

For a pH 3 solution dominated by sodium and sulfate ions at 0.035 M, the effect of proton conductivity (at the equivalent concentration of about 10^{-3} M) will be small. This electrolyte is the geological "Mother Earth" composition used by Jones. The correct IR drop for two 1.7 cm^2 electrodes separated by 2 cm, is on the order of 200 Ω. Fig. 3 shows the electroactive materials present in this electrolyte. The electrochemical potentials for their reactions as shown are expressed relative to the vacuum level. On the pH = 0 hydrogen electrode scale, the latter is +4.5-4.7 V. Ions present include Ti, Ni, Fe, H, Pd, and Au. The solution resistance is the most important voltage drop across the cell. The difference between the anode and cathode potentials is the much smaller difference between the interfacial potential drops. The actual values of the anodic and cathodic potentials will determine if the electroactive ions can indeed react at these electrodes. Thus, if we apply a constant voltage of, e.g., 5 V across the anode and the cathode, a current will flow. Its value will be adjusted by the solution resistance, and the current-dependent (i.e., potential-dependent) interfacial resistances, which themselves depend on the reactions taking place at the electrodes. The sum of the interfacial potentials and the IR drop will be equal to 5 V, but we cannot easily predict the values which the interfacial potential differences will take up. Therefore, we cannot absolutely say whether or not Ni^{2+} is being reduced to Ni^0, or indeed whether the cathode was more negative than this potential. Equally, we cannot say *a priori* whether the anode is oxidizing water to oxygen. Hence, for a given applied cell voltage the specific electrochemical reactions occurring at a given cathode at a given applied voltage depend on the spacing, on the geometry of the cell, and on the conductivity of the electrolyte.

At constant current (galvanostatic conditions) the situation is simplified. The voltage drop across the electrolyte double layers is fixed, and the interfacial resistances adjust themselves to correspond to the currents flowing, which represent the rates of the electrochemical reactions at the electrodes. This is one reason why electrochemists often prefer to operate experiments under galvanostatic control, since the reactions rates are then independent of the solution resistance.

The rates of many reactions are controlled by mass transport. In the example quoted, Ni^{2+} must diffuse to the electrode surface to discharge to Ni^0. Typical diffusion coefficients are in the range 10^{-5} to 10^{-6} cm^2/sec. This means that expressed in current terms, the diffusion rate of a typical ion in a stirred aqueous solution is about equal (in A/cm^2) to its concentration (in M/l). If the applied current density exceeds the maximum diffusion rate for a particular species, the potential of the cathode will move in a negative direction until a reaction is located which can be sustained. For example, if the applied current density is too large for the deposition of Ni^0 from Ni^{2+}, the electrode potential will go to the next potential range where reaction may occur, in this case, deposition of Fe^0 from Fe^{2+}. At this potential, both iron and nickel will be codeposited, with the latter under diffusion-limited conditions. It the current is too large to be sustained by both of these processes, along with any other cathodic processes occurring at even higher potentials, then the electrode will reach the hydrogen evolution potential. Under these conditions, gaseous hydrogen will be produced from water, and the trace metals will be codeposited. Hydrogen evolution is from water, which is present in overwhelming concentration and has an enhanced transport mechanism for H^+ and OH^- ions. Hence, no limiting current would be expected for this process in any reasonable current density range. The situation at the anode is similar for oxidative processes, with the anode ultimately reaching oxygen evolution at a sufficiently high current density. Again, this reaction will have no limiting current in the normal current density range. For information on transport limitation, electrochemists make measurements with a rotating disk electrode, which permits precise control of the steady-state diffusion layer thickness.

We will now turn to a further discussion of the implications of electrode potential. The Nernst equation for potential contains the standard reversible thermodynamic value of the potential (in cV) for a process (corresponding to $-\Delta G^\circ/nF$, where ΔG° is the standard free energy of the process, n is the number of electrons involved, and F is the Faraday), corrected for the free energy change as a function of concentration. Since free energy and concentration are related logarithmically, a 10-fold change in the latter results in a 60 mV change in reversible potential at 298°K.

In practice, these reversible potentials can be very misleading. If one measures the potential of the palladium cathode operating a high current density for hydrogen evolution, one finds that it is -0.8 V against the reversible hydrogen electrode in the same solution, i.e., the potential at which hydrogen should be evolved according to the Nernst equation.

There is also controversy regarding the actual estimate of the internal pressure of deuterium gas inside the Pd. One often hears figures as high as 10^{27} atm quoted. I would now like to tell you how this figure was obtained and what it really means physically. A typical experiment uses a two-compartment electrochemical cell with a porous separator between the compartments. On one side is a palladium

electrode in the electrolyte, which is saturated with hydrogen at 1 atm. pressure; on the other side is a high-surface-area (hence, highly catalytic) platinum electrode, also in contact with 1 atm of hydrogen. No current flows in the system. The potential of the platinum electrode is that of the reversible hydrogen electrode in that electrolyte, which we may define as zero on our reference potential scale. If the potential of the palladium electrode is -0.8 V on this scale, the question one should then ask is, "Using the Nernst equation, what hydrogen pressure is necessary to make no net current flow for the 2-electron hydrogen reaction at an electrode at -0.8 V on the hydrogen electrode scale?" The answer is 10^{27} atm. Clearly, this situation is absurd, since the atmosphere above the palladium electrode is only at 1 atm pressure. When current is flowing, the potential which is measured bears no relation to the pressure of the hydrogen produced at the surface of the electrode, or the pressure inside the electrode. Similarly, the pressure outside the system may indeed be considerably less than the pressure at the surface of the electrode, where supersaturation may take place due to gas bubble formation. The true hydrogen pressure at the surface of, or in the electrode, may be arbitrarily big or small depending on the details of the process.

The potential which is measured gives information on the phenomenon known to electrochemists as overpotential. It indicates that the electrochemistry is a high energy process, in which an electrical potential can be used to drive a reaction as an alternative to using high chemical potentials, e.g., high pressures. It is easy to apply 0.8 V, and for example, maintain zinc in a reduced state, whereas it is much more difficult to perform the equivalent via the effects of chemical potential, which would require a hydrogen pressure of 10^{27} atm.

Potentials are generally measured relative to a reference electrode with current flowing, usually under galvanostatic conditions. Alternatively, a potentiostat may be used to measure current flowing as a function of the applied potential, again relative to the reference electrode. This instrument operates by electronically adjusting the current to maintain the potential of the working electrode at the desired value. The value of the potential measured will contain the value of the interfacial potential, together with the free energy difference between the working electrode (in this case, a palladium cathode and the reference electrode). It will also contain any potential drop in the solution, or uncompensated solution resistance, which can be minimized by a special reference electrode design. The uncompensated solution resistance may be measured manually or by electronic feedback built into the potentiostat. If, for example, 0.8 V is applied to the cathode, and if the effect of the uncompensated solution resistance is determined to be 0.2 V, then the

remaining 0.6 V is a combination of the free energy differences and the interfacial potential difference. The effect of the latter can be eliminated by measuring the potential after current interruption, which shows an instantaneous drop for the effect of solution resistance between the cathode and the reference electrode, and a slower decay for the interfacial potential difference. Thus, we are left with the potential value corresponding to the free energy difference between the palladium cathode and the reference electrode. This will allow us to determine the hydrogen pressure in the palladium alloy phase.

In our laboratory, we obtained potentiostatic data for a palladium cathode in 0.1 M LiOD relative to a convenient reference, the palladium-deuterium electrode charged to the $\alpha-\beta$ phase equilibrium, rather than to a reversible hydrogen (deuterium) electrode. The former has a reversible potential of +50 mV relative to the latter. The results showed the overall current potential relationship both uncorrected, and corrected for solution resistance. After current interruption, we determined the free energy difference between the cathode and the reference electrode. It was shown that the interfacial potential difference was quite small, and that the free energy difference is the predominant potential term in this case, representing -0.7 to -0.8 V at a current density of 60 mA/cm^2. This value represents the minimum free energy difference to maintain the palladium-deuterium phase at equilibrium with no current flowing. This free energy difference tells us which electrochemical reactions are thermodynamically possible under these conditions.

Most of the University of Utah electrochemical experiments used 0.1 M LiOD as electrolyte. However, Brigham Young University's work used a 1.0 mM acidic solution. In the first case, a basic solution is used, which contains about 10^{-13} M D$^+$ ion, and correspondingly 10^{-1} M OD$^-$ ion. In the second, D$^+$ ion is 10^{-3} M. Both solutions contain about 55 M D$_2$O, which supports most of the cathodic process. In both electrolytes, the atomic fraction of deuterium in the palladium cathode can be increased from 0.8 to 0.85 by continued electrolysis. This has often been reported by measuring the weight change in the system, but this method is likely to be inaccurate, since other material can deposit on the palladium under cathodic conditions. The most effective method of determining the composition is by degassing the electrode, with volumetric or pressure determination of the gas evolved.

If we now turn to calorimetry, I would like to discuss the heat flux calculations which must be carried out in open and closed systems. In a closed system, in which the only reactions are decomposition of heavy water to deuterium and oxygen, followed by their recombination, the voltage across the cell terminals multiplied by the total cell current indicates the heat entering the cell. According to

the first law of thermodynamics and in the absence of any other effects, this value should equal the heat leaving the calorimeter.

In an open system, the applied voltage is partitioned into two quantities. The first part, when multiplied by the total current, represents the energy flow in the form of heat into the cell. The second part is the energy which is required to form deuterium at the cathode and oxygen at the anode, which escape from the open system. The standard enthalpy of dissociation of D_2O to give D_2 and O_2 is well known. This value can be converted to an equivalent voltage necessary to electrolyze D_2O by dividing the molar heat of dissociation by the number of electrons per mole (i.e., two) and the value of the Faraday. The result is 1.48 V for liquid H_2O, and 1.527 V for liquid D_2O, under standard thermodynamic conditions at 25°C. This equivalent voltage, again multiplied by the cell current, must be subtracted from the total energy supplied to the cell to determine the output heat flux.

The difference between open and closed cases therefore concerns how much of the electric input power is partitioned into the energy flux from the cell and into the energy flux escaping with the evolved gases. If the system is closed, all of the input power appears as heat energy escaping from the calorimeter. If the system is open, an amount of energy up to a maximum value, depending on the electrolysis efficiency, can escape with the gases produced. Thus, the correction would be 1.527·I, where I is the total cell current, assuming that all of the electrode reaction represents water dissociation at 100% efficiency, with no recombination. Measurements of the latter have normally shown it to be very small. It can certainly depend on cell geometry, and on whether a separator is used between the electrodes. I do not intend to speculate on whether recombination can increase to the extent of causing a substantial error. I will simply note that it is possible. It can in principle occur via two methods. First, deuterium can be transferred via the electrolyte and be oxidized at the anode. Similarly, oxygen can be transferred to the cathode and there be reduced. Secondly, instead of being electrochemical, recombination can be chemical, taking place on catalytic surfaces, such as the sides of the cell where platinum or palladium may be deposited. If the fraction of the gases which recombine is x, then the correction for the amount of energy lost via the gases evolved will be 1.527·I(1-x).

Data on heat fluxes were reported in the original Utah work. I believe that it is important to understand this data analysis, because the raw data is not widely available and has not been published to date. Furthermore, the data analysis method also is not widely known, which leads to confusion regarding the magnitude of the effects actually observed that have been ascribed to anomalous excess heating. In fact, highly exaggerated estimates of excess power have appeared both in the popular press and in some of the scientific literature based on interpretations of the meaning of the originally reported excess power figures. For example, are the anomalous effects 1000% or 400% of the heat flux into the cell, or less than these values? Based on the published data of Fleischmann and Pons, the results show that often the differences being determined are very small, and they will therefore require very accurate calorimetry for a precise determination. Since both Professors Pons and Fleischmann are here, I would like to know whether my interpretation is consistent with their actual analysis method or if we have made an error in these calculations. (Fleischmann and Pons nod in agreement.) The widely quoted 400% and 1000% excess power numbers were calculated based on the assumption that the reactions can be carried out at 0.5 V, which assumes no 1R, with one electrode evolving deuterian and the other oxidizing it. This was based on highly questionable assumptions and was never measured in actual experiments. The measured excesses are actually very small (10-30% of total input power) in most instances, and in most cases, the observed heating power is less than the total input power. Only if no recombination is established, and accurate calibration is demonstrated, can these values be considered trustworthy. It would be far better to build a calorimeter in which the claimed 50 W of excess power yielded a result that was a factor of 2 to 3 higher than the calibration curve, not a mere 5-10% higher. This should be possible to construct and will be crucial if one is to demonstrate unambiguously a substantial excess-heat effort. This is a challenge which has not been met to date, but I hope that it will be met very shortly in order to resolve this issue. In my view, much of the data obtained has been insufficiently accurate to determine such small differences. Initial data show the charging of a palladium cathode with deuterium, which presumably was not producing excess heat, because of the time required for complete charging. In order to claim that excess heat is produced, the calorimeter constant must be claimed to be indeed a constant, and its value must be known with a high precision. Significant errors can occur in calorimetry, and they must be very carefully taken into account in interpreting measurements.

This is particularly evident when no recombination is assumed in open cells. For example, at low power, the overall cell voltage may be 3V; thus, after subtraction of the voltage equivalent to the heat of dissociation of D_2O, the heat flux entering the cell will be approximately 1.5-I, where I is the cell current, assuming no recombination. This represents a total change of 50%. Let us consider that a heater is used to model the cell. If we apply the same electrical power to the heater as that applied to the cell, then if the cell showed no recombination, the heat flux from the cell would be 50% of that from the heater. The remaining energy would escape in the evolving gases. As the power into the cell (i.e., the applied current and voltage) is increased, the fraction of energy represented by that in the evolving gases will proportionately decrease. In other words, at progressively higher voltages, 1.54 V represents a smaller fraction of the total cell voltage. Thus, performing the same experiment with the power into the heater equal to the power into the cell at these higher voltages, the heat flux from the cell should approach closer to the heater calibration line. Because the effective interfacial resistance is current-dependent, the data should not fall on a straight line. As a result, I would question the precision and accuracy of the data points in this work, which was reported in a highly publicized set of experiments as having confirmed an excess-power production rate in heavy water.

In our own calorimeters, we have maintained the current constant and adjust the heater power to determine the calibration constant as a function of time. These indicate that as gas is evolved, heat is in fact lost more effectively. Finally, for each point the system appears to approach a steady state. The question at issue is whether the change in calibration constant can be distinguished from an effect which is interpreted as a change in the heat produced by the cell. There are therefore two unknowns, namely the heat produced and the calibration constant. In order to uncategorically determine both unknowns, a calibration must be carried out at each data point. To date, this has not been generally done in most systems.

Some new data were very recently obtained in a closed system calorimeter in our laboratory, and they have only been obtained in one experiment, so far without an H_2O control experiment. Since the system is closed, no thermodynamic corrections are required for D_2O dissociation. In the calorimeter, the temperature of an internal water bath is accurately measured relative to an external one using thermocouples. The system is arranged so that the temperature differences are relatively large. After calibration, the current to the internal palladium-platinum

electrolysis cell, which had a 4 mm diameter, 1 cm long cathode, is turned on. If the cell had been showing an anomalous heat flux, the point would be far beyond the calibration line. We did not observe this. The challenge in other work therefore lies in accurate calibration and proof of an effect for outside-of-system errors.

I would now like to consider the question of separation factors for deuterium and tritium. When water is electrolyzed, a kinetic isotope effect occurs, so that molecules of the lighter isotope are preferentially evolved. This effect was studied by Libby, and the process has been used for isotopic enrichment. As to the values of the kinetic separation factors of the different isotopes, much more information exists on H_2O/HD (and ultimately HD/D_2 separation factors) in H_2O/D_2O mixtures than on the corresponding D_2/DT and DT/T_2 values. Three separation factors are of interest. One is the ratio of DT in the solution compared with that in the solid palladium phase. The next is the corresponding ratio in the electrolyte compared with that in the gas phase, and the third is that in the gas compared with that in the solid phase.

The known HD separation factors are to be expected to be greater than the corresponding DT values, because of the smaller mass ratio of the latter. The most relevant DT value would be that in the gas phase compared with that in the electrolyte, since this is of primary experimental interest. In acidic solution, the HD value is approximately 5, and that for DT would be expected to be about 2. For alkaline solution, we can use Fleischmann and Dandepani's 1974 data, which show that the HD separation factor between the electrolyte and gas phases is somewhat a function of potential. For a 1 M base, the corresponding values are 8 to 10. No literature data are available for DT, but a reasonable number would be approximately 3, which would depend somewhat on interfacial potential, i.e., on current density. Thus, if the value is 3, electrolysis of 1% of a dilute tritium-containing electrolyte without makeup would cause a tritium enrichment by a factor of 1.007. The corresponding figures for electrolysis of 10% of the solution would be 1.07; for 50%, 1.59, for 90%, 4.64, and for 99%, 21.5. If the solutions are made up to their original volume, which is normally the case in electrolysis experiments, then for electrolysis of 10% of the solution, tritium enrichment would be only 1.007; for 50%, 1.30; for 90%, 1.36; and for 99%, 1.21. The maximum value will be 1.38, corresponding to electrolysis of 81% of the solution. Thus, these numbers, even if they are approximate, set an upper limit on tritium enrichment by electrolysis. With 20 ml of electrolyte, adding 2 ml each day would result in a progressive enrichment of 1.06 in 8 days or 1.48 in 56 days. If we take the upper limit value of the separation factor, i.e., infinity, the enrichment each day would be by a factor of 1.1. Hence, after 8 days under these conditions, the enrichment would be 1.21, and 208 after 56 days,

so it may be argued that extensive tritium enrichment results from some unusual change from the expected value of the separation factor. This subject therefore requires further investigation.

In concluding, I would hope that this presentation has indicated some of the pitfalls of this research.

DISCUSSION (LEWIS)

Schneider: One can speculate on reducing the input voltage to lower levels than those observed. Some of the fuel cell community feel that values as low as 0.2 V may be possible in a cell with a deuterium anode.

Lewis: I think that idea is a misconception, based on the experimental data that have been obtained for deuterium evolution on bulk palladium. The measured open-circuit polarization is about -0.8 V versus the deuterium electrode potential. I believe that this is a thermodynamic quantity, not an irreversible overpotential. The reaction therefore cannot proceed at overpotentials more positive than -0.8 V, according to the first law of thermodynamics.

Hoffman: Some of the deuterium, or tritium when it is produced, dissolves from the gas phase into the liquid electrolyte. This can be important in some types of experiment, particularly those with deuterium anodes, such as in Dr. McKubre's pressurized experiments at SRI.

Lewis: My analysis ignores any dissolved gas in the liquid phase. I also ignored any dissolved tritium in the palladium. I have assumed that the system is open, not closed, with evolving deuterium and oxygen. Other types of electrode could be used in closed systems.

Yeager: The isotope separation factors, as well as the overvoltages, are extraordinarily sensitive to a number of variables that have not been emphasized. The surface topography of the electrode is particularly important. Literature values of electrochemical isotope separation factors have often not been measured under rigorous enough conditions.

Fleischmann: There are some mysteries concerning deuterium-tritium separation factors. The values obtained in industrial processes tend to be confidential. It would be useful to have access to the separation factor values.

Bockris: We have measured values of 1.7 to 2.2. It is particularly interesting that deuterium preferentially concentrates in palladium, which points to reverse isotope effects. It is also very difficult to understand a separation factor of two between the gas and liquid phases.

Jordan: Since this presentation was intended for non-electrochemists, it would be worth emphasizing that the pressure considerations which were discussed are all related to equilibrium electrodynamics. If there are overvoltage effects due to irreversible electron transfer, it is misleading to ascribe these as being equivalent to the effect of a higher deuterium partial pressure.

Lewis: The effects of overvoltage will simply further increase the electrode potentials beyond the reversible thermodynamic values. The essential factor is how high a voltage one has to apply to carry a given current on a palladium cathode.

Appleby: Do you have corresponding data for platinum?

Lewis: Not for this type of experiment.

Appleby: Platinum seems to have a higher overpotential than palladium at the same current density in the 1 A/cm^2 range. Palladium dissolves hydrogen or deuterium, whereas platinum does not. The effects observed on both metals involve mostly irreversible kinetic overpotential.

Lewis: That may be so, but my argument is essentially thermodynamic, involving the open-circuit potential difference between the actual electrode in the cell and the reference phase of the gas atmosphere.

Section 3

CALORIMETRY OF THE PALLADIUM-D-D$_2$O SYSTEM

Martin Fleischmann

Department of Chemistry

University of Southampton

Stanley Pons*

Department of Chemistry

University of Utah

*To whom correspondence should be addressed.

CALORIMETRY OF THE PALLADIUM-D-D₂O SYSTEM

Martin Fleischmann
Department of Chemistry, University of Southampton

Stanley Pons
Department of Chemistry, University of Utah

INTRODUCTION

The strange behavior of the isotopes of hydrogen dissolved in palladium under cathodic polarization is well documented[1]. Fig. 1 illustrates a number of the important features of the discharge of D_2O and of D_2 evolution for electrolyses in alkaline media as well as of the dissolution of adsorbed D in the palladium lattice. At the reversible potential the initial state of reactions (i) a D_2O molecule interacting with its surroundings together with an electron in the Pd lattice) is in equilibrium with the final state (an adsorbed atom and a deuteroxide ion again interacting with their surroundings). For experiments close to atmospheric pressure the lattice is already in the β Pd-D phase. Increases in the difference of the galvani potential between the metal and the solution $|\Delta(\phi_m - \phi_s)|$ (shown here in a highly simplified form as a linear potential drop in potential across the Helmholtz double layer) from the value at the reversible potential stabilize the final state with respect to the initial state to an extent $\Delta(\phi_m - \phi_s)F$ joules mole^{-1}. The adsorbed atoms are therefore "driven" onto the surface and, in turn, the adsorbed species are "driven" into the FCC lattice, step (ii), where they exist as D^+ ions, almost certainly in the octahedral positions. The adsorbed species are desorbed in the further step (iii). At very negative potentials, the D^+ species behave as classical oscillators[2]. A peculiarity of the Pd/D system as compared to Pd/H and Pd/T is that the diffusion coefficient of D exceeds that of either H or T![3] It is tempting to attribute this phenomenon to the boson character of the particles but we do not wish to let our enthusiasms cloud our judgement - the phenomenon certainly requires further investigation.

The concentration of D^+ in the lattice under equilibrium conditions is already very high ($D/Pd \cong 0.6$-0.7). The composition of the lattice at high negative potentials has still not been established with precision but it would be surprising if the D/Pd ratio did not approach unity under these conditions. The dominant effect of the increase in cathodic potential must, however, be an increase in the activity of the dissolved hydrogen. The activity will be determined under steady state conditions by the rates of steps (i), (iii), and (iv) but we will restrict attention here to a quasi-thermodynamic argument based on an hypothetical equilibrium of reactions(i) and (ii). For such an equilibrium we can equate the electrochemical potentials of the initial and final states

$$\bar{\mu}_{D^+,m} + \bar{\mu}_{OD^-,s} = \mu_{D_2O,s} \tag{1}$$

or

$$\mu_{D^+,m} + \phi_m F + \mu_{OD^-,s} - \phi_s F = \mu_{D_2O,s} \tag{2}$$

i.e.

$$\mu_{D^+,m} = \mu_{D_2O,s} + \mu_{OD^-,s} - (\phi_m - \phi_s)F \tag{3}$$

In this expression $\mu_{D_2O,s}$ and $\mu_{OD^-,s}$ will be close to the standard state values. It should be noted that $\mu_{D^+,m}$, $\mu_{OD^-,s}$, and $(\phi_m - \phi_s)$ are quantities which are not accessible to thermodynamic measurement but the change in chemical potential of the dissolved D^+, $\Delta\mu_{D^+,m}$ due to a change of the galvani potential potential difference $\Delta(\phi_m - \phi_s)$, from the value existing at the reversible potential is thermodynamically defined (as is $\Delta(\phi_m - \phi_s)$).

Values of $\Delta(\phi_m - \phi_s)$ as high as 0.8 V can be achieved using conventional electrochemical systems and values even higher (in excess of 2V) could be achieved under special conditions[4]. While the energy values $\Delta(\phi_m - \phi_s)F$ may appear to be modest, they are, in fact, of astronomical magnitude. Thus, if one were to attempt to achieve the same activity of dissolved D^+ by the compression of D_2 using reaction steps (ii) and (iv) under equilibrium

conditions (as is customary in heterogeneous catalysis) we would need to satisfy the condition

$$2\mu_{D^+,m} + 2\mu_{e,m} = \mu^{\varnothing}_{D_2,g} + RT \ln P_{D_2} \qquad (4)$$

where P_{D_2} is the fugacity of the gaseous D_2. We obtain
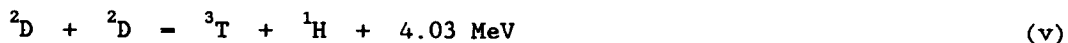
$$\mu_{D^+,m} = \mu^{\varnothing}_{D_2,g}/2 - \mu_{e,m} + RT/2 \ln P_{D_2} \qquad (5)$$

and, it can be seen that a 0.8 eV shift of the potential of the electrode corresponds to a $\cong 10^{27}$ fugacity of D_2:

$$0.8F = RT/2 \ln P_{D_2} \qquad (6)$$

Such high hydrostatic pressures are naturally not achievable on earth and, even if they were, other phenomena would intervene (formation of metallic D, collapse of the Pd lattice). The argument is instructive, however, from several points of view: in the first place it points to the importance of the "poisoning" of the desorption steps (iii) and (iv) (so as to drive (i) as close to equilibrium conditions as possible); secondly, it points to the special role of cathodic polarization in causing the "compression" of D^+ into the lattice; thirdly, it suggests that clusters of D^+ must form in the lattice under such extreme conditions by analogy to the nucleation of metals. Such clustering may well be initiated at the octahedral sites which would distort so that these sites might then be more correctly described as being parts of dislocation loops.

The starting point for our investigation was the question: would it be possible to induce the established nuclear fusion reactions[5]

$$^2D + {}^2D = {}^3T + {}^1H + 4.03 \text{ MeV} \qquad (v)$$

$$^2D + {}^2D = {}^3He + n + 3.27 \text{ MeV} \qquad (vi)$$

under these conditions? We were naturally aware of the many reasons why this might not be possible. Our discussions always ended on the note: this experiment has a one in billion chance of success. Nevertheless, there were (and still are) a number of further factors which point to the possibility of inducing nuclear reactions. The dissolved D^+ is, in fact, a very high

density, low ion temperature plasma existing in a high electron concentration. We can therefore pose the following conundrum: it would be expected that the s-electron density around the nuclei would be high but this would lead to the formation of D_2. As this is not observed the s-electron density must in fact be low. While we do not subscribe to the notion of the formation of heavy electrons, we recognize that the electron density in the clusters must be highly asymmetric and that it is necessary to develop a priori calculations about the many body problem (i.e. taking into account the presence of the lattice) before it is possible to make any predictions of the Coulomb repulsion and nuclear motion in the clusters contained in the host lattice. We also draw attention to two further relevant observations. Firstly, the source of the original reactions (v) and (vi)[5] appears to have been overlooked in all of the comment about our initial announcement[6,7]. This neglect has no doubt been due to the change of terminology since the 1930's (deuterium was called diplogen and the deuteron was called the diplon at that time so that casual searches fail to reveal the early literature). Cloud chamber work[8,9] at the time of the discovery[5] showed quite clearly that low energy deuterons undergo at the least reaction (v). Secondly, it is known that high density low ion temperature D^+ plasmas induced by electron-cyclotron resonance in D_2 gas in magnetic mirror devices generate neutrons[10] presumably by reaction (vi). This observation too appears to have been forgotten.

It is now difficult to express our astonishment at our results as they became available: it became clear that there were only very low levels of radiation in the electrolysis and that reactions (v) and (vi) only took place to extremely small extents. Nevertheless excess enthalpy over and above that supplied to the cell for the electrolysis of D_2O

$$2D_2O \; \rightleftharpoons \; 2D_2 + O_2 \qquad\qquad\qquad\qquad \text{(vii)}$$
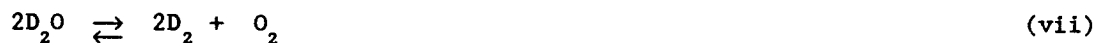
was being generated and the magnitude of the excess enthalpy was such that it could not be explained by chemical reactions. It was also clear that it was necessary to carry out large numbers of experiments for long times (the median time scale for an experiment cycle is three months) in view of the irreproducibility of the phenomena. We therefore made the low cost calorimetric investigation of large numbers of electrodes our initial prime method of investigation and we give an account of this work in this report.

<u>EXPERIMENTAL</u>

Fig. 2 illustrates the simple single compartment Dewar cell calorimeter we have adopted for most of our work. The general principles underlying the design have been described elsewhere[11]. The central palladium cathode was surrounded by an helical anode closely wound on glass rod supports and this ensured uniform charging of the cathode. Measurements using dye injection (tracer technique of chemical reaction engineering) have shown that at the minimum currents used in most of the experiments (200 mA) radial mixing is very rapid (time scale < 3 s). Axial mixing is somewhat slower($\cong$ 20 s) but,as heat injection into the system is axially uniform and, as the thermal relaxation time is $\cong$ 1600 s, the cells behave as well stirred tanks. In agreement with this prediction measurements with an array of 5 thermistors which could be displaced in the radial and axial directions have shown that the maximum temperature variation was $\pm 0.01^{\circ}$ except in contact with the bottom Kel F support where it reached 0.02°. All temperature measurements were made with specially calibrated thermistors (Thermometrics Ultrastable Thermoprobes, $\cong$ 10 kΩ, $\pm 0.02\%$ stability per year).

The cells were maintained in specially constructed thermostats (1/2" thick Plexiglas bath surrounded on 5 sides by 2" thick foam insulation bonded on both sides to aluminum foil, the whole structure being enclosed in a 1/16" thick sheet steel container); the water/air interface was allowed to evaporate freely. Stirring with oversized stirrer-temperature regulators ensured that the bath temperature could be controlled to $\pm 0.01^{\circ}$ of the set temperature (in the vicinity of 303.15K) throughout the whole space at depths greater than 0.5 cm below the water surface and to $\pm 0.003^{\circ}$ at any given point. The water level in the thermostats was controlled using dosimeter pumps connected to a second thermostat. Up to 5 cells were maintained in each of 3 thermostats at any given time.

All experiments were carried out galvanostatically (Hi-Tek DT2101 potentiostats connected as galvanostats as shown in Fig. 3). The systems could be calibrated at any given operating point using metal film resistor chains in the cells (Digikey ±1% accuracy 5 x 20Ω). The procedure adopted was as follows: after the addition of D_2O (or of electrolyte following sampling for analysis for tritium or HDO) the system was allowed to equilibrate for at least 6 thermal relaxation times. A constant current was then applied to the resistor chain (again supplied by a potentiostat connected as a galvanostat) for 3 hours (i.e. > 6 thermal relaxation times) to give a temperature rise of $\approx 2^{\circ}$ above the sloping base line and this current was then switched off and the relaxation of the system to the original sloping base line was followed. Cell parameters were monitored every 5 minutes using Keithley Model 199 DMM multiplexers to input data to Compaq 386 16 MHz computers. The measuring circuits were maintained open except during the actual sampling periods (voltage measurements were allowed to stabilize for 2s before sampling and thermistor resistances were allowed to stabilize for 8s before sampling). Data were displayed in real time as well as being written to disks. An example of a set of temperature-time plots and the associated cell potential-time plots is illustrated for one experiment at three different times in Figs. 4A-C.

Experiments were carried out on 0.1, 0.2, 0.4, and 0.8 cm diameter x 10 cm long Pd (special grade, Johnson Matthey) electrodes and on 0.1 x 10 cm Pt (Johnson Matthey) electrodes. At the highest current densities used the electrode lengths were reduced to 1.25 cm and the spacing of the anode winding was also reduced. These shorter electrodes were placed in the bottom of the Dewar cells so as to ensure adequate mixing. Measurements reported here were made in D_2O (Cambridge Isotopes) of 99.9% purity; light water levels in the cells never rose above 0.5%. Results reported here have been obtained in 0.1$\underline{M}$

LiOD prepared by adding Li metal (A.D. Mackay ^{6}Li/^{7}Li $-$ 1/9) to D_2O; 0.1$\underline{M}$ LiOD + 0.1$\underline{M}$ Li$_2$SO$_4$ and 1$\underline{M}$ Li$_2$SO$_4$ were prepared by adding dried Li$_2$SO$_4$ (Aldrich 99.99% anhydrous, ^{6}Li/^{7}Li $-$ 1/11) to 0.1$\underline{M}$ LiOD and D_2O respectively. A single batch of electrolyte was used for any given experimental series. Blank experiments were carried out both in 0.1$\underline{M}$ LiOD in D_2O and 0.1$\underline{M}$ LiOH in H_2O.

The current efficiencies for the electrolyses according to reaction (vii) were determined by measuring the combined rates of gas evolution from the cells. Surprisingly, these efficiencies were higher than 99% as was also shown by the record of D_2O additions for experiments having low cell temperatures. Such high current efficiencies have now also been reported in other work[12,13]; they can be understood in terms of the inhibition of D_2 oxidation at the anode by Pt-oxide formation and the extensive degassing of the oxygen content of the electrolyte in the cathode region by the vigorous D_2 evolution. In supersaturated, highly stirred solutions (high current densities), rapid degassing is observed even near the anode. These high current efficiencies greatly simplify the analyses of the experimental data.

Data evaluation, error analysis, and results

The "black box" representation of the calorimeters

In common with all other physicochemical and engineering devices, the
evaluation of data from the behavior of the Dewar-type electrochemical
calorimeters requires the construction of accurate "black-box" models, Fig. 5.
In this particular case the models must account for the enthalpy and mass
balances in the cell which can be combined through the current efficiency, γ,
of the electrolysis. The nature of the enthalpy flows into and out of the
"black box" will be apparent and we make the following additional comments:

a) the enthalpy flow into the cell due to the electrical input is
$(E_{cell}(t) - \gamma E_{thermoneutral,cell})I$. The term $E_{thermoneutral,cell}$ is the cell
voltage at which the electrolysis is thermoneutral; this differs from the
reversible potential of reaction (vii) since the electrolysis takes place with
an increase of entropy.

b) the current efficiency, γ, can be taken as unity (see above). This greatly
simplifies the analysis of the data.

c) in the analysis of the data we have neglected the enthalpy content of the
gas stream due to the D_2O content, $0.75\left(\dfrac{P}{P^*- P}\right)C_{P,D_2O,v}\,\Delta\theta$, as well as that
due to the evaporation of D_2O, $0.75\left(\dfrac{P}{P^*- P}\right)L$. Both these terms have been
written assuming the gas stream is saturated with D_2O at the relevant cell
temperature. The neglect of these terms causes an underestimate of the excess
enthalpy and we have throughout adopted this strategy (see further below).
The terms are relatively small for values of $\Delta\theta < 20^{\circ}$ but the second,
especially, becomes large and the dominant form of heat transfer from the cell
as the temperature approaches the boiling point. Our calorimeters are

unsuitable for measuring the heat outputs from the cells under these conditions.

d) heat transfer from the calorimeter to the surroundings can be written in a variety of ways depending on its design and properties as well as the chosen level of approximation[11]. For the Dewar-type cells, Fig. 2, heat transfer for a hypothetical steady state generation of Q watts is controlled by a mixture of radiation and conduction

$$Q = k_R \left[\left(\theta_{bath} + \Delta\theta \right)^4 - \theta_{bath}^4 \right] + k_C \Delta\theta \tag{7}$$

Similarly for the steady state following the additional injection of ΔQ watts to calibrate the system we have

$$Q + \Delta Q = k_R \left[\left(\theta_{bath} + \Delta\theta + \Delta\Delta\theta \right)^4 - \theta_{bath}^4 \right] + k_C \left[\Delta\theta + \Delta\Delta\theta \right] \tag{8}$$

The separate determination of k_R and k_C leads to an increase in the <u>random</u> errors in the estimation of the heat flows from the cells. We have therefore adopted the strategy of neglecting the conductive term while making an appropriate increase in the radiative term

$$Q \cong k_R' \left[\left(\theta_{bath} + \Delta\theta \right)^4 - \theta_{bath}^4 \right] \tag{9}$$

and

$$Q \cong k_R' \left[\left(\theta_{bath} + \Delta\theta + \Delta\Delta\theta \right)^4 - \left(\theta_{bath} + \Delta\theta \right)^4 \right] \tag{10}$$

We have shown elsewhere[11] that this leads to a small <u>systematic</u> <u>underestimate</u> of the heat flow from the cell (and hence the excess enthalpy). However, as the correct value of the radiative term can be estimated from the Stefan-Boltzmann constant and the surface areas of the cells, a correction can readily applied (if this is desired) to give the heat output from the cells to

within 1% of the enthalpy input or 1 milliwatt whichever is the greater.
These are the figures which we have always quoted in lectures describing our
initial results[6,7].

An important aspect of the approximations (9) and (10) is that any other
term linear in $\Delta\theta$ can similarly be accounted for by making an appropriate
increase or decrease in k_R (see below).

A further factor which needs to be taken into account is that for a
continuously reacting chemical system (open system) such as the
electrochemical Dewar cells, the cell contents change with time. The extent
of the radiant surface decreases with time while the length of any parallel
conduction path increases with time. To a first approximation we would
therefore expect the heat transfer coefficients to decrease linearly with time
and we write

$$Q \cong k_R^{'0} \left[1 - \frac{(1 + \lambda) \gamma It}{2FM^0} \right] \left[\left(\theta_{bath} + \Delta\theta \right)^4 - \theta_{bath}^4 \right] \tag{11}$$

where the term λ allows for a more rapid decrease of the radiant surface area
(and increase of the length of the conduction path) than would be predicted by
electrolysis alone in view of the internal solid cell components. The
superscript ^{0} here and elsewhere in this text denotes a value at a chosen time
origin.

e) a general expression for the water equivalent is

$$M = M^0 - \frac{(1 + \beta) \gamma It}{2F} \tag{12}$$

where, as for the heat transfer coefficient, the term β allows for a more
rapid decrease of the water equivalent with time than would be predicted by
electrolysis alone.

f) the term $\dfrac{\gamma I}{F} \displaystyle\int_0^t \left[0.5 + 0.75 \left(\dfrac{P}{P^* - P} \right) \right] C_{P,D_2O,\ell} \, \Delta\theta' \, dt$ is the enthalpy input to

the cell due to the addition of D_2O to make up for the losses due to

electrolysis and evaporation. Here $\Delta\theta'$ is the difference in temperature

between the cell and make-up stream. In practice it has been found convenient

to add D_2O at fixed intervals of time and, provided measurements are initiated

at times longer than 6 thermal relaxation times following this addition, the

effect of this term can be neglected in the further analysis.

We therefore obtain the differential equation governing the behavior of

the calorimeter

$$C_{P,D_2O,\ell}\left[M^0 - \frac{(1 + \beta)\ \gamma It}{2F}\right]\frac{d\Delta\theta}{dt} - C_{P,D_2O,\ell}\ \frac{(1 + \beta)\ \gamma I\Delta\theta}{2F}$$

$$- (E_{cell}(t) - \gamma E_{thermoneutral,cell})I + Q_f(t) + \Delta QH(t-t_1) - \Delta QH(t-t_2)$$

$$- \frac{\gamma I}{F}\left\{\left[0.5C_{P,D_2} + 0.25C_{P,O_2} + 0.75\left(\frac{P}{P^* - P}\right)C_{P,D_2O,v}\right]\Delta\theta + 0.75\left(\frac{P}{P^* - P}\right)L\right\}$$

$$- k'^0_R\left[1 - \frac{(1 + \lambda)It}{2FM^0}\right]\left[\left(\theta_{bath} + \Delta\theta\right)^4 - \theta^4_{bath}\right] \tag{13}$$

Equation (13) is difficult to apply because $E_{cell}(t)$ and $Q_f(t)$ are unknown

functions of time. We note, however, that since we are only concerned with

small changes of temperature at any given origin, θ^0, we can carry out a

Taylor series expansion at this point and, retaining only the first

derivatives we obtain

$$\left\{\frac{dE_{cell}}{d\theta} + \frac{d}{d\theta}\left[\frac{0.75I}{F}\left(\frac{P}{P^* - P}\right)\left(C_{P,D_2O,v}\ \Delta\theta + L\right)\right]\right\}I\Delta\theta' - \frac{\psi I}{\theta^0}\Delta\theta' \tag{14}$$

We assume also that $Q(t)$ is constant during any one measurement cycle and,

taking note also of

$$\Delta H^\emptyset_{cell} - \Delta H^\emptyset_{bath} + \sum_i \nu_i C_{P,i}\Delta\theta \tag{15}$$

as well as of b) and c) we can write (13) in the more tractable form

$$C_{P,D_2O,\ell} \left[M^0 - \frac{(1 + \beta)It}{2F} \right] \frac{d\Delta\theta}{dt} \quad - C_{P,D_2O,\ell} \quad \frac{\beta I \Delta\theta}{2F}$$

$$= \left(E^0_{cell} - E_{thermoneutral,bath} + \frac{\psi \Delta\theta'}{\theta^0} \right) I + Q_f(t) + \Delta QH(t-t_1) - \Delta QH(t-t_2)$$

$$- k_R'^0 \left[1 - \frac{(1 + \lambda)It}{2FM^0} \right] \left[\left(\theta_{bath} + \Delta\theta \right)^4 - \theta^4_{bath} \right] \tag{16}$$

Data Evaluation and Error Analysis

Analytical solutions using the linearization of the radiative heat transfer term show that the heat transfer coefficient to be used in the evaluation of Q_f from measurements at a single point is $\left(k_R^{'0} - \dfrac{\psi I}{\theta^0}\right)\left[1 - \dfrac{(1 + \lambda)It}{2FM^0}\right]$. This result would in fact also be predicted directly by applying the argument outlined in d) of the previous section to Equation (16) but would not be predicted from elementary considerations of the heat balance at a single operating point. The result highlights the need to fit the whole of the experimental $\Delta\theta$-t plot to Equation (16) in accurate evaluations of Q_f.

The analytical solutions give results which are in close accord with the experimental data for small values of $\Delta\theta$ (these solutions will naturally not be applicable for large values of $\Delta\theta$ say, $>10^{\circ}C^{(11)}$). In order to obtain approximate values of Q, $k_R^{'0}\left[1 - \dfrac{(1 + \lambda)It}{2FM^0}\right]$, and Q_f we have therefore applied the calculation scheme illustrated in Fig. 6 using equations (9) and (10). Calibrations in which an amount of heat, Q, is injected into the cell using the resistive heater, have shown that this can be accurately recovered by injecting a further amount ΔQ and by applying (9) and (10). Nevertheless the estimates of Q and Q_f based on the approach using the scheme outlined in Fig. 6 are evidently approximate, Tables 1 and 2. Accurate values of Q have therefore been obtained by fitting the whole of the transient calculated from (16) to the experimental data using non-linear regression. In this fitting procedure we have used the simplest forward integration method

$$\Delta\theta_{n+1} = \Delta\theta_n + \left(\frac{d\Delta\theta}{dt}\right)_n \Delta t \tag{17}$$

and we have used the parameters Q, $k_R^{'0}$, Q_f and $(1 + \lambda)$ estimated according to Fig. 6 as starting values for the regression procedures. The parameter ψ has

been estimated from the E_{cell} - t plot using linear regression; in this way the number of parameters to be fitted to (16) has been reduced from 5 to 4 thereby speeding the calculation. In view of the curvature of the parameter space hypersurfaces, it has also been found to be convenient to regard

$$\frac{\left(E^0_{cell} - E_{thermoneutral,bath} \right) I + Q_f}{C_{P,D_2O,\ell} M^0}$$ as one of the free parameters of

the calculation.

We have used a Marquardt-type algorithm for the fitting procedure and it should be noted that the diagonal elements of the error matrix derived in this calculation (the inverse of the matrix used in the parameter estimation) directly give the standard deviation of the parameters. In this way we have

shown that the parameter $\dfrac{\left(E^0_{cell} - E_{thermoneutral,bath} \right) I + Q_f}{C_{P,D_2O,\ell} M^0}$ can be

estimated to 0.1% throughout the operating range. This is also the error of $\left(E^0_{cell} - E_{thermoneutral,bath} \right) I + Q_f$ since the error of M^0 is $\cong$ 0.01%. Even higher precisions could well be achieved by using more structured $\Delta\theta$ - t profiles than those of Figs. 6 and 7 but we have not done this so far in our work as we have only estimated $\left(E^0_{cell} - E_{thermoneutral,bath} \right) I$ to $\cong$ 0.1% (the error of this quantity is controlled by σ_I). This error must be added to that of $\left(E^0_{cell} - E_{thermoneutral,bath} \right) I + Q_f$ to obtain the total error of the excess enthalpy listed in Tables 1 and 2.

Results

Fig. 7 illustrates the degree of fit which can be obtained by using the non-linear regression procedure outlined in the previous section and Tables 1 and 2 illustrate the results of measurements of the excess enthalpy using both the approximate and exact methods of data analysis. We have also included some data taken prior to our first publication [6,7] which were obtained using only the approximate method of data analysis.

The marked excess enthalpy production on 0.1 and 0.2 and 0.4 cm diameter electrodes, (Table 1) must be viewed in terms of the slightly negative excess enthalpies for the blank experiments, Table 2.[1] This slightly negative value is due to the method of calculation which underestimates the heat output from the cell (see previous section). In many ways we regard the "zero" result on 0.8 cm diameter electrodes (and on the sheet electrode at low current density) as the most significant blank as it shows that almost exact thermal balances can be obtained using our methodology for systems identical to those giving marked excess enthalpy. The differences between the 0.1, 0.2, 0.4 and the 0.8 cm electrodes also point to the importance of the metallurgical procedures in devising electrodes showing excess enthalpy generation.

---

[1] Much of this data was available at the time of our first publication but the Editor of Nature refused to publish a letter to correct the many erroneous statements which had been made in the Editorials of the Journal.

Discussion

It can be seen that many (perhaps all?) of the assertions e.g.[14-21] which have been made about our experiments are erroneous. We would stress here that it is perfectly possible to obtain accurate values of the heat output from the cells and, hence, the excess enthalpy provided due attention is paid to the design of the calorimeters and control of the environment and providing modern methods of data analysis are used. We would also stress the importance of deriving error estimates from a _single experiment_ rather than from the variation of a parameter (here the excess enthalpy) from a _set of experiments_ as the variability of the parameter may itself be a key feature of the phenomenon to be observed. In this context it is of interest that the variability of the results at low to intermediate current densities (which have been widely used in attempts to replicate our work) is large and far in excess of the errors of each individual experiment. This variability may point to the importance of the precise nature of the surface conditions and/or history of the electrodes in defining the phenomenon.

It can be seen that the excess enthalpies increase markedly with the current density so much so that the results have the appearance of a threshold phenomenon. However, experiments of very high precision at low current densities are required before this can be confirmed. On balance we still believe that the results confirm that excess heat generation is a bulk phenomenon, Fig. 8, although this cannot now be stated as firmly as it appeared from the results available in the spring of 1989. The levels of enthalpy generation during the duration of a typical experiment (3 months) are such (hundreds of Megajoules cm^{-3}) that they must be attributed to nuclear processes. In particular, it is inconceivable that chemical or non-nuclear physical energy could be stored in the system at these levels and then be released over prolonged periods of time[22]. The phenomenon of "bursts" in

the enthalpy production which we first described[23] shortly after the
publication of our preliminary paper[6] is also of interest in this context.
Figs. 9A, B and C illustrate the $\Delta\theta$ - t , the specific excess enthalpy - t and
the cumulative specific enthalpy - t data for the largest "burst" we have
observed to date. The total specific excess over the period of the "burst"
($\cong 16$ MJ cm^{-3} over 16 days) is again of such a magnitude that the heat release
can only be attributed to nuclear processes. The heat output during this
burst was 17 times (average value) and 40 times (peak value) of the enthalpy
input. In some cells e.g. Fig. 10, the temperature rises rapidly to boiling.
When this occurs, it is difficult to accurately measure the heat flows (see
section c above). The heat output, however, must be extremely high.

We have confined attention to the calorimetric data but here note finally
that it is perfectly feasible to observe very low levels of neutron production
(of the order 10^{-3} - 10^{-2}s^{-1}) from cells generating excess heat providing
counting is extended over prolonged periods of time[24]; tritium production up
to a level 8 times the starting concentration has been observed in experiments
in Utah following "bursts" in the enthalpy production[25]. It is hardly
possible to attribute such observations to the operation of a set of
non-nuclear phenomena. Providing adequate funding is available, an high
priority for further work must be the identification of the products of these
nuclear reactions. Our current work is concentrated on the design and
implementation of factorial experiments in which we are seeking to define more
closely the effects of the many variables which control the excess enthalpy.
The instrumentation and procedures which we are using in the execution of
these experiments are essentially the same as those described in this paper.

ACKNOWLEDGEMENTS

LITERATURE REFERENCES

1. F. A. Lewis, "The Palladium Hydrogen System", Academic Press, London, 1967.

2. B. Dandipani and M. Fleischmann, J. Electroanal. Chem. 39 (1972) 323.

3. J. Vöelkl and G. Alefeld, Eds., "Hydrogen and Metals", vol. 2, in "Topics in Applied Physics", vol. 29, Springer Verlag, Berlin (1978), chapter 12.

4. M. Fleischmann and S. Pons, to be published.

5. M. L. Oliphant, P. Harteck, and Lord Rutherford, Nature 133 (1934) 413.

6. M. Fleischmann, S. Pons, and M. Hawkins, J. Electroanal Chem. 261 (1989) 301.

7. M. Fleischmann, S. Pons, and M. Hawkins, J. Electroanal Chem. 263 (1989) 187.

8. P. I. Dee, Nature 133 (1934) 564.

9. P. I. Dee, Proc. Roy. Soc. A 148 (1935) 623.

10. W. B. Ard, M. L. Becker, R. A. Dandl, H. O. Eason, A. C. England, and R. J. Kerr, Phys. Rev. Lett. 10 (1963) 87.

11. M. Fleischmann, S. Pons, M. Anderson, L. J. Li, and M. Hawkins, J. Electroanal. Chem., in the press.

12. V. J. Cunnane, R. A. Scannel, and D. J. Schiffrin, J. Electroanal. Chem. 269 (1989) 437. .

13. L. L. Zahm, A. C. Klein, S. E. Binney, J. N. Reyes, Jr., J. F. Higgenbotham, A. H. Robinson, and M. Daniels, J. Electroanal. Chem., submitted.

14. D. E. Williams, D. J. S. Findlay, D. H. Craston, M. R. Sené, M. Bailey, S. Croft, B. W. Hooten, C. P. Jones, A. R. J. Kucernak, J. A. Mason, and R. I. Taylor, Nature 342 (1989) 375.

15. N. Lewis, M. J. Heben, A. Kumar, S. R. Lunt, G. E. McManis, G. M. Miskelly, R. M. Penner, M. J. Sailor, P. G. Santangelo, G. A. Shreve, B. J. Tufts, M. G. Youngquist, C. A. Barnes, R. W. Kavanagh, S. E. Kellog, R. B. Vogelaar, T. R. Wang, R. Kondrat, and R. New, Nature 340 (1989) 525, and 175th Meeting of the Electrochemical Society, Los Angeles, CA USA May, 1989.

16. M. Chemla, J. Chevalet, R. Bury, and M. Perie, Cold Fusion Session, 40th Meeting of the International Society of Electrochemistry, Kyoto, Japan, 11-18 September 11-18, 1989.

17. A. Bruggeman, M. Loos, C. Van der Poorten, R. Craps, R. Leysen, F. Poortmans, G. Verstappen, and M. Snykers, Studiecentrum voor Kernenergie Report, September 1989.

18. V. Eberhard, G. Fieg, K. Flory, W. Heeringa, H. V. Karow, H. O. Klages, J. Lebkücher, M. Möschke, C. Politis, J. Römer, H. Schnider, G. Völker, H. Werle, H. Würtz, and B. Zeitnitz, Report INR-1653 of the Kernforschungszentrum Karlsruhe, West Germany (1989).

19. R. D. Armstrong, Session on Cold Fusion, 40th Meeting of the International Society of Electrochemistry, Kyoto, Japan, 17-22 September, 1989.

20. H. S. Bosch, G. A. Wurden, J. Gernhardt, F. Karger, and J. Perchermeier, Report IPP III / 149' of the Max-Planck Institut für Plasmaphysik, Garching bei München, West Germany.

21. G. Kreysa International Society of Electrochemistry, Kyoto, Japan, 17-22 September, 1989 and Meeting of the Electrochemical Society, Los Angeles, CA, USA May (1989).

22. R. C. Kainthla, M. Sklarczyk, L. Kaba, G. H. Lin, O. Velev, N. J. C. Packham, J. C. Wass and J. O'M. Bockris, Inst. J. Hydrogen Energy, 14 (1989) 771.

23. M. Fleischmann and S. Pons, Meeting of the Electrochemical Society, Los Angeles, CA, USA May (1989).

24. S. Pons and M. Fleischmann, to be published.

25. M. Hawkins, NCFI Laboratories, private communication and to be published.

Table 1. Excess enthalpy observed for 0.1, 0.2, and 0.4 cm diameter palladium rods as a function of current density, time elapsed since start of experiment, electrolyte composition, and electrode batch.

Rod Dia. /cm	Batch[a] & Electrolyte[b]	Current Density /mA cm^{-2}	E_{cell} /V	Q_{input} /W	Q_{excess} /W	Approximate Specific Q_{excess} /W cm^{-3}	Specific Q_{excess} From Regression Analysis /W cm^{-3}	
0.1	1 $\mathcal{D}$ ○	8	2.754	0.0304	0.0075	0.095		
0.1^c	1 $\mathcal{D}$ ○	64	3.637	0.419	0.042	0.53		
0.1*	3 $\mathcal{Y}$ ◐	64	2.811	0.032	0.001	0.140	0.1442	±0.0002
0.1	2 $\mathcal{D}$ ◒	128	4.000	0.984	0.160	2.04	2.043	±0.003
0.1*	3 $\mathcal{Y}$ ◑	128	3.325	0.089	0.005	0.486	0.5131	±0.0006
0.1	2 $\mathcal{D}$ ◓	256	5.201	2.93	0.313	3.99	4.078	±0.007
0.1*c	1 $\mathcal{D}$ ○	512	9.08	1.51	0.17	17.3		
0.1	2 $\mathcal{D}$ ◔	512	6.085	7.27	1.05	13.4	13.77	±0.02
0.1*	3 $\mathcal{D}$ ◯	1024	11.640	4.04	1.03	105.	112.8	±0.1
0.2	1 $\mathcal{D}$ ⬒	8	2.702	0.058	0.036	0.115		
0.2^c	1 $\mathcal{D}$ ⬓	64	4.139	1.040	0.123	0.39		
0.2	3 $\mathcal{Y}$ ◧	64	4.780	1.30	0.006	0.019	0.021	±0.001
0.2	3 $\mathcal{M}$ ◨	64	3.930	0.956	0.024	0.077	0.077	±0.001
0.2	3 $\mathcal{D}$ ◨	128	8.438	5.52	1.65	5.25	5.68	±0.01
0.2*	3 $\mathcal{Y}$ ◧	128	4.044	0.250	0.028	0.713	0.714	±0.001
0.2*	3 $\mathcal{M}$ ◨	256	6.032	0.898	0.056	1.42	1.498	±0.002
0.2*c	1 $\mathcal{D}$ ⬓	512	8.25	2.68	0.66	16.8		
0.2*	3 $\mathcal{M}$ ◨	512	9.042	3.00	0.603	15.3	16.03	±0.01
0.2*	3 $\mathcal{Y}$ ◧	1024	7.953	5.13	2.80	71.2	75.42	±0.08
0.4	1 $\mathcal{D}$ △	8	2.910	0.137	0.153	0.122		
0.4^c	1 $\mathcal{D}$ ◮	64	5.137	2.88	0.502	0.40		
0.4	2 $\mathcal{D}$ ◭	64	5.419	3.10	0.263	0.209	0.214	±0.003
0.4**	2 $\mathcal{D}$ ◭	64	4.745	2.24	0.117	0.106	0.145	±0.002
0.4*	2 $\mathcal{M}$ ◭	64	3.519	0.198	0.0005	0.002	0.0023	±0.0002
0.4	2 $\mathcal{D}$ ◭	128	6.852	8.50	1.05	0.84	0.842	±0.009
0.4*	2 $\mathcal{D}$ ◮	256	7.502	2.38	0.311	1.98	1.999	±0.003
0.4*c	1 $\mathcal{D}$ ◭	512	8.66	5.70	2.18	13.9		
0.4*	2 $\mathcal{D}$ ◭	512	10.580	7.23	1.65	10.5	11.09	±0.02

(a) All rod lengths 10cm or *1.25cm or **8.75cm
(b) $\mathcal{D}$: 0.1$\underline{M}$ LiOD; $\mathcal{Y}$: 0.50$\underline{M}$ Li2SO4; $\mathcal{M}$: 0.1$\underline{M}$ LiOD + 0.45$\underline{M}$ Li2SO4. All measurements were made in the same batch of D_2O of 99.9% isotopic purity. All measurements in $\mathcal{Y}$ or $\mathcal{M}$ have been made since March,1989.
(c) Measurements made prior to March, 1989; different data set to that shown in the preliminary paper[6,7].

Table 2. Results for blank experiments on platinum and palladium rods as a function of current density, time elapsed since start of experiment, and electrolyte composition.

Rod Dia.[a] /cm	Batch[a] & Electrolyte[c]	Current Density /mA cm^{-2}	E_{cell} /V	Q_{input} /W	Q_{excess} /W	Approximate Specific Q_{excess} /W cm^{-3}	Specific Q_{excess} From Regression Analysis /W cm^{-3}	
Palladium Electrodes:								
0.1	2 W	32	3.605	0.212	-0.001	-0.009	-0.0097	±0.0002
0.1	2 W	64	3.873	0.479	-0.001	-0.014	-0.0165	±0.0005
0.1	2 W	128	5.186	1.482	-0.001	-0.001	-0.001	±0.001
0.1	2 W	256	8.894	5.931	-0.001	-0.007	-0.008	±0.006
0.1	2 W	512	11.29	15.70	-0.001	-0.008	-0.01	±0.02
b	D	0.8	2.604	1.458	-0.001	-0.000		
0.8	1 D	8	3.365	0.365	-0.001	-0.000	-0.001	±0.004
0.8	2 D	8	3.527	0.397	-0.003	-0.000	-0.0006	±0.0003
Platinum Electrodes:								
0.1	D	64	3.800	0.452	0.000	0.000	-0.0007	±0.0004
0.1	D	64	4.138	0.520	-0.001	-0.008	-0.0094	±0.0005
0.1	D	256	6.218	3.742	-0.001	-0.028	-0.032	±0.004
0.1	W	64	4.602	0.624	-0.002	-0.023	-0.0232	±0.0006
0.1	W	64	4.821	0.668	-0.003	-0.038	-0.0392	±0.0006
0.1	W	512	12.02	16.86	-0.001	-0.007	-0.01	±0.02

(a) All rod lengths 10cm.
(b) Palladium sheet electrode 8 x 8 x 0.2cm.
(c) D: 0.1$\underline{M}$ LiOD; W: 0.1$\underline{M}$ LiOH; All measurements in D_2O were made in the same batch as that used in the experiments in Table 3.

GLOSSARY OF SYMBOLS USED

$C_{P,D_2O,\ell}$ Heat capacity of liquid D_2O, $J\ mol^{-1}$.

$C_{P,D_2O,v}$ Heat capacity of D_2O vapor, $J\ mol^{-1}$.

$C_{P,i}$ Heat capacity of O_2, D_2, or $(D_2O)_\ell$, $J\ mol^{-1}$.

E_{cell} Measured cell potential, V.

$E_{cell,t=0}$ Measured cell potential at the time when the initial values of the parameters are evaluated, V.

$E_{thermoneutral,bath}$

     Potential equivalent of the enthalpy of reaction for the

     dissociation of heavy water at the bath temperature, V.

F Faraday constant, 96484.56 $C\ mol^{-1}$.

H Heaviside unity function.

I Cell current, A.

k_c Heat transfer coefficient due to conduction, $W\ K^{-1}$.

k_R Heat transfer coefficient due to radiation, $W\ K^{-4}$.

k_R^0 Heat transfer coefficient due to radiation at a chosen time origin.

k_R' Effective heat transfer coefficient due to radiation, $W\ K^{-4}$.

$k_R'^0$ Effective heat transfer coefficient due to radiation at a chosen time origin, $W\ K^{-4}$.

ℓ Symbol for liquid phase.

L Enthalpy of evaporation, $J\ mol^{-1}$.

M Heavy water equivalent of the calorimeter, mols.

M^0 Heavy water equivalent of the calorimeter at a chosen time origin.

n Iteration number (data point number).

P Partial pressure, Pa.

P Fugacity, Pa.

$P*$ Atmospheric pressure, Pa.

Q	Rate of steady state heat generation at a given temperature, W.
Q_f	Rate of generation of excess enthalpy, W.
R	Gas constant, 8.31441 J $K^{-1}mol^{-1}$.
T	Absolute temperature, K.
t	Time, s.
β	Dimensionless term allowing for more rapid time dependent decrease of water equivalent of cell than that expected from electrolysis alone.
γ	Current efficiency of electrolysis toward a given reaction.
$\Delta H^{\emptyset}$	Standard free enthalpy change, J mol^{-1}.
ΔQ	Rate of heat dissipation of calibration heater, W.
$\Delta \theta$	Difference in cell and bath temperature at a given rate of enthalpy release, K.
$\Delta \theta '$	$\Delta \theta - \Delta \theta^0$, K.
$\Delta \theta^0$	Cell temperature at a chosen time origin, K.
$\Delta \theta_n$	Difference in cell and bath temperature at the nth time interval, K.
$\Delta \theta_{n,calc}$	Calculated difference in cell and bath temperature at the nth time interval, K.
$\Delta \theta_{n,exp}$	Difference in experimental cell and bath temperature at the nth time interval, K.
$\Delta \Delta \theta$	Temperature rise in cell due to application of a calibration pulse of heat, K.
θ_{bath}	Bath temperature, K.
λ	Dimensionless term allowing for more rapid time dependent decrease of heat transfer coefficient of cell than that expected from electrolysis alone.
$\bar{\mu}_i^{\emptyset}$	Standard state electrochemical potentials, J.
$\bar{\mu}_i$	Electrochemical potentials, J.

ν_i Stoichiometric coefficients.

σ_n Sample standard deviation of a given temperature measurement, K.

χ^2 Sum of inverse variance weighted deviations between experimental data and values predicted by the model using the non-linear regression fitting algorithm.

ϕ_m Galvani potential in the metal, V.

ϕ_s Galvani potential in the solution, V.

ψ Slope of the change of cell potential with temperature, V.

Figure Legends

1. Schematic diagram of the D_2O-Pd interface, indicating the pertinent reactions at the cathode and approximate energetics of the interfacial region and of the Pd lattice. $\phi_m - \phi_s$ is the galvani potential difference across the interface.

2. The single compartment Dewar calorimeter electrolysis cell used in this work.

3. Schematic diagram of the feedback circuit used in this work for conversion of a potentiostat to a galvanostat with effective protection against electrical oscillation.

4A. Temperature above bath vs. time and cell potential vs. time data for a 0.4 x 10 cm Pd rod in $0.1\underline{M}$ LiOD solution. The applied current was 800 mA, the bath temperature was $29.87^{\circ}C$, and the estimated Q_f was 0.158 W. The time of the measurement (taken at the end of the calibration pulse) was at approximately 0.45×10^6s after the beginning of the experiment.

4B. Same as Fig. 4A except the time of measurement was at approximately 0.89×10^6s. Estimated $Q_f = 0.178$ W.

4C. Same as Fig. 4A except the time of measurement was at approximately 1.32×10^6s. Estimated $Q_f = 0.372$ W.

5. Schematic diagram of the complete "black box" model of the Dewar calorimeter used in this work (see Fig. 2).

6. Schematic diagram of the method used for the determination of the heat flow in the Dewar cell, Fig. 2.

7. Figure showing the degree of fit of the "black box" model in Eqn. (10) to actual experimental data from an experiment using a 0.2 x 10cm Pd rod cathode in $0.1\underline{M}$LiOD. The dotted line in the figure represents the fit obtained using estimated values of the several cell parameters and was obtained by the forward integration technique described in the text to force the fit of the data to the model at the starting point (t = 0), the point of application of the calibration heater pulse, the point at the end of the calibration heater pulse, and the point at the end of the experiment. The solid line (which in this figure is coincident with the experimental data) is the fit obtained to the model by using the Marquardt algorithm for the non-linear regression technique described in the text.

8. Log-log plot (Excess enthalpy vs. current density) of the data in Table 1

9. A. Responses for a large, extended "burst" of excess enthalpy The figure shows the cell temperature vs. time (upper plot) and the cell potential vs. time (lower plot) for a 0.4 x 1.25 cm Pd rod electrode in $0.1\underline{M}$ LiOD solution. The current density was 64 mA cm^{-2}, and the bath temperature was $29.87^{\circ}C$.

    B. Figure showing the calculated rate of excess enthalpy generation as a function of time, and
    C. Figure showing the total specific excess energy output as a function of time for this cell.

10. Plot of cell temperature vs. time plot for a 0.4 x 1.25 cm Pd electrode in 0.1$\underline{M}$ LiOD just prior to a period during which the cell went to boiling.

SOLUTION | PALLADIUM LATTICE

$$D_2O + e^- \rightleftharpoons D_{ads} + OD^- \quad \text{(i)}$$

$$D_{ads} \rightleftharpoons D_{lattice} \quad \text{(ii)}$$

$$D_{ads} + D_2O + e^- \rightleftharpoons D_2 + OD^- \quad \text{(iii)}$$

$$D_{ads} + D_{ads} \rightleftharpoons D_2 \quad \text{(iv)}$$

φ_s

φ_m

Fig. 1.

REFERENCE CONNECTION

HEATER CONNECTIONS

CATHODE CONNECTION

GAS OUTLET

ANODE
CONNECTION

THERMISTOR CONNECTIONS

GLASS ROD FRAMING

KEL–F PLUG

GLASS CAPILLARY

GAS OUTLET

GLASS CAPILLARY

REFERENCE
ELECTRODE

GLASS ROD
FRAMING

VACUUM JACKET

THERMISTOR

ANODE

CATHODE

RESISTANCE
HEATER

KEL–F SUPPORT PLUG

Fig. 2.

SCHEMATIC OF GALVANOSTAT

Fig. 3

Fig. 4a.

Fig. 4b.

Fig. 4c.

3-34

ENTHALPY OF GAS STREAM $\gamma \dfrac{I}{F} \left\{ \left[0.5 C_{P,D_2} + 0.25 C_{P,O_2} + 0.75 \left(\dfrac{P}{P^*-P} \right) C_{P,D_2O,v} \right] \Delta\vartheta + 0.75 \left(\dfrac{P}{P^*-P} \right) L \right\}$

$(E_{cell}(t) - \gamma E_{thermoneutral,cell}) I \longrightarrow$

ENTHALPY INPUT TO THE CELL

$C_{P,D_2O,\ell} \left[M^0 - (1+\beta) \dfrac{\gamma I t}{2F} \right] \dfrac{d\Delta\vartheta}{dt}$

$- (1+\beta) \dfrac{\gamma I}{2F} C_{P,D_2O,\ell} \Delta\vartheta$

$\longrightarrow$ Radiation and Conduction

HEAT LOSS FROM THE CELL

EXCESS ENTHALPY Q_f

CALIBRATION PULSE $\left.\begin{array}{l} + \Delta Q\, H(t-t_1) \\ - \Delta Q\, H(t-t_2) \end{array}\right\}$

$\gamma \dfrac{I}{F} \displaystyle\int_0^t \left[0.5 + 0.75 \dfrac{P}{P^*-P} \right] C_{P,D_2O,\ell} \Delta\vartheta'\, dt$

ENTHALPY OF MAKE-UP STREAM

Fig. 5.

3-35

Start
Calibration
Heater, ΔQ

$\Delta\Delta\vartheta$

CELL TEMPERATURE
RESPONSE

$\Delta\vartheta$

ϑ_{bath}

E^o_{cell}

CELL POTENTIAL
RESPONSE

TIME

Addition
Time

$t_1 = 0$ t_2

Fig. 6.

TIME AFTER ADDITION / s

Fig. 7.

Fig. 8.

Fig. 9a.

Fig. 9b.

Fig. 9c.
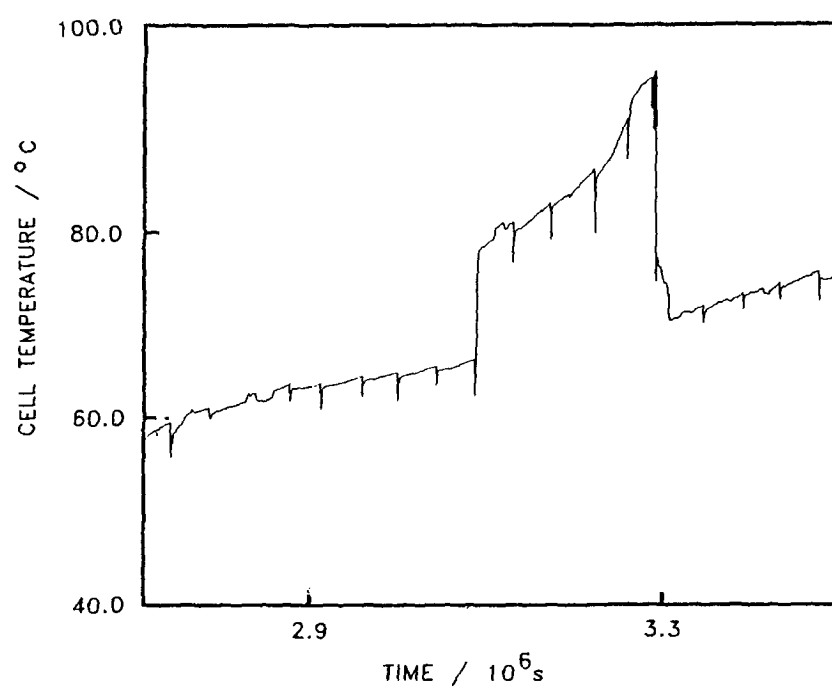
Fig. 10.

The discussions that follow refer to the papers presented at
the workshop, not the paper submitted here for publication.

DISCUSSION (FLEISCHMANN)

Mansour: Why would you expect to find the deuterium at the octahedral sites in the palladium?

Fleischmann: That is where there is most room. You would also expect it to go to the grain boundaries and defects.

Mansour: Is light hydrogen known only to exist at large sites, and based on what data?

Fleischmann: There are some low-temperature neutron diffraction data on these systems, so the information is reasonably well known. The general opinion is that the octahedral sites are occupied by deuterons.

Appleby: In reference to the depth of the energy wells occupied by deuterons, do we have data on the activation for energy for deuterium diffusion in palladium?

Fleischmann: I do not know the value under these extreme loading conditions, at high PdD ratios.

Bockris: For hydrogen in iron, it is about 5 kcal/mole.

Appleby: That value is about 8 kT, which is not as low as your classical hindered translational model seems to suggest. The well depth suggests quantized energy levels, as do the separation factors.
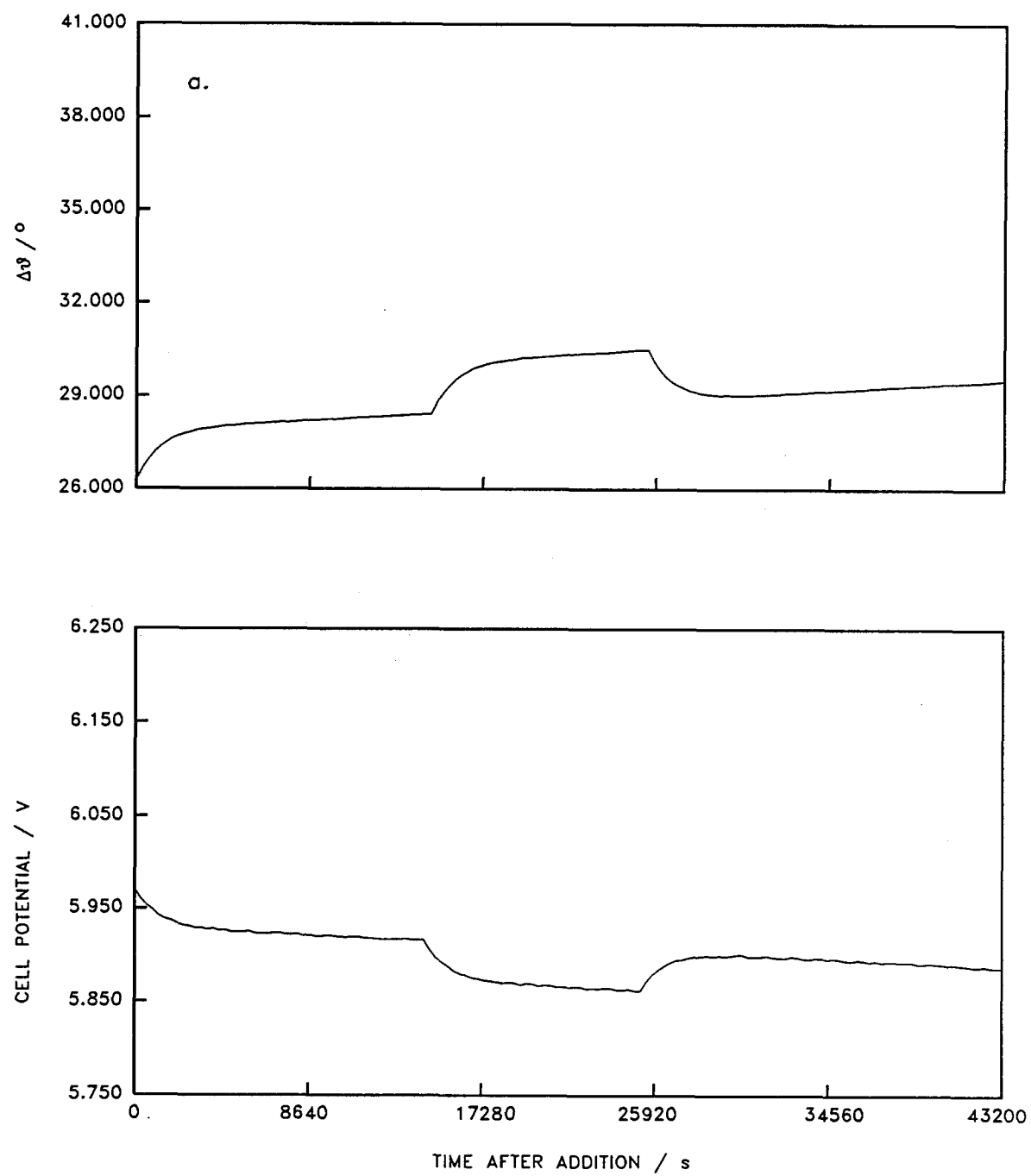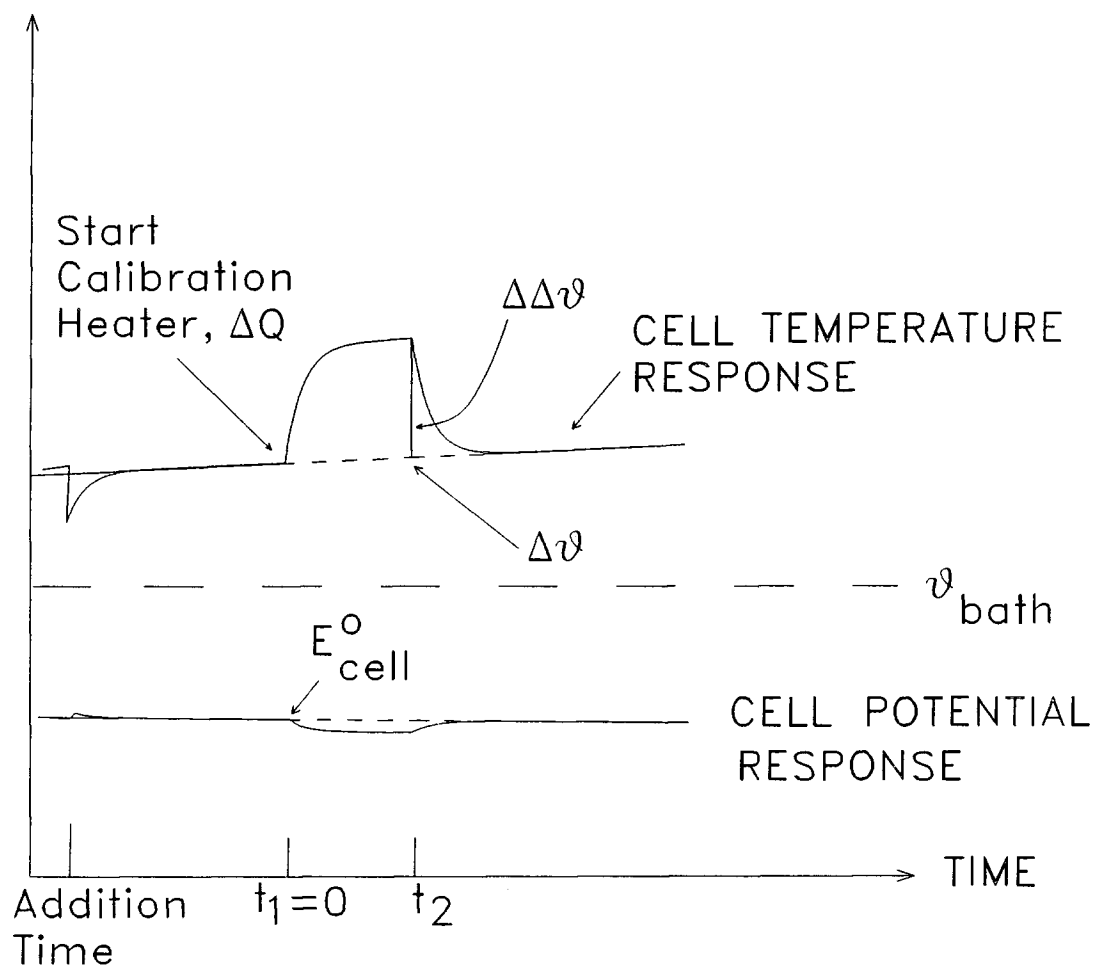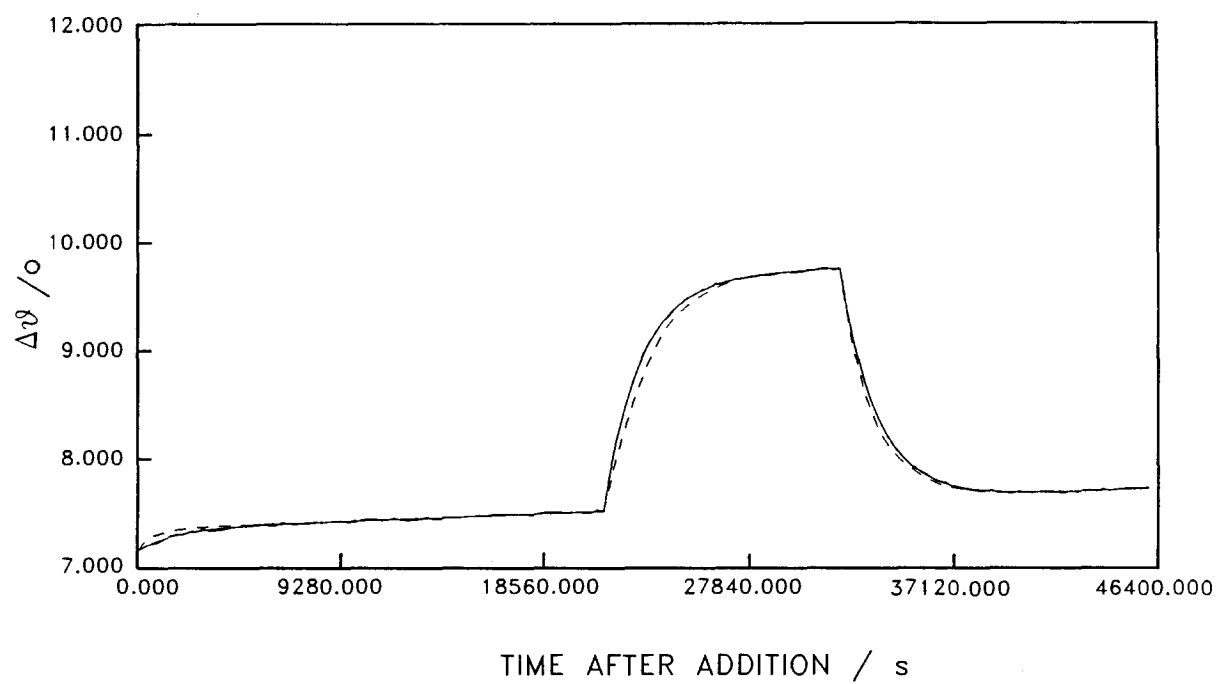
Chubb: The diffusion coefficient value is a function of the deuterium concentration. At low concentration, it is two times greater for D in Pd than for H in Pd.

Fleischmann: The diffusion coefficient for the deuterium in the palladium lattice is higher than that for hydrogen, which is a strange phenomenon. It is also higher than that for surface diffusion. I would say that you cannot explain these phenomena unless you assume the bosonic character of the deuteron and leave the question to the quantum mechanical theoreticians.

Bockris: Based on normal considerations, I would expect light hydrogen to have the greater diffusion coefficient.

Fleischmann: I agree, but there is no doubt that D diffuses faster than H in the lattice and is faster in the surface at high concentrations by about a factor of two.

Chubb: In addition, the superconducting temperature range is 2 K higher for PdD than for PdH, which runs counter to all traditional views on isotope effects.

Huggins: We repeatedly discuss these systems as fast mixed conductors. However, for hydrogen in metals such as palladium, the diffusion coefficient is so high

that one cannot use the normal lattice oscillator jump model for the diffusion process. In essence, almost every vibration becomes a successful jump. Thus, one must use some kind of a cooperative motion model with very low shallow potential wells.

Teller: When you have diffusion in a thin palladium layer, the effect of solubility may also make a difference. Protons may easily enter but may have difficulty leaving, whereas deuterons might easily go both in and out.

Fleischmann: It is important to carry out a reexamination of the diffusion of hydrogen, deuterium, and tritium, as a function of loading. The solubility of tritium also requires study.

Teller: This would be very important, and it is also of practical value. For example, experiments were conducted at Livermore some years ago on H/D and D/T separation, or deuterium and tritium.

Lewis: I have some data with me on the activation energy for diffusion of deuterium in β-phase PdD. The value is 5.7 kcal/mole. In addition, the equilibrium ratio of solubility of hydrogen to deuterium in palladium is 10, though the ratio varies somewhat with pressure. Hydrogen is therefore more soluble by about a factor of 10 at the same pressure.

Appleby: How do you reconcile the 5.7 kcal/mole value with classical potential wells? The energy levels should be quantized.

Fleischmann: It would depend on whether or not there is localized motion. The argument concerning the separation factor is based on the local behavior of the system.

Teller: Did you say that there was evidence for more than two deuterons on one side of an octahedral site and that condensation to a metallic phase might be favored?

Fleischmann: More than two may perhaps be accommodated. I don't want to go as far as saying that there is a free condensation to a metallic state, but I think it might be favored with deuterium.

Teller: This would be important, and it is relatively open to experimental investigation. At high densities the solubility of the deuteron should become greater than the solubility of the proton.

Fleischmann: Yes, there should be an inversion.

Teller: I am confused by your statement that the process is aneutronic and produces no tritium. In fusion, there are two parallel reactions: one producing neutrons, and the other producing tritium. If the process is aneutronic and produces no tritium, then you have nothing.

Chubb: Using the bosons in, bosons out rule, one could produce α-particles, which are bosons.

Lewis: Would you be satisfied with α-particle production, with no radiation?

Teller: Yes, but it is peculiar that there seems to be almost no radiation produced, which is a real contradiction. However, it is possible to obtain soft radiation in the ke V region, rather than in the Me V range.

Chubb: Alpha particles may have been detected at the Naval Research Laboratory in the higher energy range by George Chambers and coworkers. Their results were reported at the Santa Fe meeting and will appear in the conference proceedings. The results cannot be viewed as conclusive because of a later failure in their detector.

Teller: Low radiation and low neutron counts are very much outside of what is usually observed. However, α-particle production is not something that I would try to exclude.

Lewis: Have you had any problems with ignition of palladium? We have experimentally observed that palladium charged with hydrogen will melt on exposing it to oxygen.

Fleischmann: Our electrodes have never ignited.

Lewis: May I say one thing about your calorimeter calibration? I understood that you have a temperature-dependent quadratic term for radiation, plus a linear term for conduction. The heat transfer equation is therefore complex. However, you use only one temperature difference data point to determine the functional form of the equation. Is this enough to show that the $[T(^\circ K)]^4$ term dominates, or are independent experiments required?

Fleishmann: At low temperature differences, the expression linearizes.

Hoffman: Granted that your calibrations and measurements of the heat out are absolutely correct, is this always so for the heat in? A true RMS voltmeter is rarely used for galvanostatic measurements. If there is any surging due to arcing, a normal volmeter will not respond to it.

Fleischmann: The electrical system is under feedback control, so it will be extremely difficult for this system to show any surging.

Bockris: We have measured ac effects in our equipment, and we have seen about 4mV.

Lewis: The value would depend on the potentiostat, if it is used, and whether or not it is stable.

Fleischmann: Our system is stabilized against oscillation, which was one of our first precautions to obtain accurate results.

Jordan: When you said that you had at most 1 percent loss of gas by recombination, did you in fact collect the gases and measure this?

Fleischmann: Yes, we collected the gases. The effect of recombination was negligible.

Oriani: In what sense are deuterons, i.e., positive charges, present in the lattice? They must be tightly screened by electrons. How does one understand multiple occupancy of a lattice site where each species is creating a total volume expansion? Measurements of the volume of the entities in the lattice exist.

Fleischmann: There is a problem here. The concentration of deuterons or protons in the lattice is more than that in solid hydrogen. The concentration of electrons is comparable to that in silver. As one adds s-electrons, and if there is screening, one would expect the electric field gradient at the nucleus core to depend on the deuterium concentration in the lattice. A field gradient can only occur via the s-electron wave function, and we have nuclear magnetic resonance measurements. If you had a high density of deuterons and an excess chemical potential of 0.8 eV, you would expect to obtain D_2. Since that species is not formed, one probably does not have the electric field gradient. There is in fact tetrahedral distortion and an asymmetrical electric distribution.

Rafelski: Another possible explanation is that there is very asymmetric distribution of the electrons about the deuterons.

Oriani: Instead of D_2, why can you not form D^-?

Fleischmann: Some of our unpublished work shows that one can produce D^-.

DISCUSSION (PONS)

Bard: You reported originally that you used Newton's law of cooling to estimate heat flow as a function of temperature, which would give a linear dependence on temperature difference. Now you are stating that radiation, not conduction, is the primary heat loss mode, so that the Stefan-Boltzmann law with a $[T(°K)]^4$ temperature dependence term applies. Why have your assumptions changed from those in your original argument?

Pons: For small temperature differences, it does not make a significant difference whether you use a conductive or radiative heat transfer coefficient, since the higher terms in the latter linearize.

Bard: I am referring to the assumptions which you made in your presentation at the American Chemical Society meeting in April.

Pons: In April, there was a lack of understanding of the heat transfer coefficient using the linearized Stefan-Boltzmann law, as some questioners admitted. Since the calorimeter operated at low temperature differences, we used an expression of heat-conduction type to explain the simple heat transfer coefficient.

Lewis: Did you use the Stefan-Boltzmann expression to treat the original data?

Pons: We have always considered both radiative and conductive terms. Our calorimeters operated at low temperature differential, and the expression which we used then is what I indicated.

Lewis: Do you have experimental data on the calorimeter showing varying electrical power input into a resistor which demonstates the form of the heat transfer function?

Pons: Yes, those data are in our paper.

Jordan: You extrapolate your calorimetric response back approximately 45 h. Are you limited to doing this because the experiments last many days?

Pons: We extrapolate back to the time that solvent is added. This time is dependent upon how rapidly the D_2O is being consumed. At very low current densities, it may be several days before an addition is made to the electrolyte bath. At high current densities, additions are made perhaps twice per day.

Lewis: In one case, your cell temperature was 32.8°C. What was the bath temperature?

Pons: In that experiment it was 29.86°C.

Lewis: With only a 3°C temperature difference between the cell and the bath, does radiation still dominate heat transfer?

Pons: Yes.

Lewis: That seems to be unusual.

Huggins: How long is your calibration pulse?

Pons: The heaters are on for three hours for calibration.

Chu: Why does the voltage of the cell fall?

Pons: Because the temperature of the cell increases.

Bard: Did you use an oscilloscope to check for ac effects?

Pons: Yes, we observed 4 mV of oscillation.

Chu: How much excess energy did you see over the period of 8 million seconds?

Pons: About 16 MJ.

Chu: That represents more than 100 percent excess heat. What is the maximum current density which you have used?

Fleischmann: We have results up to about 5 A/cm^2.

Rafelski: When did the major excess heat event occur?

Pons: It occurred on August 1. However, the cell is still operating.

Oriani: In your excess heat results, do you subtract the 1.53 V, representing the heat of decomposition of heavy water, from the cell voltage?

Pons: The integral which I showed did have 1.53 V subtracted. In that particular cell, the gas recovery was better than 99 percent. We know how much D_2O was added. We know the cell current. The gas produced was equivalent to the heavy water added to within 1 percent. I should point out that if the excess heat is as high as that I have shown, it does not matter if 1.53 V is subtracted.

Bockris: Concerning excess heat per unit volume, at Texas A&M we consistently obtained 10-20 W/cm^3 on small electrodes. On larger electrodes results were still relatively consistent but were much lower, about 3-4 W/cm^3.

Pons: Our results on small electrodes, expressed in W/cm^3, were approximately the same as those at Texas A&M.

Bockris: Do you at present maintain that the effect is in the bulk palladium, so that W/ml units are indeed those which are appropriate?

Fleischmann: Our experimental goal was to obtain results on 1, 2, 4, 8, 12, 16, and 20 mm diameter rods to answer that question. We approached experiments on the larger rods with care, because a large electrode melted in our previous work. As it turned out, the time required for experiments on even 8 mm rods is enormous. They take three months to charge with deuterium, and we have yet to make one of these produce excess heat. We have no idea if a 2 cm diameter rod would be successful.

Menlove: During your experiments, did you monitor any fusion products apart from excess heat?

Pons: Yes. The maximum tritium level which we saw was eight times background. With simple equipment, we are looking for neutrons.

Fleischmann: We see 2.38 MeV gamma radiation when the cell is producing excess heat, as you can see on our spectrum, which includes 2.223 MeV.

Rafelski: Did you look for helium?

Pons: We are not ready to discuss our helium results, which are tantalizingly ambiguous. We have had "blank" difficulties.

Santucci: Did you sample the gases produced by electrolysis for helium?

Pons: It is not impossible to do that, but it is extremely difficult. Even if one first recombined the D_2 and O_2, it would still be difficult.

Gajewski: Do you attribute the high heat output which you have reported in your most recent cell to some special treatment?

Pons: No. I think that the heat burst outputs which we report are now measured accurately because we now have an excellent mathematical model to describe the calorimeter.

Lewis: What percentage of your small electrodes have produced excess heat?

Pons: The electrodes which we showed as blanks did not produce excess heat. We have examined a total of about 30 electrodes.

Thompson: It might be interesting to state that we have seen a consistent feature of all of the rods which proved to be positive. We have noticed a difference in the 8 mm rod returned from the University of Utah. The microstructure of the 1, 2, and 4 mm rods appears to be identical, although it requires more painstaking metallography to complete the analyses. There is a significant difference in the 8 mm rod, which was operated for approximately the same period of time as the others.

Huggins: What is the difference?

Thompson: The microstructure of the small rods is consistent with the drawing process used for forming, whereas that of the 8 mm rod has a much smaller granular structure. Whether this was caused by the long period of charging with deuterium or whether it was there initially has yet to be determined.

Santucci: What type of metallurgical tests have you carried out on the 1, 2, and 4 mm diameter cathodes?

Thompson: We have looked at transverse and longitudinal sections of the palladium rods. The structure is absolutely consistent with what a metallurgist would expect from a rod which has been cast, forged, and then drawn, which is our standard production process. This has been used for the rods that we have

supplied either commercially or to various research laboratories, including the University of Utah.

Santucci: So there are no changes that can be attributed to the excess heat effect?

Thompson: We have noticed significant recrystallization in two of the rods which produced excess heat. On rods which had been operated at 512 mA/cm^2 for long periods, XRD analysis showed that the amount of deuterium remaining was significantly lower than that in a rod charged at 64 mA/cm^2. Perhaps, the two results together may be interpreted as meaning that more excess heat was generated in the first rod than in the second.

Rafelski: Did both of the rods produce excess heat?

Thompson: Yes.

Santucci: When you say substantial recrystallization, do you mean around the bulk material or in the surface skin?

Thompson: The recrystallization was at one end of the rod. I hesitate to give further details because of the limited number of samples which we have examined. We have only examined five specimens altogether.

Bockris: Did you examine the rods for cracking and fissure formation?

Thompson: We found cracks and scratches to be surface features of virgin rods. The intensity of these features increases with the use of increasing current densities.

Bockris: Can you tell us anything about these tantalizing helium results?

Thompson: We provided samples of these for analysis externally. We have not yet received complete analytical results.

Myles: Can you describe the origin of the palladium?

Thompson: Our main supplier is South African.

Myles: What is the origin of these specimens, since this is a critical point?

Thompson: I have not been asked that question before. As far as I know, the palladium would have been of South African origin.

Kim: (to Dr. Pons) What ratio of tritium production to neutron production have you observed?

Pons: The levels which we have measured have been too small to make any reliable estimate.

Fleischmann: Without question, there was much more tritium production compared with that for neutrons. The most reliable results so far on this ratio are from Bhabha Atomic Research Center (BARC) in India.

Section 4

THE PALLADIUM-HYDROGEN SYSTEM

Ted B. Flanagan

Department of Chemistry

University of Vermont

The Palladium-Hydrogen System

Ted B. Flanagan

Chemistry Department, University of Vermont, Burlington VT.

Abstract

Some thermodynamic and material properties of the palladium-hydrogen system are reviewed. Emphasis is placed on the former properties because they may be of particular relevance to the excess heat production found in recent electrolysis experiments involving palladium-deuterium. Where data are available, differences between the palladium-protium and -deuterium systems are noted.

Introduction.

Thomas Graham found in 1866 that palladium absorbed large amounts of hydrogen (1).He called this absorbed hydrogen "hydrogenium"; he employed this term for the dissolved hydrogen in order to endow it with a metallic-like character. Since its discovery by Graham, many papers have been published on this classical metal-hydrogen system (2). This was one of the very first systems, 1895 (3), employed to demonstrate Gibbs' phase rule experimentally. It was also one of the first where hysteresis was observed for a chemical reaction. In this review we will attempt to highlight some of the important properties of this system. Hydrogen will be used to refer collectively to all three isotopes and when we wish to refer to specific isotopes the terms: protium, deuterium and tritium will be employed. Most of the data in the literature are for palladium-protium; generally the behavior of all three isotopes in palladium is similar with important exceptions being the thermodynamic and kinetic (diffusion) behavior. These isotopic differences will be discussed.

Structure.

Palladium is an fcc structure with a lattice parameter of 0.3890 nm (298 K); upon hydrogen absorption the lattice undergoes an isotropic expansion retaining its fcc structure. In the dilute, α, phase at 298 K the lattice parameter of PdH_α is 0.3894 nm reflecting its small protium content, $H/Pd \approx 0.015$, but in the protide, β, phase which co-exists with the α, the lattice parameter is

0.4025 nm and at 1 bar, where the H/Pd ratio is ≈ 0.7, $a_o = 0.4040$ nm. The volume expansion from the α to the β-phase is 10.4% (4). (These expansions are somewhat greater in the β phase if the miscibililty gap is not entered (5)). In both phases the hydrogen is disordered and hence Alefeld (6) utilized an analogy with a one component $gas \leftrightarrow liquid$ system.

For palladium-deuterium the expansions are slightly less for a given hydrogen content than that for protium (7,8). This is believed to be due to the greater zero point energy of protium and consequently the larger root-mean-displacement of protium in the interstice. The root-mean-square displacement has been measured directly using neutron scattering, i.e., 0.023 nm and 0.020 nm for H and D, respectively (9).

Very early in the history of the use of neutron diffraction for structural studies Worsham et al (10) employed neutron diffraction to determine that deuterium resides in the octahedral interstices in the fcc palladium lattice of the β phase, Figure 1. Although there have been suggestions that tetrahedral sites may be occupied (11), there is no evidence supporting this from neutron diffraction.

Neutron inelastic scattering has been employed to measure the optic mode vibrational frequencies of all of the isotopes of hydrogen in palladium in both the α and β phases. Recent studies by Rush et al(12) have determined the vibrational frequencies at very low protium contents where the effects of H-H interactions are insignificant, i.e., H/Pd=0.002. Because of the large difference in masses between the hydrogen and palladium the hydrogen optic mode frequencies are well-separated from the lattice modes and the former may therefore be described by a model of localized oscillators. The Einstein temperature for protium is 801 K; this value does not appear to change with protium content in the α phase to, at least, H/Pd =0.012. The corresponding Einstein temperature for deuterium is 540 K which gives the ratio 1.49 instead of the expected value of $\sqrt{2}$ =1.41. This is a very interesting result and indicates that the vibrations are markedly anharmonic. The Einstein temperatures for protium and deuterium for the β phase are 685 K and 460 K (12); thus, the same anharmonicity appears in the concentrated phase. Even considering the three-old degeneracy of these vibrations and the fact that they have to be multiplied by a factor of 2 for comparison to the gaseous species, they are relatively low compared to that of the corresponding gaseous molecules giving rise to interesting isotope effects on the solubilities (see below).

Preparation of Palladium Hydride.

Generally hydrogen is introduced into metals via the gas phase. In order for this absorption from gas phase to proceed, the surface of the metals should be sufficently clean so that the $H_2 \rightarrow 2H$ reaction, occurs readily, where H represents the chemisorbed state. Since any oxygen on the surface of palladium will react with H_2 to form H_2O, no special precautions are needed for palladium to absorb hydrogen other than mechanical cleaning of the surface to remove grease and other

contaminants. With a clean surface, equilibrium should be established relatively rapidly at room temperature or above between the gaseous molecular hydrogen and that dissolved in the palladium provided that the diffusion paths in the solid phase are not too great (see below). Equilibrium in bulk palladium has been obtained down to at least 195 K and even lower for films.

The thermodynamic criterion for equilibrium between the solid and gaseous phases is the equality of the hydrogen atom chemical potentials μ_H in the co-existing two phases. The chemical potential of H in the gas phase is given by

$$\mu_H = \frac{1}{2}(\mu^{\circ}_{H_2} + RT\ ln p_{H_2})$$

where the standard designation refers to 1 bar. Even at the highest pressures at temperatures below the boiling point of palladium the equilibrium concentration of H atoms in the gas phase corresponding to μ_H will be extremely small, e.g., at 300 K, $p_H = 10^{-30}$ bar. If, however, the concentration of H atoms can be increased by non-equilibrium methods, e.g., an RF-discharge, then this would greatly increase the effective hydrogen chemical potential in the gas phase providing the possibility for the introduction of large hydrogen contents into the metal phase (13). An analogous method for increasing μ_H is *via* electrochemical discharge of H^+ from solution. The gas phase method does not lead to meaningful measurements of the hydrogen chemical potential of the solid phase because a true equilibrium does not exist between the solid and gaseous phases. The chemical potential within the solid will be governed by kinetic and not thermodynamic factors, i.e., the relative rate of the recombination reaction compared to the chemisorbed→absorbed transition. For the same reason the electrochemical method cannot be readily used for thermodynamic studies electrode potentials equivalent to hydrogen pressures > 1 bar unless the surrounding hydrogen pressure is also above 1 bar. It should be emphasized that the overpotential applied during electrolysis cannot be converted to a meaningful hydrogen pressure. These non-equilibrium methods, nonetheless, provide methods to obtain high hydrogen contents if the surfaces are sufficiently inactive for the H-H recombination reaction.

The direct, but difficult, method which permits the formation of high hydrogen contents *and* thermodynamic measurements is the use of high hydrogen pressures. This method has been carried out successfully by Baranowski and his coworkers in Warsaw (14) and by Ponyatovskii and his coworkers in Moscow (15). These workers have prepared hydride phases of nickel, manganese, rhodium, iron, etc. by employing very high pressures of hydrogen. It can be remarked that at high pressures the hydrogen fugacity is the important variable for thermodynamic considerations and not the pressure. The differences between fugacity and pressure become very large indeed at high pressures, e.g., at a protium pressure of 20,000 bar the fugacity at 300 K is $\approx 10^9$ bar (16). This enormous difference helps in the successful preparation of hydride phases of metals which dissolve hydrogen endothermically, e.g., nickel, rhodium, etc. Palladium, of course, dissolves hydrogen exothermically as exemplified by the increase of hydrogen solubility as the temperature decreases.

Convincing experimental evidence does not exist supporting claims that hydrogen-to-palladium ratios in excess of 1.0 can be obtained with the exception of the introduction of hydrogen at low temperatures by ion implanatation. It has been reported that high hydrogen contents have been obtained by heating palladium films with H_2 at 873 K which, it has been reported (17), leads to formation of a tetragonal phase of stoichiometry $PdH_{\approx1.3}$. This phase has not been reported by any other workers and it would be extremely interesting if it were to be independently verified. The same authors also note that if this phase is heated to 923 K, it converts to a primitive cubic lattice (18).

When the β phase hydride is prepared at temperatures below the critical temperature, the sample is found to contain a high dislocation density (see below). The hydride phase can, however, be formed by passing around the two-phase envelope (Fig.2), i.e., above $\approx$ 575 K, and, in this case, the hydride phase is relatively dislocation-free because it has formed continuously without the abrupt volume change which accompanies hydride formation below T_c. Some properties of the heavily dislocated samples resulting from cycling through the hydride phases differ from the properties of the relatively dislocation-free hydride phase, e.g., it was noted above that the lattice expansions in the β phase differ (5).

Diffusion of H and D in Palladium.

Hydrogen diffuses relatively rapidly in palladium at 298 K although not as rapidly as it does in some bcc metals such as V. The diffusion constants for protium and deuterium at small hydrogen contents are given by (19)

$$D_H = 2.5 \times 10^{-7} exp - (21.8kJ/mol\ H/RT)m^2s^{-1}$$

and

$$D_D = 1.7 \times 10^{-7} exp - (19.9kJ/mol\ D/RT)m^2s^{-1}$$

which give diffusion constants of $3.8 \times 10^{-11}m^2s^{-1}$ and $5.5 \times 10^{-11}m^2s^{-1}$ at 298 K.

It should be appreciated that the value of Fick's diffusion constant, D(r), depends on the non-ideality of the dissolved hydrogen and in the β phase its value is approximately 4.5 times greater than in the dilute phase at 298 K (20). Fick's diffusion constant is given by $D(r) = D^*\ (dln\ a/dln\ r)$ where r is the H/Pd atom ratio, D* is the concentration independent (Einstein's) diffusion constant and a is the activity of the hydrogen. (Fick's diffusion constant is the one of practical interest, e.g., it can be used to determine the time required to load a sample with hydrogen). The magnitude of this diffusion constant for the β phase leads to the result that the root-mean-square distance that the hydrogen will move in 1 hour is $\approx$ 1 mm at 298 K.

Surprisingly the diffusion constant for deuterium is greater than for protium even though pre-exponential factor is greater for protium as would be expected from elementary models for isotope

diffusion. The difference in activation energies for H and D accounts for the more rapid diffusion of D and this has been discussed by Bohmholdt and Wicke (20); the transition state for diffusion, at least near room temperature and above, is believed to be the tetrahedral interstice where the vibrational frequency would be much higher than for the octahedral interstice and therefore the zero-point energy contribution would be such as to favor diffusion of the heavier isotope.

Thermodynamics.

The most characteristic feature of this system is that two phases form below a critical point of $T_c = 563$ K, 19 bar and r= 0.257 for protium and $T_c = 556$ K, 39 bar and r=0.257 for deuterium (21). There are no critical point data available for the Pd-T system.

The two hydrogen phases both exist within an fcc palladium matrix. They are phases in the Gibbs sense, i.e., the phase rule predicts that if two solid and one gaseous phase co-exist within a two component there should be two degrees of freedom as is observed. X-ray reflections from two sets of fcc lattices appear within the two phase envelope. For many years it was believed that the $\alpha + \beta$ miscibility gap constituted the complete phase diagram for this system despite its inconsistency with the third law requirement that disorder should disappear as T→0.

About 10 years ago Ross and coworkers (22) (see Figure 2) found low temperature ordered phases using neutron diffraction. Their finding of the low temperature phases reconciled difficulties with the third law and also clarified the origin of a low temperature anomaly in the electrical resistance and heat capacity first noted by Nace and Aston (23).

As noted above Alefeld (6) compared the $\alpha \rightarrow \beta$ transition in metal-hydrogen systems to a liquid→gas transition for a one component system. He also pointed out that the interaction energy which leads to the gas →liquid-like phase change is predicted by elasticity theory when a defect is inserted into a finite solid (24).

Metal-hydrogen systems are very convenient ones for thermodynamic studies because the chemical potential of hydrogen relative to $\frac{1}{2}H_2$(g, 1 bar), the relative chemical potential of hydrogen, can be determined from the measurement of the hydrogen pressure which is in equilibrium with the hydrogen-containing metal phase. Thus

$$\mu_H - \frac{1}{2}\mu^{\circ}_{H_2} = \Delta\mu_H = \frac{1}{2}RTlnp_{H_2}.$$

From measured isotherms the values of $\Delta\mu_H$ can be obtained and from the variation of $\Delta\mu_H$ with temperature the relative partial molar enthalpy and entropies can be obtained, i.e., ΔS_H and ΔH_H for any hydrogen content in the single phase regions (25).

Figures 3 and 4 show the variation of ΔH_H and ΔS_H with r which would be expected for temperatures above the critical where these thermodynamic quantities are continuous functions of r. The data are taken from reference 26 where they were evaluated from data over the temperature
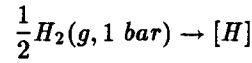
range from 250 to 650 K. For Figs. 3 and 4 the temperature has beem arbitrarily taken as 500 K which is below T_c but, nonetheless, it is assumed that a hydride phase does not form. It can be seen that the partial enthalpy and entropy both exhibit minima. The differences in values between the ideal and experimental partial entropy data correspond to the partial excess entropies. This excess partial entropy is believed to be mainly non-ideal configurational entropy $S_H^{E,c}$ and in view of the requirement that the integral molar configurational entropy must vanish at the stoichiometric composition we have

$$\int_0^1 S_H^{E,c} dr = 0$$

(26). This requirement accounts for the change of sign of $S_H^{E,c}$ from minus to plus at $r \geq 0.65$ (Fig. 4).

Figure 5 shows the dependence of the enthalpy on hydrogen content using experimental data determined at room temperature (26) where there is no longer a continuous dependence of these functions on r due to the miscibility gap. There are seen to be discontinuities at the phase boundaries although the hydrogen chemical potentials must, of course, be equal at the boundaries.

The process corresponding to the relative partial enthalpy for hydrogen solution can be indicated schematically by the following:

$$\frac{1}{2}H_2(g, 1\ bar) \rightarrow [H]$$

Its values are seen in Figure 5 to decrease in magnitude as the hydrogen contents increase in the single β phase region. The relative partial molar entropy becomes increasingly negative in this region. This circumstance makes it difficult to obtain high hydrogen contents using molecular hydrogen.

The chemical potential of the dissolved hydrogen can be expressed as (25)

$$\mu_H = \mu_H^o + RT\ ln\ (r/(1-r)) + \mu_H^E$$

where the first term on the rhs of the equal sign is the chemical potential at infinite dilution of hydrogen without a contribution from the second term on the rhs which is the partial ideal configuration term. The latter may be derived from the Bolzmann equation for thermodynamic probability, i.e., $S = Rln\Omega$, where Ω is the thermodynamic probability and, in the present case, comes from the number of ways of putting the hydrogen atoms (balls) into the identical octahedral interstices (boxes). The first two terms on the rhs are the ideal terms and describe the solubility only at low hydrogen contents. The last term on the rhs is the non-ideal or excess term; it is evaluated from pressure-composition-temperature data at hydrogen concentrations above the very dilute range. It goes to zero as $r \rightarrow 0$ and decreases as r increases from the lowest contents as shown in Figure 6. It then passes through a minimum and increases at large hydrogen contents.

This excess term (not to be confused with excess heat observed during cold fusion experiments!) is the origin of hydride formation below T_c. The initial decrease in μ_H^E is due to an H-H attractive force which is believed to arise from an elastic interaction (6,24); the increase in μ_H^E at higher hydrogen contents is believed to be due to electronic effects from the filling of the d-band of palladium by the hydrogen electrons. H-H repulsive interactions must also exist in order to account for the low temperature ordered phases but they may not be too important at hydrogen contents below 0.5.

Isotope Effects.

It was early realized that protium and deuterium had quite different equilibrium pressures in the plateau regions (27). Recently Lässer and coworkers (28) have extended the study of isotope effects in this system to include a detailed study of tritium. Some typical isotope effects are shown from Lässer's results in Figure 7 where it can be seen that at a given pressure the solubility of the lighter isotopes are considerably greater than the heavier ones. The plateau pressures also differ markedly (Fig. 8).

The large isotope effect in palladium-hydrogen has its main origin in the circumstance that the zero point energy levels differences for the isotopes differ for the gas phase molecules and for the dissolved atoms (Fig. 9). It can be seen from this figure that, relative to protium, deuterium prefers to be in the gas rather than the solid phase. Quantitative agreement between the observed solubility differences and their temperature dependences using the frequencies measured by inelastic neutron scattering has not been so far attained (29). This lack of quantitative agreement may be caused by the failure to account properly for the effects of anharmonicity on the dissolved hydrogen. The isotope effects for diffusion have already been noted under Diffusion.

The Rôle of Defects.

The types of defects which can be introduced into palladium are those which can be introduced into any pure metal, e.g, point defects such as vacancies, impurity atoms and extended defects such as dislocations, grain boundaries and external surfaces. There is no experimental evidence that vacancies in palladium contribute significantly to hydrogen solubility. This is probably because a sufficient concentration of vacancies has not been obtained for the experimental characterization of their interaction with hydrogen. Theory indicates that vacancies should serve as trapping sites for hydrogen. (Impurity atoms will be included under Palladium Alloys.) The most important hydrogen atom-defect interactions are those with the extended defects.

It was first noted by Flanagan *et al* (30) that cold-worked palladium dissolved more hydrogen than well-annealed palladium. This was attributed to segregation to the stress fields of dislocations and this work demonstrated that hydrogen can serve as an effective probe for defects. It was shown by Wise *et al* (31) that palladium which had formed and decomposed the hydride phase, contained

a large dislocation density, i.e., one which was comparable to that which resulted from heavy cold-working. Lynch *et al* (32) showed that if the subsequent dilute phase solubility was examined for palladium which had formed and decomposed the hydride without a subsequent annealing treatment ("cycled" samples), there was an enhanced solubility which was very similar to that which resulted from heavy cold-working (Fig. 10); this would be expected from the observed similarity in the dislocation densities. The only differences in behavior between cold-worked and "cycled" palladium is that there appears to be a greater non-zero intersection along the H/Pd axis for the latter samples and that these samples form some hydride phase before the plateau pressure for hydride formation p_f is reached. This is believed to be due to extensive regions of tensile stress in the latter samples resulting from the phase changes; in these regions the hydrogen chemical potential is reduced and consequently the hydride transformation occurs more readily.

In order to avoid the introduction of a large dislocation density, as pointed out in the section on Preparation of Hydrides, it is possible to prepare the hydride phase in a continuous fashion by passing around the two-phase envelope. For example, Manchester and coworkers (5) have found that the lattice parameter of, e.g., $PdH_{0.8}$ is significantly larger and, of course, broader for an sample which has been prepared by passing through the miscibility gap than one of the same hydrogen content formed by passing around the gap.

Hysteresis.

Hysteresis in metal hydrides has been recently review by Flanagan and Park (33). Isothermal, pressure hysteresis for palladium-protium is shown in Figure 11 and it can be seen that the pressure for hydride formation, p_f, is greater than for decomposition, p_d. The belief is that hysteresis results from the abrupt lattice expansion/contraction caused by hydriding or dehydriding. As noted above, hydriding and/or dehydriding introduces a large dislocation density into palladium which indicates that severe plastic deformation has occurred. When plastic deformation occurs, heat is liberated; this is a characteristic of an irreversible process. Hysteresis should be repeatable and for palladium-hydrogen this is the case. Many hundreds of cycles can be carried out with no significant of changes in the isotherms although the sample itself becomes progressively more plastically deformed.

The minimum work done on the system during a complete hysteresis cycle is $(b-a)RTln(p_f/p_d)$ where a and b are the dilute and hydride phase boundaries, respectively. This expression results from an approximation to an integral; the approximation is made that the phase boundary compositions are equal for formation and decomposition and plateau pressures are constant across the whole formation and decomposition isotherms. This work done on the system appears as heat in the surroundings. Hysteresis scans may also be carried out as shown in the figure. Such scans are always a feature of hysteresis.

4-8

Hydrogen Absorption by Alloys of Palladium.

This will not be discussed extensively here because the topic is a large one. Hydrogen solubility studies have been carried out with both substitutional and interstitial alloys of palladium and also with ordered and disordered alloys. With regard to their hydrogen solubility behavior the alloys can be divided into two broad classifications: *expanded and contracted*, where these refer to whether the alloys have expanded or contracted lattices in comparison to palladium. With the exception of Pd-Rh, palladium-rich alloys all dissolve less hydrogen than palladium at a pressure of one atmosphere hydrogen near room temperature. All of the alloys have greater terminal hydrogen solubilities than pure palladium. At a given low pressure the expanded ones dissolve more hydrogen, and the contracted alloys less hydrogen, than palladium. In comparison to pure palladium-hydrogen, the plateau pressures are smaller for the expanded alloys and larger for the contracted alloys (Fig.12).

This behavior is explained semi-quantitatively by a model in which the volume expansion of the interstices in the expanded alloys makes it easier to insert the hydrogen and therefore more dissolves. The opposite situation obtains for the contracted alloys. A seemingly different explanation, but which is, in essence, the same, is that there is a long-ranged elastic interaction between the impurity and hydrogen atoms which is attractive for those substitutional atoms whose volume is greater than palladium and repulsive for atoms which contract the lattice. It has been suggested by many workers that the presence of substitutional or interstitial atoms decrease the hydrogen solubility at one atmosphere because of electronic effects due to donation of electrons to the d-band of palladium by hydrogen, however, other explanations have been offered involving local effects, i.e., formation of unsuitable interstices for hydrogen occupation due to nearest neighbor environments of atoms other than palladium which raise the energy for hydrogen occupation to unsuitable values for occupation at 1 atm. hydrogen (34). A model incorporating both of these ideas has been recently employed (35).

Ordered and disordered alloys of the same composition have been shown to have quite different hydrogen absorption characteristics (36). It has also been shown that the hydrogen(deuterium) atoms occupy the palladium-rich interstices in the long period superstructure ordered form of Pd_3Mn (37). These results indicate that selective occupation of interstices must occur in palladium alloys.

Acknowledgements.

References.

1. T. Graham, Phil Trans. Roy. Soc.,(London), **156** 415 (1866).
2. F.A. Lewis, "The Palladium Hydrogen System ", Academic Press, New York, 1966. York (1967).
3. C. Hoitsema and H. Roozeboom, Z. Physik. Chem.,**17**,1 (1895).
4. P.Abens and W.G., Burgers, Trans. Faraday Soc., **58**,1989 (1962).

5. I.Baaba, P. Hardy, A.San-Martin, P. Coulter and D. Manchester, J. Phys.F: **17**,2041 (1987).

6. G. Alefeld, Ber. Bunsenges physik. Chem., **76** 746 (1972).

7. R. Abbenseth and H. Wipf, J. Phys.F: Metal Phys. **10** 353 (1980) .

8. J.E. Shirber and B. Morosin, Phys. Rev.B **12**, 117 (1975).

9. W. Drexel, A. Murani, D. Tocchetti, W. Kley, I.Sosnowska and D. K. Ross, J. Phys.Chem.Solids, **37**,1135 (1976).

10. J. Worsham, M. Wilkinson and C. Shull, J. Phys.Chem. Solids, **3**,303 (1957).

11. R.B. McLellen, Second Int. Cong. "Hydrogen in Metals", 2A_7, Pergamon Press, 1977.

12. J.J. Rush, J. M. Rowe and D. Richter, Z.Physik.B. **55**, 283 (1984).

13. W.A. Oates and T.B. Flanagan, Can. J. Chem., **53**, 694 (1975).

14. B. Baranowski, in "Hydrogen in Metals", G. Alefeld and J. Völkl, eds., Springer-Verlag, Berlin, 1978.

15. V. Antonov, I. Belash, V. Malyshev and E. Ponyatovsky, Plat. Met. Rev.,**28**,158 (1984).

16. A. Driessen, H. Hemmes and R. Griessen, Zeit. Physik.Chem.N.F. **143** , 145 (1985).

17. S.A.Semiletov, R. V. Baranova, Yu Khodyrev and R.Imamov, Sov.Phys.Cryst. **25** 665 (1980).

18. R. Baranova, Yu Khodryrev, R. Imamov and S. Semiletov, Sov.Phys.Cryst. **25** 736 (1980).

19. E. Wicke, H. Brodowsky, in "Hydrogen in Metals", Vol.2, G. Alefeld and J. Völkl, eds., Springer-Verlag, Berlin, 1978, 73.

20. G. Bohmholdt and E. Wicke, Zeit. Physik. Chem.N.F. **56**,133 (1967).

21. J. Blaurock, Dissertation Münster 1985.

22. I. Anderson, D. Ross and C. Carlile, Phys. Lett. **68A**, 249 (1978).

23. D. Nace and J. Aston, J. Am. Chem. Soc.,**79**,19 (1957).

24. J. Eshelby, Solid State Physics, **3**, 79 (1956).

25. W.A.Oates and T.B. Flanagan, Prog. in Solid State Chem., **13**,193 (1981).

26. T. Kuji, W.A. Oates, B.S. Bowerman and T.B. Flanagan, J.Phys.F:Metal Phys.,**13**, 1785 (1983).

27. L. Gillespie and W.Downs, J.Am.Chem.Soc.,**61**,2496 (1939).

28. R. Lässer and T.Schober, Mat.Sci. Forum, **31**, 39 (1988).

29. W.Oates, R.Lässer, T. Kuji and T.B.Flanagan, J. Phys.Chem. Solids, **47**,429 (1986).

30. T.Flanagan, J.Lynch, B. J. Clewley and B. von Turkovich J. Less-Common Met., **49**, 13 (1976).

31. M. Wise, J.Farr, I. Harris and J. Hirst, L'Hydrogene dans les Metaux, Tome 1, Editions Science et Industrie, Paris, 1972,p.1.

32. Lynch, J. Clewley, T. Curran and T.B. Flanagan, J. Less-Common Metals, **55**, 153 (1977).

33. T.Flanagan and C.-N.Park, Mat. Sci.Forum, **31**,297 (1988).

34. W.A.Oates and R. Ramanathan, 2nd. Int. Cong. on Hydrogen in Metals, $2A_{11}$, Pergamon Press, 1977.

35. R. Griessen and A. Driessen, J.Less-Common Met.,**103** 245 (1984).

36. K.Baba, Y. Niki, Y. Sakamoto, T.Flanagan, and A. Craft, Scripta Met., **21**, 1147 (1987).

37. P. Ahlzen, Y. Andersson, R. Tellgren, D. Rodic, T. Flanagan and Y. Sakamoto,Zeit. physik.Chem.N.F. **163**, 213 (1989).
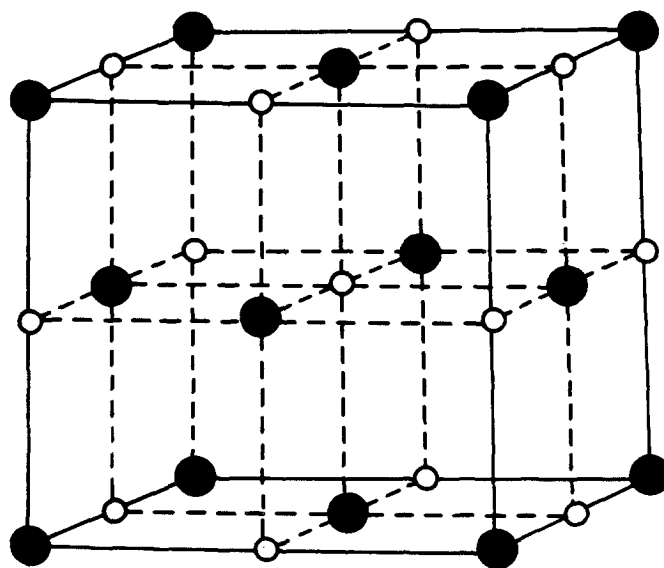
Fig. 1. Fcc palladium lattice where the Pd atoms are indicated by the large solid spheres and the octahedral interstices by the smaller open spheres. At 1 bar and 298 K, D/Pd = 0.65, i.e., 65% of the interstices are occupied by D atoms in a disordered manner.
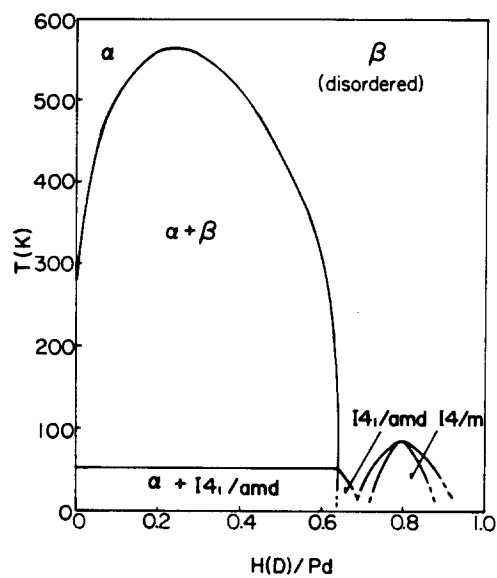
Fig. 2. Phase diagram of palladium-deuterium after reference 22.
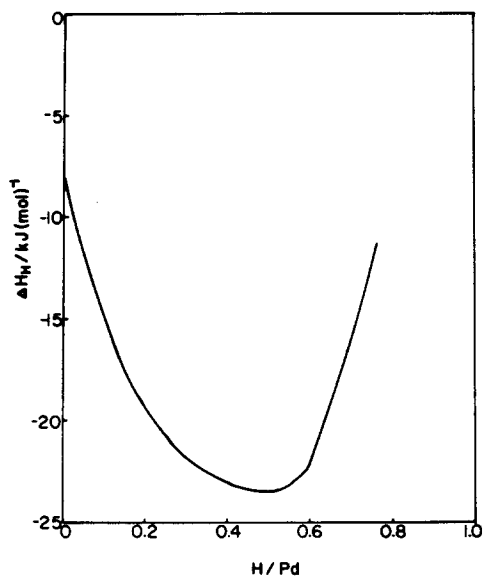
Fig. 3. Relative partial molar enthalpies of hydrogen in palladium at 500 K after reference 26.
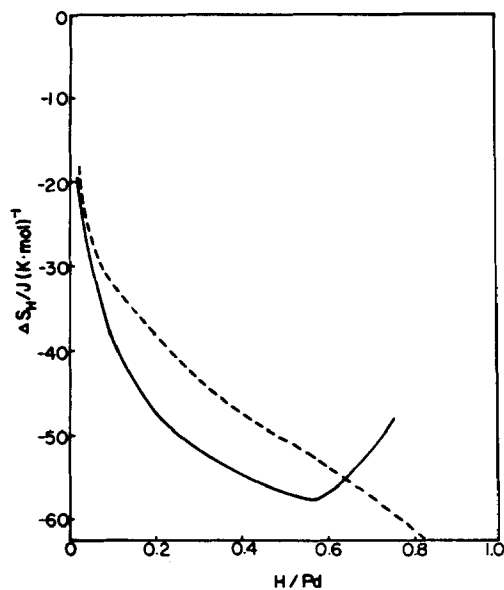
Fig. 4. Relative partial molar entropies of hydrogen in palladium after reference 26. Solid curve based on experimental data (500 K) and broken curve is the ideal partial molar entropy. The difference between the two curves is the excess partial molar entropy, S_H^E.
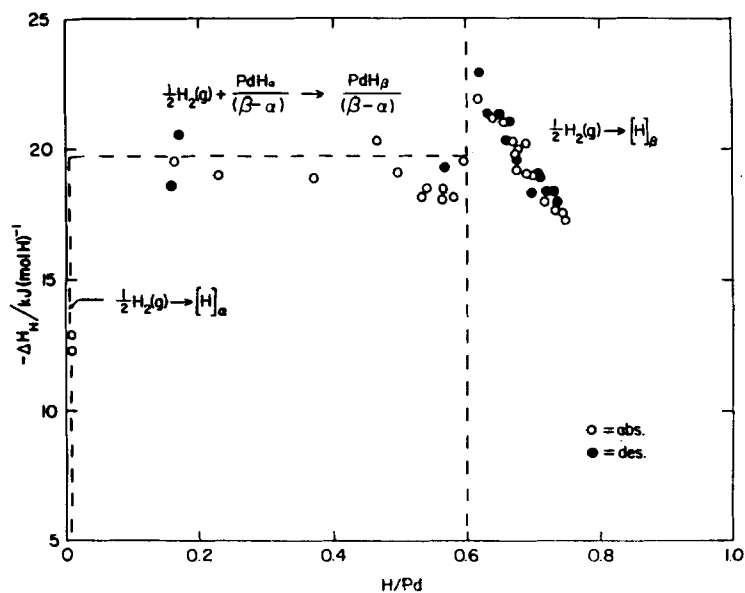
Fig. 5. Calorimetrically measured enthalpies of hydrogen solution and hydride phase formation at 298 K after reference 26; the open symbols represent data determined during absorption and the filled symbols data determined during desorption of hydrogen.
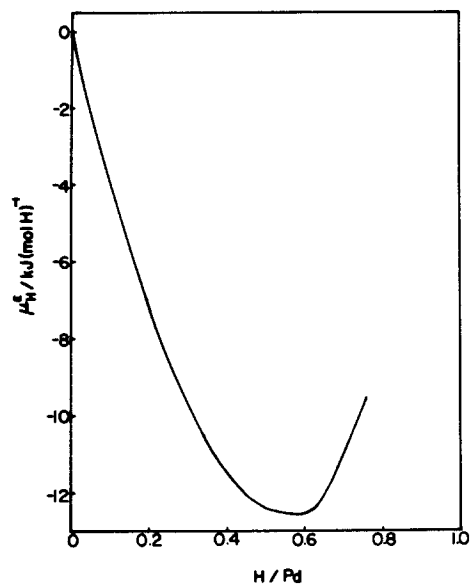
Fig. 6. The excess chemical potential of hydrogen in palladium evaluated from the results in reference 26 at 500 K.
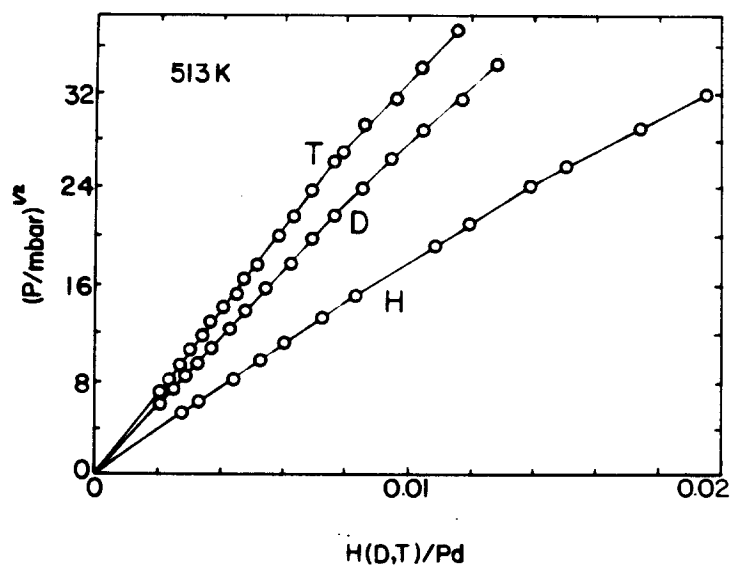
Fig. 7. Isotope effects on hydrogen solubility in the α-phase of palladium-hydrogen after reference 28 and the references therein.
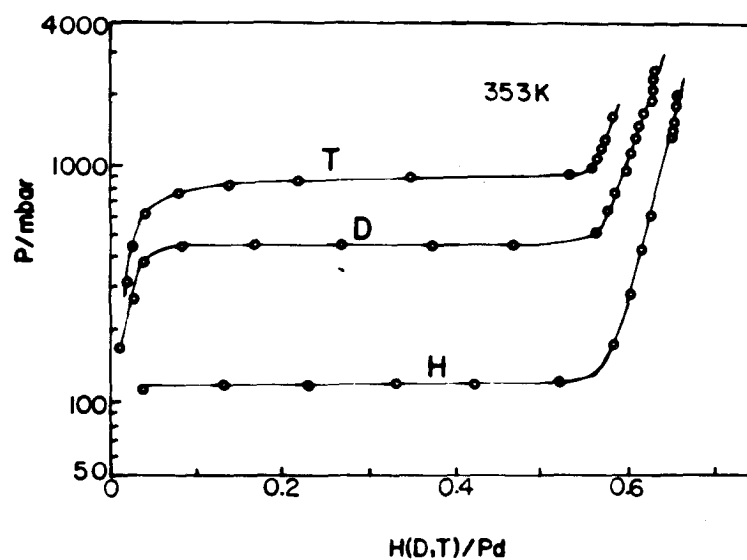
Fig. 8. Isotope effects on the plateau pressures of palladium- hydrogen after reference 28 and the references therein.
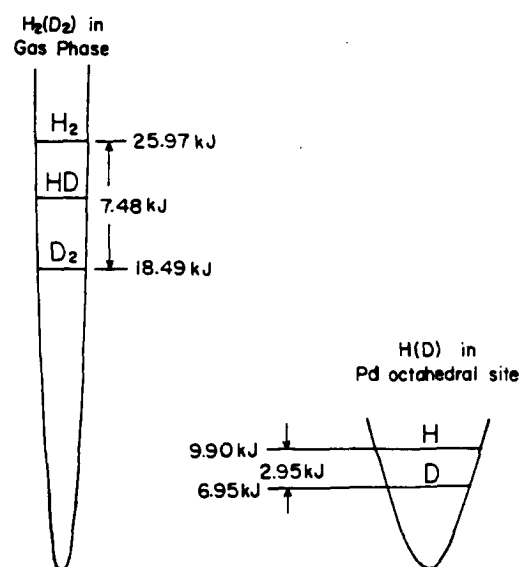
Fig. 9. The relative zero point energies of H_2 and D_2.
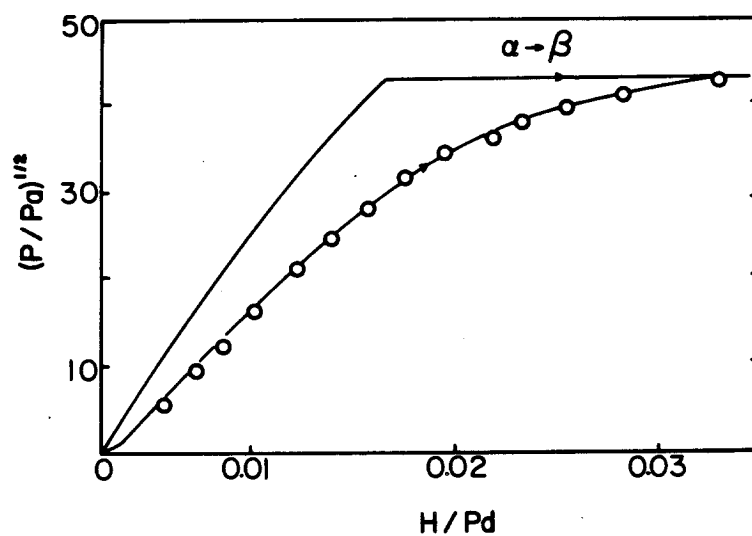
Fig. 10. The hydrogen solubility in palladium which had been cycled through the hydride phase changes, open symbols, compared to the solubility in a well-annealed sample, continuous curve without symbols (273 K) after reference 32.
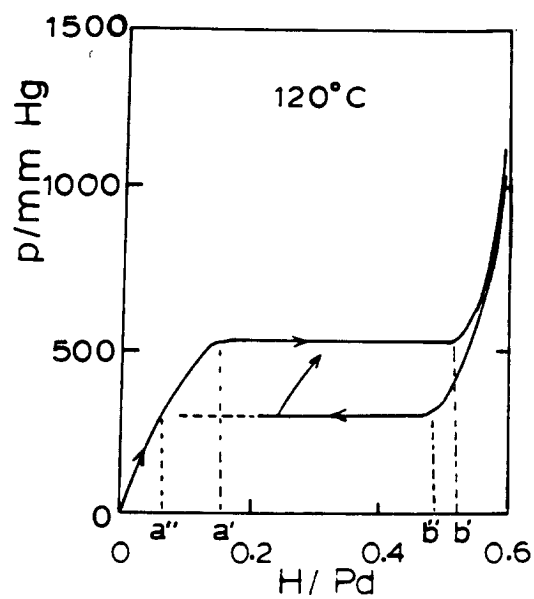
Fig. 11. A schematic isothermal hysteresis cycle for palladium- hydrogen at 120°.
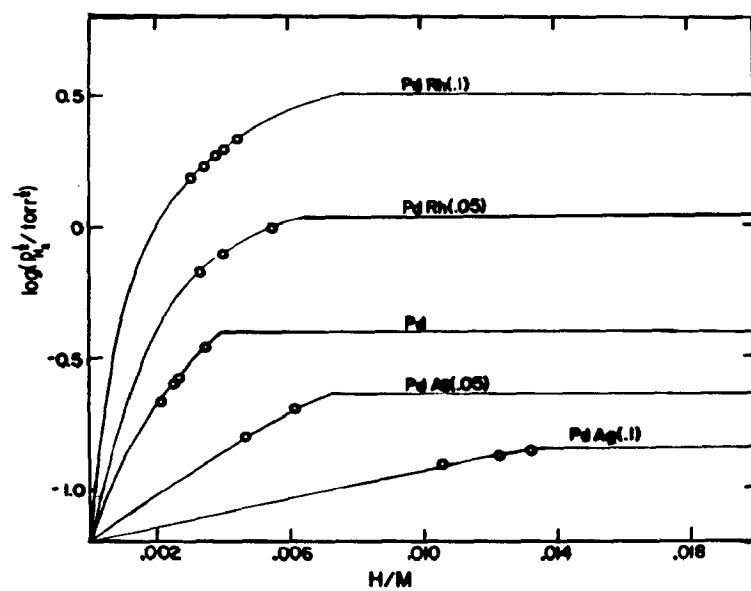
Fig. 12. Comparison of the isotherms for a typical expanded palladium alloy (Pd-Ag) with those for a typical contracted alloy (Pd-Rh). (from unpublished data of Kishimoto and Flanagan).

4-17

DISCUSSION (FLANAGAN)

Mansour: You cited Worsham's 1957 paper, which assumed that octahedral sites were occupied for the interpretation of their data. For this particular system, two indistinguishable groups of sites seem to be present.

Flanagan: Other evidence exists for the occupation of octahedral sites; for example, neutron scattering data are completely consistent with this view. Theoretical calculations also are not consistent. However, there is no serious doubt that 99 percent of the hydrogen occupies the octahedral sites. Any other explanation cannot be taken seriously.

Bockris: In contrast to what you state, there have been claims of palladium lattice expansion of up to 1.3, or more.

Flanagan: The claim is ambiguous, and it has not been substantiated.

Fleischmann: Why can the excess enthalpy in charging palladium with hydrogen become positive?

Flanagan: It can, although it is not well understood. Monte Carlo calculations have been carried out to explain it.

Fleischmann: The assumptions are really impossible unless you suppose a random distribution of particle occupancy.

Flanagan: I do not think that it is impossible. One would expect large deviations from ideality in the $D_{0.5}$ occupancy range. The hydrogens start to repel each other at short range.

Hoffman: There should be no order at all at very low temperatures.

Flanagan: There is an ordering transition at 50 K, in the palladium hydrogen system. This was an anomaly which was not understood; it was first observed by Aston and at the Naval Research Laboratory. Ross in Birmingham and Biaschko in Vienna examined the anomaly at 50 K using neutron diffraction in several papers published since 1978.

Mansour: Two references in Lewis's book _The Hydrogen Palladium System_ mention that a partial migration from the octahedral sites to the tetrahedral sites occurs below 55 K.

Flanagan: Lewis's book was published in 1967, so those references were not based on neutron diffraction data, which dates from about 1978.

Talcott: Neutron defraction data have been obtained, mostly at room temperature. While the system is a complex system, this technique is useful for identifying the locations of the hydrogen ions. Most workers in the field will state that at room

temperature, occupation is definitely octahedral. Over $PdD_{0.8}$, and as the stoichiometry approaches unity, other sites may be also involved. At $PdD_{0.7}$ that is unlikely.

Mansour: Where do you expect the hydrogens to be situated at lower temperatures?

Talcott: Workers who study ion-implanted material at low temperatures will claim that tetrahedral sites may be involved. However, little work has been done to confirm this.

Mansour: Tetrahedral sites may be involved. It is important to understand any special effects at low temperature.

Oriani: Would you care to comment on my feeling that if you have boson condensation you should expect a larger negative contribution to the entropy of solution, not a more positive one?

Flanagan: That would seem reasonable, since the disorder would be destroyed.

Appleby: There is also an electronic component to the entropy.

Flanagan: Oates and I evaluated that effect using the electronic specific heat.

Voice: If a boson condensation occurs, the material would become a superconductor.

Flanagan: I think that the effect is well understood.

Oriani: You state that a fivefold increase in diffusion coefficient is seen in the β-phase which results from the effects of nonideality. If you compare the mobilities, i.e., the kinetic terms, what is the corresponding ratio?

Flanagan: It would be approximately the same at normal temperatures. It has been examined in some detail by Wicke and coworkers.

Oriani: That is an important point.

Bockris: If one applies an external stress in the elastic region while measuring permeation as a function of time under electrolysis conditions, one finds that the measured permeation varies with stress. This is due to crack formation or healing under stress, which gives useful information from the structural viewpoint.

Flanagan: I am aware of that work. Alternatively, X-rays or dilatometry can be used.

Hoffman: You stated that after passing through the two-phase region, as occurs during electrolysis, the solubility in the α-phase then increases. Is it not also true that β-phase solubility simultaneously decreases, so the total deuterium content may be reduced after charging, degassing, and recharging?

Flanagan: I am not aware of that work. To whose data are you referring?

Hoffman: They are old data from Lewis.

Flanagan: I must look at the work carefully. I do not see any reason why this effect might happen.

Hoffman: The reason is the hardening of the palladium lattice, which prevents entry of the same amount of hydrogen in subsequent cycles.

Part 2

NUCLEAR PRODUCTS

Section 5

RECENT RESULTS FOR ELECTROLYTIC TRITIUM PRODUCTION AT LOS ALAMOS

E. Storms, C. Talcott, and M.A. David

Material Science and Technology Division

Los Alamos National Laboratory

Recent Results for Electrolytic Tritium Production at Los Alamos

E. Storms, C. Talcott, and M. A. David

Material Science and Technology Division, Los Alamos National Laboratory

ABSTRACT

Many of 90 electrolytic cells of various configurations and electrode composition have been examined for tritium production, deuterium uptake rate and palladium expansion. Low level tritium production has occurred in nine cells.

INTRODUCTION

The electrolytic study was started shortly after the announcement by Fleischmann and Pons[1]. Initially we tried to understand how high stoichiometries could be achieved. A cell was designed that would allow the cathode to be easily weighed. This consisted of a wide mouth glass jar with a small electrical socket in the lid that allowed the cathode assembly to be plugged in. The electrolyte was found to attack the solder and copper in the plug and transfer Cu, Zn and Pb to the cathode surface. Thus all cathodes up to cell #25 had a potential surface contamination of these elements. This was prevented in some later cells by coating the lead and plug with Torr seal (an epoxy). Unfortunately, the Torr seal absorbed deuterium and caused the apparent stoichiometry to be too large after about 48 hrs. Gradually, we concluded that high stoichiometries were not only impossible to achieve at room temperature, but were probably unnecessary. After the first tritium was produced, the emphasis shifted to reproducing this event. Nevertheless, some good background understanding was obtained during this early stage which will be described. Over 1400 samples have been analyzed for tritium. This large data base has given a good statistical basis for evaluating the production of tritium.

RESULTS

Twenty-five cells were studied using the design shown in Fig. 1.
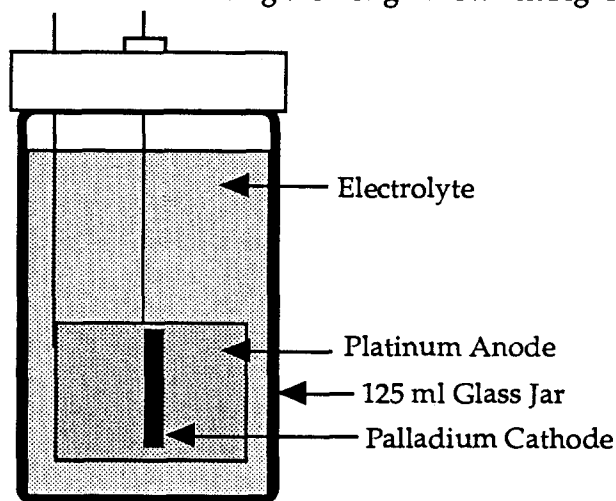
FIGURE 1. Cross-section of cell design #1.

The cathodes were Pd coins that were made by arc melting Pd powder [2] which was then rolled into a coin shape, approximately 2 mm thick and 1.5 cm in diameter. Platinum gauze anodes were usually used although solid Ni was used in two cells. Alloys of Pd+S, Pd+C, and Pd+Rh, in addition to pure Pd, were studied. On several occasions, thiourea, As_2O_3 or NaCN were dissolved in the electrolyte to function as surface poisons. A surface coat of carbon and sulfur was applied to three electrodes using a heated mixture of paraffin and sulfur. No tritium measurements were made during this early phase.

The charging rate, limiting D/Pd ratio and expansion were studied. Figure 2 shows how the D/Pd ratio changes during 10 hours after the cells are turned on. Some results obtained from later work is also shown
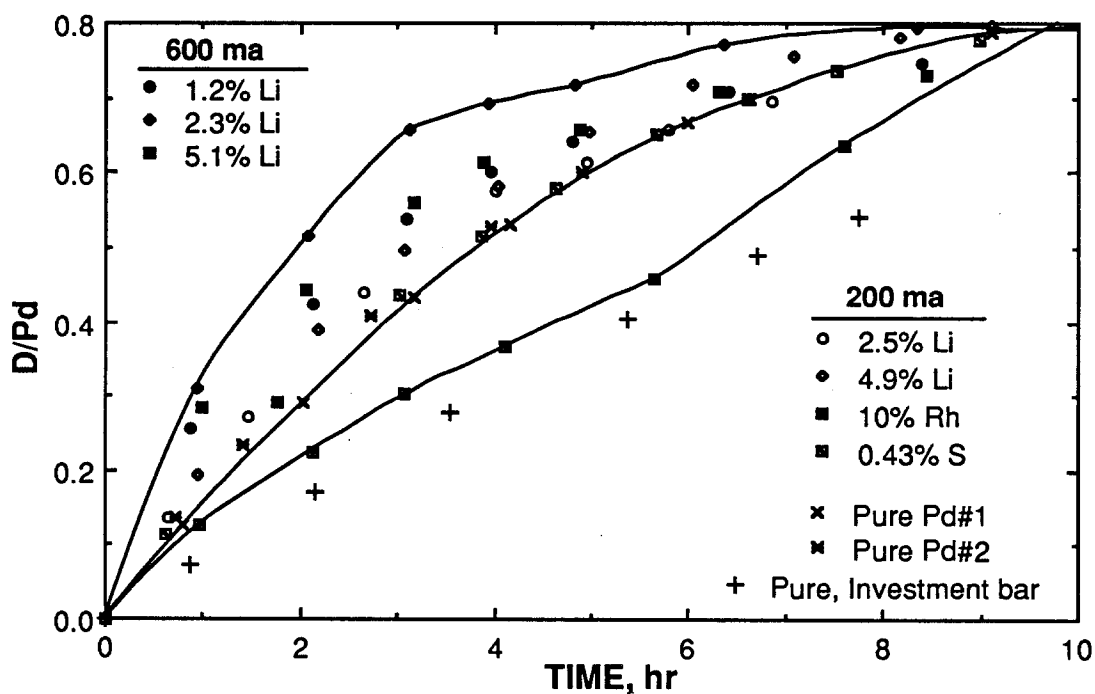
FIGURE 2. D/Pd vs time for various alloys.

The presence of Li in Pd improved the deuterium uptake. At 200 ma, the uptake was better than 97% of the D_2 produced during the first hour. Higher currents saturated the effect but showed that a Li/Pd ratio near 0.023 was best. An alloy with Rh and an investment bar (a strip cut from a 1 oz Englehard investment bar) showed a significantly lower uptake rate compared to the arc-melted powder. We also found that carbon reduced the uptake rate as can be seen in Fig. 3. We believe that because of the low solubility of carbon, the formation of graphite at the grain boundaries reduces the diffusion rate even at low concentrations. The reduced limiting composition produced by carbon is near the lower composition limit of the β phase. Apparently, once the β phase forms,

carbon becomes very effective in preventing the β phase from changing composition. When Li is added along with carbon, the effect of carbon is eliminated even at high concentrations. Perhaps the modest improvement in uptake when Li is alloyed with otherwise pure Pd is owing to the elimination of a minor carbon effect.
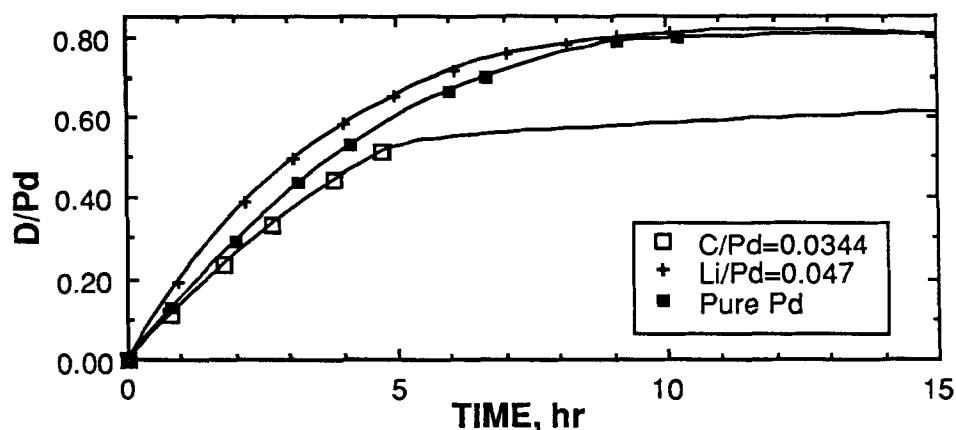
FIGURE 3. Initial charging of deuterium in Pd-C, Pd-Li and Pd.

As deuterium is absorbed, the thickness of the coin increases. As can be seen in Fig. 4, there is a break in slope near D/M=0.4. A similar break is seen in the thickness change when deuterium is removed (Fig. 5).
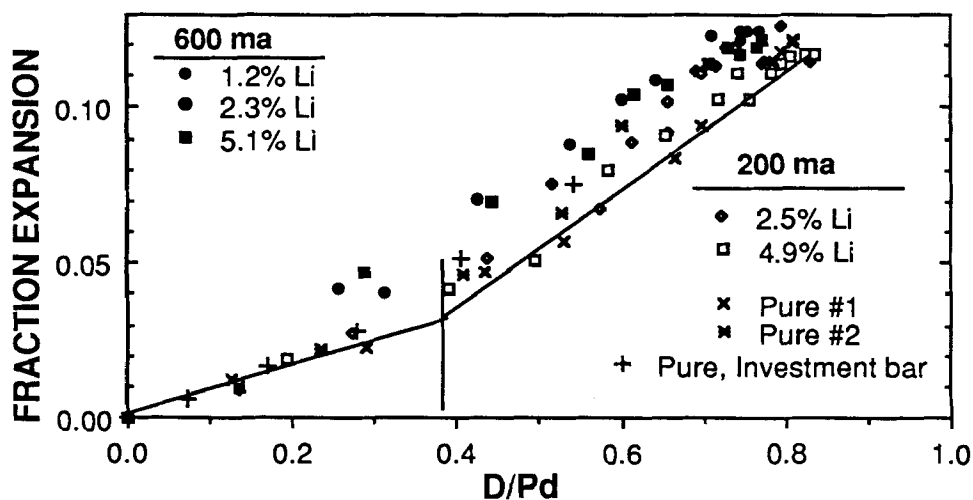
FIGURE 4. Expansion vs D/Pd for various Li-Pd alloys.

Charging lithium alloys at 600 ma produces a greater expansion compared to charging at 200 ma. The presence of Li also increases the expansion for the same D/Pd ratio. If a coin is allowed to lose by sitting in air, shown in Fig 5, the dimension does not return to
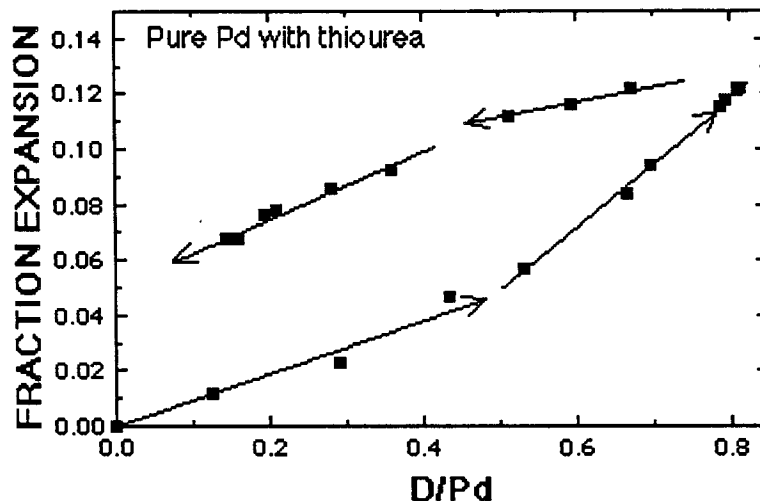
FIGURE 5. Change in thickness caused by charging in solution
and then discharging a Pd coin in air.

Other samples that have been followed until all of the deuterium was removed show
the same behavior. This residual expansion and the increased expansion when high
charging rates are used is thought to be owing to cracks and dislocations in the struc-
ture caused by stresses introduced by the α–β conversion. This happens even though
Pd and the hydride are very ductile. This internal cracking might be the origin of some
fusion reaction. Carbon may enhance this cracking because of brittle graphite in grain
boundaries.

Concentrations of Li up to 5 at. % has little effect on the ductility. An alloy contain-
ing 22 at. % Li cracks when it is rolled into a coin. However, this alloy does not appear
to be as hard as the surfaces reported by Pons after long electrolysis.

Surfaces that were coated with Li_2S or sulfided with H_2S self-heated when exposed
to air. One electrode got sufficiently hot to ignite paper. Five of the cells exploded
spontaneously because of a reaction between D_2 and O_2. No heating of the electrode
was involved and no tritium was produced.

Between cell #26 and #40, a new design was adopted. This is shown in Fig. 6
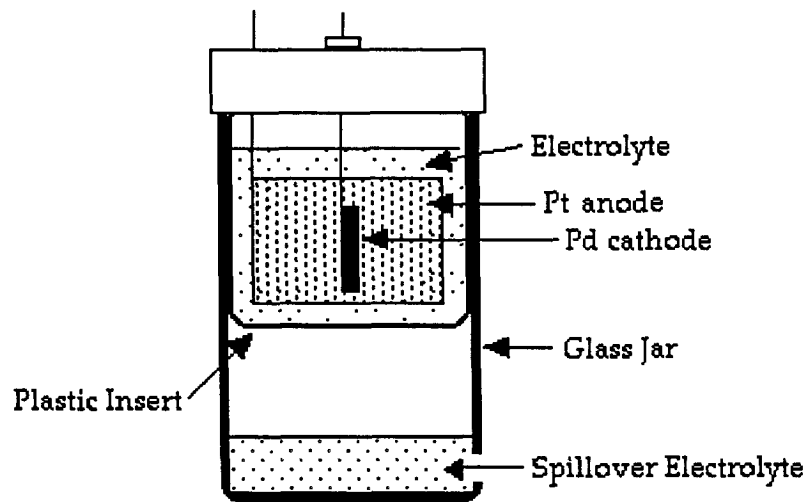
FIGURE 6. Cell design #2.

Tritium measurements were started about 13 days after the first cells of this series were turned on. Table 1 shows the materials in the cells and Table 2 lists the tritium values for cells in this initial study. Cell #38 contained tap water with 0.2N LiOH. Torr seal was applied to the lead between the cathode and the plug that was used to attach the assembly to the cell lid. In spite of this precaution, large amounts of Cu and Pb were found on the surface of cathode #30.

TABLE 1
Materials used in cells #26 to #44

#	Shape	Alloy	Surface Treatment	Pre-Treatment	Electrode Poison	Container	Lead Covering	Max D/Pd
26	coin	Li/Pd=0.047	std	none	none-thio	plastic	torr seal	0.820
27	coin	Ni	std	none	none	plastic	torr seal	0.090
28	coin	Rh/Pd=0.1	std	none	thio	plastic	torr seal	
29	coin	Pd	S	H_2S+C	thio	plastic	torr seal	tritium
30	coin	Pd	S	H_2S+C	none	plastic	torr seal	tritium
31	coin	Pd+Rh+Li	std	none	thio	plastic	torr seal	
32	coin	Pd	std	none	thio	plastic	torr seal	
A(sc)	single crystal		none	zone melted	none, Cu, Pb	glass	no	0.850
B(sc)	single crystal		none	zone melted	thio, Cu, Pb	glass	no	0.810
33	coin	Li/Pd=0.051	std	none	none-thio,Cu	plastic	no	0.770
34	coin	Li/Pd=0.023	std	none	none-thio,Cu	plastic	no	0.829
35	coin	Li/Pd=0.012	std	none	none-thio,Cu	plastic	no	0.767
36	coin	Rh/Pd=0.1	std	none	thio,Cu,Pb	plastic	no	0.861
37	coin	Rh/Pd=0.1	std	none	thio,Cu,Pb	plastic	no	0.896
38	coin	Rh/Pd=0.1	std	none	H_2O	plastic	no	0.848
40	coin	Pd	S	H_2S+C	none	plastic	no	0.835
41	wire	Pd	none	none	thio	plastic	torr seal	0.863
42	coin	S/Pd=0.0043	std	none	none	plastic	torr seal	
43	coin	Pd+B	std	none	As_2O_3	plastic	torr seal	
44	coin	Pd	S	H_2S+C	none	plastic	torr seal	0.745

coin= Arc-melted powder and rolled into coin shape

wire= 0.032" diameter

std=Sanded with 200 grit paper and washed with HNO_3

none=Cleaned only with HNO_3 or H_2O_2

H_2S+C= Heated in vapor produced by a mixture of paraffin and sulfur

H_2S+H_2O= Heated in the above gas after passing through water

thio= 0.0004 g/ml added to electrolyte

All anodes were Pt

TABLE 2

Count/min-ml in cells running when tritium measurements were started.
Numbers include a background count of 20 c/min-ml

Cell Number

DATE		26	27	28	29	30	31	33	34	35	36	37	38	40	41	42	43	44
Start=		6/1	6/1	6/2	6/5	6/5	6/8	6/15	6/15	6/15	6/17	6/17	6/17	6/20	6/21	6/24	6/24	6/26
6/13	0	77c	80	78c														
6/14	1	77	79	71	**182**		97											
6/15	2	76c	77	74c	**154**	**4204**	68											
6/16	3	103	99	87	**125**	**3711**	81	68	73	71								
6/17	4	80	78c	57	**122**	**3730**	80c	75c	78c	77c								
6/18	5	92	83	88	**c**	**130c**	83	91	85	85								
6/19	6	71c	67	70	**67**	111	72	75	70	67c	76	69	53					
6/20	7	73	71	72	**75**	78	73	c		80	80	80	60					
6/21	8	73	70c	70	**70**	80	80	69		72	83c	76	25c	65				
6/22	9	64	68	69c	**71c**		75c	66		67	67	95	26	111	70			
6/23	10			120	**74**	64	69	77		75	68	68	30	77				
6/24	11			80	**77**	75	76				66	64	31	70	69			
6/25	12	84	76	83	**99**	88					129	70		103	80	88	86	
6/26	13	c			**110**	93									110	102	**112**	
6/27	14	120			**133**	110									**128**	120	**135**	103
6/28	15	105			**120**										**118**	103	**113**	83
6/29	16	103			**121**										**105**	103	**126**	83
6/30	17				**126**										**114**	105	**123**	80
7/1	18	a			**139**										**118**	102	**128**	97
7/2	19	77			**131**										**115**	95	**118**	88
7/3	20	91			**134**										**126**	100	**114**	88
7/4	21	78			**130**										**117**	95	**122**	100
7/5	22	80			**131**											108	**128**	116
7/6	23	69			**78**										**110**	85	**108**	91
7/7	24	72			**94**										**108**	86	**111**	90
7/8	25	85			**100**										**225**	96	**113**	134
7/9	26	83			**97**											85	**102**	94
7/10	27	83			**96**											88	**109**	88
7/11	28	79			**101**											94	**102**	95

Excess tritium showed in bold type
c=electrolyte changed
a=new cell

Four cells showed an indication of tritium production. The excess values are indicated by bold type. Cell #30 give a count rate of 4204 c/min-ml which is 80 times the tritium content of the electrolyte. This level was found 10 days after the cell was started. No additional tritium was produced during the next three days. A current reversal after this time produced no additional tritium. Cell #29 showed a little excess tritium because the electrolyte had been changed about 30 hours before the tritium measurement was made. Examination of the spillover showed a counting rate of 2500 c/min-ml.

Thus, tritium was produced in this cell before the electrolyte was changed. The charging history of these two active cells is shown in Fig. 8.
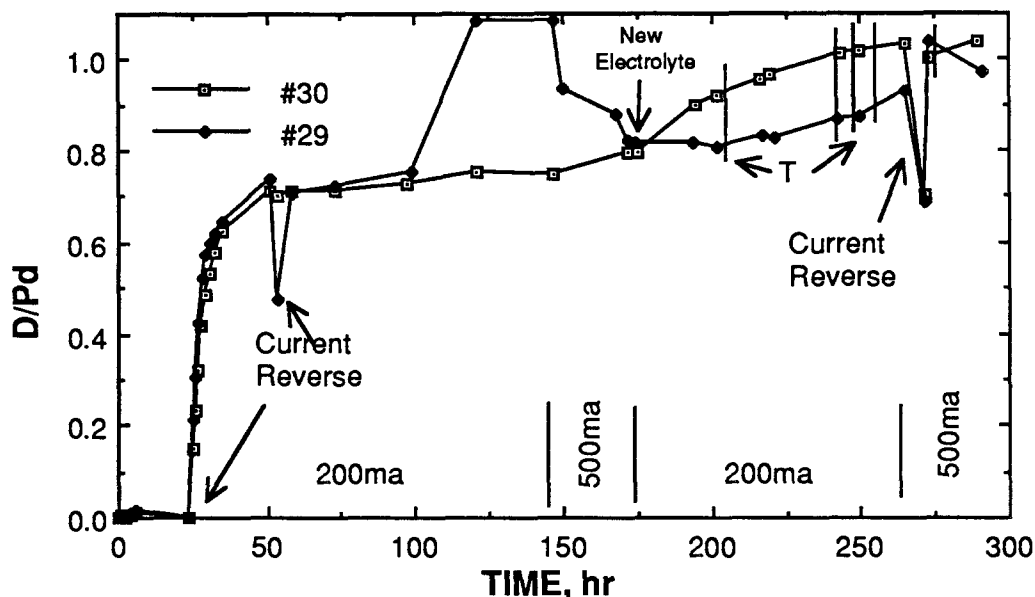
FIGURE 8. Charging history of cells #29 and #30

Other cells running at the same time, using the same heavy water, showed a counting rate between 40 and 80 c/min-ml as can be seen in Table 2. After the electrolyte in cell #29 was changed again, another small increase was seen after about 30 days from the start. Cells #41 and #43 also produced minor amounts of tritium. Cell #41 contained about a foot of 0.032″ wire that was wound into a spiral. The small tritium production was ignored at the time but later work shows that these increases were significant. The few high, isolated counting rates shown by cells #26, #28, #36, #40, #42, and #44 were ignored as being possible errors.

In order to verify that the high counts were not caused by chemiluminessence, three procedures were applied. Part of the sample (Cell #29 and #30) was neutralized, distilled and counted. The light spectra[3] was measured and compared to a known tritium sample and the undistilled sample was recounted after sitting a month. All three procedures were consistent with there being tritium in the sample. A similar result was obtained when the sample was counted by another group at the Laboratory. Nine subsequent attempts to make cells that would produce tritium failed until recently.

Gradually the cells were modified. First, plastic was substituted for glass and then recombiners were added. The recombinate was allowed to run back into the cells at first. About 16 cells were treated in this way. An examples of the tritium values are shown in the Table 3.

TABLE 3
Counting rates (c/min-ml) of closed cells run with recombiners.
A background of 20 c/min-ml is included

		Cell Number												
DATE	DAY	49	51	54	55	56	57	58	59	60	61	62	63	65
Start=		8/15	7/4	7/31	7/31	7/31	8/9	8/9	8/9	8/9	8/9	8/9	8/9	8/15
8/11	0		80	70	70	80	60	70	70	70	70	70	70	
8/14	3		75	71	68	71	79c	65	68	66	66	66	58	
8/15	4	78	77	87	80	81	78	78	79	91	82	98	89	69
8/16	5	65	79	65	67	73	67	68	d	d	67	71	75	73
8/17	6	61	71c	69	69	68	66	65	d	d	68	68	68	67
8/18	7	68	70	70	70	71	70	70	d	d	69	69	73	66
8/21	10	70	72	67	71	71	73	68	d	d	70	69	78	69e
8/22	11	71	72	70	70	65	70	66	106	71	70	73	80	68
8/23	12	64	68	72	70	69	80	71	82c	68c	63c	65	71	70
8/24	13	66	71	74	75	68	68	69	61	70	65	69	72	70
8/25	14	71	70	72	67	70	66c	66	70	68	70	71	75	66
8/26	15		82	73	75		81	80	65	70	56	73	74	71
8/27	16	60	76	70	71	71	129	73	69	73	71	72	76	72
8/28	17	68	73	68	73	72	79	72	72	68	59	68	66	66
8/29	18	67	77	72	75	67	69	74	71	74	72	76	78	69
8/30	19	67	72	73	77	71	94	66	70	75	74	68	70	65
8/31	20	73	83	71	71	69	73	70	73	80	75	77	71	63
9/1	21	66	76	72	75	71	84	68	69	77	68	69	71	66
9/5	25	71	76	72	71	74	84	69	68	70	67	70	71	73
9/6	26	71	75	69	74	73	88	71	69	73	69	71	71	69
9/7	27	68	77	74	79	76	90	74	71	72	70	70	73	66
9/8	28	74	81	73	73	82	90	74	75	76	77	73	69	68
9/11	31	73	79	74	74	75	80	77	76	81	78	72	79	70
9/12	32	69		67	74	73	76	72	67	67	72	72	74	69
9/13	33	72		69	68	76	89	70	72	80	71	73	76	67
9/14	34	50		70	70	80	90	80	70	80	70	70	70	70
9/15	35	71		71	71	70	82	74	72	75	70	73	73	64
9/18	38	71		71	76	73	83	75	76	74	75	71	73	70
9/19	39	73		75	68	71	82	70	72	77	75	73	75	68
9/20	40	81		75	74	77	84	67	80	78	73	77	78	65
9/21	41	67		68	72	76	78	70	73	72	71	70	79	70
9/22	42													
9/25	45													
9/26	46	82R					86R				85R	79R		70R

e=explosion; c=new electrolyte; R= after current reverse
d=Low count because of suspended black nickel oxide

As can be seen in Fig. 9, where two typical cells are plotted as a function of time, the tritium values were essentially constant. The line is a least squares fit to sample #62. Occasionally a high or low point is measured. However, if these isolated values are ignored, the counting rate for inactive cells is 51.1±2.8 and 53.4±3.6 for cells # 62 and #63, respectively, after the background is subtracted. All the other cells, except #57 showed essentially the same behavior. Cell #57 showed a slightly higher average and larger standard deviation because of several isolated high values.
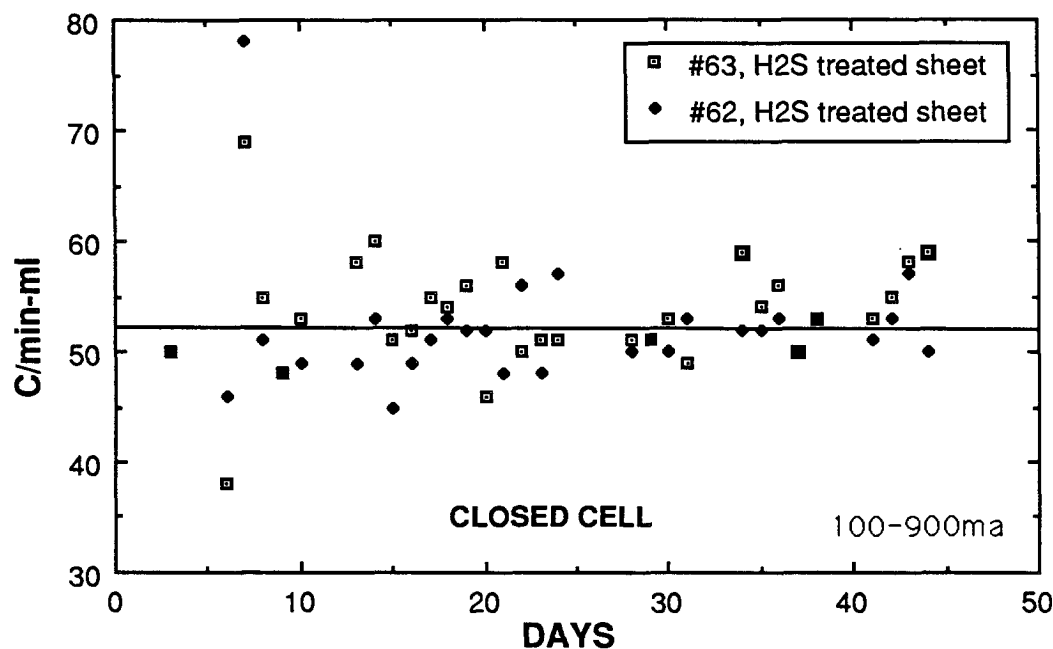
FIGURE 9. Example of closed cell behavior.

The latest group of cells have the design shown in Fig. 10. Here the recombinate is collected in an I.V. bag. The cell is glass and the anodes are either Pt gauze or Ni wire. In each case, there is a minimum distance between the anode and cathode.
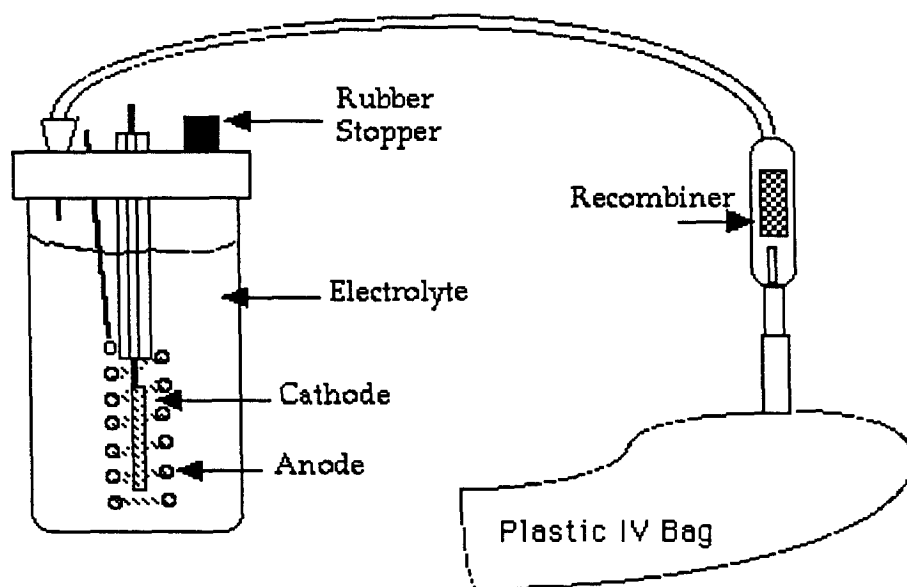
FIGURE 10. Cell design #5

Seven of the nine cells that were started at the same time and are running in series at constant current show evidence of tritium production. Two are apparently inactive. The cell construction of this group is shown in Table 4 and the counting rates are listed in Table 5.

TABLE 4
Materials used in cells #70 to #79

#	Shape	Alloy	Surface Treatment	Pre-Treatment	Anode	Date Started
70	wire	Pd, Martin	none	none	Ni wire	9/5
71	strip	Pd	C-S	paraffin, H_2S	Pt small	9/7
72	strip	Pd	C-S	paraffin, H_2S	Pt small	9/7
73	strip	Pd	C	paraffin	Ni wire	9/7
74	strip	Pd	C	paraffin	Ni+S wire	9/7
75	strip	Pd	C-S	paraffin, H_2S	Pt small	9/7
76	strip	Pd	C-S	paraffin, H_2S	Pt small	9/7
77	strip	Pd	C-S	paraffin, H_2S	Pt small	9/7
78	strip	Pd	not cleaned	none	Ni+S wire	9/7
79	wire	Pd,Martin	none	none	Ni wire+Ag	9/7

strip= strip cut from 0.05" thick sheet

wire=0.04" wire supplied by Prof. Martin, Texas A&M Univ.

C-S= Heated in paraffin and then in H_2S

C=Heated only in paraffin

none= cleaned with dilute HNO_3

Ni+S=Nickel wire heated in H_2S

Ni wire+Ag= A small piece of silver is attached to the nickel wire

Pt small= Pt gauze made into a 3/8" diameter tube

All cells are glass

TABLE 5
Count/min-ml obtained from cells #70 to #79
Values include a background of 20 c/mim-ml
Counting rate of the recombinate is shown

DATE	70	70g	71	71g	72	72g	73	73g	74	74g	75	75g	77	77g	78	78g	79	79g
9/7	64																	
9/8	79				74				59		69		84		75		67	
9/11	62		87		56		60		57		66				83		89	
9/12	64		99		80		77				90		80		84		88	
9/13	60		80		86		85		58		94		56		86		86	
9/14	70	80	100	100	90	80	100	100	70	60	100	100	90	100	90	80	100	100
9/15	73		106		97		110		73		101		113		109		103	
9/18	73		129		95		135		63		123		122		98		109	
9/19	65		116		89		128		67		119		122		106		107	
9/20	67		116		97		135		72		128		123		107		112	
9/21	71	62	109	106	93	90	122	93	70	77	119	115	117	96	105	93	101	91
9/22	74		116		105		133		72		122		121		108		112	
9/25	77		118		107		147		67		124		131		120		130	
9/26	77	63	121	98	106	87	145	121	68	73	129	107	117	101	113	96	119	93
9/27	77		121		108		153		74		120		126		120		121	
9/28	83		128		115		164		78		126		133		124		127	
9/29	76	69	118	91	106	90	144	102	72	75	129	110	133	90	124	100	126	99
10/2	86	78	132	99	107	88	147	122	85	75	136	119	123	124	141	132	122	
10/3	79		113		121		167		77		148		123		123		127	
10/4	82	75	121	110	118	95	165	117	76	97	150	124	132	108	129	100	125	
10/5	84		126		115		151		83		151		131		130		136	
10/6	78	80	115	106	106	98	124	107	80	84	122	115	122	144	115	115	118	
10/10	78		111	110	108	92	123	105	81	108	116	128	116	103	111	101	119	
10/11	78		117		107		130		81		112		133		112		116	
10/12	84		118		103		118		80		123		116		108		112	

The gas samples are based on 0.5 ml of recombinate and, therefore, have a larger uncertainty than the electrolyte.

As can be seen in Fig. 11, the two inactive cells show a slow increase in tritium content, owing to enrichment. This contrasts with the closed cell behavior seen in Fig. 9.
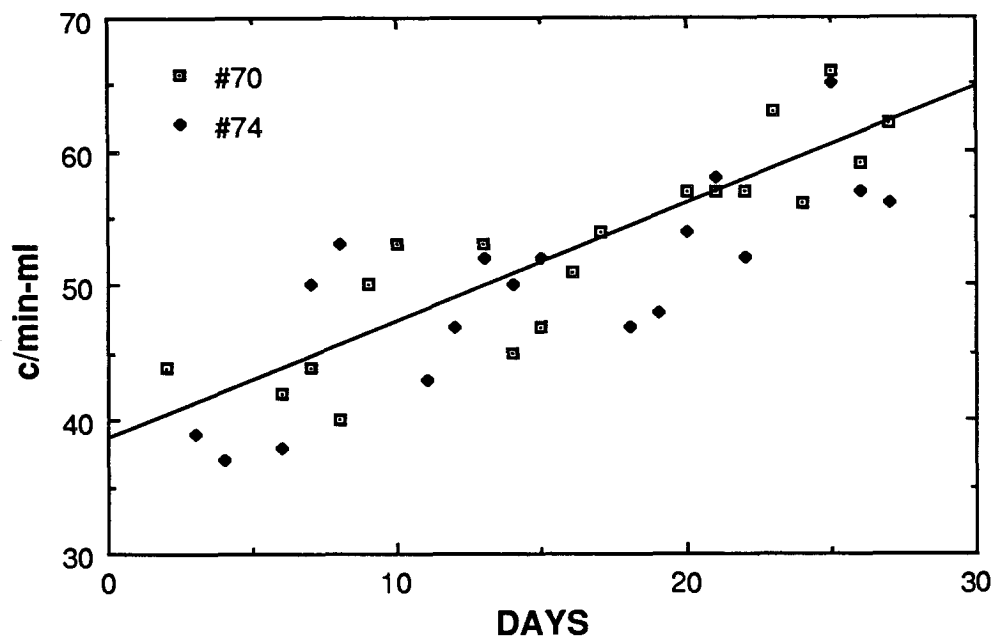
FIGURE 11. Counting rate of inactive cells

Because the current was not constant but was increased from 50 to 400 ma during this time, the enrichment rate will not be constant. However, there is sufficient scatter that this effect can not be seen. The standard deviation from the straight line is approximately ±2.4 c/min-ml which is similar to that obtained from the closed cells.

The cells that are producing tritium are compared in Fig. 12. There is a range of values but each exceeded the count rate of the inactive cells in about 3-4 days and continued to increase in steps.

FIGURE 12. Comparison between all cells in this series

Several of the cells have showed especially interesting behavior. The two highest cells are compared in Figure 13. The scatter of the values is larger than that found 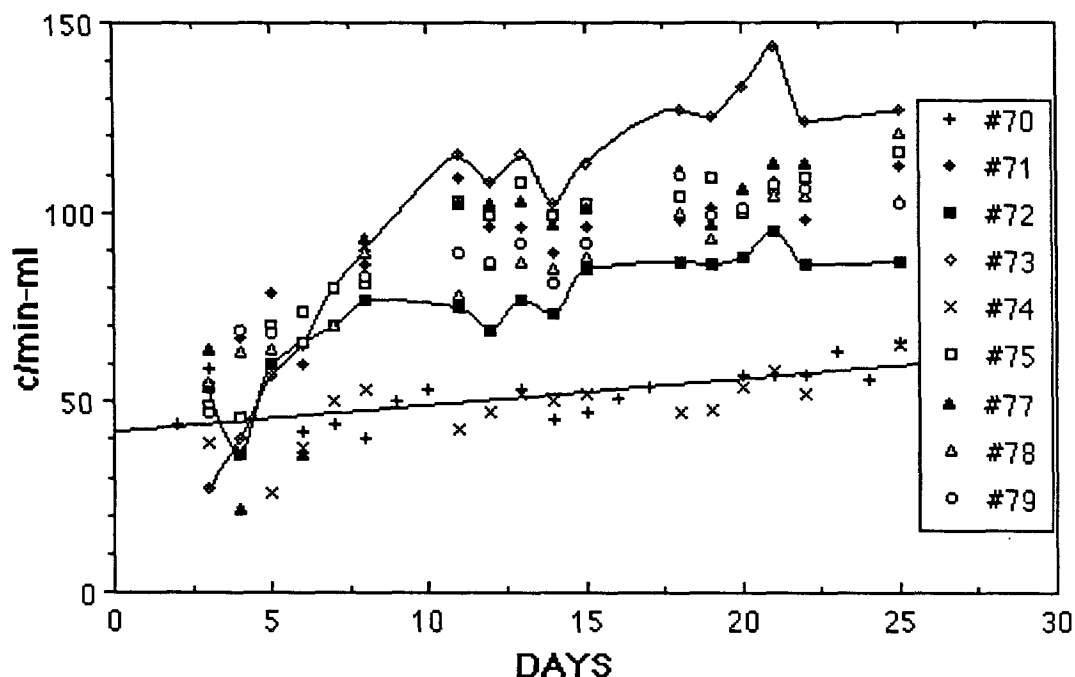for inactive cells. Perhaps the tritium is being made in bursts and the increase in activity is owing partially to dissolved tritium as DT gas which is quickly swept from the solution by the steady production of DD. The recombinate, in general, follows the count rate of the electrolyte, as shown by the data for samples #73 and #75. In general, the recombinate contains less tritium than does the electrolyte. So far, there is no indication that significant tritium is leaving the cell in the gas phase. Perhaps the production rate is small compared to the exchange rate with the D_2 that is dissolved in the electrolyte. A higher production rate such as reported by workers at Texas A & M University[4], is apparently sufficient to overwhelm the exchange reaction. A completely exchanged solution of DT is expected to have a counting rate of about 2×10^{10} c/min-ml.

One needs to realize that because the cells hold 120 ml of fluid, the same tritium production in a smaller cell, such as used by workers at Texas A&M University, would produce an activity about 10 times that measured here and more quickly saturate the liquid.
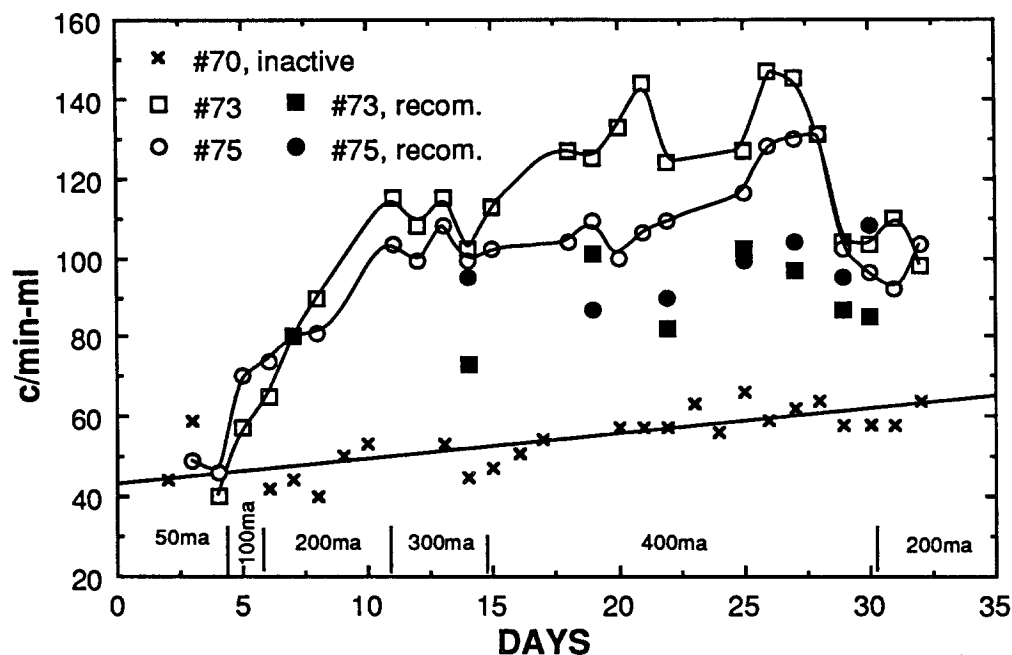
FIGURE 13. Tritium counts for two active cells and one inactive cell. The tritium activity in the recombinate is shown.

DISCUSSION

Cells #70 and #73 have been followed in sufficient detail that the enrichment factor and excess tritium can be calculated.

The excess tritium was determined by subtracting from the initial tritium content, the tritium lost to the gas phase, owing to electrolysis, and adding the amount returned to the cell when the lost electrolyte was replaced. The excess is the difference between the resulting value and the measured amount of tritium determined daily.

Cell #70 shows no sign of excess tritium production and was used to determine the enrichment factor. A minimum excess tritium is calculated for this cell if an enrichment factor of 0.9 is assumed. This value can also be obtained by comparing the tritium content in the cell to that found in the recombinate. The average gas/liquid ratio based on 11 sets is 0.87±0.03. An enrichment value of 0.9 was used to calculate the behavior of cell #73.

Cell #73 was the best of seven active cells. Tritium production started after five days and continued off and on for about 25 days with evidence of bursts as can be seen in Fig. 14. The tritium content of the recombinate was less than the electrolyte and gave a somewhat lower enrichment factor (0.80±0.04) than that obtained from cell #70. This difference is too small to have an effect on the conclusion.

We believe that DT gas was produced on the electrode at such a low rate that most or all of it was able to exchange with the dissolved D_2 gas as the gas bubbled

through the liquid. When production stopped, the DT gas was flushed out of the solution by the steady production of D_2 gas, thus reducing the tritium content. Perhaps one half of the tritium has exchanged with D in D_2O and remains fixed in the liquid.
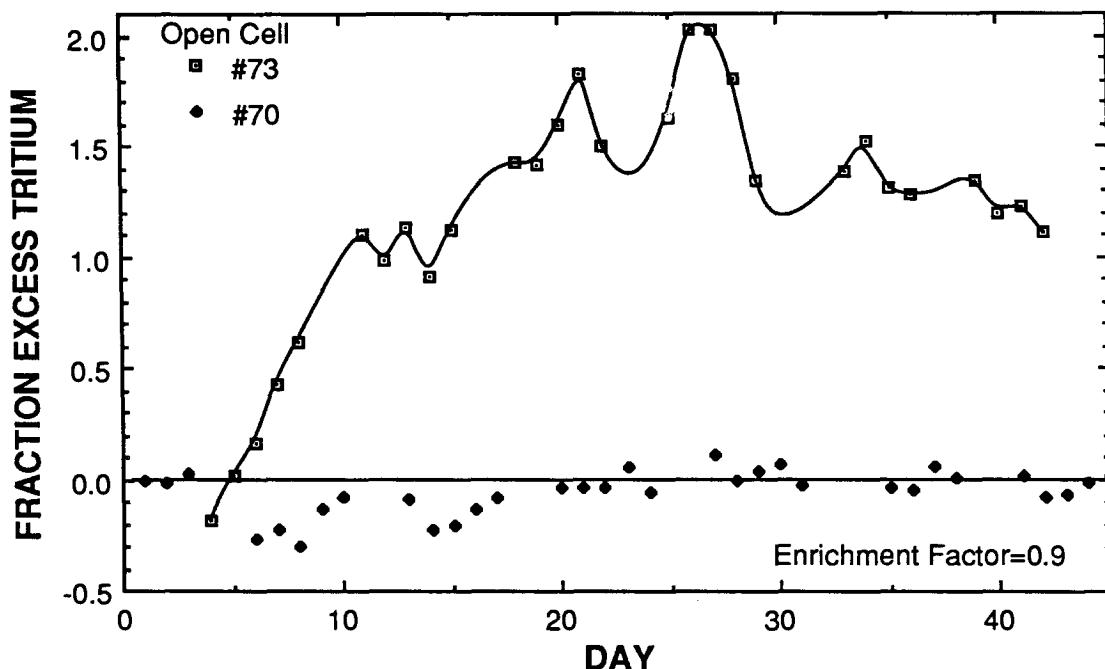

FIGURE 14. Fraction excess tritium in cells #70 and #73 assuming an enrichment factor of 0.9.

CONCLUSION

The presence of carbon at C/Pd=0.018 (7.6 wt%) significantly reduces the uptake rate and the limiting composition. Carbon may increase the likelihood of internal crack formation. The presence of Li offsets the effect of carbon and increases the takeup rate of deuterium. However, no tritium has been produced in cells containing a Pd-Li alloy.

Presence of solder and copper in the cell causes Cu, Zn and Pb to plate on to the cathode surface even though these materials were not in the electrolyte.

The electrode expands when D_2 is added but does not return to the same size when the D_2 is removed. Apparently, dislocations and cracks are formed within the metal structure.

The highest D/Pd ratio obtained was 0.88 for a C+S coated electrode although most cathodes reached a ratio near 0.7.

Tritium has been produced in 9 cells at levels between 1.5 and 80 times the starting concentration. Over 1400 tritium measurements have been made using 64 cells of various designs. The effect of chemiluminescence, counting efficiency, and other sources of error have been studied. Based on this background, we believe that the tritium is real, it is not caused by contamination and it is not a product of normal electrolysis.

However, we can not yet say what special conditions are required to produce tritium.

References

[1]   M. Fleischmann and S. Pons, J. Electroanal. Chem. **261** (1989) 301..

[2]   Johnson Matthey, Inc; 100% palladium.

[3]   The light spectra is different when luminescence is caused by beta emission compared to chemical effects.

[4]   Professor J. Bochris, comments made at the NSF/EPRI Workshop, Washington, October 16-18 (1989).

DISCUSSION (STORMS)

Lewis: Are your groups of 30 cells connected in series?

Storms: We have four stations, each with a power supply driving a series of cells. Because of their limited current requirements, this is less expensive than using a power supply for each cell.

Huggins: Were the groups of cells different?

Storms: Each group is, of course, operated at the same current, which may be different for another group. Cells can be changed from group to group if operation at different current densities is required.

Hoffman: What was the thickness of the palladium cathode?

Storms: It was about 2 mm thick and 1.5 cm in diameter.

Lewis: You weighed the electrodes after charging. What weight gains were observed?

Storms: We saw an increase of about 4 percent.

Werth: Do you know the origin of the copper and lead impurities which plate out on the cathode?

Storms: Yes, they were from the plug at the top of the cell, even though it was not in contact with the electrolyte. The plated layers were a few microns thick.

Werth: Can you tell us how you prepared the lithium-palladium alloys?

Storms: Those with higher lithium content were arc-melded from a mixture of palladium powder and lithium metal, and those with a lower lithium content were similarly made from a mixture of palladium powder and lithium nitride.

Oriani: The lithium may actually suppress the degassing of hydrogen by filling up the surface, so more gas may be detected in the metal than with palladium.

Storms: We have carried out absorption studies on lithium alloys, which show that they absorb effectively. The gas does not become irreversibly contained in the alloy.

Oriani: At what temperature does it absorb deuterium?

Storms: At room temperature.

Huggins: Carbon reduces hydrogen isotope solubility, which is restored by adding lithium. Where does the carbon go inside the palladium? It may not be a simple substitution effect.

Storms: Carbon has very low solubility in palladium. At the concentration which we studied, most of it is present as graphite in the grain boundaries. Hydrogen

or deuterium diffuses through a grain and is stopped by the impermeable graphite barrier at the grain boundary, which slows its diffusion rate.

Oriani: If a specimen is treated more than once with deuterium, does the total amount of cracking due to fissuring increase?

Storms: It rises to still higher values. Although we have not examined many absorption-desorption cycles, the tendency is for specimens to take up deuterium more rapidly than they did initially, since there are more cracks allowing entry. The total expansion of the specimen will also be greater.

Santucci: How and at what rates do you do your degassing?

Storms: The specimen simply lies on the benchtop and is allowed to degas. Depending on the sample, this may take one or two weeks.

Lewis: Does it not become warm during the process?

Storms: Some samples do and some do not. Lithium alloys do not become warm because there is no recombination on their surfaces. However, if there is any sulphur on the surface, recombination is very rapid and the specimens may become hot enough to burn paper.

Huggins: Would you explain the fall-off in tritium concentration that you observe?

Storms: The tritium is produced in the gas phase. It does not exchange with heavy water but dissolves in the electrolyte as DT molecules. Once it stops being produced, it is purged from the electrolyte by the deuterium which is constantly evolved at the cathode.

Lewis: In that case, distillation of the electrolyte should-have removed the tritium. Your analytical results must indicate exchange with the electrolyte.

Fleischmann: We also saw that the electrolyte can detritiate, which is a concern. We did not publish the time dependence of tritium production from our early work, which was extremely irregular.

Storms: I agree. We have observed that once a cell starts to produce tritium, the production rate will inevitably tend to reduce. We have not run experiments long enough to see if production eventually goes to zero.

Talcott: In this particular cell design, a spillover of electrolyte takes place on replenishing, because there is a plastic insert inside the glass. This spillover falls into the glass part underneath. So, as well as normal D_2O loss from electrolysis, one also has loss of electrolyte via spillage, which requires addition of more D_2O. The spillage showed a higher tritium content that the electolyte, since the loss rate was inevitably lower from here. Higher tritium contents were particularly seen in the spillage of cells where the electrolyte had been changed.

Lewis: What fraction of the D_2O did you replenish?

Talcott: About 10-15 ml out of 50 ml, or 20-30 percent.

Storms: The electrolyte in one cell did not show a high tritium content. Some time after the electrolyte was changed, the spillover showed 2500 counts per minute per ml. This incidently also shows that the tritium was produced in the cell and was not artificially introduced, since there was no access to the sealed spillover without contamination of the electrolyte, and the spillover material was not changed when the electrolyte was changed.

Lewis: If you consider the total amount of tritium detected, compared with the total in the amount of electrolyte added, then do a separation factor calculation, can you say that you really have made the tritium in the cell?

Storms: More tritium was detected than was introduced into the cell.

Lewis: By what factor?

Storms: By a factor of 70-80.

Hoffman: How did you convert the count to disintegrations per minute per ml (dpm/ml)?

Storms: We subtract 20 from the counts per minute per ml, representing the background at the counter, and then we divide by 0.38 to convert to dpm/ml.

Jones: When you electrochemically degas your cathodes by current reversal, your results show that tritium levels in the electrolyte hardly change. Surely, any tritium formed in the electrode would be driven out.

Storms: We believe that the tritium is produced on the electrode surface, rather than inside.

Jones: Even if it is produced in the surface layers, some should be driven off.

Storms: I agree. I am not sure that our sensitivity of detection was high enough to be able to say that no tritium came from out of the electrode, but it was not a significant amount compared to that previously in the electrolyte. It was certainly much less than 10 percent.

Bockris: To obtain greater sensitivity, have you changed electrolytes and then reversed the potential?

Storms: We propose to do that experiment.

Yeager: Concerning the electrodes which were treated with paraffin, did you leave the paraffin film, i.e., an electrical insulator, on the electrode?

Storms: The electrode was heated in paraffin, thus giving a weight increase. There was certainly a paraffin film on the electrode when it was introduced into the cell. It apparently breaks down or dissolves, since it does not affect electrochemical behavior.

Yeager: It may, of course, break down when a voltage is applied.

Storms: Certainly.

Yeager: Such experiments have some of the elements of black magic.

Storms: A problem which we face is that we do not have the resources to do this work in a sophisticated manner, as we would wish. Much of it has to be done by trial and error, in an almost accidental low-key manner, which is embarrassing when the time comes to report results. It has not been possible to use any of the high-technology techniques which are available today.

Chu: How thick was the paraffin layer?

Storms: It weighs a few tenths of a mg, corresponding to about 1 micron.

Chubb: Is it always the same thickness?

Storms: No, its thickness depended on how it was heated.

Chubb: Did you try correlating tritium production as a function of thickness?

Storms: We have attempted to do that, although results are inconsistent.

Talcott: There are a large number of variables associated with the catalytic surface, for example, its carbon composition and heat-treatment history.

Lewis: Some cells produce tritium, and some, no tritium. Could that not simply result from different electrolysis separation factors on surfaces which have received different treatment? Your curves seem to indicate that the separation factor first increased, then fell to a constant value.

Storms: The results do certainly vary a great deal. In some cases bursts of tritium seemed to occur. The raw data which I show is very new, dating from last Thursday.

Appleby: What is the electrolyte volume in the cells which we are discussing?

Storms: It is 120 ml.

Appleby: How much D_2O do you add every two or three days?

Storms: 10-15 ml.

Appleby: Let us assume that the tritium is not coming out of the solution at all, i.e., that the separation factor is infinite.

Schneider: In five days you would replace the initial electrolyte volume.

Appleby: So you would double the amount of tritium in the electrolyte in a minimum of five days, assuming the largest possible separation factor. Hence, the separation factor explanation cannot account for the observed results. The counts per minute in the unused solvent do not, of course, all represent tritium.

Storms: The starting level would be 40 counts per minute per ml with the background of 20 counts subtracted, i.e., 20 counts per minute per ml.

Rafelski: Can you characterize the electrical pulses in your neutron detection experiments?

Storms: The pulses were at about 500 V, normally at 80 Hz, lasting for about 5 microseconds.

Jones: Are your neutron data given in counts per minute or per hour?

Storms: In cumulative counts per hour.

Section 6

OBSERVATION OF NEUTRONS DURING ELECTROLYSIS OF LiOD SOLUTIONS

William G. Pitt, John N. Harb, and Cambis J. Farahmandi

Chemical Engineering Department

Brigham Young University

Observation of Neutrons During Electrolysis of LiOD Solutions

William G. Pitt, John N. Harb, and Cambis J. Farahmandi
Chemical Engineering Department, Brigham Young University, Provo, UT 84602

ABSTRACT

Electrolysis of 3M LiOD in D_2O solution was performed using an annealed cylindrical palladium cathode and a concentric wire palladium anode. The cathodic current density was 640 mA/cm^2. During 177 hr of electrolysis, neutron emission was significantly above background. No anomalous heat, tritium or helium were detected.

INTRODUCTION

This study, like many others, was motivated by the recent announcement of electrochemically induced cold nuclear fusion [1,2]. Since initial claims of excess heat, anomalous heat generation has been observed by others in similar cells [3,4]. Generation of tritium has also been reported [5], but at levels too low to account for the excess heat. Additionally, low-level bursts of neutrons have been observed from electrochemical cells with titanium [6] and palladium [7] cathodes. The purpose of the present work was to examine neutron release in electrochemical cells with palladium cathodes in LiOD.

EXPERIMENTAL

Electrochemical Cell

Figure 1 shows a schematic diagram of the electrolytic cell used in this study. The cell body was glass with a 2 cm inside diameter and a length of about 10 cm. It was surrounded by an evacuated jacket in order to improve the lower limit of heat detection in the cell which was approximately 0.1W. Temperature was measured

To vacuum system/
gas collection system

Pressure
transducer

Pt catalyst
recombination chamber

D_2 Flowmeter

O_2 Flowmeter

Thermocouples

Feedback Valve

Teflon lid
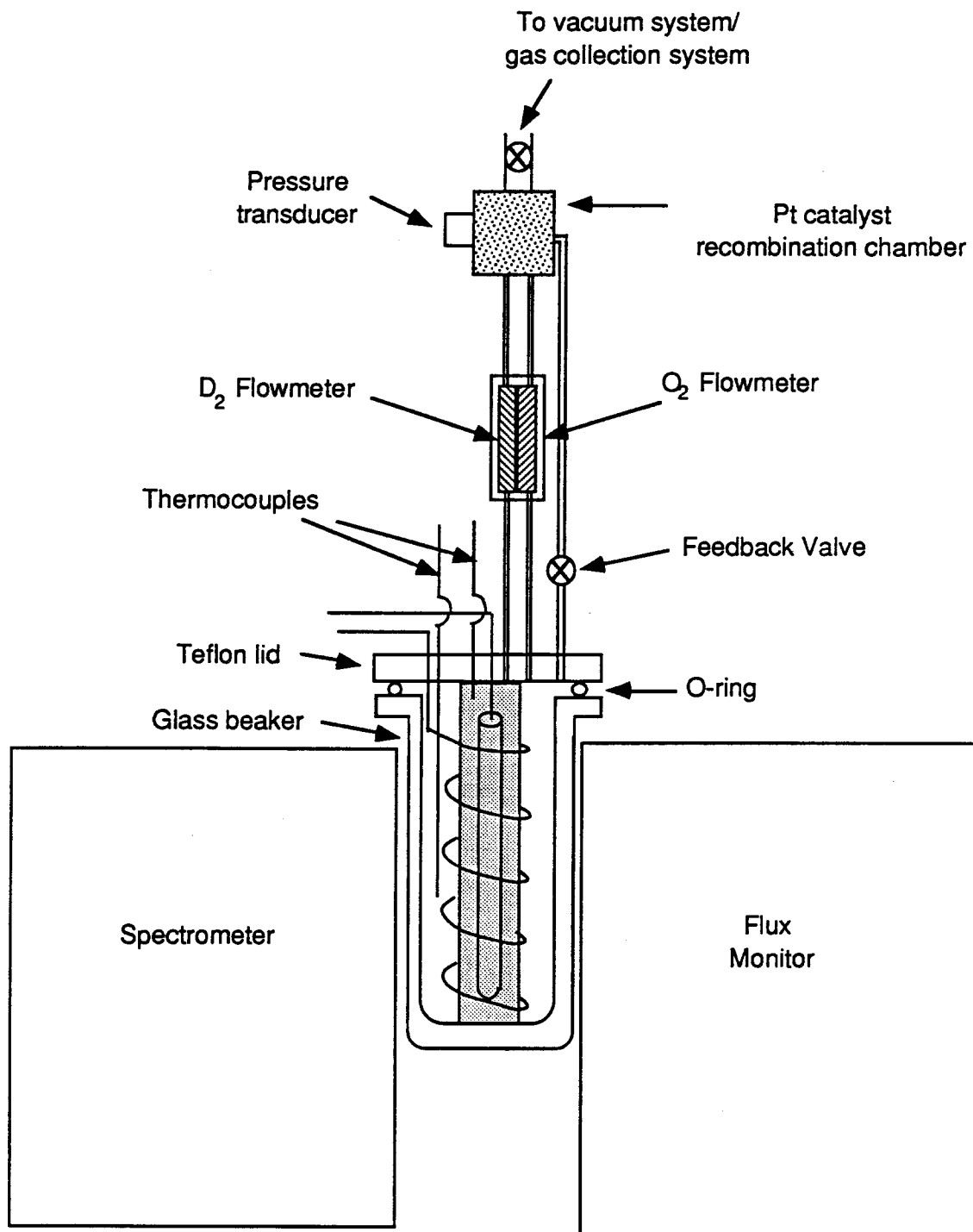
O-ring

Glass beaker

Spectrometer

Flux
Monitor

Fig. 1. Schematic diagram of electrolytic cell and recombination chamber.

with three thermocouples (type K) at different locations in the cell. The cathode was palladium wire (5 cm in length and 0.05 cm in diameter, Johnson Mathey) surrounded by a concentric anode which was also palladium to provide near uniform current densities on the cathode surface. The cathode was annealed in an argon atmosphere for 12-14 hours at 600°C prior to electrolysis. An ion exchange membrane was used to separate deuterium (or hydrogen) and oxygen inside the cell in order to prevent any possibility of in-cell reaction. The gases exited the cell separately and were fed to recombination chamber containing a Pt catalyst. The recombination water could then be returned to the cell or retained for later analysis. The experimental system was thus completely isolated from the outside environment. All experiments were conducted in 3M LiOD.

Neutron Spectrometer

Neutron emission was measured on a spectrometer in the Physics Department at Brigham Young University. Details of the spectrometer are described by Czirr and Jensen [8]. For this series of experiments, the spectrometer was operated in conjunction with a neutron flux monitor which also allowed detection of neutron emissions in bursts.

The spectrometer consisted of a 3 pieces of ^{6}Li-doped glass placed in a cylindrical glass tube (12.5 cm diameter, 12 cm Long) containing scintillation fluid. An energetic neutron entering the spectrometer was thermalized by collisions with the scintillation fluid. Light emitted from the scintillator was detected by two photomultiplier tubes (PMT) and integrated to measure the energy of the neutron. Once the neutron was thermalized, it could combine with the ^{6}Li in the glass and emit a characteristic light pulse which is detected by the PMTs. Verification of a true energetic neutron requires both signals: integrated energy of at least 1 MeV from the scintillation liquid, and the ^{6}Li capture signal. The efficiency of neutron capture of this spectrometer is 0.59%. Gamma rays also scintillate the fluid and glass, but pulse shape discrimination provides excellent rejection of spurious gamma events.

The flux monitor consisted of 3 pieces of ^{6}Li-doped glass placed in a container similar to that of the spectrometer which contained mineral oil rather than the scintillation fluid. The mineral oil thermalized the neutrons without light emission, and combination of the thermalized neutron with ^{6}Li is detected by two PMTs. The efficiency of neutron capture of this flux monitor is 1.0%.

To detect neutron bursts in these experiments, the spectrometer and flux monitor were operated in the following manner. The

spectrometer was used to measure the energy of neutrons. When the energy exceeded a threshold of 1 MeV, a gate was opened allowing the flux monitor to record neutron events within a 510 μsec time window. This window was divided into 510 periods (channels) of 1 μsec duration. Any capture event placed a count in the channel corresponding to the time of capture. Capture in the flux monitor indicates coincident or multiple neutron emission since the flux monitor is only open when a energetic neutron ($\geq$ 1 MeV) is detected in the spectrometer.

A Canberra multichannel analyzer (Meridan, CT) was used to collect and display the neutron events. This system accumulates the spectrometer and flux monitor counts for specified time blocks. In the first set of foreground (D_2O) and background (H_2O) experiments, the time blocks were on the order of 5 hours which did not permit correlation of neutrons detected in the flux monitor to the corresponding neutron event in the spectrometer. In order to achieve better time resolution, the accumulated data from the Cannberra system was dumped to a VAX computer at 60 sec intervals, giving 1 min time resolution for the second set of experiments, and providing correlation between coincident neutrons and their spectrometer event.

Tritium Detection

Samples of electrolyte or recombination fluid were neutralized to pH 6 with HCl, and 2.5 ml aliquots of this solution were placed in a glass scintillation vial along with 10.0 ml of Aquasol^{TM} scintillation cocktail. The vial was shaken vigorously for several minutes, and then placed in a Betamate scintillation counter (Beckman) and counted for 10 minutes.

Gas Analysis

An evacuated stainless steel container of 1 liter volume was attached to the recombination chamber. Gases from the chamber were vented into the container. The gas was analyzed on a Finnigan-MAT 8430 mass spectrometer in the Chemistry Department at BYU. This double-focussing reverse geometry instrument can detect down to 2.5 amu.

Scanning Electron Microscopy

Small pieces of the cathode and anode used in heavy water experiments were rinsed in D_2O, dried and attached to aluminum stubs with silver paint. The were examined in a scanning electron

microscope (SEM) which was also equipped with energy dispersive X-ray (EDX) analysis capability.

Experimental Conditions

Electrolysis was conducted under galvanostatic conditions at 500 mA corresponding to a cathodic current density of 640 mA/cm^2. After an initial transient, the cell voltage reached a constant value of 3.74 ± 0.1 V; the cell temperature was also constant at 42°C and the pressure varied between +10 and -10 psig.

RESULTS

Electrolysis in 3M LiOD in heavy water was performed in two separate experiments for a total of 177 hours. Two background experiments consisting of electrolysis in 3M LiOH in light water were also performed for a total of 261 hours. The total electrolysis time was limited at 3 to 7 days per experiment owing to deactivation of the Pd anode which increased the total cell voltage to unacceptable levels.

Anomalous Heat

Evaluation of the continuously collected cell voltage and cell temperature data showed no evidence of excess energy production or excess power production. It should be noted, however, that the size of the cathode was such that heat generation rates of 5 W/cm^3 Pd would probably not be seen.

Neutron Emission

Capture in Spectrometer. Figure 2a shows the number of neutrons detected per hour by the spectrometer in the second foreground experiment. The solid line is the average detected neutrons during background light water experiments (see Fig. 2b). Note that the emission rate with heavy water started at a level commensurate with background and then increased steadily during this experiment.

The rate of neutron production above background can be calculated by subtracting the combined background data from the combined foreground data and dividing by the spectrometer efficiency (0.53%). The resulting rate was approximately 0.09 n/s assuming the neutrons are born individually more than 510 µsec apart. If neutrons are emitted in bursts, the actual neutron rate would be higher.
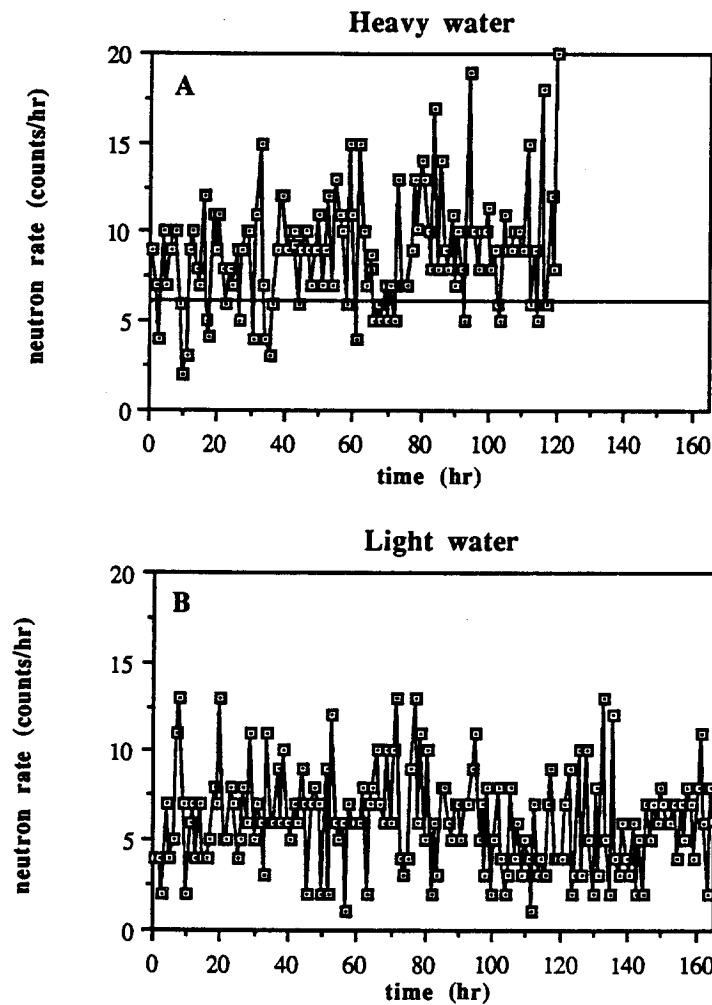
Fig. 2. Neutrons detected in the spectrometer: a) heavy water electrolysis; b) light water electrolysis.

<u>Capture in Flux Monitor</u>. Several neutron events were detected in the flux monitor indicating the probability of neutron emission in bursts. Recall that counts registered in the flux monitor are correlated with a neutron event in the spectrometer. These occurred mostly as single flux monitor captures, but there were two separate double captures in the flux monitor. Figure 3 shows the average multiple events per day for the heavy and light water electrolysis. There are significantly more multiple events (3.3 standard deviations) in the heavy water experiments.
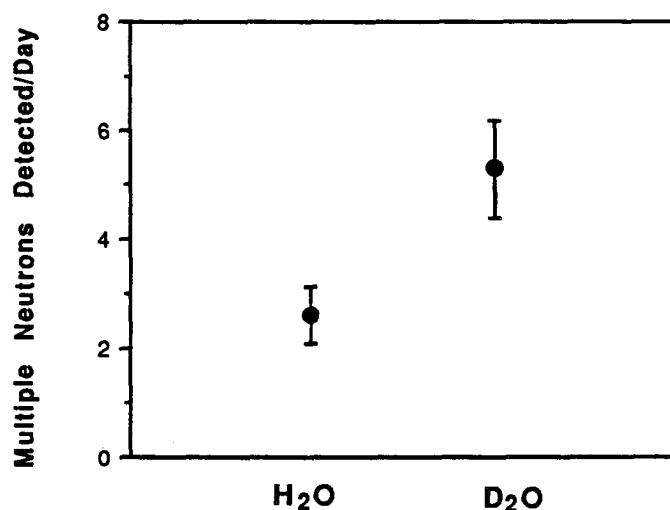
Fig. 3. Average multiple events per day for heavy and light water electrolysis.

Tritium

No significant evidence of tritium was found in either the cell electrolyte or in the recombination liquid.

Gas Analysis

Mass spectrometry of the gases in the recombination chamber showed no evidence of ^{4}He, ^{3}He, or ^{3}H.

SEM Analysis

Scanning electron microscopy of the Pd cathode showed that the surface was covered with dendrites growing radially away from the electrode. In some places the dendrites were covered with an amorphous material. EDX analysis of the dendrites and the amorphous material indicated that the surface was mostly Pd with about 1% Fe, a lesser amount of Cu, and very small traces of Zn, Pb and Mn. No Si was detected.

Analysis of the anode revealed a very smooth surface with occasional deep pits. The wire drawing scratches were still visible. EDX analysis indicated 100% Pd with no impurities.

ACKNOWLEDGEMENTS

REFERENCES

1. Jones, S.E., et al., "Observation of Cold Nuclear Fusion in Condensed Matter", *Nature*, 338 737-740 (1989).

2. Fleischmann, M., and Stanley Pons, "Electrochemically Induced Nuclear Fusion of Deuterium", Journal of Electroanalytical Chemistry, 261, 301-308 (1989).

3. Oriani, R.A., J.C. Nelson, S.K. Lee , and J.H. Broadhurst, "Calorimetric Measurements of Excess Power Output During the Cathodic Charging of Deuterium into Palladium", (preprint Aug. 25, 1989)

4. Appleby A., Young J. Kim, Charles R. Martin, "Anomalous Calorimetric Results During Long-term Evolution of Deuterium on Palladium from Lithium Deuteroxide Electrolyte", (preprint).

5. Wolf, K. L., "Neutron Emission and the Tritium Content Associated with Deuterium Loaded Palladium and Titanium Metals, Proceedings of the Workshop on Cold Fusion Phenomena, Santa Fe, NM, May 23-25, 1989.

6. Menlove, H.O., et al., "Measurement of Neutron Emission From Ti and Pd in Pressurized D_2 and D_2O Electrolysis Cells", (submitted to Nature, June 1989).

7. Mizuno, Tadahiko, et al., "Neutron Evolution From Annealed Palladium Cathode in $LiOD$-D_2O solution", Electrochemistry, 57 742-743 (1989).

8. J.B. Czirr and G.L. Jensen, "A Neutron Coincidence Spectrometer", *Nucl. Instr. Meth.*, accepted (1989).

DISCUSSION (JONES)

Santucci: Did you look for 14 MeV neutrons?

Jones: Our spectrometer is sensitive to 14 MeV neutrons, but they would not be detected because we did not go to a high enough energy range on our multichannel analyzer. This has recently been changed, but we have not seen evidence of 14 MeV neutrons.

Hoffman: Did you use the Thule station for the cosmic-ray background variations with solar flares and barometric pressure?

Jones: We used several stations, but mostly the station at Climax, Colorado.

Chubb: What were the crystallite dimensions of your high-surface-area titanium?

Jones: About 300 microns. It is my understanding that the material is made by allowing titanium crystals to grow from gaseous titanium tetrachloride around a wire.

Yeager: In the very high current density cell built by Dr. Bennion, an unusually large amount of gas would be produced. How do you handle it?

Jones: Electrolyte is pumped past the electrodes, which are separated by about 1 mm, at a very high flow rate. Under these conditions, bubbles do form on the electrodes, but in a mixing chamber, where they are collected from the center of the vortex. They are recombined on a platinum catalyst recombination chamber in a closed system.

Yeager: At those current densities, one must be careful of electrical discharge at the anode.

Jones: Dr. Bennion can supply details of the experimental design and precautions taken. For example, the system is water-cooled and maintained at 50°C.

Werth: What levels of cell voltage are seen at these ultrahigh current densities?

Jones: It is in the hundreds of volts range. Another interesting way of attaining these high energies would be by the use of impact fusion, in which deuterium and tritium are maintained in a conical cavity and impacted by a projectile. Dr. Miley, is there any ongoing work in this area?

Miley: I do not think that there is any active work at present. Certainly, that approach has been studied in the past, but it appears that higher velocity accelerators must be developed to achieve net energy production.

Jones: Professor Scaramuzzi at Frascati is proposing to use rail-guns to fire deuterium pellets into a Tokamak. He has a gun which will shoot a small 10 mg

titanium deuteride pellet at about 3 km/s. We have agreed to work together on this project.

Fleischmann: In your 9 standard deviations (9σ) event, what was the total neutron count?

Jones: The rate is about 0.1 neutron/s. Over 5 days, that would correspond to about 45,000 neutrons.

Huggins: Were the backgrounds run with two different detectors simultaneously?

Jones: We just have one pair of detectors, so we have to use one or the other alternately.

Chubb: Your lower detectable neutron energy limit is about 1.3 MeV?

Jones: Correct, so that the detectable energy range includes 2.5 MeV neutrons. Most of the background energy distribution is in a lower energy range.

Fleischmann: What is the response time or dead time of your detector?

Jones: It is 20 microseconds. Most of the neutrons which we observe are close to 2.5 MeV, but we see neutron bursts at higher energies.

Bard: How long were the electrochemical studies using palladium wire cathodes and anode at 640 mA/cm^2 operated to search for tritium?

Jones: The time was about six or seven days per run.

Santucci: Have you done acoustical measurements to detect phenomena which may coincide with low temperature neutron bursts from deuterided titanium?

Jones: Yes. Dr. Menlove will discuss these in the next presentation.

Section 7

UPDATE ON THE MEASUREMENT OF NEUTRON EMISSION FROM Ti SAMPLES IN PRESSURIZED D$_2$ GAS

H.O. Menlove and Eduardo Garcia

Los Alamos National Laboratory

S.E. Jones

Brigham Young University

UPDATE ON THE MEASUREMENT OF NEUTRON EMISSION FROM Ti SAMPLES IN PRESSURIZED D$_2$ GAS

H. O. Menlove and E. Garcia
Los Alamos National Laboratory
Los Alamos, NM 87545

S. E. Jones
Brigham Young University
Provo, UT 84602

During the Workshop on Cold Fusion Phenomena, Santa Fe, New Mexico, May 22, 1989, we reported [Los Alamos National Laboratory report LA-11686-C (September 1989)] on the measurement of neutrons emitted during pressurized D$_2$ gas experiments using Ti and Pd samples. The experimental program has continued since the Santa Fe meeting, and our data base has more than doubled.

Our recent work has included detector upgrades, background investigations, acoustical emissions, and sample preparation and procedure investigations. This report will give a brief summary of our work in the above areas.

I. DETECTOR UPGRADES

We are using four independent ^{3}He neutron detector systems for our experiments. All of the systems use ^{3}He tubes in polyethylene (CH$_2$) moderators to detect the neutrons. The detector characteristics and background levels are given in Table I.

TABLE I. Neutron Detector Characteristics

Identification	Shape	Number ^{3}He Tubes[a]	Total Efficiency[b]	Random Bkg (counts/s)	Coincidence Bkg[c] (counts/h)
System 1	Rectangular channel	18	21	0.23	1.3
System 2	Cylindrical cavity	6	26	0.092	0.35
System 3	Cylindrical cavity	16 + 5	34	0.16	2.3
System 4	Cylindrical cavity	16 + 3	31	0.39	2.3

[a]The ^{3}He tubes typically have a 30 cm active length and a fill pressure of 4-6 atm.
[b]The total efficiency was measured using a calibrated ^{252}Cf source located at the sample position.
[c]The coincidence background was measured with a 1.2-kg sample cylinder in the counting position.

A. Background Neutrons

We have reported results for both random neutron (totals) emission and time-correlated (coincidence) neutron emission. The background random neutrons originate primarily from cosmic-ray interactions in the detector, shielding, and sample, as well as from radioactive decay of uranium in the concrete shielding and α and β decay in the ^{3}He tube walls. On the other hand, the time-correlated neutrons originate from cosmic-ray spallation reactions in the sample and detector body. If the spallation reaction takes place at a significant distance from the detector tubes, the small solid angle and intervening shielding between the spallation and the detector prevent the detection of a coincidence event.

To investigate neutron background fluctuations, we counted the neutron backgrounds from the dummy sample for 3 weeks for System 4 and 2 weeks for System 3 and showed that the observed scatter of random counts (10^4-s time intervals) about the mean was no larger than the expected standard deviations (RSD) of 1.6% for System 4 and 2.0% for System 3.

Recently, the external neutron backgrounds in Systems 1, 2, and 3 have been reduced by the addition of 10 to 30 cm of CH_2 to the exterior of the detectors. These lower rates are reflected in Table I.

B. System 3 Upgrade

An electronic noise veto counter has been added to System 3. Figure 1(a) shows a schematic diagram of the upgraded system. The split of the high voltage to the external set of five ^{3}He tubes is used to pick up possible electronic noise such as voltage spikes and rf interference. The external tubes have no CH_2 and they are wrapped in cadmium so they have negligible efficiency for counting neutrons. Their coincidence rate is less than 1 count per day. A coincidence count in this external counter vetoes a count in any of the other systems.

C. System 4 Upgrade

A third ring of ^{3}He tubes has been added to System 4 as shown in Fig. 1(b). Ring 3 has completely independent electronics from the two inside rings and it measures the sample neutrons with an overall efficiency of 5%. The ratio of totals counts between the inside detector and ring 3 is 6/1 and the corresponding coincidence count ratio is 46/1.

The ring ratio can be used to show that the neutrons originated from the sample, and for larger bursts, the ratio can be used to establish the average neutron energy.

D. Neutron Die-away Time

For System 4, we have split the output from the inside detector to two different coincidence electronics, as shown in Fig. 1(b). The normal shift-register[1] has a coincidence gate of 128 μs and the second shift register has a gate of 32 μs. A ^{252}Cf source was used to show that an instantaneous burst of neutrons results in a coincidence ratio in the two gates (128 μs/ 32 μs) of 2/1. We now check that our background and sample burst events satisfy this ratio within the counting statistics. This is essentially a measure of the neutron die-away time (~50 μs) in the detector.

Typical sources of electronic noise will not satisfy this gate ratio criteria.

II. NEUTRON BURST RESULTS

We have continued to measure neutron bursts from the Ti samples in D_2 gas; however, the events are unpredictable and difficult to obtain. Table II gives a list of the samples that have yielded neutron bursts. The list shows the number of source neutrons, and the underlined values correspond to events that occurred during warm-up from liquid nitrogen (LN) temperatures at
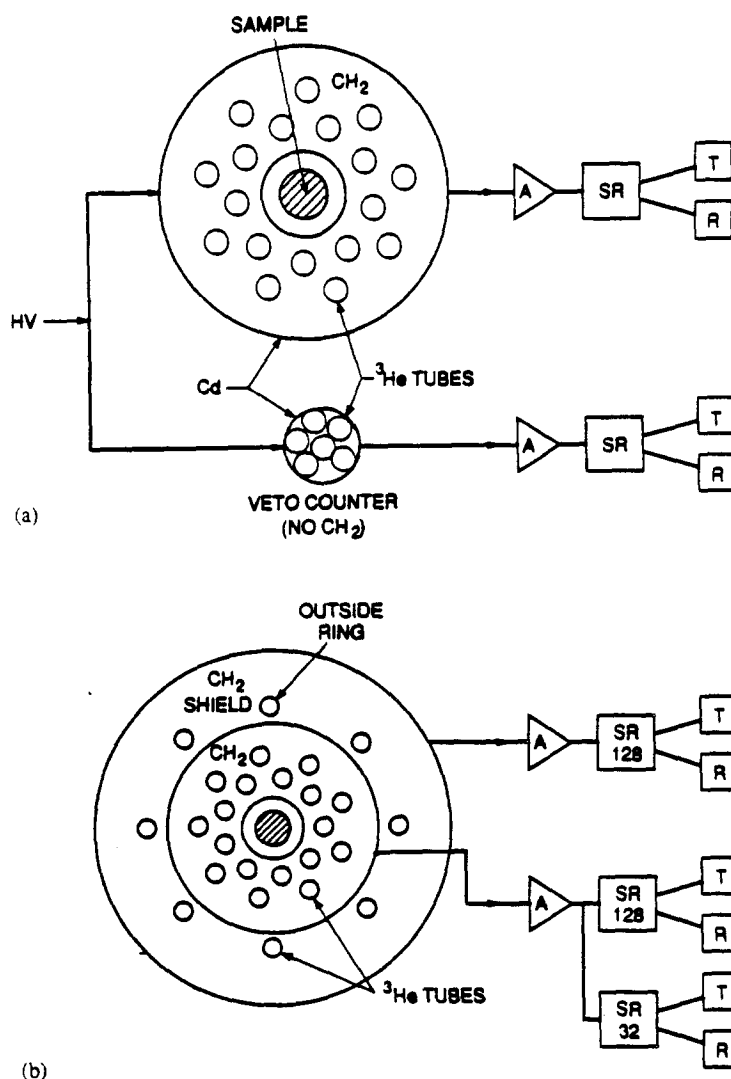
Fig. 1. (a) Schematic diagram of detector System 3 with the external electrical noise veto counter containing five ^{3}He tubes inside a cadmium absorber. (b) Schematic diagram of detector System 4 with an outside ring of detectors for splitting the signal from the inside detector and dual gate electronics for the inside tubes.

approximately -30°C. The samples in parenthesis were marginal performers, and they are on the borderline between active and inactive samples.

Table III lists the samples that were inactive in that they yielded no neutron bursts. Four of the inactive samples were H_2 gas control samples and six were deuterided Pd samples. All of the H_2 samples have been inactive and they are currently being used for the dummy samples.

7-3

TABLE II. Active Samples--Burst Results

Starting Date (Mo/d)	Sample[a]	Number of Source Neutrons[b]
4/28	Ti-1	127, 136, 85, 76
5/6	Ti-6	258, 179, 121, 70, 15, 127, 94
5/16	(Ti-10)	12, 15
5/19	DH-1	55, 15, 15, 27
6/2	DD-2	12, 85, 15, 15, 39, 142, 18, 30
6/9	(DH-4)	21
6/12	(Ti-13)	24
6/20	Ti-14	15, 91, 12, 24
6/28	Ti-16	24, 24, 12, 15, 18, 15, 15, 109, 18
7/8	DD-56	12, 279, 130, 88, 48
7/18	Ti-19	88, 15
8/18	Ti-22	55, 97
8/11	(Ti-23)	19, 23, 19
8/8	Ti-24	35, 119, 16, 16, 16, 15, 15
8/22	(Ti-25)	32
8/24	(Ti-28)	17
8/29	Ti-30	280, 13
9/11	Ti-31A	86, 34
9/12	Ti-32	23, 35

[a]The parenthesis around a sample number indicates a marginal performer that is on the borderline between active and inactive samples.

[b]The underline under the neutron yield indicates that the burst occurred during warm-up from LN temperature.

Most of the samples from Ti-12 to Ti-36 have used variations of the alloy Ti-6, 6, 2 (6% Al, 6% V, 2% Sn) or Ti-6, 4 (6% Al, 4% V). The metal bar stock is cut into small turnings (~1 by 1 by 3 mm) on a lathe.

An example of an active sample data run is shown in Fig. 2, where the coincidence counts per 2000-s time interval are plotted vs the counting time. The large emission at about 195 h occurred at the -30° temperature after removing the sample from the LN following a D_2 gas refill.

Table III. Inactive Samples

H$_2$ Gas Controls	D$_2$ Gas Ti Samples	D$_2$ Gas Pd Samples
Ti-27	Ti-2	Pd-1S
Ti-29	Ti-4	Pd-2S
Ti-31`	Ti-5	Pd-3S
Ti-35	Ti-7	Pd-4S
	DD-3	Pd-5L
	Ti-8	
	Ti-9	
	Ti-11	
	Ti-12	
	Ti-15	
	Ti-17	
	Ti-18	
	Ti-20	
	Ti-21	
	Ti-26	

The relationship between the neutron bursts and the LN temperature cycle[2] continues. The underlined values in Table II show that the majority of neutron bursts occur during warm-up from LN; however, this time period while the sample is between -100°C and 0°C represents less than 4% of the sample counting time. The dummy samples and control samples have *never* given a burst during their equivalent warm-up period.

This dramatic relationship between the LN cycle and the bursts is illustrated in Fig. 3, where the burst frequency is plotted as a function of the number of source neutrons. We see that there are a few events as large as 200-300 source neutrons; however, most events are at the low end of the distribution. Sources smaller than ~15 n are lost in the cosmic-ray spallation background.

In Fig. 3, the solid bars represent bursts that occurred at ~-30°C, and the cross-hatched bars correspond to room temperature bursts. It is highly significant that *all* of the high-yield bursts occurred during the LN warm-up at ~-30°C.

For recent experiments, we have attached an acoustic emission sensor[3] to the outside of our stainless-steel cylinders that contain the D$_2$ gas and Ti chips. The sensor can detect the cracking sounds from the hydriding of the Ti metal chips.

We have found that there is no detectable acoustical emission at the time of the neutron bursts. However, samples that have no- or low-acoustical emission are not likely to yield neutrons. Samples that we thought were the same yielded acoustical emissions that differed by an order of magnitude. Several samples have yielded many thousands of acoustical emissions without any neutron emission.

III. SUMMARY

We continue to observe infrequent neutron bursts from Ti metal chips and electrolysis residue samples in pressurized D$_2$ gas. We have been unable to pinpoint the sample characteristics that yield the neutrons. However, we have identified some negative characteristics related to inactive samples such as (1) predeuterided Ti or Pd at high temperature, (2) unstressed Ti pieces that do not crack under the LN temperature cycle. The H$_2$ control samples have all been inactive.

Ten samples have yielded large neutron bursts with at least 23 bursts at the ~-30°C temperature. A time interval of several days is required between the gas loading and the first neutron yield from the LN cycles. High-efficiency detectors, time-correlation counting, and noise rejection are required to measure the neutron bursts.
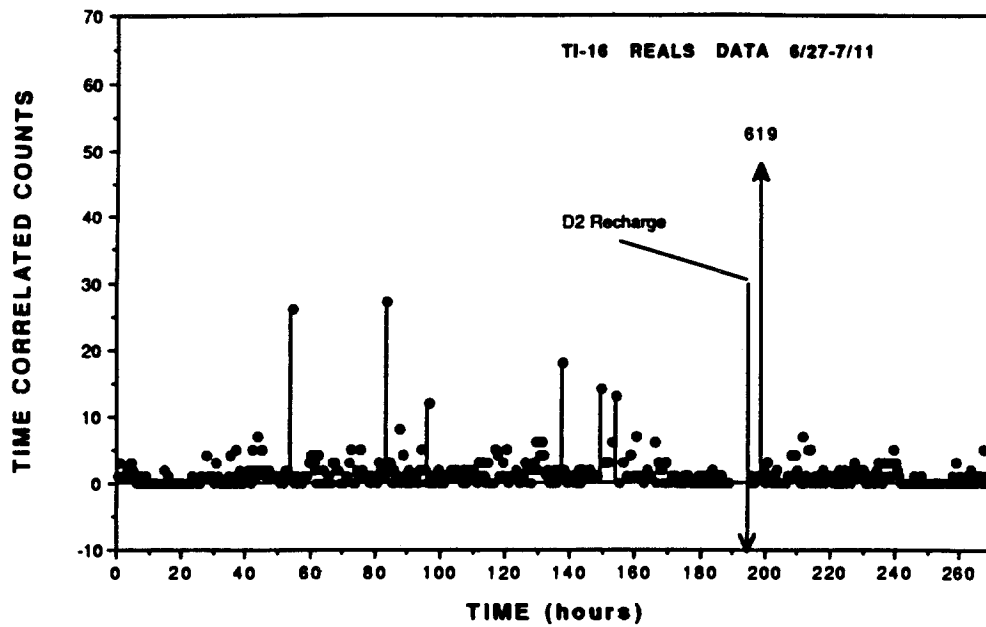
Fig. 2. Neutron time-correlated counts for 2000-s counting intervals vs time for Ti-16. The large burst at 195 h into the experiment occurred during warm-up from LN at ~-30°C following a refill of D_2 gas in the cylinder.
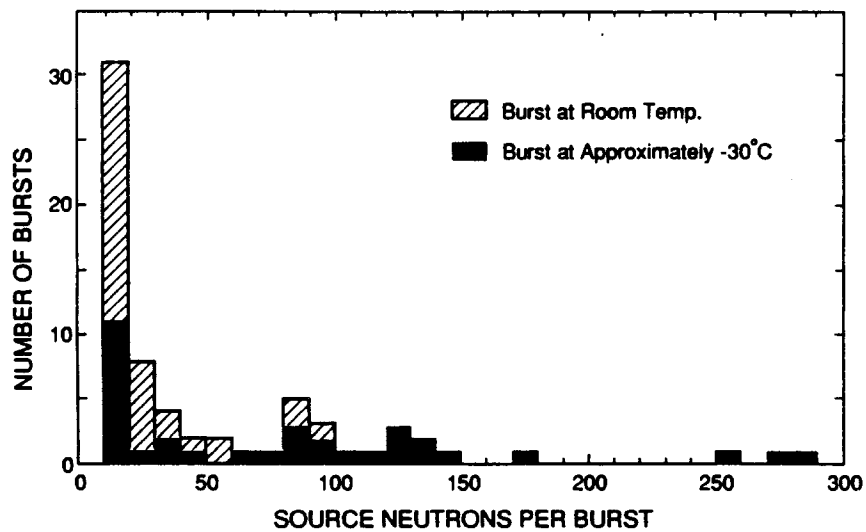

Fig. 3. The neutron burst frequency vs the yield of source neutrons in the burst. The solid bars correspond to burst events during the LN warm-up at ~-30°C.

7-6

REFERENCES

1. J. E. Swansen, P. R. Collinsworth, and M. S. Krick, "Shift-Register Coincidence Electronics System for Thermal Neutron Counters," Los Alamos Scientific Laboratory report LA-8319-MS (April 1980). Also in *Nucl. Instrum. Methods* **176**, 555 (1980).

2. H. O. Menlove, M. M. Fowler, E. Garcia, A. Mayer, M. C. Miller, R. R. Ryan, and S. Jones, "The Measurement of Neutron Emissions from Ti plus D_2 Gas," in *Highlights of Papers Presented at the Workshop on Cold Fusion Phenomena*, Santa Fe, New Mexico, May 23-25, 1989, Los Alamos National Laboratory report LA-11686-C (September 1989), p. 13.

3. E. Leonard, T. Feiertag, and H. Menlove, "Acoustic Emissions from Hydriding Ti Shavings," Los Alamos National Laboratory memorandum, September 22, 1989.

DISCUSSION (MENLOVE)

Wolf: How did you experimentally check that the veto counter in your neutron measuring equipment is more sensitive than the real counter, as it should be? What calibration procedure did you use for this?

Menlove: We only performed some artificially induced and approximate tests. For example, we induced voltage spikes in the line by switching the power supplies on and off, which were seen in both detectors. We have also used RF interference.

Hoffman: Suppose an incident cosmic ray is moderated by a person near the veto counter, which it enters. Would that mean that the veto counter would not operate in the presence of obstacles such as people?

Menlove: The veto counter would not see such an event because thermal neutrons cannot enter the counter through the cadmium screen. Its efficiency is low for faster neutrons, but it will occasionally count a neutron of this type. However, it will never see two neutrons from the same event within the required 100 microseconds. To get a coincident count the instrument must count at least two neutrons in this short time frame.

Wolf: What is your definition of the background; for example, is it that of the titanium loaded with deuterium at room temperature?

Menlove: The background corresponds to that of experimental runs using either an empty cell or dummy cell, e.g., the stainless steel cylinder. Our instrument detects the cosmic rays under these conditions.

Wolf: Do you assume that the signal from the titanium and deuterium in the dummy experiment is insignificant compared with the cosmic ray events?

Menlove: The dummy cell contains the same amount of titanium as the real experiment, but no deuterium.

McKubre: What is the time required to show coincident events?

Menlove: The data I have shown corresponds to 120 ms. In fact, events are closer in time, because to satisfy the equations all counts have to pass through the circuitry in 28 ms. If the particles originated in a period of 100 ms, when one accounts for the lifetime and the time for slowdown, the time is then more than 128 microseconds. Thus, I consider that the events probably occur in less than ten microseconds.

Santucci: Were the neutron burst results that you showed all titanium?

Menlove: The first group were electrolysis residue which were primarily titanium, but they also contained palladium and vanadium and other materials. Others were titanium 662 and 664 alloys in the form of metal chips.

Huggins: Are you certain that cracks will always give an acoustic signal?

Menlove: We are certain that cracks detected acoustically do not produce a neutron signal.

Huggins: However, were the cracks picked up by the acoustic detector?

Menlove: We are fairly certain of that. One can certainly detect the end point of hydriding. Some samples even saturated the acoustic monitor for several minutes as gas was consumed and the container became hot. We could, of course, have a case that gave neutron emission, but for which crack formation was inaudible. So I would not eliminate the possibility that cracks which are not detected acoustically may be neutron emitters. I should point out that cracking in our experiments removes the surface oxide, to allow deuteriding. Cracking is initiated by thermal stress as one goes through the temperature, so that fresh surfaces are formed which can absorb deuterium.

Santucci: Even so, the deuterium loading which you obtain is very low.

Menlove: Correct.

Lewis: Have you conducted a similar number of thermal cycles using H_2 rather than D_2?

Menlove: Initially, dummy runs were carried out, as I have already indicated. More recently, hydrogen control samples were run in thermal cycle experiments.

Chubb: The nomenclature which you use for your experiments is somewhat confusing.

Menlove: DD indicated deuterium. The D and H meant the gas used was mixed deuterium and hydrogen. We did see activity from 50/50 DH mixtures.

Lewis: Approximately how many D experiments were successful, compared to the hydrogen controls?

Menlove: With D, the success rate was 35 to 40 percent.

Wolf: Similar experiments at Sandia Laboratories were not successful. Do you understand the reasons for differences between the two sets of experiments and Sandia, or perhaps this situation has now changed?

Menlove: The Sandia workers were discouraged and discontinued their work. They typically ran experiments from a day to a few days, whereas ours operated from a week to a few weeks. Sandia had one detector, whereas we use four. They obtained detection efficiency of 10 percent, whereas ours is 34 percent. The efficiency for counting neutron bursts increases as the square of the detection efficiency, multiplied by the number one counters, i.e., a factor of 40. Sandia did see two events that might have been declared bursts if they had been reproducible, but because of the limitations of their equipment, they had to treat them as nonbursts. On the other hand, they might have seen the equivalent of 80 bursts. The question of the capability of the equipment used is therefore very important.

Wolf: Since you have shown that thermal cycling is important for correct charging, do they cycle their cells?

Menlove: Yes.

Oriani: Have you tried to change the temperature ramp rate in your thermal cycling?

Menlove: We have tried reducing it but not increasing it. When we allowed the cell to warm up over a period of several hours, we saw no positive results.

Appleby: What is the average deuterium content of the titanium?

Menlove: On average, it is quite low, certainly a long way from saturation.

Appleby: Do you know the content at the surface?

Menlove: We do not have that information, but I believe that in certain isolated areas of the material, it may reach saturation.

Rafelski: You mentioned that you are preparing DT experiments. Could you say more about that?

Menlove: They are difficult experiments to perform. We are waiting until we have a more reliable method of filling with tritium, which must be carefully controlled to avoid loss to the environment.

Section 8

A SEARCH FOR NEUTRONS AND GAMMA RAYS ASSOCIATED WITH TRITIUM PRODUCTION IN DEUTERIDED METALS

K.L. Wolf, D.R. Lawson, N.J.C. Packham, and J.C. Wass

Cyclotron Institute and Department of Chemistry

Texas A&M University

A Search for Neutrons and Gamma Rays Associated with Tritium
Production in Deuterided Metals*

K.L. Wolf, D.R. Lawson, N.J.C. Packham, and J.C. Wass
Cyclotron Institute and the Department of Chemistry
Texas A&M University, College Station, TX, 77843

Tritium activity has been measured in several Pd-Ni-D_2O electrolytic cells, as reported previously[1,2]. At the present time 13 separate cells have shown tritium at 10^2 to 10^6 times the background level of the D_2O used in these experiments. The appearance of the activity in the electrolyte and in the gas phase occurs over a period of hours to a a few days after remaining at or near the background level during 4-10 weeks of charging in 0.1 M LiOD, D_2O solution. The present paper deals with attempts to reproduce[2] the tritium measurements and to establish the source, from either contamination or nuclear reaction.

The sudden appearance of tritium activity in the cells requires the tritium to be loaded in a component prior to the beginning of cell operation in a contamination model. Release is assumed to be caused by deterioration of one of the materials used in the 0.1 M LiOD solution. In an extensive set of tests, no contamination has been found in the starting materials or in normal water blanks. Results for neutron and gamma-ray correlations have proved to be negative also. The limit set on the absence of 2.5 MeV neutrons for the t/n ratio is 10^7 from that expected in the d+d reaction, and 10^3 for 14 MeV neutrons expected from the t+d secondary reaction. Similarly, Coulomb excitation gamma rays expected from the interaction of 3 MeV protons with Pd are found to be absent, which indicates that the d(d,p)t two-body reaction does not occur in the Pd electrode.

1) K.L.Wolf,et al, Workshop on Cold Fusion, Santa Fe,N.M. 1989
2) N.J.C. Packham, et al, J. Electroanal. Chem. Oct.7,1989.

Introduction

The present paper deals with the search for the source of significant levels of tritium that have been found in Pd-Ni-D_2O electrolytic cells. Observations are given on the appearance of tritium in the cells, and two experiments are described which have attempted to correlate the tritium with neutron and gamma-ray emission. In the absence of a direct correlation with a live-time nuclear effect, a strict program of sampling and blanks must be followed in order to check for contamination. Results are given from the initial phases of such a study.

Tritium from Electrolytic Cells - Verification

Activity attributed to the beta decay of tritium was first detected in samples of electrolytes from cells at TAMU utilizing in situ liquid scintillation counting performed by the Health- Physics Department. A detector was constructed at the Cyclotron Institute for detailed measurements of the energy spectra. Figure 1 shows the results of a measurement presented as a traditional Kurie plot, in order to determine the beta endpoint energy for identification. Good agreement is obtained with the expected value of 18 keV for tritium beta decay. A comparision with a tritium standard provides agreement to the 2% level at all parts of the spectrum. Samples from four cells have been measured in this fashion, including activity from catalytic recombination of H_2 and O_2 gases evolved from a cell. An 18 keV endpoint energy from an activity carried in the gas phase leaves no doubt that tritium activity is being measured. Quantitative measurements by four outside laboratories confirm the validity of these meaurements[2], but the type of energy measurements is unknown.

The Appearance of Tritium

Table I shows a compilation of the data collected by two research groups at TAMU for 13 electrolytic cells. The background level of the tritium activity in the D_2O used is approximately 160 d/m which can be compared to the rates in Table I. Usually four times the cell volume of 15 ml has been used over the lifetime of a cell. Thus one need not consider separation factors or selective distillation in most of the samples documentated. Conservation of mass dictates the elimination of concentration mechanisms as a viable explanation. Another cell not included in Table I produced tritium at 12 times the background level, but had a titanium cathode and is not discussed here.

An activity vs time measurement was conducted in six of the 13 cells mentioned in Table I, which provides more information. Figure 2 shows the most detailed series of timed assays. After the cell was charged at a current density of 60 ma/cm^2 for four weeks, the current density was increased to 500 ma/cm^2 at the start time of Fig.2. It can be seen that the tritium activity in the electrolyte built up within a few hours. Simailarly, Fig.3 shows a plot of the tritium activity in the electrolyte vs the date of assay. A buildup of tritium occurs within a 48 hour period correlated with a period of high cell current. The constant activity levels and later decreases are interpreted as the end of production and displacement, respectively with continuuing electrolysis. Tritium activity appears during a period of high current

density or after such a period within a few days. On the basis of the six cells which have been followed with tritium assays, no significant tritium activity was detected with only low current conditions. Another significant feature involves three cells which were fitted with separate recombination catalyst cells to provide a measurement on the tritium level in the gas phase. In all cases the concentration of tritium was much higher in the recombinant D_2O compared to the electrolyte, which is opposite to that expected from separation factors. Cell C-8 in Table I produced a factor of 300 times more tritium in the gas phase, both in concentration and in integrated activity. This factor is comparable to the recombination rate measured for these cells. Cell C-8 showed the highest total amount of tritium totalling about 10^{16} atoms, but it is not the highest level observed in the electrolyte. The gas phase / electrolyte ratio of integrated amounts of tritium is quite variable. In a second larger cell C-9 with a volume of 100 ml the total activity is higher in the electrolyte. As described later, only a tritium concentration is known for the recombinant for cell D-6 with most of the remaining activity introduced into the electrolyte from the recombinant. At least an order of magnitude more tritium was produced in the gas phase than in the electrolyte from this small 15 ml cell. Many factors can be thought of which could influence the amount of tritium that exchanges with the D_2O in the electrolyte, such as the distance traveled by bubbles and the degree of saturation of gases in the electrolyte at the time of tritium emission.

Cell Design
    Figure 4 provides a schematic of the rather simple design for most of the cells used in the present study. A 12-15 ml pyrex centrifuge tube is used to provide a compact design, chiefly for a large solid angle in the neutron experiments. No cooling water was used to avoid degradation of neutron spectra, thus the cells run at elevated temperatures near boiling during high current periods. The cathode consists of a 1 mm diameter Pd wire approximately 4 cm in length. The cyclindrical anode is made of Ni mesh. Cell potentials are 2.5-3 volts while charging at 50-60 ma/cm^2 and up to 15 volts at high current density, 500ma/cm^2. Black-green NiO is formed and settles to the bottom of the cell, but does not adhere to the cathode. Cells are charged for at least a month before a 10- 12 hour period of high current is applied. This procedure is repeated until a Ni-wire electrode connection fails, up to three months. Cell C-7 in Table I showed a low yield of tritium after one week of charging and a period of high current,which is the shortest production time found.

Neutron Detection
    A system based on 3" X 5" NE213 liquid scintillators(Fig.5) has been used to provide a low background measurement for neutron emission. Pulse shape discrimination methods are used to reject gamma rays resulting in a background of 0.5 c/m for 5% total efficiency. An active cosmic ray shield of 1/4" plastic scintillator surrounds a passive shield of 10-12" thick parawax and the neutron detector situated within. The principal source of background is from the neutron component of the cosmic ray showers. The principal advantage of this type of detector is the measurement of the neutron energy spectrum. The system is sensitive to neutrons ranging from 1 to

50 MeV. Neutron energy spectra measured previously are indicative of a neutron energy of 2.5 MeV expected from the d(d,n)^{3}He reaction as shown in Fig.6, correspondig to cell C-D in Table I. The region above 2.5 MeV is found to be useful in detecting cosmic ray showers and thus can increase the sensitivity somewhat. The present paper uses the neutron data to establish limits due to the lack of 2.5 and 14 MeV neutrons in correlation with tritium measurements.

Gamma-Ray Detection

A 25% intrinsic germanium detector was active for six D_2O cells for the entire cell lifetimes in the study described later.[2] Passive lead shielding was used to minimize gamma-ray background contributions. The excellent resolution of a germanium detector provides an unambiguous identification, in this instance for the lower levels of the palladium isotopes in the 300-600 keV region. Figure 7 shows a sample spectrum covering the energy range from 80-3200 keV. Coulomb excitation of the Pd isotopes is expected by the 3 MeV protons from the d(d,p)t reaction, if it occurs. The overall efficiency of the detector is approximately 1%, which along with the probability of Coulomb excitation (10^{-7}) means the method is not one of the most sensitive. For the tritium production observed in cell D-6, a significant limit was set as discussed later.

Neutron-Tritium Correlations

Cell C-D listed in Table I showed two instances of neutron emission approximately 2 hours in duration each at levels of 20-60 n/min , and also showed tritium corresponding to 1.6 X 10^{13} atoms. The apparent branching ratio, equal to the t/n ratio, is 10^9 instead of 1:1 expected from measurements at normal fusion energies for the d + d reaction. The unknown factor here is whether or not the cell was counted for neutrons at the correct time, since cell C-D was not followed with timed assays. The next stage in the correlation was attempted with the same electrode which was melted and reformed to insure the absence of tritium, and the cell was neutron counted for 1 1/2 months. A period of neutron emission was observed but no tritium was produced above background levels.

Cell C-G was neutron counted during a period of positive tritium production as shown previously in Fig.3. The neutron count rate is plotted in Fig.8 along with the periods which were defined by the tritium assays. A small increase in the neutron rate given over 100 minute intervals shows a slight increase at the time of cell current increase, but is not regarded to be statistically significant. Over a 48 hour period a lower limit on the t/n ratio is determined to be 7x10^7. If there were a large enhancement in the t + p branch, further difficulties are encountered because of the lack of 14 MeV neutrons from the d(t,n)^{4}He secondary reaction which would be expected to occur from the 1 MeV tritons. The discrepancy here is 10^3-10^4, depending upon where the reaction takes place (surface,volume).

Tritium-Gamma Ray Correlations

The neutron measurements suggest strongly that either something quite unexpected occurs in nuclear reactions, or that we have been observing tritium contamination initially buried within the cell components. Laboratories and equipment have been checked thoroughly and it is clear that no widespread contamination is present. Samples of Pd and Ni have been checked at LANL[3] and no tritium was found.

Similarly samples of materials have been dissolved and counted in the present study, but not in the numbers necessary and not with proper sampling techniques for a model based on spot contamination. Light water blanks seem to provide an inclusive means for contamination checks, but only two light water cells were constructed in the previous studies[2], and both at the Cyclotron Institute. In the present series, 12 cells were prepared, limited by the Pd on hand, split equally between light water and heavy water electrolytes, with no other differences. The materials and methods used previously were duplicated, except for the 1mm Pd wire which was from a different batch but from the same company. Cell M-1 listed in Table I was constructed with this Pd and had shown a low level production. Table II shows the results from that study which was recently completed. All cells were charged at 80 ma for one month and then run at 600 ma for 12 hours, with no tritium activity detected above background. The procedure was repeated and again all were negative at the end of the second round of charging and high current. Cell D-6 showed a yield of approximately 5×10^{13} tritium atoms when assayed four days after the second high current period. The time profile of the activity is shown in Fig.9 with the activity concentration as a function of time in days. The recombination fraction stops at the peak because the catalyst cell (Fig.4) blew out the plunger, glass wool and catalyst beads, along with 0.5 ml of recombinant in the fume hood and into the immediate area. A wash of the catalyst beads gave 40,000 d/m of tritium activity. Approximately 3 ml of the recombinant drained back into the electrolytic cell, with only 0.2 ml remaining, which was sufficient for an assay. Thus most of the activity in the electrolyte originated from the recombinant. The rapid decrease in the activity in the electrolyte is not fully understood, but a similar effect was observed for cell C-8. It is suggested that since the closed cells operate under an appreciable positive pressure, the amount of dissolved td gas decreases as the pressure is reduced, along with the normal displacement with d_2 as the cell continues to run. During this four day period, no enhanced gamma-ray lines were observed which sets a limit for a descrepancy of a factor of 50. Due to the statistics of the matter, one D_2O cell does not prove the case one way or the other and this study will continue in the Martin group with 20 new cells.

TABLE I

TRITIUM ACTIVITY FROM PALLADIUM - NICKEL CELLS

CELL	ELECTRODE TREATMENT[a]	ELECTROLYTE[b]		ACTIVITY (d $min^{-1} ml^{-1}$)
C-A[d]	B	1		4.9 X 10^6
C-B	C	2		3.7 X 10^6
C-C	D	1		
after charging at 0.05 amp/cm^2 for 4 weeks				64
after 2 hours at 0.5 amp/cm^2				5290
after 6 hours at 0.5 amp/cm^2				5.0 X 10^5
after 12 hours at 0.5 amp/cm^2				7.6 X 10^5
C-D[c]	B	2		1.2 X 10^5
C-E	A	1		3.8 X 10^4
C-F	B	1		6.3 X 10^4
C-G	A	2		
after charging at 0.05 amp for 4 weeks; 0.5amp,12 hours				120
after additional charging for 1 week,				250
after 0.1 amp for 24 hours, 0.3 amp for 1 hour				1.5 X 10^4
C-2 (3 mm)	B	1		6.3 X 10^4
C-3 (3 mm)	C	1		0
C-1 (6 mm)	A	1		69
C-7	A	1		7.5 X 10^3
M-1	A	1		6.4 X 10^3
C-8	B	2	15 ml electr.	5.0 X 10^5
			15 ml recomb.	1.5 X 10^8
C-9 (3mm)	B	1	100ml electr.	6.7 X 10^4
			10ml recomb.	2.5 X 10^5
			100ml electr.	1.9 X 10^5
			8ml recomb.	2.4 X 10^5
D-6	B	1	14ml electr.	4.0 X 10^5
			recomb	1.3 X 10^6

a) electrode treatment: A, no treatment; B, vacuum anneal; C, acid etch; D, electroclean
b) solution type: 1, 0.1M LiOD; 2, 0.1 M LiOD + 0.1mM NaCN
c) cell JBA5 which has shown neutron activity, 50 X/min
d) verified by second ^{3}H counter at TAMU and by 5 other laboratories
All electrodes are 1mm diameter palladium except where noted.
All cell volumes are 12-15 ml except where noted
A blank count rate of 65 c/min has been subtracted before calculation of activities.

TABLE II

Cyclotron Institute 10/13/89

Reproducibility Test, Tritium Activity

6 H_2O and 6 D_2O Cells, 1mm X 4 cm Pd, Ni Mesh

CELL	d/m/ml start	max (electr)	max (recomb)
H-1	59	62	69
H-2	30	35	45
H-3	34	45	47
H-4	30	37	27
H-5	21	15	17
H-6	37	26	41
D-1	170	190	185
D-2	165	195	180
D-3	190	220	250
D-4	165	240	190
D-5	200	290	160
D-6	160	4.01×10^5	1.26×10^6

All cells were run at 500ma/cm^2 for two 12-hour periods, separated by one month of charging. Total charging time was 2.5 months.
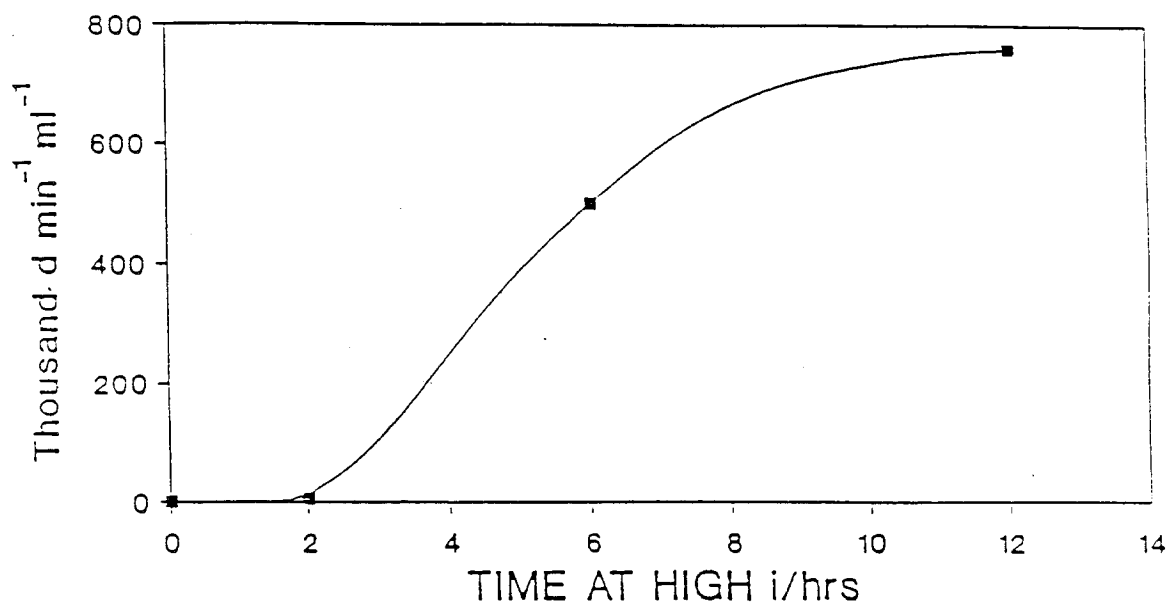
•

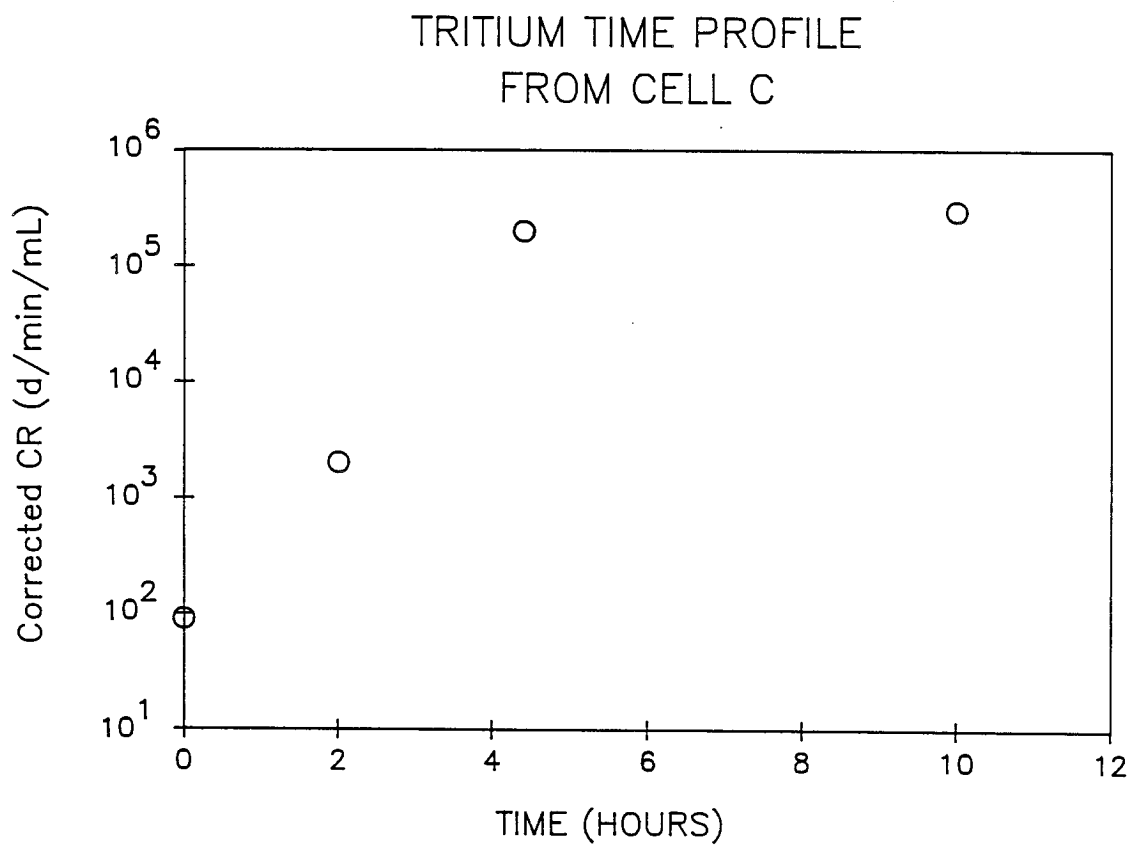# TIME PROFILE OF TRITIUM PRODUCTION FROM CELL A7

Fig. 1.

TRITIUM TIME PROFILE
FROM CELL C

Fig. 2.

Plot of Tritium Counts vs. Date Sampled for JBXR1
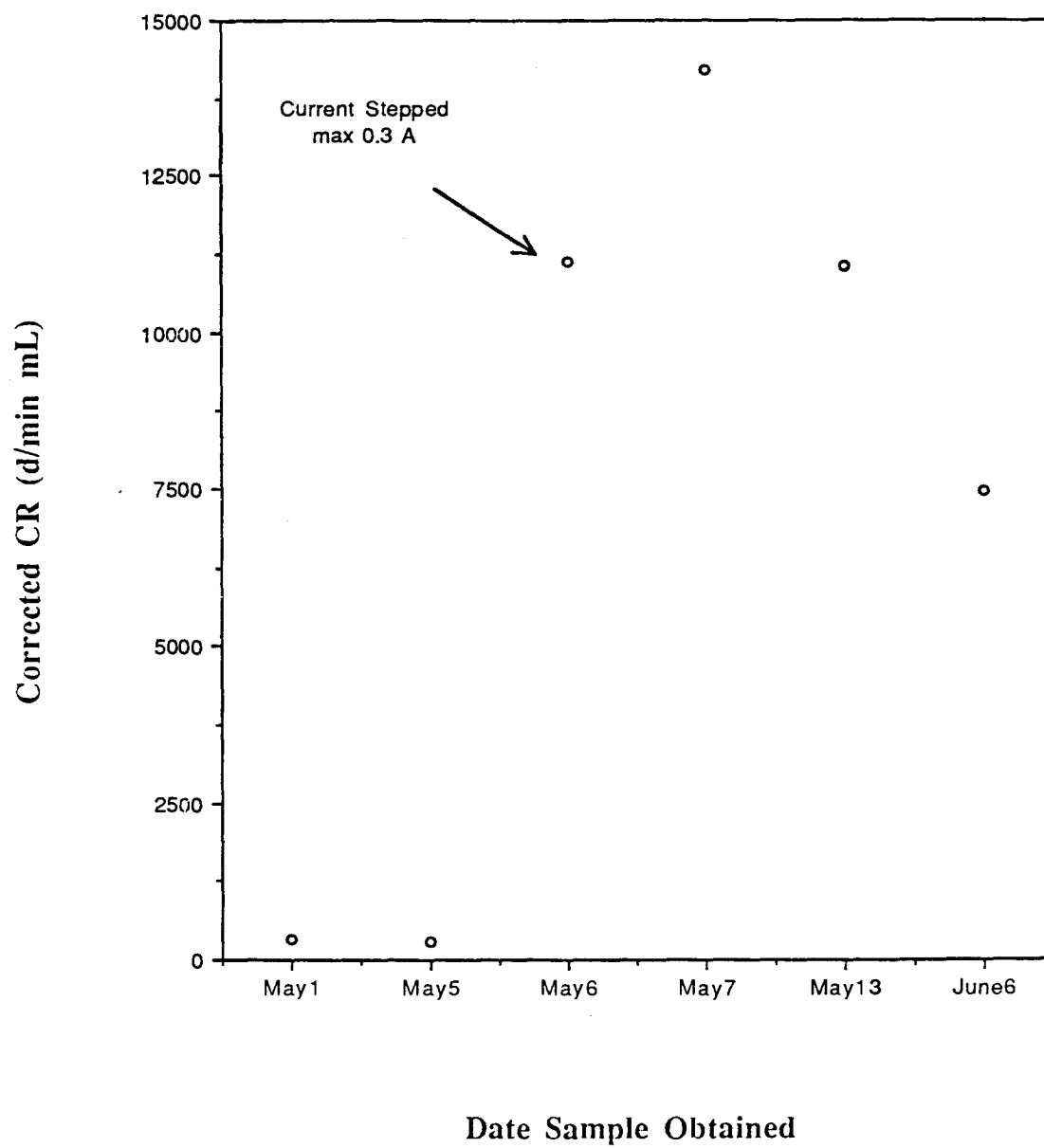
Fig. 3.

Electrochemical Cell Schematic

Plunger

Platinized Alumina
Catalyst Beads

Glass Wool

60 ml Plastic
Syringe

Septum

1 mm Pd x 4 cm

Ni Gauze
Anode

0.1 M LiOD

Septum to Prevent
Electrical Shorts
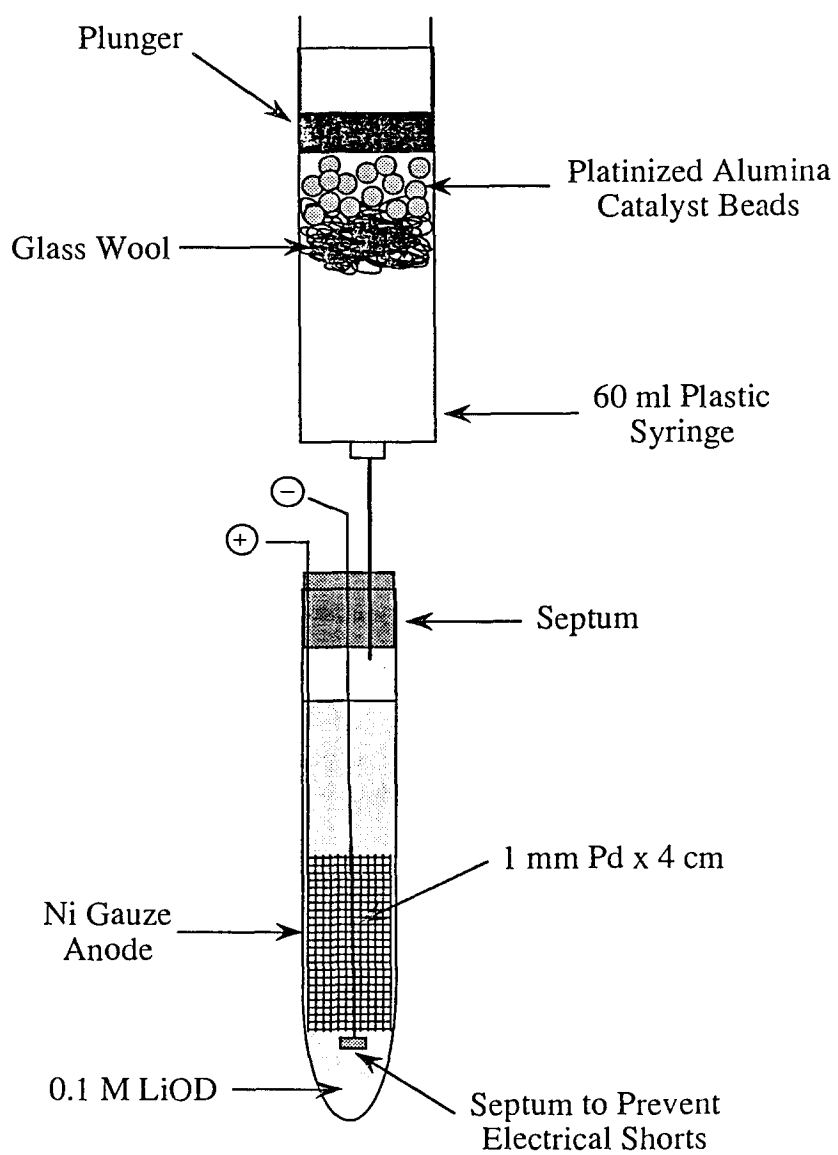
Fig. 4

Neutron Counting-
Instrument and Setup

NE 213 Liquid
Scintillator

Al Foil Wrap

1/2"
Air Gap

Black Plastic

hν

Cell

RCA 8854
PMT

Base

Anode
out

Lightguide

Temperature
Monitor

1/16" Polished
Steel Plate

Access
Door

Parrafin Wax

Fig. 5

JBA5-2 (4/27-28/89)
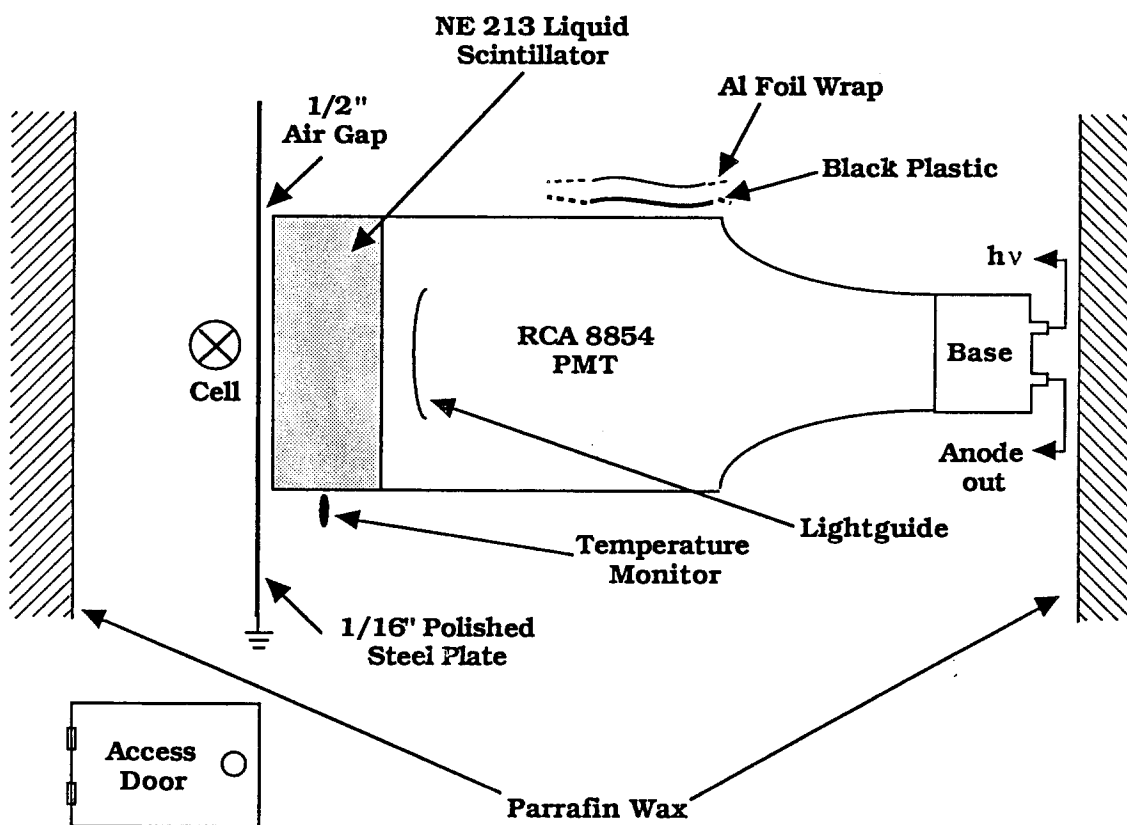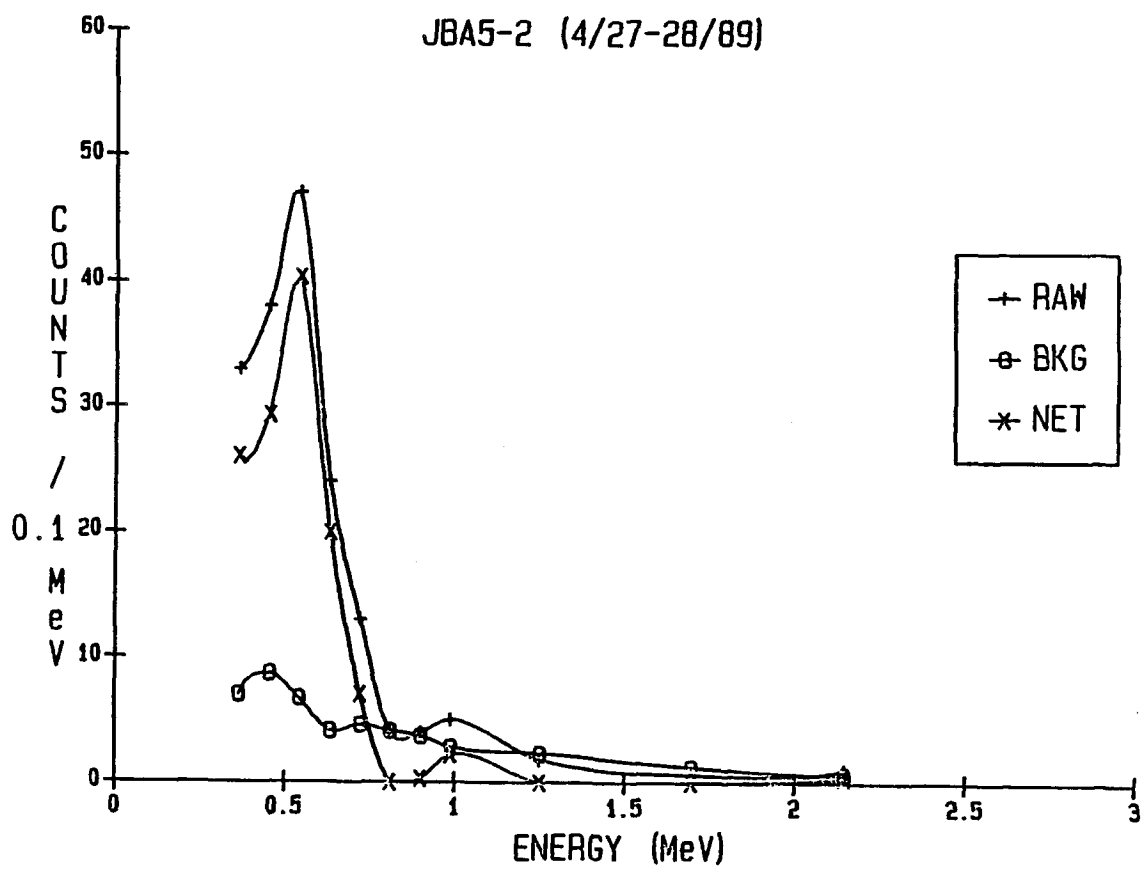
Fig. 6.

GROUP: F   VS: LOG CTS   GAIN: 8192 CHLS   OFFSET: 0000 CHLS   ID:

FUNCTION KEY

F1 ACQU	F2 ERASE
F3 GROUP	F4 SETUP
F5 ROI	F6 COLOR
F7 TRANS	F8 OVLAP
F9 EXPND	F10 MORE
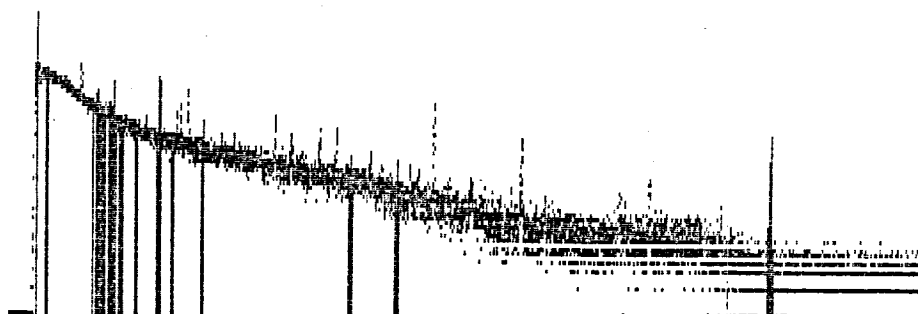
ENERGY: 507.904 KEV   COUNTS: 00000140#   REGION OF INTEREST: ON

PK #: 15 CTRD: 0.00000 KEV   FWHM: 0.00000 KEV   GROSS: 000006172   NET: 000003320

TIME   LIVE   PRESET: 000000   ELAPSED: 090802   REMAINING: ∞   SECONDS

Fig. 7.

Neutron-Tritium Correlation
May 5-8, 1989

Fig. 8.

Time Profile   D-6

Day of Electrolysis

Fig. 9.

DISCUSSION (WOLF)
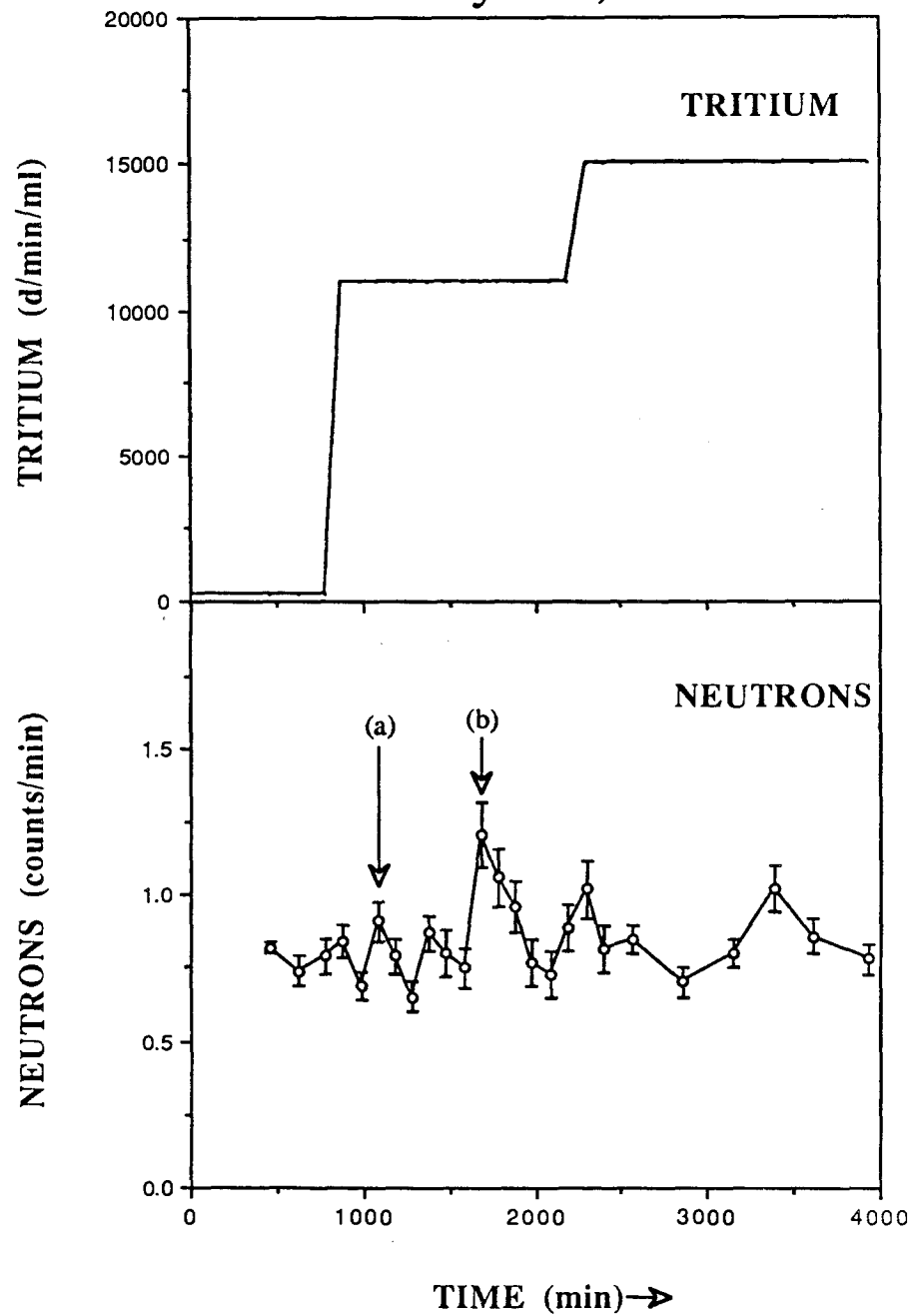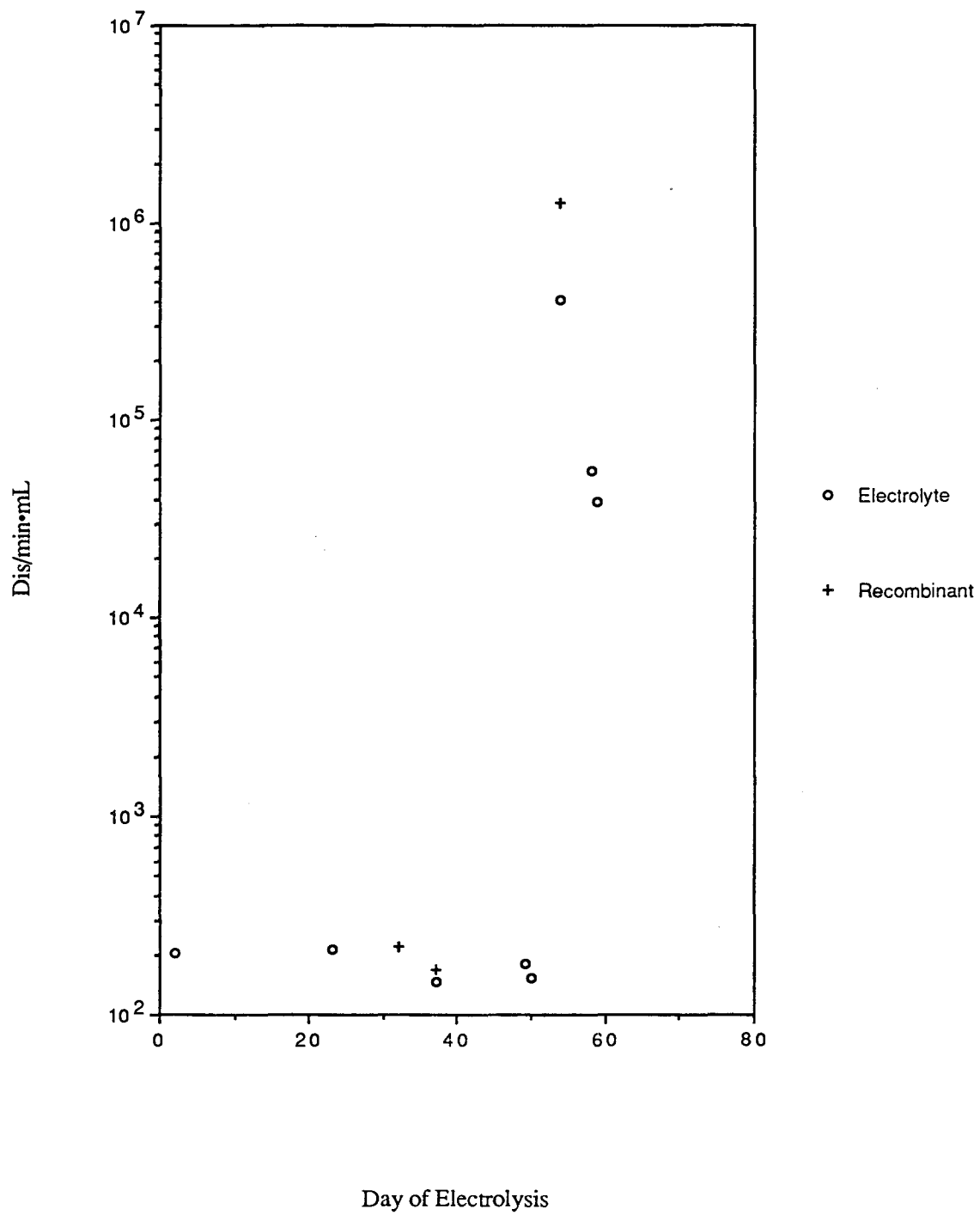
Hoffman: Do you have any iron impurity in your cells with nickel counterelectrodes?

Wolf: X-ray analysis shows iron, chromium as well as other metals present, which must be impurities in the nickel. Some impurities in the electrolyte are insignificant, whereas others are present in surprising amounts.

Yeager: Concerning the samples that were distilled before tritium analysis, how was the sample removed, and what is your opinion regarding distillation disturbing tritium analysis?

Wolf: Distillation had no effect in regard to tritium analysis on the cell liquid that we sampled.

Yeager: How did you verify the measurements?

Wolf: Solids were removed from the electrolyte by centrifuging and by filtering. Many measurements were made, including a very large number of blanks. After cells had operated up to periods of several months, high scintillation levels were suddenly seen. Proof that these indications were caused by tritium is given by the spectral shape and the proper beta end-point energy of approximately 18 keV. Are you concerned that chemiluminescence effects may be mistaken for tritium?

Yeager: Yes, since these may account for the abnormally large values which you have seen.

Wolf: No. We have hundreds of blank samples to show that it was not so. It is well known that chemiluminescence problems can occur in concentrated LiOH solutions. Thus, we examined blanks with different concentrations of LiOD. Even then, the chemiluminescence effect will eventually die out if the sample is left in the dark. All samples were double-counted. The first count was taken after leaving the sample for 30 minutes after preparation. The sample was then left in the dark and was recounted one or two days later. If any discrepancy between the two counts was seen, further testing would follow. We discovered no problem unless a concentrated LiOD solution was used, meaning 1 M or more. Samples in the present work were 0.1 M or pure D_2O from the recombination on a catalyst.

Yeager: I am concerned about impurities that may originate from the platinum or nickel counterelectrodes.

Wolf: There is always that danger. For example, the presence of nickel oxide might cause chemiluminescence and give false tritium readings, but it is removed from the solutions prior to counting. A reproducible beta end-point energy

corresponding to a tritium standard is strong evidence for the identification of tritium and is far stronger evidence than indirect tests such as distillation of the solution.

Appleby: What is your opinion about the effect of peroxides on the scintillation cocktail?

Wolf: Bleaches can certainly affect the results, but even they are eliminated with time. We confirmed that the two-stage counting procedure which we used would even eliminate the effect of deliberately added peroxide.

Appleby: The presence of ozone is another possibility, since it can be produced at the anode.

Yeager: Coming back to the point about distillation. A Case Western Reserve sample was distilled at Westinghouse before counting was performed.

Bockris: Los Alamos also distilled our samples, and results were the same before and after.

Wolf: Because of experiments of this type, we concluded that routine distillation was not necessary. At Case Western you would be far better off collecting an energy spectrum to make sure that you have tritium and not some other alpha, beta, or gamma activity from contamination, especially for the very low levels of activity.

Rafelski: In your gamma-ray experiments, what was the background count level?

Wolf: It is shown in our paper. I should point out that we used a high-resolution germanium detector measuring gamma rays, with a sensitivity limit of about 100 to 150 counts per day. Our effort was aimed at exceptions to the background, particularly in regard to energy levels corresponding to those in palladium isotopes.

Teller: You have not seen the energetic protons which you would expect from nuclear fusion reactions.

Wolf: Our results indicate that energetic protons are not present. In addition, we have seen no indications of 1 MeV tritons through the $t(d,^4He)n$ secondary reaction with 14 MeV neutrons. Any tritons present have a low kinetic energy, certainly less than the requirement for TD fusion.

Lewis: 100 keV or less?

Wolf: Our best estimate is 10-20 keV.

Bockris: I would like to point out that all the cells were isolated in a secure laboratory. No tritium had ever been used there before, and no assay showed tritium contamination. Very long periods of charging were required before significant amounts of tritium were seen in the cells, typically from 2-6 weeks. One significant result was that obtained with a cell including an external recombination catalyst. At least an order of magnitude more tritium activity was in the recombinant as compared to the electrolyte.

Wolf: In addition, the fact that distilled electrolyte showed the same results as electrolyte counted directly from the cells indicates that tritium had exchanged with D_2O.

Jones: Did your germanium detector show any evidence of palladium energy levels?

Wolf: We detected no palladium gamma rays with any degree of confidence. Over a 4-day period which produced tritium evolution from cell D-6, there was a discrepancy of at least a factor of 50 compared to the expected rate.

Jones: So something was visible.

Wolf: The background has some cosmic-ray induced gammas as well as the natural room background. Further analysis is required for setting limits on extremely low gamma rates.

Fleischmann: What is the energy range which you are examining?

Wolf: We measure over the range from 80 keV to 3.5 MeV, but the Coulomb excitation gammas cover the range of 300-500 keV, actually up to 555 keV. There are five lines that provide quite a characteristic signature for the palladium isotopes in terms of energies and intensities. Our limit, set by use of these Coulomb excitation gammas of a factor of 50, assumed that the tritium was produced during a 4-day period corresponding to the assay interval. If tritium production were continuous over a period of 60 days (the cell was counted over the entire lifetime), the factor of 50 is reduced somewhat, but discrepancy remains. The exact factor cannot be quoted now because we have yet to complete the detailed analysis of the spectra over the entire 60 days.

Santucci: What proton energy did your results represent?

Wolf: Assuming that the factor of 50 is correct, the proton energy would have been 3 MeV. The Coulomb excitation probability would, of course, be lower if the proton energy is reduced. A Coulex calculation is then required to estimate how much lower the proton energy must be below the predicted 3 MeV.

Jones: You seem to be telling us that there are no protons and that the triton energy is less than one MeV. What is your opinion concerning the theoretical possibility that a triton of this energy can be produced in a fusion process? Could it be via the type of process considered in the 1938 Oppenheimer-Phillips paper?

Wolf: We are not trying to theorize but simply trying to report our observations. We find no correlation of radiation with tritium production, and we have had two cycles of tritium production when the counters were in operation. This does not eliminate the possibility that tritium could build up from the tritium inside the palladium electrode, which would then be released as the lattice becomes cracked. The Coulomb excitation part of the energy is perhaps a better indication for the

lack of 3 MeV protons, because the gamma counter was in operation during the entire lifetime of the cell.

Kim: Some of the energetic protons that may be produced in the process should go into the electrolyte.

Wolf: If the protons are produced on or close to the surface, that would be correct, but that cannot represent more than a factor of 2-3, assuming isotropic emission of the protons.

Fleischmann: Statistically, some of the protons must go toward the interior of the electrode.

Wolf: We would take into account the solid angle effect.

Kim: Did you determine the Coulomb excitation cross section?

Wolf: Yes, it has been measured many years ago and again quite recently, explicitly for 3 MeV protons stopping in Pd.

Rafelski: If the expected energy is not present in the triton, it would be surprising to find it in the proton.

Appleby: Where do you suppose that the excess energy goes?

Wolf: I do not know. At present, all I can say about it is where it is not going. The tritium may be caused by contamination in one of the cell construction materials, so there may be no excess energy.

Teller: Some of your reactions do not appear to conserve energy.

Rafelski: You obtain a neutron signal at 2.5 MeV, yet you appear not to have tritons of the correct energy. Some rare nuclear reactions seem to conserve energy, whereas others seem to lose energy.

Wolf: The probability of 2.5 MeV neutron emission is quite low, and it is not necessarily correlated with tritium.

Rafelski: One might say that there are two kinds of cold fusion. In one, the probability of 2.5 MeV neutrons is strongly enhanced, i.e., no energy disappears.

Teller: Such reactions may be strongly enhanced, but they nevertheless occur at a level which is 10^{-8} times lower than that of the overall reaction, represented by the heat produced. Two unusual observations might be questionable, whereas three will be out of the question, unless there is some common cause which is different from anything which we have previously experienced. There is a common cause of these things. The Gamow tunneling probability is one problem. Apparent nonconservation of energy is another. The observations mean that something very different from previous observations is occurring, assuming that we are all not mistaken.

Fleischmann: When we first started to announce these observations, we acknowledged that it may all be a mistake. It still may be a mistake, but I believe that we are beginning to narrow down the possibilities.

Section 9

ELECTROCHEMISTRY, ANOMALOUS HEAT, AND TRITIUM PRODUCTION

John M. Bockris

Texas A&M University

ELECTROCHEMISTRY, ANOMALOUS HEAT, AND TRITIUM PRODUCTION

John M. Bockris
Texas A&M University

At Texas A&M we have our various groups working, and you have heard Kevin Wolf, who was our leader on the nuclear side, and we follow him in our techniques. My own area is electrochemistry, and I am going to show you a series of results (some are new, most are new), which I think to some extent will give you a correlation between heat and tritium for the first time; at least, they have been seen for the first time together.

I would like to show you two heat results. These are merely illustrative of the way we do it. Fig. 1 is a calibration graph in which we have power against temperature, and I want to stress immediately that by far the majority of the electrodes which we look at, say three out of four electrodes, up to say 90 days electrolysis, go up and down this line which is the line established by using resistance heating corresponding when we use the cells to (E-1.54)I. We vary E on the cell in such a way that we can come up and down the calibration line, and the cells do give the correct values for the classical electrochemical expected heat. So, this is a kind of internal calibration check. We calibrate every day, and sometimes we calibrate two or three times a day with heaters, and then we put the cells on to see whether they fit our calibration line, and all too many of them do exactly what we don't want them to do in one sense: they lie on the classical electrochemical curve. And from time to time, roughly speaking, I would say once every two or three weeks, we get an electrode which starts working. This one started working several weeks ago and worked for 44 hours, and during that time, it lies clearly of the line. It depends on current density and increases approximately linearly to current density. When it stops working, it goes back on the line, i.e., the line of (E-1.54)I. When the cells go back on the line, it proves the classical heat (i.e., the expected electrochemical one) supports the calibration and calorimetry.

Fig. 2 is a recent cell which operated in the last several weeks as a heat producer. This cell is producing something like 1/2 watt in 3 or 4 watts -- it operated thus for several hours. Here, we have added heat from a calibrator resistance heater, and when switched off, the value comes back to the same point, showing that we have excess heat.

In Fig 3, we see growth occur to a very high amount, 800,000 counts/min ml. The counting efficiency is about 0.3. We watched steady state being achieved in about 10 hours. We have had altogether 12 electrodes producing tritium; production goes on for between 2 and 20 hours. After the burst is over, it will go down over 2 to 3 days. I suppose, and I think Kevin Wolf said something like this, that the DT is being sparged out. The electrode has stopped producing. But D_2 continues to be produced and it pushes out the DT.

Everybody with whom we talked, of course, said contamination, contamination, contamination. So, helped by Kevin Wolf, we did a lot of analysis on everything we could.

We dissolved the nickel and sent it to Los Alamos; we sent the palladium to Los Alamos. Everything was analyzed. We had the electrolyte analyzed by many people -- by Los Alamos, but also by Battelle, General Motors, and Argonne. The results show excellent agreement. We did have a chemiluminescence when we went too high in concentrations. We distilled, we centrifuged, we filtered, and so forth. We don't do these extra checks any more.

I spoke about the cell that stops producing, and Fig. 4 is an example of what happens when it does. Here is one that was up to about 3000 counts/min ml; it stopped and started coming down here, and it took about a week to get back to background. Now, all these cells have been charging for 6 or 8 weeks before they produced any tritium. I noticed Steve Jones' remarks about tritium. He ran his cells for 6 days, and 7 days is the minimum time that we have ever seen the tritium. Usually, it is longer than that, and I think that is one of the great reasons why many people didn't see anything at all. You have to wait a long time to see anything.

Fig. 5 is the graph which I particularly wanted to show you. This is an electrode which had about 8 weeks charging before it switched on giving heat. We go up to a range between 12% and 20-22% excess heat. This heat grows over above 10 hours, and then it is relatively stable, but with this peak here it goes along like this for a long time. The electrode is still producing after a month.

After about 9 days in which plenty of heat has been produced at about 17-18% efficiency, then you see the tritium switches. This is the tritium in the liquid coming up here, and you see that in this case it looks as though there might be some kind of correlation between that rise in heat and that switch on of tritium. The solid points are the tritium in the gas, and the open points are the tritium in the liquid. You see another heat burst and then the tritium, which we would like to come, say a day later, *but the tritium comes up a little earlier*. It is in the liquid and gas phase coming up, going down again, and the heat comes up a bit afterwards, so there is only a weak suggestion of a correlation between the tritium and the heat.

If you add the gas phase to tritium together with the tritium which is insulation, then one can calculate how much heat one has produced, assuming $D + D \rightarrow T + H + 2.4$ MEV. Kevin Wolf and I did this calculation early on when we had the first burst of 10^6 tritium. In those days, we weren't measuring the gas phase. I simply assumed that Henry's law was at work so that one had an equilibrium amount of DT in the gas phase. When I did that, I got reasonable agreement with the heat. I could replicate 4-8 W or so. But if I ran the gas-phase results from the recombinant, it doesn't work so well. It gives about 0.1% of the heat.

The tritium is produced in bursts. There is a constant amount of tritium measured in the recombinant fluid, so there is a small activity of tritium production all along, but it

varies in two areas which are apart by something like 2 weeks and two bursts. There is a different meaning to the gas-phase tritium and tritium in the cell. We put the recombinant back. The tritium in the gas phase is measured daily. It represents the instantaneous or daily performance of the tritium. Thus, it should vary greatly with the activity, whereas the amount in the liquid should just go up, and you can see that roughly it is going up. Here is the amount here, and then after the next burst it has gone up. And if we put a straight line through there, it has gone up to about twice or three times and remains approximately constant, i.e., the burst has ceased.

The system is closed in the sense that D_2 and O_2 do not escape into the surroundings but recombine outside the cell and are put back into it. But you can have incomplete recombination. So, we do have a number of open cells as well.

I want to show you some things I learned on a recent visit I made to Germany, which has helped me in trying to interpret the tritium production in a surface model. I started trying to look at things in a surface-oriented way because it seemed to me to be consistent with all the irreproducibilities and all the long time that you have to wait for heat and tritium and the fact that some people get it and some people don't. Thus, I found a recent paper by Popov and Arsimovich in which they treat theoretically the time for the growth of aspirites or dendrites -- on the surface. The expression which I show here gives the ratio of the height of a protrusion at $t = 1-t_0$ to the height at $t = 0$. I am setting the ratio at 10.

In other words, I assume that there are some very tiny pyramids, perhaps 1,000 angstroms high, and that some pyramids grow, e.g., 10 times higher in the time t, from Popov's equation. Then, substituting things like diffusion coefficients, concentration of the alleged impurity in solution, one can calculate when the fast growth period for the dendrites begins. I have assumed that the impurity which deposits is 10^{-4} M, a sheer assumption, but if I do that, then I get the fast growth occurring in 20 or 25 days. That is typical of the time we have to wait. So, that is one point in favor of the surface viewpoint. It explains why the time is so much longer than the time which it takes to charge the electrodes.

Now, secondly, in my recent German trip, I visited the Fritz-Haber Institute, partly inhabited by a very large group of electrochemists. There, I discussed with Dieter Kolb the value of the field at the electrode surface, generally taken to be 10^8 volts/cm, i.e., a volt over a few angstroms. However, Kolb has a paper in press in which he has determined a field as 10^9 volts/cm.

Kolb reflects light from the surface electrode and then calculates the field from the degree of reflection. He gets 2×10^9 volts/cm in alkaline solution, and it's 10^9 in acid solution. This field is associated with surface states on the silver. It is not distributed

uniformly, as electrochemists usually think, because charges concentrate over small areas, where the local field is going to be greater.
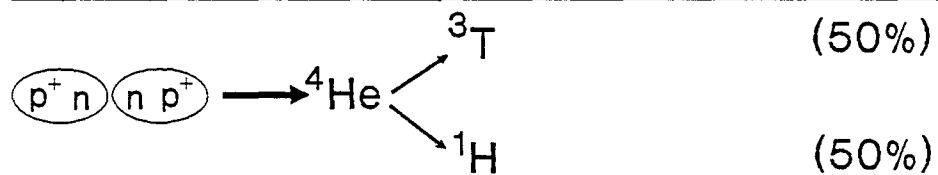
Suppose we follow this through. On the tip of one of the promontories, we have what electrochemists call the Volmer-Heyrovsky mechanism for deuterium evolution. The D is absorbed on the tip of the dendrite. The tip would be where the big field is. It is also where dielectric breakdown is most likely to begin.

Well, if you have a field of 2×10^9 volts/cm, and electrons emit from the dendrite tips, as they do in dielectric breakdown, they proceed into the gas bubble formed at the tip. There, it seems plausible to assume a reaction $D_2 + e \rightarrow D^+ + D + 2e$. The D^+ is now under the high field, and work is done in accelerating it toward the dendrite tip. If the length of passage is 50 angstroms, the work done is $50 \times 10^{-8} \times 2 \times 10^9$ ev = 1000 ev. These transitions would be local and fluctuational, for an overall cell voltage of 10 V.
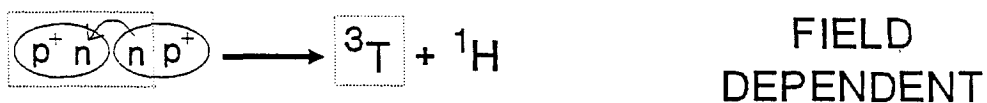
If one puts this work term into the Gamow equation, the degree of penetration is now quite high, and the calculated rate is about one-tenth that observed. There are several ways in which the model can be improved -- for example, we have neglected electron-electron screening due to the overlap of electrons from the metal. We have neglected to account for the charge on the adsorbed D. Such amendment may bring the calculation into good agreement with the facts.

DENDRITE ENHANCED TUNNELING
NEUTRON TRANSFER REACTION

CLASSICAL REACTION	BRANCHING RATIO

$$p^+ n \quad n\, p^+ \longrightarrow {}^4He \begin{cases} {}^3T \\ {}^1H \end{cases}$$

(50%)

(50%)

PROPOSED REACTION	BRANCHING RATIO

$$p^+ n \quad n\, p^+ \longrightarrow {}^3T + {}^1H$$

FIELD
DEPENDENT

TRITIUM LIQUID SCINTILLATION MEASUREMENTS
BLANK EXPERIMENTS

LKB WALLAC 1410 LIQUID SCINTILLATION COUNTER
WITH WYSE PC COMPUTER
1 mL SAMPLE IN 15 mL BIOSAFE II WATER SOLUBLE COCKTAIL

SAMPLE	CPM/ml	DPM/ml
TYGON TUBING IN NaOH	105±20	0
RUBBER STOPPERS IN NaOH	150±20	0
RECOMBINATION CATALYST IN NaOH	140±15	0
DISSOLVED SHAVINGS FROM CUTTERS	160±11	0
DISSOLVED SHAVINGS FROM VACUUM CHAMBER	164±17	0
DISSOLVED SHAVINGS FROM SPOTWELDER	155±10	0

TRITIUM LIQUID SCINTILLATION MEASUREMENTS
BLANK EXPERIMENTS

LKB WALLAC 1410 LIQUID SCINTILLATION COUNTER
WITH WYSE PC COMPUTER
1 mL SAMPLE IN 15 mL BIOSAFE II WATER SOLUBLE COCKTAIL

SAMPLE	CPM/ml	ACTIVITY (DPM/ml) BACKGROUND CORECTED
BIOSAFE II COCKTAIL	170 ± 13	- - -
H_2O ANALYSIS	161 ± 16	0
D_2O ANALYSIS	210 ± 16	100
0.1M LiOD ANALYSIS	220 ± 20	125
0.1M LiOH ANALYSIS	157 ± 12	0
DISOLVED NICKEL IN NITRIC ACID	157 ± 12	0

Fusion At Surface?

(1) Sporadicity, irreproducability

(2) Storms—no T if electrode anodic

(3) Observation dendritic growths

Popov, 1989, Mod. Aspects Electrochemistry,
Plenam, Vol. 20: Time for growth of promontories.

Days
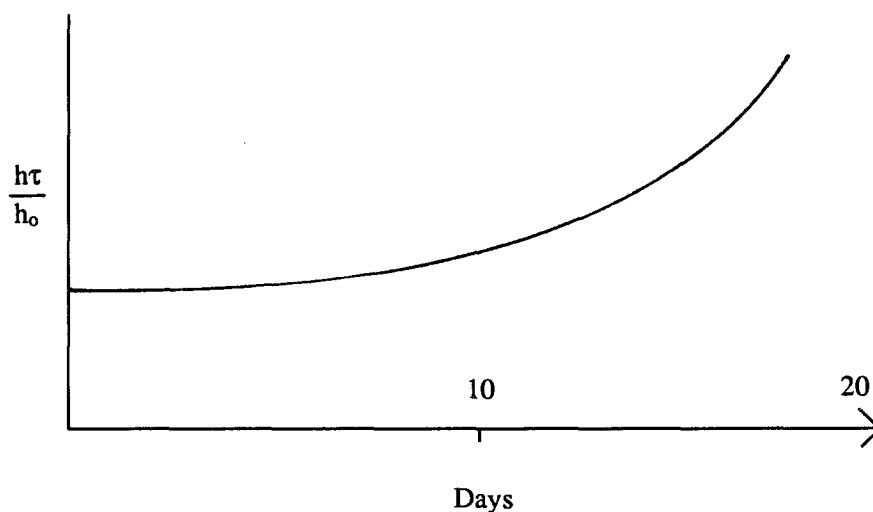
Electric Fields near electrode surface

Normally accepted order of magnitude $\approx 10^8$ volt cm^{-1}
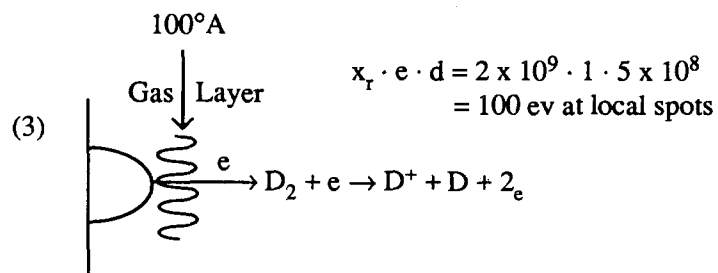
But Kolb in 1989, reflectance spectra, dependence on surface states.
Local fields $\approx 10^9$ volts cm^{-1} (Ag)

Is field further concentrated at dendrite tip? (G. gas discharge theory)

$\therefore$ Reasonable make possible field $\approx 2 \cdot 10^9$ volt cm^{-1}

Fusion At Surface

(1) Assume Volmer-Heyrovsky

$$D_2O + e_m \rightarrow D_{Ads} + OD^-$$

$$D_{Ads} + D_2O + e \rightarrow D_2 + OD^-$$

(2)

$\leftarrow d \rightarrow$

$$D \leftarrow D^+ + OD^-$$

↑ Produced local initial dielectric breakdown.

100°A

Gas Layer

(3)

$$x_r \cdot e \cdot d = 2 \times 10^9 \cdot 1 \cdot 5 \times 10^8$$
$$= 100 \text{ ev at local spots}$$

$$e \rightarrow D_2 + e \rightarrow D^+ + D + 2_e$$

CELL 4 TRITIUM AND HEAT

DPM/ml (Thousands)   % EXCESS

—•— % EXCESS HEAT   —+— TRITIUM CELL   —□— TRITIUM GAS
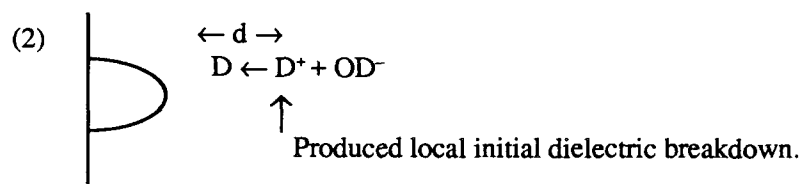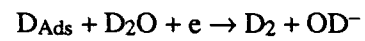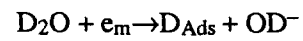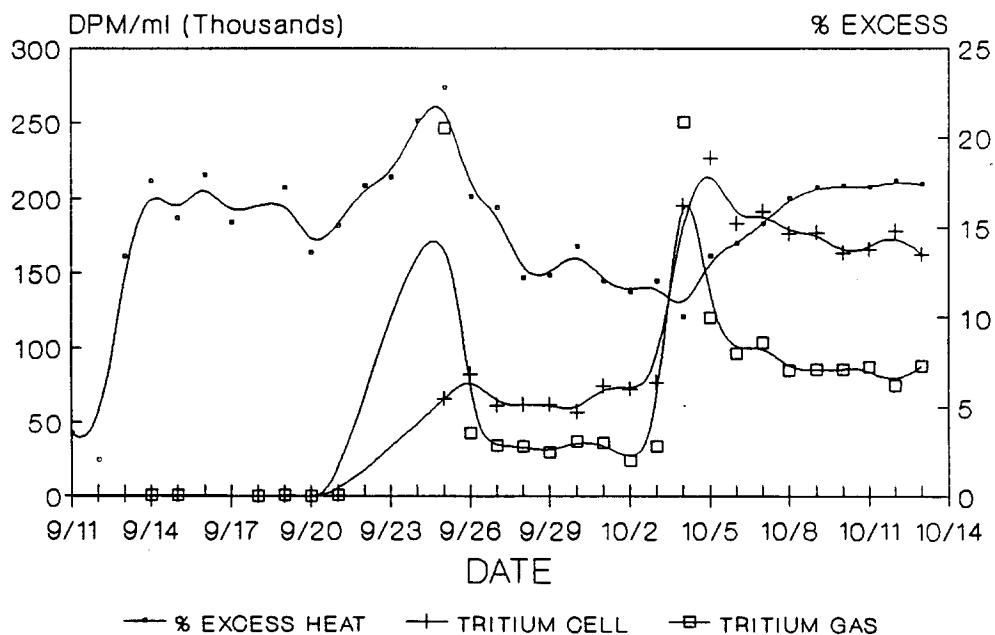
EXCESS HEAT FROM B8
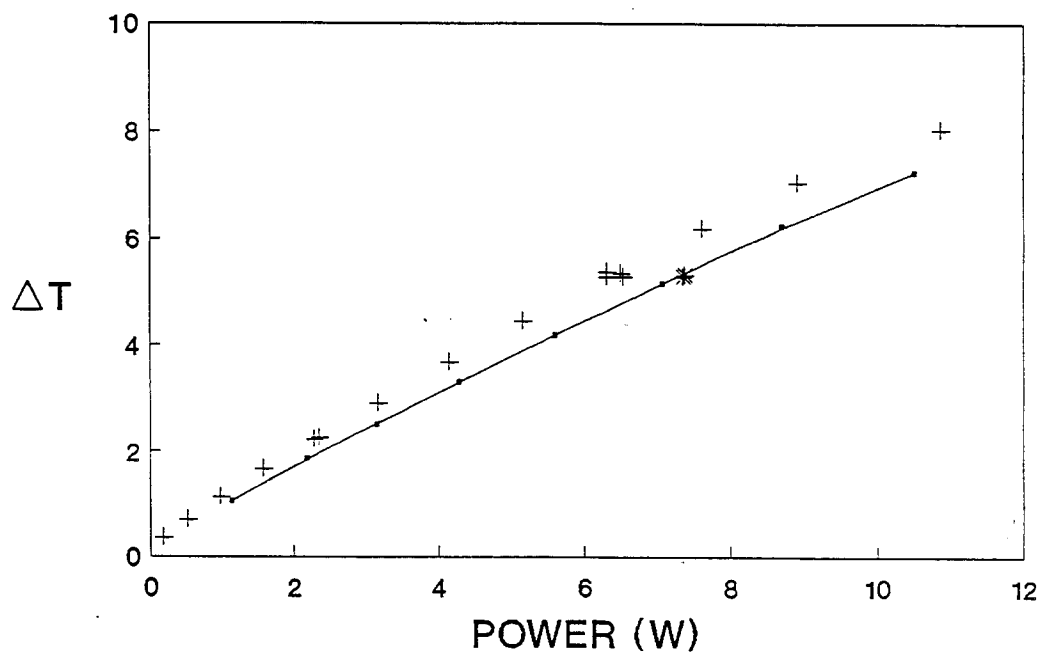
cell 4
sept 15 08:00 sept 15 17:30
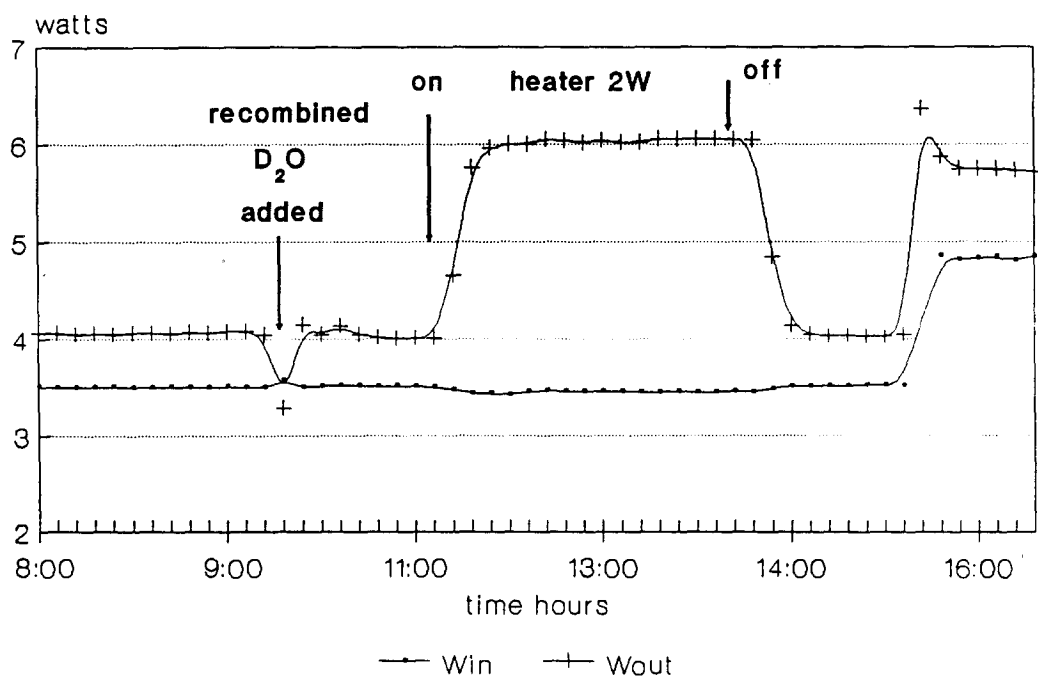
ALL ELECTRODES 1mm x 4cm 99.9% PURE Pd, Ni ANODES

	CPM/mL
ALL ELECTRODES AT 60 mAcm^{-2} TO CHARGE	
CELL A: ANNEALED AT 800 $^{\circ}$C, 10^{-6} TORR, 7 HRS 500 mAcm^{-2} FOR 8 HRS	1.6 x 10^6
CELL B: ACID ETCH TREATMENT 500 mAcm^{-2} FOR 8 HRS	1.2 x 10^6
CELL C: ELECTROCHEMICAL OXIDE REMOVAL 500 mAcm^{-2} t=0	83
t+2 HRS	1790
t+6 HRS	1.7 x 10^5
t+12 HRS	2.5 x 10^5
CELL D: ANNEALED AT 800 $^{\circ}$C, 10^{-6} TORR, 7 HRS 500 mAcm^{-2} FOR 10 HRS CELL THAT HAS EXHIBITED NEUTRON ACTIVITY	3.8 x 10^4

7 OUT OF 9 ELECTRODES HAVE SHOWN TRITIUM ACTIVITY

Tritium content of cells
AH-1 and Cell 4

Background rate 100 CPM
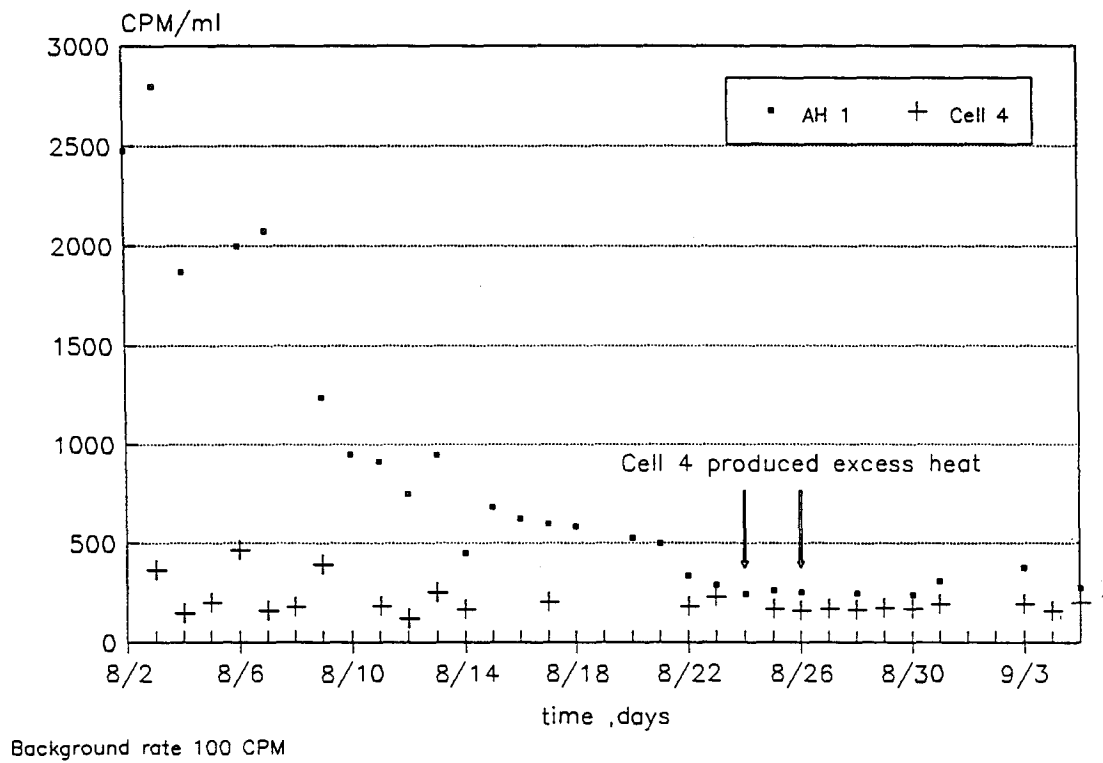
CONFIRMATORY RESULTS
TRITIIUM ACTIVITY IN CPM/ML

SOURCE	CELL A1	STANDARD
TEXAS A&M UNIVERSITY	2.13×10^6	7.23×10^5
BATTELLE LABS	1.96×10^6	8.80×10^5
ARGONNE LABS	1.96×10^6	7.59×10^5
LOS ALAMOS LABS	1.97×10^6	6.50×10^5
GENERAL MOTORS	1.80×10^6	----

DISCUSSION (BOCKRIS)

Lewis: Are your cells open or closed, and how do you calculate the excess heat?

Bockris: In general, half of our cells are open, and half are closed. The calibration of our calorimeter is as I have described.

Lewis: The excess heat seems to be 5-7 percent compared with the input power.

Bockris: It varies 10-17 percent of the total input energy, or 20-30 percent of the input energy after correction for the heat of decomposition of D_2O. We now have five or six cells which have shown 20-30 percent excess, calculated on this basis. The incubation time for excess heat production has been as little as 5 hours. The longest excess heat run has been over 3-4 weeks.

Rafelski: How much excess heat do you see over 3-4 weeks?

Bockris: About 5 MJ.

Lewis: Based on what calculation of the input?

Bockris: This represents about 20 percent of the input energy after correction for the heat of decomposition of D_2O.

Pons: Do you see any evidence of a reduction in tritium production in closed cells?

Bockris: Over our maximum duration run of 90 days, we saw no indications of such a reduction.

Lewis: Have you analyzed your cathodes for He-3 and He-4?

Bockris: Helium has not been analyzed as yet; however, we are attempting to analyze it in the gas phase. It is not easy; tritium production would represent about 10^{10} atoms per ml per second in the liquid phase and about twice that rate in the gas phase.

Fleischmann: That corresponds to about 1 percent of the excess heat detected.

Bockris: Correct.

O'Grady: What is your power input to the cells?

Bockris: It is normally in the 5-10 W range, and the excess heat production varies between 12 and 25 percent.

Rafelski: The tritium which you have detected can only account for 1 percent of the excess heat. If He-3 accounts for the rest, over the duration of your experiments you should have produced a large fraction of a ml of it somewhere in your equipment. That amount should be detectable.

Bockris: Since the neutron activity is very small, it seems unlikely that much He-3 is being produced.

Fleischmann: The product may be α-particles, rather than He-3.

Rafelski: Whatever is occurring, the heat and mass balances must be accounted for.

Santucci: Dr. Bockris, in your calculation, do you account for any tritium that might still be stored in your cathodes?

Bockris: No. We should remember that Dr. Storms detected no tritium in a fresh electrolyte on anodically polarizing his cathodes.

Lewis: Dr. Huggins has indicated that one must anneal the cathode at 75 percent of the melting point in K to remove interstitial material. Interstitial tritium may still be present in your cathodes at the start of the experiment.

Bockris: I believe that it would be detected by making the palladium an anode.

Storms: Some palladium oxide may, of course, be present on the surface in the anodic range, which could block tritium loss.

Bockris: We have studied our electrode surfaces, and they are certainly not clean after electrolysis. Nickel, iron, chromium, sulfur, and very little palladium are present at the surface, as well as silicon from glass. In our case, the nickel is probably from the counterelectrode. Iron may be from the anode or the cell heater.

Hoffman: If the gas evolution into the electrolyte is rapid, gas will pass through the electrolyte without equilibration. Tritium may therefore not have gone into the electrolyte.

Bockris: We speculate that both DT and DTO are produced.

Storms: Under anodic conditions, no gas bubbling is observed, and hydrogen can be totally eliminated from the electrode if enough time is allowed.

Bard: How often did you calibrate the heat output from your cells?

Bockris: The calibration was carried out on a daily basis. If an unusual event occurred, we recalibrated immediately.

Section 10

MASS/CHARGE ANOMALIES IN Pd AFTER
ELECTROCHEMICAL LOADING WITH DEUTERIUM

Debra R. Rolison and William E. O'Grady

Naval Research Laboratory

MASS/CHARGE ANOMALIES IN Pd AFTER
ELECTROCHEMICAL LOADING WITH DEUTERIUM

Debra R. Rolison and William E. O'Grady
Surface Chemistry Branch; Code 6170
Naval Research Laboratory
Washington, DC 20375-5000

Introduction

Among the multitude of efforts [1] to reproduce the provocative experiment of Fleischmann, Pons, and Hawkins [2], the focus has been on the production of heat, and/or the generation of neutrons, high energy gamma rays, or the expected chemical byproducts of the fusion of deuterium with deuterium, such as tritium and ^{3}He. Our approach has been to explore the surface character of Pd foils after extensive electrolysis of H_2O or D_2O solutions.

Our experiments with the electrolysis of Pd foil in D_2O did not produce large neutron fluxes, and due to the small volume of the foil, calorimetric measurements were precluded. However, surface analyses by time-of-flight secondary mass spectrometry (TOF-SIMS) of the electrolyzed Pd revealed anomalies with electrolysis. TOF-SIMS was used to survey the effect on the Pd isotopic distribution with electrolysis in D_2O and H_2O. We report here an enrichment of m/z 106 and a diminution of m/z 105 in the surface/near-surface layers of Pd electrolyzed in D_2O. No enrichment of m/z 106 was observed for the starting Pd material or for Pd electrolyzed in H_2O.

Experimental

Materials and Electrolytic Conditions

All experiments were run with samples cut from a piece of Pd foil (0.127-mm thick) obtained from the historical supply of precious metals in the electrochemistry group at the Naval Research Laboratory. X-ray diffraction [Philips/Norelco Model XRG 6000 X-ray Diffractometer] of this foil showed that it was oriented, primarily in the <200> direction.

The Pd foil cathode was cut in the shape of a flag or a rectangular strip. A spot-welded contact was made to 0.5-mm diameter Pd wire [Aldrich, 99.99% pure] for the strip electrode or to Ta ribbon for the flag electrode. The Pd-Ta join was placed well above the solution level during electrolysis. Prior to electrolysis, the Pd foil (which was dull gray) was cleaned in freshly prepared 1:1 $HCl:HNO_3$ either superficially to remove surface oxide or as follows: the Pd strip was gently moved through the acid for 90 s and then sonicated three times in fresh H_2O; this step was repeated twice; finally the foil (now shiny and showing visible facets) was sonicated in the solvent of electrolysis.

The reaction was run in two different cells. The first cell was a variation on the toroidal dispersion electrolysis cell, previously described [3,4], with an anode of Pt gauze cylindrically surrounding the Pd flag cathode (with a total surface area of 2 cm^2). Solution volume was 30 ml. The second cell was a tall-form beaker where the anode was Pt wire (Alfa, 5N pure) wrapped around the outside of a glass-rod cage, as in the Fleischmann and Pons design [2], to surround a long Pd strip (of varying area, > 1 cm^2), so that the Pd cathode is again concentrically surrounded. Solution volume of this cell was 100 ml. Unless the anode symmetrically surrounds the Pd cathode, electrolysis merely achieves the diffusion of deuterium through (and out of) Pd.

The electrolyte solution for the D_2O experiments was 0.1F Li_2SO_4 [anhydrous, Alfa] in one of two sources of 99.9% pure D_2O [MSD Isotopes or Cambridge Isotope Laboratories]. Reasoning that the pertinent half-cell electrochemical reaction, i.e., the reduction of D_2O at the cathode,

$$D_2O + e^- = D^- + OD^- \qquad \{1\}$$

occurs in both neutral and basic solutions, we opted for the less resistive and lower etchant electrolyte. One

experiment was prepared under environmentally controlled conditions, i.e., previously unopened D_2O [Cambridge Isotope Laboratories] was placed in a dry box [Vacuum Atmospheres: He atmosphere at < 1 ppm H_2O] and used to prepare 0.1F LiOD from Li metal ribbon [Alfa]. The electrochemical cell was assembled in the dry box, sealed, and removed for electrolysis. Electrolyses in light water were performed with triply-distilled (from quartz) H_2O with 0.1F Li_2SO_4.

The electrochemical loading of D or H in Pd was achieved by applying a constant current of 10 mA/cm^2 for at least one day using the galvanostatic mode of a EG&G PAR Model 173 potentiostat/galvanostat. Cell voltage was measured by connecting the reference and auxiliary electrode leads to the electrometer. After initial charging at 10 mA/cm^2, some cathodes were charged at 50 mA/cm^2 or 140 mA/cm^2, but most were maintained at 10 mA/cm^2. Some experiments were run with a neutron counter [Radiac Probe Model DT-371/PDR-70 and Radiac Model 2 Counter-Timer] placed outside of the cell.

The isotopic profile for Pd (m/z range 102-110) was performed using the static SIMS mode of a TOF-SIMS. The instrument used in these studies was built at the Naval Research Laboratory [5,6] and utilizes a pulsed alkali-ion gun, containing a thermionic emitter which produces 2-5 ns pulses of 14.0-keV cesium ions. Positive secondary ions were detected. Each intensity-amu spectrum is the averaged accumulation of two or three million spectra. Samples (sized approximately 0.5 cm x 1 cm) were argon-plasma cleaned in the analysis chamber prior to analysis.

Elemental analysis of the Li_2SO_4/D_2O solution was performed with inductively coupled plasma emission spectrometry and indicated no trace metallic impurities at sub-ppm levels.

Results and Discussion

During the initial electrochemical experiments with Pd in Li_2SO_4/D_2O, rudimentary neutron counting was performed, and although the results were statistically ambiguous, it seemed that further investigation was warranted. X-ray diffraction of the electrolyzed Pd foil showed that lines for Pd were gone and lines for a Pd deuteride phase were present.

Isotopic Distribution from TOF-SIMS

In TOF-SIMS the velocity of the secondary ions produced from the sample surface is inversely proportional to the square root of the mass/charge ratio. This allows the mass of each ion to be determined by measuring its flight time, and, thus, it is possible to reliably observe isotopic ratios in a sample.

The first TOF-SIMS experiment on a Pd foil electrolyzed in D_2O was focused on the low m/z region to gauge the presence of any Li and H/D/T isotopes. The high m/z range was coincidentally obtained, yielding the startling result that the expected natural isotopic distribution of Pd was altered in the electrolyzed Pd, with m/z 106 significantly enhanced. This is clearly seen in Figure 1, where the Pd isotope range (m/z 102-110) is contrasted for Pd blank (i.e., never-electrolyzed Pd foil) and two deuterated Pd foils: PdD#4 - Pd foil electrolyzed for an accumulated charge of $\approx 8 \times 10^3$ Coulombs with freshly opened D_2O and 0.1F Li_2SO_4; and PdD#10 - Pd foil electrolyzed for 1.4 x 10^6 Coulombs of accumulated charge with freshly opened D_2O and freshly prepared LiOD.

Figure 1 also includes the TOF-SIMS spectrum obtained for Pd foil electrolyzed in H_2O for an accumulated charge of 40.2 x 10^3 C (PdH#14). These spectra for the electrolyzed foils show peaks at the Pd isotopic values; they do not show a shifted isotopic distribution at (m+2)/z as expected for PdD or (m+1)/z as expected for PdH. This means that molecular PdD or PdH species do not predominate the ions displaced from the surface. The bond strength of PdH has been theoretically determined to be < 0.1 Hartree [7,8], thus few molecular PdD(H) ions would be expected to survive the secondary ion process.

Assigning the enhanced m/z intensity at 106 amu as due to preferential reaction of a deuteron with [104]Pd to generate [104]PdD at m/z 106 would require rewriting our chemical understanding of reactions. Isotopic effects are observed in the rate of a reaction, not in the identity of the reaction. Furthermore. $(106/104)^{1/2} = 1.010$ - which is not a large isotopic driving force.
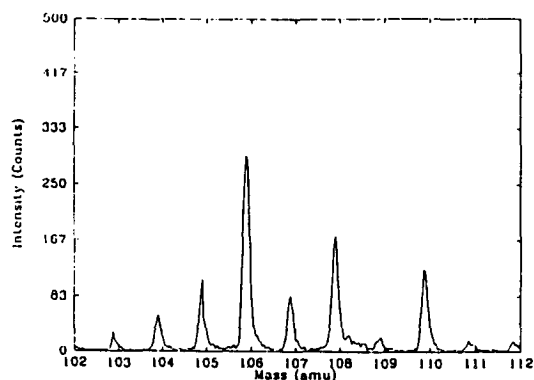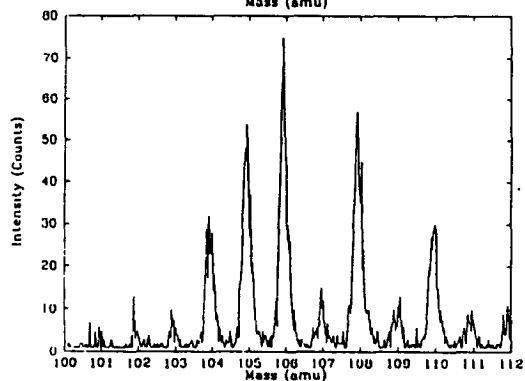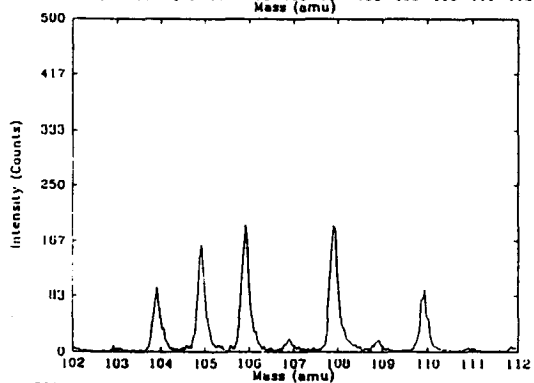
Figure 1: TOF-SIMS spectra obtained for Pd foils before and after electrolysis in D_2O and H_2O.
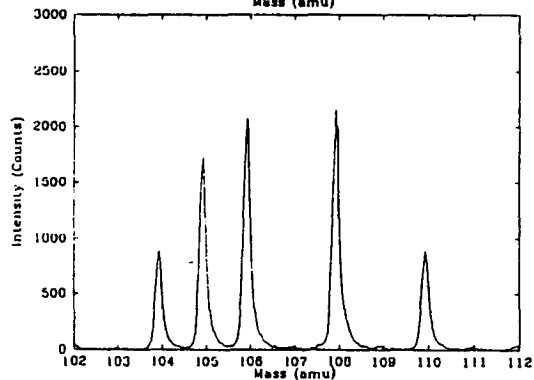
PdD#10 (0.1F LiOD/D_2O)

PdD#4 (0.1F Li_2SO_4/D_2O)

PdH#14 (0.1F Li_2SO_4/H_2O)

Pd foil

Because the samples are cleaned by generating an inert gas plasma inside the TOF-SIMS analyzer chamber, the possibility exists for contamination by constituents of the steel chamber walls; in this m/z range, chromium dimers are an especial worry. Table I lists the naturally occurring isotopes for Pd, Cr, Rh, and Ag. The greatest concern arises with respect to m/z 104, since a dimer of ^{52}Cr (83.8% abundant) would contribute to the signal for ^{104}Pd. Slighter influences from Cr dimers could also affect ^{105}Pd, ^{106}Pd, and ^{108}Pd. As the samples are placed in the chamber and analyzed separately, each experiences slightly different plasma conditions.

TOF-SIMS Analysis of Non-Electrolyzed Pd

To assess the effect, if any, of plasma-generated m/z contamination, three non-electrolyzed Pd foil samples were plasma cleaned in-situ and analyzed. Because m/z 110 cannot be affected by a chromium dimer, it was used as an internal standard: the intensities for m/z 104, 105, 106, and 108 were ratioed to that at m/z 110 for each sample. The results are listed in Table I. Also included in Table I is the percent difference between this ratio and the ratio predicted from the known isotopic abundances of Pd (also listed in Table I); this gives an estimate of the deviation from ideality.

It can be seen that for two of the blanks (Pd#1 and Pd#3) there is no obvious problem from chromium dimers for m/z 105, 106, and 108, as they vary, at most, 15% from ideality, and even m/z 104, the most susceptible m/z, is not severely affected. Pd#2, however, has an enormous excess at m/z 104 (338.7% over ideality); most encouraging, however, is the fact that m/z 105, 106, and 108 are essentially unaffected. This study with non-electrolyzed Pd shows that the use of m/z 110 as an internal standard readily highlights significant contamination ascribable to chromium dimers, and that any peculiarity at m/z 106, as seen in Figure 1, cannot be ascribed to isotopic or molecular contaminants arising from the in-situ plasma cleaning.

As a second check, the intensities were also analyzed as adjusted abundances. This was done by rejecting any information at m/z 104 and summing the areas associated with m/z 105, 106, 108, and 110 (ideally summing to 88.08% of the total), ignoring any minor contribution from m/z 102, and renormalizing to 100% (the factor is 100/88.08 = 1.135). As seen in Table I, this approach also shows that within 15-20%, the expected isotopic distribution for Pd (excluding m/z 104) is obtained, regardless of significant plasma-generated contamination as seen for Pd#2.

TOF-SIMS Analysis of Electrolyzed Pd

With this analytical footing, a number of Pd samples electrolyzed in D_2O and H_2O were analyzed by TOF-SIMS. The normalized intensities, and their percent deviation from the natural abundance, are listed in Table II. Graphically, the normalized results are depicted in Figures 2 and 3 by histograms for each electrolyzed sample and for an averaged value obtained for the three Pd blanks from Table I. Their magnitudes are contrasted with a level drawn for the ideal value.

It is immediately obvious, whether normalizing with m/z 110 (as an internal standard) or adjusting the percent abundance, that two samples, PdD#4 and PdD#10, have been significantly altered at m/z 106, by approximately 45 and 85% respectively, over what was observed for the starting Pd material which mirrors the expected values for normalized ^{106}Pd.

The isotopic distribution for two samples - PdD#4(a) (analyzed by TOF-SIMS four months after termination of electrolysis) and PdD#9 (analyzed two months after termination of electrolysis, and run with air-exposed Li_2SO_4 and D_2O) - are less clearly scrambled. If the internal standard normalization is used, there appears to be a relative enrichment in m/z 106, but not at the levels seen for PdD#4 and PdD#10. If the adjusted abundance normalization is used, these samples closely resemble the ideal ratio at m/z 106 within experimental limits.

Study of the histograms prepared for m/z 105 and 108, as in Figure 3, yields similar conclusions, i.e., clear departure from natural abundances for PdD#4 and PdD#10. In this instance the isotopic abundances of m/z 105 and 108 are clearly diminished for PdD#4 and PdD#10, by either normalization analysis, while PdD#4(a) and PdD#9 are enhanced relative to m/z 110, but appear to be normal using the adjusted abundances.

TABLE I: Isotopic Ratios from TOF-SIMS Intensities - Pd blank

Naturally Occurring Isotope, m/z	% Abundance [a]	Normalized to 110Pd	Pd#1 I_i/I_{110}	% Dev.	Adj. % Abundance	% Dev.	Pd#2 I_i/I_{110}	% Dev.	Adj. % Abundance	% Dev.	Pd#3 I_i/I_{110}	% Dev.	Adj. % Abundance	% Dev.
102Pd	0.96	0.08												
104Pd	10.97	0.93	1.26	+35.5			4.08	+338.7			0.84	-9.7		
105Pd	22.23	1.88	1.72	-8.5	20.1	-9.5	1.79	-4.8	22.6	+1.8	2.03	+8.0	21.9	-1.4
106Pd	27.33	2.31	2.43	+5.2	28.5	+4.4	2.49	+7.8	31.4	+15.0	2.65	+14.7	28.5	+4.4
108Pd	26.71	2.26	2.26	0	27.6	+3.4	1.70	-24.8	21.5	-19.5	2.50	+10.6	26.9	+0.7
110Pd	11.81	1.00			11.7	-0.8			12.6	+6.8			10.8	-8.5
50Cr	4.31													
52Cr	83.76													
53Cr	9.55													
54Cr	2.38													
103Rh	100.00													
107Ag	51.82													
109Ag	48.18													

[a]: From Reference 11.

%Deviation = [(obtained value - ideal)/ideal] x 100.
Adjusted % Abundance = (m/z)$_i$/{[sum of m/z(105+106+108+110)] x 1.135} x 100.

TABLE II: Isotopic Ratios from TOF-SIMS Intensities - Electrolyzed Pd

Sample	Accumulated Charge/10^3 C	(m/z)/amu	I_i/I_{110}	% Dev.	Adj. % Abundance	% Dev.
PdD#4 Pd/0.1F Li$_2$SO$_4$ D$_2$O	> 8	104	0.49	-47.3		
		105	1.36	-27.7	15.8	-28.8
		106	3.35	+45.0	38.9	+42.5
		108	1.88	-16.8	21.8	-18.4
		110			11.6	-1.7
PdD#4(a) Pd/0.1F Li$_2$SO$_4$ D$_2$O [a]	> 8	104	1.38	+48.4		
		105	2.65	+41.0	24.8	+11.7
		106	3.03	+31.2	28.3	+3.8
		108	2.74	+21.2	25.7	-3.7
		110			9.4	-20.3
PdD#9 Pd/0.1F Li$_2$SO$_4$ D$_2$O	254.5	104	1.14	+31.2		
		105	2.40	+27.7	23.0	+3.6
		106	3.05	+32.0	29.2	+7.0
		108	2.76	+22.1	26.4	-1.1
		110			9.6	-18.6
PdD#10 Pd/0.1F LiOD D$_2$O	1402	104	0.54	-41.9		
		105	0.95	-49.5	10.4	-53.2
		106	4.43	+91.8	48.8	+78.8
		108	1.63	-27.9	17.9	-33.0
		110			11.0	-6.8
PdD#11 Pd/0.1F LiOD D$_2$O	1402	104	0.91	-2.2		
		105	2.11	+12.2	22.9	+3.2
		106	2.18	-5.6	23.6	-13.5
		108	2.84	+25.7	30.8	+15.2
		110			10.8	-8.1
PdH#14 Pd/0.1F Li$_2$SO$_4$ H$_2$O	40.2	104	0.89	-4.3		
		105	1.84	-2.1	22.2	0
		106	1.99	-13.9	24.0	-12.1
		108	2.47	+9.3	29.9	+12.0
		110			12.1	+2.5
Pd Blank (not electrolyzed) [Average of 3 samples]	0	104				
		105	1.85±0.16	-1.6	21.5±1.3	-3.2
		106	2.52±0.11	+9.1	29.5±1.7	+9.9
		108	2.15±0.41	-4.9	25.3±3.3	-5.2
		110			11.7±0.9	-0.8

[a]: Sample was a portion of Pd foil ribbon used to contact the flag portion of PdD#4, but analyzed 4 months later.

%Deviation = [(obtained value - ideal)/ideal] x 100.
Adjusted % Abundance = (m/z)$_i$/{[sum of m/z(105+106+108+110)] x 1.135} x 100.
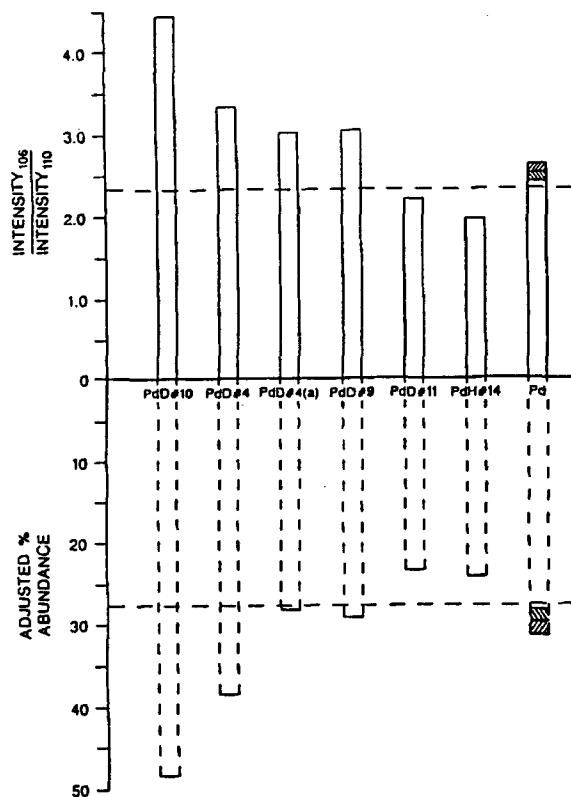
10-5

Figure 2: Histograms of the m/z 106 intensity normalized to the m/z 110 intensity (above the x-axis) and normalized as an adjusted % abundance (below the x-axis) for Pd foils before and after electrolysis in D_2O and H_2O. The horizontal dashed line represents the ideal value for m/z 106 by either normalization method.
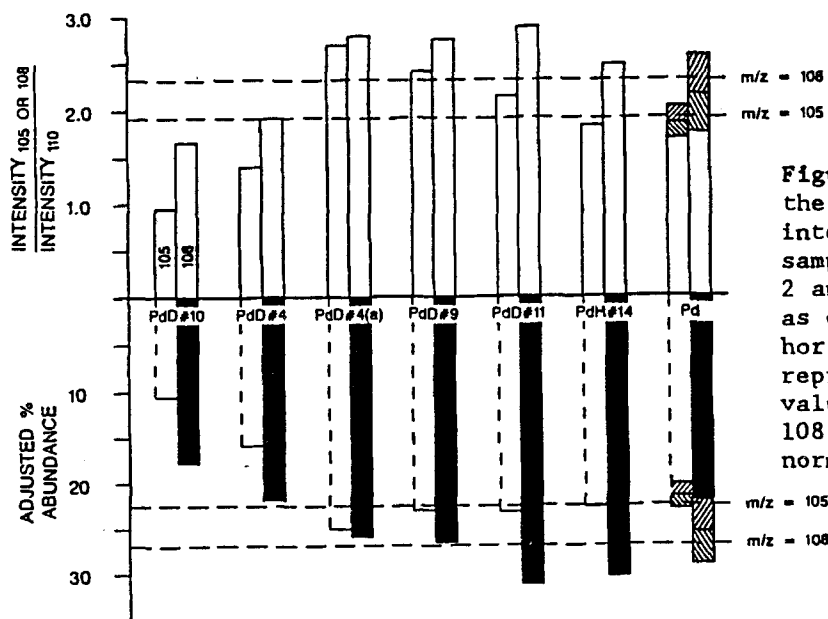

Figure 3: Histograms of the m/z 105 and 108 intensities for the samples shown in Figure 2 and normalized as described above. The horizontal dashed lines represent the ideal values for m/z 105 and 108 by either normalization method.

The isotopic distribution for Pd electrolyzed in H_2O (PdH#14, analyzed by TOF-SIMS two months after termination of electrolysis) has an essentially normal isotopic picture, by either normalization analysis, and resembles the averaged non-electrolyzed Pd values: see Table II and Figures 2 and 3. Only the Pd samples electrolyzed in D_2O exhibit an abnormal isotopic distribution.

Curious as to the depth of this m/z anomaly, we acid etched a piece from PdD#10 - the sample with the most pronounced enhancement at m/z 106 (and diminution of the remaining naturally occurring isotopes) - with 1:1 $HCl:HNO_3$. The etching removes on the order of micrometers of material from the surface. After the acid etch the foil was once again shiny and crystal facets were again visible, i.e., it looked just like acid-cleaned, non-electrolyzed Pd foil. The TOF-SIMS results (Table II and Figures 2 and 3) show that this treated sample (PdD#11) is indistinguishable from the Pd blank. While the depth of the acid etch is on the order of 10 μm, the mass/charge anomaly is clearly not a bulk phenomenon.

Conclusions and Concluding Speculations

During prolonged electrolysis of D_2O at Pd, in addition to stuffing the Pd lattice with deuterons, other processes are occurring, including enrichment of Pd bulk impurities such as Rh and Ag at the surface [9]. The apparent scrambling of the normal isotopic distribution for Pd, which occurs only after electrolysis in D_2O, is another. The possibility of stable, non-Pd isotopes contributing to the m/z 106 signal can be ruled out as follows: (1) the only other stable 106 isotope is [106]Cd (1.22% naturally abundant) [10,11]; at the magnitude of the change in m/z 106, the more abundant Cd isotopes ([112]Cd, 24.07% and [114]Cd, 28.86% abundant) would also be present in the TOF-SIMS spectrum; the intensities at m/z 112 and 114 are at background; and (2) a doubly charged 212 amu isotope is even less plausible, as all 212 amu isotopes are radioactive [10].

The fact that the interior of the Pd remains isotopically normal implies two things: (1) that any isotopic scrambling is near surface; and (2) that the enhancement of m/z 106 does not derive from a long range isotopic separation - an isotopic redistribution which leaves the middleweight isotope enriched relative to the light- and heavyweight isotopes is puzzling, especially when the separation factors (calculated as the square root of the ratio of the masses) differ only by parts-per-thousand.

A surface-sensitive, high-resolution mass spectrometric analysis is required to determine if the intensity at m/z 106 is due to only [106]Pd or to a mix of [106]Pd and another m/z 106 species. Contributions to the m/z 106 intensity by the most plausible plasma-generated polyatomic candidates have been ruled out, as summarized in Table III.

Subsequent to the NSF-EPRI meeting of 16-18 October 1989, high-resolution surface-sensitive mass spectrometric measurements have shown that PdD#10 was contaminated during the electrochemistry with a trace of ZrO_2 [12] (also confirmed by X-ray photoelectron spectroscopy). Zirconium has an isotopic range of:

90 (51.45% natural abundance)
91 (11.32%)
92 (17.19%)
94 (17.28%)
96 (2.76%)

This makes for a coincidental, and unfortunate, overlap of ZrO ions with the Pd isotopic region. [90]Zr[16]O has a mass of 105.8992; [106]Pd has a mass of 105.9032 making the high-resolution aspect of the mass spectrometric analysis even more critical.

PdD#4, the sample with a nearly 50% enrichment at m/z 106, shows no m/z intensities consistent with zirconium isotopes in its TOF-SIMS spectrum, so the enrichment observed for this sample is not due to this happenstance interference. This sample was dissolved shortly after termination of charging for bulk analysis, so, unfortunately, it does not exist in a form permitting high-resolution, surface-sensitive mass spectrometric analysis. The origin of the m/z 106 enrichment and m/z 105 diminution for PdD#4 is still unknown, but it is not due to either plasma contamination from the conditions of the TOF-SIMS experiment or the zirconium contamination seen for PdD#10.

Table III: Possible Contributing Species to m/z 106

Possible Species	Contributor to m/z 106?	Experimental Evidence
$(^{104}PdD)^+$	no	1. Do not see peaks at $(m+2)/z$; for the enhancement seen at m/z 106, a peak at m/z 112 (for ^{110}PdD) would be apparent and is not.
$(^{105}PdH)^+$	no	1. No reflection of the Pd isotopic distribution at $(m+1)/z$ for Pd electrolyzed in H_2O or D_2O, in particular, no signal above background at m/z 111 (for ^{110}PdH) is observed. 2. No $(PdH)^+$ species seen for Pd from trace H and H_2O species in the spectrometer.
$^{53}Cr_2{}^+$, $(^{52}Cr^{54}Cr)^+$	no	1. Control experiments with non-electrolyzed Pd show that plasma-imposed Cr contamination, even when overwhelmingly present, does not contribute to m/z 106 intensity. 2. Electrolyzed Pd shows no dominating increase in m/z 104 intensity.
$(^{52}Cr_2D)^+$	no	1. For this species to cause a 50% increase in m/z 106, m/z 104 should be enormously enhanced (as $Cr_2{}^+$ would be more probable than $(Cr_2D)^+$), but is not.

$(^{52}Cr^{54}Fe)^+$; $(^{50}Cr^{56}Fe)^+$	no	If plasma conditions generate Fe ions as well as Cr ions from the walls of the analyzer chamber, the level of m/z 106 enhancement seen would require:
		    a. A large enhancement at m/z 104 for $^{52}Cr_2{}^+$ (^{52}Cr is 83.8% abundant, while ^{54}Fe is only 5.8% abundant), which is not seen.
		    b. A large enhancement at m/z 104 for $^{52}Cr_2{}^+$ (^{50}Cr is only 4.3% abundant) with a large signal at m/z 112 (for dimers of 91.7% abundant ^{56}Fe) - also not observed.
		    c. Control experiments with non-electrolyzed Pd show that plasma-imposed Cr contamination, even when overwhelmingly present, does not contribute to m/z 106 intensity and no increase in m/z 112 intensity above background is observed.

$^{106}Cd^+$	no	1. ^{106}Cd is 1.2% abundant; at 50% enrichment, significant intensity at m/z 112 (24.1% abundant ^{112}Cd) and m/z 114 (28.9% abundant ^{114}Cd) should be observed and are not.
Silicate molecular ions	no	1. Such a species would have to be observed for Pd electrolyzed in light water, if not at m/z 106 (for a $(Si-O)_n$ species charge balanced by alkali) then at m/z <106 for OH forms. PdH #14 has background intensities from m/z 73 to m/z 104.
$(^{53}?)_2{}^+$	no	1. ^{53}Cr (9.6% abundant) is the only stable 53 amu isotope.
$(^{106}?)^+$	no	1. ^{106}Pd and ^{106}Cd are the only stable 106 amu isotopes.
$(^{212}?)^{2+}$	no	1. All 212 amu isotopes are radioactive.

It is possible that the additional intensity is due to a radioisotope and not ^{106}Pd. The 106 amu radioisotopes, their half-lives, and their decay products are listed in Table IV. The most promising candidate in terms of half-life is ^{106}Ru. Ru is unfortunately difficult to surface analyze by XPS or Auger in this particular chemical system due to interferences from characteristic lines for other elements also present in high concentrations at the surface.

TABLE IV: Possible Radioactive Isotopes at 106 amu [10]

Radioisotope	Half-life	Decay Product
Ru	1.0 y	^{106}Rh
Rh	30 s	^{106}Pd
Ag	8.3 d/24 m	^{106}Pd
In	5.3 m	^{106}Cd

The diminution of m/z 105 in PdD#4 reacted in D_2O implies a reactive or diffusional loss that cannot be explained away by non-Pd species at this m/z value. We are at a loss to explain this near-surface isotopic redistribution (enrichment of m/z 106 and diminution of m/z 105) - admittedly only for a single sample - by polyatomic interferents, leading us to the speculation that the redistribution may be nuclearly induced. (d,p) reactions with ^{104}Pd and ^{105}Pd, while also thought to be as improbable as deuterium-deuterium fusion in the Pd lattice, have been recently proposed for this system [13,14]. Isotopic analyses from 100-112 amu of known heat-producing Pd cathodes will be needed to extend (or discount) our provocative experimental observation.

Acknowledgments

References

1. *The Wall Street Journal*, 23 March 1989 - present.
2. M. Fleischmann, S. Pons, M. Hawkins, *J. Electroanal. Chem.* **261**, 301 (1989); errata, **263**, 187 (1989).
3. M. Fleischmann, J. Ghoroghchian, D. Rolison, S. Pons, *J. Phys. Chem.* **90**, 6392 (1986).
4. D. R. Rolison, E. A. Hayes, W. E. Rudzinski, *J. Phys. Chem.* **93**, 5524 (1989).
5. S. M. Hues, R. J. Colton, R. L. Mowery, K. J. McGrath, J. R. Wyatt, *Appl. Surf. Sci.* **35**, 507 (1988-89).
6. S. M. Hues, R. J. Colton, J. R. Wyatt, J. A. Schultz, *Rev. Sci. Instrum.* **60**, 1239 (1989).
7. N. A. Baykara, J. Andzelm, D. R. Salahub, S. Z. Baykara, *Int'l J. Quantum Chem.* **29**, 1025 (1986).
8. B. I. Dunlap, D. W. Brenner, R. C. Mowrey, J. W. Mintmire, P. P. Schmidt, C. T. White, *Canadian J. Chem.* submitted.
9. D. R. Rolison and W. E. O'Grady, manuscript in preparation.
10. *Chart of the Nuclides* (United States Atomic Energy Commission, 1965).
11. John Emsley, *The Elements*, Clarendon Press: Oxford, 1989.
12. D. R. Rolison, W. E. O'Grady, R. J. Doyle, Jr., P. P. Trzaskoma, *Proceedings of the 1st International Conference on Cold Fusion*, Salt Lake City, UT, 28-31 March 1990.
13. D. Mueller, L. R. Grisham, *Fusion Tech.* **16**, 379 (1989).
14. F. E. Cecil. D. Furg, T. E. Furtak, C. Mader, J. A. McNeil, D. L. Williamson, *Proceedings of the Workshop on Cold Fusion*, Santa Fe, NM, 23-25 May 1989.

DISCUSSION (ROLISON)

Rafelski: What atomic numbers are the peaks at mass number 107 and 109?

Rolison: They are silver impurities in the palladium, and they are in the expected ratio of 49:51. The secondary-ion mass spectrometry (SIMS) technique does not have the resolution to determine the masses to a high enough degree of accuracy to identify each isotopic species.

Teller: Does the technique only sample the palladium surface?

Rolison: SIMS is surface sensitive, because the secondary bombarding ions are of low energy and only ionize the surface.

Teller: What is the depth of penetration?

Rolison: Essentially only one or two atomic layers.

Appleby: If you take the Pd-105 peak and add it to the Pd-106 after testing, do you see the same total amount of Pd isotopes as those in the starting sample?

Rolison: Because of the possibility of iron and chromium contamination, we use Pd-110 as an internal reference standard which cannot be compromised by such contamination. On palladium blanks we have seen compromisation at mass number 104, indicating the presence of chromium, i.e., $^{52}Cr_2$. However, if one sums the areas of the peaks, it corresponds rather well to the initial natural abundances of the two isotopes.

Hoffman: Did you try progressive evaporation of surface layers?

Yeager: Using that technique, you would be able to obtain a concentration-depth profile.

Rolison: Such an experiment would have been very useful, but unfortunately our spectrometer does not have that capability.

Bockris: How long was your palladium sample exposed to electrolysis?

Rolison: The lithium sulfate solution in D_2O was electrolyzed for only four days. The thin foils charge with deuterium within a short time, about 1-2 hours. We have typically charged at 10 mA/cm^2 or less. The platinum anode was of 99.999 percent purity. Electrolysis in the LiOD solution corresponded to 1.4 million Coulombs over 26 days.

Yeager: Your palladium surface would certainly not be clean after electrolysis.

Bockris: How did you clean it before obtaining the SIMS results?

Rolison: We cleaned our surfaces using a modified aqua regia etch before electrolysis. After electrolysis, the surface is dull gray; it becomes bright

after etching, and it is quite clean. After exposure to lithium sulfate solution, little silicon contamination from glass was seen by XPS.

Appleby: Do you see platinum on the surface?

Rolison: Yes, the result is shown on one of my figures.

Werth: Were the cell potentials the same in the H_2O and the D_2O solutions?

Rolison: They are a little lower in the H_2O solutions, as one might expect.

Lewis: Even so, the H_2O and D_2O solutions might contain different contaminants which would affect both overpotential and surface composition.

Rolison: They were both analyzed by ICP (inductively coupled plasma atomic spectrometry) to look for problems of metal contamination, and they were both shown to be very clean.

Werth: I asked my question about the cell voltage or overpotential, because if some impurity were coming from the platinum anode, different amounts might be seen at the surface at different overpotentials.

Rolison: One surface analysis which we have carried out in detail is XPS. Results of this kind would certainly stand out if they were important.

Teller: A neutron removed from an atomic species like palladium requires about 7 MeV. If a proton is simultaneously removed, 11 MeV would be required to go from Pd-108 to Pd-106. Instead of an energy input, an excess energy seems to be observed.

O'Grady: The mass number 106 species may not be palladium. What we see is only a mass analysis, not an elemental analysis.

Chubb: We must also account for the apparently missing proton that should be formed with the tritium. Loss of a proton from Pd-106 could conceivably yield a mass number 105 species, going down the periodic table. A silver isotope is also a possible product. When I heard of this result, my immediate reaction was a conclusion that perhaps nuclear physics is indeed happening at the palladium surface.

Rolison: I would like to make a first point. The two electrolyte samples in which palladium electrodes appeared to give a strong enrichment were kept relatively dry, following some of Dr. Huggins' comments about making sure that the D_2O does not absorb water. The lithium sulfate used was sealed and was freshly opened before use, using as much care as possible. With the LiOD solution, all possible precautions were taken, which included loading the cell with electrolyte in a glovebox, followed by sealing.

A further point is that there is only one other stable 106 isotope, namely Cd-106. It has a natural abundance of only 1.2 percent. If it were present, one would expect to see very large peaks for two more abundant Cd isotopes, which are not observed. Other species may still be responsible for this peak. For example,

deposition of silicates on the surface is in principle possible. However, I believe that our light water controls rule out that possibility. One is then left with the possibility of dimers of atomic mass unit (AMU)-52 and -53 species, particularly Cr-53. A doubly-charged AMU-212 is in principle possible, but that would be a radioactive species, since there are no stable 212 isotopes. Other species may still, of course, be possible: for example, ^{90}ZrO, which would add up to 106.

Finally, taking a thickness of 1000 angstroms as that of the reaction zone at the palladium surface, and knowing the enrichment of the AMU-106 species, one can calculate how many new atoms of 106 palladium have been generated in that layer during the time of electrolysis. The results showed apparently about 10^{11} events per second.

Appleby: How large was the surface area of your electrodes in this work?

Rolison: They varied, though they were always more than $1\text{-}cm^2$ facial surface area, including the front and back sides.

Appleby: The order of magnitude of excess heat that we observed, for electrodes of this size, would certainly correspond to about 10^{11} event/s.

Rolison: That was certainly our impression, although we did not carry out heat or tritium measurements.

Hoffman: Is there a possibility that the Naval Research Laboratory could provide a service for researchers to have their cathodes examined after electrolysis?

Rolison: It would appear that the next generation of experiments will require the use of surface-sensitive equipment, particularly high-resolution surface-sensitive mass spectrometry. We may have that capability at NRL.

Lewis: Could you show us the entire SIMS data over all the AMU range?

Rolison: Unfortunately, I do not have all the data, but our emphasis was on the lower AMU range.

Lewis: Did you also obtain data for the higher AMU range? For example, have you detected any $^{102}RuD_2$ or some other compound whose AMUs might add up to 106?

Rolison: That's what we tried to consider. We can see the cations for chromium and iron, for instance.

Lewis: What other elements did you find in the SIMS?

Rolison: Chromium and the iron were always present, even in the light water blanks. In the higher AMU region, any species seen would have to be molecular. We did not observe anything of this sort. The blank data in light water show that traces may be there, but they do not show any signals in the higher AMU range. One can argue that the 106 species must be ^{104}PdD. Of course, that is ludicrous, since it is impossible to conceive of a preferential isotopic chemical reaction of D with ^{104}Pd.

Kim: It may, of course, be $^{52}Cr_2$.

Rolison: We have ruled that out. If Cr_2 were a problem, it would be seen at AMU 104 in the absence of Pd. We do not see it.

Teller: I continue to be concerned about the ^{108}Pd peak. If you cannot account for this via molecular impurities, its presence is very difficult to explain. To produce it would require energy input, so the laws of physics would be violated.

Kim: There is one possible chain process which could do it: neutron capture by ^{108}Pd producing gamma rays. And gamma rays are about 6 MeV, which could disintegrate deuterons and produce more neutrons.

Rolison: As I have emphasized, our SIMS results lack high resolution for the AMU values detected. Our XPS results show atom percent concentrations of various elements present at the surface relative to palladium. Platinum is an important impurity, and the total amount of it is a function of cumulative charge, so the longer electrolysis is carried out, the more platinum is present on the surface. This is easy to explain, since some platinum goes into the solution at the anode and plates out at the cathode. As one would expect, platinum results are similar in heavy water and light water.

The XPS results, which are highly surface sensitive, show significant amounts of silver and rhodium at the palladium surface, but they are not present in the electrolyte or in the anode. However, they are initially present in our palladium cathode. Analysis of the 99.9 percent pure palladium which we used showed that it contained 100 ppm of silver and 50 ppm rhodium. Both metals form continuous solid solutions with palladium. It has been considered surprising that they segregate at the surface. However, migration is not impossible, since their solubility characteristics may be different in Pd deuteride.

The palladium surface is cleaned using a plasma etch before the SIMS results are obtained. The sample which showed a large surface enrichment of AMU 106 using SIMS showed only the bulk level of rhodium at the surface using XPS, after an acid etch. Before etching, XPS showed 3 atom percent of rhodium at the surface. Reaching this rhodium level in a 0.1-micron surface layer from a bulk value of 50 ppm in a 127-micron foil implies a great deal of segregation. In fact, it indicates that all of the rhodium is in the 0.1 micron surface layer sampled by XPS. Because our palladium was not 99.999 percent pure, and we did have a bulk presence of these elements, we either must say that they are completely segregated near the surface, making the metallurgists unhappy, or that they were produced there by nuclear transformations. Rhodium and silver are near neighbors to palladium in the periodic table, and there are certainly a number of neutron processes that can generate their nuclei.

Bard: What were the results of a similar analysis in the light water samples?

Rolison: At present, we do not have the data.

Lewis: Do you have results on a platinum, not palladium, cathode as a control in the same D_2O electrolytes?

Rolison: We did try that experiment, but the platinum cathode was not ultrapure either.

Voice: Would you review the relative change in AMU 105 and AMU 106 compared with that for AMU 108?

Rolison: The results are shown in detail in our paper.

Bockris: Do you have plans to successively evaporate the surface layers to determine the progressive change in composition?

Rolison: I have already pointed out that we cannot do that in our instrument, and I am not sure if we can do it elsewhere. Such experiments will in any case be criticized, since the surface can be rearranged during the higher energy ion bombardment required for evaporation.

Hoffman: You are using AMU 110 as the internal standard to determine your ratios.

Rolison: Correct.

Hoffman: Have you tried making AMU 108 the internal standard instead, to see the results obtained under those conditions?

Rolison: We have not attempted that. However, we did examine two methods of evaluating the ratios. One was with AMU 110 as an internal standard, and the other used an adjusted percent abundance for the isotopes. Since AMU 104 may possibly be due to chromium dimer contamination, we ignored that peak. In consequence, we added the total of the natural abundances of ^{105}Pd, ^{106}Pd, ^{108}Pd, ^{110}Pd, giving 88 percent. We matched the expected abundances for the light water blank. For heavy water specimens, the results using this alternative method showed an enrichment in ^{106}Pd, with a diminution in the ^{105}Pd and ^{108}Pd.

Voice: If you use ^{108}Pd as a standard, all of the other isotopes appear to be increasing in mass. For example, ^{104}Pd and ^{105}Pd go to ^{106}Pd, and ^{108}Pd goes to ^{110}Pd.

Rolison: Maybe, but we do not obtain a relative increase in AMU 112.

Voice: Relative to ^{110}Pd, does ^{108}Pd become reduced in abundance?

Rolison: Yes.

Voice: Relative to ^{108}Pd as a standard, both ^{110}Pd and ^{112}Pd increase. Using this standard, all of the other isotopes increase in mass.

Rolison: Different methods of analysis will give different results. The important point is that a redistribution of isotope abundances occurs in the case of the D_2O specimens.

Hoffman: If some people are concerned that the surface concentration of ^{108}Pd is reduced, the analysis can be adjusted so that it is no longer a problem.

Voice: But then one has the difficulty that ^{110}Pd is increasing.

Schneider: Alternatively, some other method of treating the raw data should be used which would allow one to extract additional information that one cannot obtain from calculations based on these different hypotheses.

Jordan: Some assumptions can be made based on the various possible nuclear reactions that have been hypothesized.

Rolison: An initial examination of our data might make many groups rush to find a surface-sensitive mass spectrometer.

Rafelski: Could you tell us again how the surface of the specimen was treated after electrolysis for a few hours and before surface analysis?

Rolison: The cathode was charged at the low current density of 10 mA/cm^2 for a time that is probably an order magnitude longer for charging than would be estimated based on diffusion into the palladium volume. The cathode was then either left at this same current density or exposed to a higher current density equal to about 100 mA/cm^2. Before electroylsis, the palladium was cleaned with a 50/50 nitric and hydrochloric acid mixture, which polishes its surface.

Storms: Have you measured the tritium level which you may have developed in your cell?

Rolison: No. In my opinion, the next hurdle in this work will involve heavy isotope analysis, particularly SIMS peak resolution measurements along the AMU axis. These will allow us to follow the Pd isotope enrichment processes, if this process is really applicable. For example, it will allow us to determine if the AMU 107 peak is ^{107}Pd, which has a 6.5 million year half-life. As an alternative, it may be ^{107}Ag occurring without ^{109}Ag.

Section 11

COMMENTS ABOUT DIAGNOSTICS FOR NUCLEAR REACTION PRODUCTS FROM COLD FUSION

George H. Miley and Magdi Ragheb

Fusion Studies Laboratory

University of Illinois

Heinrich Hora

Department of Theoretical Physics

University of New South Wales

COMMENTS ABOUT DIAGNOSTICS FOR NUCLEAR REACTION
PRODUCTS FROM COLD FUSION

George H. Miley and Magdi Ragheb
Fusion Studies Laboratory, University of Illinois

Heinrich Hora
Department of Theoretical Physics, University of New South Wales

INTRODUCTION

An uncertainty still remains about whether or not cold fusion actually exists. Experiments that support this possibility have been reported by some laboratories but a number of negative experiments have also been obtained by very reputable groups. In the present discussion, however, we will simply make the assumption that the phenomenon occurs and proceed to discuss diagnostic requirements to confirm the production of nuclear products and shed light on possible reaction mechanisms.

Since the reaction mechanism(s) is(are) presently unknown, we must consider a wide variety of diagnostics. Much of the focus to date has been on use of calorimetry to measure excess heat production. This is an important diagnostic but requires extremely careful control. Also, taken alone, it will not resolve the issue of the existence of fusion reactions, i.e., the need to simultaneously confirm the generation of fusion reaction products. In that respect, neutron measurements have been a primary focus, but this approach has faced many problems due to the low signal-to-noise ratio typically involved. Thus we must consider other possible reaction products. Helium is frequently mentioned, but in view of the variety of products that could occur, an appropriately diagnosed experiment should consider a wide range of possibilities. This is illustrated in Fig. 1.

Indeed, the problem becomes even more complex when we consider that different mechanisms may be operative in different experiments. This can confuse and cloud the issue unless this possibility is recognized in advance and incorporated into the diagnostics plan. For example, some experiments appear to have neutron bursts associated with high-field acceleration of

deuterons caused by crack propagation in the electrode. In that case, one

would expect conventional d-d reactions to occur as a result of beam-target

- Neutrons

- Gammas, x-rays

- Charged Products:

  protons, ^{4}He, ^{3}He, tritium, betas (β^+ and β^-)

- Transmuted Pd isotopes

Note: different mechanisms may occur in various
      experiments, resulting in a different grouping
      of products.

Figure 1. Reaction Product Possibilities

type fusion. Then equal rates of neutron and tritium production should occur.

On the other hand, if an entirely different mechanism is found under different

experimental conditions, (e.g., tunneling through the Coulomb barrier combined

with the high density at the reaction site), this could possibly lead to a

different channel for decay of the compound nucleus created in fusion. As a

result, uneven ratios of tritium/neutrons or even different reaction products

might occur. Consequently, until these experiments are better understood, the

observation of different nuclear products in different experimental

arrangements does not necessarily indicate an inconsistency. Further,

experimenters must remain alert to the possibility of a variety of reaction

products and provide the necessary array of diagnostics to handle this

situation.

TWO-BODY REACTION PRODUCTS

    To illustrate the many of possibilities involved, we begin by briefly

surveying the reaction products that can occur through two-body reactions. As

summarized in Table I, Mueller and Grisham[1] have provided an excellent

survey of the spectrum of two-body reactions that should be considered in cold

TABLE I

Possible Two-Body Reactions, Their Products, and Q Values

Reactants	Product 1	Product 2	Product 3	Q Value (MeV)
$p + d$	^{3}He	γ		5.4
$d + d$	t ($\beta t_{1/2} = 12.3$ yr)	p		4.03
	^{3}He	n		3.27
$p + {}^6$Li	^{7}Be ($\epsilon t_{1/2} = 53.3$ days)	γ		5.61
	^{3}He	α		4.02
$p + {}^7$Li	^{8}Be ($2\alpha t_{1/2} = 0.07$ fs)	γ		17.25
	α	α		17.35
$d + {}^6$Li	^{8}Be ($2\alpha t_{1/2} = 0.07$ fs)	γ		22.28
	α	α		22.37
	^{5}He (α, $n\Gamma = 0.6$)	^{3}He		0.84
$d + {}^7$Li	^{3}He	α	n	1.80
	^{7}Li	p		5.03
	^{7}Be ($\epsilon t_{1/2} = 53.3$ days)	n		3.38
	^{5}Li (α, $p\Gamma = 1.5$)	t ($\beta t_{1/2} = 12.3$ yr)		0.60
	^{9}Be	γ		5.61
	^{8}Be ($2\alpha t_{1/2} = 0.07$ fs)	n		15.03
	^{5}He (α, $n\Gamma = 0.6$)	α		15.16
	α	α	n	15.12
$p + {}^{12}$C	^{13}N ($\epsilon t_{1/2} = 9.96$ min)	γ		1.94
$d + {}^{12}$C	^{14}N	γ		10.27
$p + {}^{16}$O	^{17}F ($\epsilon t_{1/2} = 64.5$ s)	γ		0.6
$d + {}^{16}$O	^{18}F ($\epsilon t_{1/2} = 110$ min)	γ		7.53
$p + {}^{102}$Pd	^{103}Ag ($\epsilon t_{1/2} = 1.10$ h)	γ		4.24
	m (IT$t_{1/2} = 5.7$ s)			4.11
$p + {}^{104}$Pd	^{105}Ag ($\epsilon t_{1/2} = 41.3$)	γ		5.01
	m (ϵ, IT$t_{1/2} = 7.2$ min)			4.97
	^{101}Rh ($\epsilon t_{1/2} = 3.3$ yr)	α		2.85
	m (ϵ, IT$t_{1/2} = 4.34$ days)			2.69

(Similar reactions in ^{106}Pd, ^{108}Pd, ^{110}Pd: see Ref. 1)

$d + {}^{102}$Pd	^{103}Ag ($\epsilon t_{1/2} = 1.1$ h)	n		2.01
	m (IT$t_{1/2} = 5.7$ s)			1.88
	^{103}Pd ($\epsilon t_{1/2} = 17.0$ days)	p		5.38

(Similar reactions in ^{104}Pd, ^{105}Pd, ^{106}Pd, ^{108}Pd and ^{110}Pd: see Ref. 1)

Nomenclature

d = deuteron

IT = isomeric transition (gamma-ray and conversion-electron decay)

m = isomeric state

n = neutron

p = proton

t = triton

$t_{1/2}$ = half-life

α = alpha decay

β = negative beta decay

ϵ = positive beta decay including electron conversion

Γ = level width for particle-unstable nuclides (MeV)

fusion experiments. Their compilation assumes that the reactants involved include protons, deuterium, Li-6, Li-7, Carbon-12, Oxygen-16 and palladium; but the reactions are restricted to those with a positive Q value. Additional assumptions include conservation of neutrons and protons plus a measurable half-life for all species. The latter assumption deserves a special note since it excludes products that are unbound to neutrons and protons. For example, the often cited[2] reaction: d+d → α + 23.85 MeV involves a product alpha without a bound state. In contrast, in the "conventional" d-d reaction, the compound nucleus decays by breakup to either ^{3}He + n or t + p. This decay occurs so rapidly (10^{-20}s) that this decay channel would normally be expected to dominate, ruling out the direct alpha reaction.

Most reactions in Table I result in either gamma or neutron emission. If the heat producing reaction is as strong as reported earlier and it involves two-body reactions of these types, the emissions should be detectable. The reaction rate (sec^{-1}) is ~ 6.3 P(w)/Q(MeV) (where P is the power obtained and Q is the reaction energy). Then, for example, a cell producing ~ 20 watts, as suggested by the original Pons-Fleischmann experiments, would have a gamma emission rate of ~ 10^{13} per second. Such a gamma flux would be easily detectable, assuming the gamma energy is high enough (as is expected for most of these reactions). Corresponding strong neutron emission is also predicted and should be well above any background. Of course, as is well known, such strong gamma and/or neutron emission rates have not been observed, and this is one of the fundamental "mysteries" of cold fusion to date.

If a cell were to operate at 20 watts for 10 hours, "typical" two-body reactions would, on average, produce the order of 5×10^{17} to 2×10^{18} alpha particles and/or 6×10^{17} tritons. Such a production of either helium or

tritium would be measurable and this should be an important focus for experimental study. Indeed, as noted later, tritium production has been reported from several experiments, but the production rate appears to be well below that predicted from heating observations using the above two-body reaction logic. This could suggest several independent reactions occur simultaneously, or that two-body reactions should not be assumed. Thus the tritium issue remains unresolved and deserves strong study. Likewise, the question of helium production remains uncertain, the few measurements attempted to date being inconclusive.

Note that some reactions in Table I involve proton or deuterium reactions with palladium. This would result in a variety of products including stable palladium isotopes and various beta emitting isotopes of Rh, Ag and Pd. The existence of these isotopes could be determined through a mass spectrographic analysis of electrode material. Also, electrodes with isotopically enriched palladium could be used to further pinpoint these reactions. This important issue of palladium reactions is discussed in more detail in a later section.

OTHER REACTION POSSIBILITIES

Some additional reaction possibilities that have been suggested are summarized in Fig. 2. Since this can serve as an important guide to nuclear product diagnostics we will discuss each briefly in turn from that point of view.

The NATTOH model, proposed by T. Matsumoto[3], assumes that deuterons are compressed in the metal electrode to such a high effective pressure so that three or more can "condense" to form a cluster. With cluster formation, many-bodied fusion reactions of the type illustrated in Fig. 3 are possible. Indeed, Matsumoto has reexamined the radiation spectrum reported by Pons and

. Nattoh model (T. Matsumoto, Ref. 3)

$$\text{many body} \rightarrow {}^6\text{Li}^*,\ {}^8\text{Be}^*,\ {}^{10}\text{B}^* \rightarrow \text{MeV } \gamma\text{'s}$$

. Fast ion slowing, knock ons, chaining (R. Bussard, Ref. 4)

$$d + d \rightarrow t + p + 4\text{MeV}$$

$$E_T \rightarrow \begin{cases} 0.071 \text{ to d} \rightarrow \text{up scatter} \rightarrow <\sigma v>\uparrow \text{ etc.} \\ 0.276 \text{ to Pd} \rightarrow \alpha + \text{Rh}^* \ (\text{Ag}^*) \\ 0.653 \text{ to e} \end{cases}$$

[Note: 14 MeV neutrons from t + d]

· Neutron chain (Jackson, Ref. 5)

$$n + {}^{104}\text{Pd} \rightarrow {}^{105}\text{Pd} + \gamma$$
$$\gamma + d \rightarrow p + n$$
$$n + d \rightarrow p + 2n$$
[Note: Pd transmutation]

. Neutron Chain (Y. E. Kim, Ref. 6)

$$n + \begin{cases} {}^6\text{Li} \rightarrow {}^4\text{He} + t \\ {}^7\text{Li} \rightarrow {}^4\text{He} + t + n \end{cases}$$

$$\rightarrow + d \rightarrow {}^4\text{He} + t$$

[Note: ${}^7\text{LiOD} \rightarrow \text{ht}\downarrow$; $H \rightarrow \sigma^n_{Abs}$

$$N + {}^{108}\text{Pd} \rightarrow {}^{109}\text{Pd}^* + \gamma (<6.2 \text{ MeV})$$

$$\gamma + d \rightarrow p + n \ (< 2 \text{ MeV})$$
[Note: Pd transmutation products]

. Nuclear Mass Resonance (R. McNally, Ref. 8)

$${}^6\text{Li} + d \rightarrow {}^8\text{Be} + 22.28 \text{ MeV}$$

$$\begin{cases} \rightarrow 2\alpha \\ \rightarrow n, p, d, \alpha \ldots \end{cases}$$
[Note: variety of nuclear products]

· Neutron and Deuteron Tunneling (G. Collins, Ref. 9)

$${}^6\text{Li} + {}^6\text{Li} \begin{cases} {}^7\text{Li} + p + \alpha + 3.6 \text{ MeV} \\ \alpha + t + p + \alpha + 1.1. \text{ MeV} \end{cases}$$

α, t products; also rate $\sim n^2_{Li}$

$$d + d + e^- \rightarrow {}^4\text{He} \ (20 \text{ MeV}) + e^- \ (3.7 \text{ MeV})$$

$$\rightarrow t \ (0.08 \text{ MeV}) + p \ (0.23 \text{ MeV})$$
[Note: t, e^-, X-ray products]

. Oppenheimer-Phillips (M. Ragheb and G. Miley, Ref. 11)

$$d + {}^A\text{Pd} \rightarrow {}^{A+1}\text{Pd} + p + \sim 4.8 \text{ MeV}$$
$$d + d \rightarrow t + p + 4.03 \text{ MeV}$$
[Note: represents "deuteron disintegration" (vs.
fusion); transmuted Pd isotopes are products]

Figure 2. Other Reaction Possibilities.

**Attention is called to key products of
interest for diagnostics in the notes.**

$$3D \rightarrow {}^6Li* \rightarrow {}^4He + d$$
$$\searrow {}^6Li + \gamma$$

$$4D \rightarrow {}^8Be* \rightarrow 2\,{}^4He$$
$$\searrow {}^8Be + \gamma$$
$${}^7Be* + n$$
$${}^7Li* + p$$

$$5D \rightarrow {}^{10}B* \rightarrow 2\,{}^4He + d$$
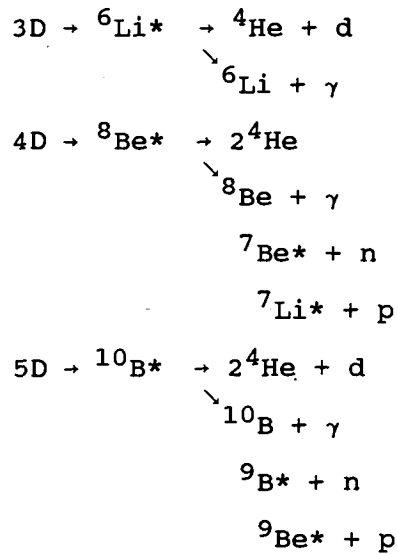$$\searrow {}^{10}B + \gamma$$
$${}^9B* + n$$
$${}^9Be* + p$$

Figure 3. Typical Cluster Reactions (Ref. 3).

Fleischmann and concluded that an alternate explanation for it is that the main peak of the gamma rays observed may correspond to the 2.185 MeV gamma from $*Li^6$ while $*Be$ contributes to the "wings" of the spectrum (see Fig. 4).

R. Bussard[4] has considered an interesting explanation for mechanisms in cold fusion. We cannot consider details of his theory here, but of particular interest for diagnostics is the fact that he predicts energetic reaction products which transfer energy to background d, Pd and electrons as they thermalize. He finds in a typical case that tritium from d-d reactions would slow down transferring about 7% of its energy to the deuterium. Of the remaining energy, about 28% goes to palladium and about 65% to electrons. The energy going to palladium would ultimately fill up via reactions leading to alphas and Be and subsequent reactions led to radioactive Ag. One "telltale" product from this process would be 14-MeV neutrons caused by d+t reactions
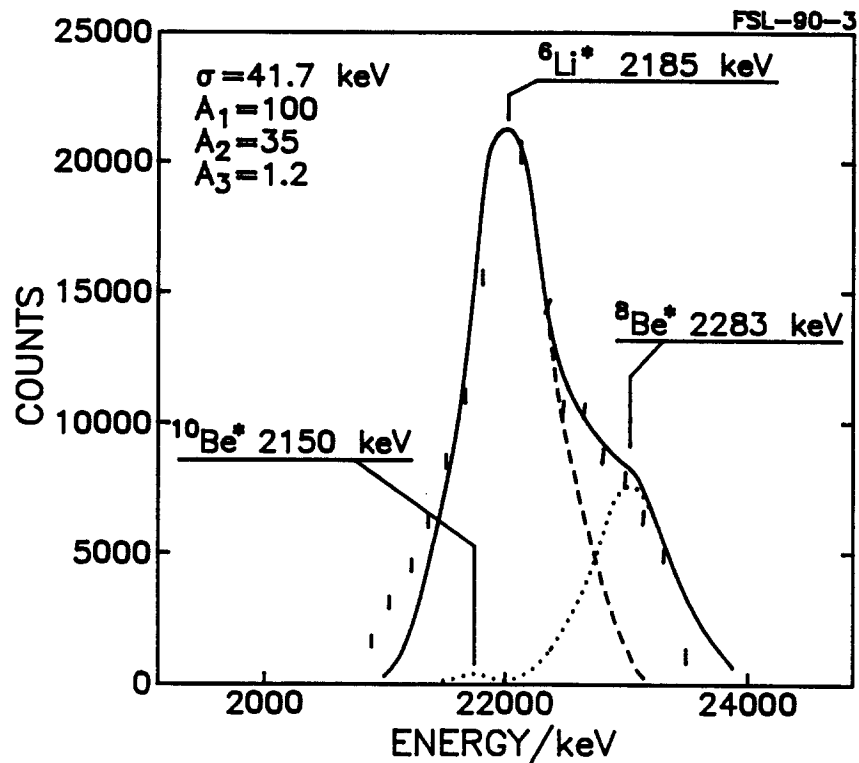
Figure 4. Alternate explanation for the spectrum around 2.2 MeV proposed by Matsumoto[3].

during the slowing down of the tritium. R. Bussard estimates a tritium slowing down time of the order of 3×10^{-8}s, in which case sufficient 14-MeV neutrons should be emitted to be detectable. Indeed this is an important issue that relates to several other proposed mechanisms where energetic tritium is produced from d-d reactions. Thus far 14-MeV neutrons have not been reported, but a continued search for this possibility seems warranted.

Several theories involve neutron chain reactions. For example, Jackson[5] has proposed a neutron chain where neutrons interacting with palladium produce gammas which in turn interact with the deuterium to produce a neutron. This neutron continues the reaction and would be multiplied through an n-d reaction, giving 2n. Jackson observes that a key signature of this chain would be the palladium transmutation products. This issue is

discussed further in the later section on palladium transmutation.

Another neutron chain mechanism has been proposed by Y. Kim[6]. His concept includes both the possibility of neutrons interacting with lithium in the electrolyte and with the palladium. Like Jackson, he views neutrons as a chain carrier and obtains neutron multiplication from γ + d reactions. Exactly how these chains could be self-sustaining, however, is not clear without an extensive reaction kinetic calculation. At any rate, palladium reaction products and low energy neutrons should provide telltale signals for this mechanism. An interesting point is that some recent experiments where heat production decreased with the use of Li^7 enriched lithium in the electrolyte[7] seem to be consistent with predictions from this theory. However, there are alternate explanations so this observation alone is not a conclusive demonstration of the mechanism.

R. McNally[8] has considered the possibility of a nuclear mass-energy resonance. This would lead to direct production of ^{4}He from d-d reactions. He also considers another possible resonance reaction that involves deuterium interacting with Li^6 in the electrolyte, perhaps on the electrode surface. The beryllium produced in this case could undergo various reactions releasing alphas, neutrons, protons, etc., so a careful search for these products would identify the mechanism.

An interesting possibility suggested by D. Collins[9] involves neutron or deuterium "tunneling." He points out that this might occur with either deuterium or Li^6 reactions. However, the most intriguing scenario for cold fusion cells follows from the compound nucleus energy level diagram illustrated in Fig. 5. Collins postulates that the high density of electrons in the palladium lattice allows an electron to carry off 3.7 MeV. Then the 20-MeV level could decay to a t + p pair with relatively low energies, namely,

Excitation (MeV)

25.5

23.85 d+d

22.1

21.1

20.6 ³He+n

20.1

19.8 Triton+Proton
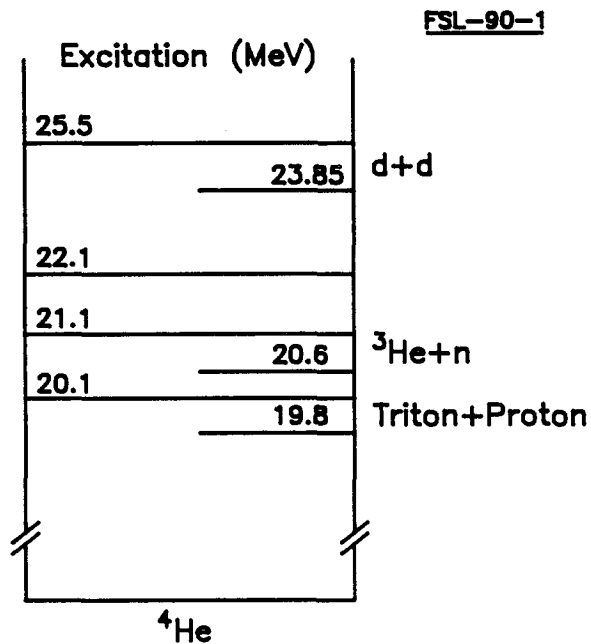
⁴He

Figure 5.   Energy Level Diagram (by Collins, Ref. 9). Electron
             collisions would remove 3.7 MeV, allowing low energy
             t + p products.

0.08 MeV and 0.023 MeV, respectively. Such tritons would have too low an

energy to produce many d-t reactions during thermalization. This could

explain the absence of "secondary" 14-MeV neutrons, which, as noted earlier,

have not yet been observed experimentally. The primary reaction should be

directly observable through the high energy electrons and subsequent X-ray

production. Thus a key diagnostic required would be X-ray detectors and cells

constructed with appropriate "windows" to allow the X ray to escape. Only a

few experiments have been arranged to look for X rays to date, and

unfortunately no definitive results have been reported[10]. A basic problem

appears to be that cells which have employed good X-ray diagnostics may not

have been operating, i.e., not undergoing "cold fusion."*

*This situation has occurred with other diagnostics also. Clearly more
 collaborative experiments are needed so the best diagnostics can be
 brought to bear on the best operating cells.

Another possible reaction involving energy transfer to electrons is illustrated in Fig. 6 where 23.8 MeV is removed, allowing decay directly to 4He. This process is analogous to reactions discussed by McNally, Hagelstein, and others where the 23.8 MeV is carried off by gamma emission. Energetically, however, this seems less likely than the t + p channel. Again, X-ray diagnostics should provide a distinctive signal.

Finally, we note that Ragheb and Miley[11] have discussed the possibility of (d,p) reactions in the palladium electrode itself based on an Oppenheimer-Phillips type deuteron disintegration mechanism. In other words, as the deuterium's wave function comes into palladium's Coulomb field, it becomes polarized so that the neutron component penetrates the field first. Consequently, the neutron component is captured while the proton component, which has not yet penetrated far into the field, is "split off." Reference 11 shows that this reaction produces a net energy of about 4.8 MeV which could, in principle, explain the heating as well as the failure to detect copious neutron emission (see Fig. 7). However, there is no known process of barrier penetration (tunneling, etc.) that would explain the high reaction rate, i.e., the many watts of power, found in some cold fusion experiments.* The claim is simply that should a mechanism be found to allow "easy" penetration of the Coulomb barrier, this reaction would be favored. For example, as shown in Fig. 8, for low-energy deuterium and a high-Z target, the Oppenheimer-Phillips reaction is favored by orders of magnitude over the Gamow penetrability of the potential barrier of the nucleus. From this point of view, the tritium

---

*The authors recently prepared a paper with H. Hora that examines the possibility that this may be explained in terms of an electrostatic double layer at the electrode surface (in press, "Plasma and Surface Tension Model for Explaining the Surface Effect of Tritium Generation at Cold Fusion," Nuovo Cimento, 12, 393, 1990).
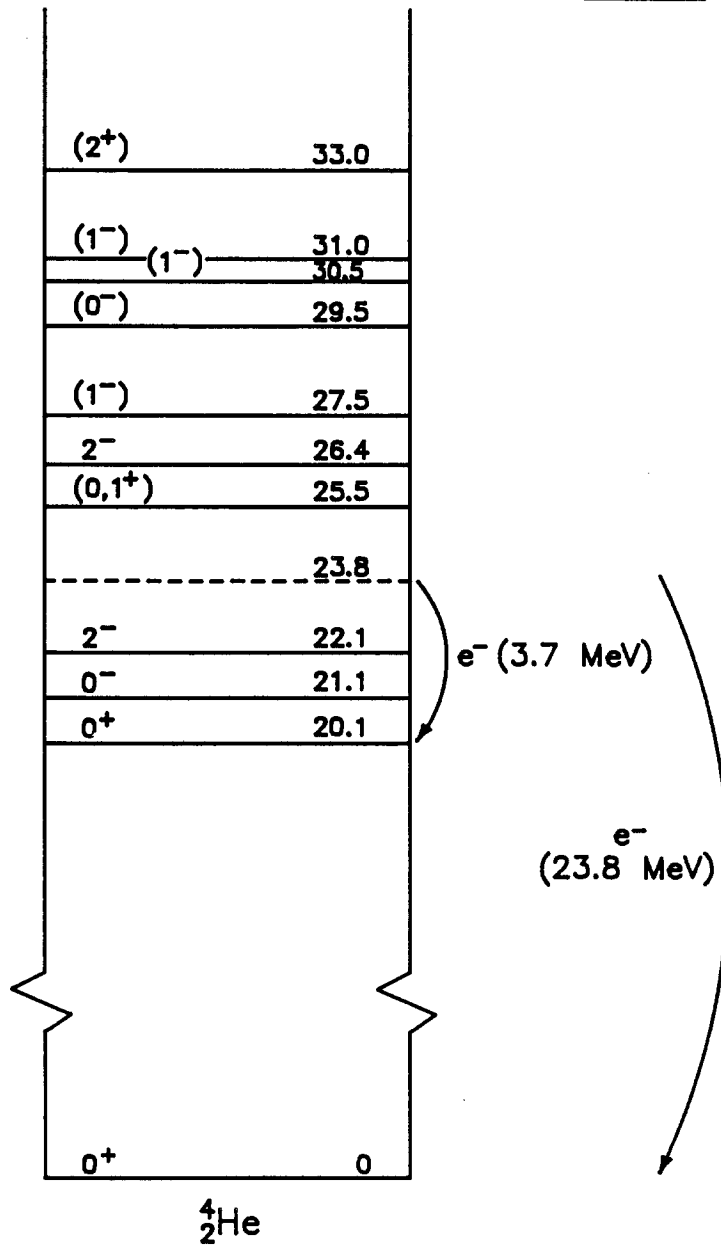
Figure 6. Energy Level Diagram (by Collins, Ref. 9). Energy transferred to electrons allows direct decay to ^{4}He.
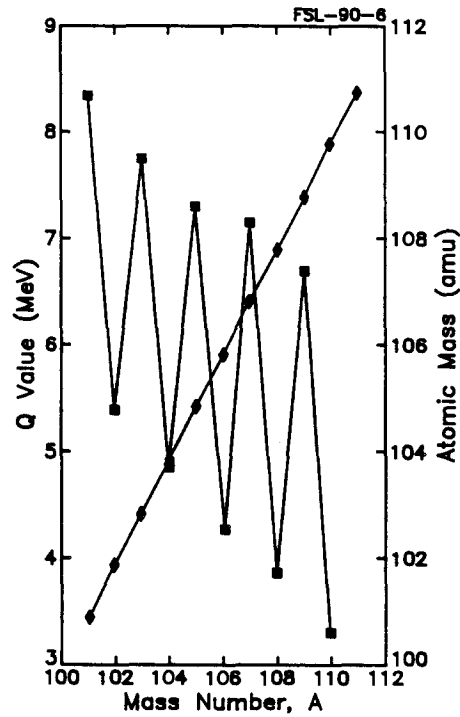
Figure 7.   Values of Q for the neutron capture reaction in
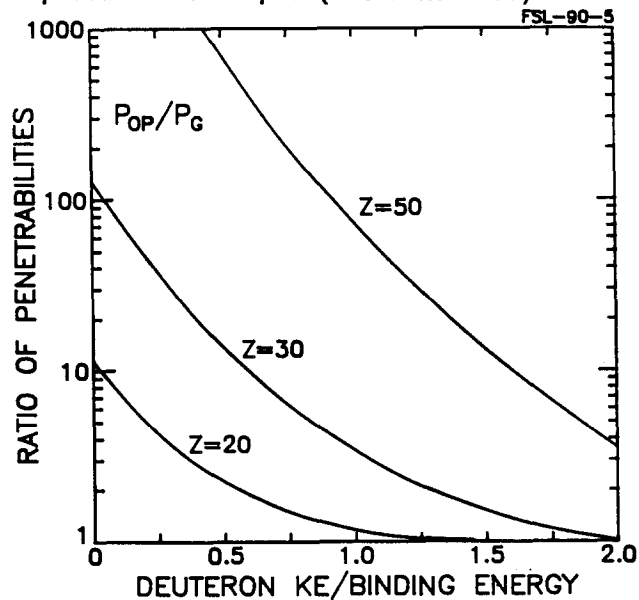palladium isotopes (after Ref. 11).

Figure 8.   The ratio of the Oppenheimer-Phillips to the Gamow penetrability of
the nucleus potential barrier for different values of the atomic
number Z as a function of the ratio of deuteron kinetic energy to
its binding energy, as reported by Bethe[12].

production observed in some cells would be attributed to the Oppenheimer-Phillips reaction for d-d which results in t + p production. This reaction would occur simultaneously with d,p reactions in the palladium, the latter producing the large heat rates.

One reason that the Oppenheimer-Phillips reaction is favored with deuterium is the remarkably low binding energy of deuterium relative to other nuclei (Table II). Indeed the only other nucleus having a lower binding energy is beryllium-9. Thus as suggested in the original discussion by Ragheb and Miley[11], alternate cold fusion reaction cells that might be considered could be based on beryllium reactions. Another possibility would be to use thorium or uranium electrodes in order to obtain an even higher Z which should be favorable (cf Fig. 7). The uranium or thorium electrode concept[11] is of particular interest for diagnostic tests since any neutrons produced would probably cause fission reactions. The resulting energy release (200 MeV/fission) would be even more significant and measurable than fusion neutrons. Also, the fission products could provide the basis for a sensitive detection technique based on their beta and γ-ray emissions.

Table II. Binding Energy (BE) for Typical Nuclei

Nuclide	BE(MeV)
^{2}H	2.2
^{3}H	8.5
^{3}He	7.7
^{4}He	28.8
^{6}Li	32.0
^{7}Li	39.2
^{9}Be	1.6
Average per nucleon	7-8

REACTIONS INVOLVING PALLADIUM TRANSMUTATION

Since several potential reaction mechanisms discussed earlier involve palladium transmutation by neutrons, we will consider this process in more detail here. Unique diagnostics, e.g., high resolution mass spectrometer analysis of electrode material, would be required to study this possibility. (Unknown to the authors when they prepared this paper for the EPRI/NSF workshop, a mass spectrometer analysis of electrode material is in progress at NRL by W. O'Grady and D. Rolison who described their work at the NSF/EPRI workshop.) In contrast, the detection of the other nuclear products such as neutrons, gamma rays, and X rays involves more conventional nuclear diagnostics while tritium can be measured by detection of its beta emission.

The natural abundances of the Pd isotopes are listed in Table III. If a neutron chain reaction occurs, the relative abundances would be modified according to their respective neutron capture cross sections. For example, average neutron cross sections are listed in Table III assuming a thermal neutron flux. Here the first line corresponds to the metastable state formation, and the second line to direct-ground-state formation. For illustration, note that neutron capture is favored in Pd 105. Thus one would expect its abundance (22.2 a/o in natural Pd) to be lowered relative to the other isotopes while that of Pd 106 (27.3 a/o) would be increased.

"Free" neutron reactions would occur if the mechanism involves a chain reaction such as suggested by Jackson and by Kim. Then the reaction rates would follow roughly* the neutron cross-section in Table III. In contrast, if a neutron splitting deuteron disintegration reaction (Oppenheimer-Phillips reaction) such as suggested by Ragheb and Miley occurs, the reaction

---

*A correction for the average neutron energy would be required.

Table III. Abundances and Neutron Cross Sections for Pd

Isotope	^{102}Pd	^{104}Pd	^{105}Pd	^{106}Pd	^{108}Pd	^{110}Pd
a/o(atomic %)	1.0	11.0	22.2	27.3	26.7	11.8
σ_γ (barns) *	5.0	?	10.0	0.013	0.20	0.02
**		10.0	90.0	0.28	12.00	0.21

  *   metastable state formation

  **   direct-ground-state formation

probability in the palladium would be roughly independent of the isotope involved. Then the reactions with large "free" neutron cross sections would no longer be favored over others. Consequently, a precise mass spectrometer resolution of the various palladium isotopes after operation of the cell should be capable of distinguishing between these two mechanisms. This should be a key objective of such experiments if palladium transmutation is confirmed.

A full understanding of the build-up of decay products due to neutron transmutation requires a computer study of various decay chains. This has not been reported to date so here we can make some general observations. For example, based on the half lives of the Pd radioactive isotopes (see Table IV), we would expect the long half-life isotope ^{107}Pd to start appearing in an electrode composed of natural Pd which does not contain significant ^{107}Pd. For "free" neutrons, the effect is somewhat inhibited by the low cross section for ^{106}Pd. However the effect could be enhanced for diagnostic purposes by

Table IV. Half Lives of Pd Isotopes

Isotope	Half-Life
^{103}Pd	17d
^{107}Pd	6.5×10^6y
^{107m}Pd	21.3s
^{109}Pd	13.43h
^{109m}Pd	4.69m
^{111}Pd	22m
^{111m}Pd	5.5h
^{112}Pd	21.1h
^{113}Pd	1.5m
^{114}Pd	2.4m
^{115}Pd	37s
^{116}Pd	14s
^{117}Pd	5s
^{118}Pd	3.1s

m: isomeric state

use of an isotopically enriched sample of ^{106}Pd. This would not be so crucial, however, should the Oppenheimer-Phillips reaction occur since ^{106}Pd transmutation would be relatively strong (but subsequent ^{107}Pd transmutations would quickly saturate its build-up).

In general, neutron capture either results in stable isotopes such as ^{106}Pd and ^{109}Ag or some radioactive species which will in turn decay to stable species. Figure 9 summarizes the major transmutation and decay chains. Interesting products that should be found after long runs include various isotopes summarized in Table V. Since ^{106}Pd and ^{108}Pd have the largest natural
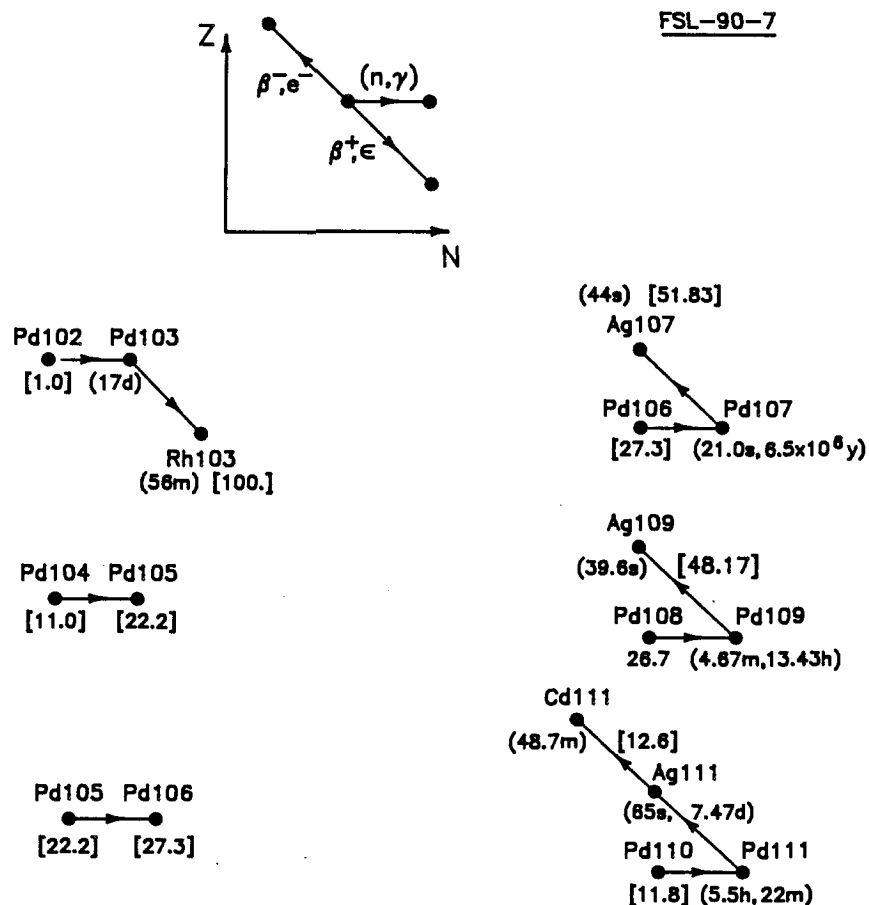
Z

β^-, e^- (n, γ)

β^+, ϵ

N

Pd102 Pd103
[1.0] (17d)

Rh103
(56m) [100.]

Pd104 Pd105
[11.0] [22.2]

Pd105 Pd106
[22.2] [27.3]

(44s) [51.83]
Ag107

Pd106   Pd107
[27.3]   (21.0s, 6.5x10^{6}y)

Ag109
(39.6s) [48.17]

Pd108   Pd109
26.7   (4.67m, 13.43h)

Cd111
(48.7m) [12.6]

Ag111
(85s, 7.47d)

Pd110   Pd111
[11.8] (5.5h, 22m)

Figure 9. Major Transmutation and Decay Chains for
Palladium Isotopes. Square brackets [] indicate
natural abundances. Half lives of isomeric
states given in parentheses () with s: seconds,
m: minutes, h: hours, y: years.

Table V. Possible Stable or Long-Lived Palladium
Isotopes Transmutation Products

From	Long Half Life	Stable
^{102}Pd		^{103}Rd
^{105}Pd		^{106}Pd
^{106}Pd	^{107}Pd (6.5x10^{6}y)	^{107}Ag
^{108}Pd		^{109}Ag
^{110}Pd		^{111}Cd

isotopic abundances in the Pd isotopes, the [109]Ag silver isotope and the long-lived [107]Pd should be prominent products. Mass spectroscopy or activation analysis could be used to detect the silver isotopes. Cadmium has a large neutron cross section, so activation analysis might also be used to detect it.

As silver is produced, depending on the amounts accumulated, a silver alloy of Pd would be formed. This would ultimately affect the metallurgical properties of the electrode in a measurable fashion. However, such an effect would only occur after very lengthy runs.

For convenience, Fig. 10 summarizes the decay schemes for several key species involved. The half-lives and branching probabilities will be needed to model the decay process. Also as seen from this figure, some of the decay emissions might be considered for diagnostic purposes.

CONCLUSION

The objective of nuclear product diagnostics is to identify the mechanism(s) involved in cold fusion. Thus the choice of diagnostics must be tied to a hypothesis (or conjecture) about the mechanism and the products involved. Any consideration of mechanisms must revolve around two key issues: how to explain the high reaction rates implied by some experiments and how to explain the unique branching ratios for reaction products that are observed. For example, there appears to be an indication from experiments at Los Alamos, Texas A&M, and Bombay[7,13,14] that the tritium production rate is a factor of 10^8 to 10^9 higher than the neutron production rate. Also, there is some possible confirming evidence for a large branching ratio from [3]He measurements during the cluster experiments at BNL[15]. However, it appears that the tritium production rate is still only able to account for 1 to 5% of the heating rate reported. These factors put together represent a very unique,
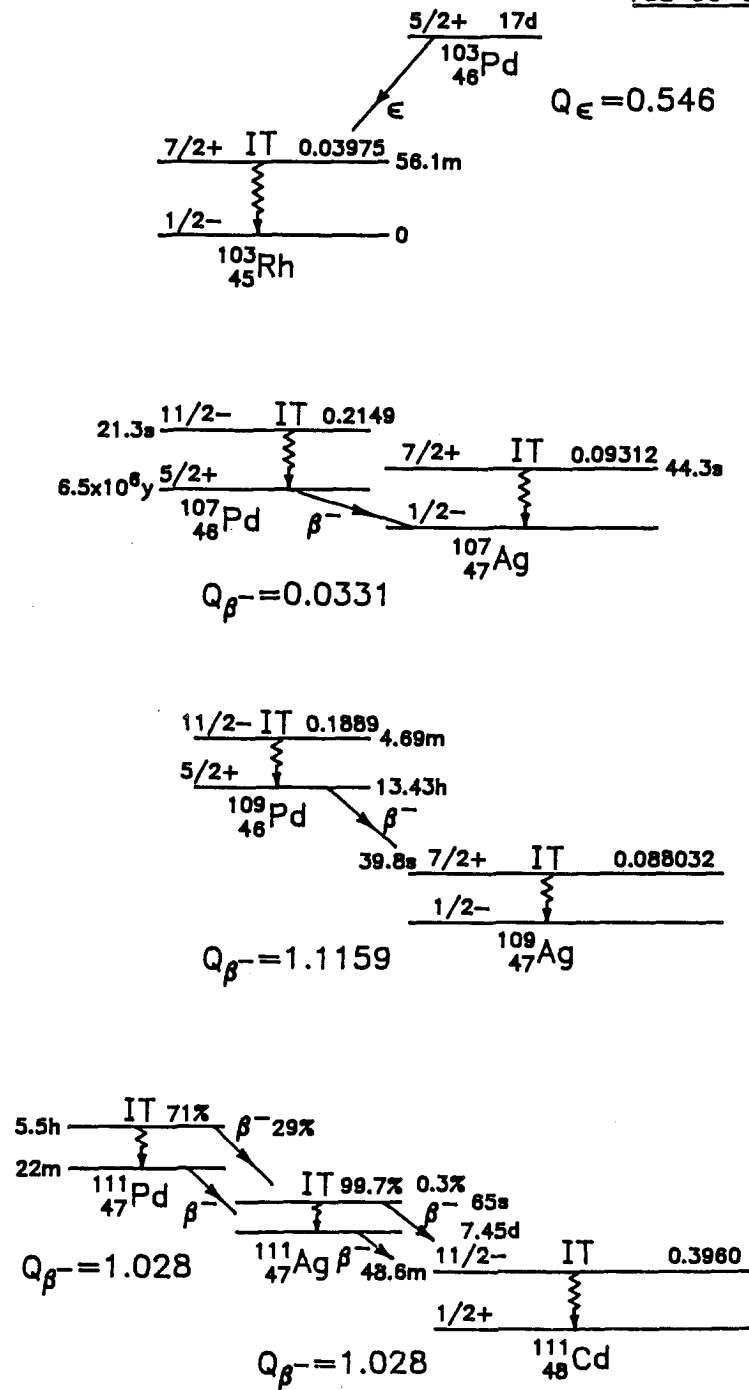
5/2+   17d
$^{103}_{46}$Pd

ϵ

Q_ϵ=0.546

7/2+ IT 0.03975 56.1m

1/2−   0

$^{103}_{45}$Rh

21.3s 11/2−   IT 0.2149

6.5x10⁶y 5/2+

$^{107}_{46}$Pd β^-

7/2+   IT 0.09312 44.3s

1/2−

$^{107}_{47}$Ag

Q_{β^-}=0.0331

11/2− IT 0.1889 4.69m

5/2+   13.43h

$^{109}_{46}$Pd β^-

39.8s 7/2+   IT 0.088032

1/2−

$^{109}_{47}$Ag

Q_{β^-}=1.1159

5.5h   IT 71% β^-29%

22m $^{111}_{47}$Pd β^-

IT 99.7% 0.3%
β^- 65s
7.45d

$^{111}_{47}$Ag β^- 48.6m 11/2−   IT 0.3960

1/2+

$^{111}_{48}$Cd

Q_{β^-}=1.028

Q_{β^-}=1.028

Figure 10.   Decay Schemes and Energy Levels for Key Species.

but, in some ways a mutually exclusive set of circumstances. At present it is very difficult to explain how the high reaction rates can occur. Various mechanisms that have been proposed however, might explain the branching ratios between reactions. For example, if the reaction were due to neutrons splitting (deuteron disintegration via Oppenheimer-Phillips reactions), the heating would occur from (d,p) reactions in the palladium. However, the tritium and neutron production would be attributed to the corresponding Oppenheimer-Phillips reaction of deuterium with itself, perhaps near the electrode surface. This would rationalize the high ratio of tritium/neutron production rate. Still it is not clear how tunneling (or whatever mechanism is involved) in the palladium would result in a higher rate for d,p reactions in the palladium than the corresponding d-d reaction.

The other possibility for tritium production, which might be more plausible in combination with heating via the d,p reaction in palladium, would be neutron/deuterium tunneling as suggested by Collins and discussed earlier. This would provide d-d reactions with low energy tritium production, avoiding 14-MeV neutron production.

While this line of reasoning provides some "clues," the mechanism involved remains a "wide open" issue. Thus we come back to the earlier discussion and again conclude that, in addition to an examination of the electrodes in search for palladium transmutation products and embedded helium (both He^4 and He^3), it is important to continue the search for neutrons, gamma rays and X rays with the objective of ultimately establishing both energy spectra and time history. In addition, certainly the study of tritium production which has already begun, should be continued with the goal of obtaining online measurements that can be time correlated with other products, e.g., with neutrons and heating rates. Other studies should focus on the

issue of the possible existence of the very low fluxes of 14-MeV neutrons due to the secondary reactions of product tritium with deuterium.

The above remarks concentrate on the broad range of reaction products. However in some specific experiments, more restricted objectives may be desirable. For example, in a number of instances neutron emission has been reported but the neutron energy was not measured. In those cases, neutron energy resolution is an obvious goal. Also diagnostics should be considered with the objective of explaining the nonreproducibility and long delay times preceding rapid rises in the reaction rates that are reported in some experiments. Whether or not these observations are unique to certain classes of experiments, e.g., cases involving crack propagation, dendrite formation, etc. (vs. generic characteristics associated with all experiments) is not clear. It is essential to resolve this issue in order to solve the "mystery" of cold fusion. However, the explanation will probably require a combination of nuclear product detection and a variety of other diagnostic techniques, e.g., a metallurgical examination of electrodes and electrode surfaces.

In closing, we would stress that the main thrust for fusion product detection should be to provide a correlation between several reaction products, thus shedding light on the mechanism involved, as well as unique characteristics such as the neutron bursts, delay times, etc. This will probably require an interdisciplinary team approach since the diagnostics involved span a variety of areas and optimized "operating" cells are difficult to obtain clearly a combination of the two requires experts input from several disciplines.

REFERENCES

1. D. Mueller and L. R. Grisham, "Nuclear Reaction Products that Would Appear if Substantial Cold Fusion Occurred," Fusion Technology, 16, 379, 1989.

2. P. L. Hagelstein, "A (Slightly Revised) Simple Model for Coherent DD Fusion in the Presence of a Lattice," Abstracts, Workshop on Cold Fusion Phenomena, Santa Fe, NM, May 23-25, 1989.

3. Takaaki Matsumoto, "'NATTOH' Model for Cold Fusion," Fusion Technology, 16, 532, 1989.

4. Robert W. Bussard, "Virtual-State Internal Nuclear Fusion in Metal Lattices," Fusion Technology, 16, 231, 1989.

5. J. C. Jackson, "Cold Fusion Results Still Unexplained," Scientific Correspondence, Nature, 339, 345, 1989.

6. Yeong E. Kim, "New Cold Nuclear Fusion Theory and Experimental Tests," Abstracts, Workshop on Cold Fusion Phenomena, Santa Fe, NM, May 23-25, 1989.

7. S. Srinivasan, Y. J. Kim, O. H. Murphy, C. R. Martin, and A. J. Appleby, "Evidence for Excess Heat Generation Rates During Electrolysis of D_2O in LiOD Using a Palladium Cathode: A Microcalorimetric Study," Workshop on Cold Fusion, Santa Fe, NM, May 23-25, 1989 (Los Alamos National Laboratory, Report LA-11686-C, p. 1, 1989).

8. J. Rand McNally, "On the Possibility of a Nuclear Mass-Energy Resonance in D + D Reactions at Low Energy," Fusion Technology, 16, 237, 1989.

9. Gary S. Collins, "Deuteron Tunneling at Electron-Volt Energies," Abstracts, Workshop on Cold Fusion Phenomena, Santa Fe, NM, May 23-25, 1989.

10. R. Fleming, F. Donahue, S. Mancini, G. Knoll, and B. Neuser, "An Attempt to Measure Characteristic X-Rays from Cold Fusion," Workshop on Cold Fusion, Santa Fe, NM, May 23-25, 1989 (Los Alamos National Laboratory Report, LS-11686-C, p. 17, 1989).

11. Magdi Ragheb and George H. Miley, "On the Possibility of Deuteron Disintegration in Electrochemically Compressed D+ in a Palladium Cathode," Fusion Technology, 16, 243, 1989. Also see: Abstracts, Workshop on Cold Fusion Phenomena, May 23-25, 1989, Santa Fe, New Mexico (to be published Journal of Fusion Energy).

12. H. A. Bethe, "The Oppenheimer-Phillips Process," Physical Review, 53, 39, 1938.

13. E. K. Storms and C. Talcott, "Attempts to Understand and Reproduce Cold Fusion," Abstracts, Workshop on Cold Fusion Phenomena, Santa Fe, NM, May 23-25, 1989.

14. BARC Studies in Cold Fusion (eds. P. K. Iyengar and M. Srinivasan), Bhabha Atomic Research Centre Report BARC-1500, 1989.

15. M. Rabinowitz and D. Worledge, "An Analysis of Cold and Lukewarm Fusion," Fusion Technology, 17, 344, 1990.

Section 12

SOURCES OF EXPERIMENTAL ERROR IN MEASURING NUCLEAR
PRODUCTS ASSOCIATED WITH THE ANOMALOUS BEHAVIOR OF
DEUTERIUM/PALLADIUM SYSTEMS

Nathan J. Hoffman

ETEC

SOURCES OF EXPERIMENTAL ERROR IN MEASURING NUCLEAR PRODUCTS ASSOCIATED WITH THE ANOMALOUS BEHAVIOR OF DEUTERIUM/PALLADIUM SYSTEMS

by   Nathan J. Hoffman, ETEC, Rocketdyne

Introduction

Many experimenters are attempting to measure ^{3}He, ^{4}He, neutrons, tritium and isotopic changes while exposing deuterium-rich palladium to an environment high in deuterium under non-steady-state conditions. In this chapter we will discuss sources of error in the quantitative analyses of those products. Each of these five possible nuclear effects will be discussed in terms of sampling, background, and analysis technique.

^{3}He

^{3}He Sampling:

^{3}He is analyzed by evaporating between 10 and 30 mg of palladium cathode material in an especially adapted mass spec capable of resolving DH from ^{3}He masses.

The lower limit of detection of ^{3}He is approximately 10^9 total atoms within the mass spec. Since a typical cathode mass is greater than 1000 mg, usually less than 1 percent of the cathode is used. Therefore, the minimum number of ^{3}He atoms that can be detected is $\sim 10^{11}$ atoms. If the ^{3}He was generated within the palladium during one thousand seconds of a 3×10^6 second electrolysis, any ^{3}He generation rate of $<10^8$ events/second would be non-detectable. If ^{3}He is generated in the D_2 gas bubble phase on the PdD surface, the ^{3}He will not diffuse into the PdD. Only the fraction driven in would be present within the cathodes.

^{3}He Background:

There is no ^{3}He background problem.

^{3}He Analysis:

The presence of a large number of DH molecules in the mass spec can result in a false positive reading for ^{3}He (Figure 1). This is avoided by extensive gettering of all hydrogen isotopes within the mass spec. Other sources of false positive readings would be contamination from tools used to prepare the 10 mg mass spec sample or belching of ^{3}He from the walls of the mass spec because of inadequate cleaning of the instrument.

^{4}He

^{4}He Sampling:

Considerations involving the relative masses of mass spec specimen to cathode are the same as for the ^{3}He.

^{4}He Background:

Although helium does not diffuse through metal, most glasses do not prevent the serious contamination of sample gas by the helium in air.

An additional background problem for the measurements occurs because ^{4}He implantation is sometimes performed on drawn palladium wire in order to create nanometer grain sizes on the very surface of cathodes. Such ultra fine-grained surfaces often show very high heat of hydrogen adsorption[1] and may be important in anomalous palladium behavior in deuterium versus protium. Any such ^{4}He implantation varies widely in the number of ^{4}He atoms per square mm of surface along the length of the same palladium wire, obscuring any possible reading of created ^{4}He results.

^{4}He Analysis:

^{4}He is much easier to distinguish from D_2 than ^{3}He from DH.

Helium Summary

Measuring no He within a cathode still allows a total of 10^{11} He producing events to have occurred uniformly with the solid. If the He is postulated to be created within the bubble phase on the surface, any level of the He production may have occurred.

Neutrons

Neutron Sampling:

Most experimenters that find neutrons observe bursts of several hundred neutrons occurring within 10 or 15 minutes of a stepped change in electrolysis conditions. The "storage bin" time must be short enough to distinguish such bursts from background (obviously, a 3600 second collection time with one stepped change will add a minuscule ~0.1 neutrons/second to the background). On the other hand, a sufficient number of bins must be sampled to show no bursts occur during steady state electrolysis.

Neutron Background:

Microphonic phenomena in the amplification circuits are often mistakenly assumed to be neutron events even by experienced neutron scientists used to working at higher flux levels than those of interest here. The true neutron background due to cascades of neutrons from interactions of cosmic rays (usually high energy protons) with matter in the vicinity of the detector changes from day to day and even has a diurnal pattern.[2] Such variations are shown in Figure 2. Movement of mass in the vicinity of the detectors will create a difference in background. In particular, neutron detectors that do not contain large amounts of heavy metal are very susceptible to neutrons cascading from interactions of cosmic rays and human bodies. Tons of lead are added to the detectors used to monitor the daily neutron background at Climax, Colorado, and Thule, Greenland, for example, just to avoid the peaks created by humans in the detector room. Measuring very low neutron levels is an art quite different from the usual neutronics work done around reactors or radioactive sources. The reader is referred to the very extensive literature by Simpson of the University of Chicago on this subject.[3]

Changes in the neutron background because of solar activity are quite marked. In general, the quieter the sun, the higher the neutron counts due to cosmic rays. An active sun, however, can change the geomagnetic cut-off at a particular geomagnetic latitude, allowing lower energy cosmic rays to get through to the earth's surface than normally would be allowed. There is a service in Boulder, Colorado, that will provide the hourly neutron background as measured at one of their stations (Climax, Colorado, by Leadville, in the United States).

Neutron Analysis:

Individual detectors have been built and checked out for these types of experiments, and the reader is referred to these papers for characteristics unique to each setup.

Neutron Summary

Microphonic artifacts and changes in background can result in false positive readings. Extensive experience in neutron measurements at higher flux levels does not assure that measurements taken at near background levels will be taken correctly. Burst events in the hundreds of neutrons will be missed if collection times are on the order of one hour or more. These neutron bursts are associated with step changes in electrolysis conditions, and measurements are needed at the appropriate times.

Tritium

Tritium Sampling:

Tritium is the principal nuclear product reported in the palladium/deuterium experiments. The deuterium gas within the palladium cathode usually does not contain the created tritium. The tritium buildup appears to be a dissolved DT gas within the electrolyte or in the gas bubbles leaving the palladium surface. If the gas is oxidized and returned to the electrolyte, the time between experiment and electrolyte analysis is not critical (the tritium half-life is just over 12 years). If the gas is not oxidized and returned to the electrolyte, the dissolved gas will leave the liquid phase within a day. Time requirements for sampling the palladium cathode is also

on the order of a day due to the ultra rapid diffusion (Figures 3 and 4), even when the cathodes are stored at dry ice temperatures.

Tritium sampling should always be performed on a liquid (i.e., oxidized) phase as gaseous analyses of D_2 are too insensitive in practice to be of use.

Tritium Background:

If protium buildup occurs within the electrolyte, the electrolyte can build up in tritium due to the preferential loss of D_2 as compared to DT.

If the milliamps/milliliter of electrolyte is unity or less, the buildup in the electrolyte is negligible. When protium is a serious contaminant, tritium buildup can be over two hundred percent if milliamp/milliliter values are greater than unity.

As-received heavy water or deuterium gas can have quite a variation of initial tritium values and should always be measured before any experiments are initiated.

Contamination of sample by inadvertent tritium addition is perhaps the most serious background problem. Running a sufficient number of blanks along with the cell of interest, combined with duplicate handling procedures, is the best contamination check.

Tritium Analysis:

Tritium analysis experts maintain that the characteristic tritium beta signal in the scintillation technique is unmistakable. Since tritium is the dominant nuclear produce claimed to be observed and various laboratories have confirmed each other's readings on the same liquid solution, the assignment of the observed spectra to tritium and only tritium is a critical technical assumption. Every tritium analyst contacted maintained that the tritium signature is unmistakable. If this is true, the problems in tritium measurement lie in sampling and background, not in the analysis technique.

Tritium Summary

The main problems in tritium measurements relate to missing tritium because of improper sampling techniques or measuring too much tritium because of contamination.

Isotopic Changes

Isotopic Changes Sampling:

Palladium cathodes almost always become covered with impurities during electrolysis. These impurities can be highly localized in whiskers or dendrites or uniform as in a solid layer. Some of these impurities overlap the atomic weight range of the palladium isotopes. SIMS analyses to measure atomic weight should be done at several locations to minimize the chances of missing a localized region.

Isotope Changes Background:

A major effort is being made to look for the enhancement of palladium 106 isotope at the expense of the 105 isotope. ZrO, a SIMS molecule formed from ZrO_2 surfaces, Cr_2D, and $Cr(OD)_3$ are all surface contaminants that can register as mass 106. Auger analysis should always accompany SIMS work to differentiate between identical masses of sputtered surface species.

Isotope Changes Analysis:

The surface science techniques for measuring surface chemistry are straightforward although preferential sputtering can distort quantitative analyses.
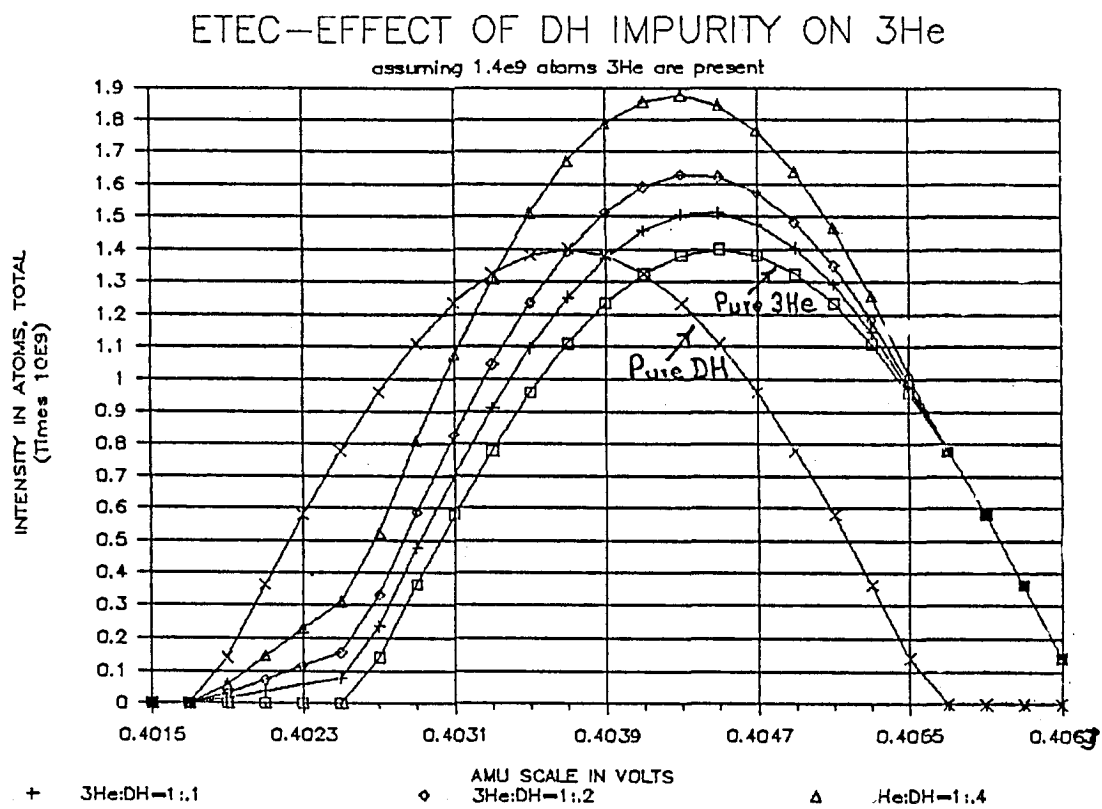
Isotope Changes Summary

The main problem with measuring surface isotope changes on palladium cathodes is the tramp elements that plate out on the cathode surface. Although these tramp elements may be

beneficial in producing nuclear products (such as iron dendrites and whiskers) or deleterious to the point of shutting down the production of such products (ZrO_2 layers), these deposits complicate any measurement of isotope changes.

REFERENCES

1. P. Chou and M. A. Vannice, "Calorimetric Heat of Adsorption Measurements on Palladium, I: Influence of Crystallite Size and Support on Hydrogen Adsorption," Journal of Catalysis, Vol. 104, p 1-16 (1987)

2. R. B. Mendell, H. J. Verschell, M. Merker, E. S. Light, and S. A. Korff, "Time Dependent Worldwide Distribution of Atmospheric Neutrons and of Their Products, 3. Neutrons from Solar Protons," Journal of Geophysical Research, Vol. 78, No. 16, p 2763-2778 (June 1, 1973)

3. J. A. Simpson, "Neutrons Produced in the Atmosphere by the Cosmic Radiations," The Physical Review, Vol. 83, No. 6, p 1175-1188 (September 15, 1951)

ETEC—EFFECT OF DH IMPURITY ON 3He

assuming 1.4e9 atoms 3He are present

VARIATION OF ³He READINGS WITH VARYING ³He/DH RATIOS

FIGURE 1
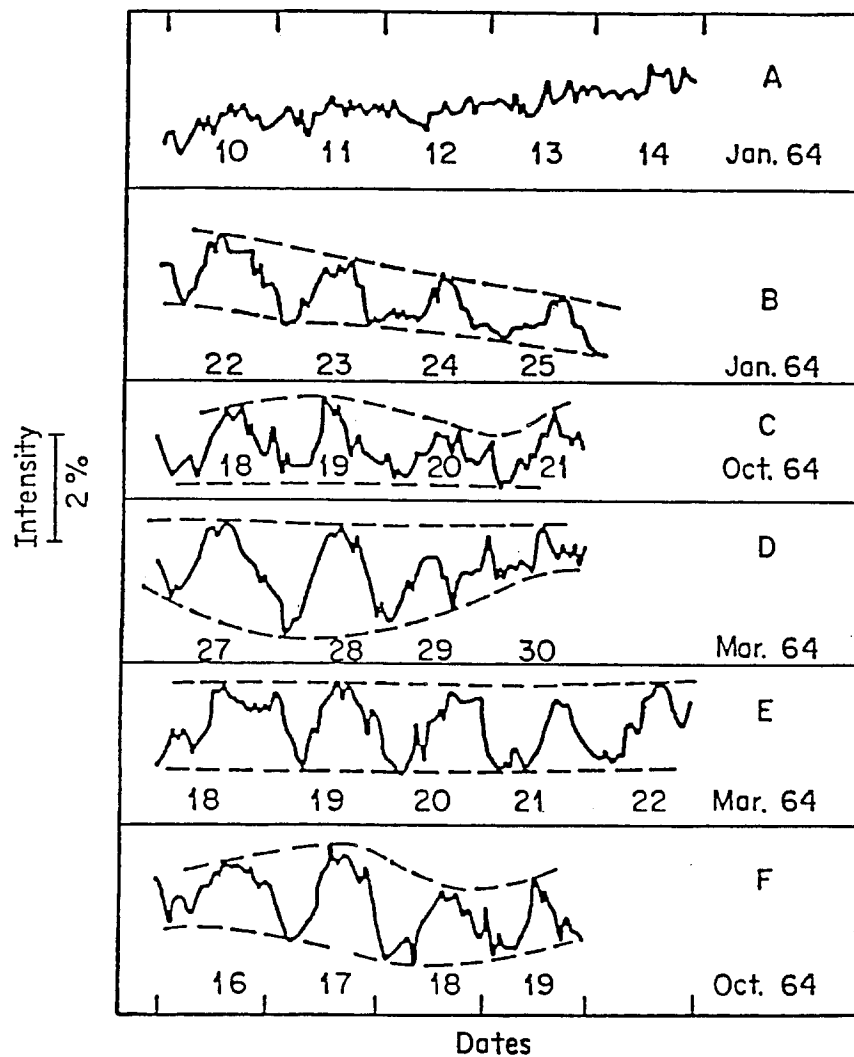
FIG. 11.40. Some sample patterns of diurnal variation in the year 1964. The curves show the deviations in the averaged rate for neutron monitors at Sulphur Mountain, Climax, and Calgary in North America. [*From Kane* (1965).]

FIGURE 2
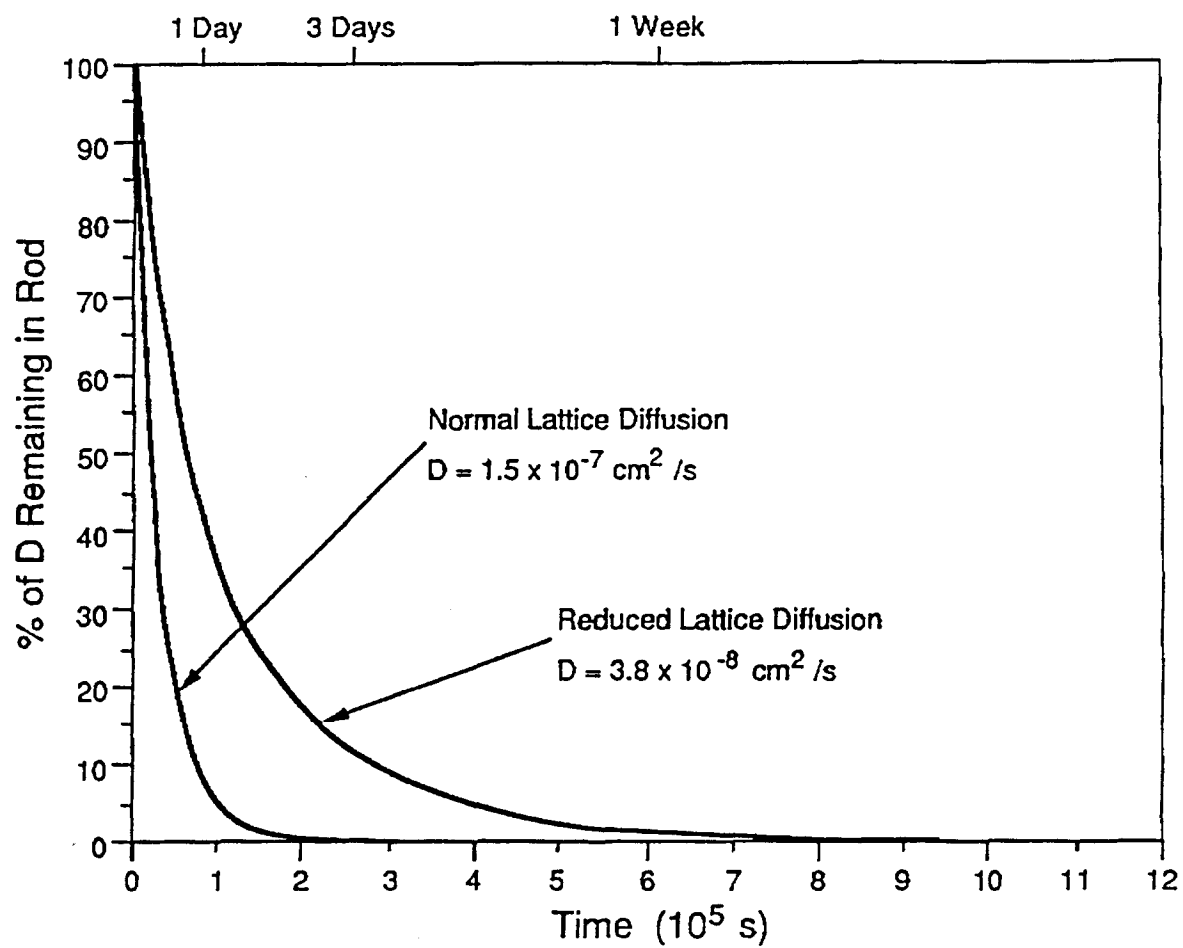
RETENTION OF DEUTERIUM IN 3 MM DIAMETER PALLADIUM RODS
IF STORED IN ICE (273)K)

FIGURE 3

12-11
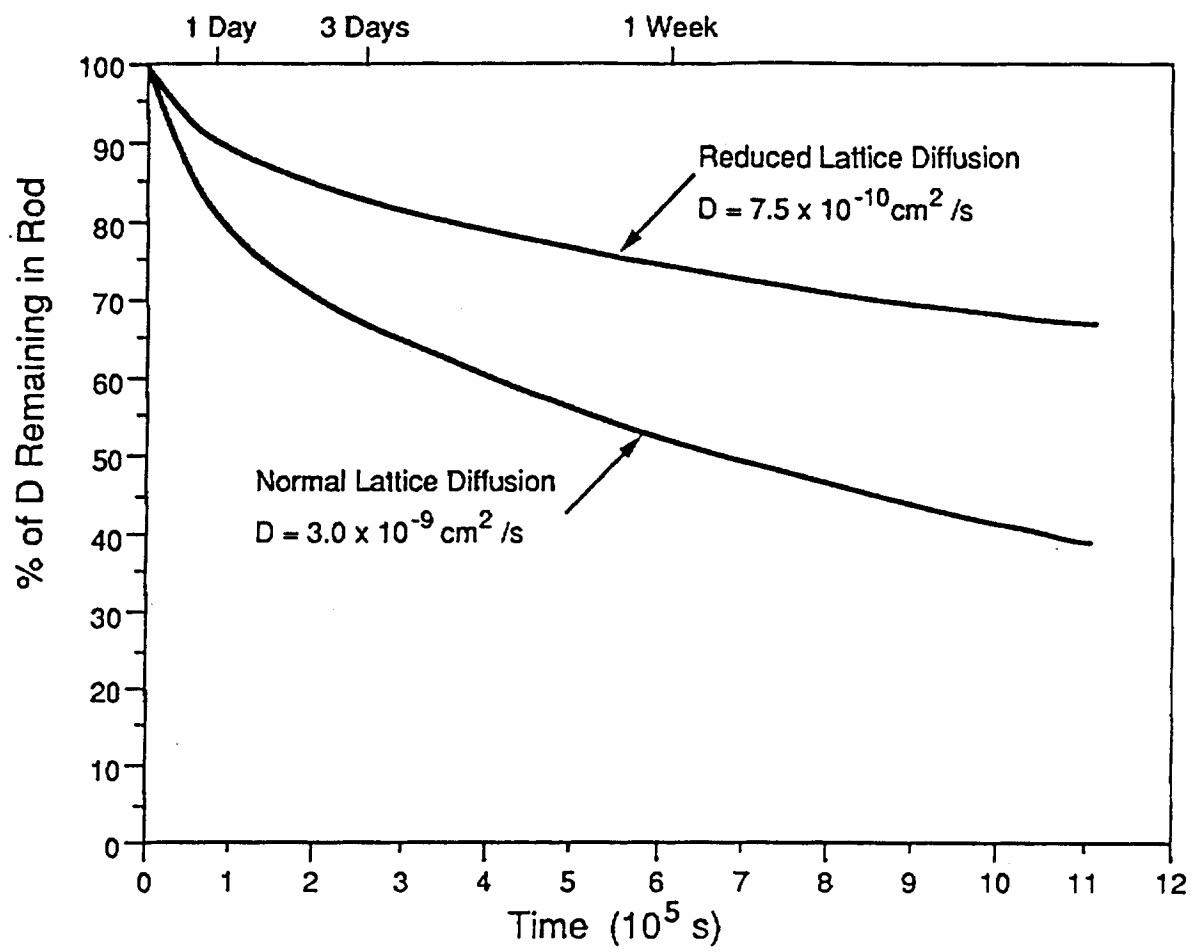
RETENTION OF DEUTERIUM IN 3 MM DIAMETER PALLADIUM RODS
IF STORED IN DRY ICE (195K)

FIGURE 4

DISCUSSION (HOFFMAN)

Fleischmann: What size sample did you use for the ^{3}He measurements?

Hoffman: The sample weighed about 2 g. The specimen evaporated for assay weighs about 10 mg.

Jones: What percentage average diurnal variation in cosmic ray neutrons was measured at Climax?

Hoffman: Typically, it is about ± 3 percent during the day, although the range can change. However, it is that order of magnitude at the altitude of the station, which is about 10,000 ft.

Jones: Can a neutron counter make measurements of cosmic ray events as precisely as you state?

Hoffman: The counter is a combination of three separate ^{3}He detectors, and it is sensitive to neutrons over a wide energy range.

Talcott: What was the stoichiometry of the PdD samples? Was it assumed that they were $PdD_{0.7}$, PdD, or some other value?

Hoffman: The stoichiometry was 0.7. The samples were in the β region at the PdD_0.7 composition.

Tritium Measurement: Methods, Pitfalls, and Results

C. Talcott, E. Storms, R. Jalbert, and M.A. David
Los Alamos National Laboratory

Let me begin this note with a conclusion: I see no way the large (10^3 to 10^6) tritium values reported throughout the world could be in error. The smaller values (10^2) type range require more scrutiny, but even those are unlikely to be in error.

There are a few places errors could be made in establishing these tritium numbers. The majority of these actually yield lower, not higher values. Those which could produce high values are
1) Droplets adhering to the outside of the pipette
2) Not changing pipette tips after sampling a high tritium level sample
3) Getting high tritium level into the shaft of the pipette
4) Using incorrect blanks and/or standards
5) Not allowing chemiluminescence to die away
6) Using an uncalibrated spectrometer
7) Using a single photomultiplier/non-coincidence spectrometer
8) Counting the sample for too short a time
9) Using contaminated supplies

Tritium Measurement: Methods, Pitfalls and Results

C. Talcott, E. Storms, R. Jalbert, and M. A. David
Materials Science and Technology Division, Los Alamos National
Laboratory

Roland A. Jalbert

*25 years working with tritium and tritium detection

*involved in the development, design, and inplementation of tritium
    instrumentation for 15 years

*for 12 years he has had prime responsibility for the design, implementa-
tion, and maintainance of all tritium instrumentation at a major fusion
technology development facility (Tritium Systems Test Assembly).

*Consultant on tritium instrumentation to other fusion energy facilities
    for 10 years (Tokamak Fusion Test Reactor at Princton)

Outline of Talk

General overview of how we take a measurement

Explain where errors may occur and the functioning of
   a liquid scintillation system

Show statistical evaluation and express why we are
   certain of our tritium data

Offer general questions you could ask anyone to
   reassure yourself of the accuracy of their data

Basic Steps in Tritium Content Evaluation for Cold Fusion

Select cell of interest and pipette 1 ml of fluid into plastic vial

Add blank and standards (D_2O, LiOD,H_2O tabletop) to plastic vials

Add scintillator and shake

Run vials in scintillation detector multiple times (we use 10 minute runs)

IF TRITIUM IS DETECTED:

Take a second,third and fourth sample

Neutralize and distill sample two

Run both for 24 hours nonstop in detector

Acquire an energy spectrum of the sample radiation

Send samples three and four to another lab for confirmation

Possible Sources of Error in Tritium Measurements

*pipetting
*blanks and sample containers
*scintillators and chemiluminescence
*quenching: chemical or optical
*machine stability or age
*pmt age
*natural radiation levels
*statistics

Pipetting Errors

Equipment error   0.12%

User error   ?
*bubbles in sample volume
*drops on outside of tip
*pipetting tip not on tightly
*incorrect lever use
*not changing pipette tips
*fluid into pipette shaft

Using the Right Blank

Enrichment appears too high if blank is rated artificially high

70cpm-ml	-50cpm-ml blank	20cpm-ml starting
100cpm-ml	-50cpm-ml blank	50cpm-ml final
	Yielding 2.5X enrichment	

70cpm-ml	-20cpm-ml blank	50cpm-ml starting
100cpm-ml	-20cpm-ml blank	80cpm-ml final
	Yielding 1.6X enrichment	

70cpm-ml	-50cpm-ml blank	20cpm-ml starting
220cpm-ml	-50cpm-ml blank	170cpm-ml final
	Yielding 8.5X enrichment	

70cpm-ml	-20cpm-ml blank	50cpm-ml starting
220cpm-ml	-20cpm-ml blank	200cpm-ml final
	Yielding 4X enrichment	

Chemiluminescence vs. time using Two Fluors

Time in Minutes (data is plotted at midtime of counting)
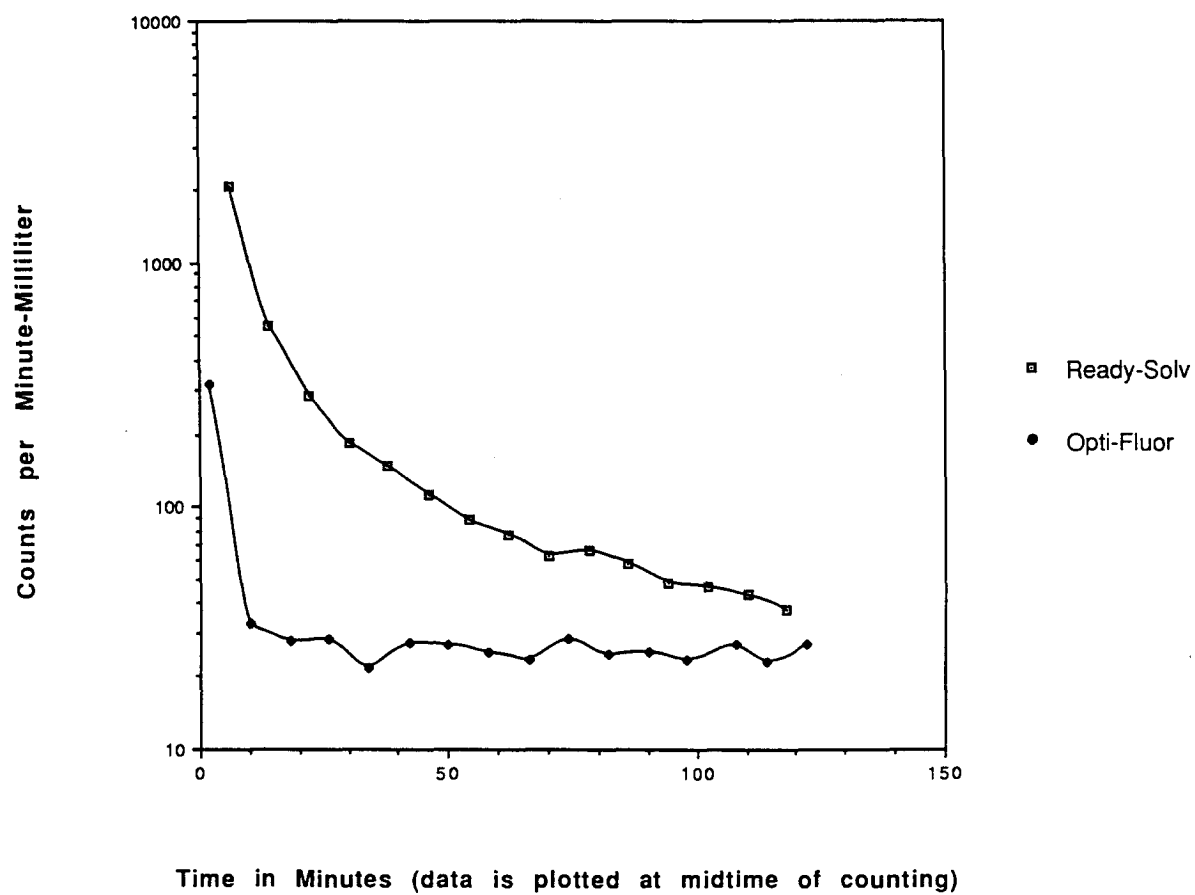
Molarity, Luminescence and Darktime
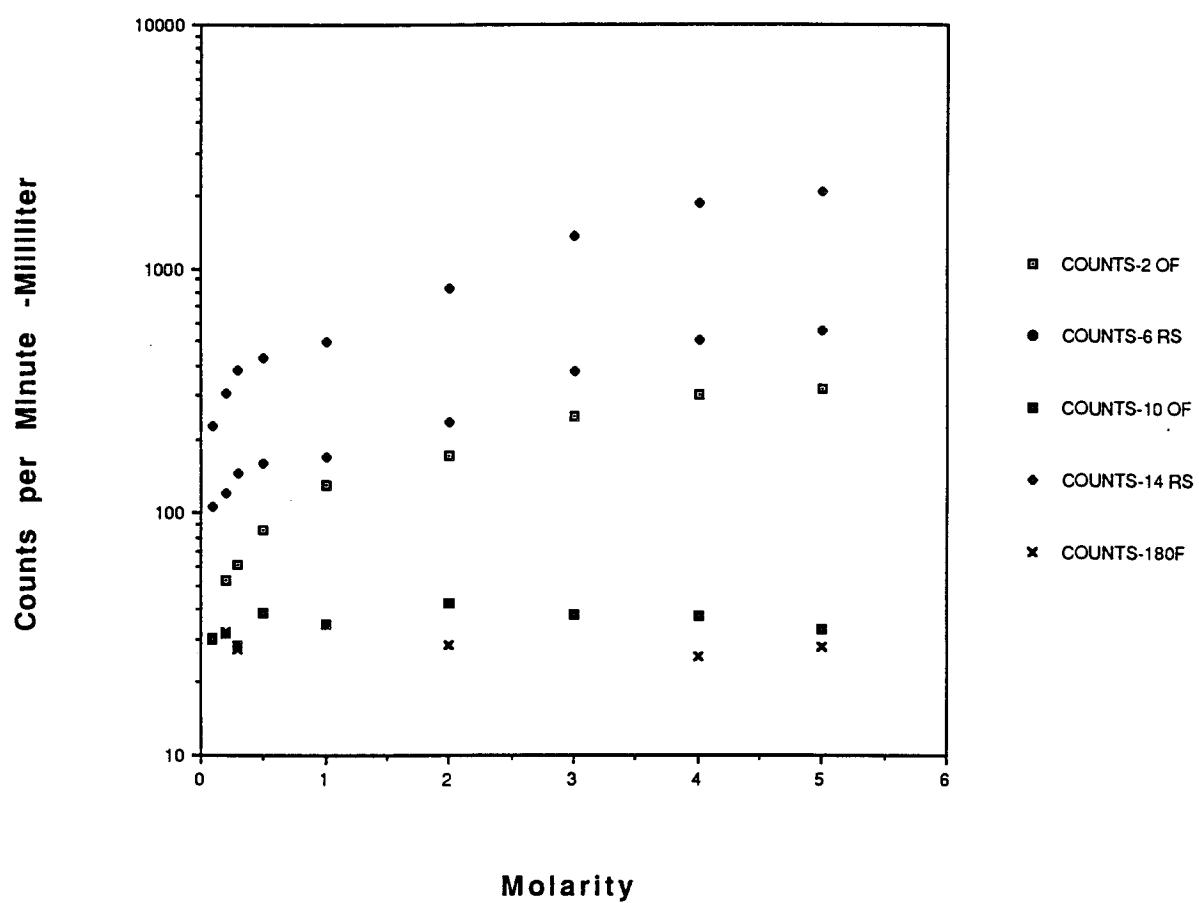
PACKARD

MATERIAL SAFETY DATA SHEET

HEALTH	1
FLAMMABILITY	1
REACTIVITY	1
PERSONAL PROTECTION	B

Alkylbenzene	CASRN	123-01-3
PPO	CASRN	92-71-7
bis-MSB	CASRN	13280-61-0
Tributyl phosphate	CASRN	126-73-8

PACKARD INSTRUMENT CO., INC. • 2200 WARRENVILLE ROAD • DOWNERS GROVE, IL 60515

PREPARER: G. Russell   DATE: 1/89   REVISION #: E

CHEMICAL NAME: Blend of long chain alkylbenzenes with scintillators PPO and bis-MSB and emulsifiers

SYNONYMS: None   CHEMICAL FAMILY: N.A.

FORMULA: N.A.   MOLECULAR WEIGHT: N.A.

TRADE NAME AND SYNONYMS: OPTI-FLUOR™

PHYSICAL DATA

BOILING POINT, 760 mm, Hg	518-590°F/271-312°C	FREEZING POINT	<-94°F/<-70°C
SP. GRAVITY (H₂O = 1)@20°C	0.900	VAPOR PRESSURE AT 20°C	<0.1 mm Hg
EVAPORATION RATE (BUTYL ACETATE = 1)	N.D.	SOLUBILITY IN WATER, % by wt. at 20°C	Slight, 0.1
% VOLATILES BY VOLUME	<1	VAPOR DENSITY (AIR = 1)	N.D.
APPEARANCE AND ODOR	Clear blue-violet fluorescent liquid with mild odor.		

HAZARDOUS INGREDIENTS

MATERIAL	%	OSHA PEL	ACGIH TLV	OTHER LIMITS RECOMMENDATIONS
Tributyl phosphate	<3		0.2ppm	

FIRE AND EXPLOSION HAZARD DATA

FLASH POINT (test method)	300°F/150 °C Tag closed cup	AUTOIGNITION TEMPERATURE	(BTU Value=134,713/gallon) 752°F/400 °C
FLAMMABLE LIMITS IN AIR, % by volume		LOWER 0.45	UPPER 10.7

EXTINGUISHING MEDIA	Dry chemical, carbon dioxide or foam
SPECIAL FIRE FIGHTING PROCEDURES	None
UNUSUAL FIRE AND EXPLOSION HAZARDS	None

EMERGENCY PHONE NUMBERS

DAY: 312/969-6000   NIGHT: D. MRKVICKA   312/858-0684
     800/323-5891   G. RUSSELL   312/ 972-0823

Legal responsibility is assumed only for the fact that all studies reported here and all opinions are those of qualified experts.

N.D. - NOT DETERMINED   N.A. - NOT APPLICABLE   < LESS THAN   > GREATER THAN
MSB-28

HEALTH HAZARD DATA

EFFECTS OF OVEREXPOSURE (ACUTE ANO CHRONIC)	Contact may cause slight irritation of eyes, skin and mucous membranes. May cause nausea, diarrhea or vomiting if ingested. No chronic effects are known.
ROUTE(S) OF ENTRY	INHALATION ☐ SKIN ☒ INGESTION ☒
EMERGENCY ANO FIRST AIO PROCEDURES	Remove to fresh air. Wash affected areas with soapy water. Flush eyes with running water for 15 minutes and seek medical attention if irritation persists.
CARCINOGENICITY	N.T.P. ☐ I.A.R.C. MONOGRAPHS ☐ OSHA ☐
MEDICAL CONOITIONS GENERALLY AGGRAVATED BY EXPOSURE	None

REACTIVITY DATA

STABILITY	CONDITIONS TO AVOID	
UNSTABLE ☐ STABLE ☒		Oxidation; ignition sources
INCOMPATIBILITY (materials to avoid)		Strong oxidizers
HAZARDOUS OECOMPOSITION PRODUCTS		None
HAZARDOUS POLYMERIZATION	CONOITIONS TO AVOIO	None
May Occur ☐ Will not Occur ☒		

SPILL OR LEAK PROCEDURES

STEPS TO BE TAKEN IF MATERIAL IS RELEASED OR SPILLED	Remove ignition sources, ventilate area. Absorb small spills with paper, diatomaceous earth or equivalent, with evaporation in a fume hood.
WASTE DISPOSAL METHOO	Sanitary sewer or incinerate in accordance with government regulations.

SPECIAL PROTECTION INFORMATION

RESPIRATORY PROTECTION (specify type)		None required		
VENTILATION	LOCAL EXHAUST	None	SPECIAL	None
	MECHANICAL (general)	Satisfactory	OTHER	None
PROTECTIVE GLOVES		Chemical proof	EYE PROTECTION	Splash-proof safety goggles
OTHER PROTECTIVE EQUIPMENT		None		
HYGIENIC PRACTICES		No eating, drinking or smoking in area. Wash after use.		

SPECIAL PRECAUTIONS

PRECAUTIONARY LABELING	WARNING! Contains the mildly irritating solvent alkylbenzene. Avoid contact with eyes and skin, prolonged breathing of vapor. Avoid sparks and open flame.
OTHER HANDLING ANO STORAGE CONOITIONS	Keep tightly closed. Protect from light. Store in a cool dry place with adequate ventilation.

PCN 8840021
MSB-28

Color Quenching

Raw Sample 5 Minute Counts

4286*   *low count from initial cloudiness

4532   (would be discarded statistically)

4510

4527

4557

4573

4583

4536

4528

Neutralized Samples with Discoloration over Time

initial	2 weeks later	3 months later
4828 (13203)	2108 (12400)	857 (9021)
4580 (12066)	2259 (12994)	916 (8724)
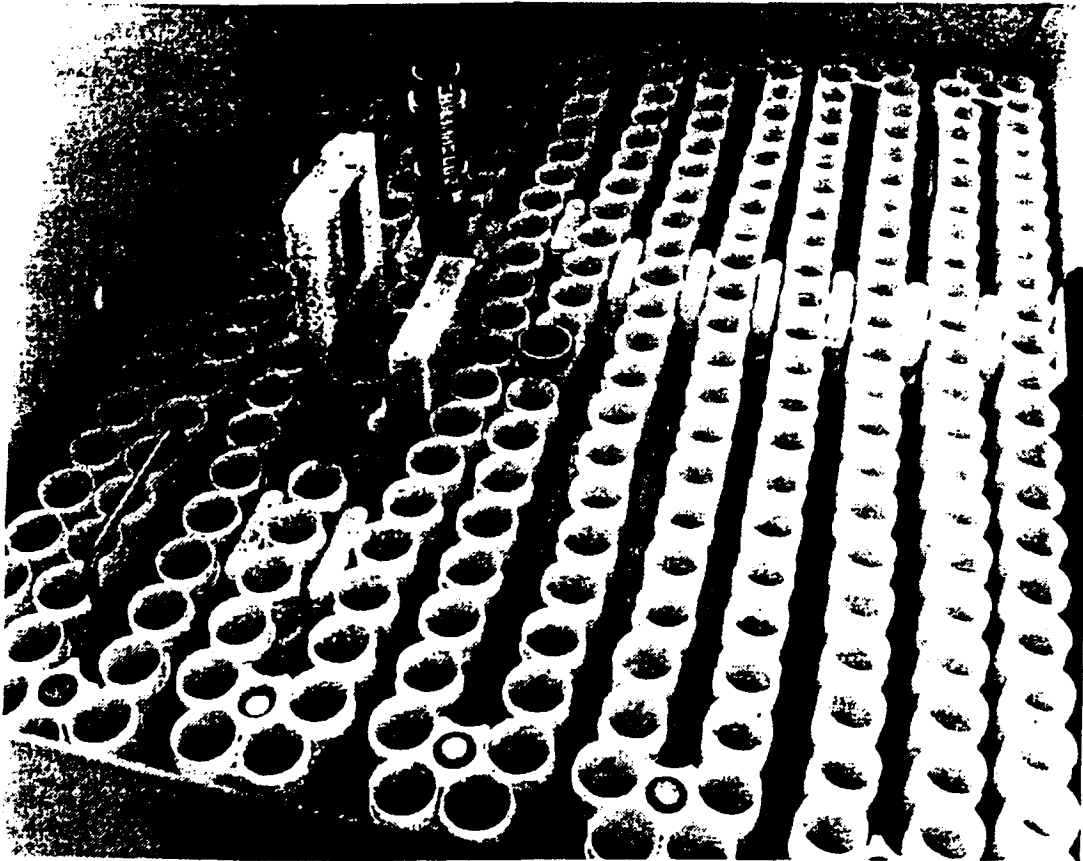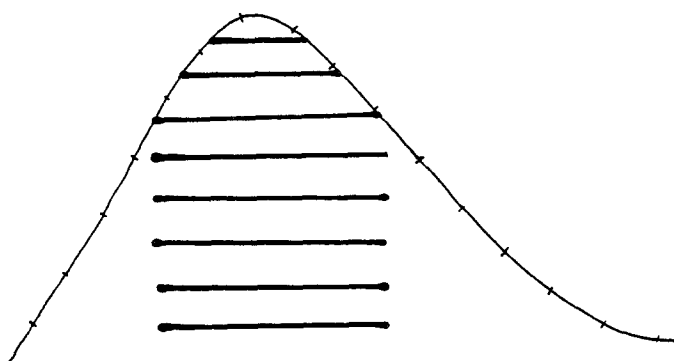
Figure 1-2. Sample Changer

COINCIDENCE

PMT

VIAL

PMT

H.V.
SUPPLY

COIN-
CIDENCE

SUM-
MATION

GAIN

B

ULD

A

LLD

REJECTION
GATE FOR
PULSES
EXCEEDING
ULD

COINCIDENT
ACCEPTANCE
GATE

RED
SCALER

GAIN

D

ULD

C

LLD

GREEN
SCALER
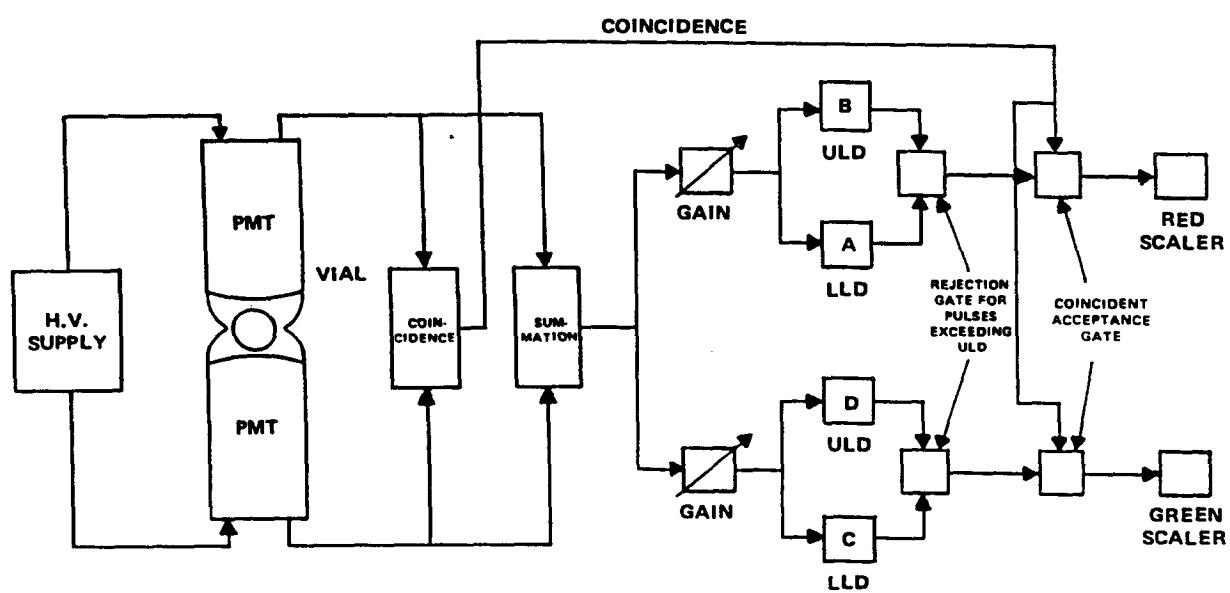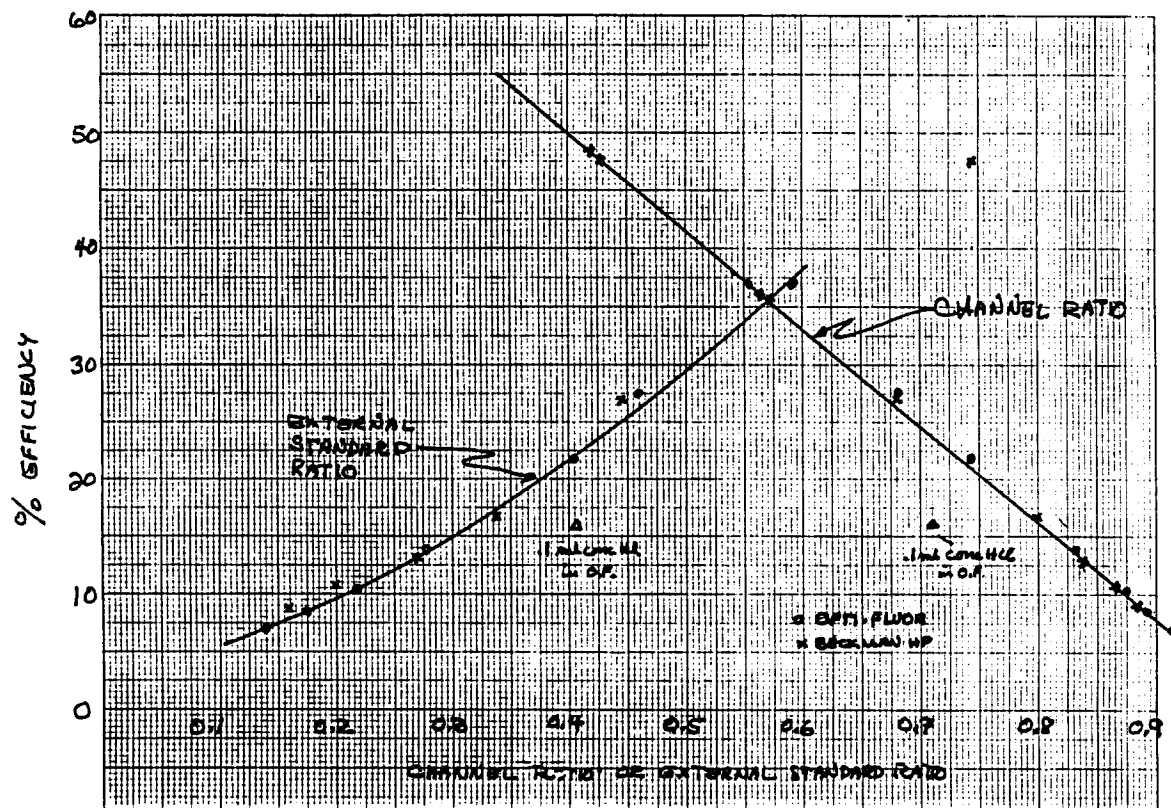
Channel Ratio Effect of Luminescence

—+— Higher Energy Spectra

SPECTRUM PLOT

1 KEV/POINT

```
   0   CPM                                                      797
  . . . . . . . . . . . . . . . . . . . . . . . . . . . . . . . . . . . . . . . . . . . . . . . .
  ******************************
  *****************************************************  .
  ***************************************************************************
  **********************************************************
  ********************************************
  *****************************
  ****************
  ********
  ******
  ***
  ***
  **
  *
  .
  .
  .
  .
  *
  *
  *
  *
  *
  *
  *
  *
  *
  *
  *
  *
  *
  .
  30   KEV
```

SPECTRUM PLOT
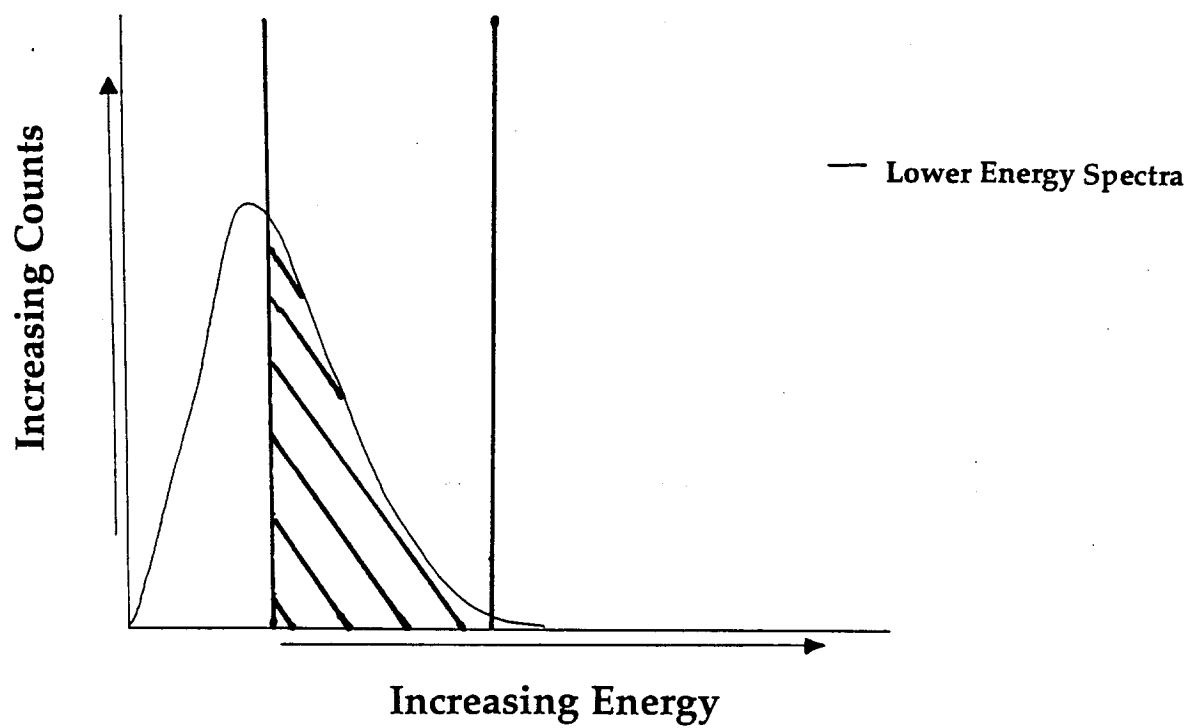
1 KEV/POINT

0 CPM   796
. . . .
¥*¥*¥*********¥***********¥****
¥***¥*****¥*¥****¥*****¥****¥****¥*******
¥***¥**¥*¥********¥**¥****¥***¥************¥*****¥*¥**
¥*¥**¥****K****¥***¥*****¥***¥*******¥****
¥****¥****¥**¥*¥***********¥****
¥***********¥******¥*
¥***¥***¥***¥
¥******¥
*****
***   THO spike from NBS (NIST) to show
**   Energy Specta for T containing sample

30 KEV

Statistics for Tritium Counting

Sample count rate = $\dfrac{N \pm \sqrt{N}}{T}$

N = Total Sample Count
T = Sample Counting Time
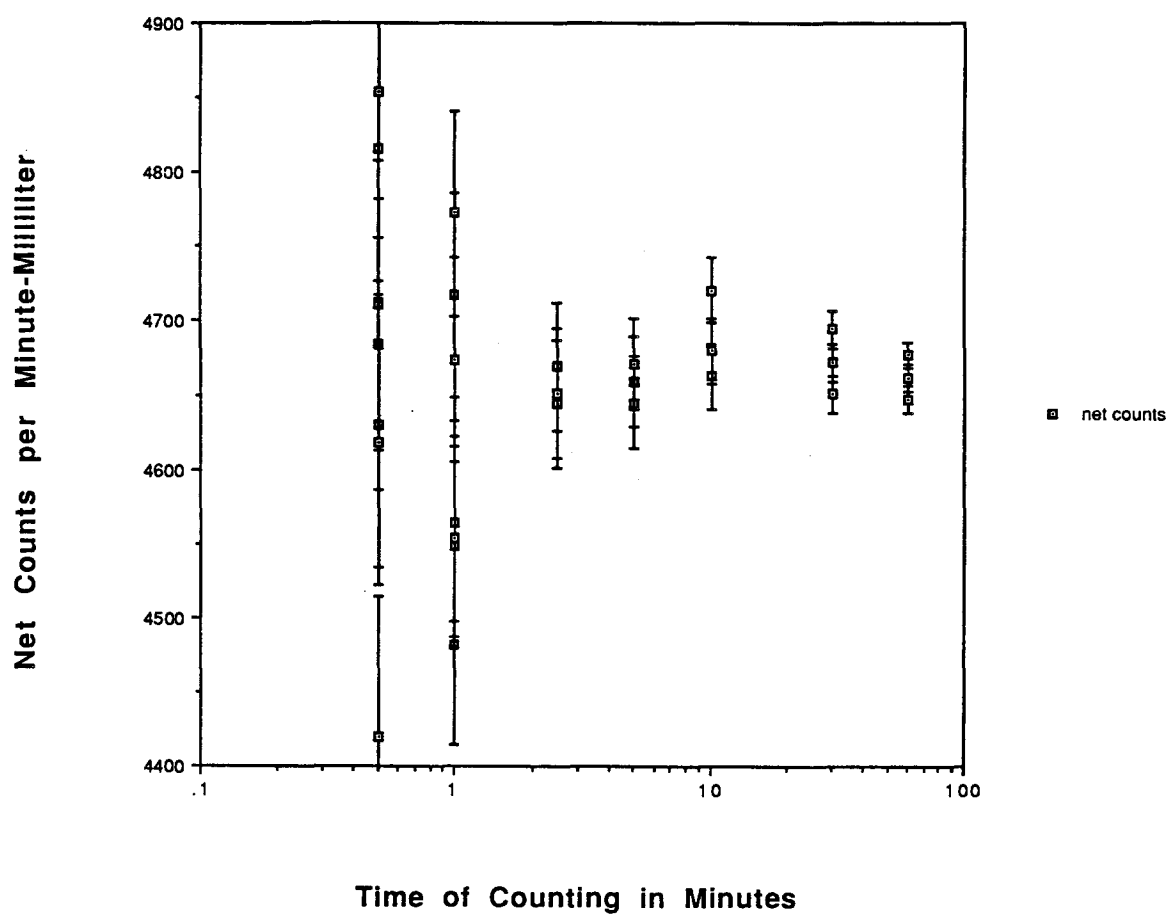
Background = $\dfrac{B \pm \sqrt{B}}{T'}$

B = Total Background Count
T'= Background Counting Time

Net sample count rate = $\dfrac{N}{T} - \dfrac{B}{T'} \pm \sqrt{\left\{ \left(\dfrac{\sqrt{N}}{T}\right)^2 + \left(\dfrac{\sqrt{B}}{T'}\right)^2 \right\}}$

Several observations $\sigma = \sqrt{\dfrac{\Sigma (N - \bar{N})^2}{n - 1}}$

n = Number of observations

Effects of Counting Time on Standard Deviation

Net Counts per Minute-Milliliter

Time of Counting in Minutes

net counts

Net Counts and Percent Error in Single Value Ten Minute Counts

counts (per min)	net counts (per min)	1 sigma	percent
25	5	2.1	41.2
50	30	2.6	8.6
75	55	3.1	5.6
100	80	3.5	4.4
150	130	4.1	3.2
200	180	4.7	2.6
300	280	5.7	2.0
400	380	6.5	1.7
500	480	7.2	1.5
1000	980	10.1	1.0

Chauvenet's Criterion for Rejecting a Value[a]

n	k	n	k	n	k
2	1.15	7	1.80	20	2.24
3	1.38	8	1.86	25	2.33
4	1.54	9	1.91	30	2.40
5	1.65	10	1.96	35	2.45
6	1.73	15	2.13	40	2.50

[a] n is the number of observations and k is the factor that, when multiplied by the standard deviation, defines the range from the mean beyond which values may be rejected for that n.

Questions You Might Ask to Reassure Yourself About Tritium Data

1) Are pipette tips changed after each sample is taken?
2) Do you run background and standards with each set of samples?
3) What type of scintillator do you use and what is your dark time?
4) Have you calibrated your equipment and is the channel ratio of your sample near 0.5?
5) What are you using for your blank?
6)* Is your detection system a dual pmt coincidence counter?
7) How long was each sample counted?
8)* Do you have an energy spectrum from the sample? If so, does the spectra match that of a tritium standard?

* If the answer to these questions is yes and the tritium count is   high,

Tritium Data for Spiked and Unspiked Samples
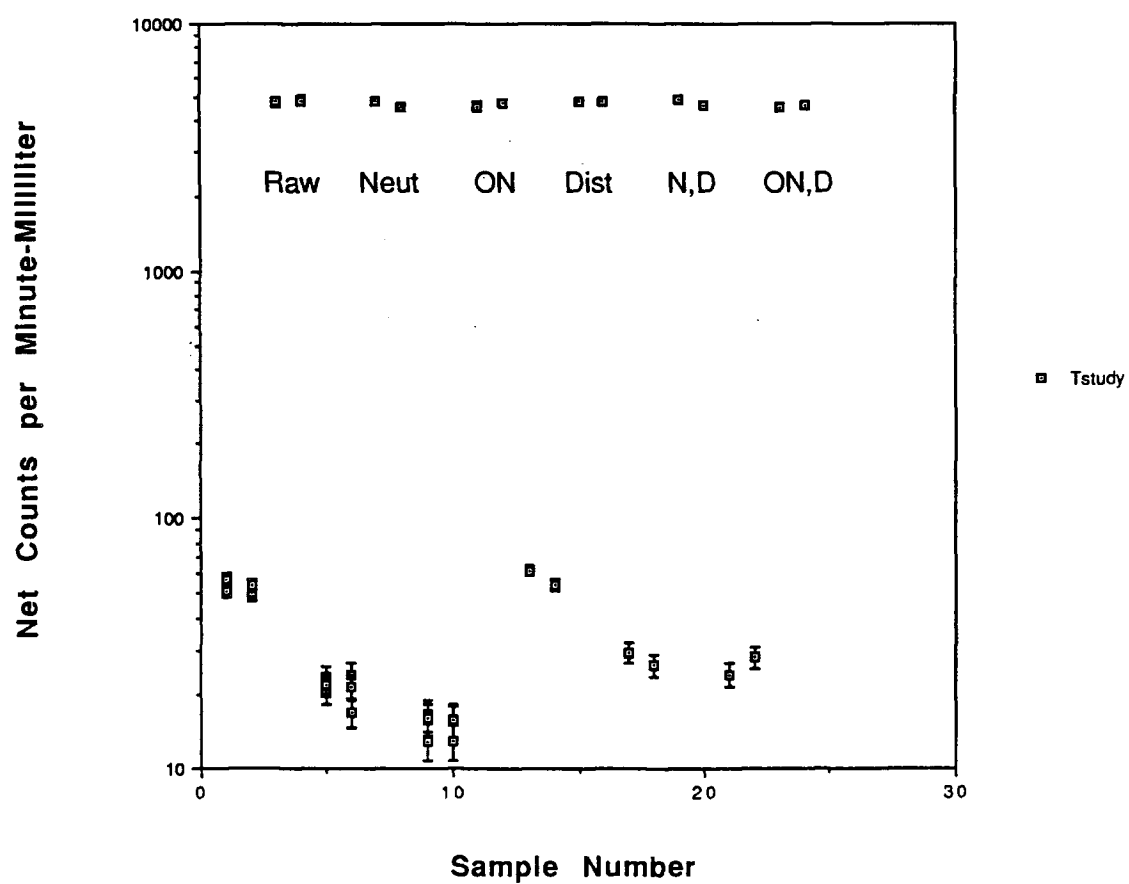
DISCUSSION (TALCOTT)

Hoffman: It is clear that measuring tritium concentrations accurately is much more difficult than the act of buying a scintillator. Many precautions must be observed. As you know, I did send blind samples containing known amounts of tritium to various laboratories, and the range of results reported back tended to produce some lack of confidence in procedures.

Talcott: That is correct, but the samples which you gave had very low tritium contents. The measurements which are significant for this work are not in the same concentration range, so uncertainty would be very much reduced.

Hoffman: I believe that it would be valuable if your laboratory, for example, could circulate a round robin of reasonably low level tritium samples, sending them to the various laboratories for comparative measurement.

Talcott: Would the participants at this Workshop be interested in such a plan? If so, please let me have your names. We would certainly be interested in such a program.

Lewis: The suggestion is important, and we will certainly collaborate.

Yeager: I have a technical question. What happens to the variation in results when one adds hydrogen peroxide to the samples?

Talcott: We have not examined the effect of hydrogen peroxide.

Yeager: This point is important, since it may be produced as an impurity in the electrolyte.

Hoffman: I will determine its effect in the typical electrolytes used in this work.

Wolf: In our experience, it only results in a longer-lasting chemiluminescence.

Bockris: That should be correct, since it decomposes in the air within 2 to 3 hours.

Lewis: Nevertheless, its effect does depend on the scintillator used and on the solution pH.

Bockris: Repeating the count after several hours is all that is necessary to obtain accurate results.

Wolf: I agree. In our experience, its effect is eliminated by the second count in our procedure, which is taken 24 h later.

Talcott: If the precautions which I have outlined are taken, a significant amount of tritium in the electrolyte would be difficult to miss.

Section 14

REVIEW OF CALORIMETRIC DATA

Allan J. Bard

Department of Chemistry

University of Texas at Austin

REVIEW OF CALORIMETRIC DATA

Allan J. Bard

Department of Chemistry, University of Texas at Austin

My appointed task, this evening, is to review the material up to the time of the Santa Fe workshop. However, it seemed to me to be more meaningful to focus particularly on the calorimetric results which have been obtained. I therefore intend to discuss my observations and those of my colleagues on the Energy Research Advisory Board (ERAB) committee which resulted from our visits to the laboratories engaged in this work during June, 1989 and from our consideration of the literature and materials made available to the committee through October, 1989. I will put these observations in the context of the open literature on calorimetry.

The chronology of the events is shown in Fig. 1. Fleischmann and Pons announced their results on March 23, 1989. For me the most important aspect of their report was the claim that large amounts of steady-state excess heat were produced when deuterium was evolved in a simple experiment on deuterium-saturated palladium. In some cases, they claimed a heat output equal to four times the input heat. In consequence, a large number of laboratories attempted to repeat their experiment. The paper by Fleischmann, Pons, and Hawkins appeared in April in the Journal of Electroanalytical Chemistry. Further details were given at the American Chemical Society meeting in Dallas on April 12th. To my knowledge, the first confirmation of this effect was by Martin, Gammon, and Marsh at Texas A&M, where a rather different type of calorimeter was used. However, this confirmation was later retracted, after they determined that there was an electrical fault in their experimental equipment.

From April 12 to April 30, there were a number of other news reports on other claimed confirmations of the Fleischmann-Pons work. At the same time, some negative reports were beginning to appear. At the meeting of the American Physical Society in Baltimore on May 1, Dr. Lewis gave a presentation in which he stated that no anomalous calorimetric results had been observed in work at Caltech. On May 9, a number of presentations were given at the meeting of the Electrochemical Society in Los Angeles, and several groups reported positive reports, including those of Appleby at Texas A&M, Landau at Case Western Reserve, and Huggins at Stanford. At this meeting, Pons and Fleischmann reported a so-called heat burst for the first time. I will return to the question of heat bursts later in this presentation. Confirmations were again presented at the Santa Fe workshop later in May, particularly by Appleby, Srinivasan, and coworkers and by Bockris' group, with the latter reporting the presence of tritium in the electrolyte. Negative results also continued to be noted.

The basic electrochemical cell used in this work is by now familiar to most of you. However, for those who have not seen it, it consists of a palladium rod cathode and a platinum anode, as is shown in Fig. 2. For reliable measurements, a stirrer should be included in the cell, which is immersed in a constant temperature bath. A suitable power supply provides the input current and voltage.

The power into the cell in Watts is given by the applied voltage times the instantaneous current. This is equal to the heat flux in Joules per second. In the cell, liquid D_2O is decomposed into D_2 and $1/2O_2$. Thus, part of the input energy is converted into chemical energy, equivalent to the heat of combustion of the deuterium evolved. The remaining energy is lost in the overpotentials at both electrodes and in the internal resistance of the solution. Both of these losses appear in the cell as heat. If all of the current goes into the decomposition of liquid D_2O, i.e., if this reaction has a coulombic efficiency of 100%, then that part of the input power appearing as chemical energy is $i(1.527)$, where i is the cell current and 1.527 eV is the heat of combustion of gaseous deuterium and gaseous oxygen in their standard states to produce liquid D_2O and 25°C. Corrections to this term for the partial pressure of water vapor above the electrolyte are small, as is the effect of evaporation of D_2O. The remaining energy in the cell is degraded to heat, so that the cell voltage minus 1.527, multiplied by the current, should be the heat output as determined by the calorimeter, according to the First Law of Thermodynamics. Excess heat output, if observed, will be in addition to this value.

The different types of electrochemical cells which have been used are shown in Fig. 2. The above analysis refers to so-called open cells, in which the gases produced are allowed to freely exit the cell. Since the gases can, in principle, recombine on a catalytic surface, any active metal components, particularly the electrical leads, must be covered to avoid this reaction. Since D_2O is progressively consumed, its level will drop as a function of time, and eventually the electrodes or their leads may be exposed. Thus, a danger of recombination of deuterium and oxygen will then exist. Hence, careful attention must be paid toward making up the liquid level in the cell. Whether any recombination can in fact take place under these conditions is a problem which has been incompletely addressed.

In addition to the possible recombination of gases which have been electrolytically evolved, it is well known that the current efficiency for D_2O and O_2 production in cells of this type may not necessarily be 100%. Open cells can certainly be used for calorimetric experiments, but in my view the results obtained will always be open to doubt because of the possibility of coulombic inefficiencies. In addition, other processes involving heat losses will occur, for example, evaporation and the loss of heat in the escaping gases and entrained water.

A second type of cell, which I believe is better for calorimetric measurements, is operated closed. Here the cell is sealed, and it contains a recombination catalyst. Platinum or some other active material, for example, heated palladium, may be used for

this purpose. The catalyst is included in the cell volume above the electrolyte, where any evolved gases will recombine. Thus, an amount of heat equal to i(1.527) is evolved during recombination on the catalyst, exactly compensating for the amount of energy absorbed in the electrolysis reactions on the electrodes. No corrections involving unknown coulombic efficiencies and recombination losses are required, and in addition, there are no changes in the D_2O level or loss of the latter by evaporation. From the First Law of Thermodynamics, at steady state the energy into the cell should exactly equal the energy out under normal chemical conditions. Therefore, the closed cell is the simplest type for reliable calorimetric measurements.

A third type of cell is one which is sealed, but in which the recombining surface is outside of the calorimeter. It is a recombination cell in the sense that the evolved gases do react within a closed system, and consequently the total D_2O level can be keep constant in a properly designed cell. However, it is not a recombination cell in the calorimetric sense, because energy is absorbed in electrolysis as in the open cell and is transferred to the recombiner on the outside of the calorimeter. Hence, this type of recombination system has the disadvantages of the open cell in regard to the corrections for the coulometric efficiency of electrolysis.

The final type of cell has so far been used, to my knowledge, by only one group at SRI. However, it was discussed in the original paper by Fleischmann, Pons, and Hawkins. It consists of a closed cell in which the cathode evolves D_2, which is subsequently oxidized at the anode, so that no oxygen is produced. To obtain satisfactory anodic current densities for D_2 oxidation, the system is operated pressurized. This cell is a closed system in which the energy absorbed in the cathodic half-cell reaction is exactly compensated by the amount liberated in the anodic half-cell. One advantage is that it contains no oxygen anode; therefore, it can, in principle, operate at a much lower voltage than that of the normal closed cell. While this is advantageous, in practice the system is difficult to construct and operate at high pressure. My personal feeling is that convincing calorimetry should be conducted in sealed cells, either incorporating an efficient recombination surface in the calorimeter, or a deuterium anode. It will be difficult to produce entirely convincing calorimetric results in open cells.

A further problem concerns the type of calorimeter which would be most advantageous. Some of the available calorimeter designs are shown schematically in Fig. 3. The isothermal heat leak calorimeter is the variety which has been most discussed in the workshop today. It is the type of instrument used by Pons and Fleischmann. I refer to this type of instrument as Iso-A. In this system, the cell contains one or more temperature-measuring devices, e.g., Beckmann thermometers, thermistors, resistance thermometers, or

thermocouples. Other temperature-measuring devices are in the thermal bath outside of the calorimeter. The cell also includes a heater for calibration and is separated from the bath by some medium which controls the heat leak. To my knowledge, this was a vacuum jacket in all of the Pons and Fleischmann experiments. The heat loss by conductivity will then be very small. In other instruments, a jacket containing air or glycerin or some other medium may be used. The heat loss from the cell is then determined by Newton's Law of Cooling, which predicts a linear dependence of heat flux on the temperature gradient between the cell and the external bath. The cell is calibrated via an internal heater to yield the constant K for heat transfer as a function of the temperature difference, T_c - T_b, between the cell and the bath.

Another method of measuring the heat flux has been used by Martin, Gammon, and Marsh at Texas A&M. In this method, the internal heater is continuously operated in the cell, and its output is reduced after the electrolysis current is switched on, so T_c - T_b is maintained constant. The heat flux from electrolysis is then equal to the difference between the power input to the heater with and without electrolysis. This method has the advantage that T_c - T_b remains small and constant during the whole range of measurement. In my view, this technique, referred to as Iso-B, is an improvement on Iso-A, but it still suffers from a number of experimental problems. For example, it assumes that the cell constant does not change during electrolysis, which is not necessarily true because of gas bubble formation and liquid level changes. While it is possible to obtain good data with an isothermal heat leak calorimeter, it is the most difficult technique to use in an open electrolysis system, especially one operating over long periods of time. I think that this view is widely accepted.

A more appropriate type of calorimeter, of which several commercial models exist, operates on the isothermal heat flow principle. These are referred to as Iso-C. Instruments of this type have been used by several contributors to this meeting, including Lewis, Appleby, and Oriani. In these, the cell is maintained in good thermal contact with a very large bank of thermocouples which surround it. The signal from the parallel-connected thermocouples is proportional to the heat flux from the cell. A sealed cell can be used, and the heat flux measurement can be directly calibrated using a built-in heater.

Another calorimetric technique which has been used rather effectively is flow calorimetry. In instruments using this principle, the external bath is not used as an isothermal heat sink. Liquid from a constant-temperature bath is allowed to flow at a constant rate around the cell, and its inlet and outlet temperatures are measured. The heat flux may be determined from the flow rate and the heat capacity of the liquid. Flow

calorimeters of this type have been used by several groups, and they are effective, especially from the viewpoint of steady-state measurements.

Some experimental problems which arise in calorimetry are shown in Fig. 4. All calorimeters, particularly those operating on the isothermal principle, have calibration problems. Some of these were discussed this morning by Lewis. In particular, there may be variable and undefined heat transfer properties in the cell as a function of time. The most important factor in long-term electrolysis experiments with open cells is the fact that the liquid level changes. A paper by the group at Harwell points this out. If the liquid level varies with time as electrolysis takes place, the heat transfer characteristics will change, giving a so-called sloping baseline. Similarly, there can be undefined changes in the cell constant in the presence and absence of gas bubbles.

A critical question which must be addressed in calorimetric experiments is the quantitative consideration of systematic and random errors. Calorimetric data must always be shown graphically, including error bars. These errors are often much larger than we would normally expect. When we performed some calorimetric measurements in our laboratory with less care than usual, we obtained errors of $\pm 5\%$. In my view, this would not be an unusually large error in many calorimetric experiments. It is vitally important to show the standard deviation for blank experiments to determine the overall precision of anomalous measurements.

We should be on the lookout for the possibility of electrical artifacts which may affect measurements. This possibility has been raised several times at this and previous meetings. I will return to some of these problems later. Other potential sources of error exist. One which was identified is the position of the thermocouple in the cell when an isothermal heat leak calorimeter is used. With a thermocouple, temperature measurements are expressed in microvolts. The electric field in an electrochemical cell can be quite large. For example, if 10 V is applied between the electrodes, the average field may be 10 V/cm or greater. If the thermocouple is placed in the wrong spot in the electrochemical cell, part of this field may be registered. Since we are discussing measurements of microvolts compared with volts, the error can be serious.

Another pitfall concerns unrecognized chemical processes which may occur in the cell. In an open cell, the possibility of recombination is one of these. However, there may also be others. For example, contamination with carbon dioxide in open cells may occur, which may result in side reactions. The LiOD system is an excellent carbon dioxide scrubber. Carbon dioxide has been shown by Wrighton and others to be readily reduced to formate on palladium. The formate produced can be as readily oxidized on platinum, so a

CO$_2$-formate shuttle can exist between the two electrodes. If this occurs, it may introduce serious errors.

Finally, researchers have generally conducted an inadequate number of blank experiments. This is especially so if it is claimed that the alleged events are uncommon and sporadic. Such events might also occur sporadically in blank systems. It is not justifiable to operate 14 palladium-LiOD electrolysis cells, and then claim that 1 out of the 14 cells exhibits anomalous behavior, alongside the only one LiOH blank in which nothing anomalous occurs. If one is examining a system in which low probability events are alleged to occur, equal numbers of observation samples and blank controls should be operated. I believe that this point is one which all workers in this field must address.

Let us now review a selection of the results which have been reported. The latest which were available to the DOE ERAB committee are shown in Figs. 5-7. They are based either on published papers, papers which are in press, or papers which have been submitted for publication and which have been made available to the committee. I must stress that they do not represent the latest work, but rather the work available in writing at the time of the evaluation. Other results are certainly now available, for example, those of Oriani and Hutchinson, which are being discussed at this workshop, and those of Landau, which were verbally presented at the Los Angeles Electrochemical Society Meeting in May. Since the commitee did not have access to their data in writing, and since we did not visit their laboratories, we were unable to evaluate their work. Hence, the committee's conclusions were based on the results shown in Fig. 5, taken together with the negative results (Figs. 6 and 7) which could be at least partially evaluated.

Starting with the positive results, Fleischmann and Pons used Iso-A calorimeters with an open cell. They reported values of anomalous heat varying from 5% to 111% of the input energy, corrected for the decomposition of D$_2$O. A commercial Tronac Iso-C microcalorimeter, again with an open cell, was used by Appleby and Srinivasan at Texas A&M University. Heat conduction considerations in this instrument dictated the use of a stainless steel cell. Excess heat results with the palladium-LiOD systems varied from 6-30% of the corrected input energy. They also reported control experiments on palladium LiOH and on platinum-LiOD. Huggins and coworkers at Stanford used an Iso-A calorimeter with an open cell using current densities in the 10-1000 mA/cm^2 range at cell voltages of 3-15 V. They reported 10-30% excess heat. Finally, Bockris at Texas A&M also used open cells with an Iso-A calorimeter, reporting 5-25% excess heat in 3 out of 10 cells. They also performed platinum-LiOD control experiments. The above positive results were the only ones available to the committee in which the data could be evaluated.

The results which were evaluated and did not show excess heat are shown in Figs. 6 and 7. First, Hayden's group at the University of British Columbia performed very careful experiments with a flow calorimeter using closed cells operating at current densitites up to 2.2 A/cm^2. They observed no excess heat in their longest runs, which were up to 10 days. Platinum-LiOD cells were used as controls. Wrighton and co-workers at MIT used an open cell in an Iso-B calorimeter. They did not operate a large number of cells, but they included one 200 h run. At Caltech, Lewis used two different types of calorimeter, with one a Tronac heat-flow type. Like Wrighton's group, they observed no excess heat over 5 days.

Miles and coworkers at the Naval Weapons Laboratory used an open cell in an Iso calorimeter and saw no evidence of anomalous effects over 10 days. The Sandia Laboratories group, using a similar arrangement , operated for the particularly long period of 36 days. Fleming, Law, and coworkers at AT&T Bell Laboratories performed particularly careful experiments using both open and closed cells in a commercial Setaram flow calorimeter. They operated at current densities of 16-512 mA/cm^2 for up to 40 days, and they observed no excess heat.

At Argonne National Laboratory and in Kreysa's group at the Free University of Berlin, a wide current density range was again used for periods of time between 10 and 20 days without the appearence of excess heat. Other groups reporting no excess heat were those at EG&G Idaho, at Ohio State, and at the University of Newcastle-upon-Tyne. Not shown on Fig. 7 are the results of a particularly careful study performed by Williams and coworkers at Harwell using two different types of calorimeter. Results were obtained with open cells over a wide current density range in more than 11 cells over periods of up to 33 days. Their work included many different control experiments, and it included a very careful error analysis. They recorded no excess heat.

I would next like to address the question of so-called heat bursts. A burst may be defined as an abrupt change in cell temperature, which appears sporadically, often follows a change in operating conditions, and lasts for an undetermined length of time. Since sporadic phenomena are very hard to address, I have no satisfactory explanation of such bursts. However, I believe that several possible explanations exist, as Fig. 8 shows.

The first of these is the obvious occurance of an instrumental artifact. Another may be the release of stored intrinsic energy. In this connection, it has been argued that deuterium-saturated palladium cathode or the deuterium gas on the catalytic surface, becomes exposed to oxygen and then reacts. This argument may not be valid, and it is hard to see that such a process would last long enough to explain the amount of heat reported in a burst. Pauling has suggested that phase changes in the palladium may provide an

explanation. Birnbaum at the University of Illinois believes that deuterium dissolved in palladium as a solid solution undergoes a change to a hydride phase. The energy difference between the heat of formation of a deuterium solid solution and that of a palladium deuteride phase is then evolved as heat. Again, it is uncertain that the amount of energy which might be released in this manner would account for a heat burst over an extended period of time. It would be useful if information on exactly how much energy has been observed in an apparent burst, together with its duration, can be provided by the participants at this workshop. A further explanation which requires discussion is the question of an unrecognized increase in the input electrical energy. This has been raised most recently in a paper by a Belgian group. If a cell operating at constant current starts to develop a high resistance, which has been seen in our own laboratory, large voltage changes can then occur. Another electrical error will occur if the cell potential starts to oscillate at a high frequency, when an a.c. current will be superimposed upon the d.c. current from a power supply, which will not be registered by a d.c. measuring device. This will depend on the potentiostat, if used, or on the electric characteristics of the power supply and the cell. The impedence of the palladium cathode also changes with time, as charging with deuterium occurs. If apparent heat bursts are observed, any a.c. component of the current should be examined using an oscilloscope. If all of these explanations fail, then perhaps a nuclear process is occurring. However, all other explanations must be eliminated before this possibility can be suggested.

In conclusion, how can one evaluate the available data today? The DOE committee was charged with this task, asking the further question: what is the possibility of cold fusion? The committee concluded, after assessing the reports from the different laboratories, that they did not feel that "the steady production of excess heat has been convincingly demonstrated." Moreover, they felt that "the present evidence for the discovery of a new nuclear process termed cold fusion is not persuasive." I believe that there are four major questions which must be answered by the proponents of cold fusion. These are shown in Fig. 9. The first is the lack of reproducibility of the excess heat which has been apparently observed in cells evolving deuterium from palladium cathodes in D_2O solutions under the conditions reported. Excess heat, or a heat burst, may be observed, but under conditions which are not within the realm of a reproducible scientific experiment. The second major question, which is being addressed at this workshop, is that there must be a correlation between the quantities of fusion or other nuclear products and the reported levels of excess heat. The correlation must be reasonably close if the argument that the excess heat results from a nuclear process is to be convincing. When tritium is observed, its reproducibility is the critical factor. Some groups have determined that it is present, but
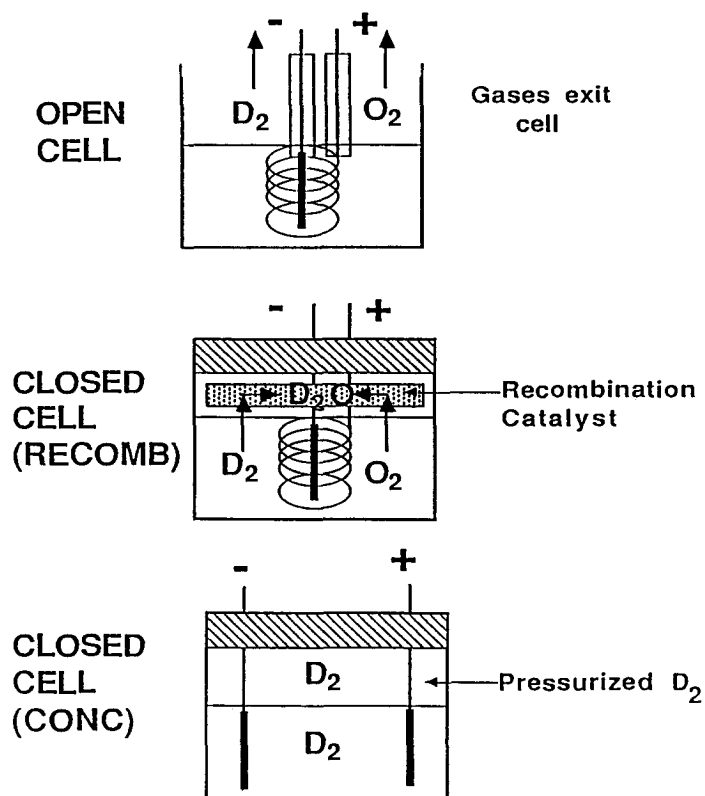
only sporadically. Others in the same location using the same experimental conditions, are unable to detect it. Until its presence becomes a reproducible phenomenon, it will remain suspect. The other problem is the apparent absence of secondary neutrons or subsecondary radiation. If the process involves fusion, it is generally agreed that neutrons from the secondary fusion of high-energy tritium should be observed. As far as I am aware, these have not been detected. Finally, there are the objections of the theorists, which also must be answered.

I would like to finish with an interesting quotation from Lavoisier, which is much truer than I would have thought before these questions were raised. During the period between the American and the French Revolutions in 1784, he was appointed by Louis XVI to a commission to investigate Mesmerism or "animal magnetism." The commission included Benjamin Franklin and Dr. Guillotin, the inventor of the guillotine. I must point out that I do not mean to put the subject of this Workshop in the same category as Mesmerism; I am only using the quotation. Lavoisier's report contains the following statement, "The art of concluding from experiment and observation consists in evaluating probabilities and estimating if they are high or numerous enough to constitute proof. This type of calculation is more complicated and more difficult than one might think."

CHRONOLOGY

1. MARCH 23-28, 1989 INITIAL PRESS
   RELEASE BY FLEISCHMANN AND PONS

2. APRIL 10, 1989 PAPER APPEARS IN
   J. ELECTROANAL. CHEM. WITH FURTHER
   DETAILS

3. APRIL 11, 1989 CONFIRMATION OF
   EXCESS HEAT EFFECTS BY MARTIN ET.
   AL. (LATER RETRACTED)

4. APRIL 12-30, 1989 SEVERAL OTHER
   NEWS REPORTS OF CONFIRMATIONS AND
   NEGATIVE RESULTS

5. MAY 1, 1989 AMERICAN PHYSICAL
   SOCIETY MEETING - NEGATIVE REPORTS

6. MAY 9, 1989 ELECTROCHEMICAL SOC.
   MEETING - SEVERAL CONFIRMATIONS
   AND NEGATIVE RESULTS. FIRST MENTION
   OF "HEAT BURST"

7. MAY 23-25, 1989 SANTA FE WORKSHOP
   A FEW CONFIRMATIONS AND MANY
   NEGATIVE REPORTS

Fig. 1

OPEN CELL

Gases exit cell

CLOSED CELL (RECOMB)

Recombination Catalyst

CLOSED CELL (CONC)

Pressurized D_2

TYPES OF ELECTROCHEMICAL CELLS

Fig. 2

ISOTHERMAL HEAT LEAK

ISOTHERMAL HEAT FLOW

FLOW
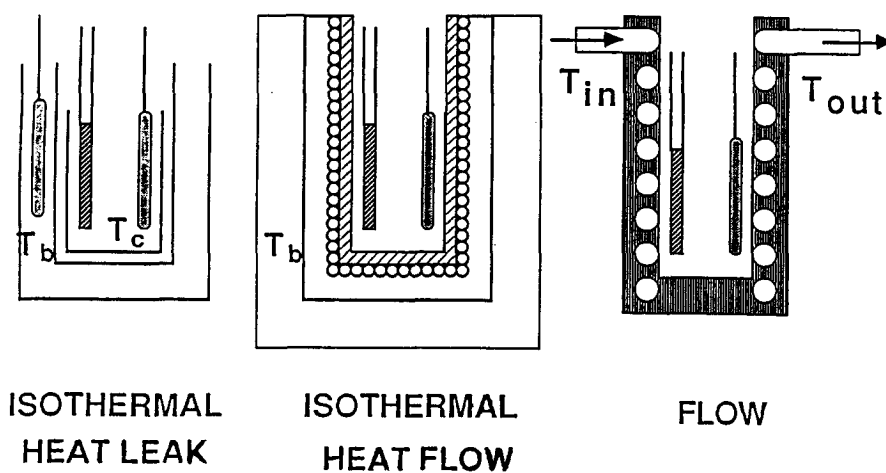
TYPES OF CALORIMETERS

Fig. 3.

14-11

EXPERIMENTAL PROBLEMS
IN CALORIMETIC MEASUREMENTS

1. Calibration problems

2. Variable and undefined heat
   transfer properties of cell

3. Inadequate quantitative
   consideration of systematic
   and random errors

4. Electrical artifacts

5. Unrecognized chemical
   processes, e.g. recombination

6. Inadequate number of blank
   experiments

Fig. 4

SUMMARY OF CALORIMETRIC RESULTS
GROUPS OBSERVING EXCESS HEAT

Research Group	Calorimeter, Cell	Current Density, Voltage	Results	Controls
1. Univ. of Utah Fleischmann, Pons et al.	ISO A open	8, 64, 512 mA/cm^2 3-10 V	5-111 % (9) [n, t ,γ]	none
2. Texas A&M Univ. Appleby, Srinivasan et al.	ISO-HF (Tronac) open (s.s.)	0.3, 0.6, 1.0A/cm^2 3.4-5.6 V	6-30 %	H$_2$O Pt
3. Stanford Univ. Huggins, Gür et al.	ISO A open	10-1000 mA	10-30 % 3-15 V	H$_2$O
4. Texas A&M Univ. Bockris et al.	ISO A	100-500 mA/cm^2	5-25 % (3 of 10)	Pt

Fig. 5

SUMMARY OF CALORIMETRIC RESULTS
GROUPS NOT OBSERVING EXCESS HEAT

Research Group	Calorimeter, Cell	Current Density, Voltage	Results	Controls
1. U. British Columbia Hayden et al.	Flow closed	to 2.2 A/cm^2	none (10 d)	Pt
2. M.I.T. Wrighton et al.	ISO B open	69 mA/cm^2 2.9 V	none (> 200 h) [no t, n]	H$_2$O
3. Caltech Lewis et al.	ISO B, ISO C (Tronac) open	72-140 mA/cm^2	none (5) [no t,n,He]	H$_2$O
4. Naval Weapons Ctr. Miles et al.	ISO open	100-200 mA/cm^2 3-5 V	none (1-10 d) [no n,γ]	Pt H$_2$O
5. Sandia N.L. Roth et al.	ISO A open	320 mA/cm^2	none (17, 36 d) [no n, t]	

Fig. 6

14-13

GROUPS NOT OBSERVING EXCESS HEAT

Research Group	Calorimeter, Cell	Current Density, Voltage	Results	Controls
6. AT&T Bell Labs Fleming, Law et al.	ISO C (Setaram) closed&open	16-512 mA/cm^2 2-10 V	none (1-40 d)	Pt H$_2$O
7. Argonne N.L. Redey et al.	ISO B, ISO C open	15-500 mA/cm^2	none (460 h)	H$_2$O
8. Free U. Berlin Kreysa et al.	ISO A open	1.2 A 9 V	none (10 ?) [no n,t,γ]	H$_2$O
9. EG&G Idaho Longhurst et al.	ISO A ISO C open	0.1 ma-5.7 A 3.3-5.1 V	none (> 20 cells) (120 h) [no n,t,γ]	H$_2$O
10. Iowa St. U. Hill et al.	open	0.7-1 A/cm^2	none [no n,γ]	
11. U. Newcastle-upon-Tyne Armstrong et al.	Flow open	100 mA/cm^2 15-20 V	none (8 d) (2)	Pt(H$_2$O)

Fig. 7

TEMPERATURE BURSTS

Abrupt changes in cell temperature which appear sporadically, often following a change in operating conditions, and last for an undetermined length of time.

1. Instrumental artifacts

2. Release of stored or intrinsic chemical energy

3. Changes in heat transfer characteristics of cell

4. Unrecognized increases in input electrical energy

5. Nuclear process

Fig. 8

MAJOR QUESTIONS TO BE ADDRESSED

1. Lack of reproducibility of excess heat experiments

2. Lack of correlation of fusion product levels (especially T, n, He) with reported heat levels

3. General lack of confirmation of high T levels and absence of secondary n

4. Theoretical objections

Fig. 9

DISCUSSION (BARD)

Appleby: In regard to your statement about the use of the Newton's Law of Cooling by Fleischmann and Pons for the calibration of their calorimeter, which suggests that heat loss is by conduction, I would point out that they used a vacuum jacket. Heat loss is then by radiation, and the Stefan-Boltzmann law will apply.

Bard: An explanation of heat loss in terms of radiation is new. In their original paper and during the visit of the ERAB committee to Utah, the calibration term was given as $(T_c - T_b) \times K$.

Yeager: In the steady state, calibration should cause no problems in a closed system. The problem is that one is never in a steady state.

Bard: However, the assumption is made that the incoming and outgoing heat fluxes are in equilibrium.

Appleby: You mentioned the problem of CO_2 contamination in the electrolyte. In the dilute solutions used, there should be a pH gradient between the electrodes at high current density. It may be sufficient to eliminate CO_2 at the anode.

Bard: I believe that this consideration is another reason to perform experiments in closed-cell systems.

Bockris: Heat, tritium, and neutrons appear to come in bursts. The results are not consistent in this respect. What is your view on heat bursts?

Bard: Impedance changes in the system can occur, and I believe that if heat bursts are seen, an oscilloscope should be used to examine the cell voltage to see if there is any high frequency ac superimposed on the dc signal.

Bockris: We do it routinely.

Bard: However, do you measure the ac during the burst?

Bockris: We do it during the burst. That is when the measurement is most important. In my view, the main issue which Dr. Bard addressed is the lack of reproducibility of the results. I believe that all of us at Texas A&M will agree with that conclusion. Dr. Bard points out that the criterion for science is that it should be reproducible. Many people would agree. There is no doubt that results in this work are not reproducible. However, it would be misleading to indicate that the consistent repetition of the experiment showing positive excess heat is rare, as Dr. Bard suggests. He has stated that he knows of only four experimental results showing this effect. I know of 10 universities within the United States and a larger number outside the country who claim to see excess effect. The overriding factor is not these positive results, but rather the much

larger number of people who have apparently obtained negative results. One ingredient may be missing in all this work: that is patience. One needs a great deal of patience, because with large cathodes results may not be seen for 20, 50, or even 90 days. Few people are prepared to wait that long. I would like to give rebuttals to two arguments. The first is the possibility that the energy is stored in a chemical form. We have carefully examined this question and have published a paper. Insofar as we can tell, no chemical explanation can account for even 1 percent of the excess heat that has been observed. Thus, I see no possibility of explaining these observations in terms of chemical effect. The second is the possibility that the phenomena may result from ac electrical effects. During our heat bursts, we have seen voltage oscillation, but they are only a few mV, far below the level required as an explanation. While I believe your use of the Lavoisier quotation is reasonable, let us be reminded what Rutherford is purported to have said in 1923 when he obtained some evidence of atomic fission, namely, "This is a darned interesting thing academically, but it will never have any practical application."

Werbos: Concerning positive experiments, I have a list here of an additional 11 cases which we have attempted to evaluate. As Dr. Bockris points out, the problem is that I also have a list of 12 negative results from laboratories which include Brookhaven National Laboratory, Lawrence Berkeley Laboratory, and General Motors Research Laboratories. The problem with many of the positive results is that one cannot deal with hearsay, as Dr. Hoffman pointed out this morning. The results must be seen to be obtained, and we must see reviewed and published data. Until we can do that, we cannot evaluate any results.

Bockris: Of course, publication usually takes nine months, so we must wait longer.

Werbos: Concerning time in a different context, those workers who have seen excess heat have talked about a variety of lengths of time for it to appear. At Texas A&M and in other groups, excess heat was seen right from the beginning, or at least within hours. The original Fleischmann and Pons paper states that one must wait 10 hours to charge a 1 mm rod without seeing excess heat. If they had persevered for 10 days longer, they might have been successful.

Bockris: Many people have failed to realize that to see excess heat, one must electrolyze at a current density which is outside of the normal range.

Werbos: Some of those who have used very high current densities also report negative results. My feeling is that after evaluating all of the data, simple explanations may explain all of these. They would include the type of palladium used, the current density used, and the length of time one waits.

Appleby: Following your quotation of Lavoisier, let me quote Sir William Grove, the inventor of the Fuel Cell in 1839. It is well known that he anticipated Helmholtz in discovering the Law of Conservation of Energy, but he could never publish his conclusions. As he said, this was "because of the opposition usual and proper to novel ideas."

Bard: Let me point out that Lavoisier was not considering any particular idea. He was simply stating that it is difficult to evaluate data which are not reproducible.

Part 3

EXCESS HEAT

Section 15

CALORIMETRIC MEASUREMENTS OF EXCESS POWER DURING THE CATHODIC CHARGING OF DEUTERIUM INTO PALLADIUM

R.A. Oriani, J.C. Nelson, S.K. Lee, and J.H. Broadhurst

University of Minnesota

<u>Technical Summary</u>

Calorimetric Measurements of Excess Power During
the Cathodic Charging of Deuterium into Palladium

R.A. Oriani, J.C. Nelson, S.K. Lee, and J.H. Broadhurst
University of Minnesota

<u>Calorimetric technique</u>

Large-diameter concentric cylindrical metal shells enclose 1961 copper-constantan

junctions in series which generate a thermoelectric emf proportional to the radial heat flux

from whatever source of power is within. Inhomogeneous temperature distribution within

electrolysis cell is of no importance at steady state. The calorimeter, held in a

thermostatically controlled bath, is calibrated electrically by relating the steady-state emf, E,

to the product of current I through the resistor and the applied voltage V. The calibration

factor is determined within $\pm$ 0.3%.

<u>Electrochemical cells</u>

A. Anode: Pt spiral. Cathode: 1 mm diameter, 99.9% Pd. Electrolyte: 0.1 M

LiOH or LiOD. Relatively high electrical resistance cell because of effort to keep evolved

gases separated. This effort failed; gases mixed within cell.

B. Anode: Pt spiral with short length of Pd wire attached. Cathode: 1 mm

diameter Pd, either 99.9% or 99.999% pure. Electrolyte: 0.1 M LiOH + H_2SO_4, or 0.1 M

LiOD + D_2SO_4. Relatively low electrical resistance cell, with gases mixing within cell.

<u>Results with high-resistance cell</u>

EMF vs. I(V-1.48) for H_2O dissociation coincides exactly with EMF vs. V for

electrical calibration, showing that recombination of gases within cell is negligible. EMF

vs. I(V-1.53) for D_2O dissociation coincides exactly with H_2O results, showing that

anomalous energy was not generated. Largest current density achieved was 0.42 A/cm^2.

Results with low-resistance cell

EMF vs. I(V-1.48) for H_2O dissociation in acidic electrolyte and encompassing higher current densities has a slope different by 2.5% from that of the high-resistance cell because of better heat extraction in the calorimeter with the low-resistance cell. With H_2O dissociation the calorimeter signal remains constant for many hours within 0.02 mV, which translates to a constancy of heat flux within 0.04 watt.

EMF vs. I(V-1.53) for D_2O dissociation in acidic electrolyte with the 99.9% Pd cathode shows coincidence with H_2O line at lower current densities, but positive deviations (i.e., larger calorimeter EMF signals) from the H_2O line for same abcissa values. This is definite indication of excess power generation. Considerably larger positive deviations from the H_2O line are observed with the purer Pd cathode. As much as 3.6 ± 0.2 watts of excess power, with 13.37 net input watts, were observed. In one episode 1.78 ± 0.2 watts of excess power were observed over a time of 560 minutes of quasi-steady state, or 59.8 kJ of excess energy were produced. Summing up also over the non-steady excess power evolution in this one episode at 10.68 net watts input, the excess energy developed was 82.3 kJ. This episode developed 67 watts of excess power per cm^3 of Pd cathode. Another episode produced 106 watts of excess power per cm^3 Pd. When excess power is being produced the calorimetric signal is not steady with time showing possibly the sporadic or intermittent nature of the generation of excess power. The highest current density employed in the two successful D_2O runs was about 1.7 A/cm^2.

Supplemental Information and Comments

Table 2 presents the overall cell resistance corresponding to the enumerated data points in Fig. 3 for each of the steady states. It is seen that data points 1, 4, and 9 which lie on or very near the calibration line are accompanied by $R \geq 4.96 \, \Omega$, whereas episodes

that show significant anomalous power evince R values averaging 3.43 Ω. Episode 2, which shows a small amount of anomalous power, has R = 4.34 Ω, an intermediate value. The first group, those on the line, show the expected decrease in R with increasing temperature (caused by the increasing power dissipated in the cell.)

It looks as if there is a casual relationship between reduced R and anomalous power generation. This is probably an interfacial phenomenon which merits careful consideration.

Table 2. OVERALL CELL RESISTANCE IN SECOND D_2O EXPERIMENT IN THE LOW-RESISTANCE CELL.

Episode	Applied Volts	Current, A	Cell Resistance, Ω
1	6.58	1.28	5.14
2	8.64	1.99	4.34
3	7.52	2.23	3.37
4	7.24	1.46	4.96
5	7.01	1.95	3.59
6	6.64	1.83	3.63
7	7.43	2.25	3.30
8	7.30	2.21	3.30
9	4.87	0.87	5.59
10	7.18	2.11	3.40
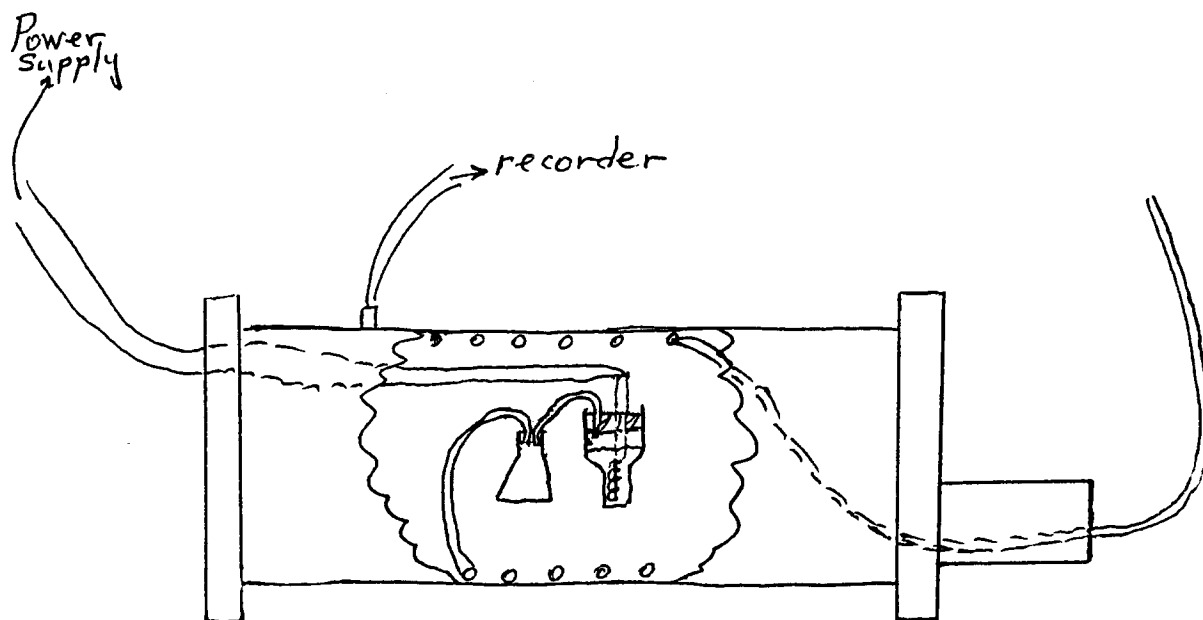
Nuclear aspects
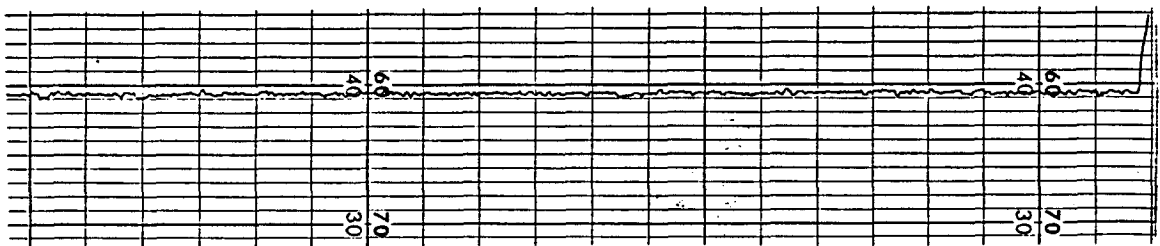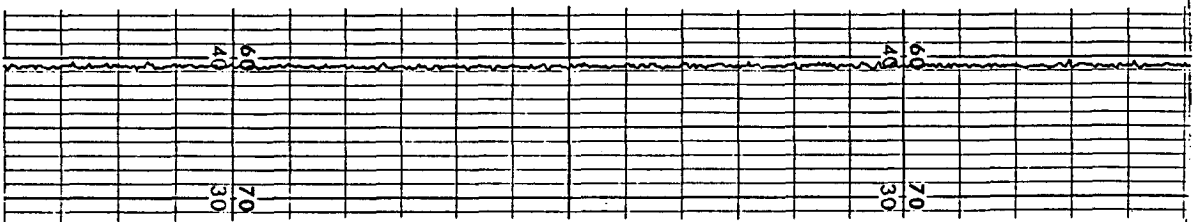
Tritium was looked for, but was not found significantly above background, in the deuterium charged into the Pd cathodes, in the electrolyte, or in the off-gases in the two successful D_2O runs at high current densities. Neither neutrons, x-rays nor tritium was
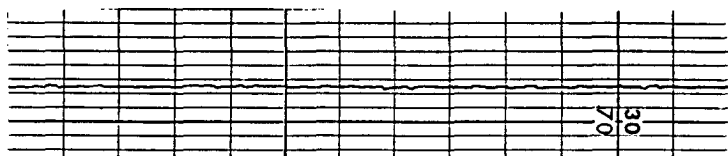
observed in measurements made on D_2O dissociation cells with LiOD and operated at low current densities.
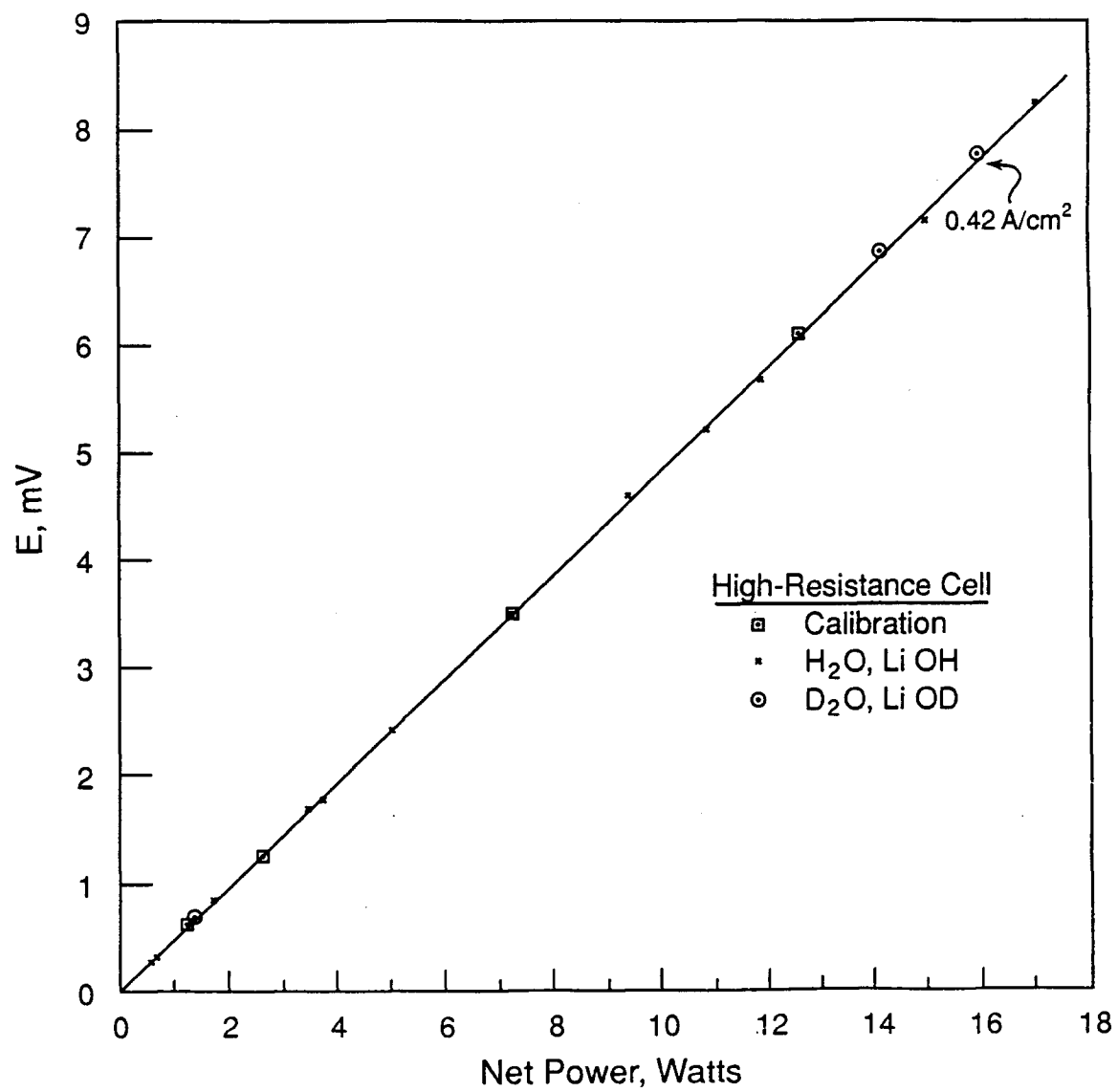
Conclusions

The development of excess (anomalous) power is a reality. Because we cannot attribute it to any chemical reaction nor to a storage and relaxation mechanism, and because we have not seen any manifestation of nuclear fusion, the mechanism for the development of the excess power is as yet mysterious. This problem merits intensive further research.
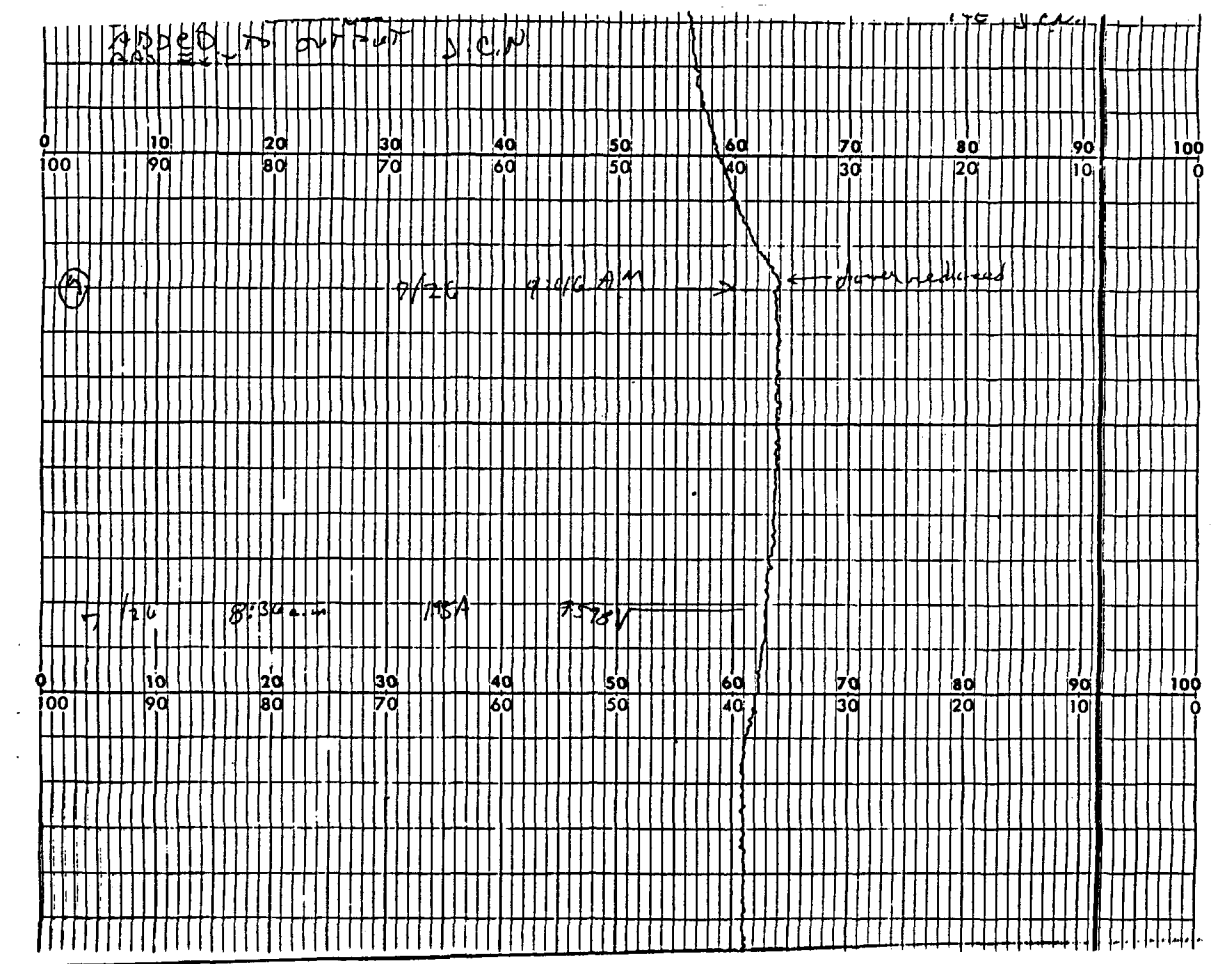
Power
Supply

recorder

15-5

Scale change 1.0 mV

10 min.

0.1 mV

15-6

ADDED O₂ TO OUTPUT D.C.W.

| 0 | 10 | 20 | 30 | 40 | 50 | 60 | 70 | 80 | 90 | 100 |
| 100 | 90 | 80 | 70 | 60 | 50 | 40 | 30 | 20 | 10 | 0 |

9/26   9:16 AM   →   ← power reduced

↑ 9/26   8:30 a.m.   15A   ↑ 58V

| 0 | 10 | 20 | 30 | 40 | 50 | 60 | 70 | 80 | 90 | 100 |
| 100 | 90 | 80 | 70 | 60 | 50 | 40 | 30 | 20 | 10 | 0 |
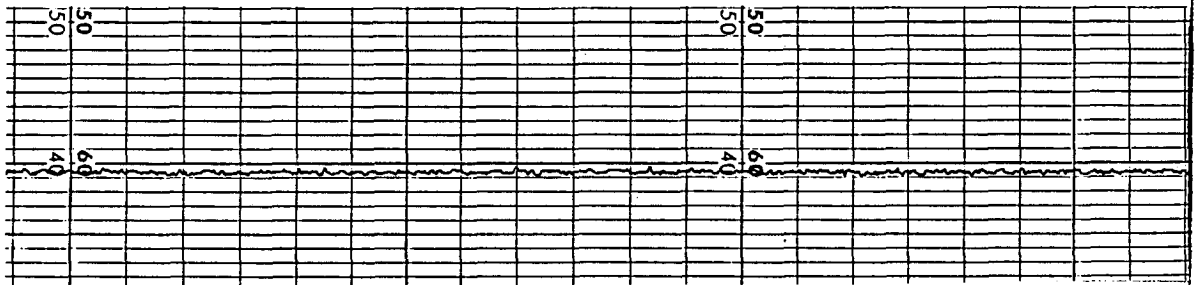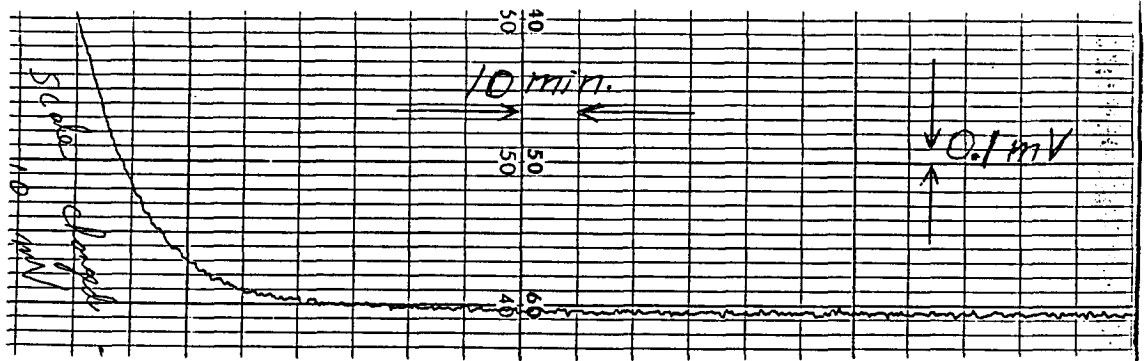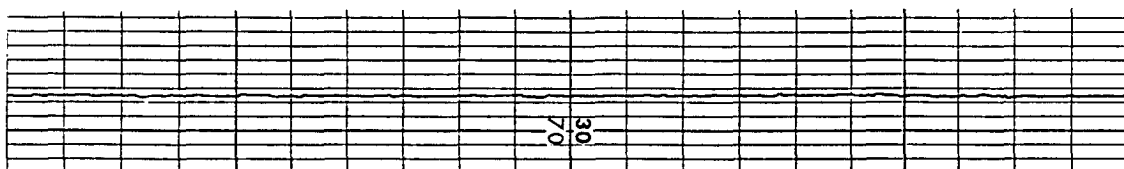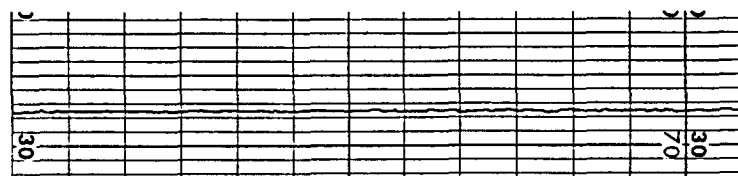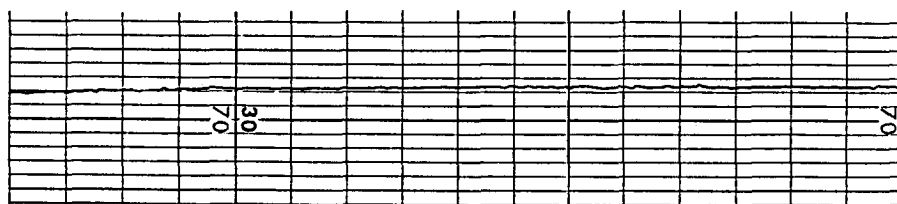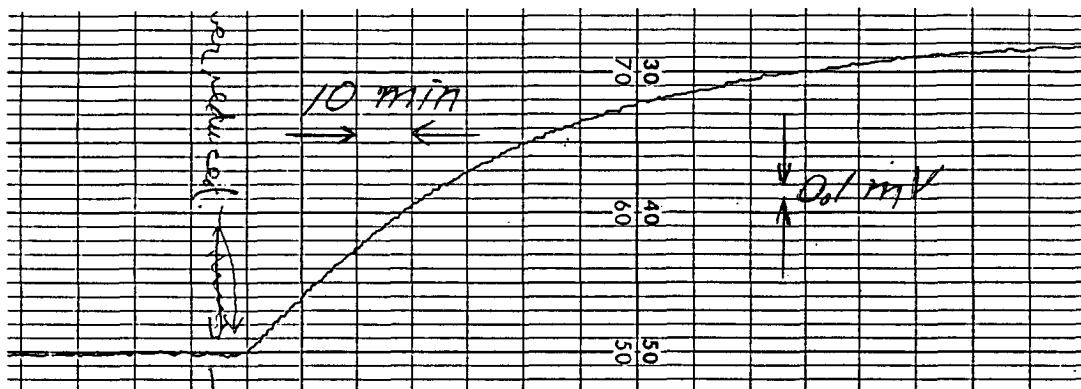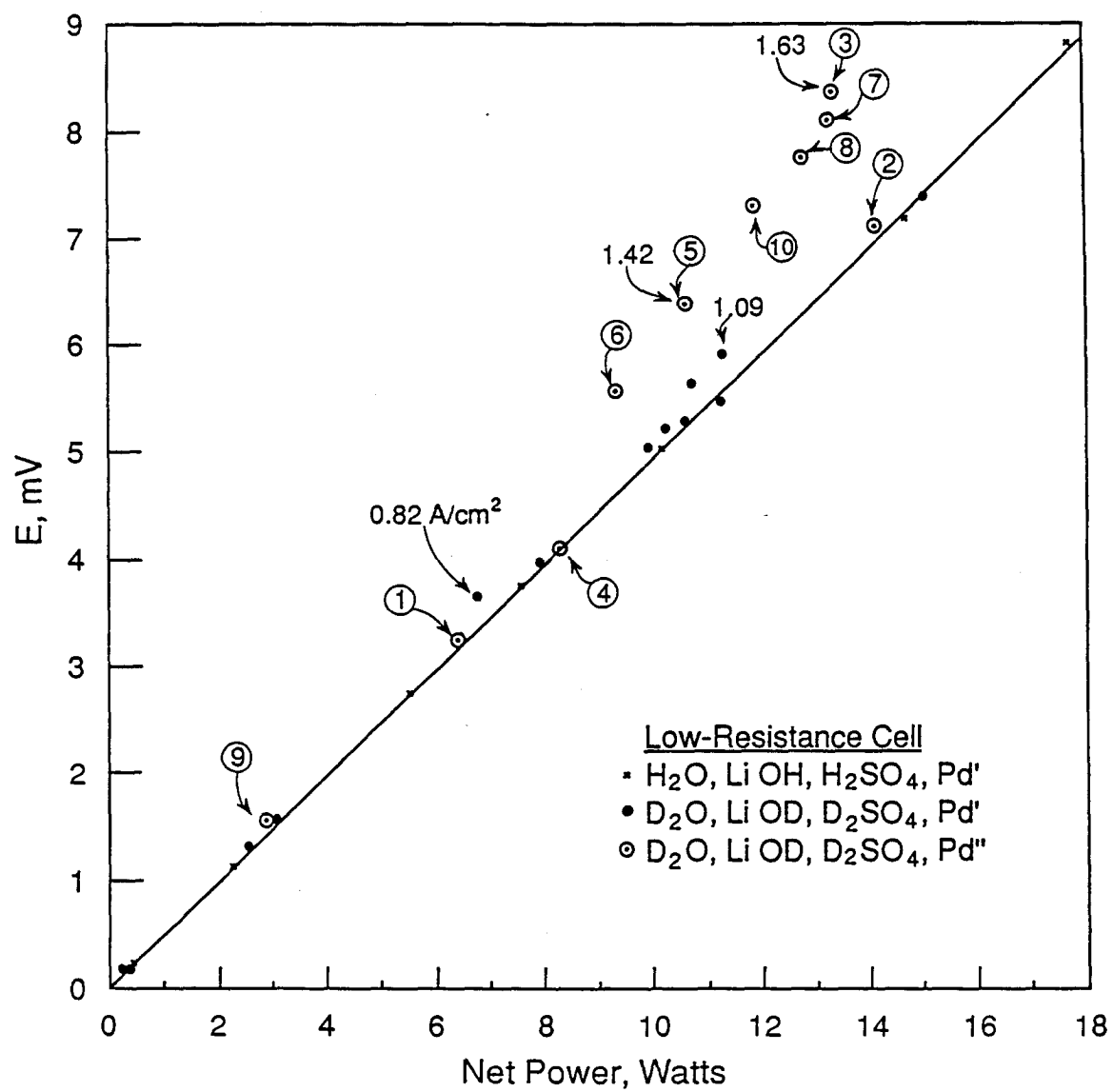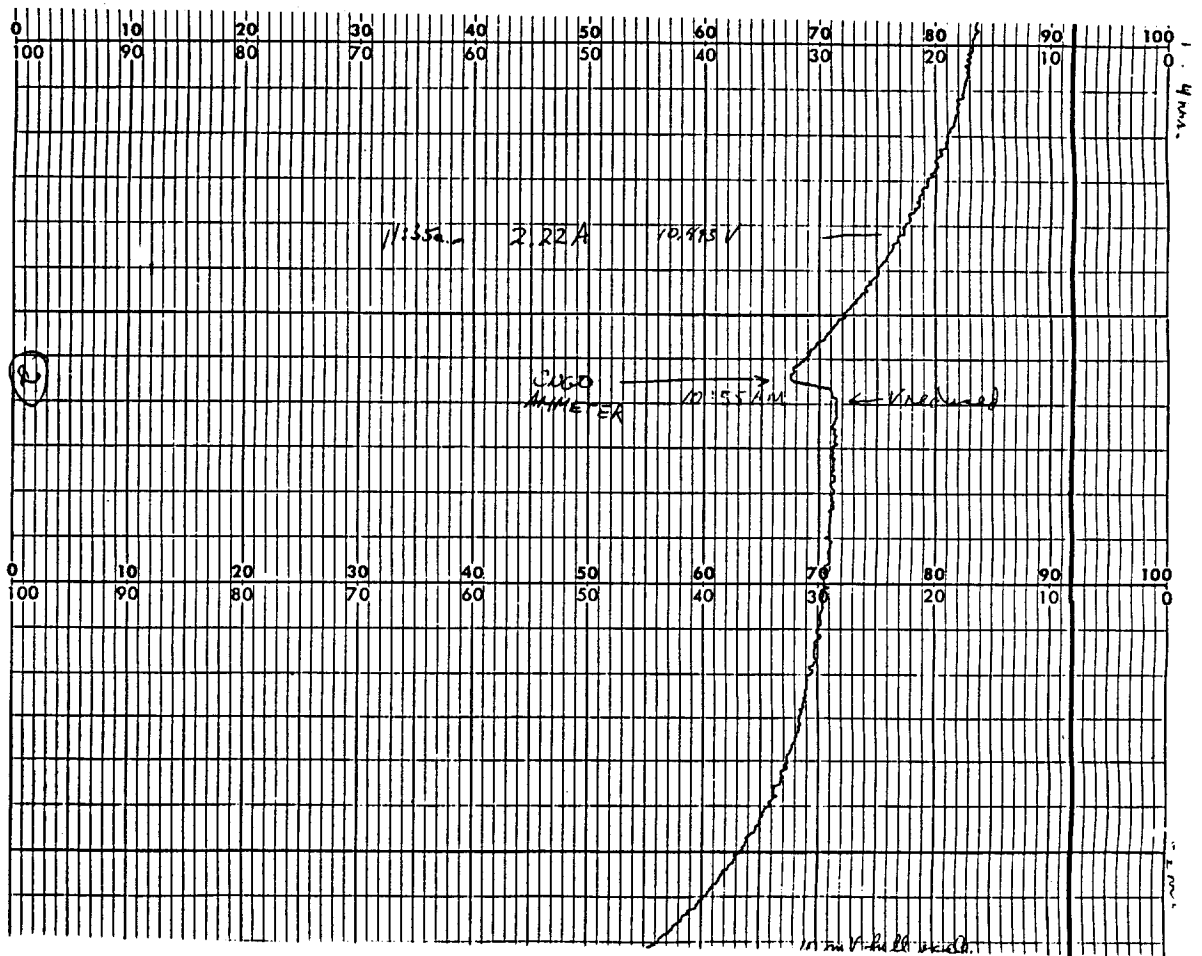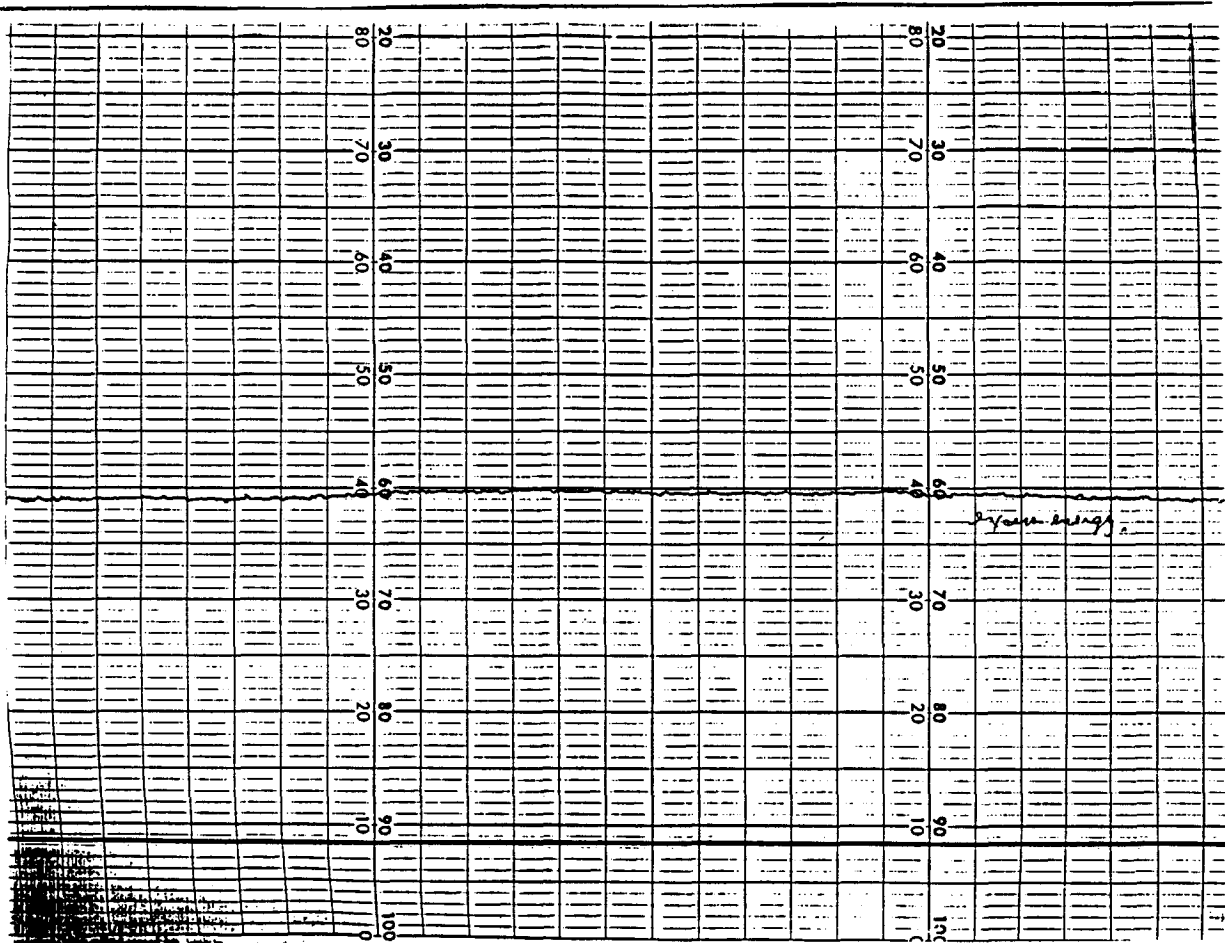
Table I. Characteristics of the Second D_2O Experiment in the Low-Resistance Cell

Episode	Input Watts		Duration, min	E,mv	E_0,mV	Input Energy		Excess Quantities	
	Net	1.531				Net kJ	Total kJ	Watt	kJ
1.	6.465	1.957	985(t)	3.25(s)	3.25	382.1	497.7	0	0
2.	14.16	3.04	156(t)	7.15(r)	6.95	132.5	160.0	0.4±0.1	--
3.	13.37	3.41	90(r)	7.8(a)	6.58	72.2	90.6	2.5±0.2	13.5
	13.37	3.41	150(s)	8.35(s)	6.58	120.3	151.0	3.6±0.2	32.4
4.	8.33	2.24	320(t)	4.09(s)	4.09	159.8	202.8	0	0
5.	10.68	2.98	30(r)	--	5.23	19.2	24.6	--	--
	10.68	2.98	120(r°)	5.8(a)	5.23	76.9	98.4	1.16±0.2	8.4
	10.68	2.98	560	6.1(s)	5.23	358.8	459.0	1.78±0.2	59.8
	10.68	2.98	103	6.35(a)	5.23	66.0	84.4	2.29±0.2	14.1
6.	9.36	2.80	77(d)	--	4.60	43.2	56.2	--	--
	9.36	2.80	70(s)	5.56(s)	4.60	39.3	51.1	1.96±0.1	8.2
7.	13.27	3.44	17(r)	--	6.52	13.5	17.0	--	--
	13.27	3.44	63(r°)	7.5(a)	6.52	50.2	63.2	2.00±0.2	7.6
	13.27	3.44	68(s)	8.1	6.52	54.1	68.2	3.23±0.2	13.2
8.	12.76	3.38	42(d)	--	6.28	32.2	40.7	--	--
	12.76	3.38	33(s)	7.78(s)	6.28	25.3	32.0	3.07±0.1	6.1
9.	2.903	1.33	167(d)	--	1.34	29.1	42.4	--	--
	2.903	1.33	770(s)	1.56(s)	1.34	134.1	195.6	0.45±0.2	21
10.	11.91	3.23	44(r)	--	5.85	31.4	40.0	--	--
	11.91	3.23	109(r°)	7.0(a)	5.85	77.9	99.0	2.4±0.2	15.4

Key: E is the observed calorimeter signal, E_0 is the calorimeter emf of the calibration curve (H_2O dissociation line) at same net power input, (t) refers to total, over the entire episode; (r) and (d) refer, respectively, the rising and decreasing signal portions of the episode; (r°) refers to the rising portion when $E>E_0$; (s) means steady state: (a) means a value averaged over the indicated duration.

High-R Cell	Low-R Cell
Max c.d. $\approx$ 0.42 A/cm^2	c.d. $\geq$ 1
0.1 M LiOD in D$_2$O	0.1 M LiOD + D$_2$SO$_4$ in D$_2$O
Pt anode I Pd cathode	Pt + Pd anode I Pd' and Pd" as cathodes
"Separated"	gases Mixed gases

DISCUSSION (ORIANI)

Chu: How do you calculate the current density?

Oriani: Using the total cathode area.

Chu: In superconductivity, we use the cross section.

Oriani: In electrochemistry, it is the area of the electrolyte-metal interface.

Bard: Do you use a constant-current or constant-voltage power source?

Oriani: We have used both, but normally we use constant voltage.

Bard: Is the smaller voltage in the H_2O cell due to a lower cell resistance?

Oriani: That is right, although the dimensions of the arrangement are not exactly the same.

Bard: How do you know that there is no recombination in your open system with mixed gases?

Oriani: One can infer that from the congruence of the H_2O calibration line and that for D_2O in the absence of excess power, after subtracting 1.48 V and 1.53 V, respectively, from the cell voltage.

Lewis: Did the copper which you detected in the D_2O case result from some reaction? Copper should not react in H_2O, but H and D could be different in principle.

Oriani: Copper is present in the system only as an impurity.

Lewis: You have a copper tube in the cell.

Oriani: If copper were reacting, it would be expected to do so in H_2O as well as in D_2O, unless you measured some huge isotope difference.

Yeager: What was the pH and the deuterium ion concentration?

Oriani: I am sorry to say that we did not measure it. However, we added 0.5 ml of concentrated H_2SO_4 or D_2SO_4 to the cell, which would have given a pH of about 3.

Yeager: At the current densities which you use, you will have a very strong concentration gradient between the electrodes because of hydrogen ion transport limitations.

Fleischmann: The cathode surface will be alkaline.

Oriani: We do observe a larger uptake of hydrogen into the ferrous alloys under these conditions and would expect the same result with palladium.

Miley: The excess heat which you generate seems to occur when the current increases. Is that correct?

Oriani: Because I use a constant-voltage power supply, the current increases slightly when the temperature of the cell increases, and that is when excess heat is produced.

Miley: You stated that there is a threshold current density for the appearance of excess heat. Do you know what that current density is?

Oriani: I would like to be cautious and say that I suspect that there is a threshold current density, but I really do not know for certain if this is so.

Miley: The results seem to show a very definite threshold.

Lewis: The numerical precision of your results is very high. With this precision, would you be able to detect excess heat at the lower current densities used by Dr. Pons on the Johnson-Matthey palladium?

Oriani: In some experiments run for 30 hours in LiOD, I did not see any excess heat production at a current of 4.2 A. I should certainly have been able to see 0.2 watts excess heat output.

Fleischmann: 0.2 watts is far above the level which we can measure. Our limit of accuracy is 1 percent or ± 1 mW, whichever is greater.

Oriani: My accuracy is ± 0.02 watts. As you can see, my calorimeter is not as sensitive as yours. It is a heat-integrating calorimeter, and if there were short-lived heat bursts, I would not see them. However, I suspect that my quasi-steady state under excess power conditions does in fact represent sporadic heat bursts which are integrated over the long response time.

Jordan: How many thermocouples have you in your thermal pack?

Oriani: 1,961.

Jordan: They are, of course, outside of the electrolytic solution?

Oriani: Of course. They are between the two concentric shells.

Jordan: Am I correct in saying that the measurements are totally immune to any errors in temperature?

Oriani: That is correct, yes.

Jordan: I happen to know this calorimeter.

Oriani: It was homemade about 18 years ago.

Jordan: Have you considered building another calorimeter of this type?

Oriani: No. The reason for that is that I regard this as a credible calorimeter to test my credibility, in other words, to convince myself that a real phenomenon is taking place. I have found it rather difficult to use. Next, I would prefer to construct a flow calorimeter, which I believe will give much more flexibility and much faster heat detection to allow burst information to be obtained.

Bard: Were the electrodes in the second series of experiments of different sizes from those in the first set? I noticed that 0.42 A/cm^2 was on the extreme right of

the first set, whereas on the other set 0.42 A/cm^2 would have been well down the list.

Oriani: That is correct.

Bard: What was the main difference between the two sets?

Oriani: I used a closer spacing between the electrodes in the first set.

Bard: So that the I^{2}R term is much lower?

Oriani: That's right. The largest current density with the first configuration represents about the same input voltage as the lowest current density in the second configuration.

Jordan: I would hope that you will continue to perform these calorimetric experiments. I believe that the best calorimeters available today are actually home-built.

Oriani: We have now reconstructed the calorimeter. We will be using an air thermostat, which has taken us some time to stabilize. In case we have another explosion, the air thermostat will absorb the shock wave rather than transmit the energy to the instrument, as the water bath did.

Bard: Do you intend to use closed cells with recombination?

Oriani: I was hoping to do that, using catalyst from Chalk River. My feeling is that we will not learn anything more by using a closed cell, compared with what we have learned from these experiments. However, to convince skeptics, we will try closed-cell experiments, after we have learned to use the recombination catalyst safely.

Voice: What were the dimensions of the piece of palladium attached to the anode?

Oriani: It was 0.25 mm diameter and 1.5 cm long, spot-welded to the anode. The two successful D$_2$O runs used this feature.

Wolf: Did health physics survey the people involved in this explosion?

Oriani: Yes, indeed.

Wolf: Did they find any tritium to be present?

Oriani: As I have mentioned, we had no nuclear manifestations resulting from the catalytic recombination. I looked for tritium in several places. First of all, the explosion did not damage the flask for collecting the D$_2$O, only the calorimeter and its contents. We looked for tritium in the recombined off-gases. We conserved the palladium cathodes from the two successful runs and electrochemically oxidized the deuterium in each one. The cathode from the first D$_2$O run had been stored in liquid nitrogen. After the explosion, it required two hours to find the cathode sample in the wreckage. We therefore lost some of the deuterium, but we stored the sample in liquid nitrogen for a month and a half before dissolving out the deuterium. However, the amount was very small, and no

tritium was detected. Finally, we washed the recombination catalyst with H_2O.
Again, we saw no tritium.

Flanagan: It would appear that your conditions were quite different from those
described by the previous speaker. You analyzed your samples for deuterium
content, but you did not measure high values.

Oriani: Correct.

Section 16

METALLURGICAL ASPECTS OF THE ELECTROCHEMICAL
LOADING OF PALLADIUM WITH DEUTERIUM

S. Guruswamy, J.G. Byrne, J. Li, and M.E. Wadsworth

Department of Metallurgical Engineering

University of Utah

METALLURGICAL ASPECTS OF THE ELECTROCHEMICAL LOADING OF PALLADIUM WITH DEUTERIUM

by

S. Guruswamy, J.G. Byrne, J. Li, M.E.Wadsworth

Department of Metallurgical Engineering
University of Utah
Salt Lake City, Utah

INTRODUCTION

Since Pons and Fleischmann's startling announcement of the possibility of electrochemically induced nuclear fusion of deuterium atoms in solid palladium cathodes at room temperature, there has been international activity to replicate as well as explain their observations. Embrittlement of metals under hydrogen loading has been an important area of study for decades, but rarely, in these studies, is the degree of loading as extensive as that required in the P-F experiments. While there is a very large literature base on the embrittlement of metals under hydrogen loading and the ability of several metals and alloys to store hydrogen, understanding at the atomic level of hydrogen in metals has been eluding the physical metallurgists and solid state physicists. Pons and Fleischmann moved into a hitherto unexplored area of voltage induced heavy hydrogen/deuterium loading of metals; to levels much larger than normally encountered in electroplating, corrosion or conventional metals processing. The properties of metals under such conditions are very important in view of the proposed solid state fusion reactions. This laboratory embarked on a program, which included the operation of electrochemical cells, to determine changes in metallurgical characteristics, composition and structural integrity of cathodes under conditions of high deuterium loading. After several weeks of charging 0.4 cm. X 10 cm. palladium cathodes in 0.1 M LiOD solutions at high overvoltages, modest to large heat releases were observed.

CELL CONFIGURATION AND OPERATION

The large cells used in this study are shown in Figure 1. These cells contained a single thermocouple. Make-up heavy water was added manually once or twice a day. Recently, the cell design has been modified to include features such as continuous heavy water addition to the cell using syringe pumps, removal of electrolytic gases both with and without recombination, multiple temperature sensors and the flexibility to use various sizes of electrodes. Cells are operated mostly in a constant current mode. Temperature, voltage, current and other signals are sampled every 10 seconds and recorded every 1 minute. When sudden changes in cell operating conditions are sensed, recording then occurs every 10 seconds. Thermal calibration is done by performing electrolysis at different power levels as well as by using an internal heater.

The temperature is measured near the cell wall both in the cell and in the bath. Calibration curves are used to determine the heat transfer constant for the cell. The cells have a wall thickness of approximately 2 mm with a corresponding calibration constant of approximately 2.5 watts/degree Celsius, varying ±0.5 watts/degree from cell to cell. Continuous recording of the temperature on either side of the cell wall provides a means to measure the power output level. Because of the large cell constant, this method is applicable for moderately large heat excursions only. This degree of accuracy was considered adequate since the purpose was to examine cathode materials which had experienced large heat excursions as reported by Pons and Fleischmann.

Laser Doppler measurements of bubble velocities in the cell (Figure 2) demonstrate excellent stirring by the evolving gas bubbles except for the very bottom of the cell. Laterally the temperature variation is within 1 $^\circ$C over the length of the cathode. In Figure 2, bubble velocity is shown for each 1 cm interval and is proportional to the length of the arrow. There is an upward movement of bubbles at each electrode of approximately 5 cm/sec and a downward movement of bubbles along the wall of about 0.2 cm/sec for a 9 watt cell input. Figure 3 illustrates the thermal response of three thermocouples in a single cell located one-quarter, one-half and three-fourths of the way down parallel to the cathode and approximately 2 mm from the inner wall surface. Figure 4 illustrates a calibration curve for one of the cells. Each cell thermocouple was calibrated before operation and after a period of time, depending on the behavior of the cell, to make certain it was functioning properly during any thermal response.

Experimental variables considered in an initial series of six cells have been the shape of the platinum anode, the relative anode-to-cathode surface area, the anode-to-cathode distance, with separation of deuterium and oxygen using a Nafion cation membrane, preloading of deuterium under high-pressure deuterium gas, and with variations in the heat and surface treatment of the palladium cathode. Two of the cells used Johnson & Mathey (J-M) Pd cathodes (99.95% Pd) 0.4 cm X 10 cm and 0.3 cm X 10 cm respectively. Four used Metallor cathodes (99.995% Pd). All of the latter were 0.4 cm X 10 cm.

Originally gold contacts were used in soft glass cells. Severe contamination of the electrode surface resulted. The electrode surface was covered by silicates, iron, copper, zinc, and platinum, from the leaching of glass and the gold electrical leads by LiOD. All operating cells were shut down and contacts were made by spot welding of platinum/ palladium lead wires to the cathode. Fresh solutions of the electrolyte were used. All new cell bodies were made of quartz.

TEMPERATURE EXCURSIONS SHOWING EXCESS POWER GENERATION

During the first week of May, 1989, frequent explosive popping of the cells occurred, some with minimal damage and some with the destruction of the assembly. Temperature excursions were associated with some of these events, which were initially dismissed as being due to deuterium and oxygen recombination. Again in the third week of May, 1989, a heat excursion of about 12°C in the cell temperature and lasting about 90 minutes was observed (Figure 5). At this time, the cell was operating in a constant current mode with a current setting of 0.95 amperes (≈ 100 ma/cm^2. The voltage was recorded continuously while the current was recorded manually. The temperature excursion was interrupted after 90 minutes by the addition of heavy water. The temperature-time profiles showed a similar pattern to an earlier temperature excursions for the same rod which had been attributed only to D_2/O_2 recombination. The data for the earlier excursion were accessed and showed an interesting bimodal pattern of excess heat generation. The results are presented in Figure 6. During the time shown in Figure 6, the cell was being operated in a constant voltage mode and the voltage and current readings were recorded manually. Explosive popping of the cell interrupted the large heat burst after 40 minutes. The cell head had been readjusted immediately and the cell temperature remained at an elevated level for 30 hours. The input during this period was about 9.6 watts. After the 30 hour period, a second explosion occurred ending the run. Excess heat generated during these two events was about 240,000 joules during the 90 minute burst and approximately 1.2 Mj during the 40 minute burst plus the 30 hour period. This level of energy output could not be explained by burning of all the deuterium stored in the palladium, by the heat of solution of deuterium in palladium, nor by the heat of formation of PdD_x.

The heat excursions shown in Figures 5 and 6 were for the same J-M rod. The charging time for the first excursion (Figure 6) was approximately 19 days. The rod was polished with fine alumina abrasive and reassembled in a new cell. After approximately 17 additional days of charging the second excursion (Figure 5) occurred. Figure 7 shows a heat excursion for the 0.3 cm X 10 cm J-M cathode. This level of heat generation continued for approximately three days. Figures 8 and 9 illustrate two consecutive heat excursions from a single Metallor rod. The first (Figure 8) occurred after 9 days charging time. The second, (Figure 9) occurred 4 weeks later. A third burst occurred after an additional 1 week of charging time. The cathode showed extensive cracking along its length.

The possibility of storing energy in the solution in the form of peroxide was examined. Analysis of electrolyte samples from all the operating cells showed peroxide concentration was less than 10^{-4} moles/cm^3 as expected from the instability of peroxide under high cathodic overvoltage conditions and in basic solutions. After

degassing of the electrode that showed the 90-minute heat burst, the tritium levels in the electrolyte and in the starting solutions were checked by 3 different laboratories. The level of tritium was found to have increased by a factor of 3 to 4. We are doubtful that this is a significant effect.

METALLURGICAL EXAMINATION

The palladium electrode which had the two heat bursts illustrated in Figures 5 and 6 was degassed by opening the circuit. The open circuit degassing was continued until D_2 evolution was no longer evident. The electrolyte was then sent out for tritium analysis. The electrode was cleaned with distilled water and dried. Resistance measurement by a four probe technique showed a two-fold increase in resistivity. The electrode was then examined by a positron annihilation technique. The Doppler line broadening of the electron-positron annihilation peak at 512 Kev showed a 6% change in the Peak/Wing ratio, which indicates a large increase in defect density. The surface hardness along the length was first measured using a Vickers indentor at 1 Kg load. Soft and hard spots at adjacent locations were observed. Smaller lengths were cut from the lower half of the electrode and hardness measurements were made on the cross section. The hardness values obtained were very uniform showing values of 102 ±5 VHN. The hardness value for this material before the cell exposure was 69 VHN. Thin slices cut from this electrode were mechanically polished and then electrochemically thinned for observation of the internal structure. The electrode after the cell operation showed extensive deformation and, as expected, much larger dislocation density compared to the annealed starting material. The damage observed may be due to the large strain associated with β hydride phase formation and/or the deformation resulting from high-pressure hydrogen bubbles. In the future it will be very important to make a comparison of the internal damage for identical rods, only one of which has experienced excess heat generation. Surface chemical analysis by CAMECA 50 SX electron microprobe showed only palladium with trace amounts of Rh and Br. Rhodium contamination from the platinum anode is possible. However, SIMS analysis shows an enhanced Li surface concentration along with a number of other elements. The amount of palladium in the near surface region is surprisingly small. The sputtered depth over which the SIMS analysis was performed was about 5000 °A. Bulk analysis by atom probe and Differential Scanning Calorimetry to measure damage energy release rates are currently in progress.

CONLUSIONS

The experiments reported here support observations from other laboratories of excess heat generation by electrochemically charged Pd cathodes in heavy water. No evidence of nuclear reactions producing gamma radiation or neutrons was obsrved. There was a 3 to 4 fold increase in Tritium for the cell showing the largest heat

generation, but this level could result from various separation factors and is not considered to be conclusive. Initiation of heat generation by bursts is very random in time. The possibility of excess heat from peroxides in solution was examined as a possible chemical source of heat. The level of peroxide in solution was well below the detection limits and thus too low to have any bearing on heat generation. As yet a chemical explanation for excess heat generation has not been found.
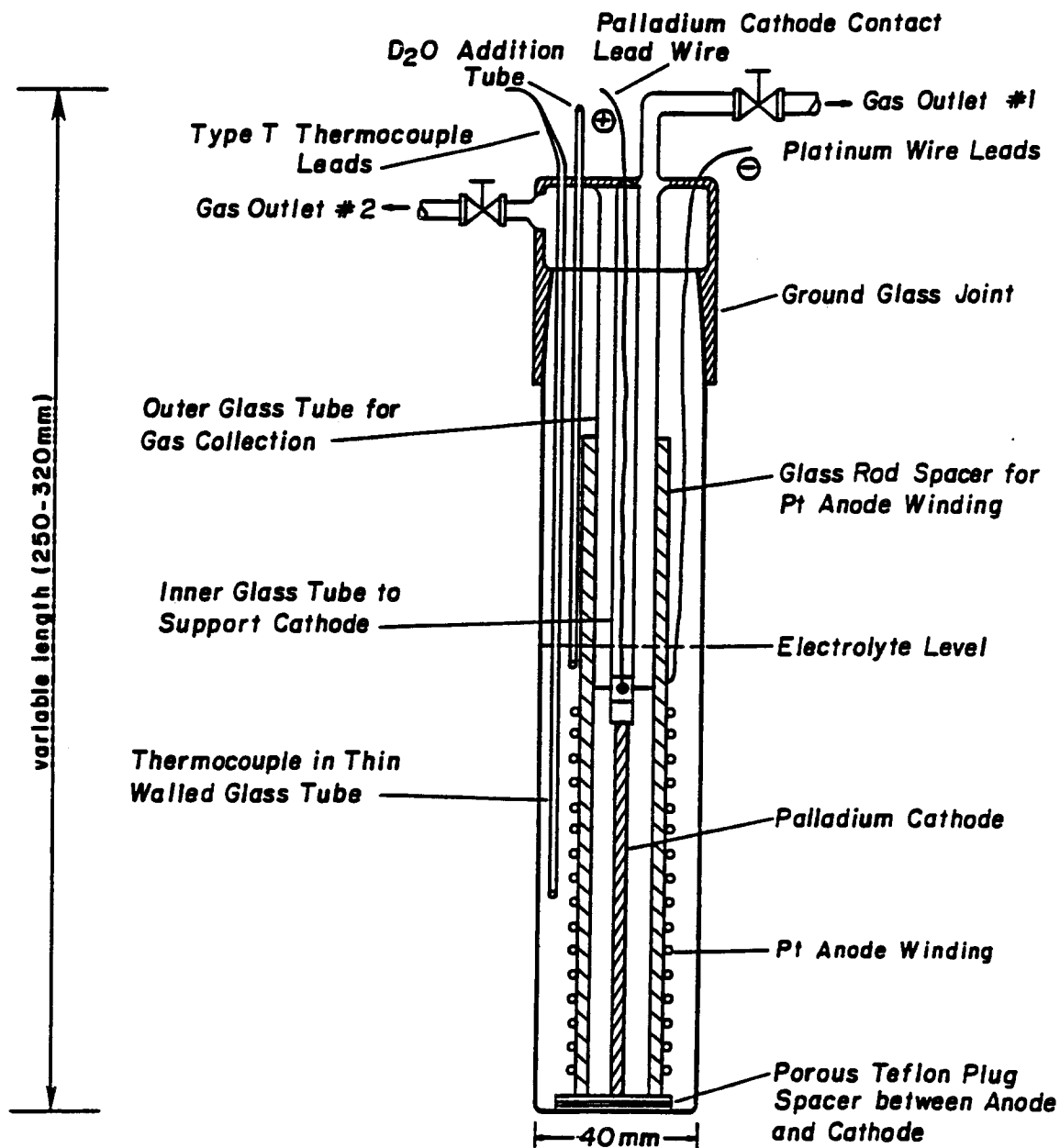
Figure 1.   Electrochemical Cell Construction.
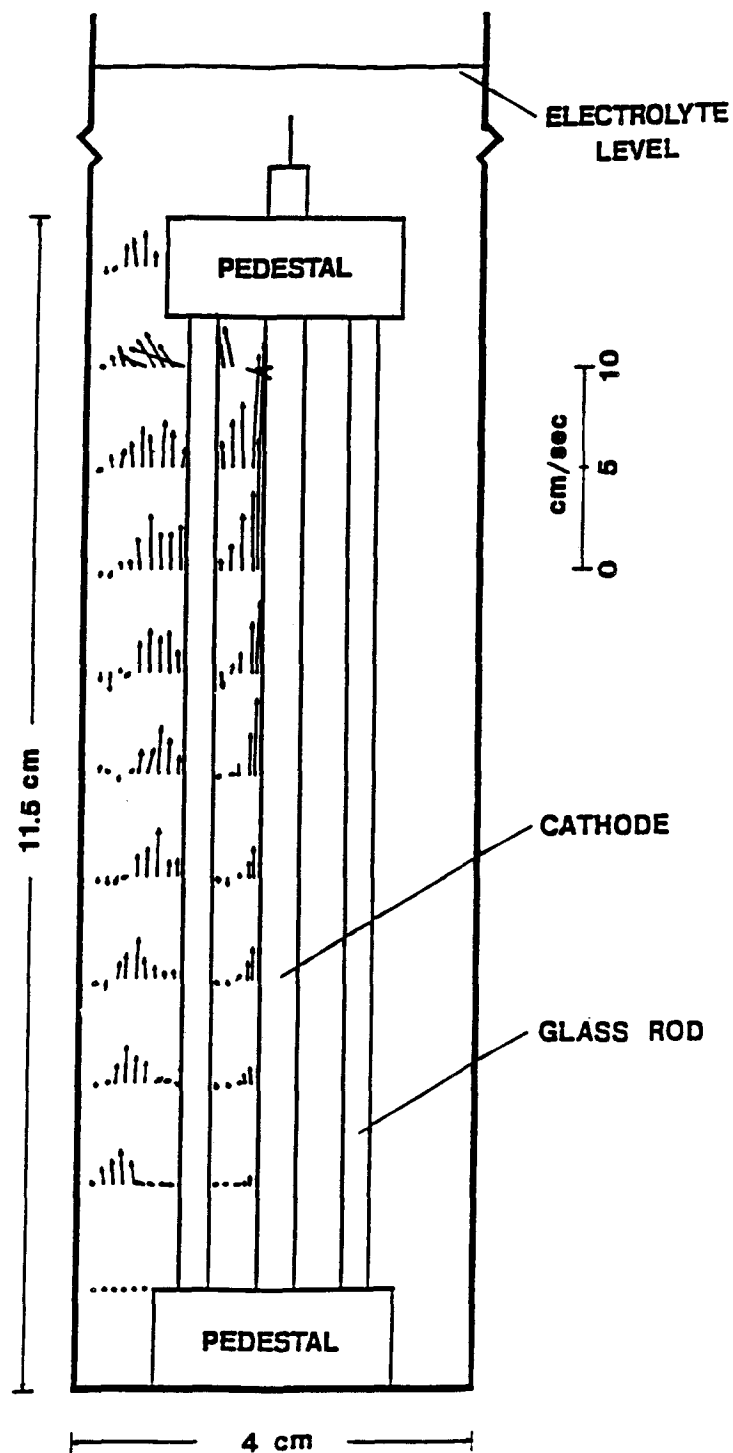
Figure 2. Laser Doppler Results Showing Velocity of Bubble Movement in Electrochemical Cells.
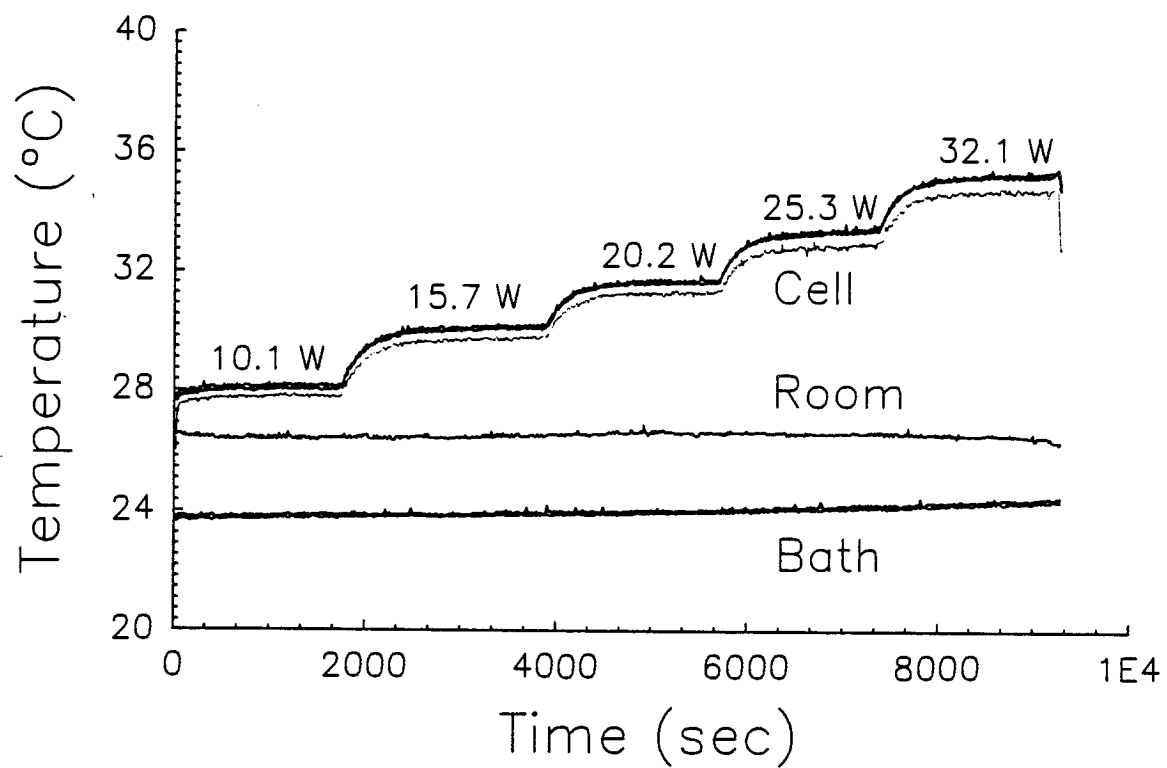
Figure 3. Thermal response of three separate thermocouples in a single cell.
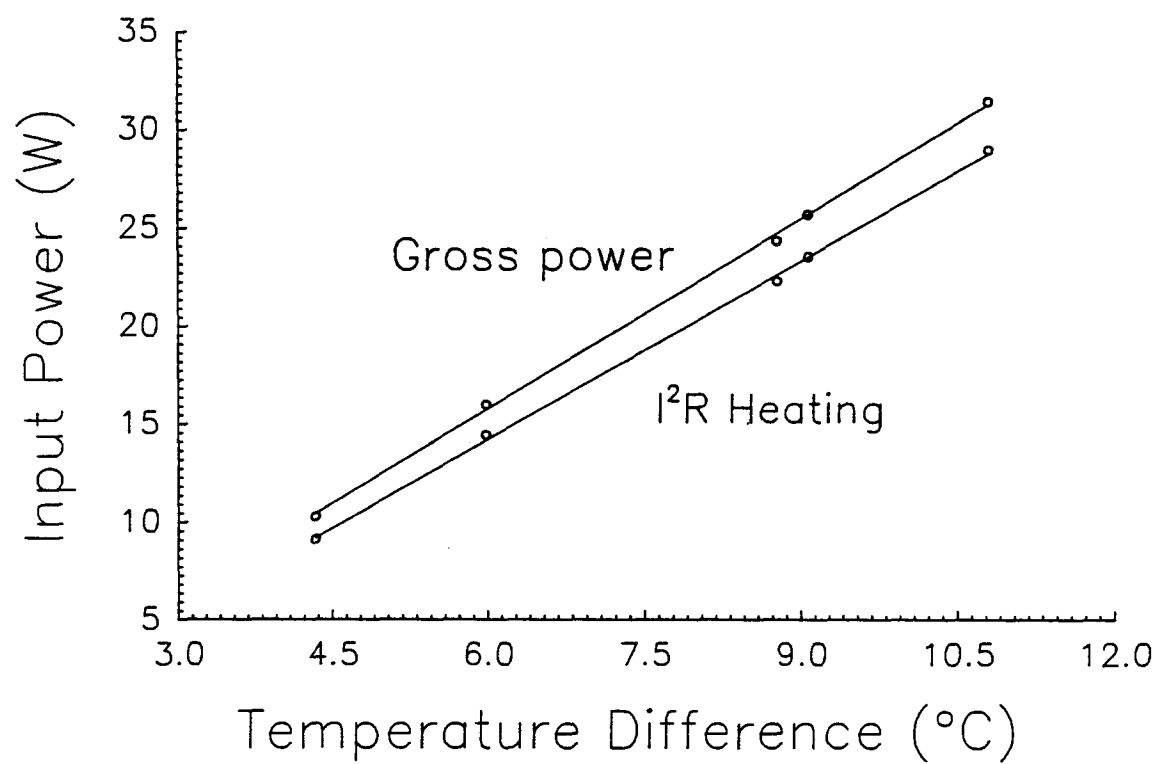
Figure 4. Calibration curve of an electrochemical cell.
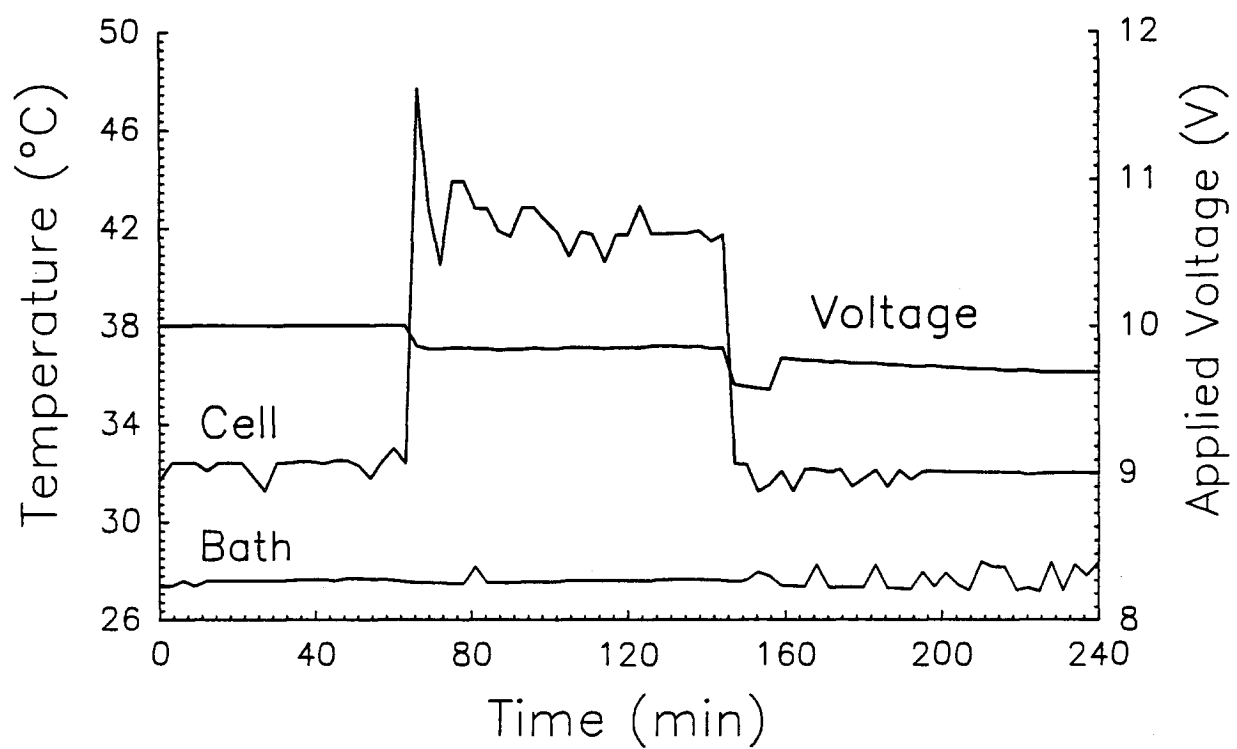
Figure 5. Heat excursion for the J-M cathode 0.4 cm x 10 cm.
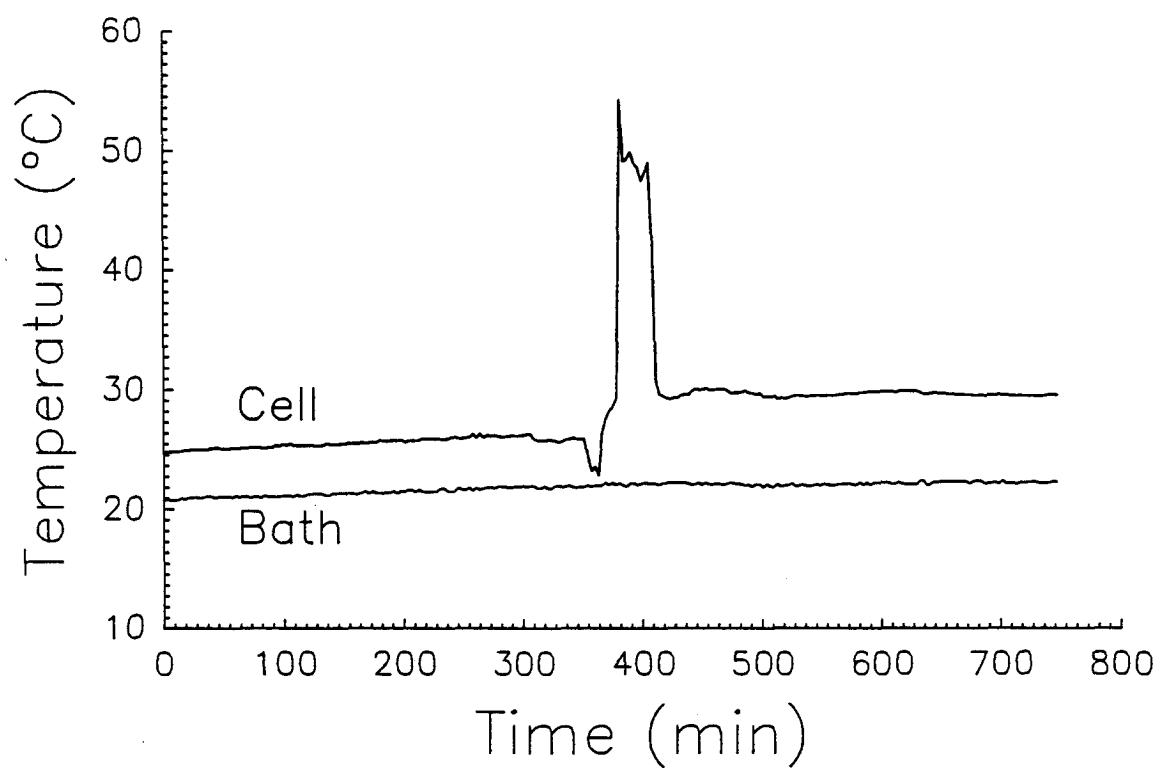
Figure 6.   Previous heat excursion for the cathode of Figure 5.
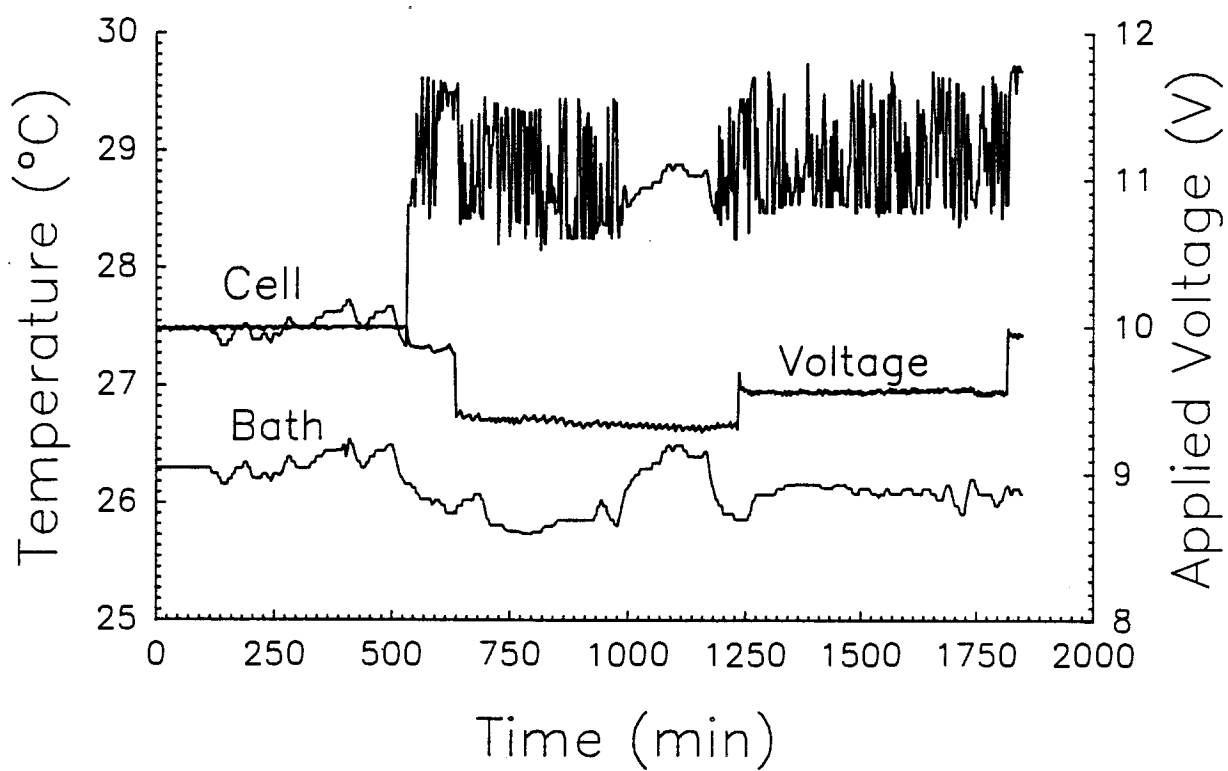
Figure 7. Heat excursion for the J-M cathode 0.3 cm x 10 cm.
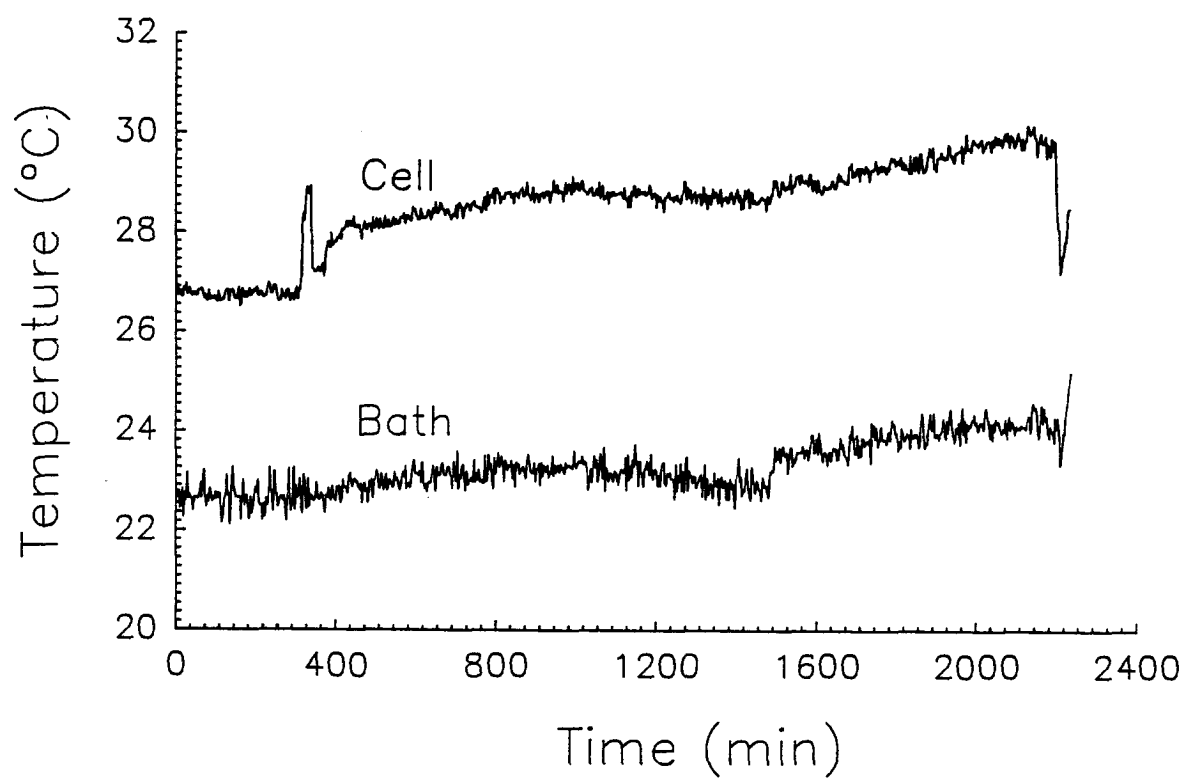
Figure 8. Heat excursion of a metallor Pd cathode.
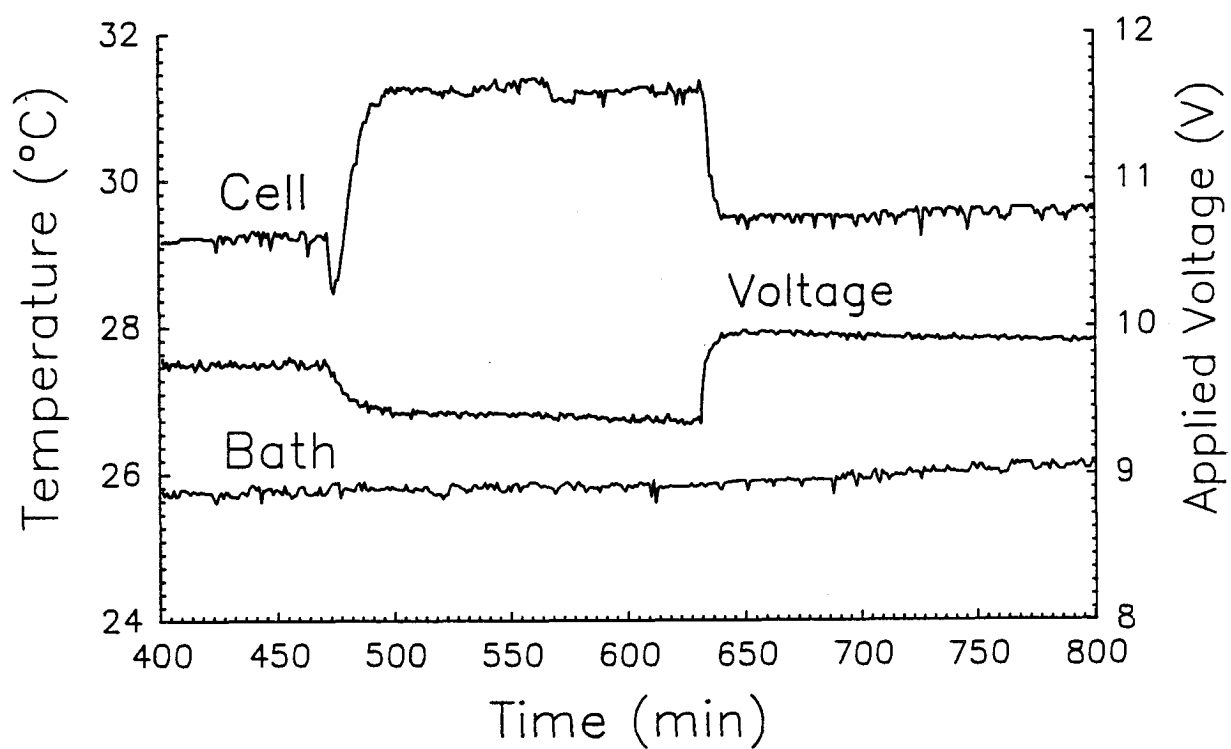
Figure 9. Second excursion of metallor Pd cathode.
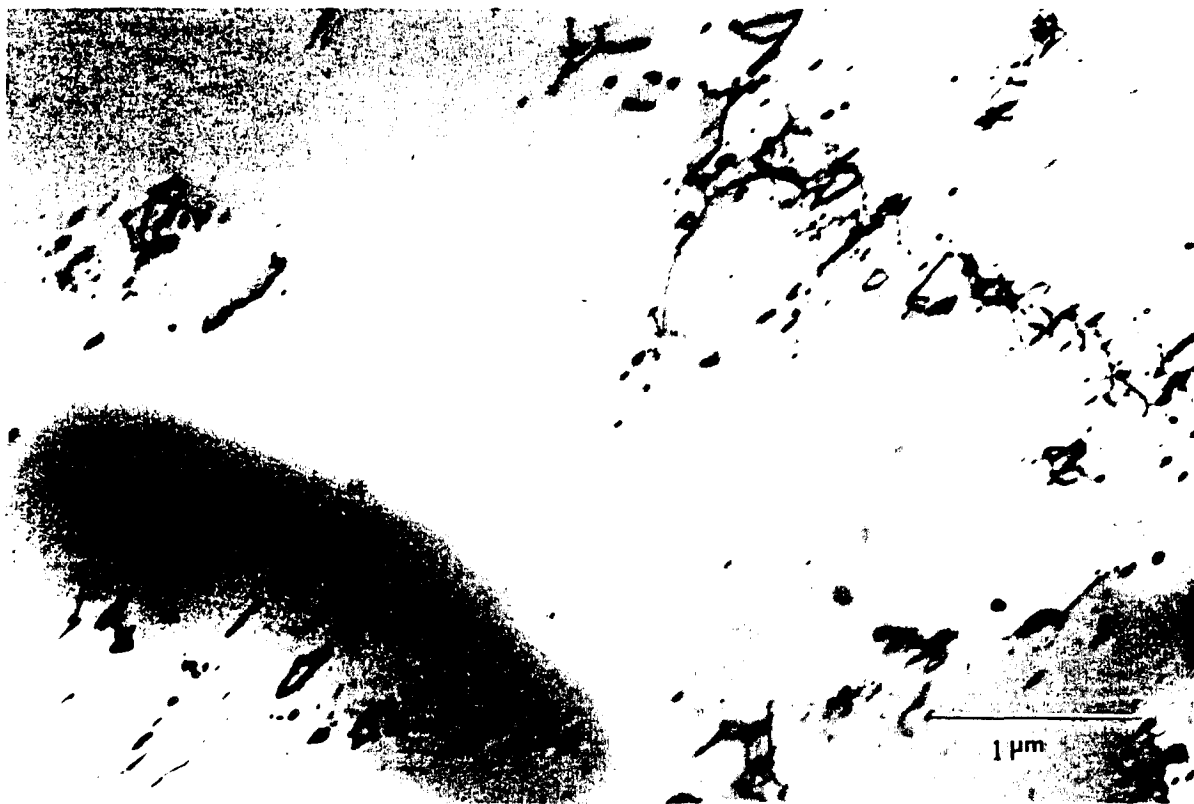
Figure 10a.   Transmission Electronmicrograph of J-M Pd after
               Annealing.
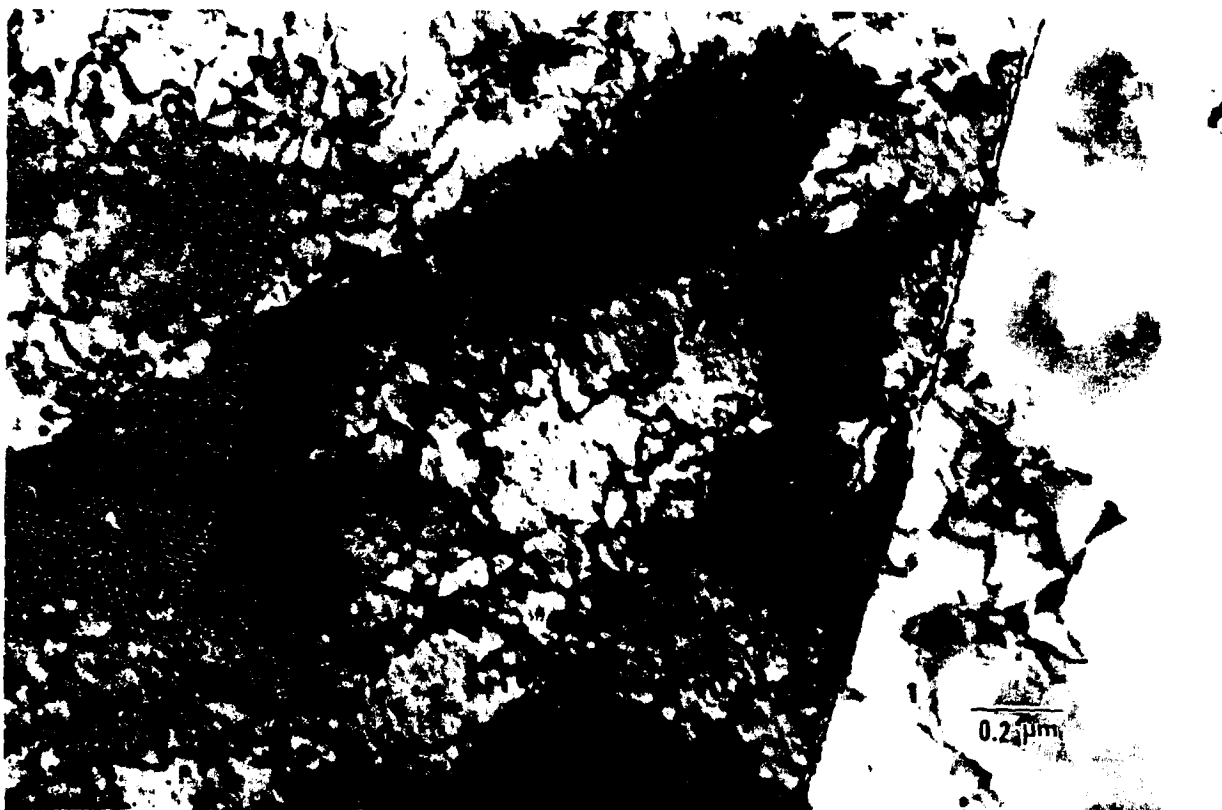
Figure 10b.   Transmission Electonmicrograph after Heat Excursions
                   Shown in Figures 5 and 6.

DISCUSSION (WADSWORTH)

Santucci: Do you know if the silica which you detected in your cells was there before the experiment, or was it deposited after you turned off the current?

Wadsworth: I cannot give you a definitive answer. The cell was removed, washed, and then sent out for analysis. After experiments with soft glass cells we immediately went to a quartz apparatus. My results refer to a series of quartz cells which had approximately linear calibration constants.

Lewis: What was the temperature difference between the bath and the cell in your experiments?

Wadsworth: Rather than considering the temperature difference, we should consider the calorimeter constant. It was about 2.5 $\pm$0.5 W/K taken over a series of experiments.

Lewis: I suppose that it would represent about 2 W per cell?

Wadsworth: Yes. I should point out that our calorimeter is good for rapid response, but that it is rather poor for measuring a small constant heat output. We had the same degree of frustration as that reported by other groups who have operated PdD electrolysis cells. Our cells were operated for a very long time before any interesting results were seen. Thus, our first impression was that our cells would run forever without showing anomalous effects. I must point out that we had gas explosions, so we put blow-off tops on the cells. However, I have to admit that we did not check the system for tritium. Our experiments convinced me that we were looking at problems concerning hydrogen-oxygen recombination. In 1964, I worked on this topic at Oak Ridge National Laboratory. It is an important consideration in breeder reactor technology, since neutrons can cause water breakdown. If the latter does occur, one must be able to recombine the gases faster than they are generated. We examined this problem, and we found out that first-order oxygen-hydrogen recombination occurs routinely on catalytic particle surfaces. Such a recombination phenomenon should be very regular and should follow a first-order recombination process. My initial impression was that once in a while the process may become out of control and explode. This was true until one Sunday morning, when the cell temperature definitely increased for the first time. My first thought was that it was an artifact.

Oriani: Was there an explosion at that time?

Wadsworth: No.

Bard: Did your cell use a constant-current power system?

Wadsworth: Yes.

Bard: Your results show that the cell voltage dropped during electrolysis, but the excess heat dropped when electrolyte was added.

Wadsworth: Electrolyte was added once or twice a day, as was necessary. Often, when it was added, it quenched the cell. So, if the excess heat process is a nuclear reaction, it can apparently be quenched with 10 ml of D_2O.

Oriani: Was the electrode fully covered by electrolyte in every case?

Wadsworth: In this particular case, we had 3-8 mm of the top of the electrode outside of the electrolyte because of contact problems.

Oriani: When you added additional D_2O, did you cover more of the electrode active area?

Wadsworth: We consistently used a total electrolyte volume of 120 ml. We added about 10 ml of D_2O per day, so that our level has been changing by about 10 percent.

Rafelski: Was the electrode exposed to the gas phase during the experiments?

Wadsworth: Yes, it was. However, my paper has evidence to show that it was not always the case. As much as 17 days of charging time was used.

Santucci: Did the current remain constant while you added the electrolyte?

Wadsworth: We normally never changed the cell current.

Rafelski: Is it possible to generate the amount of heat which you see via a chemical process involving hydrogen in the palladium cathode?

Wadsworth: This was the first question we asked ourselves. However, the heat which we measured was 38 times the amount of energy one would obtain by burning the deuterium absorbed in the cathode, assuming the composition to be PdD. The total quantity of deuterium would then represent 0.1 moles.

Storms: How can the cell temperature change as rapidly as your plots show?

Wadsworth: The data points were taken three minutes apart, and the thermocouple will respond within that time. Unlike the previous speaker's calorimeter, our system does not integrate the heat output.

Bard: Did your voltage measurement show the same oscillations as the heat output response?

Wadsworth: Yes, there is a correlation.

Bard: How many microvolts do the temperature oscillations at the thermocouple represent?

Wadsworth: They are on the order of 10 microvolts.

Storms: Are the thermocouples shielded?

Wadsworth: There was only one thermocouple in the cell. It was shielded by a small quartz tube, making it easy to replace.

Rafelski: Why does the plot representing the bath temperature vary?

Wadsworth: It represents the change in air conditioning temperature in the building.

Chubb: How were your anodes and cathodes arranged?

Wadsworth: The anode was a spiral on a cage outside the cathode rod in the center.

Chubb: Are the heat oscillations associated with any special type of experimental arrangement?

Wadsworth: We saw no heat oscillations in the other cells which we examined. If it were an endemic phenomenon, one would expect to see it every time.

Yeager: What caused the surge in cell voltage at 1,200 minutes?

Wadsworth: This was simply an input power adjustment, where the cell current was increased.

Yeager: How deeply is the cell immersed in the bath? Is the top of the cell in contact with the air in the laboratory?

Wadsworth: About 8 cm is exposed above the bath.

Yeager: Variations in room air conditioning temperature would be expected to affect the calorimetric results, with a large portion of the cell exposed.

Wadsworth: It was necessary because of our cell connections. I agree with you that it may have caused some slight error. However, our objective was not to do accurate calorimetry, but rather to detect the relative changes represented by heat bursts.

Miley: How many joules were released during the time that your cell temperature rose by 2°C?

Wadsworth: About 8 W over 3 days, or 2 MJ.

McKubre: Could you comment on your results on cells using cathodes other than palladium?

Wadsworth: Out of a total of eight cells, six have palladium cathodes, one has zirconium, and one has titanium. We have not seen any heat excursions in the cells with zirconium or titanium cathodes after three or four months of operation.

McKubre: Do you see any corrosion of zirconium or titanium in alkaline electrolyte?

Wadsworth: The electrodes are intact.

Thompson: You said that some of your rods showed cracks and fissures, but that there were none in the Johnson-Matthey cathode. Was that active for excess heat production?

Wadsworth: The Johnson-Matthey specimen did produce excess heat. We did not see the gross fissures in it that were seen in the other samples.

Thompson: That is consistent with our analytical results on rods returned from experiments conducted by Fleischmann and Pons. Cracks and scratches are surface

features of virgin rods, and the intensity of these features increases with the use of increasing current densities.

Chubb: At what point in the experiments was cracking identified?

Wadsworth: The cracking which I described was seen shortly after we observed the first heat burst. The electrode was operating in a cracked condition during the next two bursts. It is interesting that the metal is still capable of operating with the kind of gross damage that it has sustained. Another specimen did not crack but suffered severe internal damage. More important metallurgical studies are required on these specimens.

Oriani: I would not expect any marked differences in microstructure between an active and an inactive electrode. Any damage should occur during loading with hydrogen or deuterium.

Santucci: Is the damage in the bulk, or mostly at the surface?

Wadsworth: The damage penetrates to the bulk material. The metal becomes full of voids and dislocations.

Oriani: Did you say that one would not expect this damage in the normal course of events?

Wadsworth: I would say that the damage goes far beyond that which is normally seen in hydrogen embrittlement.

Oriani: I would maintain that it is not abnormal.

Wadsworth: I will accept that, but it does represent a great deal of damage.

Flanagan: Normal hydrogen embrittlement does not occur with a 10 percent volume expansion. It is not like embrittlement in iron or steel, where the amount of hydrogen involved is small, and no expansion occurs.

Lewis: I would like to say that I find both your results and those reported by Dr. Pons very believable. Can you identify any differences in your experiments which might explain why you have had no successes in two months, after previous experiments were successful?

Wadsworth: The only thing which I can think of is the fact that we are now using a different lot of metal.

Rafelski: Perhaps it is due to a different lot of heavy water. May I ask what you have done with the old palladium which you used in the successful experiments?

Wadsworth: We still have some samples, and we sent the remainder to Battelle-Northwest.

Rafelski: Could you not reuse the old material?

Wadsworth: You mean the material which showed the oscillations in heat output. We are still operating it in a cell, and it is showing some low-grade excess heat after several months of operation.

Huggins: Have you determined if there is a threshold value of the current density for production of excess heat?

Wadsworth: No.

Myles: You mentioned heat-treatment of your electrodes. Exactly what pretreatment did you use?

Wadsworth: Both the Johnson-Matthey and Metallor electrodes were annealed at 900°C. The other two electrodes were annealed at 600°C.

Myles: Which were successful?

Wadsworth: Electrodes which had received both 900°C and 600°C heat treatments were successful.

Myles: How did the palladized electrode behave?

Wadsworth: It showed the largest amount of excess heat. We plan to do another experiment using an electrode which has received only anodic treatment followed by cathodic treatment. Anodic treatment and cathodic plating would be conducted in a separate experiment. There are many other variables which we would like to examine.

Hoffman: Did you see any dendrites on the surfaces of any of your specimens?

Wadsworth: No.

Hoffman: Did you specifically look for them?

Wadsworth: No. The surface examination was carried out at General Electric. There were pocketlike areas on one surface which were about about 100 microns long. Inside these pockets, oxide patches and silicate deposits were visible. Battelle-Northwest reported some enhancement of lithium, although GE did not identify it as being present. Aluminum, sodium, lithium, calcium, iron, carbon, and cadmium contaminants were present on the surface. The amount of palladium which is detectable on the surface of the electrode is surprisingly small. After electrolysis, the composition of the electrode was about $PdD_{0.7}$.

The possibilities of localized hot regions in the top sections of the cell was a concern. Different situations that were considered are catalytic burning of deuterium on the exposed top section of the electrode, catalytic recombination under the electrolyte in the vicinity of the anode, and occasional development of convectional current patterns leading to hot fluid moving down near the inner cell glass. Experiments were conducted early on simulating localized burning at the top exposed section of the electrode. The localized heat was supplied either by electrical resistive heating and by hydrogen flame. Electrical resistive heaters, having different winding configurations located near the electrolyte level, delivered power at levels of between 1-10 watts, and the temperatures at different points of the cell were probed at steady state. The convection in the liquid was maintained by electrolysis as well as by bubbling air. The temperature

differences observed were less than 4-5°. In another simulation, a hydrogen flame burning near the top of the electrolyte level was used to deliver localized heat, and it was observed that the temperature changes sensed were less than 2 or 3°. We have not observed the large temperature excursions since we have completely covered the electrode with the electrolyte. However, we believe that sustaining large temperature differences over a long period of time, as observed in our cells by localized burning, is likely. Temperature measurements, along with laser Doppler measurements of fluid velocities, performed to find out the flow patterns and temperature variation between different points in the cell, were small. It should be pointed out that in the latter experiments different lots of palladium and heavy water were used.

Section 17

ANOMALOUS CALORIMETRIC RESULTS DURING LONG-TERM EVOLUTION OF DEUTERIUM ON PALLADIUM FROM ALKALINE DEUTEROXIDE ELECTROLYTE

A. John Appleby, Young J. Kim, Oliver J. Murphy, and Supramaniam Srinivasan

Center for Electrochemical Systems and Hydrogen Research

Texas A&M University

ANOMALOUS CALORIMETRIC RESULTS DURING LONG-TERM EVOLUTION OF DEUTERIUM ON PALLADIUM FROM ALKALINE DEUTEROXIDE ELECTROLYTE

A. John Appleby, Young J. Kim,
Oliver J. Murphy, and Supramaniam Srinivasan

Center for Electrochemical Systems and Hydrogen Research
Texas Engineering Experiment Station
Texas A&M University
College Station, Texas 77843, USA

Abstract

Evidence of anomalous thermal fluxes on palladium cathodes in LiOD solutions is provided. Compared with previous work, effects are only seen at a relatively low level, and they appear to decrease with decreasing electrode surface/volume ratio. They are also observed in a sealed cell with gas recombination, which requires no thermodynamic corrections. The effect of lithium ion is seen to be specific, and the effect seems to involve only the palladium surface layers.

Introduction

In a recent publication, Fleischmann, Pons and Hawkins[1] have alluded to anomalous enthalpy production when deuterium is evolved on palladium from solutions of lithium deuteroxide in deuterium oxide after polarization over long periods of time. These experiments were conducted using a classical calorimetric technique, in which temperature changes were measured using Beckmann thermometers. The authors concluded that nuclear reactions of unknown type involving deuterons dissolved in palladium beyond the composition corresponding to that of the end of the $(\alpha+\beta)$ phase were taking place, since no significant neutrons or γ-radiation much above background were observed. The total excess thermal energy (4MJ), observed over a period of 120 hours, was much greater than the heat output from any possible chemical process. Such results have not been reported for cathodes which do not significantly absorb deuterium (e.g., platinum), or during hydrogen evolution on palladium from light water. In this paper, we report the results of work on anomalous heat production from palladium cathodes during deuterium evolution from lithium deuteroxide solutions in deuterium oxide. We also present results of control

experiments with platinum cathodes evolving deuterium under identical conditions, and with palladium electrodes evolving hydrogen from lithium hydroxide-light water solutions.

Experimental

The investigations were conducted using an automatic precision heat conduction microcalorimeter (Tronac Model 350, Orem, UT). This is a differential heat conduction instrument with a noise level of less than 0.3 μW and a precision better than 1 μW. The temperature fluctuations of the water bath in the microcalorimeter are controlled to $\pm 0.0002°C$. The instrument operates by electrically comparing the voltage signal ΔV across a thermoelectric junction assembly mounted around the working chamber with a similar signal from a reference chamber in the instrument, which avoids fluctuations in the baseline or in the instrument constant. The voltage determined is proportional to the temperature difference across the ends of the thermoelectric pile, and thus to the heat flux. The instrument includes a built-in calibration resistor (about 1000 Ω), with a maximum heat output of 25 mW. Since this level was much below the heat outputs measured, we constructed an extended calibration curve using a standard resistor of smaller value inside the electrochemical cell with and without electrolyte (Fig. 1). It includes any effects of temperature change inside the cell, and is linear over a wide heat flux range. The voltage signal ΔV is monitored using a high-impedance digital voltmeter and the instrument also provided a continuous chart-paper printout of these data, which is available for inspection. The heat flux from the calorimeter is given by $\Delta V.C$, where C is the slope from Figs. 1a and 1b, the calibration plots for the two chambers of the calorimeter. Since the bath temperature of the calorimeter can be adjusted in the range 2°-30° C, it was possible to verify the temperature-independence of the the calibration. The value of C was 184.0 with a standard deviation of ± 1.23.

Heat generation rates were measured in a closed stainless steel cell, which was used because of its high thermal conductivity. The cell fitted snugly in the working chamber of the microcalorimeter (1cm x 5cm x 5cm) which was located in a large aluminum block in contact with a water bath maintained at 25°C. The latter temperature could be varied by means of a freon bath. Preliminary results established negligible corrections for the heat generated by oxidation of the stainless steel cell in the electrolyte.

Electrochemical cells were assembled with palladium wire cathodes (1 cm long, 0.05 cm diameter) surrounded by spirally wound platinum wire anodes (99.9995% pure, Alfa Products). All cathodes were cut from the same batch of palladium wire (99.997% pure, Alfa Products). Platinum wire leads (0.05 cm diameter) were spot welded to one end of the palladium cathodes and isolated from the solution by means of Teflon. In control cells,

a similar electrode configuration was used with a platinum wire substituted for the palladium. All electrode specimens were cleaned using acetone followed by thorough rinsing with ultrapure water. The electrolytes initially used were 0.1 M lithium deuteroxide in 99.8% pure deuterium oxide (Aldrich Chemical Company), and 0.1 M lithium hydroxide in ultrapure light water. Both solutions were prepared by dissolving natural lithium metal ("^{n}Li" 99.9% pure containing 93% ^{7}Li, Aldrich Chemical Company) in light and heavy water. The cells with the palladium cathodes were examined in the heavy and light water electrolytes, and those with platinum cathodes in the deuterium oxide electrolyte only. In later experiments, 0.1 M NaOD, 1.0 M ^{n}LiOD, 0.1 M ^{7}LiOD and 0.17 M ^{6}LiOD electrolytes were used. They were prepared by dissolving "nuclear" grade sodium metal sealed under argon (Alfa Products), ^{7}Li (99.9% chemical purity, 99.8% isotopic purity, Eagle-Picher Industries) and ^{6}Li (99.97 chemical purity % pure, isotopic purity 98.67%, Oak Ridge National Laboratory). The ^{7}Li isotope was supplier-sealed under argon, whereas the ^{6}Li was under oil, and was Soxhlet-extracted with hexane before use.

The electrical circuits were carefully checked for leakage currents to ground via the metal cell and it was verified that the working and counter electrodes connected to a constant-current power supply were indeed floating. Any AC component from the power line was verified to be less than 20 mV in 5 V. The cell voltage (V) was continuously monitored using a high-impedance digital voltmeter.

After allowing the stainless steel cell and its contents to thermally equilibrate in the microcalorimeter, palladium working electrodes were polarized cathodically 0.1 M ^{n}LiOD at 0.06 A/cm^2 for 40 hours to allow saturation of the palladium with hydrogen or deuterium beyond the end of the ($\alpha+\beta$) phase composition. In preliminary work, this was immediately followed by the application of current densities of 0.6 A/cm^2, 1.0 A/cm^2, and 0.3 A/cm^2 for various times (see for example Fig. 2). In this example, the cell currents were 97.2 mA, 161 mA and 49.2 mA, respectively. The voltages were about 4.5V, 5.6V and 3.4V. Some voltage variation, discussed below, was seen as a function of time. While the cells were being polarized, the rates of heat generation were monitored. The heat input could be determined from instantaneous readings of the cell voltage, which could be read to within three (but not four) significant figures. The voltage at constant current showed a random noise in the range ±2 to ± 10 mV due to variations in effective cell resistance resulting from gas evolution. The cell current, which showed small variations with time, could be determined to a precision of 0.1%. The calorimeter output was a low noise signal typically in the range 1500 to 2500 μV, which was read by a digital voltmeter to a precision of ±10 μV.

Solvent was periodically added every 48 h to the cell to maintain constant volume due to loss of solution by electrolysis and any entrainment by evolved gas. The measured amount of solvent was 1.7 ml at a current density of 0.6 A/cm2. This quantity corresponds to the theoretical amount for 100% dissociation of the electrolyte to hydrogen or deuterium and oxygen at a total cell current close to 0.1 A. In no case was the electrolyte level allowed to fall so that platinum or palladium wires were exposed above the electrolyte. After each addition, the cell and its contents were allowed to reequilibrate before further recordings were made.

Results

Plots of the cell potential and of the excess rate of heat generation, recorded as a function of time for a palladium wire cathode in 0.1 M ^{n}LiOD, are presented in Figure 2. The rate of excess enthalpy generation, ΔQ, is given by:

$$\Delta Q = Q - \{E - (\Delta H/F)\} I \qquad (1)$$

where Q is the total rate of enthalpy generation, E is the cell potential, ΔH is the heat of formation of gaseous D_2 or H_2 and O_2 from liquid D_2O or H_2O, as appropriate, F is the numerical value of the Faraday in joules, and I is the current passing through the cell. The value of DH/F is 1.527 V for D_2O (rounded to 1.53 V) and 1.48 V for H_2O. The excess enthalpy flux for D_2O was therefore:

$$\Delta Q = \Delta V.C - (E - 1.53)I$$

(2)

The correction for evaporation of solvent was determined to be small (certainly less than -2 mW at a cell temperature maintained close to 25°C by the heat conduction calorimeter), compared with the order of magnitude of the heat flux changes sought. Consideration of the precision of reading ΔV, E and I, along with the standard deviation of C, suggests the the error in determining ΔQ using Equation 2 is ±3 mV. However, to verify that Equ. 2 can be used to accurately calculate the irreversible heat flux, it is necessary to show that recombination of the gases is small. Although it is possible to estimate the extent of recombination from the measured amount of solvent periodically added to the cell, for a more precise determination gas volumes from the operating cell were measured using a gas burette during electrolysis, both on the bench and in the calorimeter. Results obtained were always slightly less than, but within about 1% of, the theoretical value, indicating a small

amount of recombination, presumably by diffusion of oxygen through the electrolyte to the cathode. If the fraction of gases recombining during the experiment is x, the heat flux input to the calorimeter will be (E - [1.53][1-x])I. If x is indeed 0.01, then the error in ΔQ will be positive and equal to about +1.5 mW. Thus, a small amount of recombination will tend to compensate the heat loss resulting from evaporation. Since these corrections are within the overall estimated errors bars, the latter are shown as $\pm$ 3 mV on the plots of the experimental results. Breaks are shown in the plots corresponding to the re-equilibration times for the calorimeter after the cells were opened for verification or electrolyte addition. These corresponded to intervals of 1-2 hours.

The result in Fig. 2 shows an excess rate of heat generation (i.e. over and above the rate of heat generation due to irreversible losses in the electrochemical cell) several hours after the current density was increased to 0.6 A/cm^2 from 0.06 A/cm^2, the current density for charging of palladium with deuterium. It is interesting to note that at current densities of 0.6 and 1.0 A/cm^2, the excess rate of heat generation was 38 mW, whereas at 0.3 A/cm^2 it decreased to 29 mW. As a percentage of the irreversible heat flux input to the calorimeter, the excess heat was 6.1%, 13.2%, and 31.5% at 1.0, 0.6, and 0.3 A/cm^2 respectively. The fact that the rate of excess heat evolution increases as heat input (i.e., the reaction rate) to the calorimeter decreases is a strong argument against a spurious chemical explanation of this effect, particularly anomalous (and unobserved) recombination of deuterium and oxygen. The highest heat generation rate observed (at 0.6A/cm^2) corresponded to 19.3 W/cm^3 of Pd, which is comparable to that reported by Fleischmann, Pons and Hawkins (26 W/cm^3).

A similar experiment to that shown in Figure 2 was carried out using a platinum cathode in 0.1 M ^{n}LiOD for a period of 80 hours. Since platinum does not form a hydrogen or deuterium bulk alloy, a current density of 0.6 A/cm^2 was applied from the beginning of the experiment. From the data in Figure 3, it is clear that there was no excess heat generation in this case. In a third experiment, electrolysis of H_2O from 0.1 M ^{n}LiOH using a palladium cathode, and the same current density sequence as in Fig. 2, did not reveal any excess heat generation, as shown in Figure 4. These results again demonstrate that recombination of evolved oxygen and deuterium gases within the electrochemical cell should not be a chemical source of the excess rate of heat generation observed for deuterium evolution on a palladium cathode from the ^{n}LiOD electrolyte. The experiments in Figures 3 and 4 have been repeated three times with palladium cathodes in ^{n}LiOH electrolyte, and three times with platinum cathodes in ^{n}LiOD electrolyte, each giving identical results to the examples shown.

The sequence of current densities shown in Fig. 2 for palladium cathodes in ^{n}LiOD electrolyte was repeated for several different specimens of different dimensions, origins, and pretreatments. In all cases, some excess heat generation was observed, the quantity varying according to the nature of the specimen. All results are shown in Table 1. Following Fleischmann and Pons, anomalous heat flux results are expressed in W/cm^3. The highest value obtained (about 25 W/cm^3) was for an annealed wire, 0.05 cm diameter, from the same lot as that used for Fig. 2. These results are shown in Fig. 5. Relatively lower values (6-12 W/cm^3) were obtained on a spherical electrode, 0.2 cm diameter, prepared by melting another sample of the same wire. A further result was obtained on a 0.1 cm diameter wire of "investment" quality. Before stepping up the current density to 600 mA/cm^2, charging was this time conducted at 0.06 A/cm^2 for two weeks. Results for this wire, expressed in terms of raw data (i.e., ΔV.C and [E - 1.53]I), are shown in Fig. 6. It can be seen that from the start of deuterium evolution at 0.6 A/cm^2, this electrode produced an excess heat flux at a low level. However, after about 12 hours, about 30-60 mW excess heat flux was produced, corresponding to 4-7 W/cm^3. In the case of the specimens shown in both Fig. 5 and Fig. 6, the anomalous heat production was associated with a falling cell potential as a function of time, although this was not consistently true of the other specimens studied. In contrast to the results shown in Figs. 2 and 5, some decay of anomalous heat occurs after 25 h in this case.

Results for two experiments for 0.5 mm diameter annealed Pd wires in 0.1 M ^{n}LiOD and ^{n}LiOH are shown in a more detailed form as a function of time in Table 2. In ^{n}LiOH solution, the cell voltage starts at 4.325 V and shows a slight initial rise as electrolysis proceeds, which we suggest may be due to the effect of impurities. This is followed by a fall as electrolysis proceeds and as the solution becomes more concentrated, hence more conductive. On adding 1.7 ml of solvent, the voltage increases to a value 200 mV greater than that initially observed, which again falls smoothly by 200 mV as the solvent is consumed. In all cases, the heat output from the calorimeter is slightly less than the heat input corrected assuming 100% Faradaic efficiency for electrolysis. In contrast, the cell voltage in ^{n}LiOD solution starts at a considerably higher voltage, reflecting its lower conductivity than that of ^{n}LiOH. This voltage initially falls as the solution concentrates over the first 24 h, then it shows a rise as the production of anomalous heat becomes more evident.

More results are shown in Fig. 7 for a 0.05 cm diameter "as-received" palladium wire initiated in ^{n}LiOD solution show an excess rate of heat generation starting about 3.5 h after the current density was increased to 0.6 A/cm^2 from 0.06 A/cm^2. After a rise time of a further 14 h, excess enthalpy generation had reached a maximum value of 36 mW,

equivalent to 18.3 W/cm^3, compared with 19.3 W/cm^3 observed in Figure 2 for a specimen cut from the same wire sample. However, a rise time of 50 h was required to show the maximum effect in this case. After allowing the excess enthalpy generation to stabilize for 10 h, 0.1 M NaOD electrolyte was substituted, giving a rapid decay of the effect, most having disappeared after 4 h. The cell potential was about 340 mV lower in the NaOD solution, whose specific conductivity is higher than that of 0.1 M ^{n}LiOD. After 24 h, the excess heat flux had fallen to 4 mW and the electrolyte was again changed to 0.1 M ^{n}LiOD. The excess heat flux then rapidly redeveloped, reaching a maximum similar to that earlier within 12 h. After a further 12 h, the electrolyte was changed for 1.0 M ^{n}LiOD. In this case build-up of the excess heat after recovery from switching off the current was slow, perhaps due to impurity accumulation by plating-out on the electrode surface from the more concentrated solution, in which the cell voltage was about 3.5 V, compared with about 5.2 V in 0.1 M ^{n}LiOD. The final rate of excess heat production was similar to that in the latter.

After 23 h the current was switched off and heat generation was allowed to decay. Fig. 8 shows the cell voltage and absolute heat decay rates on switch-off. The former is very rapid: After a change of scale, an open-circuit voltage of about 1 V is observed, corresponding to that for the oxidized platinum anode against the deuterium-charged palladium cathode. Within about 1 hour, the open-circuit voltage has decayed to about 350 mV, which is followed by a slow decay as deuterium is lost from the palladium and the platinum surface becomes reduced. The rate of heat decay is the same as that for a heated electrical resistance within the cell, hence it can also be described as instantaneous, corresponding in practice to the time constant of the microcalorimeter.

A similar set of results is shown in Fig. 9 for an annealed wire. In them, 0.1 M ^{7}LiOD electrolyte, rather than 0.1 M ^{n}LiOD, was substituted for 0.1 M NaOD. Results are broadly similar to those shown in Fig. 7, however, while time from changing the current density tenfold to the appearance of excess enthalpy production on the palladium cathode was rapid (about 1 h), the rise time was slower (about 20 hours instead of 14 hours). It was also much slower than for the annealed wire studied in the same electrolyte in Fig. 5, where initiation of the phenomenon from switching the current density from 0.06 A/cm^2 to 0.6 A/cm^2 took only 2.2 h, reaching close to the maximum value after a further 3.5 h. The maximum excess enthalpy production was this time 34 mW, or 94% of that in Fig. 7. In the previous work reported, a similarly treated annealed wire produced 49 mW (25 W/cm^3). These differences may be due to the presence of trace impurities, since the palladium cathode surface blackens and roughens with use. Surface examination by the SEM shows mossy surface growths, and SIMS and Auger data (to be reported separately)

show the presence of transition metals other than Pd, as well as a relatively large amount of Li, at the surface.

Fig. 10 shows similar data to those on Fig. 9, this time on an annealed wire immersed from the beginning in 0.17 M ^{6}LiOD electrolyte. Initiation time from the application of 0.6 A/cm^2 was almost instantaneous, and the slope of the rise was about the same as for ^{n}LiOD in Fig. 8.

The final result obtained in this series of experiments is given in Fig. 11, which shows results for an untreated palladium electrode 2 mm in thickness cut from a 4 mm diameter rod (Johnson-Matthey) cut from the same rod stock used by the authors of Ref. 1. The disk-shaped electrode was immersed in 0.1 M ^{n}LiOD in a sealed cell containing a platinum black fuel cell electrode for gas recombination. In this case, no thermodynamic corrections at all are required in evaluating the results, which are shown in tabular form in Table 3. After precharging at 60 mA/cm^2 for two weeks, the maximum excess enthalpy production was similar to that in other cells, about 30 mW, however it represented only about 3% of the maximum heat flux input of 900 mW. Because of limitations in the power supply used, the maximum current density was limited to 400 mA/cm^2. The most interesting effect noted is the abrupt fall in excess enthalpy production on reducing the current density from an initial value of 350 mA/cm^2 to 200 mA/cm^2, which is followed by a slow rise over 20 h. A further change to 400 mA/cm^2 results in a short horizontal characteristic, followed by a further slow rise. This may be interpreted as suggesting that 200 mA/cm^2 is perhaps close to a threshold current density for the anomalous heat phenomenon to occur, at least under the conditions used by us.

Discussion

The detailed results reported above show that excess enthalpy production during electrolysis of D2O solutions on Pd is a real effect, at least in certain electrolytes, and we thus confirm at least some aspects of the rather limited details given in the paper by Fleischmann, Pons and Hawkins[1]. By expressing their results in terms of the excess heat flux per unit volume of the electrode, these authors presumably assumed that they were observing a bulk phenomenon. However, their data scarcely suggest this, since in their reported work[1] at 0.008 A/cm^2, a change of electrode volume by a factor of 16 increased the excess heat flux by only 28%. The corresponding increase at 0.064 A/cm^2 was 38%, and at 0.512 A/cm^2, 257%. For a wire of diameter similar diameter to that in Fig. 6, Fleischmann and Pons obtained 8.33 W/cm^3 excess enthalpy production at 0.512 A/cm^2. Hence, the high values for the 0.05 cm diameter wires used in this work, particularly the annealed specimen, may be atypical.

The results shown in Figs. 7, 9 and 10 above show that excess enthalpy production required the presence of lithium in the electrolyte, indifferently ^{6}Li or ^{7}Li isotopes. Replacement of lithium-containing alkaline electrolyte by sodium causes a rapid fall in excess enthalpy production. The rate of this fall suggests that it is due to lithium leaching from the surface. This strongly suggests that a superficial chemical process underlies the effect, although it does not necessarily mean that the excess heat is of chemical origin. Furthermore, the results on the platinum cathodes, compared with those obtained with palladium, indicate that the effect is not exclusively at the metal surface, but appears to be only associated with dissolved (i.e., alloyed) deuterium (and not protonic hydrogen) present in the surface layers of palladium. When the current to the cell was switched off, rapid decay of the excess heat occurred, since ΔV decayed as a function of time in the same way as heat produced by an electric heater inside the cell. If we can discount continuously-occurring chemical explanations such as gas recombination for this phenomenon, other chemical events also seem unlikely. For example, 15 W/cm^3 for 80 h represents over 40,000 kJ/mole or 0.45 keV/Pd atom, which is far greater than either the bond strength of palladium (about 0.67 eV/Pd atom) or the latent heat of sublimation of the metal (4 eV/Pd atom). Even if all of the electrolyte had been involved in some chemical or physical change, this must involve about 17 kJ/mole, which should have been detected.

In the present work, the specific effect of lithium has been shown. This should be contrasted with the recent results of Iyengar[2], which show anomalous heat, with tritium formation, in 5M NaOD at current densities in the 0.2 -0.3 A/cm^2 range at Pd-Ag alloy electrodes. While lithium metal (deposition potential from pH 13 LiOH solution -2.310 V vs H$_2$ under the same conditions) is unlikely to plate out on the palladium cathode, LiD (deposition potential of LiH -806 mV on the same scale) may well do so. We therefore suggest that the deposition of lithium deuteride layer from a concentrated, i.e., almost D$_2$O-free electrolyte, at the cathode surface under high current density conditions for deuterium evolution may be responsible. Such a coating, once formed, may easily lose lithium ions into the palladium lattice, to form a superficial lithium alloy. Similarly, D$^-$ could lose its two electrons and also pass into the metal. Sodium deuteride, whose deposition potential close to that of LiD, would also be expected to form on the electrode surface from NaOD solutions, but it may be less likely to alloy with the palladium lattice. With Pd-Ag electrodes and a 5M NaOD solution[2], the situation is evidently different. When electrodes exposed to LiOD solution are exposed to NaOD under the conditions used in this work, the superficial compounds formed may leach out, and anomalous enthalpy production stops. The NaOD data reported here are highly reproducible, and have been repeated a total of five times to date on different palladium cathode samples.

Whether nuclear events are responsible for anomalous heat production depends on the detection of the correct amounts of nuclear products. In parallel work at this University, Wolf et al.[3] have examined neutron fluxes from cells containing the same 0.1 cm palladium wires reported in Figure 6, again operating in the 0.6 A/cm^2 range. Results have been inconsistent, neutrons occasionally being observed at a level of about three times background, i.e., many orders of magnitude less than that corresponding to the level of the excess heat flux observed, assuming the usual approximately equal branching ratios for ^{2}D + ^{2}D → ^{3}He + ^{1}n or ^{3}T +^{1}p. Iyengar[2] has suggested a branching ratio of 10^8. Our collaborators at this University (Bockris et al.[4]) have observed high levels of tritium in the electrolyte (> 10^6 counts/ml/min, compared with background values (200 counts/ml/min) at the start of experiments. Their work showed that more tritium was formed in the gas phase than was present in the electrolyte. However, results have been sporadic, suggesting that tritium is formed within the electrode, at least initially. If the tritium formed corresponds to the anomalous heat, about 10^{16} atoms, or 0.01% of the total palladium atoms present, should be formed in the cell over 80 h. High tritium levels in the electrolyte are only observed after charging for long times (2-6 weeks) at 0.06 A/cm^2. We have observed no significant amounts of tritium in the electrolyte during the course of the relatively short-term experiments reported above.

Samples of 0.05 cm and 0.1 cm diameter palladium wires in "as-received" form and after serving as cathodes in the above experiments were analyzed at Atomics International Division of Rocketdyne Corporation, Canoga Park, CA, and at Lawrence Livermore National Laboratory. Neither ^{3}He nor ^{4}He were observed above background (10^{12} and 2.5 x 10^{11} atoms per ml respectively). However, if no significant neutrons are observed, ^{3}He as a primary reaction product would not be expected. It is usually considered that ^{4}He is an improbable fusion product in a plasma phase, but perhaps it is not in a lattice, as a recent paper by Walling and Simons[4] notes. We should note that lack of ^{3}He in the bulk of the palladium indicates that no known deuterium fusion process involving the classical branching ratio between the ^{4}He + ^{1}n and ^{3}T + ^{1}p channels is occurring in the bulk at a enthalpy production level greater level greater than a fraction of 1 μW. Similarly, the quantitative upper limit for tritium production in the bulk palladium in an electrode that was assayed 5 days after a series of experiments was about 1.5 x 10^{15} atoms/ml, about 3000 times less than the amount expected from the enthalpy evolved. However, this electrode had degassed, and tritium and deuterium would have been lost both from the surface layers and the bulk. Further work is clearly needed to clarify the origin of the observed heat flux.

The ensemble of results however show that chemical enthalpy resulting from spurious gas-

phase processes is a highly improbable explanation of the heat flux effects seen with LiOD isotopic species present. The results also persuasively show that the phenomena do not appear to be true bulk effects, but that the occur within the surface skin. The time-integrated results are much too large[1] to be explained by continuous chemical processes taking place in a thin superficial skin of palladium. It is also improbable that they can be cyclic chemical processes, for example lithium deposition taking place in surface cracks, followed by its dissolution to produce hydrogen, as one reviewer of this paper suggested. This would be akin to an a.c. impedance effect, and as such it should be detectable at the levels observed. The anomalous heat effects are however chemically initiated by Li ions, and they may well not be identical to those noted by Fleischmann, Pons and Hawkins[1]. Indeed, with larger electrodes, the excess enthalpy production observed here is relatively low grade compared with that reported by the latter authors. Our results on 0.1 cm diameter wires were about the same as those reported in Ref. 1, but as stated above, those with 0.05 cm diameter wires were significantly higher. We presently have no explanation of either this, or as to why the excess heat went through a maximum in the experiment shown in Fig. 2, or for the fall shown at 24 h in Fig. 6.

If the excess enthalpy production is due to nuclear processes, lithium ions seem unlikely to be involved due to their s-electron screen and the apparent lack of an isotope effect. Further evidence is required to say whether they are due to some unusual form of $^2D + {}^2D$ fusion associated with the presence of the palladium lattice[4]. Finally, the fact that surface phenomena initiate the anomalous enthalpy production effects may explain the lack of success of many laboratories in reproducing the Fleischmann-Pons results, since such reactions are known to be very sensitive to surface pretreatment and to the effect of impurities which might be present.

References

1. M. Fleischmann and S. Pons, *J. Electroanal. Chem.* **261**, 301 (1989).
2. P. K. Iyengar, Proc. Fifth Intl. Conf. on Nuclear Energy Systems (ICENES V), Karlsruhe, FRG, July 3-6, 1989.Iyengar, P. K.
3. K. L. Wolf, N. J. C. Packham, D. R. Lawson, J. Shoemaker, F. Cheng, and J. C. Wass, J. Fusion Tech. (in press). This volume, p. xxx.
4. N. J. C. Packham, K. L. Wolf, J. C. Wass, R. C. Kainthla, and J. O'M. Bockris, *J. Electroanal. Chem.* **270**, 451 (1989).
5. C. Walling and J. Simons, *J. Phys. Chem.* **93**, 4593 (1989).

Table 1:   Excess Enthalpy Production from Various Pd Specimens in 0.1 M LiOD at 0.6 A/cm^2.

Table 2:   Enthaply Data for Annealed 0.5 mm Diameter Pd Cathode in 0.1 M LiOD and 0.1 M LiOH Electrolytes.

Table 3:   Excess Enthalpy Production in a Sealed Cell, Pd Disk Cathode.

LIST OF FIGURES

Figure 1:   Calibration curve for microcalorimeter.   : With built-in resistor (limited to 25 mW);   : With resistor in cell without electrolyte;   : With resistor in cell containing electrolyte.

Figure 2:   Cell potential and excess rate of heat generation on a 0.05 cm diameter as-received palladium cathode at various current densities as a function of time in 0.1M LiOD in D$_2$O.

Figure 3:   Cell potential and excess rate of heat generation on a 0.05 cm diameter as-received platinum cathode at 600mA/cm^2 as a function of time in 0.1M LiOD in D$_2$O.

Figure 4:   Cell potential and excess rate of heat generation on a 0.05 cm diameter as-received palladium cathode at various current densities as a function of time in 0.1M LiOH.

Figure 5:   Cell potential and excess rate of heat generation on a 0.05 cm diameter annealed palladium cathode at various current densities as a function of time in 0.1M LiOD in D$_2$O.

Figure 6:   Heat flux: - entering calorimeter and   - leaving calorimeter, for deuterium evolution at 0.6 A/cm2 in 0.1M LiOD in D$_2$O on a 0.10 cm diameter as-received palladium cathode after charging for two weeks at 0.06 A/cm^2 as a function of time.

Figure 7:   Excess enthalpy generation rates during electrolysis of D_2O on a Pd cathode in alkaline solutions showing the specific effect of lithium cation.

Figure 8:   Chart recorder tracings showing the rapid decay of enthalpy generation rate on interruption of the electrolysis current. The decay of the open-circuit potential of the cell is apparent.

Figure 9:   Excess enthalpy generation rates during electrolysis of D_2O on a Pd cathode in alkaline solutions showing 0.1 M electrolyte changes in the sequence $^nLiOD \rightarrow NaOD \rightarrow ^7LiOD$.

Figure 10:   Excess enthalpy generation rates during electrolysis of D_2O on a Pd cathode in 0.17 M ^6LiOD as a function of time, showing the decay of excess heat flux to negligible values when the electrolyte was changed to 0.1 M NaOD.

Figure 11.   Excess enthalpy generation rates on a palladium disc cathode in 0.1 M LiOD in a sealed cell.

TABLE 1

Exp. #	Electrode Material		Electrolyte	Current Density	Rate of Excess Heat Generation
	Cathode	Anode		mA/cm^2	W/cm^3 of Pd
1	as-received Pd 0.5mm dia. 10mm long	Pt	0.1M LiOD	300 600 1000	16.3 19.3 18.5
2	as-received Pd 1.0mm dia. 10mm long	Pt	0.1M LiOD	600	4-7
3	annealed Pd 0.5mm dia. 10mm long	Pt	0.1M LiOD	600	22-25
4	arc-melted Pd 2.0mm dia. sphere	Pt	0.1M LiOD	600	6-12

TABLE 2A (LiOD)

Date	Time	Cell Current (mA)	Cell Voltage (V)	Power In (mW)	Power Out (mW)	Excess Heat (mW)
5/11	10:30	98.18	5.26	366	385	19
5/11	12:50	98.02	5.13	353	381	28
5/11	16:15	97.79	5.06	345	382	37
5/12	08:45	97.81	4.91	331	368	37
5/12	12:10	97.80	4.92	332	371	39
5/12	16:00	97.91	4.97	337	375	38
5/12	17:00	98.20	5.04	345	382	37
5/12	21:45	97.80	4.90	330	371	41
5/13	11:00	97.53	4.75	314	359	45
Calorimeter opened at 11:00 on 5/13 to measure electrolyte volume--1.7 ml/2 days consumed. 1.7 mls of D_2O was added.						
5/14	09:00	97.03	4.70	308	341	33
5/15	08:00	97.03	4.75	312	350	38

TABLE 2B (LiOH)

Date	Time	Cell Current (mA)	Cell Voltage (V)	Power In (mW)	Power Out (mW)	Excess Heat (mW)
5/27	11:30	96.40	4.325	274	272	-3
5/27	13:00	96.35	4.335	275	272	-3
5/27	18:00	96.40	4.330	275	272	-3
5/28	10:00	96.55	4.295	272	272	0
5/28	11:30	96.60	4.295	272	272	0
5/28	20:00	96.61	4.280	270	268	-2
5/29	08:10	96.60	4.232	266	265	-1
Calorimeter opened at 08:15 on 5/29 to measure electrolyte volume--1.7 ml/2 days consumed. 1.7 mls of H_2O was added.						
5/29	12:00	96.58	4.532	295	294	-3
5/29	15:00	96.56	4.525	294	292	-2
5/29	17:00	96.45	4.520	293.5	292	-1.5
5/29	22:00	96.60	4.500	292	290	-2
5/30	08:10	96.61	4.450	287	286	-1
5/30	11:00	96.58	4.430	285	284.5	-0.5
5/30	15:30	96.55	4.410	283	283	0
5/31	08:00	96.60	4.330	275	274	-1
5/31	15:30	96.58	4.320	274	274	0

TABLE 3 (LiOD, Sealed Cell)

Date	Time	Cell Current (mA)	Cell Voltage (V)	Power In (mW)	Power Out (mW)	Excess Heat (mW)
7/4	08:00	100.75	4.440	447	466	19
7/4	10:30	175.60	6.175	1084	1122	38
7/4	12:50	175.25	6.090	1067	1111	44
7/4	15:10	175.25	6.030	1057	1096	39
7/4	16:25	175.70	6.010	1056	1089	33
7/4	22:55	175.70	6.050	1063	1100	37
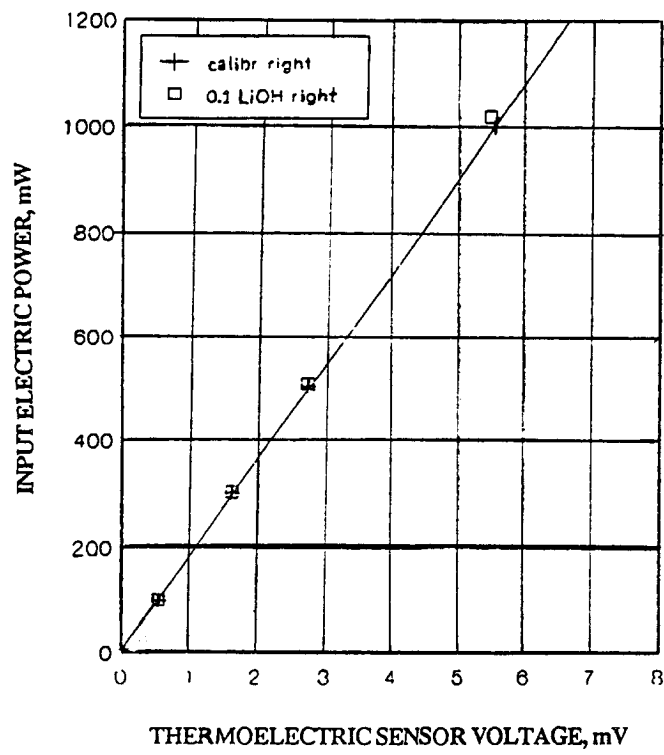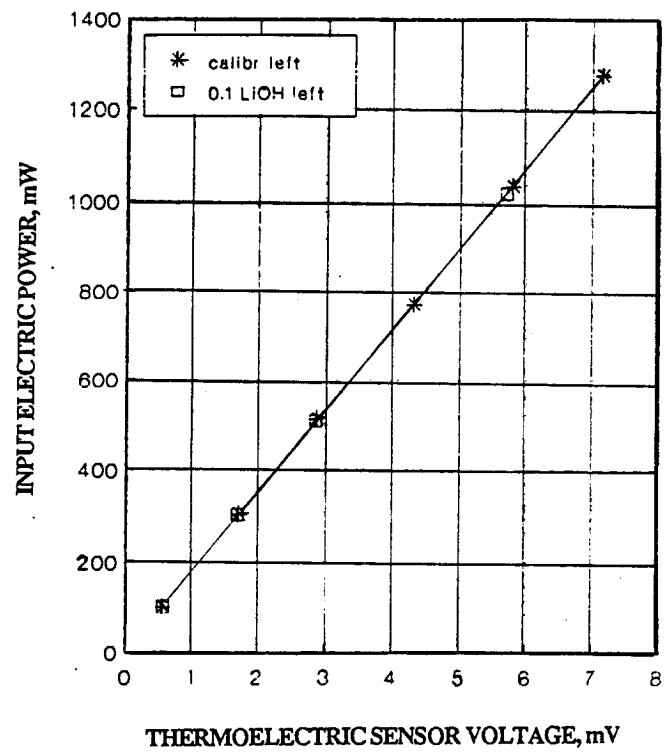
Figure 1
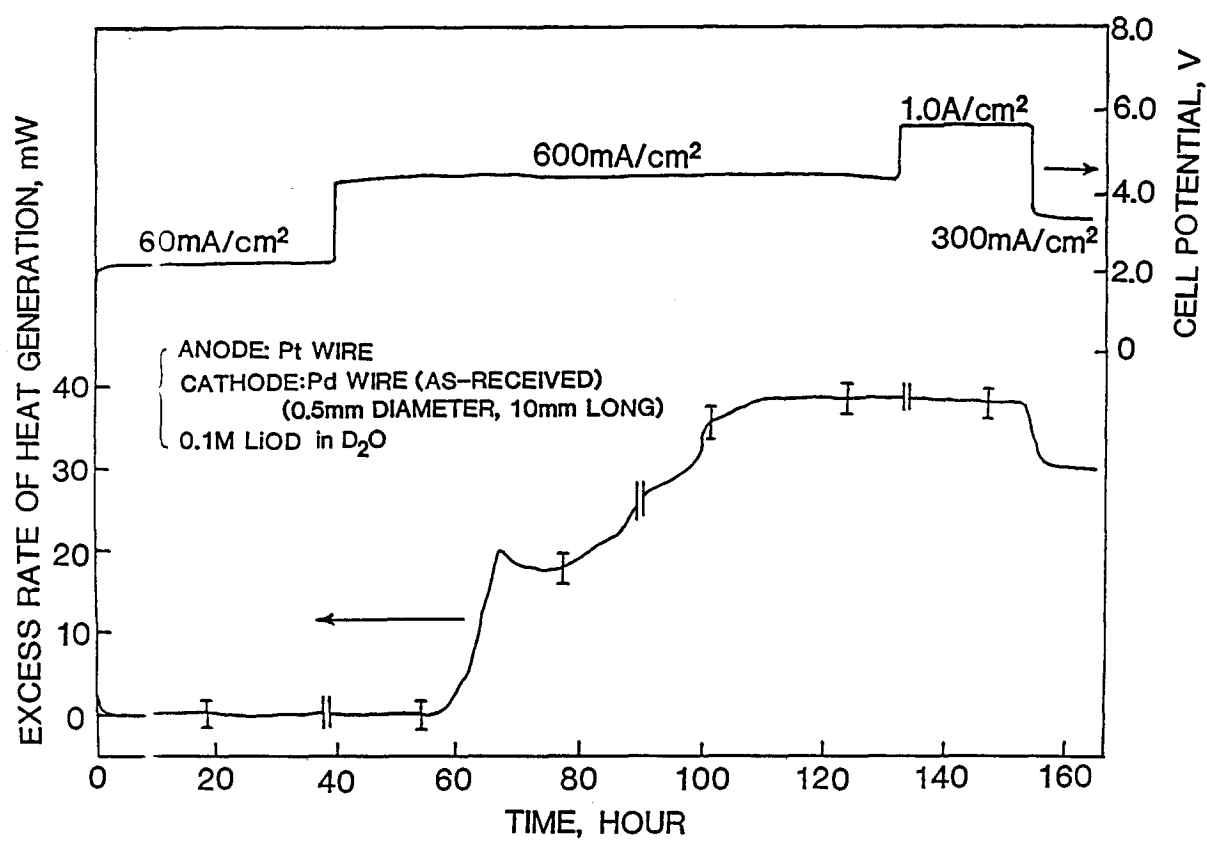
Figure 2
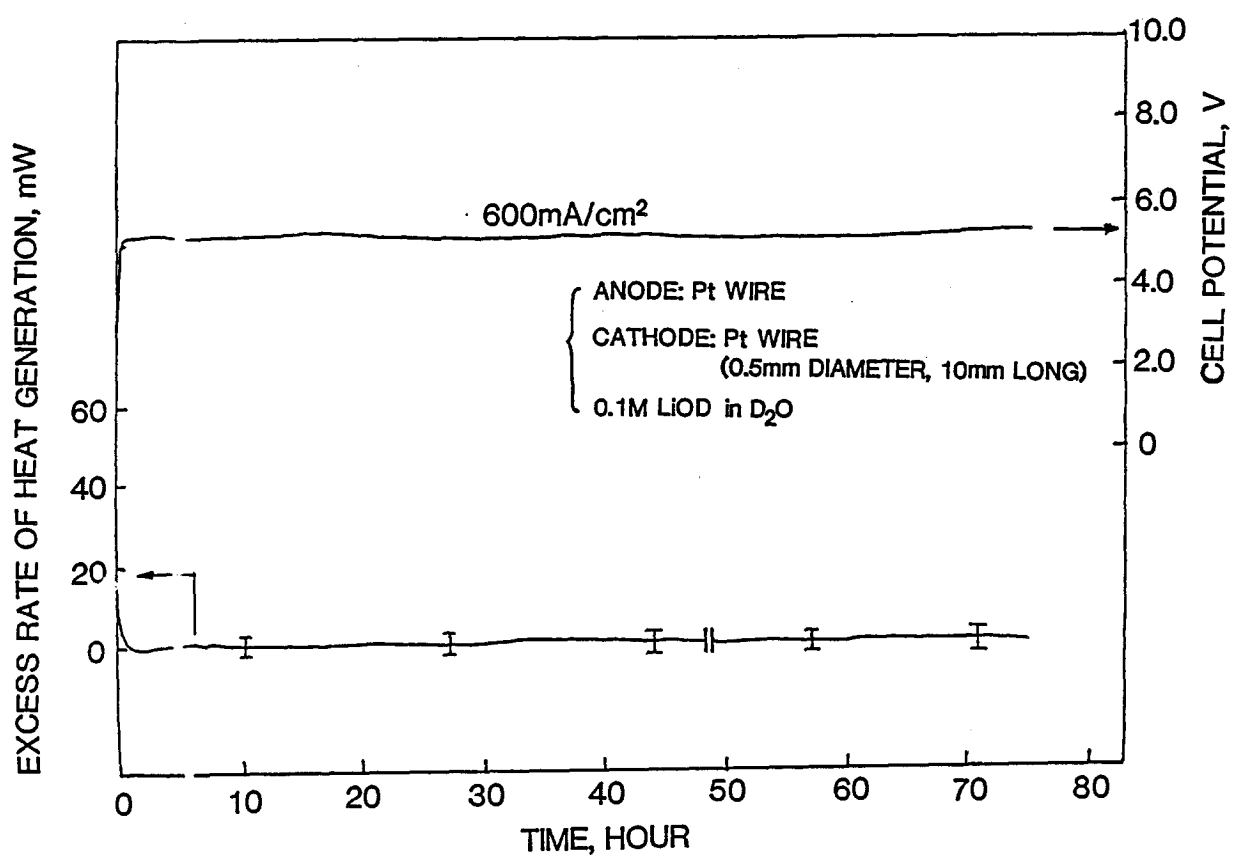
Figure 3
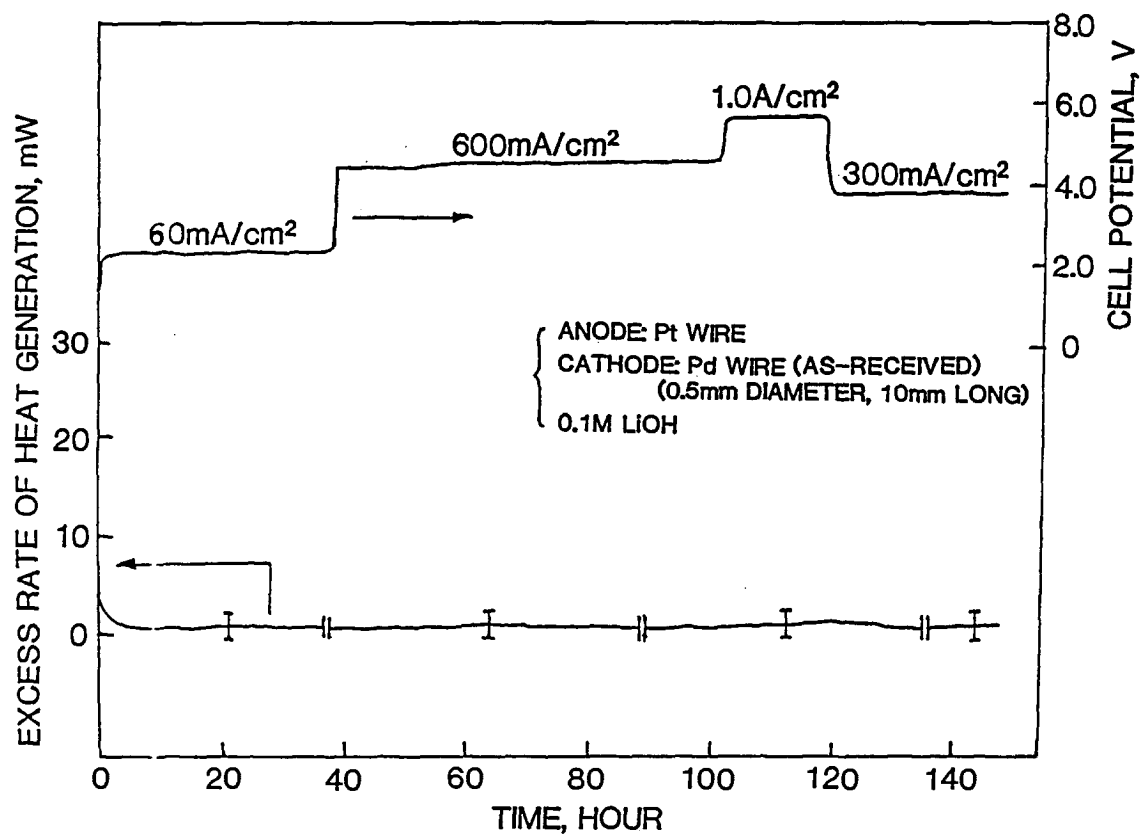
Figure 4
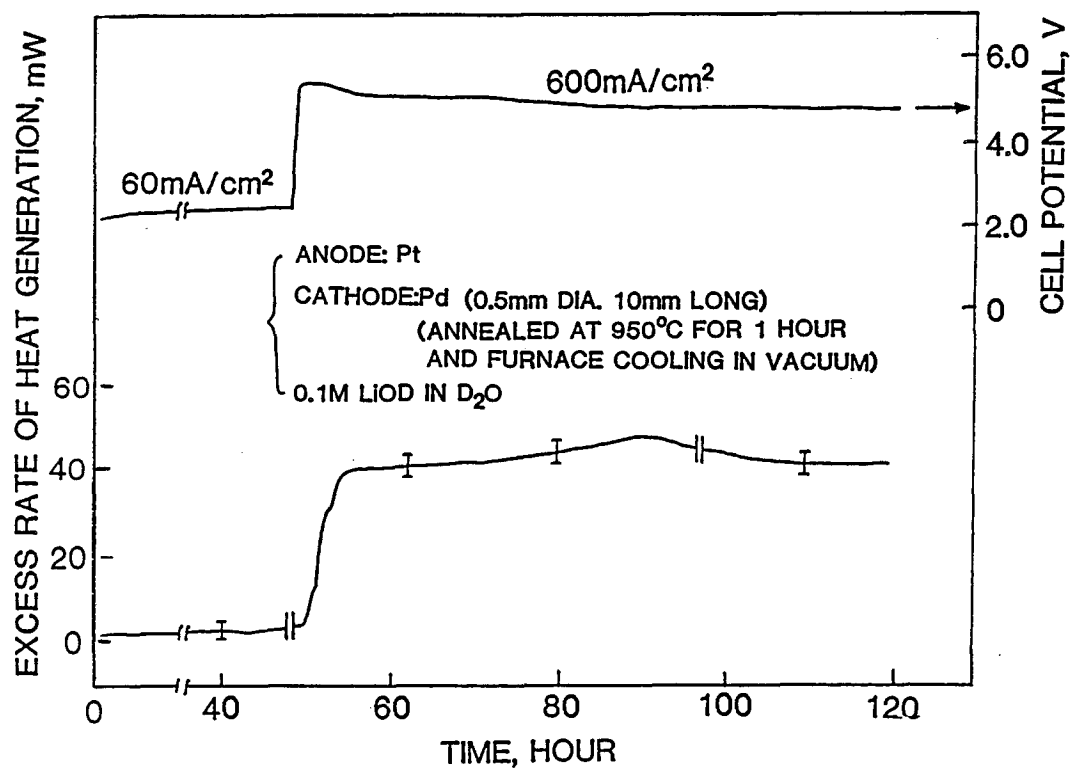
Figure 5

Figure 6

Figure 7

17-23

Figure 8

Figure 9

17-25

Figure 10

17-26
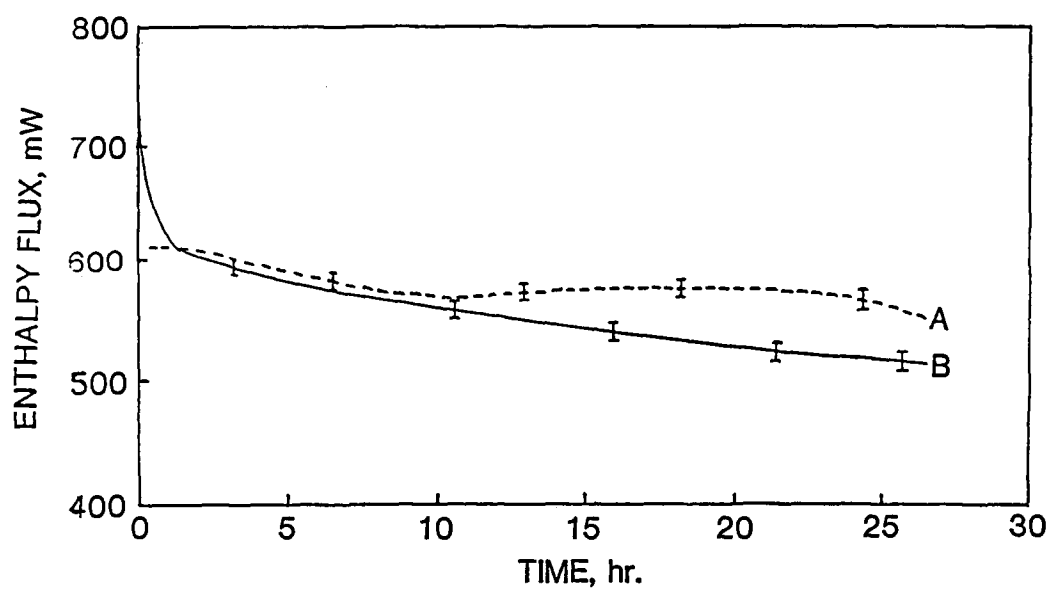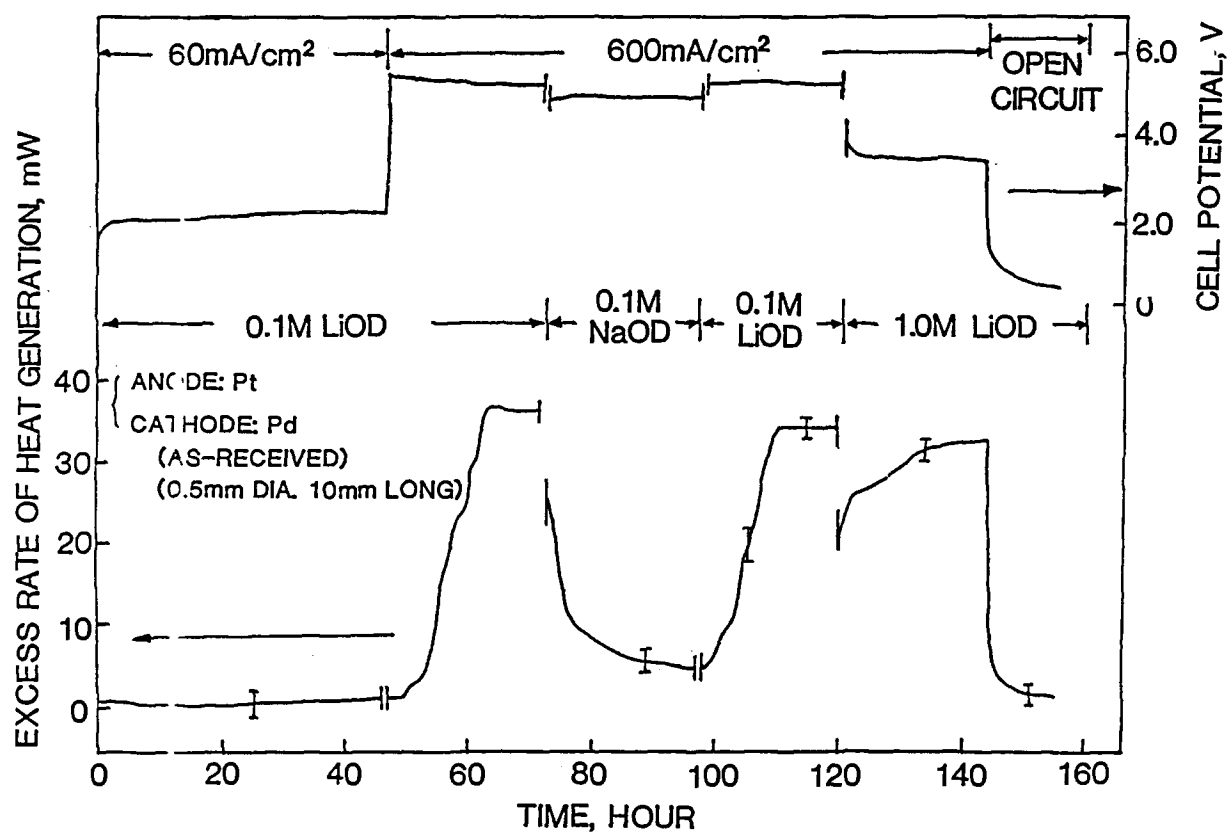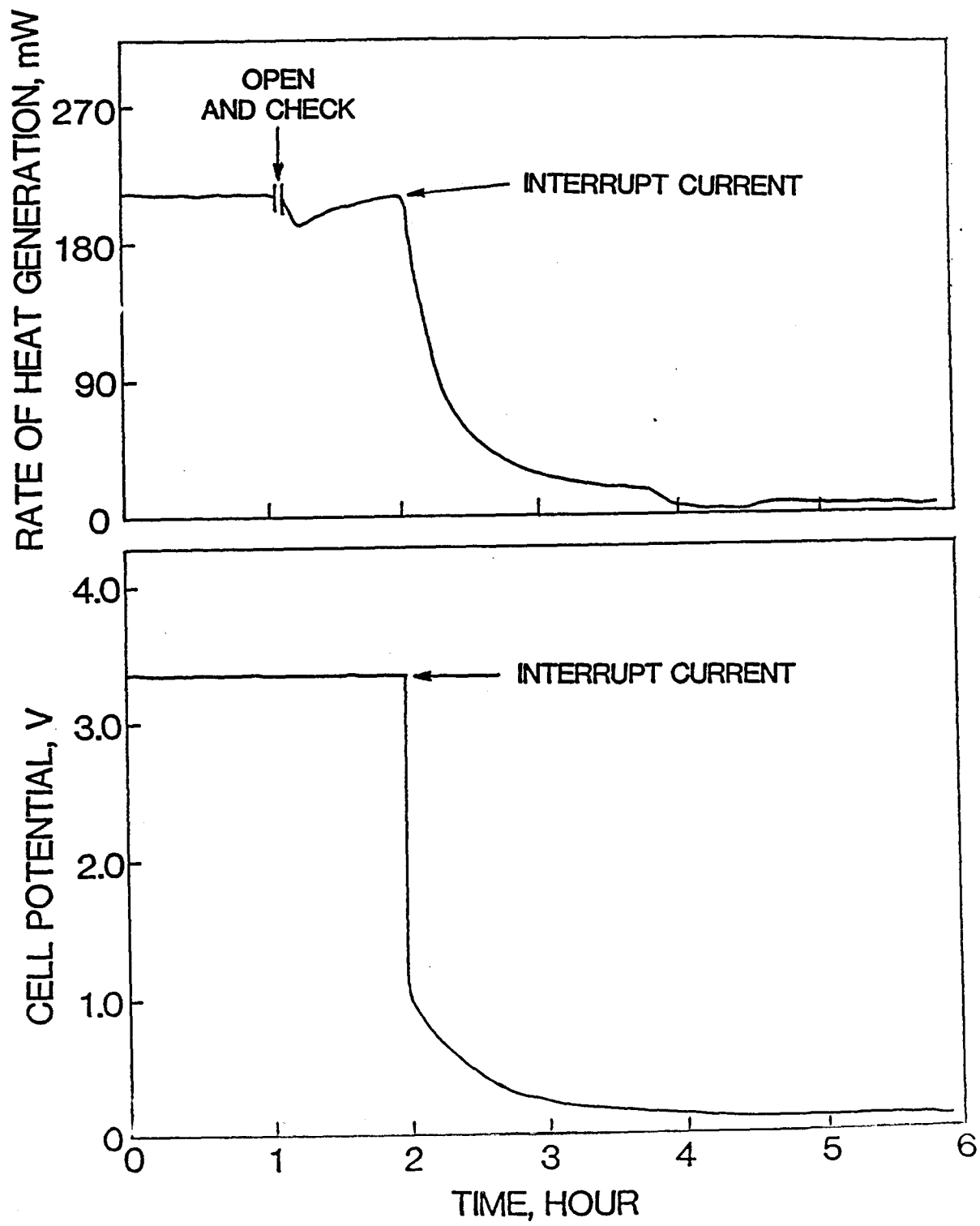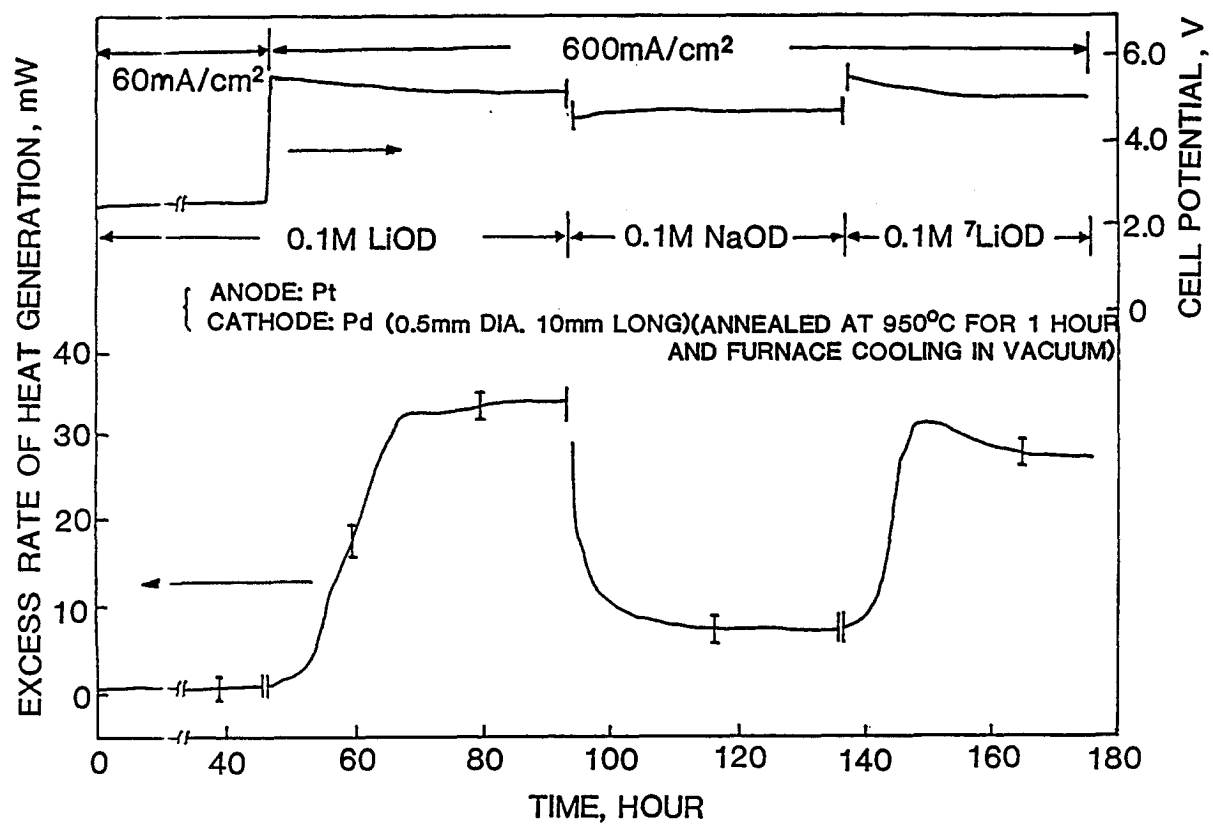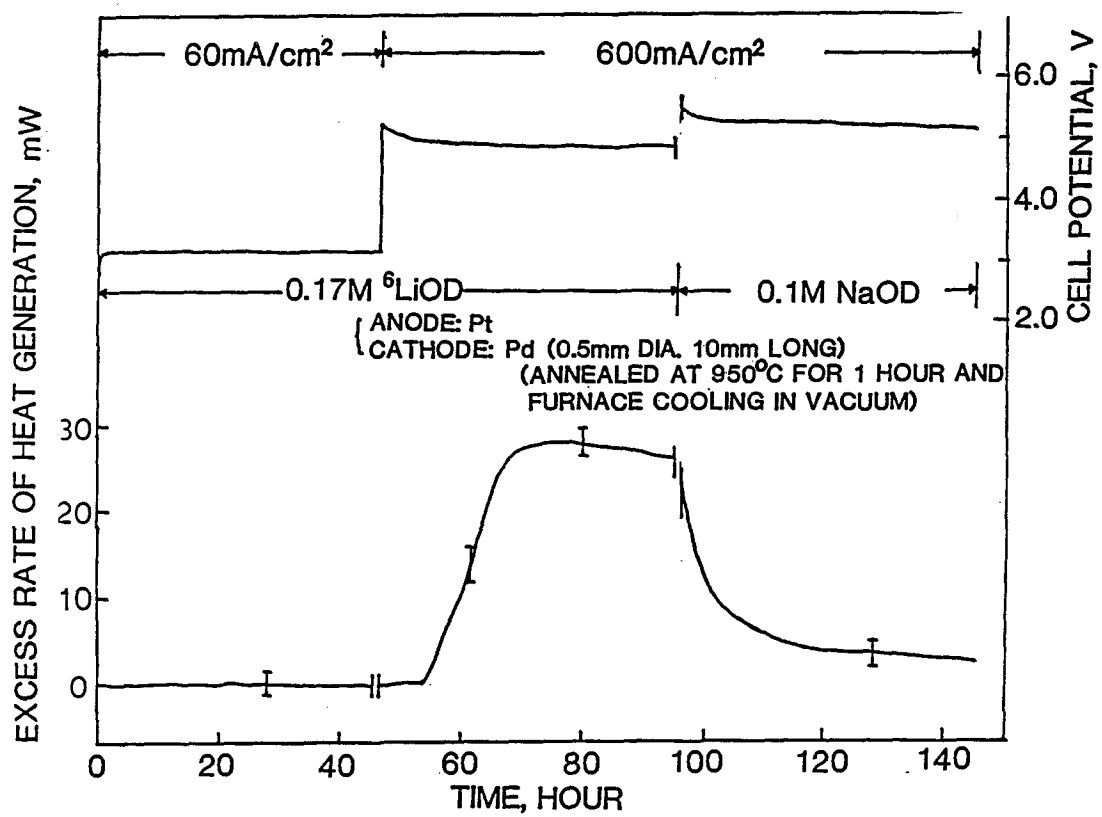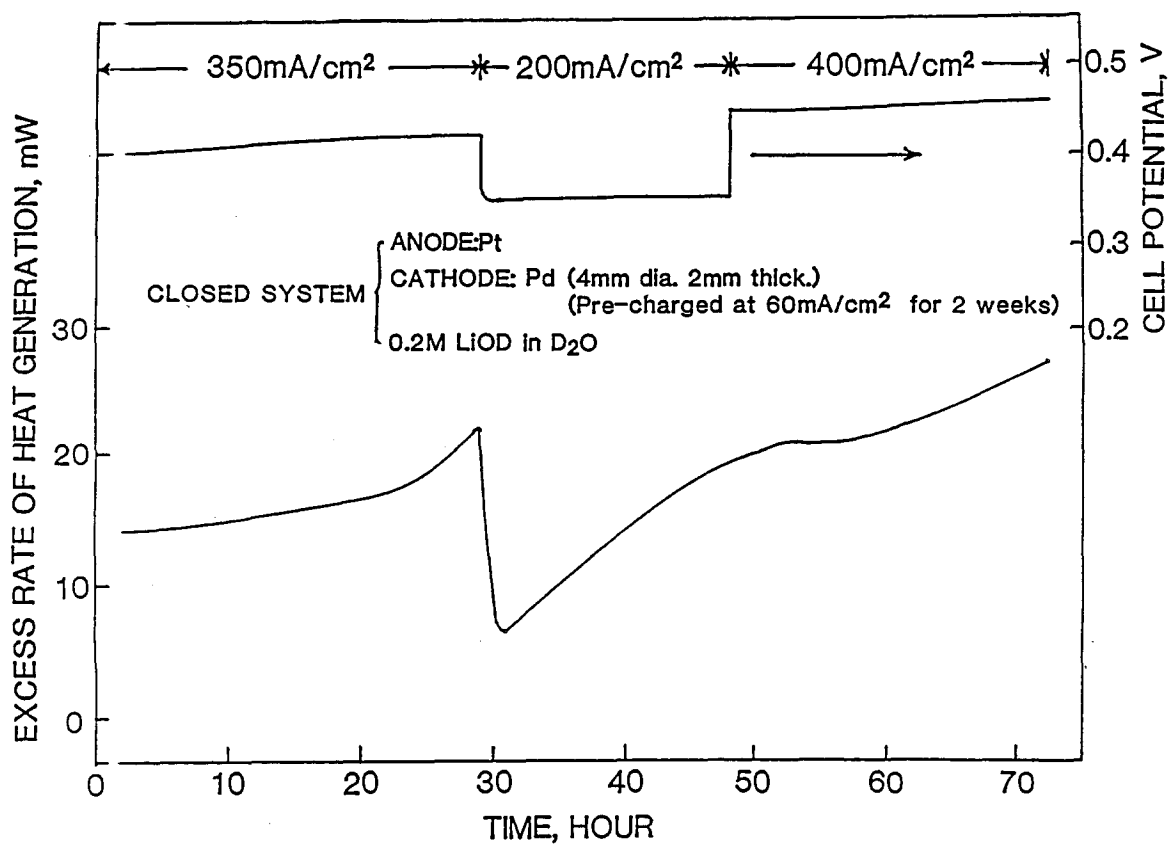
Figure 11

DISCUSSION (APPLEBY)

Rafelski: Do you have a photograph or diagram of the calorimeter?

Appleby: No, but it's about the size of an office desk, and it has a considerable thermal mass.

Oriani: Is the calibration carried out as a differential calorimeter or as an absolute instrument?

Appleby: As a differential calorimeter.

Yeager: Did excess heat change when current density was changed?

Appleby: The effect is shown in Fig. 2. Reducing the current density from 600 mA/cm^2 to 300 mA/cm^2 resulted in an absolute decrease, but a relative increase in the amount of excess heat, whereas increasing the current density to 1000 mA/cm^2 caused little absolute change or a relative decrease in the amount.

Rafelski: The anomalous heat effect is only of significance if it is there on demand. Have you run several times in heavy water, with each instance giving a positive result?

Appleby: In every single case where we have tested palladium in heavy water, we have had positive results, though in some cases the effects were small. However, the more changes one makes in operating conditions on a given electrode, the less the effect seems to become a function of time.

Chu: Have you tried LiOH with heavy water?

Appleby: No, not to this point. However, we plan some substitutional experiments of this type.

Teller: Have you always had the experience that excess heat appears with the delay of a few hours?

Appleby: Yes, although in some cases, the delay is quite short, a matter of 2-4 hours. Sometimes it was 12 hours or more. It was about 20 hours in the case of the first nonannealed wire shown in Fig. 2. For annealed wires, we saw a much more rapid rise time with hardly any delay. We feel that this is probably significant.

Myles: Were the electrodes saturated with deuterium?

Appleby: Presumably. If one evolves deuterium on very small diameter wires at 60 mA/cm^2 for a long time, some degree of saturation will clearly be reached.

Myles: Did you measure the saturation level?

Appleby: No. We found that the small wires degas very quickly, as one would expect.

Rossi: What was the temperature rise inside the calorimeter?

Appleby: In the heat conduction calorimeter, it is minimal.

Rafelski: In some cases, your plots show that the power out remains constant, whereas the power in varies with time.

Appleby: That is so. In many cases, the power out remains more or less constant. The power in falls because the voltage decreases as a function of time as we operate the cell. The decrease in voltage is substantially more than one would expect from changes in the resistance of the solution as D_2O is consumed. This is not the case in LiOH solution.

Hoffman: If you had dendrite growth or whisker growth on the palladium cathode, its area would increase tremendously.

Appleby: I agree. Dendrite growth does occur much more in D_2O than in H_2O. This is probably because the D_2O solution is much less pure than the H_2O solution which we used.

Teller: Concerning the disappearance of the anomalous heat when LiOD solution was replaced by NaOD, was the lithium in the palladium exchanged before the electrode was placed in the NaOD solution?

Appleby: No.

Teller: So that palladium must contain all of the lithium which had been intercalated.

Appleby: That is correct; however, the indication from the excess-heat/time curves is that the lithium diffused out after about 20 hours in NaOD solution.

McKubre: The disappearance of the anomalous heat is not complete on your plots. If one waited long enough, the heat production might recur.

Appleby: It might indeed have increased again. There are still large uncertainties in the experiments.

Yeager: Do you remove the cells from the calorimeter to change the electrolyte, or is it carried out using syringes?

Appleby: The cell was removed from the microcalorimeter.

Hoffman: Some of the surface poisons which are undoubtedly present may be more soluble in NaOD than in LiOD. It is interesting that changing 0.1 LiOD to 1.0 M concentration seems to have little effect on the generation of anomalous heat.

Fleischmann: My impression is that the overpotential in LiOD solutions is much higher than in NaOD, so this may be associated with the results that you show, which seem to reflect changes in surface chemistry. On your plots, you do see a significant drop in the cell potential in NaOD solution. It may be all at the cathode. Before we reach any conclusion about the effect of lithium, one of the most important points is whether its effect is not just due to changes in the overpotential.

Appleby: That may be so. A question that I would pose is whether the anomalous heat phenomenon is driven by current density or by overpotential. One can imagine a scenario whereby one has a bulk palladium deuterium absorber on which is superimposed a very high surface area of catalytic dendrites. Under these conditions, one can apply a high current density as far as the bulk material is concerned, though at a lower overpotential than on a smooth surface. It is also significant that the NaOD solution used here was 0.1 M. Iyengar's work at the Bhabha Research Institute (BARC) in India showed positive results in NaOD. It was carried out in 4 M solution.

Chexal: They used a palladium-silver alloy cathode in their work.

Appleby: That is correct.

Teller: What effect did they see at the higher sodium ion concentration that they used?

Appleby: They found anomalous heat, tritium, and neutrons.

Teller: You may be seeing a LiD reaction, which at first sight is even more absurd than one involving DD, because it has an even higher potential barrier. The potential barrier for DD is already prohibitive, so something must occur to modify it. If it can be modified to accommodate DD, then why should LiD also not occur? The latter react very well under the right conditions.

Fleischmann: The possibility of LiD reactions was always part of our scenario. However, we are still at the beginning of trying to understand the effect.

Rafelski: Nevertheless, there appear to be no differences between Li-6 and Li-7.

Appleby: That is correct, so a nuclear effect due to lithium may seem to be excluded. However, please understand that all these conclusions are based on the results of a very limited number of experiments.

Teller: If a neutron is transferred, it must be from deuterium to lithium, rather than the other way around. Thus, if this is the case, from Li-6 one should obtain Li-7, and from Li-7, Li-8, which is a very strong β-emitter. The latter should therefore occur if you use natural lithium, but not if you use Li-6.

Fleischmann: So you should have some type of scintillator in the cell. How large is the energy for this transformation?

Teller: About 12.5 MeV. Li-8 transforms to Be-8, which is followed by α-particle production. Any α-particles should be detectable.

Jones: Do you have a γ-ray or neutron detector in your equipment?

Appleby: No, it could not be fitted into the microcalorimeter. We rely on Dr. Kevin Wolf for these measurements.

Fleischmann: You could probably incorporate particle track detectors, e.g., using photographic film.

Appleby: That may be possible in modified future equipment.

Werth: If Li-6 and Li-7 both give about the same amounts of excess heat, does that not make it unlikely that lithium has anything to do with a direct nuclear reaction?

Appleby: After the earlier discussion, I would not like to speculate further.

Chubb: Li-6, stripped of its electrons, is a boson, whereas Li-7 is not. Using the "bosons in, bosons out" rule, Li-7 would appear rather as an impurity in an overall process involving lithium nuclei.

Appleby: Because of our results on the substitution of LiOD electrolytes by NaOD, we feel that whatever is occurring must be initiated by a chemical process taking place in the surface skin of the electrode. As we reported at the Santa Fe Workshop, our electrolytes appeared to contain no tritium, and they contained no significant amounts of He-3 or He-4. However, if only a surface skin is involved, the helium isotopes, if present, may not be readily detected after the degassing of the electrode at the end of the experiment.

Teller: Would any lithium which is plated out stay on the palladium surface?

Appleby: It should alloy with the palladium. Lithium metal should not plate out at the thermodynamic potentials observed in this work, unless a phenomenon known as underpotential deposition occurs. Under the conditions of deuterium evolution which I have described, lithium deuteride can be produced at the surface as a feasible thermodynamic product. In the absence of D_2O, which would be the case at high current density, this could form a lithium-deuterium alloy with palladium.

Teller: Then is it possible that palladium is not the reacting material, but rather lithium deuteride?

Appleby: I am open to suggestions.

Section 18

EXPERIMENTS ON EXCESS HEAT GENERATION UPON ELECTROCHEMICAL INSERTION OF DEUTERIUM INTO PALLADIUM

Steven Crouch-Baker, Joseph A. Ferrante, Turgut M. Gür,
George Lucier, Martha Schreiber, and Robert A. Huggins

Department of Materials Science and Engineering

Stanford University

Experiments on Excess Heat Generation Upon Electrochemical Insertion of Deuterium Into Palladium

Steven Crouch-Baker*, Joseph A. Ferrante, Turgut M. Gür, George Lucier, Martha Schreiber, and Robert A. Huggins

Dept. of Materials Science and Engineering, Stanford University, Stanford, CA 94305

*Present address: Dept. of Materials Science and Engineering, University of California, Los Angeles, Los Angeles, CA 90024

Introduction:

Martin Fleischmann and Stanley Pons announced on March 23, 1989 that they had performed electrochemical experiments involving the insertion of deuterium into palladium that produced excess heat generation, neutrons, gamma rays, and tritium (1), and claimed that these must be due to some previously unrecognized form of atomic fusion. If this is found to be correct, it might represent a very important breakthrough in the search for a source of energy that is widely available, relatively inexpensive, and not accompanied by severe radiation hazards or environmental pollution.

Two sets of careful calorimetric experiments are reported in this paper. The first group was designed to provide a direct comparison of the thermal behavior during electrolysis of the deuterium - palladium system with that of the chemically and metallurgically similar hydrogen - palladium system under comparable experimental conditions. These experiments employed "open cells", in which the deuterium and oxygen gases formed during electrolysis were allowed to exit the system.

The second group of experiments employed a new design of calorimeter and "closed cells" in which the gases evolved from the electrolytic dissociation reaction were internally recombined.

Except for neutron and gamma ray monitors used for safety purposes, no radiation detection or reaction product measurements were undertaken in this work.

Experimental Aspects:

Experiments were conducted using isoperibolic calorimetry. This is a two - compartment steady state power balance method in which heat is generated within one compartment, and is conducted through an intermediate thermally - conducting wall into the other compartment, which is maintained at a fixed lower temperature. Under steady state conditions, a temperature distribution is established in which the temperature difference across the thermally - conducting wall between the two compartments transports heat at a rate that just balances the power generated within the first compartment. Thus, measurement of the difference in the temperature of the two compartments $(T_1 - T_2)$ provides information about the thermal power generated in the first compartment, P_{therm}, that is passed out as heat flux through the thermally - conducting wall into the second compartment. This can be expressed as

$$\text{Thermal power generated} = P_{\text{therm}} = K \ (T_1 - T_2) \tag{1}$$

where K is the calorimeter calibration constant.

As will be shown below, if power is introduced into the first compartment electrically, the thermal power generated P_{therm} is not equal to the applied electrical power P_{appl} if the electrical power causes a chemical or electrochemical reaction to occur that involves a change in the enthalpy of the system. This is the case when an "open cell" is used. As a result, the resultant temperature difference is less than would be the case if the electrical power produced only Joule heating.

On the other hand, if a "closed cell" design is used, so that no enthalpy is tranported out of the first compartment, P_{therm} and P_{appl} will be equal if there is no other heat generation process present. Any difference must be due to some additional power generation process taking place inside the cell.

Principles of Isoperibolic Calorimetry When Electrolysis is Taking Place

If we introduce power to the cell electrically by passing current I_{appl} at voltage E_{appl}, the power applied to compartment 1, i.e. the electrolysis cell, is

$$P_{\text{appl}} = E_{\text{appl}} \, I_{\text{appl}} \tag{2}$$

If we have only a simple resistive impedance Z_R in the cell,

$$E_{\text{appl}} = I_{\text{appl}} \, Z_R, \tag{3}$$

and the applied electrical power is all converted to thermal power

$$P_{\text{appl}} = P_{\text{therm}} = I_{\text{appl}}^2 \, Z_R \tag{4}$$

Under steady state conditions, this thermal power generated in the cell passes across the thermally - conducting wall, and from equation (1)

$$P_{\text{appl}} = P_{\text{therm}} = I_{\text{appl}}^2 \, Z_R = K \ (T_1 - T_2), \tag{5}$$

However, in an electrochemical cell passing current so that electrolysis is taking place, we must take cognizance of the thermal effects of that process. We can divide the externally applied voltage across the cell into several parts, a chemical term, and a purely resistive term

$$E_{\text{appl}} = E^0 + I_{\text{appl}} \, (Z_c + Z_a + Z_e) \tag{6}$$

where E^0 is the equilibrium thermodynamic voltage due to any difference in the chemical potentials at the two electrodes, and Z_c, Z_a, and Z_e are the impedances at the cathode/electrolyte interface, the anode/electrolyte interface, and in the bulk of the electrolyte, respectively. The products $I_{\text{appl}} \, Z_c$ and $I_{\text{appl}} \, Z_a$ are often called overvoltages in the electrochemical literature.

The applied electrical power can therefore be written as

$$P_{appl} = I_{appl} E^O + I_{appl}^2 (Z_c + Z_a + Z_e) \tag{7}$$

In experiments that involve the electrolysis of H_2O or D_2O, the values of E^O are related to the reactions

$$H_2O = H_2 + 1/2\ O_2 \tag{8}$$
and
$$D_2O = D_2 + 1/2\ O_2 \tag{9}$$

respectively, and each can be related to the respective standard Gibbs free energy change per mole ΔG^O, following the convention that E^O is positive in an electrolytic reaction, by

$$E^O = \Delta G^O/2\ F \tag{10}$$

where F is the Faraday constant. Furthermore, the Gibbs free energies can be divided into their enthalpic and entropic components:

$$\Delta G^O = \Delta H^O - T\Delta S^O \tag{11}$$

where ΔG^O, ΔH^O and ΔS^O are all positive.

We can thus write from equation (7) that

$$P_{appl} = I_{appl} (\Delta H^O - T\Delta S^O)/2\ F + I_{appl}^2 (Z_c + Z_a + Z_e) \tag{12}$$

The enthalpy change can be converted to an associated voltage, the thermoneutral voltage E_{tn}, which is the voltage that can be applied across the electrochemical cell that causes no heat evolution, and thus neither generates nor consumes heat as a result of the chemical reaction taking place. It is also the open circuit voltage of the electrochemical cell at 0 K.

$$E_{tn} = \Delta H^O / 2\ F \tag{13}$$

Thus we can rewrite equation (12) as

$$P_{appl} = I_{appl} E_{tn} - I_{appl} (T\Delta S^O)/2\ F + I_{appl}^2 (Z_c + Z_a + Z_e) \tag{14}$$

From elementary thermodynamics, one can relate the enthalpy change of a system ΔH to the difference between electrical work done on it and the heat evolved. Thus in the presence of electrolysis, the thermal power generated will be less than the electrical power introduced.

This can be expressed as

$$P_{therm} = P_{appl} - I_{appl} E_{tn} \tag{15}$$

or

$$P_{therm} = I_{appl}(E_{appl} - E_{tn})$$ (16)

The values of ΔH° for such reactions are essentially independent of temperature, and are reported to be + 286 kJ/mol for the electrolysis of H_2O, and + 297 kJ/mol for the electrolysis of D_2O. Thus the values of E_{tn} are 1.48 V and 1.54 V, respectively.

Hence we see that the positive values of ΔH° in the reactions of equations (8) and (9) mean that a cell in which such reactions are occurring should be generating less heat than an identical cell containing only resistive components by an amount corresponding to the value of $I_{appl} E_{tn}$, and from equations (12) and (16)

$$P_{therm} = -I_{appl}(T\Delta S^\circ)/2 F + I_{appl}^2 (Z_c + Z_a + Z_e)$$ (17)

The thermal power generated is thus the result of entropic cooling and Joule heating. It is important to note that the latter is related to the sum of the impedances in the cell, and the distribution between them is of no consequence.

If, in addition to the endothermic electrolysis phenomenon and the exothermic resistive behavior included in equation (17), there were some other phenomenon present in the cell that produced thermal power, P_{int}, it would add an additional term, giving

$$P_{therm} = -I_{appl}(T\Delta S^\circ)/2 F + I_{appl}^2 (Z_c + Z_a + Z_e) + P_{int}$$ (18)

and therefore an increase in $(T_1 - T_2)$ over that for the case of only endothermic electrolysis and exothermic resistive behavior given in equation (17) for any level of P_{appl}, in accordance with equation (1).

Additional endothermic phenomena will, of course, provide a negative value of P_{int}, and decrease the measured temperature in the electrochemical cell, and therefore $(T_1 - T_2)$. Any heat leakage that does not go through the thermally - conducting wall into the second compartment (the external water bath) will also lead to a reduction in the temperature of the electrochemical cell compartment relative to what would be the case if only resistive phenomena were present. This could include heat transport up wires, tubing, electrical connectors, etc. In addition, any sensible heat carried out of the cell by the gases evolved, entrained liquid, and the evaporation of the solvent (H_2O or D_2O) could contribute endothermically to the observed behavior.

In addition to the resistive components in equation (17), other exothermic phenomena can also be present related to chemical phenomenon taking place within the cell, and contribute positively to P_{int}. One of these is the heat of solution when hydrogen or deuterium is inserted into the palladium, and the enthalpy change related to the α - β phase transformation. The magnitudes of these effects are relatively small, 9.55 kcal/mole for the α - β transformation in the H-Pd case, and 8.55 kcal/mole in the D-Pd case (2) and only contribute to the observed behavior when these particular processes are under way. As the insertion into the interior is relatively slow in the time span of a particular measurement these produce only relatively small effects in comparison to the large thermal effects of the electrolysis phenomenon itself. In addition, the rate of the insertion reaction decreases with

time (approximately proportional to $t^{1/2}$) and so this effect becomes less and less important the longer the cell has been in operation.

Experimental Considerations - Open Cell Experiments

The electrochemical cells were submerged inside a large, well stirred cold water bath, which acted as the second compartment. The intermediate thermally - conducting wall thus was the glass container surrounding the electrochemical cell.

Two closely comparable electrochemical cells were employed, one containing a 0.1 M solution of LiOH in light water (H_2O), and the other a 0.1 M solution of LiOD in D_2O as electrolytes. Each also contained a resistance heater for calibration purposes, and a protected thermocouple for temperature measurements. There was also a thermocouple to measure the temperature of the surrounding water bath.

Electrolysis voltages in the range 3 to 15 V were applied to the cells in both increasing and decreasing directions, and the currents varied between 10 and 1,000 mA. Temperatures, as well as the cell currents were monitored for steady state conditions. The temperature differences between the cells and the water bath ranged up to about 10 °C.

The palladium was obtained by arc melting pieces cut from a palladium crucible that contained an appreciable amount of hydrogen, and other possible impurities. In order to get rid of such contaminants, the samples were re-melted at least 10 times, using an arc-melting apparatus with a water cooled tungsten electrode and a water cooled copper hearth, which acted as the other electrode. The environment was argon, and the procedure consisted of first melting some titanium sponge in order to getter species from the argon, such as oxygen, just prior to melting the palladium. After melting the palladium, the argon atmosphere was replaced, and the procedure repeated again. It was quite obvious from the change in the color of the arc during repeated melting that the impurity content of the palladium was gradually being changed. This process was repeated until re-melting caused no further visible change in the arc color.

The resulting palladium, in the form of a distorted sphere, was then mechanically converted into coin - shaped disks 2 - 4 mm thick and roughly 1 cm in diameter, with weights in the range of 1 to 2 grams each. Fine gold wire was employed as the current collector.

The anodes were made from approximately 2 meters of fine platinum wire, and were coiled just inside the cell periphery in order to be as far away as possible from the palladium samples, which were attached by gold wire to the calibration heater in the center of the cell.

Heavy water is a getter for light water, and therefore precautions were taken to prevent contact between the palladium and (moist) air or water, both during assembly and operation of the cells. The cell components were stored, as well as assembled and loaded into the cells, inside a dry nitrogen - filled glove box. Gases were allowed to exhaust from the cell through a simple one - way bubbler system containing silicone oil.

In order to be sure that there was sufficient stirring, both cells were mounted in a gyrotary water bath shaker. This provided additional mechanical motion, and therefore stirring, both within the cell and in the external water bath.

Calibration measurements were made over the whole range of electrolysis power level by adding to the electrolysis power three different values of additional heater power for each data point. By measuring the change in $(T_1 \cdot T_2)$ as a function of the additional electrical power supplied to the heater, one can determine the calibration constant over a specified range of total input power in the presence of the convective stirring. Thus, every data point that was obtained was accompanied by a direct calibration of the calorimeter. The characteristic relaxation time of the calorimeters was of the order of 15 to 20 minutes.

Experimental Results - Open Cell Experiments

The relation between the thermal power out through the calorimeter system and the applied electrical power was determined for cells containing light water. The output thermal power during electrolysis was found to be lower than that when the electrical power was put into the calibration heater due to the entropic cooling. Measurements taken at different times showed that there is essentially no time dependence to this behavior.

On the other hand, in experiments with heavy water cells, the thermal behavior under electrolysis conditions was found to vary with time. This is illustrated in Figure 1, which shows the temperature difference between the two compartments of the calorimeter system with the heavy water cell as a function of applied electrical power for three situations. The data on the middle line are those obtained when the electrical power was applied to the calibration heater. The data on the lower line are those which were obtained initially when a fresh piece of palladium not containing deuterium was inserted into the cell and the electrolysis reaction was made to occur. One sees that the endothermic behavior related to electrolysis in an open system was initially present in this case, as with the light water cell mentioned earlier.

However, over a period of time the temperature in the heavy water electrolysis cell rose relative to its initial value, in contrast to the light water case. The data on the upper line were obtained after electrolysis had been under way for 66 hours. This indicates that there was some process taking place, generating heat, and giving P_{int} a positive value.

In this case, at any applied electrical power level, the thermal power out had increased beyond that observed when electrical power was applied to the resistive calibration heater. Thus under these conditions P_{int} was greater than $I_{appl} E_{tn}$, and the electrochemical cell was producing excess power P_{exc} above and beyond that which was being input electrically, P_{appl}, where

$$P_{exc} = P_{therm} - P_{appl} = P_{int} - I_{appl} E_{tn} \qquad (19)$$

Thus the cell in which an appreciable amount of deuterium had diffused into the palladium had an additional exothermic phenomenon present producing P_{int} that was not observed in the case of the light water cell where hydrogen was inserted into the palladium.

Measurements have been taken of the ratio of power out, P_{therm}, to the power supplied electrically, P_{appl}, at various values of time after the insertion of a fresh palladium electrode.

$$P_{therm} / P_{appl} = (P_{appl} + P_{exc}) / P_{appl} \qquad (20)$$

Two sets of such data are shown in Figure 2. At the beginning, one sees the electrolysis cooling effect, but this is gradually overcome with time by an additional phenomenon that produces P_{int}, so that after about 60 hours we see that P_{exc} becomes greater than zero, and the thermal power evolved P_{therm} is greater than the electrical power applied P_{appl}.

Four sets of light water/heavy water comparisons were run. In every case, there was no time dependence to the behavior of the light water cell, in which hydrogen is inserted into the palladium. In the heavy water cells, with deuterium insertion into the palladium, there was always a time - dependent generation of additional power P_{int} above that which is due to the exothermic Joule heating and the endothermic electrolysis process. Over time, the values of thermal power out of the cell come to exceed the electrical power input, so that the value of P_{exc} becomes positive.

New Calorimeter Design

Questions have been raised about possible errors in calorimetric measurements upon electrochemical cells in which electrolysis is taking place. Except for the question of the possible role of recombination in open systems, the key issues have involved the calibration process whereby the value of K is determined, and the comparability of the measurements of T_1 and T_2 during the calibration and during the actual experiments.

Of special concern have been questions such as the influence of the physical locations at which heat is produced and at which the temperatures are measured in the two cases, and the magnitude of the stirring of the electrolyte fluid, which should have some influence upon thermal homogeniety.

In order to avoid these potential problems a new type of isoperibolic calorimeter was designed in which, under steady state conditions, essentially all the heat generated within the electrochemical cell passes to the external environment radially through a pair of concentric heavy aluminum cylinders that are separated by a well - defined thermal conduction layer.

Instead of relying upon measurement of the temperature within the electrochemical cell itself, as well as the assumed homogeneous environment, this design involves the measurement of the temperatures of the two aluminum cylinders. Because of their dimensions, the temperature is homogenized within the cylinders, so that the questions of the location of the heat sources and temperature measurement within the electrochemical cell, and the amount of stirring, are not relevant.

The design of this new type of calorimeter is shown schematically in Figure 3. The electrochemical cell within it is 1.16 inch in diameter, and 4 inches long. The inner (T_1) aluminum cylinder is 4 inches long, and the outer (T_2) cylinder is 7 inches long. The inner diameter of the T_1 cylinder is about 1.16 inches, and itse outer diameter 2.0 inches. The inner diameter of the T_2 cylinder is 2.25 inches, and its outer diameter is 3.0 inches. Thus the gap across which the heat conduction takes place, and the temperature difference measured, is 0.125 inches.

Calibration

The calibration procedure involved the introduction of several levels of Joule heating power and the measurement of the temperature difference between the two

aluminum cylinders (T_1-T_2) in each case. One result of this procedure is illustrated in Figure 4, in which the calculated value of the calibration constant K is shown as a function of time, during which the calibration power input was stepped among several values. It can be seen that the K values are quite consistent, lying in a band approximately 1 % wide, except during the periods of equilibration after the input power level was varied.

Experimental Considerations - Closed Cell Experiments

The experimental arrangement within the closed cells was essentially the same as in the open cells described earlier, except for three items. One was the inclusion of a teflon/nickel/platinum catalyst in the gas space above the electrolyte to produce recombination of the deuterium and oxygen generated during the electrolysis.

The second was the replacement of the large surface area fine platinum wire anode by a large area thin ribbon of palladium, produced by rolling from its initial rod shape. The purpose of this modification was to continuously deposit a layer of fresh palladium upon the cathode surface in order to cover up any potentially blocking metallic or other impurities that might be deposited during the electrolysis process.

The third difference from the earlier cells was the inclusion of a second cathode of platinum wire. Passing current between this platinum cathode (instead of the palladium) and the anode caused only the generation of Joule heat, so that measurement of the electrical input to this configuration provided a simple calibration method, with gas generation, bubble - driven stirring, and recombination of the same character as that which took place during electrolysis with the palladium cathode. Of course, one had to be sure to open the platinum electrode circuit during operation with the palladium cathode to insure that there was no electrical cross talk between the two cathodes.

These cells were inserted into the new design calorimeter described earlier, and connected to a bubbler system to allow the escape of gas in the amount of the uncombined oxygen. Observation of the time behavior of the bubble evolution provided information about this process, and showed that it ceased as the palladium cathode became saturated with deuterium.

The palladium was prepared as before, with thorough repeated arc melting in an argon atmosphere, followed by mechanical deformation to produce a "fat dime" shape. The cathode current collector was changed to palladium wire, which was covered by a thin teflon tube to prevent appreciable current flow to it, rather than to the cathode.

Comparison of The Behavior of a Cell Containing Light Water With Those Containing Heavy Water.

As was the case with the earlier experiments with open cells, the question of whether there is a difference of the behavior of light water and heavy water cells was addressed with the new closed cell design.

As before, it was found that no excess thermal power was generated in a cell containing H_2O and LiOH instead of D_2O and LiOD. The time dependence of the total energy balance of a heavy water cell early in an experiment is illustrated in Figure 5. It is seen that the cell achieved a condition of energy balance after about 120 hours.

Discussion:

A direct comparison has been made, using careful calorimetric techniques, of the behavior of the light water (H_2O) - palladium system and the heavy water (D_2O) - palladium system under conditions in which electrolysis was taking place at high rates in both open and closed systems.

It was found that these two systems behaved quite differently. In the light water case, the electrochemical cell temperature was lower than that expected from Joule heating alone, because of the endothermic electrolysis reaction taking place. This behavior was found to be independent of time.

On the other hand, electrolysis of the heavy water system showed different behavior. Initially, such electrochemical cells behaved in a manner directly analagous to the light water cells, showing the combination of Joule heating and electrolysis cooling. However, with time, the cell thermal power output gradually increased, and over time reached values greater than the input electrical power in both open and closed systems.

These experiments thus demonstrate not only a different behavior in the case of the hydrogen - palladium system and the deuterium -palladium system, but also the generation of significant excess power in the deuterium case.

Our calorimetric measurements give no information about the mechanism causing the internal generation of this excess power. However, the observations which have come from several different laboratories of the generation of tritium in such cells are especially interesting, and deserve further consideration. If, indeed, tritium is an important product of the reaction occurring in the electrochemical systems that are producing P_{int}, it is an indication that some type of nuclear process must be taking place.

Acknowledgements

References:

1. M. Fleischmann and S. Pons, Jour. Electroanal. Chem. 261, 301 (1989)
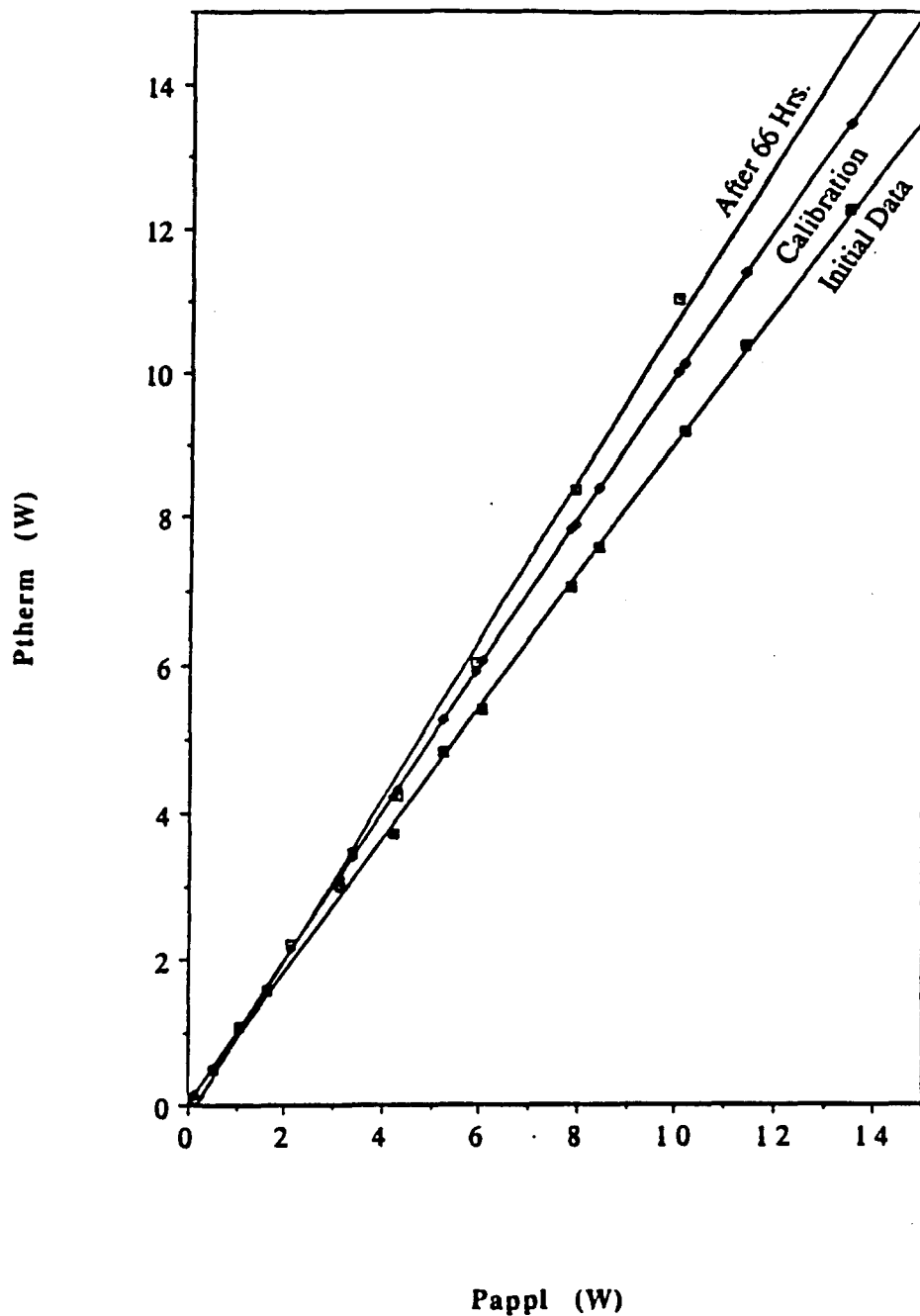2. A. Maeland and T.B. Flanagan, Jour. Phys. Chem. 68, 1419 (1964)

Figure 1. Variation of the relation between the thermal power output and the applied electrical power in a heavy water cell with time. The data on the middle line were obtained by the use of a resistive heater. Those on the lower line were from electrolysis shortly after the introduction of a fresh palladium sample, and those on the top line were measured after electrolysis for 66 hours.
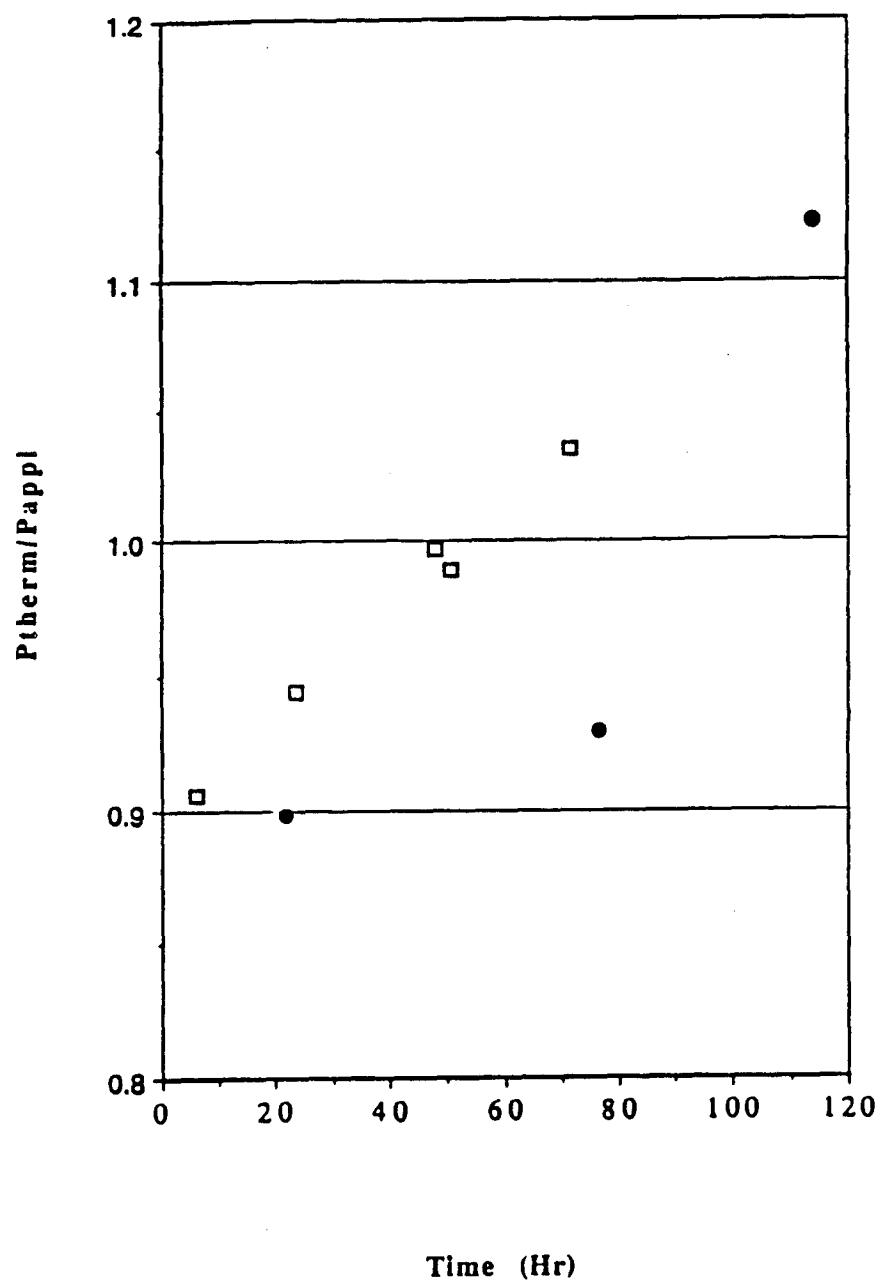
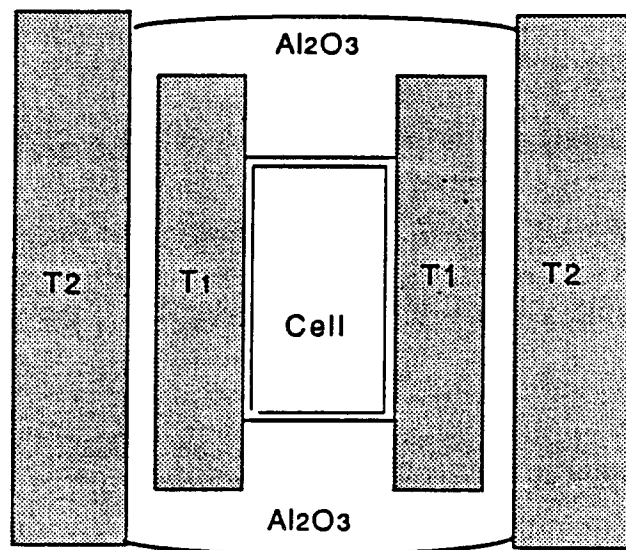Figure 2. Variation of the output/input power ratio with time for two different heavy water cells.

Figure 3. Schematic cross-sectional view of the concentric cylinder isoperibolic calorimeter. Thick layers of powdered Al_2O_3 above and below the cell and the inner cylinder insure that the heat flow is primarily in the horizontal radial direction. The thermal power output is evaluated by measurement of the difference between the temperatures of the heavy aluminum cylinders.
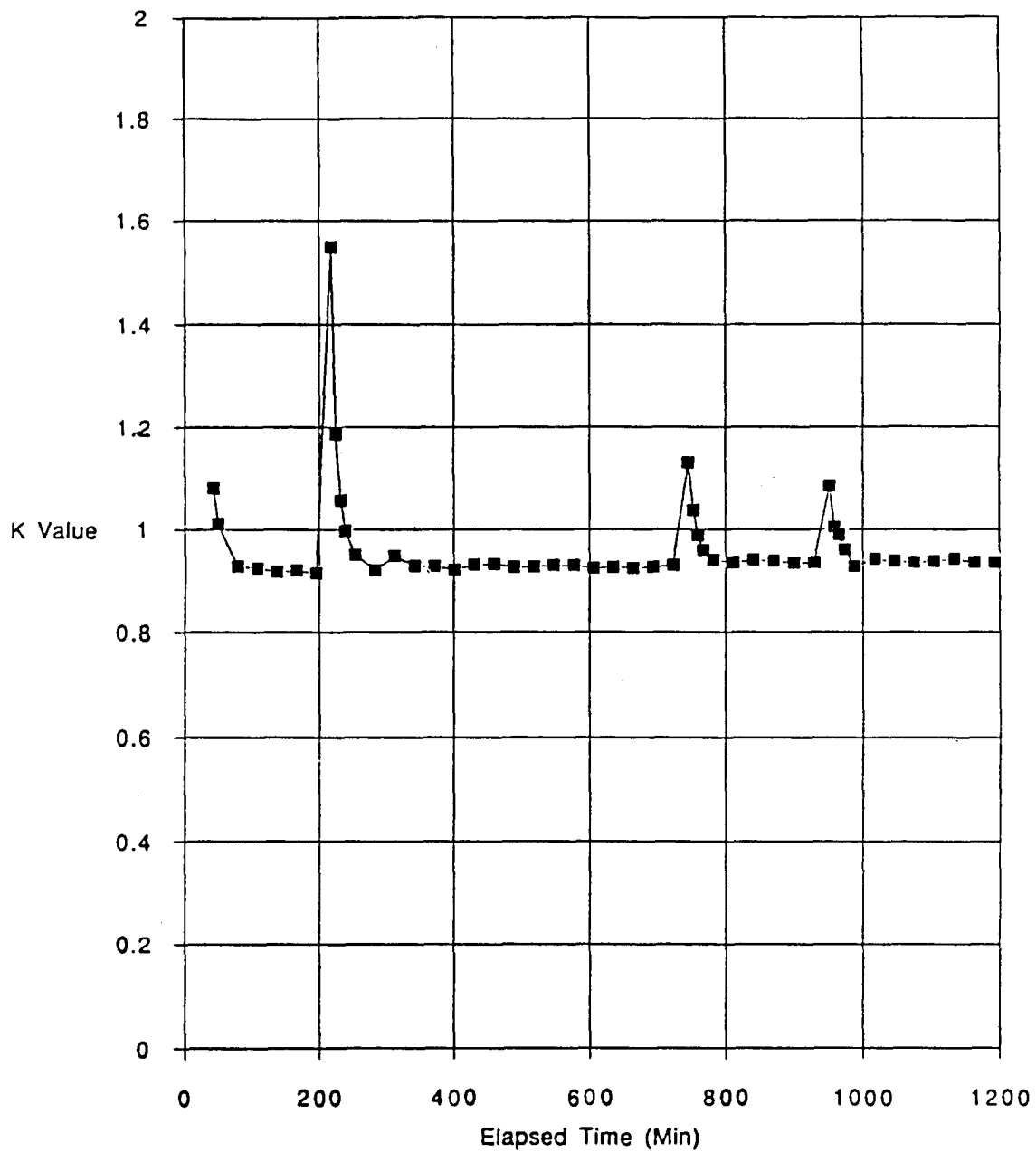
Figure 4. Variation of the calibration constant K with time while stepping the calibration heater power. Heater power levels were approximately 2, 4, 6, and 8 watts. The transients are due to the time delay between the change in the input power level and the equilibration of the calorimeter temperature response.
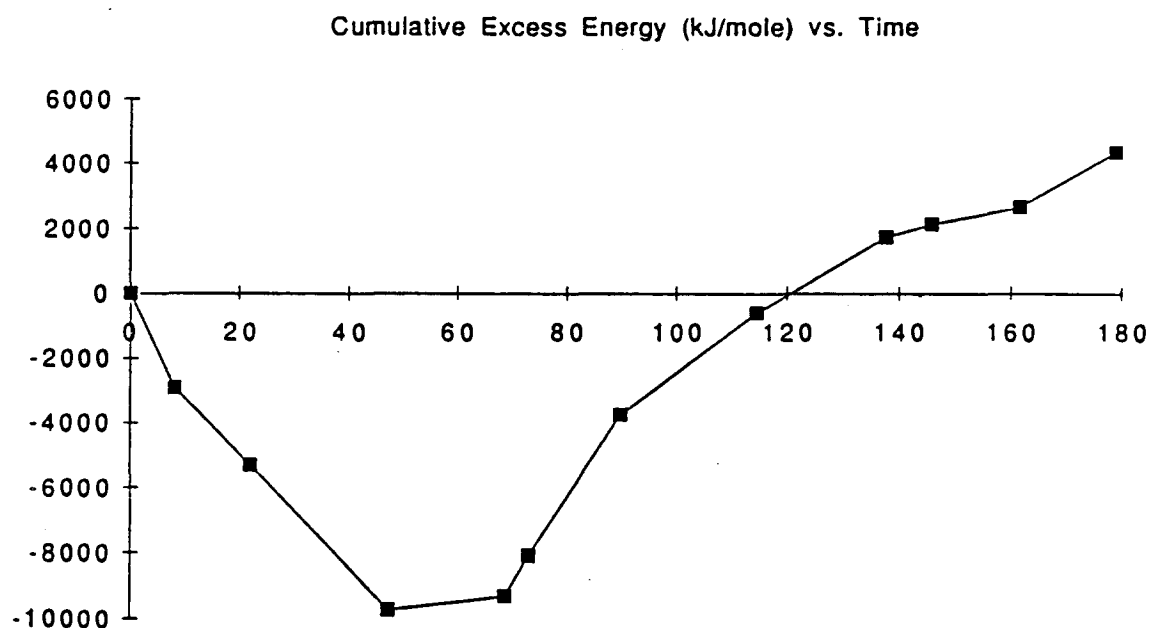
18-13

Cumulative Excess Energy (kJ/mole) vs. Time

Figure 5. Energy balance of a heavy water cell versus time. It is seen that energy breakeven was achieved after about 120 hours in this case. A power ratio greater than unity was reached after about 50 hours.

DISCUSSION (HUGGINS)

Myles: What were the details concerning your electrode samples and electrolytes?

Huggins: The details are in the paper, but I will add that the cell was a glass container, with about 30 ml of heavy water. The 1-2 g palladium samples were disk-shaped, in the form like fat coins, made from parts of a crucible of Engelhard origin. The platinum anode was a fine wire, about 2 m long, wrapped around outside the cathode, near the inner surface of the glass container.

Bard: What were the typical temperature increases which you determined?

Huggins: Up to about 10°C.

Oriani: If your plots represent steady state, why do they curve up or down in some cases?

Huggins: Because they are only tending toward steady state, which has not been exactly reached in the cases you mention.

Bard: I do not understand why some of your plots show excess heat production rising so sharply with time.

Huggins: I do not know the answer to that. However, our results show large jumps in cell temperature.

Appleby: Your results are shown without the 1.53 eV correction for the electrolysis of D_2O?

Huggins: That is correct. We have done this to be ultraconservative regarding possible recombination.

Bard: Even though this is not a closed cell?

Huggins: This one is an open cell, but we also have closed-cell data.

McKubre: Could you define the temperatures on your plots?

Huggins: The T_2 temperature is that of the outer cylindrical aluminum block, and T_1 that of the inner cylinder. We assume that the cell is close to equilibrium with the temperature of the inner block.

McKubre: The amount of Joule heating in the cell depends on the electrolyte temperature. If you cannot quantify this, you cannot estimate the Joule heating effect.

Huggins: We have measured the power inputs and resistance changes. All Joule heating effects, regardless of origin, have exactly equal power inputs and outputs, and they are thus taken into account by measuring the input parameters.

Appleby: Does not the fact that T_2 varies somewhat affect the value of the power going into the cell, thus making the calibration nonlinear?

Huggins: Yes, the calibration constant varies somewhat with temperature if steady state is not attained.

Appleby: Even so, this is in effect a heat-conduction calorimeter.

Huggins: That is correct. We used a layer of 1/8 inch of aluminum oxide powder between the inner and outer cylinders of the calorimeter. The heat is being conducted, not radiated, through this space.

Myles: Your results show instantaneous, not integrated, energies. How can you tell if energy is not being stored, then released?

Huggins: We could not distinguish the two effects.

Teller: The excess energy output which you calculate is approximately what percentage of the input power?

Huggins: The plots show 10-12 percent excess, which is reduced to 6 percent excess over the electrical power input, if no correction is made for the decomposition of D_2O.

Teller: You seem to seeing strong evidence that the excess heat output is fluctuating so that heat release occurs in bursts.

Huggins: There are certainly fluctuations.

McKubre: The time constant of the calorimeter is about 1 hour.

Huggins: Correct. It requires about 1 hour for the apparatus to achieve equilibrium after a fluctuation. The inner block temperature is moving up and down somewhat, but the outer block temperature is very stable.

Bard: What is the error bar in the larger deviation? About 2 percent?

Huggins: Approximately 1 percent. It seems certain that the effects are sporadic. The output power varies with time; it is not a steady-state phenomenon.

Myles: Is it possible that your periodic peaks represent a charging phenomenon?

Huggins: A charging system would indeed be periodic, but we do not believe that our results indicate charging. The orders of magnitude are too large for that. Other experimental data given at this meeting show that the system is not acting like a battery.

Rafelski: What is the power input?

Huggins: Most results shown were at about 4 W, though some of the early results were larger. The absolute excess heat output is larger if the input power is higher.

Bard: What is the approximate current density?

Huggins: At a power input of 4 W, it is about 100 mA/cm^2.

McKubre: In regard to the unusual results which you obtained in closed cells, is it possible that there is a time shift between the data points which you are measuring for time and temperature?

Huggins: The results could be an artifact. However, they were obtained using a PAR potentiostat in the constant-current mode.

Bard: Do the changes show the cell temperature rising, or the input voltage decreasing?

Huggins: Apparently, the voltage, which is controlled by the potentiostat, is going down. However, the temperature of the inner block of the calorimeter does change somewhat, for example, going from 36.0°C to 36.2°C, i.e., by 0.1°C to 0.2°C. While there was not a thermocouple in the cell itself, there were three sets of thermocouples between the two blocks. All three showed the same general behavior during these measurements.

Bard: Do you have the cell voltage variation on the same time scale as the temperature changes?

Huggins: I do not have the results plotted, but the voltage was reduced about 30 percent during these excursions. Even so, the temperature which we measured still showed an increase.

Oriani: What was the time scale for these events?

Huggins: Each change took a few minutes.

Hoffman: I have brought up this point several times before. If arcing were occurring between the electrodes, the circuit could oscillate. If you do not have a true RMS voltmeter, which is apparently the case, you would not see the true voltage changes or power input. The dc power would appear to go down.

Bard: Your inner block temperature seems to have a fairly long time constant. My impression is that oscillations can in fact account for the percentage of excess heat which you measure.

Huggins: The observed temperature rise itself cannot account for the 50 percent excess heat flux which we observed.

Werbos: Does the time constant for the temperature rise match that for heat conduction from the cell to the inner block of the calorimeter?

Huggins: I have no data on that. Heat conduction is quite rapid from the electrode area to the inner aluminum block. From there to the outer cylinder, it requires 30-60 minutes before steady state is reached.

Werbos: So, from the cell to the inner block, heat transfer might take only about two minutes.

Huggins: Yes, that sounds reasonable.

Appleby: Would it not be helpful to have another thermocouple in the side pocket of the calorimeter to obtain a better idea of what is occurring?

Huggins: It would be useful, but I do not think that it would change the general effect. The computer measures the cell current, determines the potentiostat voltage, and then multiplies the two to obtain the input power.

Appleby: Obviously, there would be a time lag between the temperature rise and the voltage change, as Dr. McKubre has pointed out.

Huggins: Yes, of course.

Appleby: It should be integrated from minute to minute, on the scale of your plots. The voltage which you show is very large compared with data from other groups, on the order of 40 V.

Huggins: We would like to do that, but we do not have all of the information to do so. The lag should be about 2-3 minutes, as far as we can tell.

Jones: To make correlations of the sort which you suggest, independent of the available data, may be dangerous. First, it would help to see the error bars. Second, you are showing correlations over only a short timeframe.

Huggins: We have examined the effect over short and long timeframes, with essentially the same results.

Jones: However, it is surprising that you see the jerking effects in the data. Why should these occur?

Huggins: It may be related to the behavior of the potentiostat, changing the voltage when current excursions occur.

Myles: Could the variations be due to something spalling off the surface of your electrode, dendrites, for example?

Huggins: It may be due to cracks in the palladium. Whatever it is, it appears to be very interesting. However, the potentiostat has a very rapid response time, on the order of a millisecond, so it should keep up with electrical changes.

Werth: I have a question for both Dr. Oriani and Dr. Appleby, concerning what Dr. Huggins has stated about the endothermic effect during the charging phase on the palladium. Were endothermic effects observed in these cases?

Voice: We did not measure any such effects. However, if storage of deuterium occurs involving lattice straining, then a negative heat output deviation should be seen. We have not observed that effect, but its magnitude would not be large.

Bard: I would like to raise one other question, which would pertain to both Dr. Huggins' and Dr. Appleby's talks. The nature of the phenomenon should be independent of the way in which it is measured. As one went from an open to a closed cell, changing the calorimetric conditions in a small way, the excess heat effect went down from 15 to 20 percent to only 5 to 8 percent, forgetting transient effects. Is that not a fair appraisal?

Oriani: I would now say that the general range of values that we have observed for open and closed cells was about the same. It seems to vary a great deal, going from 5 percent one day to 15 percent the next. The largest range that we have seen is 30-35 percent.

Hoffman: In the Appleby work, the numbers seemed to be generally lower in closed cells compared to open cells.

Voice: For systems operating in the closed mode, the startup period is difficult to interpret, since oxygen is being released from the system, whereas hydrogen or deuterium is being absorbed in the palladium phase. What particular issues arise in this case?

Voice: We use a closed cell in which the cell itself is connected by a tube to a bubbler. Initially, the bubbles which are seen are oxygen. Since there is a recombination catalyst, once bubbling stops, both gases must be produced at the same stoichiometry. For completely sealed cells in opaque containers, the situation is more difficult.

Teller: Can we determine if there has really been some effect which has been established by everybody who has seriously looked at these phenomena, or is there solid evidence in the opposite direction?

Voice: I think that there is substantial disagreement as to how to respond to your question. There seems to be substantial evidence that those who have made serious efforts to search for excess heat have not necessarily found it, but at the same time, the experimental parameters are such that it is impossible to say that everyone has in fact been doing the same thing.

Oriani: In our work, there are indeed instances where we saw excess heat with deuterium and LiOD, in what we considered were very good measurements.

Fleischmann: Many groups claim that they have seen nothing.

Teller: So we can agree that there is disagreement, or at least we can agree that there are arguments for one effect or another. I would like to be unconfused.

Chu: Perhaps, we should examine all of the factors which may influence results, and in essence, agree on disagreeing. A decisive factor might be electrode treatment, which for some people is important. Current density is another factor, as is whether closed or open cells are used.

Bard: We are clearly tending to focus on materials problems. However, the key experiment which must be done should involve a cell producing excess heat for one group being given to a group which does not find excess heat. Rumor, for example, says that one of the Utah cells was given to Harwell. Is that true?

Fleischmann: That is not true. One electrode was given to Harwell. I do not know its subsequent history; indeed, there are only rumors.

Bard: A way to settle some of these problems would be to give away the whole cell, including the D_2O and the electrodes, when it appears to work.

Santucci: A cathode was given to Dr. Oriani.

Bard: But he was producing positive results anyway. I suggest that we give a producing cell to someone who is a nonproducer.

Appleby: One well-publicized set of negative calorimetric results are from the Harwell Laboratory. They deal with a very large number of different cells. Their current-density conditions were such that, based on our own work, only their last cell, at a current density of about 500 mA/cm^2, would have produced a positive anomalous heat result.

Teller: Other cells do not produce positive results?

Appleby: In my opinion, almost all their cells produced small positive results with LiOD solutions, though it was felt that the results were within their error bars.

Teller: You mean within, say 2 percent?

Appleby: Yes.

Fleischmann: Some extraordinary statements are made about statistics. I would like to perform a reductio ad absurdum. First, I would like to pose a question familiar to all electrochemists. If we impose an alternating voltage as a function of time about a mean voltage, and if the variation of that imposed voltage is less that two standard deviations (2σ), then using normal statistical considerations one would conclude that all of the measurements are unsound. However, one can perform a Fourier analysis, or some time average. If the process is stoichastic, the treatment is not so obvious. Anomalous heat data from many groups, at Harwell in particular, have shown a small positive excess that is within 2σ. In reality, things cannot be examined in that way. Overall, to be statistically significant, the results should show as many minus as plus data. For example, we may have eight neutron counts in a cell. All are with 2σ of background, yet the net result is positive in separate experiments. In consequence, I think that there is a great deal of confusion between what are acceptable and unacceptable statistics. I do not know how this issue will be resolved, since I think that people will argue about this particular point. For example, certain groups may really have seen low levels of heat with positive deviations, but they have assumed the results to be zero.

Bard: That may not be true with the Harwell data.

Teller: I would like to put one question to those with positive results. Although there are some variations, there is agreement that you do not see the effect at once. There is an induction period, sometimes a fraction of an hour, sometimes several hours. My question is how long will you then see positive results after you have turned off such a cell?

Huggins: In our case, if you turn the power off, the effect dies away immediately.

Teller: If you turn on the power again, does the effect return after, say 5 hours?

Rafelski: Dr. Appleby turned off the power for 10-minute intervals, and the effect returned after a short time.

Teller: How long does one have to wait until this memory effect goes away? An hour, a day?

Appleby: The effects are confused by the time constant of the calorimeter. When NaOD solution switched off the effect in our work, the process was slower than the time constant of the calorimeter. Thus, the loss of memory, due to lithium loss, was on the order of hours.

Rafelski: However, when the lithium was put into the palladium surface again, the effect returned.

Schneider: After a period of several hours?

Appleby: Quite quickly.

Yeager: Some of our experiments indicate that lithium stays in the surface and that it persists for long periods of time. It does not appear to come out in a matter of hours.

Miley: I would like to ask Dr. Huggins a question. On one of your early slides, you indicated that you thought that you were seeing a bulk effect, rather than one at the surface. This seems important, in view of the claims of other investigators.

Huggins: The only argument for the bulk effect is time dependence, and that is not strong. It is possible that it is a surface reaction.

Chubb: The surface effects seem to relate to conventional nuclear products, such as tritium. Perhaps α-particles from the interior interact with the surface, so that not only surface effects influence the anomalous heat phenomenon.

Section 19

ELECTROCHEMICAL KINETIC AND THERMAL STUDIES OF THE Pd/LiOD SYSTEM

Michael C.H. McKubre, Romeu C. Rocha-Filho, Peter C. Searson, Stuart I. Smedley, Francis L. Tanzella, and Robert D. Weaver

SRI International

Bindi Chexal, Thomas Passell, and Joseph Santucci

Electric Power Research Institute

ELECTROCHEMICAL KINETIC AND THERMAL STUDIES OF THE Pd/LiOD SYSTEM

Michael C.H. McKubre, Romeu C. Rocha-Filho, Peter C. Searson, Stuart I. Smedley,
Francis L. Tanzella, and Robert D. Weaver
SRI International

Bindi Chexal, Thomas Passell, and Joseph Santucci
Electric Power Research Institute

INTRODUCTION

Thermal and electrochemical kinetic processes were examined in a cell comprising a Pd cylindrical cathode and concentric Pt coated Ni anode, containing 0.1N LiOD in D_2O. Experiments were performed using an electrochemical overvoltage to load deuterium into the Pd lattice, at a cell voltage below that of electrolysis of D_2O, in an overpressure of D_2 gas.

A separate series of experiments was performed in cells which permitted electrolysis to occur at ambient pressure. These experiments were designed to investigate the effects of physical variables on the rate and extent of loading of D into a Pd lattice, and to examine the electrochemical kinetic processes occurring at a highly loaded $PdD_x/LiOD$ interface.

Anomalies were observed in both the thermal behavior evidenced by the calorimetric response, and the kinetic behavior obtained from the interfacial impedance, measured as a function of D_2 loading, as inferred from axial resistance measurements of the Pd electrode.

CALORIMETRY AND ELECTROCHEMISTRY

A differential calorimeter was constructed employing two identical high pressure electrochemical cells. Deuterium was used as the pressurizing gas: this served to depolarize the anode reaction and to enhance the solubility of D_2 in the Pd cathode. Both cells were mounted in a temperature controlled water bath, maintained at 4°C. One cell contained

a pure Pd cathode, 7 mm in diameter and 5 cm in length, and the other a palladized Cu rod of identical dimensions. Both cells contained 0.1 M LiOD prepared by dissolving Li metal in D_2O. The intent was to prepare two cells of identical thermal and electrochemical properties but with different electrodes. Calibration was made by comparing the electrochemical power with the temperature differential between each cell and the bath.

This procedure calibrates the cell against a constant background and is useful only in identifying "bursts" of excess power. The computerized data collection system recorded cell voltages, cathode voltages with respect to a Pt electrode, cell current and cell and bath temperatures. Periodic measurements were made of the electrochemical interfacial impedance, and of the resistance of the Pd cathode in the axial direction. The latter measurement provides an indication of the D/Pd ratio in the cathode.

The advantages of this approach are principally those of having a closed system for calorimetry, and tritium measurement. It also facilitates a high loading of deuterium, and enhances electrochemical measurements because bubble formation at the electrode is minimal or nonexistent.

The Pd electrode was prepared by annealing at 800°C for three hours in a vacuum and then cooling in D_2 gas; aqua regia was used to etch and "activate" the surface before installation into the pressure vessel.

Electrochemical effects, and in situ measurements of the D/Pd ratio, were studied in glass cells which contained a 3 mm diameter x 10 cm long Engelhardt Pd electrode and a helically wound wire Pt electrode. One of these cells also was equipped with a Pt reference electrode and multiple

temperature sensors: three in the electrolyte and two in the gas phase above the electrolyte. The electrolytes studied were 0.01M, 0.1M and saturated LiOD, prepared by dissolving Li in D_2O (in the latter case to the point where no further metal would react with the electrolyte). The electrodes were prepared by annealing in a vacuum, subsequent D_2 treatment at 1 Atm. and then etching before insertion into the cell.

RESULTS

Calorimetry

Several different types of events were observed: "excess" temperatures from both the Pd and the palladized Cu electrode, and voltage excursions on the Pd electrode.

The "excess" temperature excursions of the Pd electrode were interpreted as "excess" heat bursts. Seven were observed with peak power up to 9 W that in total sum to ~ 20 W Hr of energy over the total duration of the experiment of approximately one month. It is worth noting that the electrochemical power input to each cell was approximately 1 kW Hr in that same time. A typical temperature profile during such a heat burst is illustrated in Figure 1.

Electrochemistry

The resistance of Pd is a known function of the D/Pd ratio, and the rate of change of the resistance ratio $R/R°$ (where R is the temperature corrected resistance and $R°$ is the electrode resistance of pure Pd at the reference temperature) is proportional to the flux of absorbed D at the Pd cathode surface. The flux or current of adsorbed D thus calculated is shown in Figure 2 as a function of time; it is also compared with the total cell current. It is noticeable how i_{abs} increases at first with increasing current, then passes through a maximum and continues to decline. This is
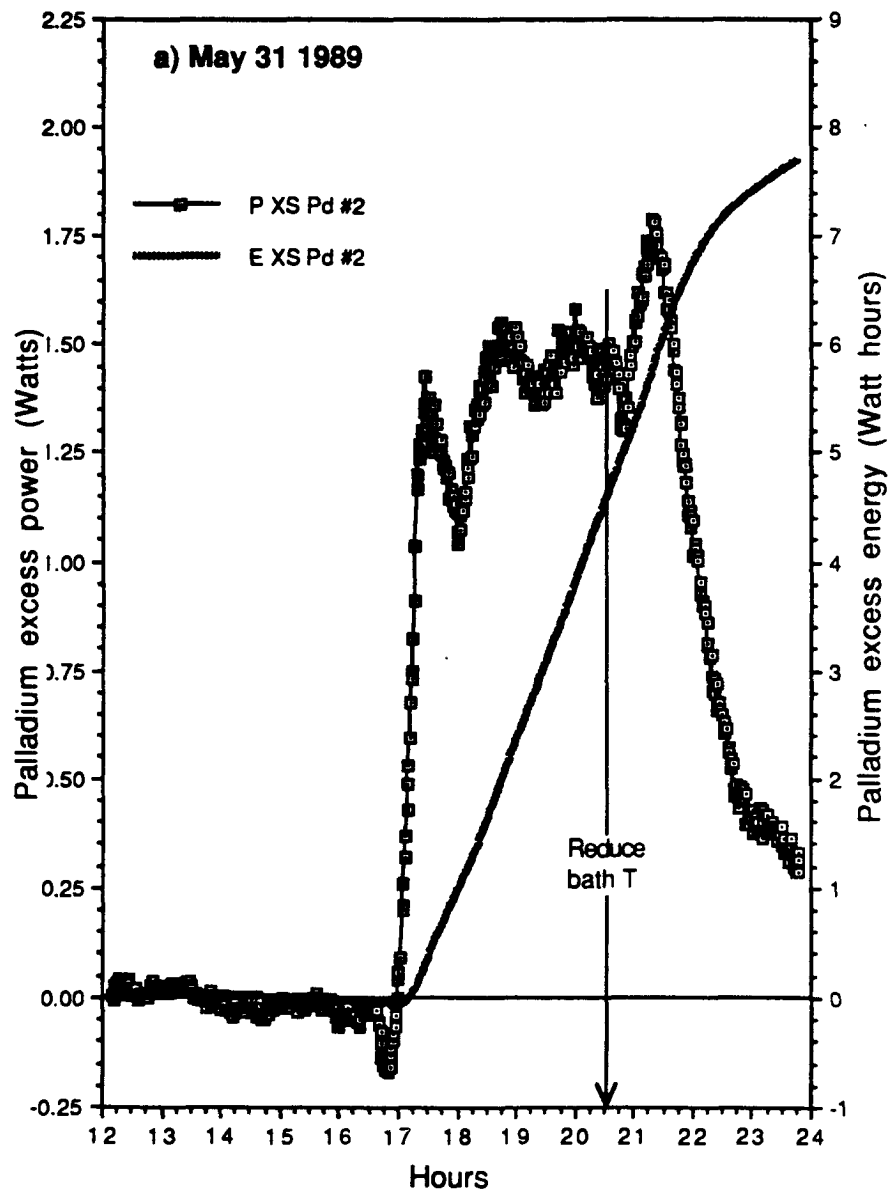
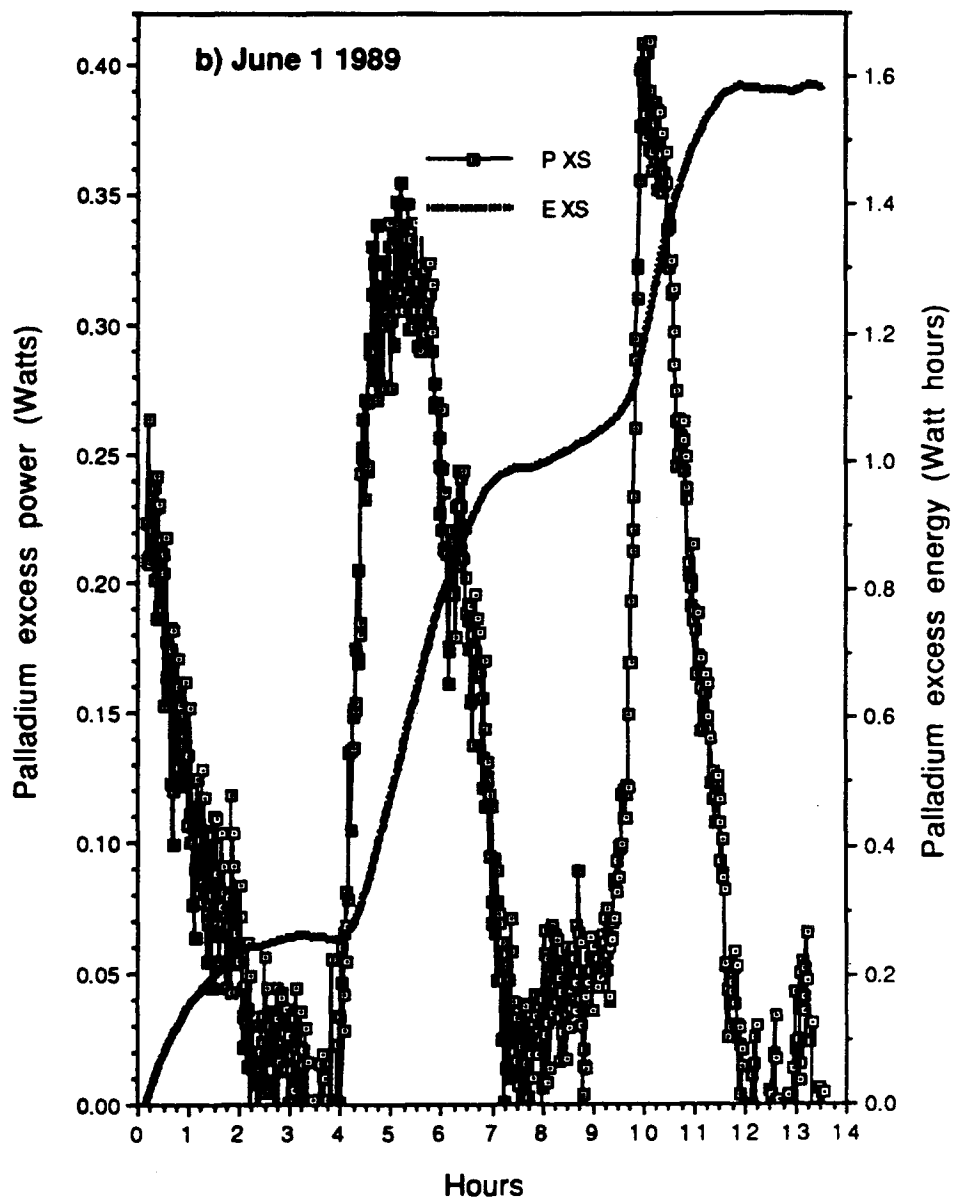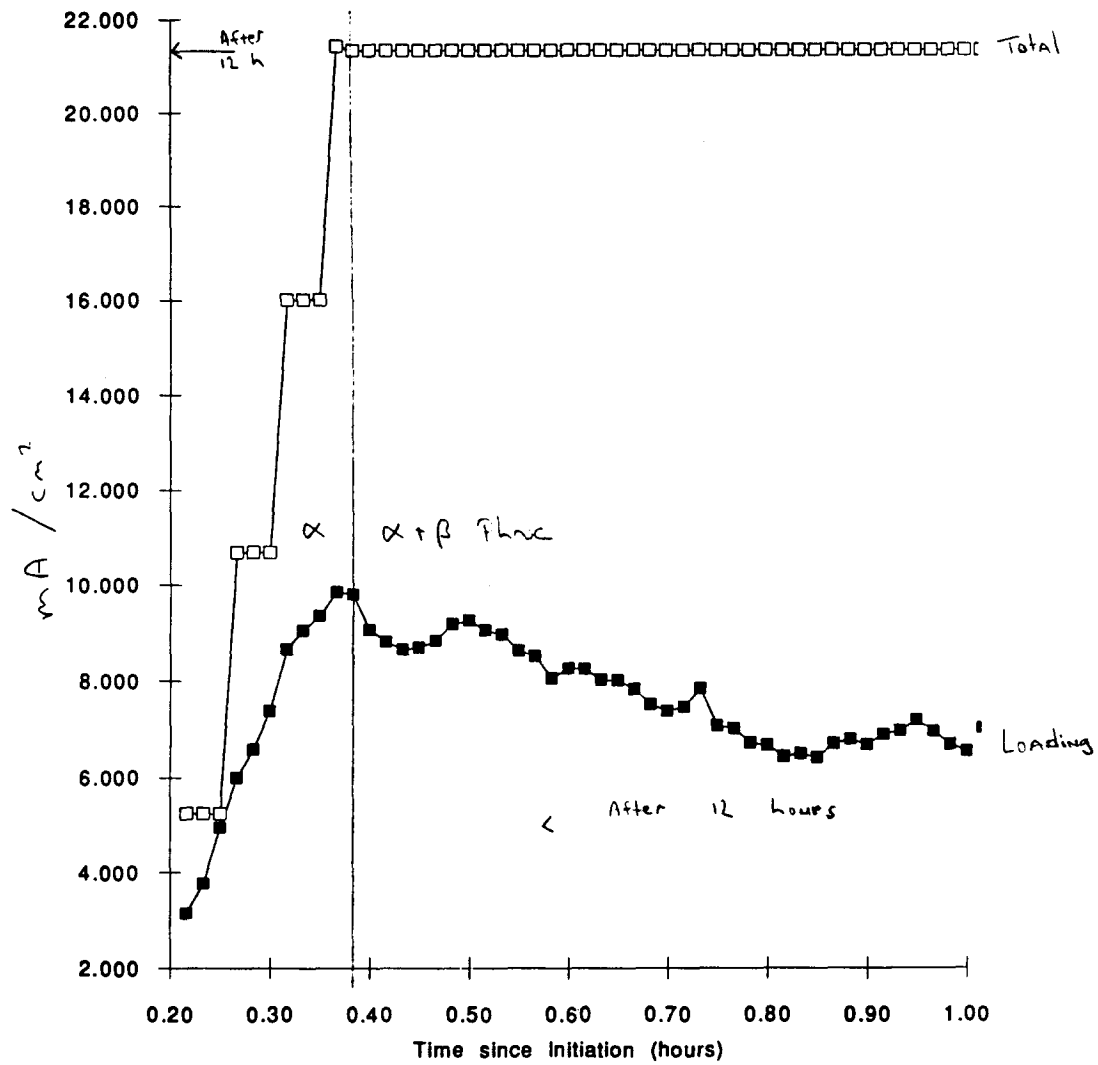**Figure 1   Differential Calorimeter Excess Power**

Figure 1   Differential Calorimeter Excess Power

Chexal 1

Total and Loading currents   versus time

presumably due to the diminution in the concentration gradient of D in the Pd as the electrode becomes increasingly charged.

By extrapolating the resistance versus loading behavior of the Pd/D system, in a manner parallel to the known behavior of the Pd/H system, we can obtain approximate values of the loading of a Pd electrode at very high mole fractions of D. On this basis, we have demonstrated in some experiments that it is possible to obtain D/Pd loadings in excess of 0.8 and even approaching 1.0. In other experiments with nominally identical electrolytes, we have been unable to load a Pd electrode, beyond the maximum in the resistance versus loading curve (at D/Pd ~ 0.72). The key elements in achieving a high D/Pd loading in alkaline electrolytes appear to be: activation of the Pd surface, high temperature loading with D_2 gas, high current densities, low temperatures. Obviously some of these requirements are exclusive, and we have found it desirable to use electrolytes more concentrated than 0.1 Molar in order to achieve high loadings. The degree of loading is however not stable, and we have observed instances where, at constant current pressure and temperature, the electrode resistance spontaneously decreases and then increases over a period of ~5 hours. This can be interpreted as a spontaneous decrease and increase in the D/Pd ratio, which may be stress induced.
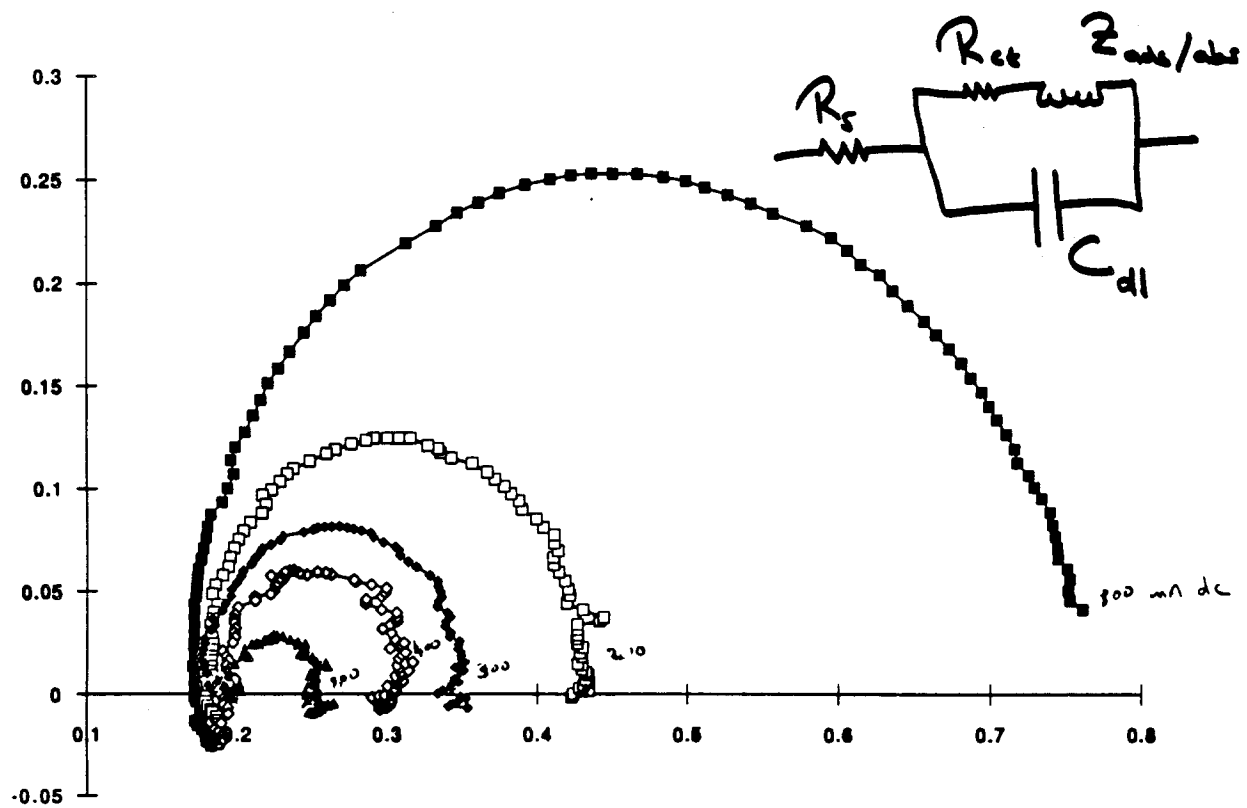
Electrochemical impedance measurements of the palladium/electrolyte interface can provide a useful insight into the kinetic processes that govern the deuterium reduction, D adsorption/absorption and D_2 recombination reactions. Such measurements also may provide information on the kinetic effects of surface adsorbed species other than D,

and the presence of surface films. At moderate loadings D/Pd ⪴ 0.75, the impedance locus describes a nearly perfect semi-circle, offset from the origin by a small real component due to the resistance of the electrolyte volume between the tip of the reference electrode and the cathode surface. The simple semicircular, single time constant response suggests that the concentration of absorbed D is not significantly a function of current density up to moderate loadings and cathodic current densities.

This simple picture changes for a heavily loaded electrode (D/Pd > 0.75) and at very high cathodic current densities. Figure 3 shows data obtained in saturated LiOD in an electrolysis cell with internal recombination. As the cathodic current density is increased from 10 mA cm^{-2} to 80 mA cm^{-2}, the single time constant, semicircular response changes to show evidence of a "pseudo-inductive" or positive phase shift response at low frequencies. This effect is shown more clearly, and extends even down to moderate current densities, for a very highly loaded Pd electrode. Figure 4 shows results obtained in 10 M LiOD under an overpressure of 850 psi of D$_2$ gas at 25°C.

The frequency dependent data in figures 3 and 4 can be modelled as a parallel RC combination and a pseudo-inductance. The RC combination consists of charge transfer resistance of the deuterium reduction reaction in parallel with the double layer capacitance. Charge transfer resistances are inversely related to the rate of the rate determining reaction, which in this case decrease approximately with increasing exponential current. The pseudo-inductive effect can be ascribed to a change in the concentration of some absorbed species that is out of phase with the applied waveform. This surface active species could be adsorbed or absorbed D atoms.
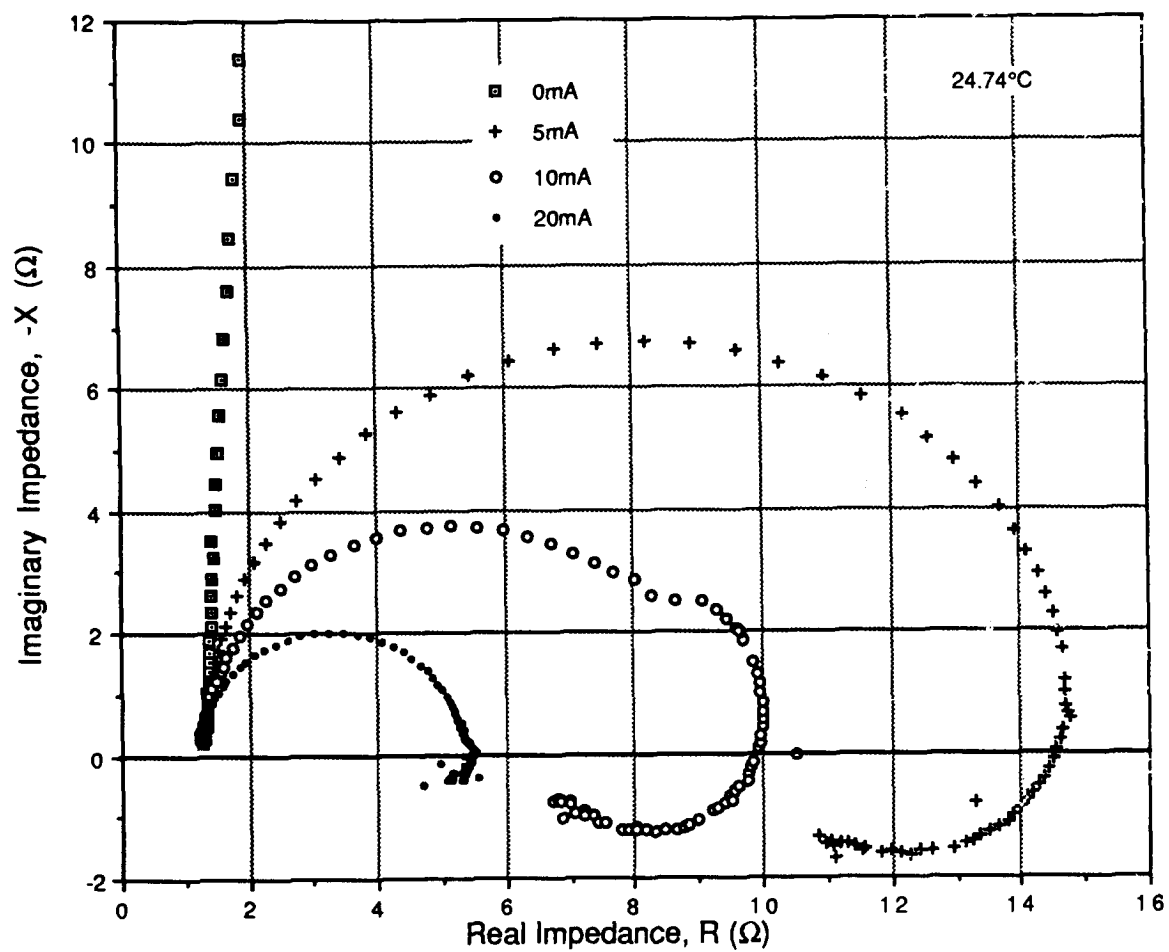
Z1 9/29; Reducing Icell in sat LiOH

Figure 4   Pressurized Cell P2 Impedance Data

CONCLUSION

Measurement of the metal phase resistivity provides a good indication of the degree of loading of a palladium electrode. While the resistance ratio still needs to be calibrated for the Pd/D system at loadings D/Pd $\gtrsim$ 0.6, this nevertheless provides a good qualitative indicator of the effect of external variables on the concentration [D], that is presumed to be the reactant species of any nuclear processes that may occur in the palladium lattice. Using this method we observe that high loadings may be achieved at high current densities and low temperatures, following pre-loading with D_2 gas at high temperature and surface activation by an acid rinse. The absorption of D appears, however, to be controlled by a unknown factor that may prevent loading beyond D/Pd ~ 0.6 to 0.7.

Measurement of the interfacial impedance provides valuable insight into the electron transfer and adsorption/absorption processes that control the loading kinetics. These also can be useful in identifying the existence of adsorbed species other than D that may influence the charge transfer kinetics or prevent the achievement of high loadings.

Temperature excursions in excess of the shady state values have been observed for a Pd electrode, and also for a palladized copper electrode, both in 0.1 M LiOD, in a pressurized differential calorimeter. These have been interpreted as "excess" heat bursts, although in the case of the palladium coating the associated "excess power" was small. For the bulk palladium electrode, "excess heat" was observed only after the electrode had been loaded to an apparently very high level (D/Pd ~ 1.0 ± 0.1) by a combination of static gas pressure and D^+ reduction current. In this condition we also observe considerable irregularity in the cathode voltage. It is possible that the thermal and potential anomalies may be characteristic of the highly loaded D/Pd system.

DISCUSSION (MCKUBRE)

Oriani: What can you say about the effect of dislocations which are produced during loading with deuterium?

McKubre: The resistance returns to its original value after negative-positive cycling of the electrode. The method is a well-understood technique, and dislocations do not significantly add to the resistance of the electrodes.

Appleby: What was the maximum pressure which you used?

McKubre: We have gone as high as 1000 psi.

Appleby: What about the question of copper stability under anodic conditions?

McKubre: The copper is fully coated with both nickel and palladium and is not exposed to the electrolyte.

Oriani: What was the magnitude of the excess power which you saw at any time?

McKubre: About 9 W, or about 100 percent in our closed cell.

Jones: Did you see any negative fluctuations?

McKubre: No.

Jones: What about endothermic fluctuations?

McKubre: Nothing significant. There were some at the beginning of experiments, but the instrument stays on or above the calibration line. The calorimeter can be used in a differential mode or as a single-cell instrument. In the latter mode, correct data treatment can handle the problem of negative excursions.

Flanagan: If you leave a sample charged to $PdD_{0.92}$ on open circuit, what effects are seen?

McKubre: We have examined a sample under these conditions with a superposed ac signal as a diagnostic tool. Nothing anomalous was seen.

Bard: What is the D_2 concentration in the electrolyte under your pressure conditions? This would determine mass transport to the anode. What was your anode current density?

McKubre: The solution is supersaturated and contains fine bubbles, which enhance mass transport. The anode current density was 200 mA/cm^2.

Appleby: With supersaturation, the deuterium concentration may have been as high as 0.1 M under the pressure conditions used.

McKubre: The solution is certainly supersaturated; otherwise, the observed current densities could not be accommodated.

Hoffman: When you introduced the deuterium into the palladium, what temperature was used?

McKubre: 850°C.

Hoffman: If you load through the miscibility gap, as you do electrochemically, the specimen will usually crack, so that an unusual electrical resistance will be observed.

McKubre: Normally, the electrode is in the β-phase region when it is placed in the cell. Electrochemical loading does not cause a problem.

Bard: However, is the resistance-loading relationship understood for high loadings? It must be a bi-valued function. Do you determine the composition via the change of resistance as loading proceeds?

McKubre: You can determine the side of the function which you are on by changing the conditions, e.g., the current density. The highest loadings that we achieved were at a current of 15 A, or 1.6 A/cm^2.

Mansour: Dr. Flanagan, I thought that you made a strong argument yesterday that loadings would not go above unity. Over this value, all the octahedral sites will be filled, or there will be mixed occupancy between octahedral and tetrahedral sites.

Flanagan: I do not see any evidence that Dr. McKubre's results go beyond unity.

Talcott: Did you try a LiOH-H$_2$O blank? Lithium may also be present in the octahedral sites in the palladium, which may affect the resistance. This could be confirmed with an experiment involving LiOH.

McKubre: I would like to do that in the future. These experiments are not easy to perform, and we decided to examine blanks after we had obtained results with LiOD.

Section 20

INVESTIGATION OF PHENOMENA OCCURRING DURING
D$_2$O ELECTROLYSIS AT A PALLADIUM CATHODE

R.R. Adzic, D. Gervasio, I. Bae, B. Cahan, and E. Yeager

Case Center for Electrochemical Sciences and Department of Chemistry

Case Western Reserve University

INVESTIGATION OF PHENOMENA OCCURRING DURING

D_2O ELECTROLYSIS AT A PALLADIUM CATHODE

R. R. Adzic*, D. Gervasio, I. Bae, B. Cahan, and E. Yeager

Case Center for Electrochemical Sciences
and the Department of Chemistry
Case Western Reserve University
Cleveland, Ohio   44106

ABSTRACT

Measurements have been carried out on the phenomena reported by Fleischmann and Pons to occur during the electrolysis of D_2O solutions with a palladium cathode. The measurements include: 1) the determination of tritium concentrations in the cells 2) the determination of the D/Pd ratios by coulometry; 3) surface analysis of the Pd cathode; and 4) neutron radiation measurements. Enhancement of tritium in the D_2O solution was found in two open-type glass cells as well as in four other cells with Ni anodes. The largest enhancement factor found was ~50. The source of this enhancement remains unexplained. Surface analysis revealed a number of impurities on the Pd surface including Si, Pt (with Pt anodes) and Li. The latter was found to penetrate 200 nm into the Pd bulk. The neutron measurements were inconclusive.

INTRODUCTION

Fleischmann, Pons and Hawkins [1] and Jones et al. [2] have reported evidence for the nuclear fusion of deuterium electrochemically injected into palladium. Excess heat generation, neutrons and γ-rays emission and tritium enhancement in the electrolytic solution were found by Fleischmann et al. [1] and neutron emission by Jones et al. [2]. These results have been met with much skepticism, especially after several reports of negative results by other workers [3-5]. Subsequently there have been a number of reports of excess heat generation [6-8] and tritium enhancement [9,10] or both [11].

The present research was motivated by the necessity for experiments under well defined conditions. In order to verify excess heat generation calorimetric measurements were done with a modified Fleischmann-Pons (F-P) type open cell and also with a closed cell with internal D_2/O_2 recombination. Some excess heat generation was observed. These results, however, require further evaluation and will be reported at a future date. Careful determination of tritium was done in the electrolytic solution and also in the water obtained from the recombined gases outside the cell. Surface analysis of Pd cathode

---

*Permanent Address: Institute of Electrochemistry, ICTM, University of Belgrade, Belgrade, Yugoslavia.

was performed and the D/Pd ratio determined. Neutron radiation measurements were attempted, but difficulties in making background corrections interfered with the measurements.

EXPERIMENTAL

Electrodes

Pd from several sources was used for the cathodes. The rods 0.2 x 10 cm were obtained from the Engelhard Corporation. Wire of 0.5 mm diameter and 99.9% purity, was obtained from Johnson Matthey - Aesar. 1 mm wire (grade A) and 4 mm rod of 99.9% purity were obtained from Johnson-Matthey, England. Engelhard's Pd was also used by Westinghouse to prepare 2 mm rods by recasting, drawing and swaging. One or more of the following pre-treatments were used with various samples (as indicated in the tables):

1. Annealing in a vacuum with a small amount of Ar for 24 h at ~950°C, followed by cooling in D_2 for some samples

2. Recasting, drawing and swaging of some samples

3. Electrochemical oxidation of H_{abs} in 0.1 M LiOD at E = ~0.5 V vs. S.C.E. for 24 h, followed by immediate transfer into the calorimetry cells for most samples.

The anodes were made of Engelhard's Pt ribbon or wire cages of 99.9% purity Pt or Ni foil (99.9%), obtained from Fischer Scientific Co.

Electrolytes

0.1 M LiOD was used as the electrolyte in all glass cells, while 0.1 M and 1 M LiOD were used in Ni encased cells. LiOD attacks glass, which leads to a deposition of Si and other constituents of glass onto the Pd. The SIMS measurements showed that even in 0.1 M LiOD after several weeks Si could be easily detected on the Pd surface. The electrolytes were prepared from once distilled Norell (99.5%) or Isotech (99.9%) D_2O. 1 M LiOD was prepared from Li_2O (99.9%) Cerac, Inc. in a glove bag. Upon diluting this stock solution, 0.1 M LiOD was obtained. The blank experiments in 0.1 M LiOH in H_2O have not yet been carried out.

Tritium Measurements

The analyses of the solution for tritium were performed by Westinghouse Electric Company using liquid scintillation counting on a Packard 4030 counter. The liquid scintillation cocktails were prepared with OPTI-FLOUR scintillator. Typically, four consecutive 60 min. counts were recorded and averaged. Another precaution against any possible complications caused by components in the electrolyte solution was the separation of the water from the cell electrolytic solution by distillation at reduced pressure before the tritium measurements. While this procedure minimized the possibility of interference effects with some constituents of the electrolyte, it causes loss of dissolved T_2 and DT. For this reason some experiments were done without distillation after neutralization of the alkaline electrolyte. The electrolytic solution from the cells with Ni anodes was neutralized,

filtered and centrifuged to remove suspended nickle oxide particles. Distillation was also used with a centrifuged sample which showed high counts in order to ensure that solid particles within the electrolytic solution were not responsible for the high count rate.

Neutron Radiation Measurements

The neutron detection was attempted by using two BF_3 counters coupled with a multichannel analyzer. The authors are not satisfied that the background was adequately taken into account with this experimental arrangement and hence the results are considered inconclusive. Solid state track recorders may prove attractive for such measurements in the future.

RESULTS AND DISCUSSION

Tritium Measurements

Fleischmann and Pons (1) reported enhancement of tritium concentration in the electrolyte as one evidence for a cold fusion of deuterium. The enhancement factor (see Eq. 4) is, however, close to the deuterium/tritium separation $S_{D,T} \simeq 2$, as recently determined by Corrigan and Schneider (11). Bockris et al. (13) and Wolf et al. (14) reported recently enhancements of 4 to 7 orders of magnitude over the background. In this work we have measured tritium concentration in open F-P cells, closed cells with the Ni casing and in four open cells designed for studying the tritium enhancement.

In open cells a change in tritium concentration will occur due to the addition of D_2O containing T and due to its removal by electrolysis. The isotopic separation factor of T to D is defined as

$$S = (n_D/n_T)g/(n_D/n_T)s \qquad (1)$$

where n_D and n_T are numbers of deuterium and tritium atoms in the gas (g) and solution (s) phases respectively, at steady state. It can be shown (14) that the enhancement of tritium in the electrolytic solution at time (t) obeys the following expression:

$$n_T(t)/n_T(o) = S-(S-1)exp(-t/T) \qquad (2)$$

where T is the tritium build-up time constant.

Thus, at very long times the tritium concentration in the solution due to isotopic separation is S times the tritium concentration in the original solution.

If the recombination of D_2 and O_2 is carried out in the cell or outside the cell and the D_2O returned to the cell, only change in tritium concentration in the electrolyte could be brought about either by having substantial tritium in the palladium or other cell components or by a nuclear reaction. The palladium was stripped of hydrogen and its isotopes by electrochemical oxidation for 24h in LiOD solution. This treatment should have removed any tritium present in the Pd samples.

In all of the experiments in which an enhancement of T was observed, a

long time electrolysis of the order of several weeks was necessary before observation of the increase in tritium concentration. In two out of five open-type cells with Pt anodes excess tritium was found. These cells also were the only ones out of five which generated excess heat.

Table 1 gives the cell parameters for which enhancement of tritium concentration was observed. The four open cells, which were designed to study tritium accumulation and generation, were essentially test tubes 3 cm in diameter with a Teflon cell top. The cathodes were 5 cm long, spot welded to a nickel ribbon as an electrical contact; 0.25 cm thick Ni foil was used as anode. During a long term electrolysis a black residue, most probably nickel oxide, accumulated in the electrolyte in only two cells. The electrolyte was filtered and centrifuged to remove these particles and then neutralized by HCl before determination of T. When large tritium counts the solution was distilled and counted again. In some instances (cells 1, 2) the solution was distilled and only the distillate was added to the scintillation liquid to avoid possible complications with various species in the solution.

The results are given in Table 2. All measurements were done in four runs during several to 24 h. The average of 4 counts is given with the standard deviation indicated. The decrease in the count rates for distilled vs. neutralized samples was usually negligible. The samples were taken in intervals of 15-20 days. According to Bockris et al. (13) after reaching the maximum level, the tritium content considerably decreases after a few days, eventually down to the separation factor. If this is applicable to our experiment, it may mean that we have not observed the maximum amount of tritium probably due to a low frequency of sampling. The calculation of the tritium concentration was done in the following way:

$$\text{Net count rate/c ml}^{-1} = \text{average count rate/c ml}^{-1}\text{-blank count rate/c ml}^{-1} \quad (3)$$

$$\text{Enhancement ratio} = \frac{\text{sample net count rate}}{\text{D}_2\text{O net count rate}} \quad (4)$$

The number of disintegration per min per ml was calculated by dividing the net count rate with the efficiency factor, which is 0.224 c/d for this instrument.

$$\text{dpm ml}^{-1} = \frac{\text{net count rate/cpm ml}^{-1}}{0.224 \text{ c/d}} \quad (5)$$

For cells number 1 and 2 for which some excess heat generation was observed, the tritium level amounted to 766.43 and 1730 dpm ml^{-1} respectively.*

Let us compare the excess power generated in these open cells with the amount of T found. If all of the energy were coming from the tritium generating reaction,

---

*The tritium concentrations in the samples of electrolyte from the cells in the present work have been checked by S. Landau of Case Western Reserve University and Z. Minevski of Texas A & M University, whose help in this matter is acknowledged.

$$D + D \rightarrow T + H + 4.03 \text{ MeV} \tag{6}$$

this would produce 4.03 MeV = 4.03 · 10^6eV · 1.6022 · 10^{-19}J/eV = 6.46 · 10^{-13} J/reaction. If 1 mW of heat is produced in a cold fusion reaction per 1 cm^3 of Pd the corresponding number of T atoms would be 10^{-3} W/(6.46 x 10^{-13} W s/reaction) = 1.55 x 10^9 reactions/s; i.e. 1.55 x 10^9 T atoms would need to

be produced. Tritium decays by the reaction

$$T \rightarrow {}^3\text{He} + \beta^- + \bar{\nu} \tag{7}$$

where β^- is a beta particle and $\bar{\nu}$ is a antineutrino. Tritium decay is, as with all radioactive nuclei, first order. For N atoms of T, the decay rate is (16)

$$\frac{dN}{dt} = -\lambda N \tag{8}$$

The decay constant, related to the half life is (16)

$$\lambda = 1.782 \times 10^{-19} \text{ s}^{-1}$$

For 1 mW one should observe

$$- \frac{dN}{dt} = (1.782 \times 10^{-9} \text{ s}^{-1}) (1.55 \times 10^9) = 2.76 \text{ dps} = 166 \text{ dpm of T} \tag{9}$$

Therefore, the observed 766 and 1730 dpm ml^{-1} can account only for ≃ 4-10 mW, i.e., three orders of magnitude below experimental observations (1). Much smaller, but still significant, enhancement of tritium was found in the gas phase for cells 1 and 4 after recombination of O_2 with D_2 and TD. Based on the separation factor one would expect a lower concentration of tritium in the gas phase, if tritium originates from the solution phase. Smaller concentrations of T in the gas phase then in the liquid phase were found by Bockris et al. (13) for long electrolysis times. In certain short intervals, e.g., one day, however, a higher concentration in gas phase was observed. The frequency of our measurements was not sufficient to detect such short-lived changes.

The impurity layers on the Pd cathodes in the glass and nickel cells can seriously perturb the processes occuring at the cathode surface. Despite this layer, the palladium is still charged with deuterium. Definitive work, however, requires that these impurities are eliminated so that the behavior on clean palladium can be achieved. Then, the impurity effects can be tracked by the addition of each impurity under well defined condition. Such a study is needed but will prove very time consuming and expensive. Furthermore, if tritium is present in some of the materials used in the cell, it is necessary to explain why the large enhancement occurs only after long electrolysis times. One remote possibility, however, is that the Pd contained a relatively stable metal tritide which did not decompose at the temperatures involved in the vacuum pre-treatment of the Pd (e.g., 900°C). If this compound is quite stable and present in a separate phase, then the diffusion of this tritide to the Pd

surface would be extremely slow and probably at a negligible rate even on a time scale of weeks and months. The charging process, however, produces stress cracking and this would then provide a possible mechanism by which the electrolyte solution could reach this tritide and become contaminated with T.

AES and SIMS Analyses of the Composition of Pd Cathodes

Auger electron spectroscopy (AES) and secondary ion mass spectroscopy (SIMS) were the *ex situ* analytical techniques used for examining the surface of the palladium cathodes used to electrolyze D_2O in deuterated aqueous 0.1 $\underline{M}$ LiOD solutions. The electrodes were removed from the cell, blotted with towel paper, and dried. A dry electrode was introduced into the vacuum chamber ($\sim 10^{-8}$ Torr), where the surface composition was examined with AES and SIMS. The surface was sputtered with an Argon ion beam in order to remove an aproximately 90 Å thick layer (sputter rate $\sim$ -5 Å/s; time interval $\sim$ 18 s), and the newly exposed surface was then analyzed. A depth profile of the electrode composition was obtained by repeatedly sputtering for a fixed interval of time and then analyzing the newly exposed surface. The depth profiling was continued until the AES and SIMS responses were virtually constant.

The Pd cathodes were examined from the two different types of cells. The major difference in the construction of these two cells, as it pertains to these surface spectroscopy studies, is that the F-P type cell was made of glass, whereas the cell used in the Tronac calorimeter was made of nickel.

Figures 1 and 2 show the Auger spectra for the Pd cathode used in the glass cell for 75 days when the sample was first introduced into the vacuum chamber (Fig. 1) and after an $\sim 3,000$ Å thick layer was sputtered off (Fig. 2). The spectra are markedly different. The spectrum of (Fig. 1) shows peaks for Si, C, O, Mg and Al, but there is no peak for Pd. The spectrum of the surface after sputtering (Fig. 2) showed one major peak characteristics of Pd.

The AES depth profile (Fig. 3) suggests that the composition found for the electrode surface (Fig. 1) prior to sputtering persists for $\sim 1,300$ Å, and then the composition of the electrode gradually changes to the Pd rich bulk surface composition (Fig. 2) between 1,300 to 1,800 Å . No further noticeable changes were observed in the depth profile between 1,800 to 3,000 Å.

A second piece of the same Pd cathode cut off after the electrochemical measurement was examined with SIMS. In principle, the SIMS technique should parallel the AES technique and also should be useful for detecting elements not observable with the AES technique, particularly lighter elements such as Li. There are pronounced peaks for masses 6 and 7 in the SIMS data for the surface (Fig. 4) before extensive sputtering. These peaks, which represent Li^6 and Li^7, are larger than the peaks at mass 16, corresponding to O^{16}, which gave a prominent peak in the Auger spectrum for this surface (Fig. 1). The SIMS peaks for Li persist even after sputtering ~ 9000 Å off the original surface.

Figures 5 and 6 show the Auger spectra for the Pd cathode 1 nm diameter wire used in the Ni cell, when the sample after two weeks of use in the electrochemical cell was first introduced into the vacuum chamber (Fig. 5) and after an $\sim 10,500$ Å thick layer was sputtered off the original surface (Fig. 6). The spectrum of the unsputtered surface shows peaks for C, Ni and O (Fig.

5), but none for Pd. The spectrum of the surface exposed after sputtering shows only one major peak characteristics of Pd (Fig. 6). The AES depth profile (Fig. 7) suggests that the composition found for the virgin surface persists for ~1,000 Å, and then the composition gradually becomes richer in Pd and poorer in C, Ni and O between 1,100 to 6,300 Å. The Pd rich bulk spectrum (Fig. 6) persisted between 6,300 tO 10,500 Å from the original surface.

These *ex situ* studies show impurities masked the Pd from the surface for Pd cathodes used in both the F-P type and Ni cells. Ni was found only in the Pd cathode used in the Ni cell, and probably came from the Ni cell case. Si, Mg and Al were found only in the Pd cathode used in the glass cell, and probably these came from the glass cell case.

Coulometric Determination of D Absorbed in Pd Cathodes

Metallic palladium absorbs D to form a solid PdD_x solution during the electrolysis of D_2O at the cathode. The electrolysis of D_2O in the Pd is sensitive to the conditions at the Pd surface. A coulometric stripping technique was used to analyze the amount of D absorbed in the Pd during the electrolysis. The working electrode was a coil of Pd wire (diameter = 0.025 cm, area = 1.86 cm^2, mass = 0.12 g; 99.997%, Puratronic grade, Johnson Matthey) crimped together with the end of a gold wire (d = 0.05 cm; 99.9985%, Puratronic, Johnson Matthey) which served as the lead to the potentiostat. During all electrochemical measurements, the Pd coil of the working electrode was completely submerged in an anaerobic electrolyte solution consisting of 0.1 $\underline{M}$ LiOD in D_2O. A three compartment electrochemical cell was used. The electrolyte in the working electrode chamber was continuously and vigorously degassed with N_2 (99.995%, Ultrapure, Matheson). The counter electrode, a coil of Pd wire (A = 2 cm^2), was in a chamber connected to the working chamber by a glass tube filled with a glass wool plug. The reference electrode was a reversible deuterium electrode (RDE) which was submerged into the reference chamber which in turn led to the working electrode chamber via a Luggin capillary. All potentials are given versus RDE unless stated otherwise.

The working electrode was rinsed with 0.1 $\underline{M}$ LiOD in D_2O and cycled between 0.25 and 1.35 V until the steady state voltammogram shown in Fig. 8 (dashed line) was obtained. The cell was then rinsed and refilled with fresh electrolyte solution and sparged with N_2 gas. The steady state voltammogram was observed after only a few cycles. When the cell was left at open circuit for several days, it came to rest at +0.83 V, and it always returned to +0.83 V at open circuit whether it was offset to more positive or negative potentials.

Figure 9 shows the chronoamperometry curves for the charging of Pd with D at -0.3 V (negative current) and discharging of D from Pd at +0.83 V (positive current). During the charging at -0.3 V, O_2 was clearly seen evolving at the counter electrode, but when the N_2 bubbler was lifted out of the electrolyte solution in the working electrode chamber, there was no noticeable D_2 gas evolution at the working electrode. This suggests that when D is formed on the Pd surface at -0.3 V, initially most of the D is absorbed into the bulk Pd. During charging at -0.3 V, the magnitude of the current was ~10 mA in the first minute, gradually dropped to ~1.5 mA after 10 hours, and finally stabilized at ~0.7 mA after 1 day.

There is an inflection in the chronocoulometry charging curve at ~0.3 V

(Fig. 10, bottom curve) after 10 h. It was also noticed that after 10 or more hours that if the N_2 bubbler was lifted out of the electrolyte solution, D_2 bubbles were visible and slowly nucleating at the Pd surface. These observations suggest that after 10 h the charging of the Pd with D is nearly completed. Most of the charge measured before 10 h can probably be associated with the absorption of D by Pd, and the charge measured afterwards is probably associated mostly with D_2 evolution at the Pd surface.

The endpoint of the charging process was difficult to assign since PdD_x formation and D_2 evolution can occur simultaneously as discussed above. The discharging process at +0.83 V was easily spotted because the current goes to zero when discharge is complete. Although the charging of D into Pd (bottom curves in Figs. 9 and 10) took over 10 h, discharging of D from Pd at +0.83 V (see top curves in Figs. 9 and 10) was completed after ~70 minutes. The relatively quicker discharging versus charging of D through Pd is consistent with a greater D concentration gradient and Pd lattice spacing within the electrode expected during the discharging compared to the charge process.

Several other charging potentials were tried, but the optimal charging potential was ~-0.3 V vs. RDE. The rate of charging Pd with D was impractically slow at lower overpotentials (i.e., potentials more positive than -0.25 V). On the other hand, the rate of charging Pd with D was not noticeably increased at greater overpotentials (i.e., more negative than -0.3 V), although the rate of D_2 evolution did appear to increase with increasing overpotential. This is evidenced by two observations: 1) the nucleation of bubbles within minutes of starting the charging of the Pd with D at -0.35 V compared to after ~10 h of starting the charging of the Pd with D at -0.3 V and 2) the difference in the chronocoulometry curves for charging at -0.3 versus -0.35 V. Figure 9 shows the chronocoulometry curve for loading D into Pd at -0.35 V (see bottom curve). Comparing this and the analogous curve in Fig. 10 for loading at -0.3 V, one can see that at any given time there was more total negative charge for the loading of -0.35 V versus at -0.3 V. Furthermore, even though the total charge collected at -0.35 V (-255 C) was greater than the total charge collected at -0.3 V (-142 C), both experiments gave roughly the same total value for discharge at +0.83 V, namely +107 C. Similarly, the total charge collected at -0.4 V was -289 C (and was accompanied by even stronger D_2 bubble evolution), but still discharging the Pd cathode loaded this way gave just +122 C.

The mass of the Pd in the electrode was 0.12 g, which corresponds to 1.1 x 10^{-3} moles of Pd. Assuming that the positive charge collected at +0.83 V is due only to the discharge of D from Pd, the moles of D in Pd can be calculated from Faraday's law, moles(D) = Q(discharge)/nF, in which n is 1 for the discharge of 1 D from Pd and F is Faraday's constant (9.65 x 10^4 C/equivalent). The results are summarized in Table 3. All three cases indicate that there was one D absorbed per Pd atom in the electrode over this range of loading potentials with 0.1 $\underline{M}$ LiOD and D_2O as the electrolyte solution.

The loading and discharging processes were essentially reversible when the loading potentials were more positive than -0.4 V. When larger overpotentials, e.g., -0.6 V vs. RDE, were used the value of the subsequent discharge fell to ~+90 C, i.e., the corresponding ratio of D to Pd in the charged electrode was ~0.8. <u>This suggests that charging Pd cathodes at high overpotentials (or alternatively at high constant currents) may result in irreversible damage to the electrode, which may prevent attaining higher ratios of D to Pd.</u>

GENERAL DISCUSSION AND CONCLUSIONS

The results reported here support, to a certain extent, the claim of tritium generated in the electrolysis of D_2O on Pd of deuterium reported by Fleischmann, Pons and Hawkins (1). The following conclusions have been reached:

1. Enhancement of tritium was found in two out of five open cells with Pt-anodes and four out of four cells with Ni-anodes. The largest enhancement factor with respect to D_2O is ~50.

2. The ratio of deuterium to palladium atoms was found to be 1 for 0.25 mm wire, charged at E = -0.3 - 0.65 V.

3. Surface analysis using AES and SIMS revealed a number of impurities on Pd surface after a long time electrolysis including Si, Pt or (Ni) and Li which was found to penetrate into the bulk of Pd.

4. The neutron radiation measurements were inconclusive due to the uncertainty in determining the background correction.

In general, on the experimental side there are many questions to be answered in order to increase the understanding of this phenomenon, These include the irreproducibility and sporadicity of the phenomenon, necessity for a prolonged electrolysis before the excess heat or tritium production occur, the role of the microstructure and of the trace impurities of palladium, the difference between the amount of excess heat in open and closed cell, the role of surface impurities and the role of lithium, if any.

On the theoretical side the questions appear even more difficult. Table 3 lists possible fusion reaction of deuterium. According to the accepted theories the evidence for fusion of deuterium requires, besides the heat generation, a corresponding amount of neutrons, tritium and ^3He. The branching ratio of reaction A and B (Table 4) is approximately one. The cross section for reaction C is on the order of 10^7 lower than for A and B (16). γ-rays should be observed if the reaction K occurs in the electrochemical cell.

The proposition that electrochemically induced fusion is involved does not satisfy these requirements. In order to overcome these difficulties several new mechanisms of fusion have been proposed. These include the mechanisms in which the energy from the reaction C dissipates into the lattice as heat rather than γ-photon (7, 8), or in which two deuterons as bosons are squeezed together in a sphere of an octahedral site (19). Dendrites on Pd surface have been suggested as a explanation for tritium generation, due to increased electric fields around the dendrite tips (3). Fracto-fusion was also mentioned as a possible explanation in anology with the explanation of neutron generation upon fracturing LiD single crystals (19). There is, obviously, a need for more work in order to estimate the merits of these explanations, as well as to reach an complete understanding of the Fleischmann and Pons phenomenon.

ACKNOWLEDGEMENTS

REFERENCES

1. M. Fleischmann, S. Pons and M. Hawkins, J. Electroanal. Chem 261 (1989) and Errota 263 (1989) 187.
2. S. E. Jones, E. P. Palmer, J. B. Czirr, D. L. Decfer, G. L. Jensen, J. Thorne and S. F. Taylor, Nature, 338, 737 (1989).
3. M. Gai, S. L. Rugori, R. H. France, B. J. Lund, Z. Zhao, A. J. Davenport, H. S. Isaacs and K. G. Lyun. Nature, 340, 29 (1989).
4. N. S. Lewis, et. al. Nature, 340, 525 (1989).
5. D. E. Williams, D. J. S. Findley, D. H. Creston, M. R. Sene', M. Bailey, S. Croft, B. W. Hooton, C. P. Jones, A. R. J. Kucernak, J. A. Mason and R. I. Taylor, Nature, 342, 375 (1989).
6. A. J. Appleby, S. Srinivasan, A. J. Appleby, O. J. Murphy and C. R. Martin, Workshop on Cold Fusion Phenomena, Sante Fe, May 22-25, 1989.
7. R. A. Huggins, Workshop on Cold Fusion Phenomena, Sante Fe, May 22-25, 1989.
8. R. A. Oriani, J. C. Nelson, S. K. Lee and J. H. Broadhurst, The Electrochemical Society Meeting, October, 16-20, 1989, Hollywood, Florida.
9. N. J. C. Packham, K. L. Wolf, J. C. Wass, R. C. Kainthle and J. O'M. Bockris, J. Electroanal. Chem., 270, 451 (1989).

10. P. K. Iyengar, Fifth International Conference on Emerging Nuclear Energy Systems (ICENESV) Karlsruhe, West Germany, July 1989.
11. U. Landau, The Electrochemical Society Meetings, October 16-20, 1989, Hollywood, Florida.
12. D. A. Corrigan and E. W. Schneider, submitted to J. Electroanal. Chem.
13. G. H. Lin, R. C. Kainthle, N. J. C. Packham, O. Velev and J. O'M. Bockris, p. 3. Manuscript submitted to J. Electrochem. Soc.
14. K. L. Wolf, N. J. C. Packham, D. L. Lawson, J. Shoemaker, F. Cheng and J. C. Wass, Manuscript submitted to J. Fusion Energy.
15. D. Albolgi, R. Ballinger, V. Commoroto, X. Chen, R. Crooks, C. Fiore, M. Gaudreau, I. Hwang, C. K. Li, P. Linsay, S. Luekhardt, R. R. Parker, R. Petrasso, M. Schoh, K. Wenzel and M. Wrighton Manuscript submitted to the Journal of Fusion Energy.
16. P. Clark Souers, Hydrogen Properties for Fusion, Energy, University of California, Berkely 1986.
17. P. L. Hagelstein, Proc. of the Cold Fusion Workshop, J. Fusion Energy, in press.
18. J. Rafelski, M. Gaide, D. Harley and S. E. Jones, unpublished results.
19. B. V. Deryagin, V. A. Klyuev, A. G. Lipson and Yu. T. Toporov, Kolloiidnyi Zhurnal, 48, 12 (1986).

13. G. H. Lin, R. C. Kainthle, N. J. C. Packham, O. Velev and J. O'M. Bockris, p. 3. Manuscript submitted to J. Electrochem. Soc.
14. K. L. Wolf, N. J. C. Packham, D. L. Lawson, J. Shoemaker, F. Cheng and J. C. Wass, Manuscript submitted to J. Fusion Energy.
15. D. Albolgi, R. Ballinger, V. Commoroto, X. Chen, R. Crooks, C. Fiore, M. Gaudreau, I. Hwang, C. K. Li, P. Linsay, S. Luekhardt, R. R. Parker, R. Petrasso, M. Schoh, K. Wenzel and M. Wrighton Manuscript submitted to the Journal of Fusion Energy.
16. P. Clark Souers, Hydrogen Properties for Fusion, Energy, University of California, Berkely 1986.
17. P. L. Hagelstein, Proc. of the Cold Fusion Workshop, J. Fusion Energy, in press.
18. J. Rafelski, M. Gaide, D. Harley and S. E. Jones, unpublished results.
19. B. V. Deryagin, V. A. Klyuev, A. G. Lipson and Yu. T. Toporov, Kolloiidnyi Zhurnal, 48, 12 (1986).

Table 1: Cell parameters for Tritium measurements

Cell	Electrode size d x 1 (cm x cm)	Supplier	Pretreatment	Anode	Current (mA/cm^2)
1	0.4 x 6	JM[a]	oxid. of H_{abs}	Pt	5-400
2	0.2 x 10	E[b]	"	Pt	60-120
3	0.1 x 5	JM	"	Ni	10-120
4	0.2 x 5	E	"	Ni	10-120
5	0.1 x 5	JM	Annealing	Ni	10-120
6	0.2 x 5	E	"	Ni	10-120
7	0.2 x 10	E	"	Pt	10-120

[a] - JM refers to Johnson Matthey.
[b] - E refers to Engelhard.

Table 2 : Tritium Measurements

Cell	Days	ACR[a] (cpm)	NCR[b] (cpm)	$\dfrac{NCR^{sample}}{NCR^{D_2O}}$	DPM/ml[c]
1	42	21.13	5.13	1.6	44
	48	20.72	16.72	1.5	148
	58	35.08	19.08	6.5	170
	68	107.63±1.20	85.99±0.99	24.6±8.3	766
gas phase	68	42.66±2.32	24.06±0.93	8.3±2.3	114
	75	34.05	18.05	6	160
gas phase	75	20.93	4.93	1.6	44
2	25	209.27±0.80	193.80	6.2	1730
	45	120.06±0.49	103.06	4.1	920
3	26	159.14±1.83	143.24±1.88	49.4±13.8	1278
gas phase	26	26.53±0.86	9.63±0.96	3.3±0.9	85
	36	39.14±1.95	22.73±1.97	14.2	202
4	26	91.58±1.58	75.68±1.64	26.1±7.3	675
	36	36.94±0.54	20.53±0.60	12.8	183
5	26	58.11±0.27	42.21±0.51	14.6±4.1	376
	36	40.24±0.34	23.83±0.43	14.8	212
	76[d]	37.03±0.40	19.63	9.67	87
gas phase	76[d]	29.00±0.40	11.60±0.71	5.71±1.94	51
6	26	80.54±0.48	64.64±0.64	22.3±6.2	577
gas phase	26	39.40±0.86	23.50±0.96	8.1±2.3	209
	36	25.35±0.37	8.94±0.46	5.5	79
gas phase	56[d]	33.88±0.55	16.48±0.81	8.12±2.75	73
	76[d]	35.94±0.55	16.48±0.81	9.13±3.09	82
gas phase	76[d]	26.62±0.38	9.22±0.70	4.54±1.56	41
7	16	22.21±0.49	6.31±0.65	2.18±0.65	56
	36	20.93±0.86	4.52±0.63	2.8	40
	76[d]	21.76±0.86	4.36±1.04	2.15±0.88	19

[a] ACR - average (4 replicates) count rate per 0.5 ml.
[b] NCR - net count rate per 0.5 ml.
[c] DPM - disintegrations per minute.
[d] Sample size - 1 ml.
   Typical background count rate - 16 cpm.
   ACR(Norell D_2O) - -46 cpm; ACR(Isotech D_2O) - -19cpm.

TABLE 3

Summary of the Calculated Amount of the D

Loaded in Pd[a] at Different Overpotentials

η(volts)	$Q_{discharge}$(C)	moles D
-0.30	106.5	1.1×10^{-3}
-0.35	170.0	1.1×10^{-3}
-0.40	111.7	1.2×10^{-3}

[a] Mass of Pd electrode was 0.12 g before and after the experiment. This corresponds to 1.1×10^3 moles Pd.

TABLE 4

Nuclear Fusion Reactions

Reaction	Equation
A	$D + D \rightarrow n$ [2.45 MeV] + ^{3}He [0.82 MeV]
B	$D + D \rightarrow H$ [3.02 MeV + T [1.01 MeV]
C	$D + D \rightarrow \gamma$ [23.0 MeV] + ^{4}He [0.08 MeV]
D	$D + {}^6$Li $\rightarrow n$ [2.96 MeV] + ^{7}Be [0.43 MeV]
E	$D + {}^6$Li $\rightarrow {}^4$He [11.2 MeV] + ^{4}He [11.2 MeV]
F	$D + {}^6$Li $\rightarrow H$ [4.39 MeV] + ^{7}Li [0.63 MeV]
G	$D + {}^7$Li $\rightarrow n$ [13.36 MeV] + ^{8}Be [1.67 MeV] $\rightarrow n$ [13.36 MeV] + ^{4}He [0.85 MeV] + ^{4}He [0.85 MeV]
H	$D + {}^7$Li $\rightarrow \gamma$ [16.7 MeV] + ^{9}Be [0.02 MeV]
I	$D + {}^7$Li $\rightarrow p$ + ^{8}Li (endoergic, -1.01 MeV) $\rightarrow \rightarrow p$ + ^{4}He [8.05 MeV] + ^{4}He (8.05 MeV]
J	$D + {}^7$Li $\rightarrow T$ + ^{6}Li (endoergic, -1.81 MeV)
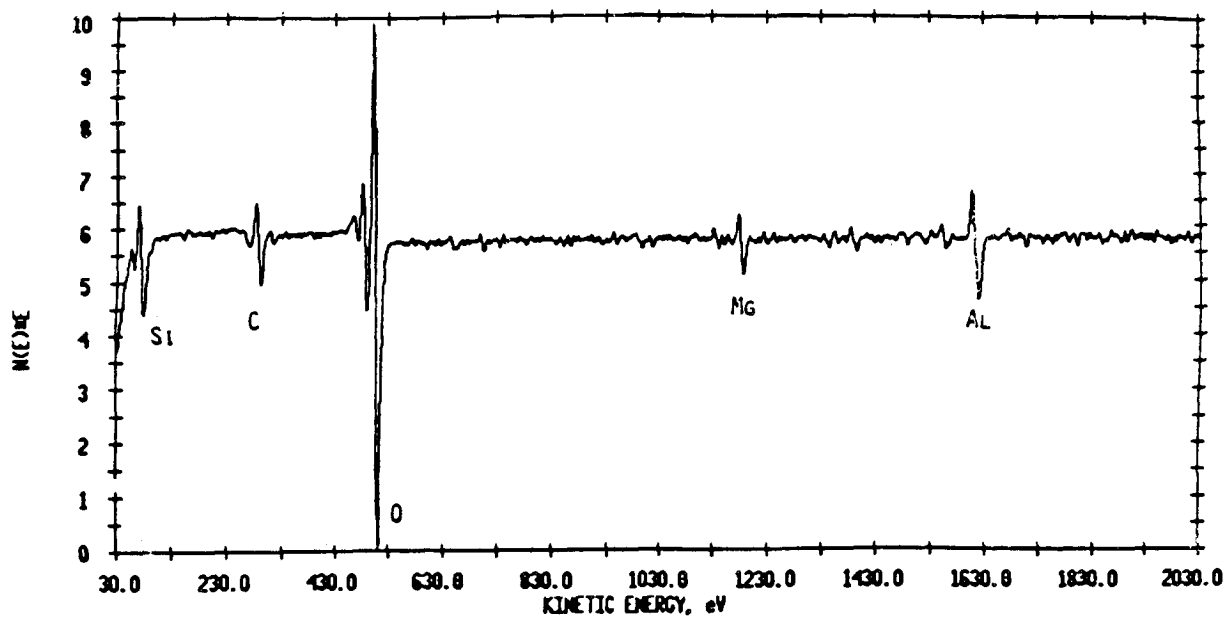
Fig. 1. Auger electron spectrum of Pd cathode (Johnson Matthey, "Fusion rod") used in a glass cell for the electrolysis of D_2O in 0.1 $\underline{M}$ LiOD. As introduced into the spectrometer with no sputtering of the surface. Incident beam energy = 10 KeV. Sampled area 25 x 25 μm^2.

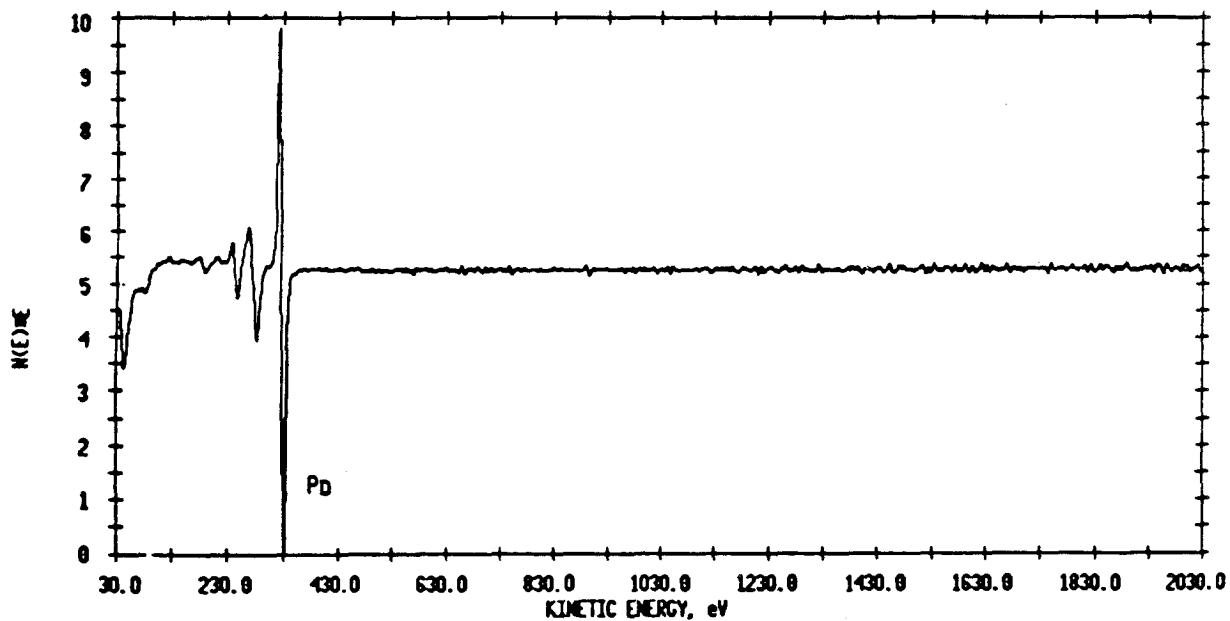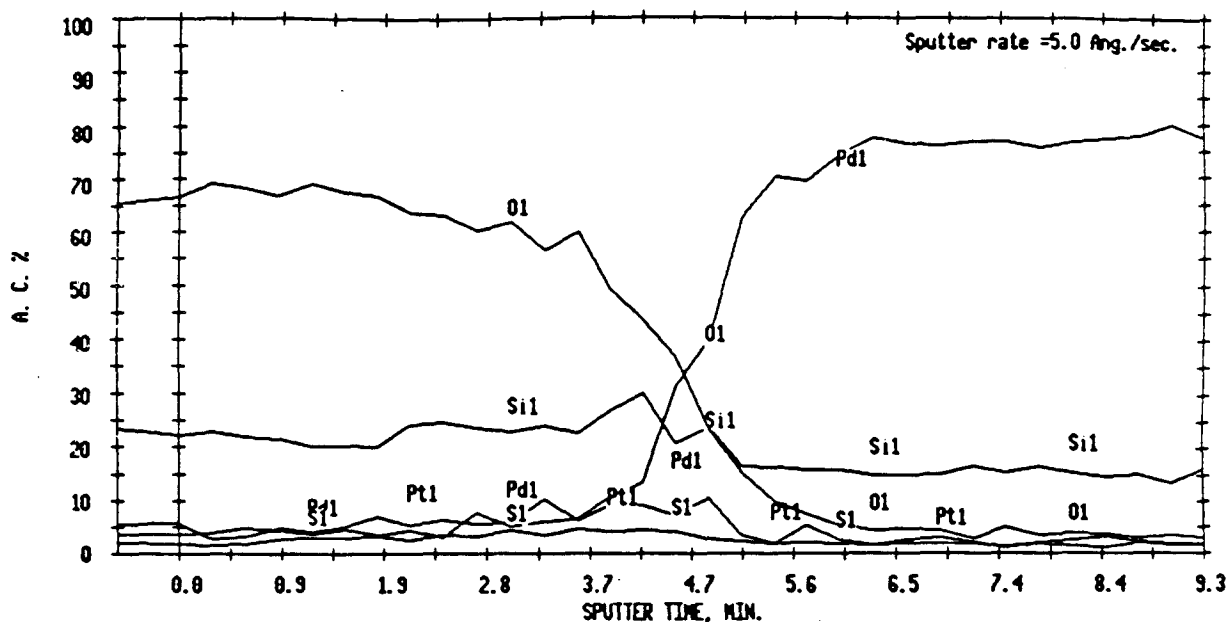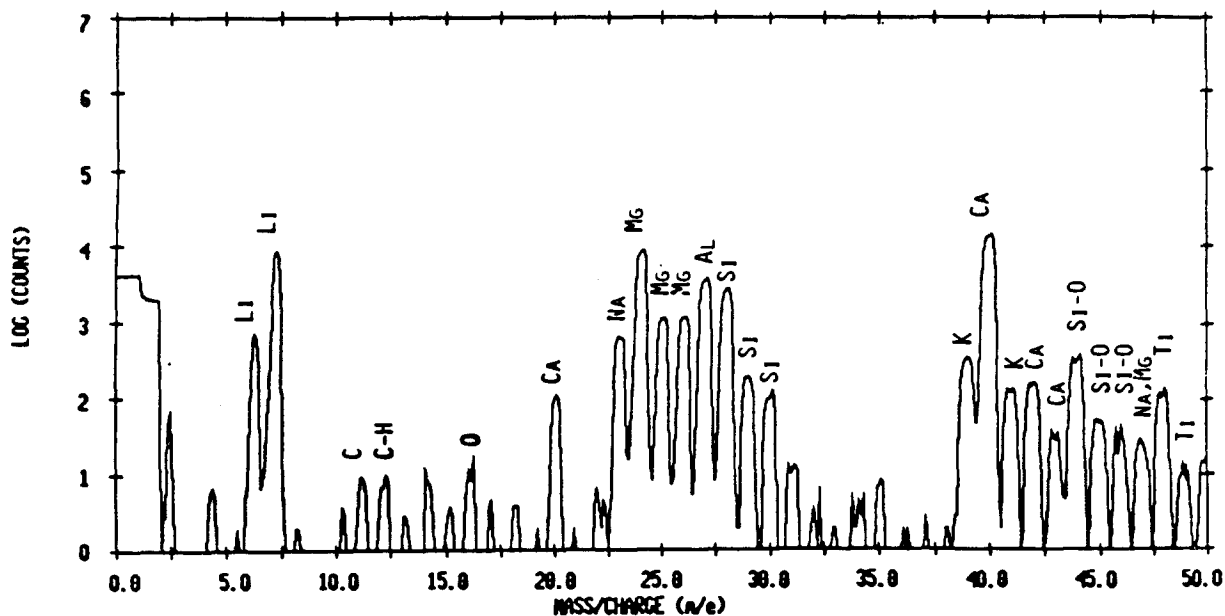Fig. 2. Auger electron spectrum of Pd cathode (Johnson Matthey, "Fusion rod") used in a glass cell for the electrolysis of D_2O in 0.1 $\underline{M}$ LiOD. After a ~3000 Å layer was sputtered off the original surface. Incident beam energy = 10 KeV. Sampled area 25 x 25 μm^2.

Fig. 3. Auger electron spectrum depth profile of Pd cathode (Johnson Matthey, "Fusion rod") used in a glass cell for the electrolysis of D_2O in 0.1 M LiOD. Sputter rate = ~5 Å/sec. Incident beam energy = 10 KeV. Sampled area 25 x 25 μm^2.

Fig. 4. Positive Secondary ion mass spectrum survey of the Pd cathode (Johnson Matthey, "Fusion rod") used in a glass cell for the electrolysis of D_2O in 0.1 M LiOD. Incident beam energy = ~3 KeV. Ion current = ~4 μA. Sampled area 1 x 1 mm^2.
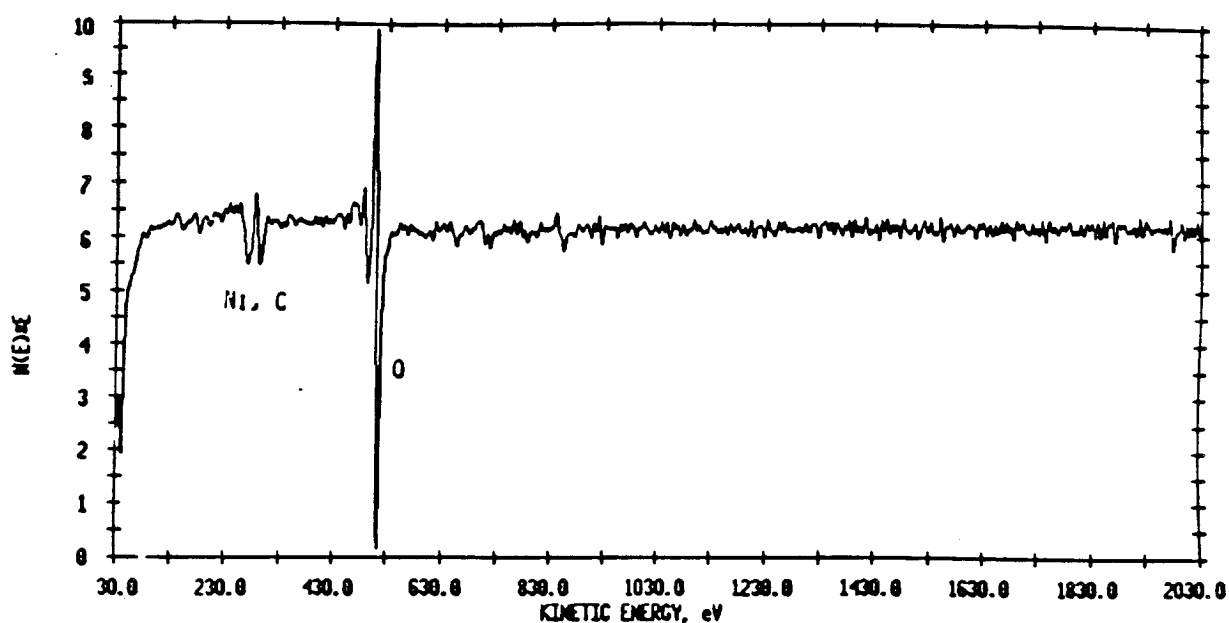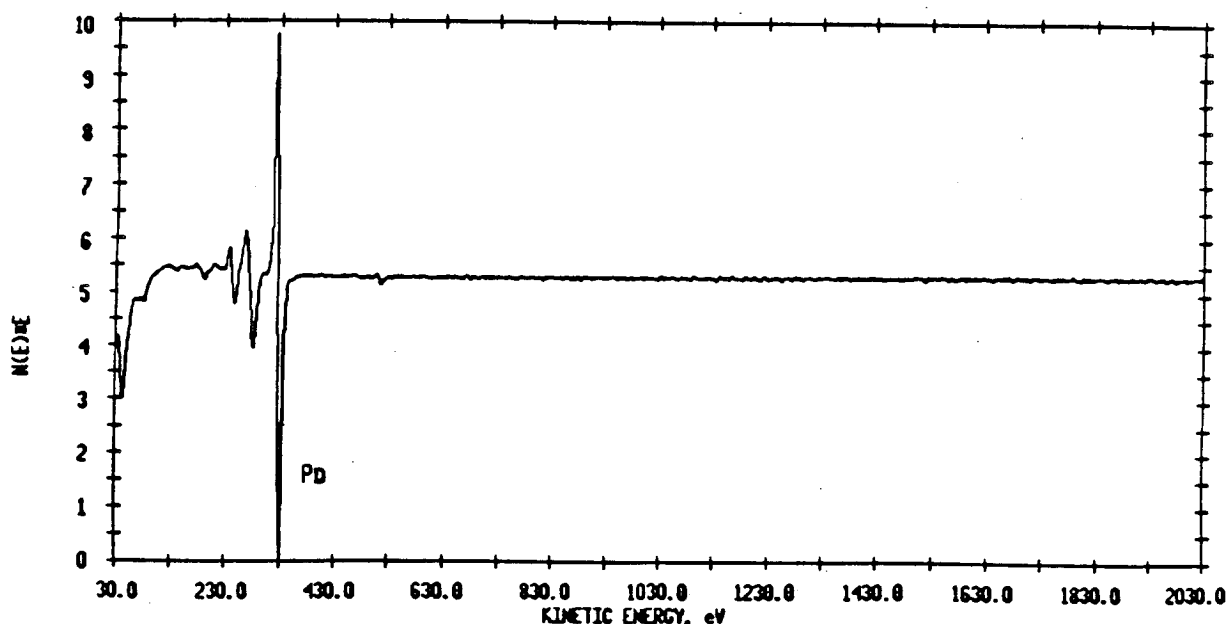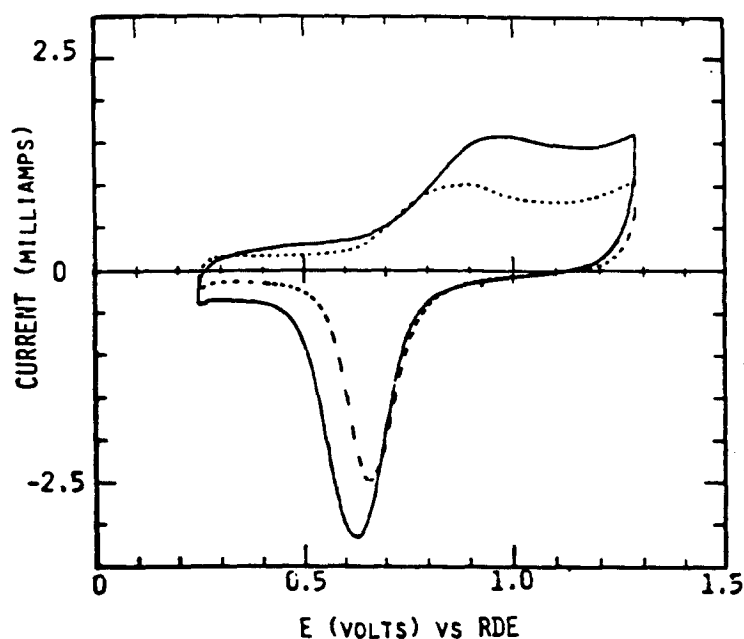
20-15

Fig. 5. Auger electron spectrum of Pd cathode (Englehard) used in a Nickel
cell for the electrolysis of D_2O in 0.1 $\underline{M}$ LiOD. As introduced into
the spectrometer with no sputtering of the surface. Incident beam
energy − 10 KeV. Sampled area 25 x 25 μm^2.

Fig. 6. Auger electron spectrum of Pd cathode (Englehard) used in a Nickel
cell for the electrolysis of D_2O in 0.1 $\underline{M}$ LiOD. After 10,500 Å
thick layer was removed from the original surface. Incident beam
energy − 10 KeV. Sampled area 25 x 25 μm^2.
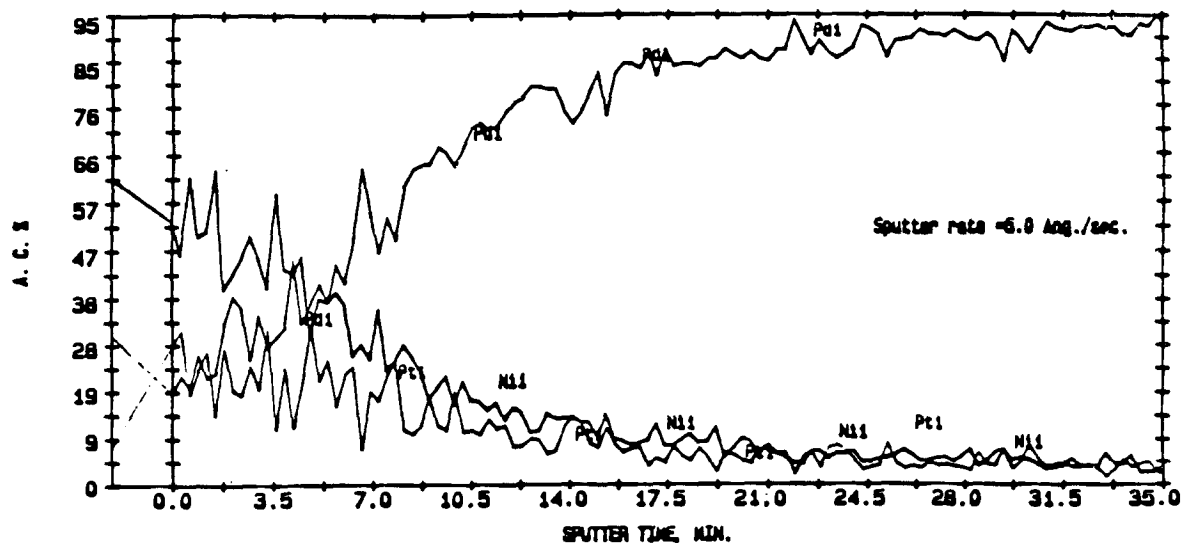
Fig. 7. Auger electron spectroscopy depth profile of Pd cathode (Englehard) used in a Nickel cell for the electrolysis of D_2O in 0.1 $\underline{M}$ LiOD. Sputter rate - 5 Å/sec. Incident beam energy - 10 KeV. Sampled area 25 x 25 μm^2.

Fig. 8. Cyclic voltammograms of Palladium wire (d - 0.03 cm) in D_2O with 0.1 $\underline{M}$ LiOD under a N_2 atmosphere. Dashed line is the steady state voltammogram. Solid line is the voltammogram recorded after charging the Pd with D at -0.4V for 24 hours, followed by discharging the D at +0.83 V for 60 minutes. Scan Rate - 100 mV/s. Electrode area - 1.86 cm^2. Counter electrode: Pd.
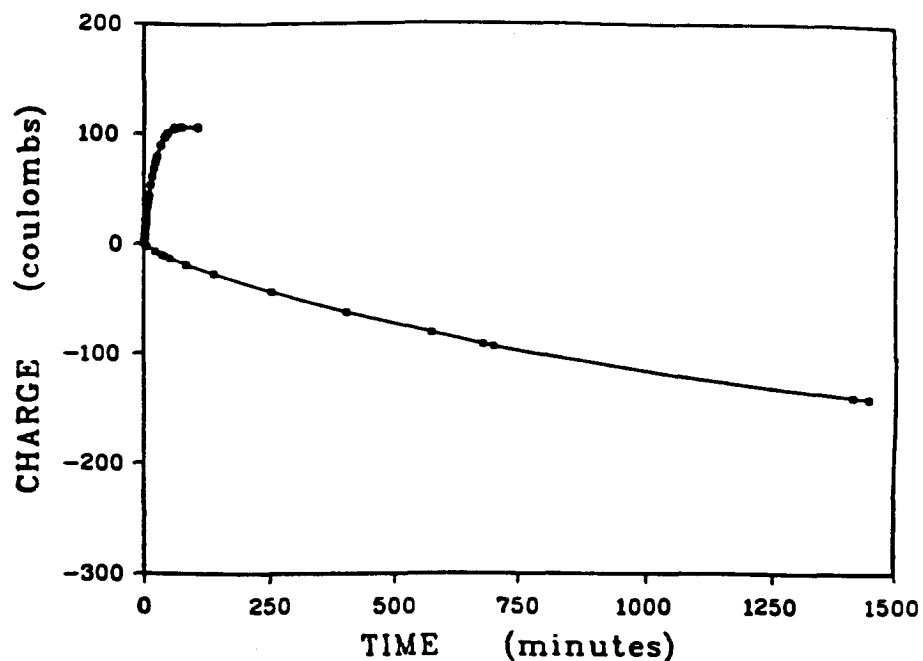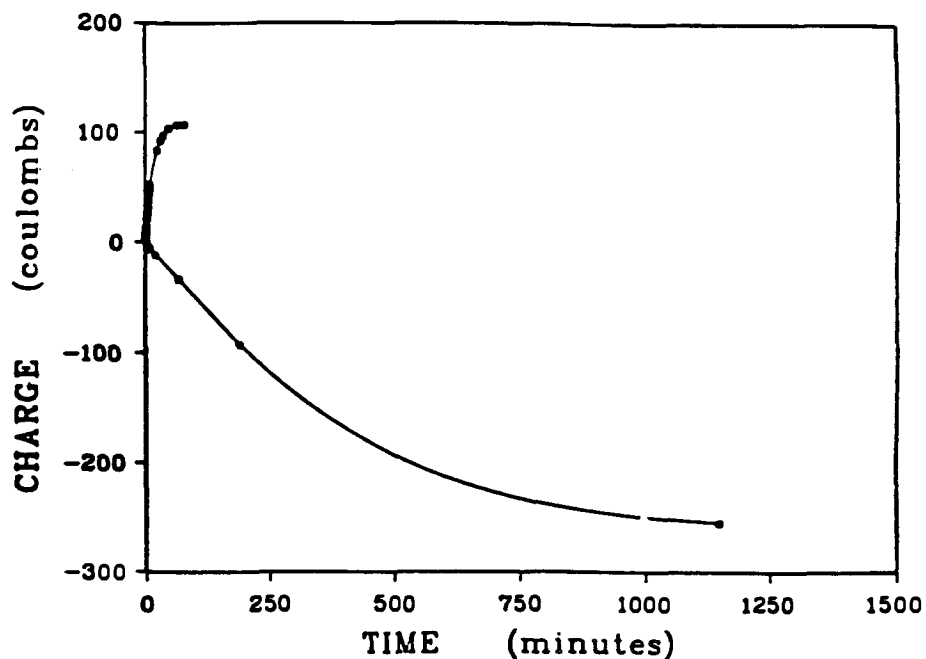
Fig. 9. Chronocoulometry curve for the charging (negative charge) and discharging (positive charge) of D into palladium wire (d=0.03 cm). Electrode area = 1.86 cm^2. Electrode mass = 0.12 grams. Electrolyte: 0.1 $\underline{M}$ LiOD in D_2O. Charging potential = -0.3 V vs RDE. Discharging potential = +0.83 V vs RDE.

Fig. 10. Chronocoulometry curve for the charging (negative charge) and discharging (positive charge) of D into palladium wire (d=0.03 cm). Electrode area = 1.86 cm^2. Electrode mass = 0.12 grams. Electrolyte: 0.1 $\underline{M}$ LiOD in D_2O. Charging potential = -0.35 V vs RDE. Discharging potential = +0.83 V vs RDE.

20-18

DISCUSSION (YEAGER)

Menlove: How long was the experiment run before excess heat was observed?

Yeager: 50-60 hours. In another case, 1 percent excess was seen at 306 hours, and 5 percent for a period following that time.

Miley: If tritium is being produced along with the anomalous heat, what percentage of the heat would be attributed to tritium?

Yeager: Only a very small fraction, since the amount of tritium which we have detected is much less than that reported by Dr. Bockris and his group.

Section 21

REMARKS MADE AT THE NSF/EPRI WORKSHOP

J.W. Bray

General Electric Research Development Center

REMARKS MADE AT THE NSF/EPRI WORKSHOP
(J.W. BRAY)

We have seen no positive results in our own work. All of our results have been negative for calorimetry. We have tried. All I want to do is make a point about differential calorimetry that we think is important.

Of course, in any cell, one can write an equation like this.

$$MC_p \frac{dTc}{dt} = IV + Q_h + Q_{xs} - Q_L - IE$$

The thermal mass of the cell MC_p times the time derivative of the cell temperature dTc/dt is equal to a number of terms; basically, the input power minus the output power. Not surprisingly, the input power is IV where I is the cell current and V is the cell voltage. If you're putting any calibration power Q_h into the cell, that is also an input. If you are getting any excess heat Q_{xs} produced by the cell through some other unknown process within the cell, that is also an input.

The outputs are of course the loss of heat Q_L from the cell and a voltage term EI which represents other losses, such as losses which come from evaporation of the fluids in the cell. If it is an open cell, the major (non-heat) losses come from the gases which are being electrolyzed, so E contains a voltage equivalent for that. That is the E = 1.53 or 1.54 volts you have seen, of course.

The loss term Q_L also is fairly obvious. It has been talked about by a number of people already. It can have a conductive component and a radiative component generally. Every cell will have these components, perhaps dominated by one or the other. The radiative term may be very small in a particular case or it may be larger in any given circumstance.

Now, when T_c is constant and there is no excess heat, the loss term Q_L must be equal to the power IV being put into the cell plus any heater power Q_h used in

the calibration minus once again those loss terms IE that I've already
described due to evaporation or electrolysis gases leaving the cell.

Now, one can take data from the operation of a real cell and use it to plot
Q_L in these two possible forms (conduction plus radiation, and input minus
output), one form on the x axis and the other on the y axis. The slope and
intercept of such a plot will give the relative coefficients of conduction and
radiation loss for the cell.

So far, it is pretty elementary. When one is doing differential calorimetry
(by this, I mean any circumstance in which one is adding to an operating cell
an incremental heater power), you've got a cell which is operating under some
current I and are adding to it some additional heater power Q_h in order to get
a calibration point.

When one turns on the heater, going from zero to some power Q_h, the point to
remember is that one can affect <u>a number of variables of the cell</u>. You do not
just affect the temperature of the cell T_c by turning on the heater.

You can possibly affect the excess heat if you have any in a cell. We have no
knowledge, any of us, whether or not we would affect that. We don't know what
it is. We don't know what it is caused by. Presumably, it could change due
to the fact that one is causing the heater to go on. God forbid that this
would happen, but it is uncontrolled and unknown.

You will affect the products leaving the cell which are saturated by heavy
water vapor; the saturation will presumably increase due to the fact that you
have added a heater pulse to the cell and increased the temperature of the
cell slightly. This increase of T_c will also slightly change the equivalent
voltage for electrolysis products coming out of the cell. Finally and perhaps
most importantly, the change of T_c will change the voltage of the cell V (in a
constant-current mode).

Now the point is that the changes do occur. The question is: How big are
they in any given circumstance?

And the only way you can know that is by putting in numbers from the cell that you are working with. That is the bottom line.

If you put in numbers from cells that we have worked with and that we have looked at, we find that some of these correction terms are negligible. For instance, changes caused by Q_h on the evaporation products and on the electrolysis voltage itself usually are in the 1 percent range or so until you get up to temperatures which are fairly high compared to the boiling point of water. We usually find that the correction is quite negligible below about 60 degrees centigrade, for instance.

However, we find that the change of V is not negligible. The voltage of the cell is changed when one puts in a heater pulse because one has changed the temperature of the cell and therefore, inter alia, the cell electrolyte resistivity.

I noted with pleasure that Bob Huggins pointed this out in his talk. He was using a situation in which he was running cells at constant voltage. When he turned on his heater for the differential calibration, he showed you that the current of the cell increased under a constant voltage. This was because he increased the temperature of the cell and that reduced the resistivity of the electrolyte. So, in order to maintain constant voltage with this reduced resistance, the mechanisms that control the cell cause the current of the cell to increase, and the power into the cell IV increased. If you happen to be running a constant current cell, the opposite will happen. There, once again, the resistance of the cell will be increased. But, in that case, you will find that the constant current source will cause the voltage to be reduced because the resistance of the cell decreases.

This effect is not negligible. We have found, for typical operations, a 15 percent correction from this term not hard to get at all. How large it is depends on how large I is for the cell at the time you're doing the calibration, so it varies. Of course, if I is zero, there is no effect from this term. But, if I is large, you could get a very large effect from this term.

The point is that it is important to take it into account, and the correction is in the opposite directions, depending on whether you are running at constant current or at constant voltage.

Now, if you are taking just one data point, of course, you cannot satisfy conditions needed to derive both the radiative and conductive loss components for a cell. If you have both conduction and radiation as important terms for your cell, there is no way with one measurement that you can do it. You need at least two.

In a circumstance where only one term is used, it is most conservative to use just the radiative term. If you have a strong radiative loss component to your cell, it has the strongest variation with T_c and therefore can lead to the larger estimates of Q_L. There is some danger in doing this, however, that one may underestimate the errors (variability) of the cell, since the neglected conductive term will have some nonzero error associated with it.

This is really all the message I wanted to give you. It is important when one is doing differential calorimetry to do it correctly, and if one does it correctly, then one can get correct results.

DISCUSSION (BRAY)

Chu: To see zero excess heat, did you make all the differential calorimeter corrections which you mentioned?

Bray: Yes, when we did not observe false excess heat.

Bard: At what false excess heat level?

Bray: It is not difficult to see a 15 percent false excess. It depends on the current flowing through the cell when the calibration is performed.

Fleischmann: This morning, Dr. Pons showed that following our data analysis one can predict precisely the effect of the calibration heat pulse on the calorimeter. I contend that if your method of analysis is used, the measured heat output will in fact be low.

Bray: I disagree.

Fleischmann: In our type of calorimetry, which has its weaknesses, progressive electrolysis takes place, leading to a sloping baseline. Your analysis is the same as ours, but you do not take the baseline slope into account.

Bard: I agree. If you have a situation where the cell constant is changing as a function of time, where the electrolyte level, hence the radiation area, is changing, then the relative proportions of conduction and radiation will vary with time.

Appleby: Instead of using this calibration method, why not use substitutional calorimetry?

Fleischmann: There is a good argument for changing to that technique.

Chexal: If you have enough data points with electrolysis and the heater operating at the same time, and the calibration is carried out correctly, there is no reason why the sloping baseline terms are not already included in the calibration curve.

Bray: I agree, if indeed you perform the calibration correctly.

Bard: Bockris's calorimetric technique is different. He calibrates with the heater to obtain an integral heat transfer coefficient before electrolysis begins. However, I think that a critical point being made here, Dr. Fleischmann, is the validity of the single-point heat calibration, forced back to the origin on the time axis.

Fleischmann: I will make our data and calculations in our model available to anyone who asks for them. We know the values which we estimate, and we know that our estimate is low, as I pointed out yesterday.

Huggins: One can avoid this question by the use of a recombination cell, so that the baseline is time-invariant. Similarly, a constant-power input, rather than a constant-current system, will simplify matters. We are now operating some of our cells in this way.

Appleby: Substitutional calorimetry using a built-in internal heater, which always operates, and whose output is controlled electronically to yield a constant-power output (rather than input) is another way to avoid these problems.

Bray: One can also lower the bath temperature and add enough internal heater power to maintain the cell at constant temperature. Using this method, one avoids the complications to which I referred.

Section 22

INITIAL CALORIMETRY EXPERIMENTS IN THE PHYSICS DIVISION--ORNL

D.P. Hutchinson, C.A. Bennett, and R.K. Richards

ORNL Physics Division

J. Bullock IV and G.L. Powell

Y-12 Development Division

INITIAL CALORIMETRY EXPERIMENTS IN THE PHYSICS DIVISION–ORNL

D. P. Hutchinson, C. A. Bennett, and R. K. Richards
ORNL Physics Division

J. Bullock IV and G. L. Powell
Y-12 Development Division

ABSTRACT

Four calorimetry experiments were performed with palladium cathode electrolysis cells to investigate the possibility of cold fusion heat production based on the reported results of Fleischmann and Pons. Two of the cells contained 6.35-mm-diam × 10-cm-long palladium cathodes in a 0.2-M ^{6}LiOD electrolyte; one cell contained a similar cathode in a 0.1-M ^{6}LiOD electrolyte solution; and one cell used a cast 1.27-cm-diam × 10-cm long palladium rod in a 0.2-M electrolyte. All four cells were constructed with platinum wire anodes. One of the cells exhibited an apparent 2-3 W power excess for a period of approximately 300 hours of a total operating time of 1800 hours; each of the remaining cells remained in power balance for the 1800 hour period.

INTRODUCTION

Immediately following the announcement by Fleischmann and Pons[1] at the University of Utah of the discovery of cold fusion in an electrolysis cell containing a palladium cathode, several experiments were begun at ORNL to investigate this claim. A number of electrolysis cells were constructed using palladium foil cathodes and platinum gauze anodes in an attempt to measure cold fusion produced neutrons. A neutron counter was assembled using NE213 scintillator detectors, which employed pulse shape discrimination to reduce the effective gamma ray background. The background count rate of this detector was approximately 90 events per hour. Another detector located near the primary system was used to monitor any changes in the background level. No neutrons above the background rate were detected during these initial experiments. We then focused our attention on the report of excess heat result also made by the University of Utah group.

EXPERIMENTAL APPARATUS

Four calorimetry cells were constructed with an electrolyte volume of 300 cc in a 54-mm-o.d. quartz envelope. A diagram of the calorimetry cells is shown in Fig. 1. Each cell contained a Teflon plug in the top of the container with a number of penetrations for electrical connections, heavy water refilling, and sampling. Two 6.35-mm Teflon rods projected through the top plug to support the palladium cathode rod in the center of the envelope. The Teflon rods were spring loaded to allow for expansion of the palladium electrode during charging with deuterium. The anode was helically wound from platinum wire on the inside of a perforated quartz tube. The anode helix was wound on a mandrel and allowed to spring against the inside of the quartz tube for support. No internal recombiner was used to catalyze the recombination of the gases produced by electrolysis back into heavy water. The D_2 and O_2 gases were allowed to escape through a vent hole in the top Teflon plug. The quartz cells were placed inside Teflon cylinders that in turn were immersed in a temperature controlled water bath. A 2.5-mm gap between the quartz and the Teflon cylinder was filled with D_2O and contained a platinum resistance temperature detector (RTD). Another platinum RTD was placed in the water bath adjacent to the Teflon socket. A cell containing a resistance heater similar in size to the palladium cathode and identical in construction to the actual cells was placed into each Teflon socket, prior to activation of the cells, for calibration. Varying amounts of electrical power were applied to the resistance heater, and the temperature difference across the Teflon was noted for each setting. Calibration curves for three of the cells are shown in Fig. 2. The calibration data were fitted with a fourth order polynomial for use with the cell calorimetry data. The second order term was very small and the third and fourth order terms nearly zero. The cells were periodically re-calibrated during the course of the experiments, as well as whenever the bath temperature was altered. A shielded neutron counting chamber was prepared next to the constant temperature baths to permit neutron counting of the cells during operation without interruption of the electrolysis.
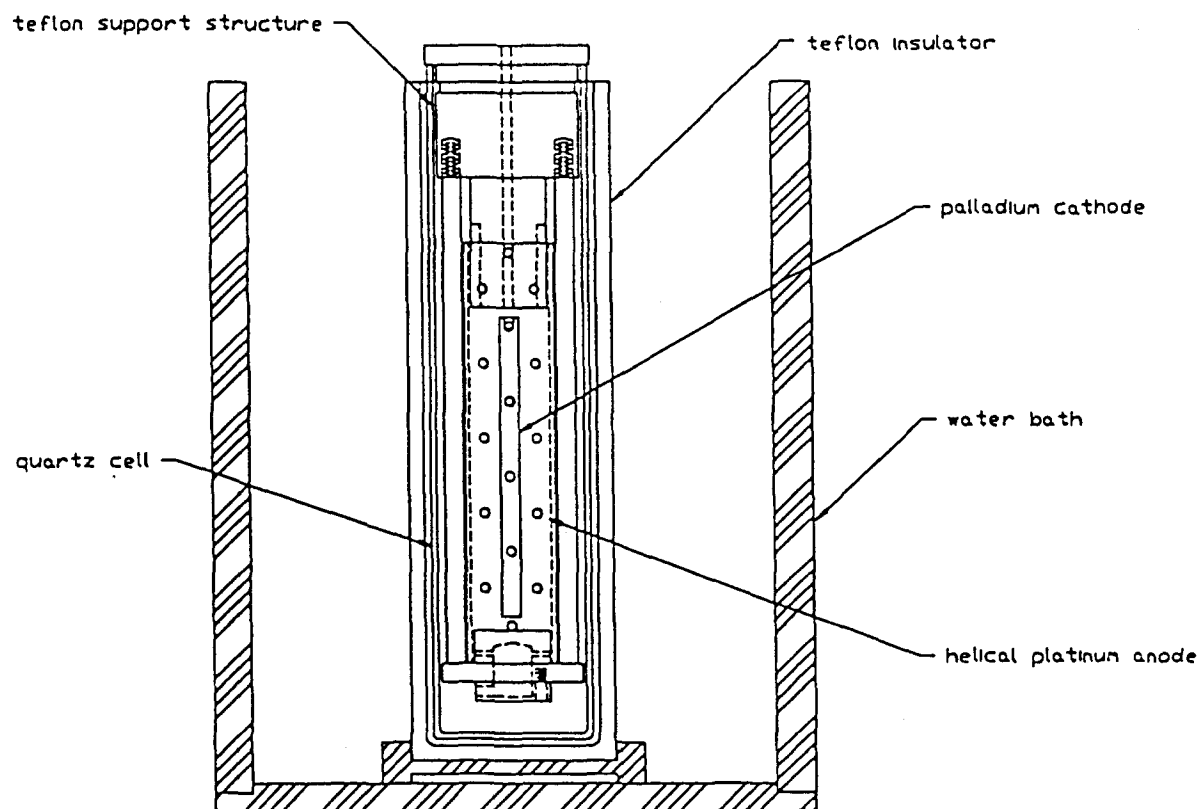
teflon support structure

teflon insulator

palladium cathode

water bath

quartz cell

helical platinum anode
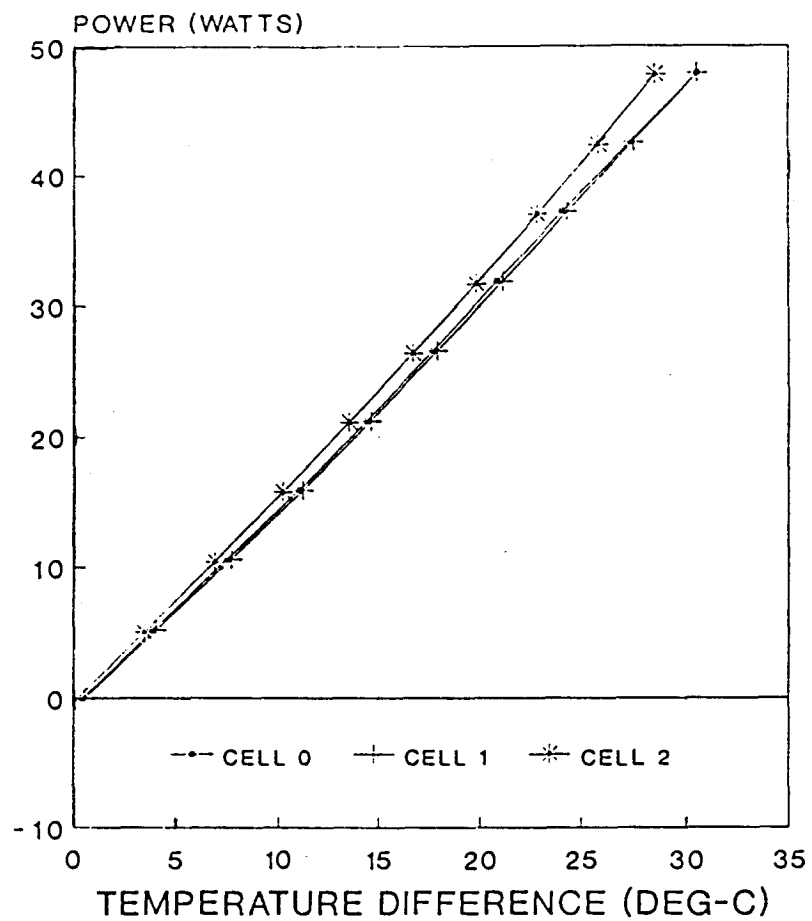
Fig. 1. Diagram of the design of the calorimetry cells.

Fig. 2. Calibration curves for three of the calorimetry cells.

ELECTRODE PREPARATION

Two of the cells contained 6.35-mm-diam × 10-cm-long annealed palladium cathodes, one of which was pre-charged in D_2 gas to a stoichiometry of 0.6, in a 0.2-M ^{6}LiOD electrolyte; one cell contained a pre-charged annealed cathode in a 0.1-M ^{6}LiOD electrolyte solution; and one cell used a cast 1.27-cm-diam × 10-cm-long palladium rod in a 0.2-M electrolyte. Annealing was performed by heating the rods to a temperature of 900°C for 4 hours in vacuum. The cast 1.27-cm-diam rod and the 6.35-mm-diam non-pre-charged rod were baked at 200°C in vacuum for 24 hours to remove any residual protium before being placed in operation. The experimental parameters for the palladium cathodes are summarized in Table 1. The three 6.35-mm-o.d. rods were purchased from Johnson-Matthey. The cast rod was fabricated from stocks of palladium obtained at ORNL.

RESULTS

The cells were operated at an initial current density of 50 mA/cm^2 for 48 hours and then at a current density of 250 mA/cm^2 for over 1800 hours. Referring to the cell numbering from Table 1, cells #1,#2, and #3 have remained in power balance within an experimental uncertainty of ±1 W for the duration of the experiments. However, cell #0 exhibited an apparent excess power level of approximately 3 W for a 300 hour period beginning 180 hours after the beginning of the experiment. This imbalance was approximately 10% of the input power. Our calorimetry cells did not use an internal catalyst to promote the recombination of the electrolyzed gases back into heavy water. D_2O was added to the cells every twelve hours to replace the water depleted by electrolysis. By carefully recording the water usage rate, we were able to determine that no recombination was occurring in the cells.

The power balance for our cells was determined from the equation

$$P_{imbalance} = \text{heat output} + \text{electrolysis} - \text{electrical input} .$$

The heat output of the cells was measured by the calibrated platinum RTDs. The electrolysis term was determined by measuring the make-up water for the cells assuming the exhaust gases were 100% humidified. The electrical input was determined by

Table 1. Experimental parameters

Cell No.	Electrode Configuration	Electrolyte Concentration	Electrode Conditioning
0	6.35 mm diam	0.2 M LiOD	Annealed
1	6.35 mm diam	0.2 M LiOD	Annealed/ pre-charged/ arsenic added
2	6.35 mm diam	0.1 M LiOD	Annealed/ pre-charged
3	12.7 mm diam	0.2 M LiOD	Cast

Note:
1. All rods were 100-mm long.
2. The 12.7-mm-diam rod was dropped cast in a chilled copper mold. The rod was x-rayed to identify any possible voids.
3. All rods were heated in vacuum to remove residual protium.
4. Current density = 250 mA/cm^2.

monitoring the voltage and current going to the cells. The electrolysis cells were driven by computer-controlled constant current sources and the voltages across the electrodes were monitored by a digital-to-analog converter in the control computer. The constant current power supplies were calibrated prior to the experiment. At an operating current density of 250 mA/cm^2, the total current to the 6.35-mm-diam rod cathodes was 5.03 amps. At this current, 1.88 grams of D$_2$O were electrolyzed per hour of operation, resulting in volumetric water usage rate of 1.702 cc/hour. Using the value of 70.41 kcal/mol for the heat of formation of heavy water, this electrolysis rate results in 7.635 W of power consumption. Assuming that the exhaust gases have a relative humidity of 100%, the total water consumption rate we calculate is 1.88 cc/hour corresponding to a total electrolysis power level of 7.77 W, including power due to evaporation. The consumption of D$_2$O was monitored over the entire course of the experiment. Figure 3 shows a graph of the measured replenishment rate for the first 21 days of the experiment. The open circles are the measured values and the straight line is a straight line fit to the data points. The fitted value of 1.87 cc/hour is in excellent agreement with the predicted value of 1.88 cc/hour. Using this result the heat balance equation becomes

$$P_{imbalance} = heat + 7.77 \ W - V_{cell} \times I_{cell} \ .$$

In addition to control of the power supplies and constant monitoring of the cell parameters, the control computer was programmed to sweep the cell current once each hour. The duration of the current sweep was 5 seconds. The slope of the I-V curve is the electrolyte resistance.[2] By multiplying the square of the cell current by this quantity, the ohmic power deposited in the electrolyte may be determined. Figure 4 contains a plot of the measured parameters of cell #0 for the first 600 hours of operation. The lower curve, represented by the dots, is the ohmic power, $I^2_{cell} \times R_{electrolyte}$, deposited in the electrolyte. The curve represented by the asterisks is the measured calorimeter power output determined by comparing the temperature difference across the Teflon with the calibration curve obtained with the electrical resistance heater. The curve represented by the x's is the electrical input power to the cell, $V_{cell} \times I_{cell}$. Finally, the curve represented by the (+) symbol is the sum of calorimeter plus the electrolysis power value of 7.77 W. During the initial 75 hours of the experiment, cell #0 exhibited a slight negative heat
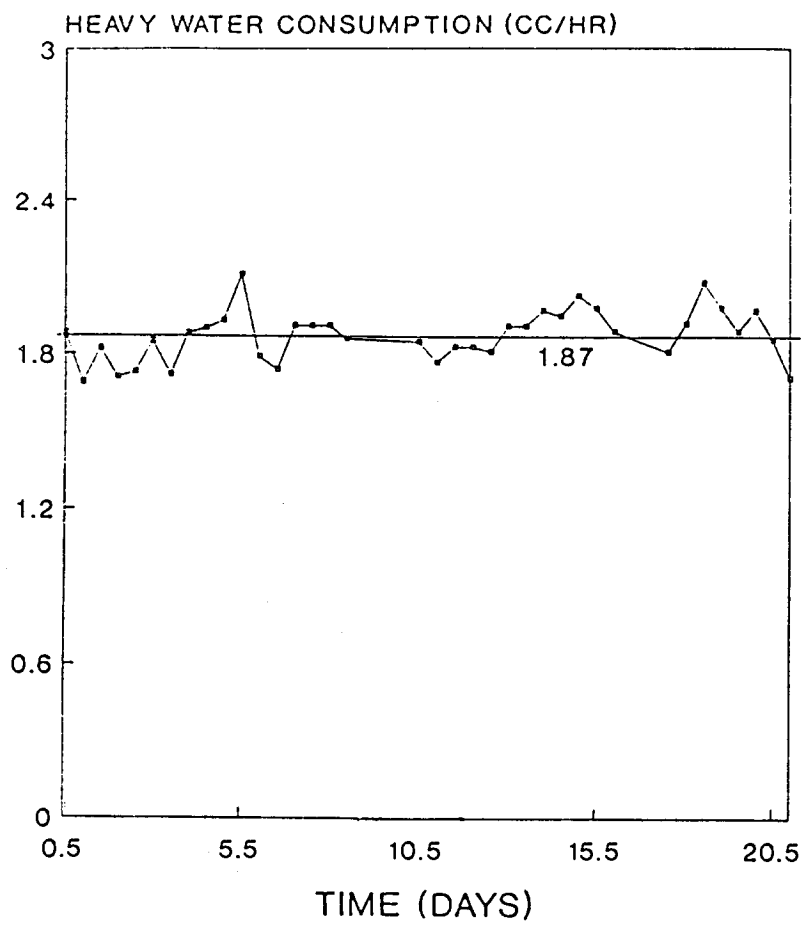
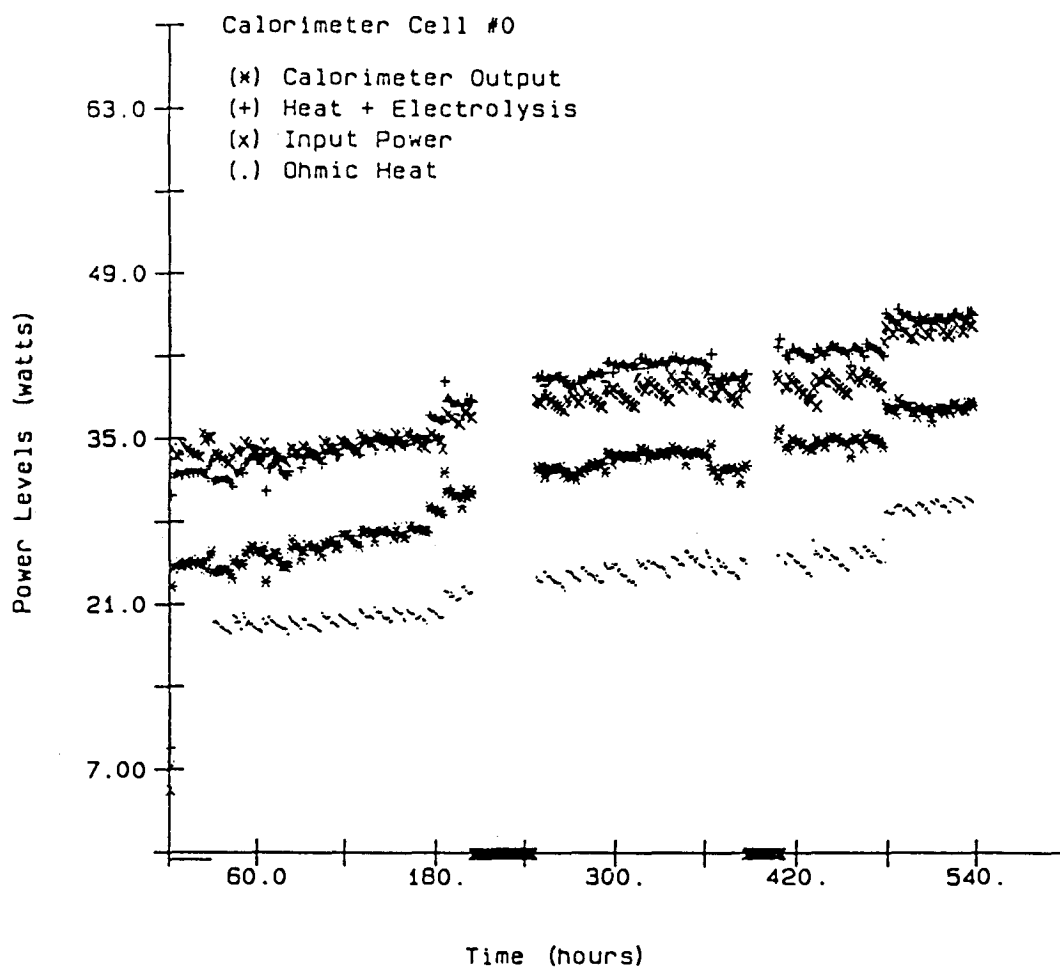Fig. 3. Heavy water consumption in cell #0 for the first 21 days of operation.

Fig. 4. The measured output parameters of cell #0.

balance. At a level of less than 2 W tapering to zero at approximately 75 hours, this indicates an energy storage of approximately 270 kJ. This far exceeds the hydride heat of formation value of approximately 3 kJ calculated for these rods. Cell #0 remained in balance until the 180 hour mark when a positive imbalance of 2 W was observed. Twelve hours after this apparent excess heat event began, the temperature of the water bath was inadvertently changed from an initial value of 18°C to 13°. The ohmic power increased at this point due to the increased electrolyte resistance at the lower temperature. The input power also increased with the increased electrolyte resistance because the cells were driven by constant current sources. The calorimeter output also increased with the lower temperature and maintained the 2 W excess. The sawtooth behavior, which is most evident on the input power and ohmic power curves, with a period of approximately 12 hours, occurred because of the changing level of liquid in the cell due to electrolysis and the periodic refilling twice a day. As the liquid level decreases, the heat transfer area changes and the electrolyte resistance decreases as the molality increases. Although the effect of these changes is not accurately known, we only use data taken at the peaks of the sawtooth, where we know the calibration is accurate, for evaluation. The gap in the data represents a period when the cell was removed from the calorimeter socket for 30 hours. During this period, the socket was re-calibrated at the lower temperature and the cell was placed in the neutron counter. All of the parameters of the cell were monitored during this time except heat output. We arbitrarily chose to display data taken only when the cell was in the socket. The imbalance increased slightly until the 370 hour mark when the temperature of the bath was deliberately raised to 18°C. The imbalance nearly disappeared but recovered and increased over the next 120 hours to slightly over 3 W. At approximately 480 hours the cell bath temperature was lowered to 5°C in an attempt to study the effect of temperature changes on the imbalance. The excess power disappeared at this point and repeated temperature and current cycling failed to reproduce the effect. The power balance for cell #0 for the first 25 days of operation is shown in Fig. 5. The data were averaged over a twelve hour period for this graph. We continued the experiment for a total period of 1800 hours with no recurrence of the excess heat observation. The other cells remained in accurate power balance during the entire
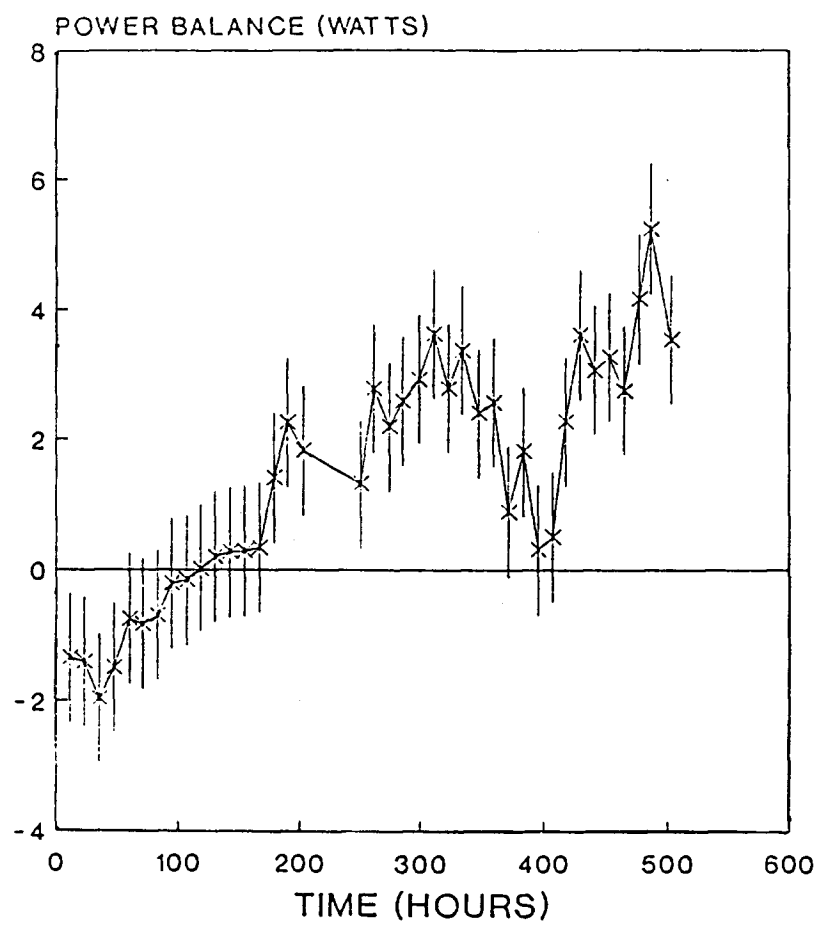
Fig. 5. Power balance plot for cell #0.

experimental period. During the observation of heat imbalance in cell #0, cells #0 and #1 were switched in their calorimeter sockets to verify that the apparatus was working properly. The power readings for each cell during this period were consistent with the calibrations for both cells, the measured imbalance in cell #0 remained irrespective of the calorimeter socket used.

ADDITIONAL MEASUREMENTS

Shortly after the power imbalance was discovered, cell #0 was removed from the calorimetry socket and placed in a shielded neutron counter containing a pair of NE213 scintillator detectors with pulse shape discrimination. The neutron emission level of the cell was determined to be less than 1×10^{-24} neutrons/sec/d-d pair, as set by the background level of the counting system. The tritium level of the initial electrolyte fill of D_2O was measured to be 1.0×10^6 dpm/cc and increased to a level of 1.3×10^6 dpm/cc 50 hours after the beginning of the apparent excess power production. The accuracy of the tritium measurement was at best 10%; because of this uncertainty we draw no conclusions from our measurement.

CONCLUSIONS

During a period of approximately 300 hours, one cell of four exhibited a positive power imbalance of 2-3 W after a short period of negative imbalance. The mechanism responsible for this behavior has not been identified; it appears to be a transitory effect with some dependence on temperature.

REFERENCES

1. Martin Fleischmann and Stanley Pons, J. Electroanal. Chem. <u>261</u>, 301-8 (1989).

2. J. S. Bullock, IV, G. L. Powell, and D. P. Hutchinson, <u>Electrochemical Factors in Cold Fusion Experiments</u>, TM Y/DZ-490, Visuals prepared for Workshop on Cold Fusion Phenomena, Santa Fe, New Mexico, May 23-25, 1989, Martin Marietta Energy Systems, Inc., Oak Ridge Y-12 Plant, May 1989.

DISCUSSION (HUTCHINSON)

Teller: The excess heat flux amounts to how much? About 3 percent?

Hutchinson: Our input is about 30-35 W, and its value is about 3-5 W, or 8-10 percent.

Chexal: Are all four cells identical?

Hutchinson: They are identical in structure. Two of the palladium rods were purchased from Johnson-Matthey and annealed. The other two were melted in the laboratory, extruded into quarter-inch diameter bars, and given vacuum treatment at 250°C for 24 h. They were not annealed.

Santucci: What is the ΔT at an excess power level of 9 W?

Hutchinson: It corresponds to 32-33 W input power, 40 W output, and from the calibration curve a ΔT across the Teflon of 25°C.

Santucci: What is the operating voltage?

Hutchinson: About 7 V, corresponding to 5 A at 35 W.

Santucci: What is your net integrated energy balance?

Hutchinson: After charging at 1 A for 130 h, we increase the current to 5 A, and excess heat appears almost immediately. However, I believe that we do not yet have a value for the integrated excess power out.

Mansour: What type of surface measurements did you perform?

Hutchinson: Dr. Farrell in our Solid State Division is starting a wide range of analyses. Results will be available in about a month, including helium measurements.

Mansour: You do find iron present, which correlates with Dr. Hoffman's remark that he has seen it without exception in palladium cathode samples which he has examined.

Hutchinson: We have stainless steel heaters in our cells, which are used to check calibration for every current operating point.

Bard: The use of metal heaters can be a source of error. If the heater is accidently grounded, there can be additional heat input.

Hutchinson: Our heaters are definitely floating, and they are located outside of the teflon insulation, effectively outside of the cell. The platinum anodes are grounded.

Bard: But you still detect iron deposition at the cathode?

Hutchinson: Yes, but the currents to the heater are very small, because of the Teflon liner.

Jones: You saw few neutrons. Did you detect any tritium?

Hutchinson: In our initial experiments we used reactor heavy water, containing about 106 dpm/ml. More recently, we have used heavy water with 12-15 dpm/ml. After one week of operation, the value is the same. Since we have an external recycle, we collect samples every two days. We also conserve our recombined water for analysis.

Teller: So your excess level is perhaps 108 times higher than any tritium formed so far.

Hutchinson: At least.

Huggins: What current density did you use?

Hutchinson: 250 mA/cm^2, that is, 5 A and 20 cm^2.

Chubb: You mentioned that you did not detect lithium in the palladium.

Hutchinson: After our first run with excess heat, we cut and polished the palladium cathode, then scanned for lithium. We found none. The other rods will be analyzed in turn.

Jones: You have done no control experiments on light water?

Hutchinson: Correct. That work is planned.

Jones: Did you see any helium, particularly He-3?

Hutchinson: The first rod has been sent for helium analysis. Any He-3 present was below background.

Part 4

THEORY

Section 23

DR. EDWARD TELLER: THE MESHUGANON

A Catalytic Neutron Transfer ?

by Edward Teller

We have seen some interesting data during the last two days. They may not be statistically significant. Yet, if proved correct, some new phenomena may be at work.

I say new phenomena and not Cold Fusion. Cold fusion is excluded for two strong reasons. One well-known reason is the Gamow factor. This prevents the reaction by many orders of magnitude.

The second reason, of comparable force, is the relative frequency of the D + D -> He_3 + n and the D + D -> T + P reactions. The rates should be nearly equal. But measurement of neutron production and triton production indicate that the second reaction is 10^8 or 10^9 times more likely than the first reaction.

While there is some evidence suggesting the production of tritium, the D + D -> T + P reaction does not proceed in the usual manner: no gamma rays or X-rays are observed. Yet, they should be present due to the fast charged particles. Furthermore, the fast tritons should produce 14 MeV neutrons in interaction with the deuterium, and they are also not observed.

Finally, the excess heat ascribed to cold fusion never occurs at the beginning of the electrochemical experiments. It is claimed to appear with a variable delay.

If the production of tritium and of excess heat should be firmly established, a new physical phenomenon must be involved. I would like to propose a new particle which catalyzes the transfer of a neutron from one deuteron to another. In the reaction with the first deuteron, a proton would be left behind; in the second reaction, a triton would be formed.

My friends have remarked that this proposal is "meshuge," which means crazy but not necessarily repulsive. I accept this criticism and call my particle Meshuganon.

The most frequent argument against the meshuganon is that it does not fit into the systematics of new particles. An even stronger negative argument is that the Meshuganon does not explain the absence of gamma-rays, X-rays and 14 MeV neutrons. The contradiction with experiments is reduced because the energy of the D + D -> T + P reaction is delivered in two steps, rather than in one. In

addition, a considerable part of the energy is carried off by neutral particles which can produce heat without giving rise to X-ray or gamma-ray emission.

The Meshuganon designated as M should be neutral to escape direct observation. It may be produced in a small fraction of the D + D fusion reactions. These reactions could occur in very rare cases due to strong electric fields at cracks or surface irregularities. These reactions would account for the few observed neutrons. The doubly rare production of Meshuganons would eventually give rise to the presence of enough Meshuganons to catalyze the neutron transfer which then proceeds at a considerably higher rate. The mass of the Meshuganon would, of course, be limited by the energy available in the D + D reactions.

My proposed catalytic chain involves two reactions: D + M -> (Mn) + P and (Mn) + D -> M + T. Here (Mn) stands for a neutral particle composed of a neutron and a Meshuganon. Its binding energy must be greater than the binding energy in the deuteron but less than the binding energy of the second neutron in the triton. The binding of a proton to a Meshuganon (MP), must not occur because the production of (MP) would break the chain. Since the Meshuganon has a mass comparable to that of an electron, one can describe its behavior in its interaction with nuclear particles according to the Bom-Oppenheimer method. It is plausible that in the field of a deuteron, the Meshuganon will have not more than one bound state. In that case, during a dissociation of the deuteron into a proton and a neutron, the Meshuganon will almost exclusively stay with the particle to which it is bound most strongly. Therefore, the systematic absence of (MP) as a reaction product is in no way absurd.

It seems necessary to assume that the Meshuganon have a finite lifetime but can accumulate so that in the presence of this catalyst the energy production and the generation of tritium can proceed at an unusually fast rate. Models that can accomplish this may be constructed.

In the presence of beryllium, the reaction Be + M -> (Mn) + α + α might be observed. In the presence of U_{235}, one might expect U_{235} + (Mn) -> M + fission. This should yield observable fission-products and considerable release of heat. Neither of these reactions is a necessary consequence of my assumptions. The observation of either would be most interesting while the absence of both would make the hypothesis of a Meshuganon more unlikely to represent reality.

My conclusion is that the experimental work on "cold fusion" should continue until a decision is obtained. The Meshuganon may give a possible but not a probable explanation. In any case, the experimental observations, if they are confirmed, must be explained by means that are outside of conventional nuclear physics.

Section 24

CALORIMETRIC MEASUREMENTS ON ELECTROCHEMICAL CELLS WITH PdD CATHODES

L. Redey, K.M. Myles, D. Dees, M. Krumpelt, and D.R. Vissers

Electrochemical Technology Program

Argonne National Laboratory

CALORIMETRIC MEASUREMENTS ON ELECTROCHEMICAL CELLS WITH Pd-D CATHODES

L. Redey, K. M. Myles, D. Dees, M. Krumpelt, and D. R. Vissers

Electrochemical Technology Program
Chemical Technology Division
Argonne National Laboratory

ABSTRACT

Two series of experiments were performed to determine the conditions of cell operation that produce sufficient excess heat to be useful for the production of energy. In the first series, the results from a differential temperature analysis of identical light- and heavy-water electrochemical cells were too ambiguous and, thus, not suitable for evaluating excess heat effects. In the second series, two Pd-D/LiOD-saturated D_2O/Pt cells were operated at current densities between 15 and 500 mA/cm^2 in a constant-heat-loss-rate twin calorimeter for 460 hours. Water loss measurements during the experiments indicated that the recombination reaction ($D_2 + O_2 \rightarrow D_2O$) did not occur. The D/Pd ratio was determined gravimetrically during the experiments. No excess heat was found within the sensitivity (0.13 W, 0.082 W/cm^3 of Pd, 0.013 W/cm^2 of Pd) and precision ($\pm$0.3 W) of the calorimeter.

CALORIMETRIC MEASUREMENTS ON ELECTROCHEMICAL CELLS WITH Pd-D CATHODES

L. Redey, K. M. Myles, D. Dees, M. Krumpelt, and D. R. Vissers

Electrochemical Technology Program
Chemical Technology Division
Argonne National Laboratory

INTRODUCTION

The purpose of these experiments was (a) to investigate the energetics of the electrochemical formation of Pd-D, (b) to verify the claims of excess heat generation reported by Fleischmann and Pons,[1] and (c) to ascertain whether an electrochemical cell could be operated to produce sufficient excess heat for the production of useful energy. These experiments were not designed to detect any nuclear radiations and, thus, to verify the results of Jones.[2] This article is based on the presentation given at the Workshop on Cold Fusion Phenomena, Santa Fe, NM.[3]

TECHNICAL APPROACH

Two series of experiments were performed: (a) differential temperature analyses of identical light- and heavy-water electrochemical cells and (b) calorimetric measurements of operating heavy-water electrochemical cells.

In the first series of experiments, the temperature difference between identically constructed Pd-H/LiOH-saturated-H_2O/Pt and Pd-D/LiOD-saturated-D_2O/Pt cells was monitored. It was anticipated that the temperature difference would be close to zero until the onset of "cold fusion," when the D_2O cell would become noticeably hotter. However, it proved to be impossible to maintain identical electrochemical conditions in both cells. For example, to maintain the current densities the same in the two cells, the cell

operating voltage of the heavy-water cell became higher than the light-water cell; this in turn caused the temperature to be also higher. When the current densities and the cell voltages were both made the same by manipulating the cell resistance, the light-water cell became very slightly warmer (0.8 K). We concluded that the results from this kind of experiment were too ambiguous and, thus, not suitable for evaluating the occurrence of excess heat as has been reported.[4]

In the second series of experiments, Pd-D/LiOD-saturated-D_2O/Pt cells were operated in a constant-heat-loss calorimeter that was sensitive enough to detect the levels of excess heat previously reported.[1,4,5] Excess heat has been generally defined as that heat output from the cell, after suitable corrections have been made to account for several concurrent side reactions, that is greater than the heat equivalent of the electrical energy that was put into the cell. Details of this series of experiments and the associated calculations are described below.

EXPERIMENTAL

The Calorimeter

The schematic of the constant-heat-loss-rate water calorimeter that was built for the specific purpose of this experiment is shown in Fig. 1. The electrochemical cell, located in the water of the calorimeter, was controlled at 30.0°C. The constant-temperature bath that surrounded the calorimeter was held at 21.0°C by flowing the water through a controlled-temperature circulator. A heat-loss-rate control gap regulated the rate of heat transfer between the calorimeter and the bath. The heat loss rate (Q_c) was varied by placing air in the gap for levels of cell heat production up to 5 W and water

in the gap for levels up to 30 W. The bath was thermally insulated from the surroundings by thick layers of styrofoam. The cover was insulated to prevent any significant direct heat loss to the ambient air through the top of the cell. The heat loss from the calorimeter was calibrated with a precision electrical heater that was placed into the electrolytic cell. A stirrer kept the water temperature of the calorimeter uniform; however, in this type of calorimeter, neither the temperature of the electrochemical cell nor any nonuniform temperature distribution in the cell affects the precision of the heat measurement. Prior to operation of the electrochemical cell, the calorimeter was calibrated by introducing known resistive heat inputs.

The principle of the calorimeter is illustrated in Fig. 2. To maintain the temperature of the calorimeter constant, the rate of heat loss from the calorimeter to the bath (W_L) was precisely compensated for by adjusting the heat input from the electrical heater (W_H). When the electrochemical cell was off, $W_L = W_H$; when the electrochemical cell was on and produced heat, the heater input was decreased in accord with the following relationship:

$$W_L = W_H + Q_c. \tag{1}$$

The constant temperature bath contained twin calorimeters so that two electrochemical cells could be identically operated; thus, the results would emphasize any unusual occurrences that may occur in one of the cells. The electrical circuit diagram for the electrochemical cells is shown in Fig. 3. The power source was a potentiostat (Princeton Applied Research Model 375) operated in the galvanostatic mode. The cell voltage was measured by high precision digital meters.

The overall precision of the heat flux, determined to be ± 0.3 W at low Q_c and ± 0.4 W at high Q_c, was limited by some slight temperature oscillations experienced by the calorimeter, which were in the range of 0.1°C. Because these oscillations were quite slow (less than 0.1°C/6 h), the sensitivity of the calorimeter was better—approximately 0.13 W over a period of one hour. The time constant of the calorimeter to reach steady state after changing the current density was about 10 minutes. Included in these values are all the experimental errors related to the measurements of the temperature, cell voltage, heater voltage, and current. When related to the volume, surface area, and weight of the starting Pd cathode, the sensitivity of the calorimeter was 0.082 W/cm^3, 0.013 W/cm^2, and 0.068 W/g respectively. Considering that the reported levels of excess heat[1,4,6] have been around 10 W/cm^3, this precision was more than adequate for the present experimental purposes.

The Electrochemical Cell

Details of the electrochemical cell are shown in Fig. 4. A wrought Pd rod cathode was supplied by Johnson Matthey (AESAR's #12557) and had the following characteristics: 99.96% pure, 0.63 cm diameter, and 5 cm long (1.58 cm^3, 10.29 cm^2, 19 g). The rod was degassed, either at temperatures below 100°C or at high temperatures in vacuum, and then was heat treated before each experiment at 650°C for an hour in air and, finally, at 600°C in vacuum for about 18 hours. A Pt wire anode was supplied by Johnson Matthey (AESAR #10285) and had the following characteristics: 99.95% pure, 0.1 cm diameter, and 100 cm long. The anode wire was wound into a 3.2 cm ID coil to snugly fit into the cell.

The electrolyte was about 40 cm^3 of LiOD-saturated D$_2$O. The LiOD-saturated D$_2$O was prepared from 99.9% pure Li metal, supplied by Johnson Matthey (AESAR #10767), and 99.8% pure D$_2$O, supplied by Aldrich (#15,188-2). Saturated LiOD electrolyte (about 12 w/o) was used to lower the resistivity, compared with that of the 0.1 M LiOD solution used by Fleischmann and Pons[1], produced less irreversible heat during electrolysis and, thus, improved the precision of the experiment. The cell was covered, leaving only a small gap to allow escape of the electrolyzed gases, to minimize the back diffusion of H$_2$O vapor from the ambient atmosphere. Nevertheless, some H$_2$O did contaminate the electrolyte as was shown by the post-experiment chemical analysis.

The Pd cathode was supported by a stainless steel tube current lead that was covered by a Nalgene tube to preclude any involvement of the stainless steel in the electrochemical reaction. A thermocouple, inserted through the tube, was in physical contact with the Pd cathode to monitor any rapid temperature excursions that might occur.

Six extended duration experiments were carried out under a wide variety of conditions. The cumulative electrolysis time was 1500 h. The duration and charge input of the longest experiment were 460 h and 700 Ah, respectively. During the course of the experiments, the following measurements were made in addition to the calorimetric ones: (a) the weight of the Pd cathode to calculate the D/Pd ratio, (b) the potential of the PdD$_x$ cathode on closed and open circuit versus a Hg/HgO reference electrode filled with LiOD-saturated D$_2$O, and (c) the weight of the heavy water added to maintain the electrolyte level in the cell constant to within 0.3 cm.

At the end of the experiment the electrolyte was chemically analyzed. A H/D ratio of 0.02 was found after 460 h of cell operation, presumably the

result of some D_2O/H_2O exchange from the atmospheric moisture. An analysis for tritium in the electrolyte (269 d/m/ml) at the end of the same experiment indicated no significant change over that in the as-received heavy-water (138 d/m/ml). The Pd cathode was degassed after the experiment, and the original weight of the palladium still remained. However, the outcoming gas had an average H/D ratio of 0.06 which means that the actual concentration of deuterium in the PdD_x cathode was slightly less than that calculated from only the weight measurements.

DATA EVALUATION

Power Balance

During the operation of the electrolytic cell, several well-identified electrochemical, chemical, and electrical processes occur and produce heat effects in the cell. These processes must be quantified before any assessment of excess heat generation can be made. The processes are those associated with the cell resistance, the electrolysis of heavy water, the absorption of deuterium into the palladium lattice, and the loss of water from the cell. It is assumed in this analysis that no significant amount of recombination had occurred during electrolysis.

The cell impedance includes the ohmic resistance of the cell (R), the polarization of the Pd cathode (η_c), and the polarization of the Pt anode (η_a). The rate of heat generation from these processes is the sum of the individual effects (Q_{IRR}) given by

$$Q_{IRR} = I (IR + \eta_c + \eta_a), \qquad\qquad (2)$$

where I is the cell current. Q_{IRR} is an exothermic process and is often referred to as electrochemical irreversible heat that arises from performing the electrolysis reaction at a finite rate. It can be shown that

$$Q_{IRR} = W_E - I(\Delta G/2F) = I (E - 1.2570), \qquad (3)$$

where E is the applied cell voltage, $W_E = I E$ is the electrical power to the cell, $\Delta G = 242.6$ kJ/mol D_2O at 30°C[6,7] is the free energy change in the electrolysis of heavy water, F is the Faraday constant, and 1.257 volts is the thermodynamic voltage.

Even when carried out at a reversible rate, the electrolysis of heavy water (and any other reaction for that matter) produces heat effects equal to the change of entropy (ΔS) multiplied by the absolute temperature (T). For heavy water electrolysis, this heat effect is endothermic, and the rate of heat adsorption (Q_{REV}) at a finite rate is given by

$$Q_{REV} = I (T\Delta S/2F) = 0.269 I, \qquad (4)$$

where $\Delta S = 170.8$ J/K mol D_2O at 30°C[6,7], and 0.269 volts is the value.

The heat generation from the absorption of deuterium becomes negligibly small as the D/Pd ratio in the Pd cathode approaches 0.7.

The water loss processes include the saturation of electrolyzed gases with D_2O vapor and the entrainment of liquid D_2O in the gas leaving the electrochemical cell. An evaluation concluded the sum of all these effects is negligible (less than 1% of the total heat effects) for the present experiments.

Assuming that no excess heat is generated, the net heat output from the electrolysis cell (W_Q) is given by the sum of all the above effects, or

$$W_Q = Q_{IRR} - Q_{REV} = W_E - I (\Delta G + T\Delta S)/2F = W_E - I(\Delta H/2F) = I(E - 1.526), \quad (5)$$

where ΔH = 294.4 kJ/mol D_2O at 30°C[6,7] is the enthalpy change in the electrolysis of heavy water and the thermal neutral is 1.526 volts is the value. Intuitively, the enthalpy term in Eq. 5 arises because it is the quantity of power input to the electrolysis cell that produces chemical energy without heat evolution. Therefore, W_Q can be thought of as the adjusted electrical input to the cell.

The excess heat generated can be determined by

$$\text{Excess Heat} = Q_C - W_Q, \quad (6)$$

where Q_C, which is the measured heat-generation rate of the electrolysis cell transported to the calorimeter, is defined in Eq. 1.

Energy Balance

The energy balance is based on the comparison of the $\int Q_C dt$ and $\int W_Q dt$ integrals calculated for a period of time starting at time t_1 and ending at time t_2. Ideally, the integrals should cover the entire span of the experiment; but, because of the nature of the instrumentation available, it was only possible to calculate the integrals over periods of constant current density of 10- to 50-h durations with acceptable accuracy.

Mass Balance

A mass balance was performed to evaluate how much water was lost from the electrolytic cell due to the saturation of the electrolyzed gases with D_2O

vapor and the entrainment of liquid D_2O in the gas leaving the cell. The mass balance was also used to determine the extent that the electrolyzed gases had recombined in the cell. The mass balance was calculated by determining the rate at which water had to be added to the cell to keep the electrolyte level constant and comparing it to the cell current (knowing that each ampere of current consumes heavy-water at a rate of 6.22 mg/min due to electrolysis and an additional 0.41 mg/min at 30°C due to the saturation of the gases). The loss by entrainment was three orders of magnitude smaller than the loss by electrolysis.

RESULTS AND DISCUSSION

The following chemical processes were addressed in the analysis of the experimental results: the electrolysis of water,

$$2D_2O = 2D_2 + O_2; \tag{7}$$
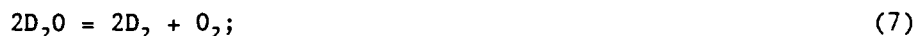
the recombination of the split D_2 and O_2 gases,

$$2D_2 + O_2 = 2D_2O; \tag{8}$$

The formation of PdD_x from gaseous D_2,

$$xD_2 + 2Pd = 2PdD_x, \tag{9}$$

and from liquid D_2O,

$$Pd + xD^+ + xe^- = PdD_x; \text{ and} \tag{10}$$

the decomposition of PdD_x,

$$2PdD_x = 2Pd + xD_2. \tag{11}$$

Whereas the actual reaction steps may be much more complicated than these processes would indicate, the energy calculations only require a knowledge of the beginning and end of the process. Of these processes, the electrolysis of water (Eq. 7) is of primary importance because it dominates the energetics of the experiments.

The electrochemical formation of PdD_x (Eq. 10) made a significant contribution to the power, energy, and mass balances (PEM balances) only during the comparatively short periods in the experiments when the formation of PdD_x was rapid. During most of the experiment, the compositional change of PdD_x was slow, and this reaction then contributed less than 1 percent to the PEM balances, as was deduced from the measured current efficiencies shown in Fig. 5. It should be noted that PdD_x can be formed directly from the gas phase (Eq. 9) at ambient temperatures and pressures only up to about $x = 0.6$; higher concentrations require electrochemical charging.

The decomposition of PdD_x (Eq. 11) occurs when the cell is on open circuit. The rate of decomposition is dependent on the concentration of deuterium in the PdD_x, (Fig. 6) and on the elapsed time after current interruption in accord with Fick's law of diffusion.

The extent that the evolving D_2 and O_2 gases recombine (Eq. 8) must be carefully considered in calculating the PEM balances. The recombination rate is directly related to the rate that the heavy water had to be replenished to keep the level constant in the electrolytic cell. In all of these experiments, the measured replenishment rate was essentially equal (Fig. 7) to the rate that the water was electrolyzed, as calculated with Faraday's law and the measured current input, and increased by the amount of heavy water needed

to saturate the evolving gases at 30°C. Because no recombination of deuterium and oxygen was observed, no correction for recombination was included in Eqs. 2-6.

The lack of recombination in our experiments does not exclude the possibility that, under other investigators' experimental conditions, recombination might have occurred and have been overlooked. If recombination does occur, the factor 1.526 in Eq. 5 must be reduced in proportion to the recombination rate. Whereas recombination is slow in liquid D_2O itself because of the low solubility and slow diffusion of D_2 and O_2, there are conditions when fast recombination can occur. For example, on exposed electrolyte-free surfaces of the Pd or Pt electrodes or in the electrolyte when O_2 gas bubbles admix with D_2 gas bubbles on the surface of electrode and recombine. Further, pH changes can occur in the surface layers of the electrodes at high current densities, which can be very pronounced in dilute electrolytes, and create favorable conditions for recombination or peroxide formation. Peroxide, or other impurities, can set up heat-producing irreversible reactions or electrochemical-chemical cycles.

The concentration of deuterium in the Pd cathode was determined by gravemetric measurements. Because some deuterium escaped from the Pd electrode as the measurements were being made, time plots were necessary to extrapolate the weights to when the current to the cell was first interrupted. The decomposition of PdD_x (Eq. 11) produced a very distinct cooling effect while the PdD_x electrode was being weighed. Up to about x = 0.7, the deuterium uptake in the PdDx electrode was relatively fast, as is reflected by the observed high current efficiency (Fig. 5). However, very energetic electrochemical conditions were required to achieve higher deuterium

concentrations. A manifestation of this is the low electrode potential measured at high concentrations. In the compositional range of the α and $\alpha+\beta$ PdD_x phases, the electrode had potentials in agreement with the literature[8,9], that is, about 30 mV at x<0.4 and a gradual decrease to about zero as x reached 0.6 (these potentials are relative to a $Pt(D)/D_2$ electrode prepared with the same electrolyte, and assuming that the Hg/HgO reference electrode used in the measurement had a 920 mV potential against this electrode). At concentrations greater than x = 0.6, however, the open-circuit potential of the PdD_x electrode shifted to approximately -90 mV, indicating that the deuterium had a high fugacity and was very energetic in the PdD_x electrode. This negative potential was not stable but did persist for long periods (10-20 minutes) after the current was interrupted and then slowly drifted to less negative values. This behavior was probably due to the decrease in the deuterium in the surface layers of the PdD_x electrode.

The results of the PEM balances are plotted in Figs. 8 and 9. The heat output of the cell (Q_c) and the adjusted electrical input (W_Q) show agreement well within the accuracy limits of the measurements. Thus, no excess heat was found within the limits of the sensitivity and precision of the calorimeter as operated under the described experimental conditions. The experimental conditions encompassed many of the factors that have been suggested as influencing the onset of "cold fusion." These are (a) the Pd cathode had sufficient mass and surface area to meet the reported claims for both bulk effects[1] and surface effects[2]; (b) the applied current densities covered the wide range from 12.5 to 500 mA/cm^2 (Fig. 10); (c) the duration of the experiment was long enough to maintain a high concentration of deuterium in the Pd cathode for hundreds of hours (Figs. 10 and 11); and (d) the ratio of

D/Pd in the PdD_x electrode approached 1.0, that is, PdD. The data in Fig. 11 have been corrected for the measured H/D ratios. It should be noted that the deuterium concentration did fluctuate (Fig. 11), even at constant current density for unknown reasons. Because the deuterium concentration in the PdD_x electrode was measured relatively infrequently, the instantaneous rate of change of x is unknown. However, the examination of the continuous temperature record of the PdD_x electrode showed that to within $\pm 0.025°C$ no sudden temperature changes occurred. Furthermore, our calorimeter could detect a change in x of 0.1 within a 10 minute period assuming an enthalpy of 33 kJ/mol D_2.[8,10,11]

CONCLUSION

No excess heat was observed in Pd/LiOD-saturated D_2O/Pt cells during long duration experiments conducted with a high sensitivity, constant-heat-loss-rate calorimeter. The experimental conditions covered a wide range of parameters that have been described as being important to the production of excess heat. Additionally, quantified were the power/energy/mass balance, deuterium concentration and potential of the palladium cathode, degassing of Pd-D, and tritium level of the electrolyte. All of the observed heat effects were accountable by established electrochemical, chemical, electrical, and thermodynamic processes.
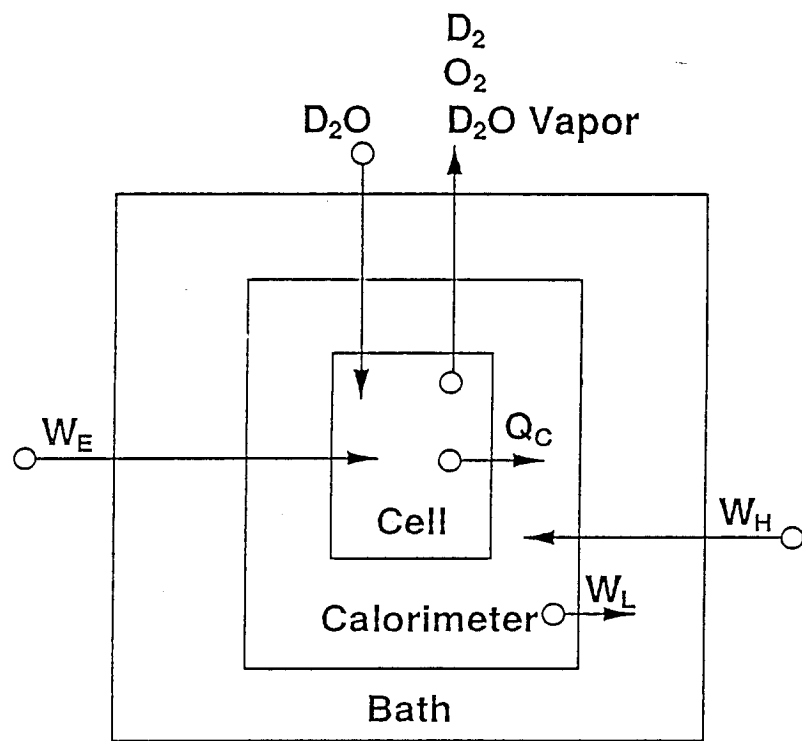
ACKNOWLEDGMENT

REFERENCES

1. M. Fleischmann and S. Pons, J. Electroanal. Chem., 262, 301 (1989).

2. S. E. Jones, E. P. Palmer, J. B. Cirr, D. L. Decker, G. L. Jensen, M. J. Thorne, S. F. Taylor, and J. Rafelsky, Nature, 338, 27 (1989).

3. L. Redey, K. M. Myles, D. Dees, M. Krumpelt, and D. R. Vissers, Workshop on Cold Fusion Phenomena, May 23-25, 1989, Santa Fe, NM.

4. A. Belzer, U. Bischler, S. Crouch-Baker, T. M. Gur, M. Schreiber, and R. A. Huggins, ibid.

5. A. J. Appleby, S. Srinivasan, Y. J. Kim, O. J. Murphy, and C. R. Martin, ibid.

6. CRC Handbook of Chemistry and Physics, 59th Ed., CRC Press, Cleveland, OH, p. D-71 (1978/79).

7. JANAF Thermochemical Tables, Third Edition, Part II, Vol. 14, 1985, Supplement #1; M. W. Chase Jr., C. A. Davies, J. R. Downey Jr., D. J. Frurip, R. A. McDonald, and A. N. Syvernd, J. Phys. Chem. Ref. Data, p. 1007.

8. T. B. Flanagan, J. Physics. Chem., 65, 280 (1961).

9. S. Schuldiner, G. W. Castellan, and J. P. Hoare, J. Chem. Phys., 28, 16 (1958).

10. D. M. Nace and J. G. Aston, J. Amer. Chem. Soc., 79, 3627 (1957).

11. W. M. Mueller, J. P. Blackledge, and G. G. Libowitz, Metal Hydrides, Academic Press, New York, p. 642 (1968).
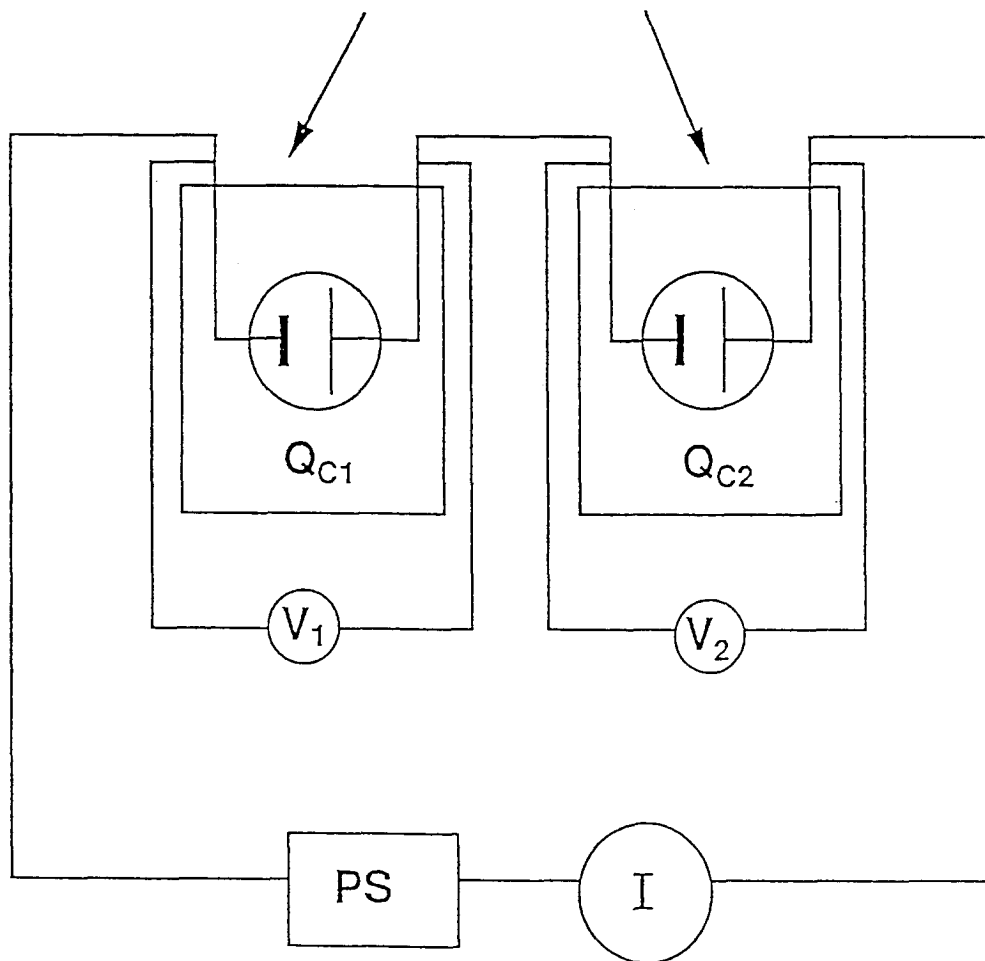
FIGURE CAPTIONS

Fig. 1   Constant Heat-Loss-Rate Calorimeter

Fig. 2   Mass-, Energy-, and Power Balance Considerations

Fig. 3   Circuit Diagram for Calorimetric Experiments

Fig. 4   Electrolytic Cell for Calorimetric Experiments

Fig. 5   Current Efficiency of PdD_x Formation at Low Current Density ($i < 25$ mA/cm^2)

Fig. 6   Degassing Rate of PdD_x at 2 min. after Current Interruption

Fig. 7   Water Loss Rate for the Experiment

Fig. 8   Comparison of the Heat Output of the Cell (Q_c) and the Adjusted Electrical Input (W_Q)

Fig. 9   Difference of Heat Output (Q_c) and Adjusted Electrical Input (W_Q)

Fig. 10   Current-Density Program for the Experiment

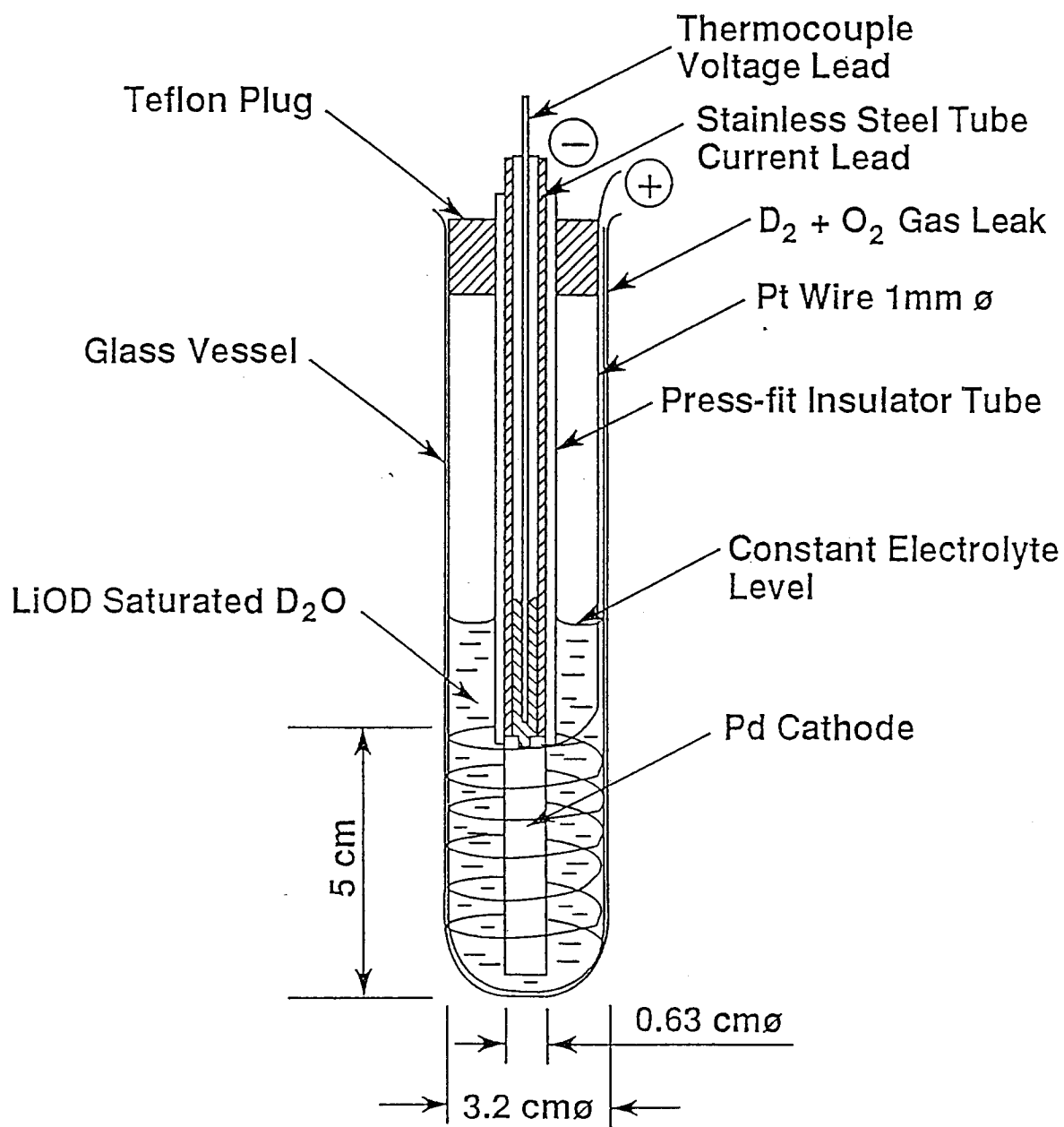Fig. 11   Deuterium Concentration Variation During the Experiment
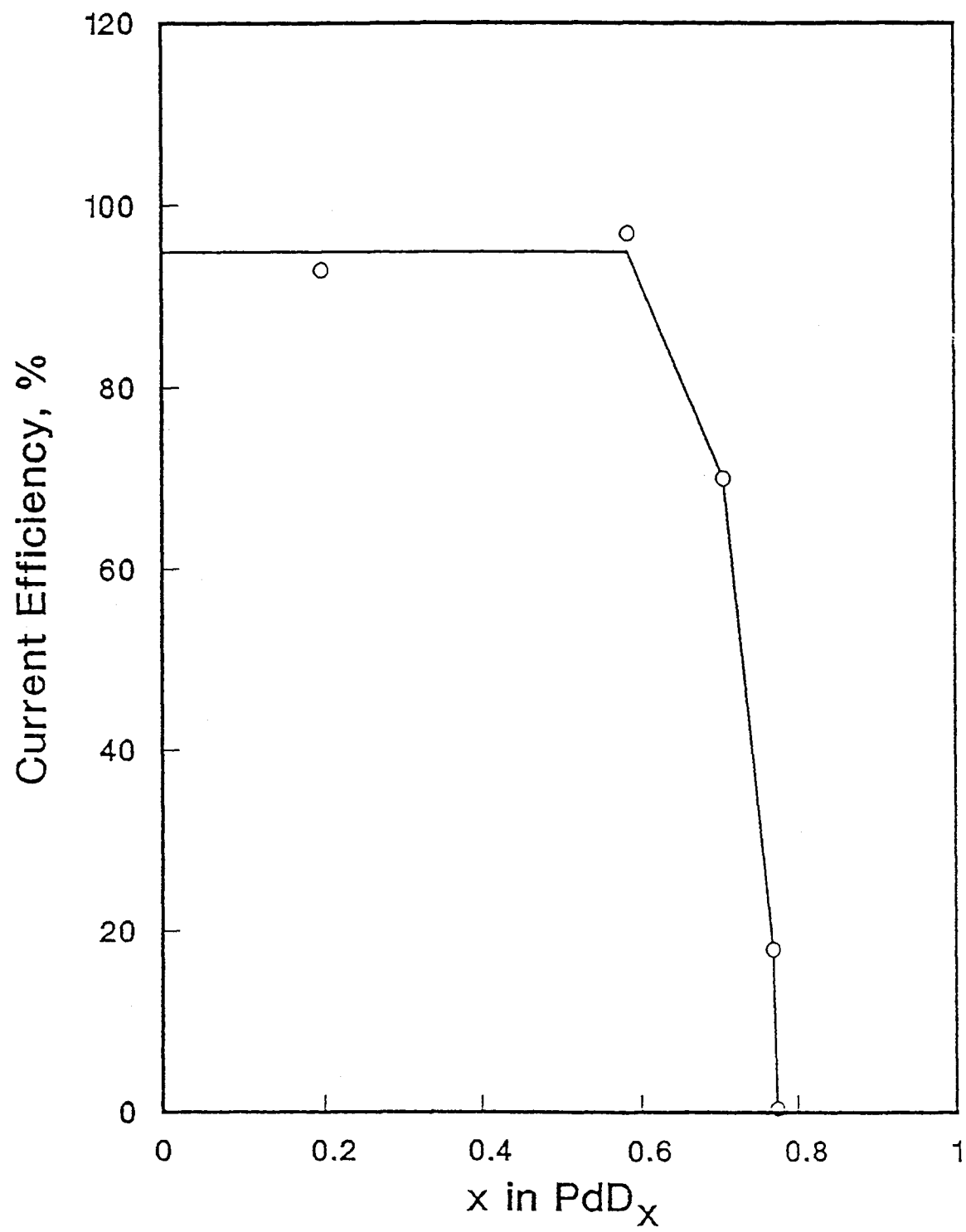
Thermocouples   Stirrer
Electrical Heater

$\ominus$ $\oplus$

Back to
Controlled
Temperature
Circulator

Cell

Heat-Loss-
Rate Control
Gap

30°

Constant
Temperature
Calorimeter

21° C

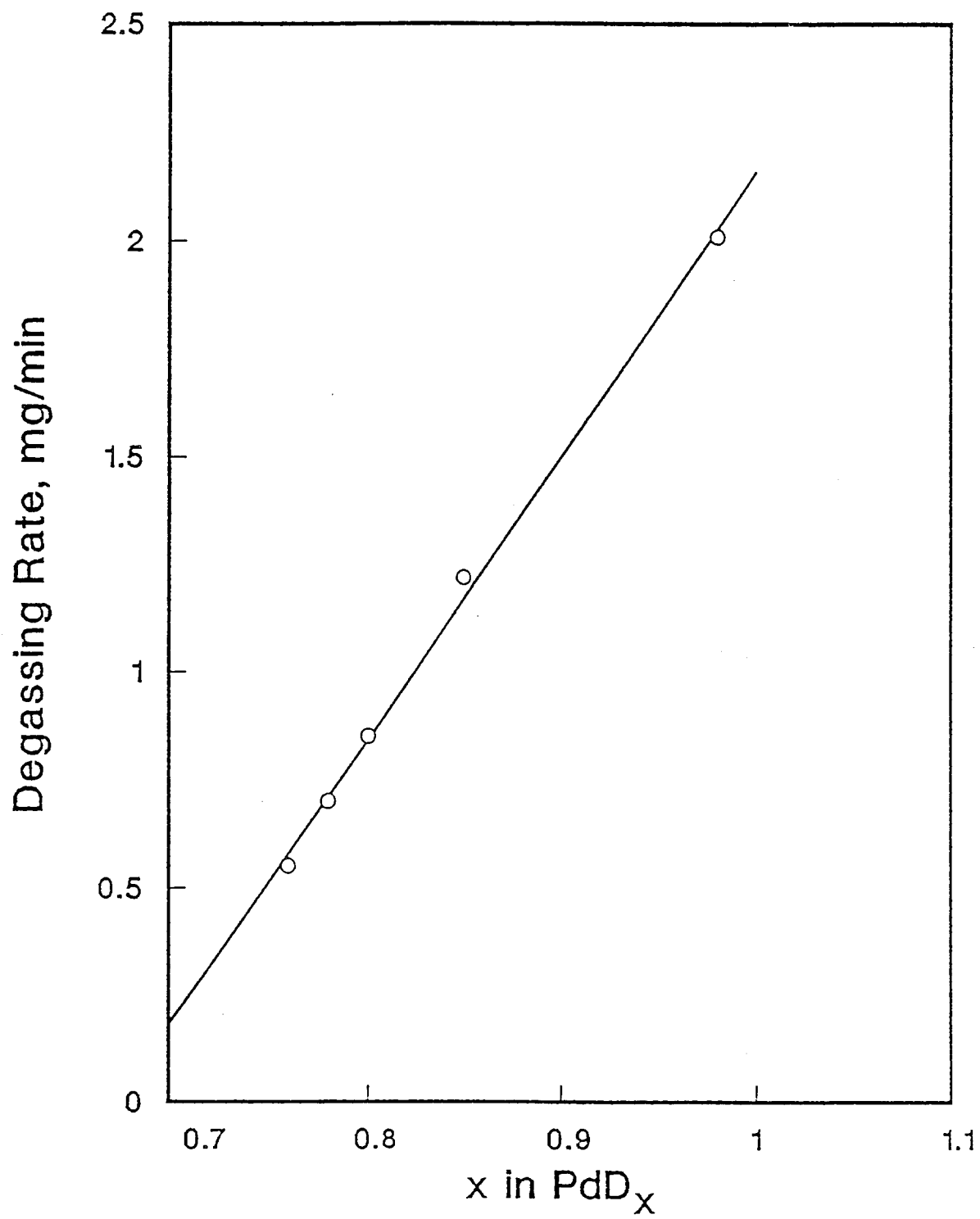Constant
Temperature
Bath
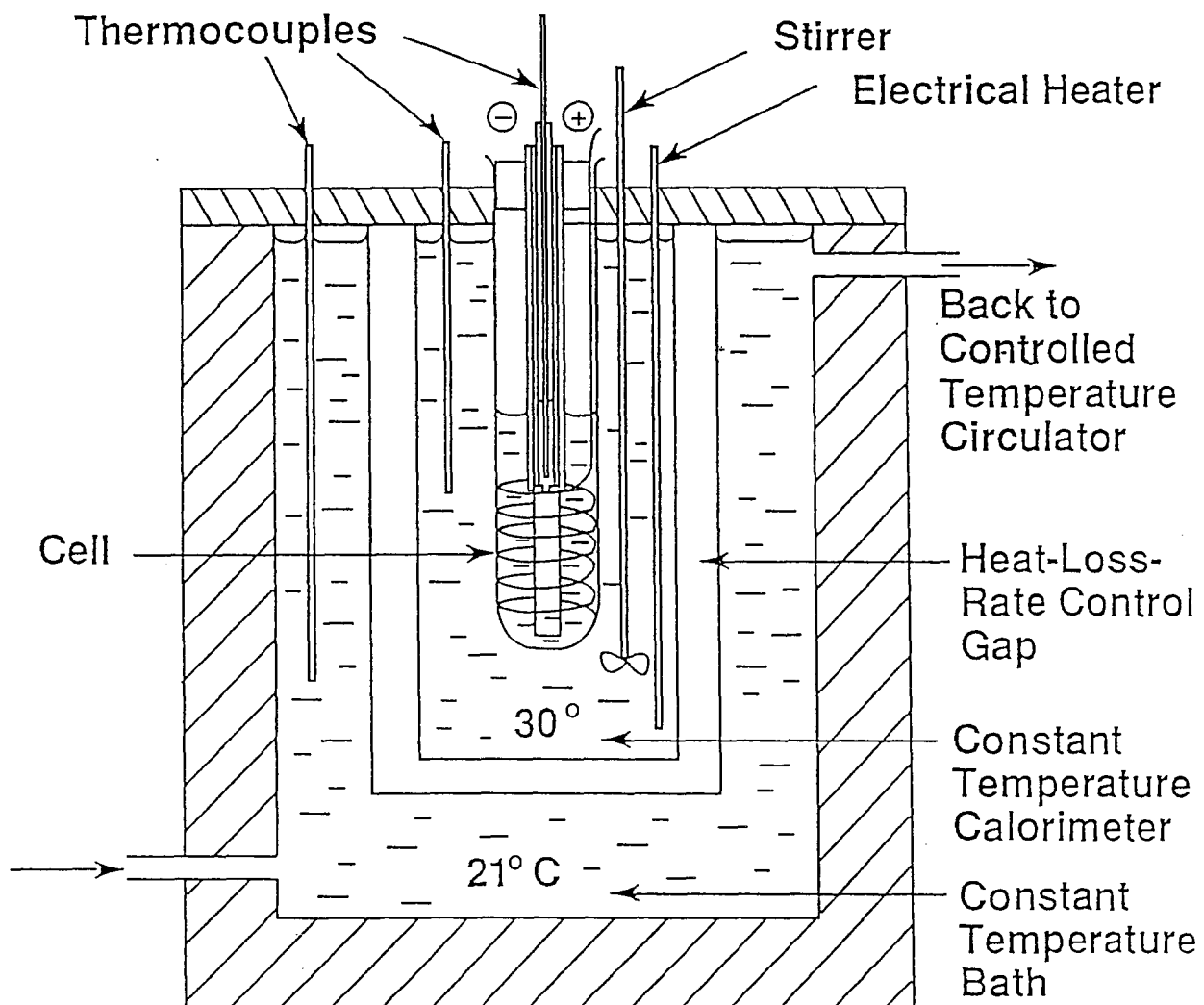
W_L : Heat-loss rate from calorimeter to bath
W_H : Electrical heater power to calorimeter
W_E : Electrical power to cell
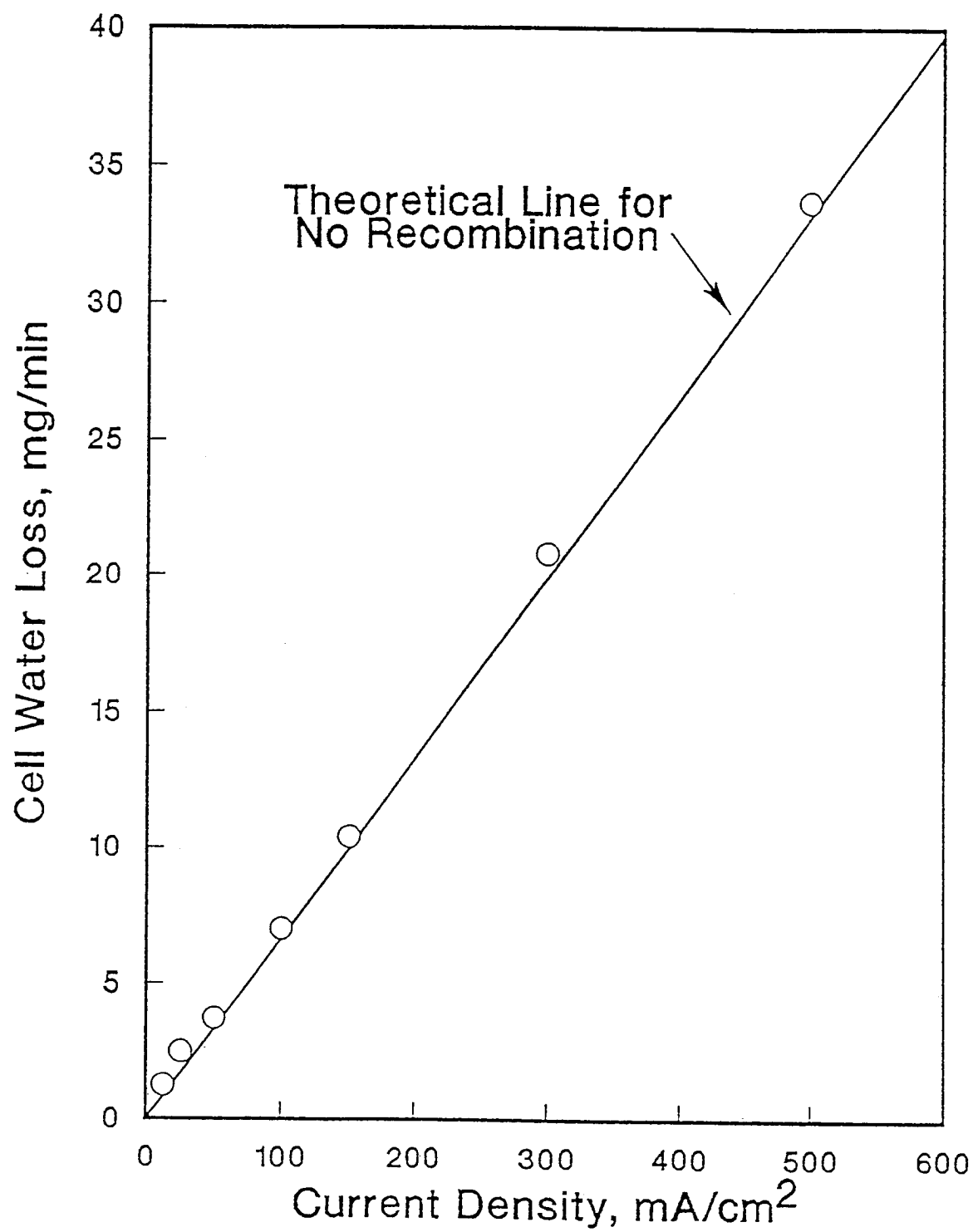Q_C : Heat-generation rate of cell transported to calorimeter

Calorimeters in Common Bath

Q_{C1}

Q_{C2}

V_1

V_2

PS

I

Thermocouple
Voltage Lead

Stainless Steel Tube
Current Lead

Teflon Plug

$D_2 + O_2$ Gas Leak

Pt Wire 1mm ø

Glass Vessel

Press-fit Insulator Tube

Constant Electrolyte
Level

LiOD Saturated D_2O

Pd Cathode

5 cm

0.63 cmø

3.2 cmø

24-20

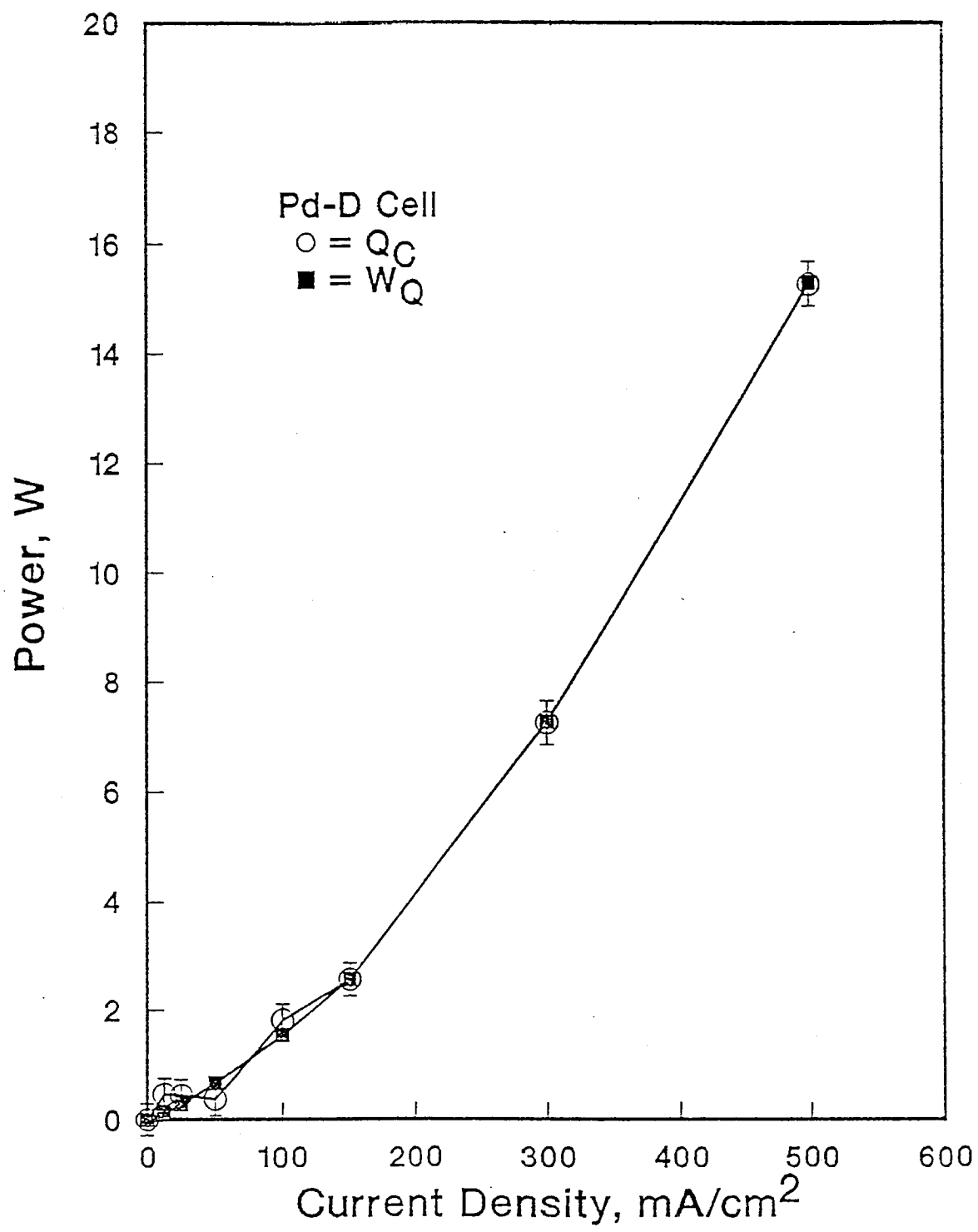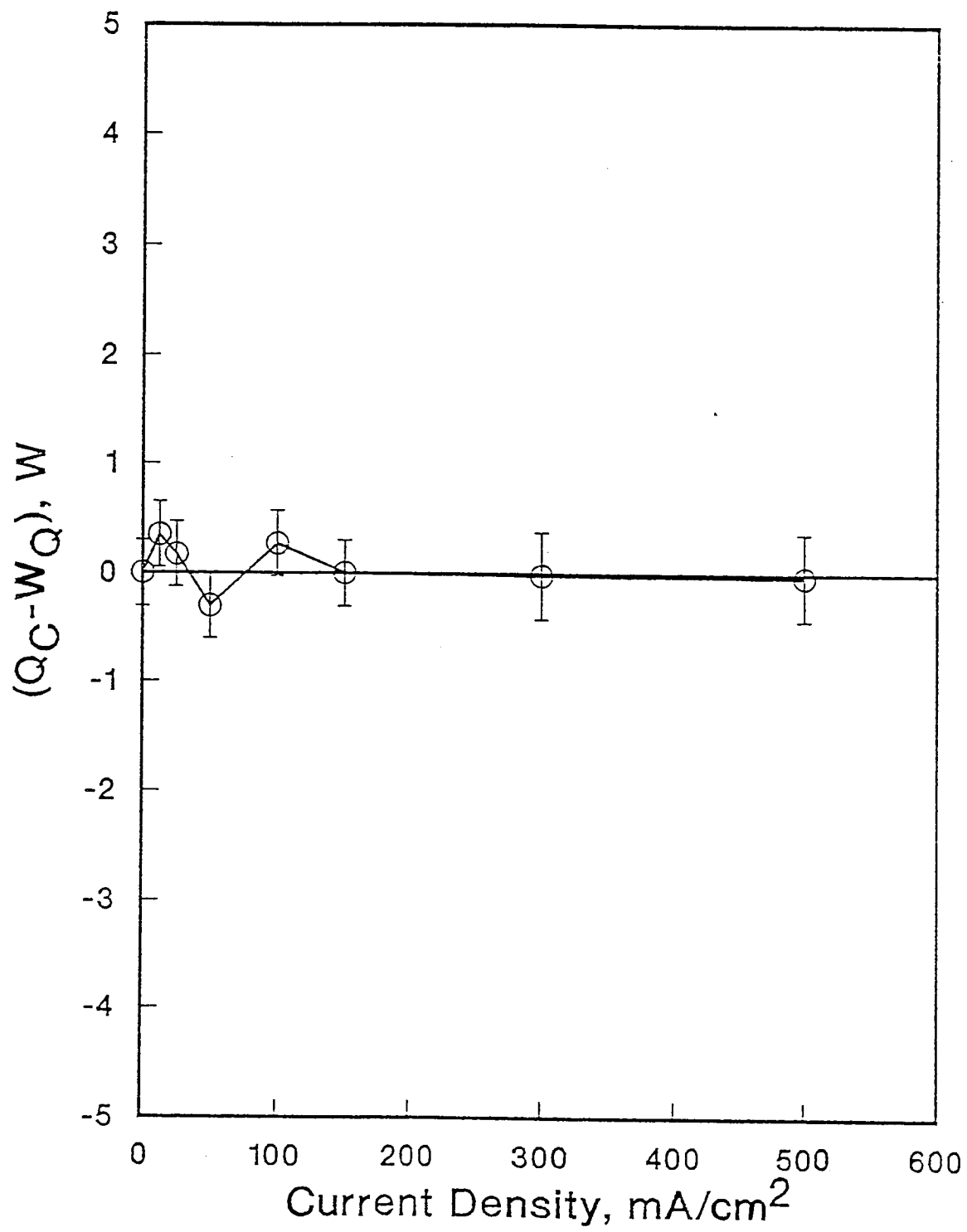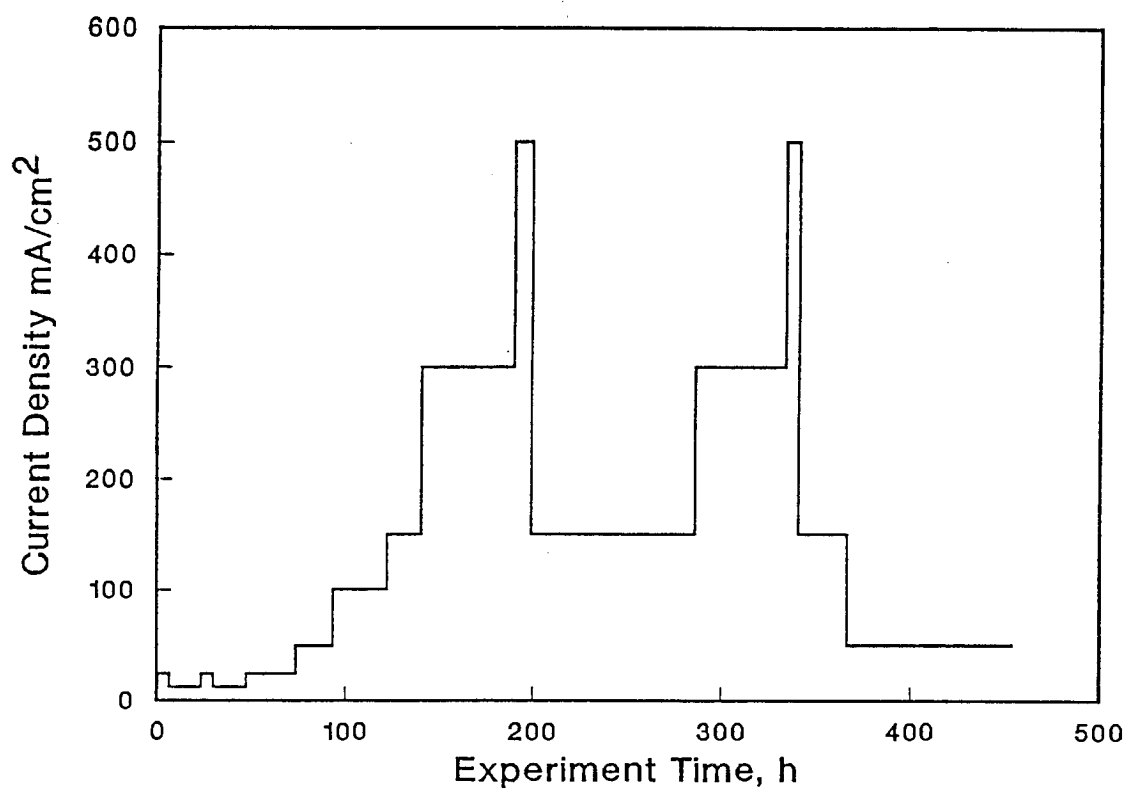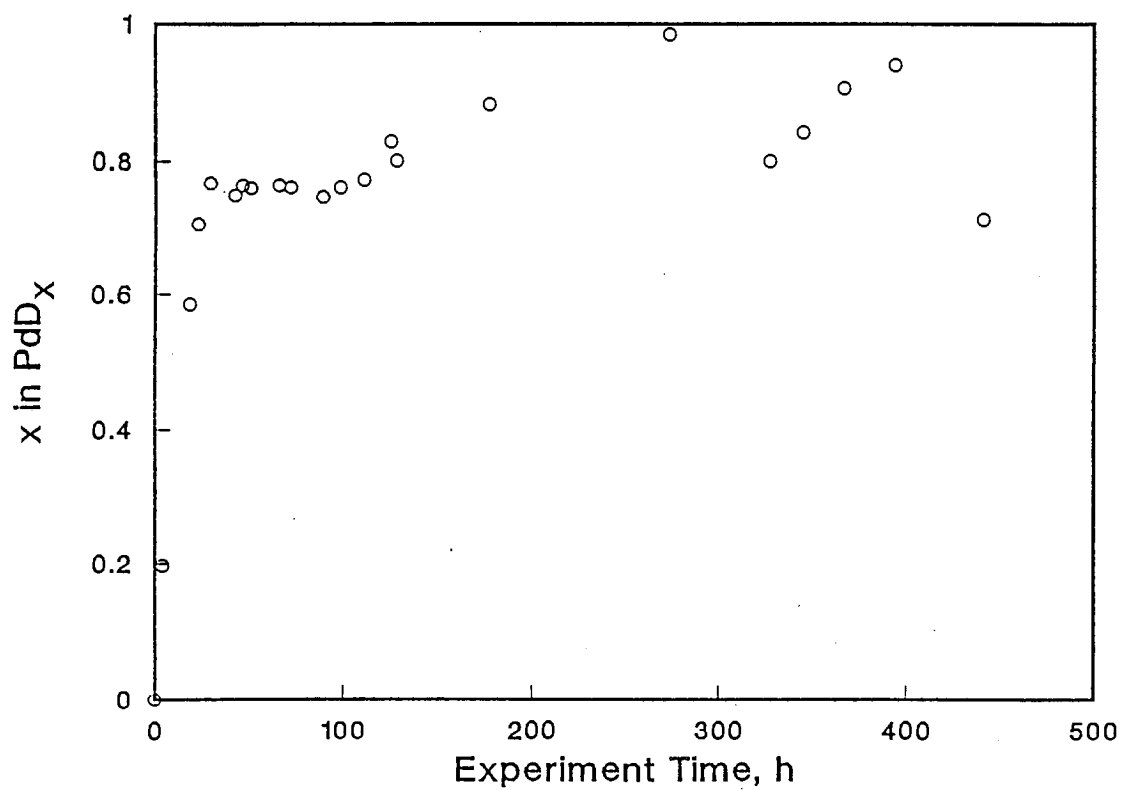Theoretical Line for
No Recombination

DISCUSSION (MYLES)

Bard: Is the heat output in your substitutional calorimeter controlled automatically?

Myles: Yes. The internal heater is automatically controlled by a data acquisition system. At Argonne we have an electrochemical technology laboratory for fuel cell and battery development work, which has the instrumentation in situ. The calorimeter was home-built. It also contained a home-built counter for thermal neutrons.

Yeager: How accurately is the calorimeter temperature controlled?

Myles: To less than 0.1°C. The information is given in the paper.

Hoffman: You use the Intense Pulse Neutron Source (IPNS) to determine the location of the deuterium in the palladium while electrolysis takes place?

Myles: Exactly.

Talcott: How do you handle the D_2O background in the IPNS?

Myles: I am sorry, but I was not responsible for the data analysis, which started only one or two weeks ago.

Talcott: Is Dr. Gian Felcher doing this work?

Myles: That is correct.

Chu: On one of your graphs, you showed a point indicating that your final composition for PdD_x gave an x value equal to unity. Was this determined by a single weighing?

Myles: All of our results involved multiple weighings over several weeks of repeated experiments. There are possible losses of deuterium when the specimens are removed from the cell, so that the gravimetric data are probably low.

Chu: How long was your palladium cathode typically charged?

Myles: Charging was typically for 6 weeks, although some specimens have operated for longer periods, up to several months. For specimens of the diameter which we used, based on the size of specimen reportedly used by Pons and Fleischmann, these times may have not been long enough. In further work, we would like to examine smaller-diameter cathodes.

Section 25

EXACT UPPER BOUNDS ON BARRIER PENETRATION IN MEDIA: SOLID-STATE EFFECTS CANNOT ENHANCE FUSION RATES ENOUGH

Gordon Baym

Department of Physics

University of Illinois at Urbana-Champaign

EXACT UPPER BOUNDS ON BARRIER PENETRATION IN MEDIA: SOLID-STATE EFFECTS CANNOT ENHANCE FUSION RATES ENOUGH

Gordon Baym

Department of Physics, University of Illinois at Urbana-Champaign,

1110 W. Green Street, Urbana, Illinois 61801, U.S.A.

In two recent papers,[1,2] A. J. Leggett and I developed an exact quantum mechanical upper bound on the rate at which two deuterium atoms in palladium in equilibrium can overcome their repulsive Coulomb barrier and tunnel to zero separation, thus giving rise to a fusion reaction. Underlying the mathematics is the very simple physical observation that from the point of view of the solid-state environment, two deuterium at zero separation look to the medium like a ^{4}He atom. If solid-state effects favor having two deuterium at zero separation, then one should also find enhanced binding of ^{4}He.

Experimentally the deuterium affinity, K_d, is[3] 2.4 eV in Pd. While we were unable to discover any published direct measurement of the helium atom affinity, K_4, for Pd or Ti, the fact that at room temperature ^{3}He desorbs[4] from Ti and forms bubbles[5] in Pd suggests that, as for other metals, K_4 is at best very small ($\ll$ 1 eV). While it would be very useful to have accurate data for the ^{4}He affinity, there is no evidence of solid-state enhancement of the binding of ^{4}He.

The technical argument can be summarized as follows: first, writing the tunneling rate from radius r as usual as e^{-B}, we demonstrate, by judicious choice of variational wavefunctions for the exact many-body ground state, the inequality:

$$B(\mu, r, E) \geq B_0(\mu, r, E),$$

where μ is the reduced mass of the tunneling nuclei, and B_0 is the rate that would be calculated in the lowest Born-Oppenheimer approximation for tunneling from any radius r in the classically inaccessible region of that approximation. Second we combine this result

with an exact lower bound for B_0 employing the affinity data, to show that for two isolated deuterons in Pd or Ti a very conservative upper limit on the probability density of two deuterons to be at the origin at zero temperature is $2 \times 10^{-31}/\text{cm}^3$. This number is to be compared with the value of order $10^{-7}/\text{cm}^3$ needed to understand the more conservative claims for a positive fusion rate. In other words, equilibrium zero-temperature solid-state physics provides an upper limit some 23 order of magnitude too small.

As discussed in ref. 1, to attain the necessary $\sim 10^7$ enhancement in equilibrium at room temperature would require unprecedented long range thermal effects of distant particles on the tunneling process. Similarly to attain the necessary enhancement by means of collective processes among the deuterons, would require a totally unphysical value of the deuteron pair correlation, $\sim 10^7$, at atomic separations.

One should note that these arguments place strong constraints on any model for enhanced fusion in solids; as a minimum, such a model should be tested for its prediction of the binding energy of ^4He in the solid. It is too easy to produce inter-deuteron potentials that yield large fusion rates, if the potentials are not constrained at zero separation to describe correctly helium in the solid.

References

1) A. J. Leggett and G. Baym, Phys. Rev. Letters **63**, 191 (1989).

2) A. J. Leggett and G. Baym, Nature **340**, 45 (1989).

3) R. Lässer and G. L. Powell, *Phys. Rev. B***34**, 578 (1986).

4) P. Bach, *Radiation Effects (GB)* **78**, 77 (1983).

5) G. J. Thomas and J. M. Mintz, *J. Nuc. Mat.* **116**, 336 (1983).

Theory (Topical Discussant: Gordon Baym, University of Illinois)

It is completely appropriate that the summary of theory come last in this meeting, since we are searching for new experimental phenomena in an area in which theory must be supported by consistent, systematic data. Any search for "anomalous phenomena" is, in its early stages, an experimentally, not theoretically, driven field. It is all to easy at this point for theorists to construct theories to explain one or another bit of data, independent of what other experiments are revealing.

To summarize the major theoretical issues, discussed in the earlier gathering of the theorists here, one must distinguish three classes of phenomena. First is the question of equilibrium versus nonequilibrium processes, involving conventional physics as we know it. The second is the question of whether one is confronting some kind of exotic nuclear physics – of which many suggestions were offered– or is there yet other new physics, for example, the possibility that one is seeing a breakdown of elementary quantum mechanics for events having very small probability. This latter issue has not, in fact, been adequately tested in the laboratory. As agreed by the theorists present, it is necessary to stay as close as possible to conventional physics for as long as one can hold out, and only when driven up to the wall should theorists start to invoke new physics. It is very important, in particular, that one should study the limits imposed by conventional physics. I gave an example in the theory session of the theoretical limits on fusion in the equilibrium ground state of a system. What other limits does conventional theory impose?

Coming down to particulars, one can identify two future directions for theoretical research: materials problems, on the one hand, and nuclear reaction mechanisms on the other. The materials issues can be divided into static, i.e., basically equilibrium, problems, versus dynamic, although this distinction is a rather artificial, since there is a large overlap between the two.

Most important is to have a strong understanding, through good systematic studies, of the elementary properties of the various materials being dealt with, as well as studies of possible variations of the materials. Theorists need to understand better the energetics involved in these materials, carrying out more extensive calculations of their electron band

structure, including fundamental determinations of electron screening effects.

While much is already known, one could use further studies of questions such as where, as a function of hydrogen concentration, the different isotopes of hydrogen prefer to sit in the lattice; in which states is tritium, for example, expected in palladium. Do there exist special sites, which may be due to impurities, where tritium and the other hydrogen isotopes prefer to live? How strongly does ^{4}He bind to palladium? What does deuterium do in systems such as palladium at large concentrations? Should one expect yet-to-be discovered clustering phenomena? Does there exist a phase transition beyond a critical loading in the β-phase to a state with large numbers of clusters? What are the expected dynamics associated with clusters, if there is in fact cluster formation? Theory will require considerable experimental information, obtained by neutrons, x-rays, and other methods, on highly loaded materials. Unfortunately, we have a paucity of data on many of these questions, data that will be needed for a fuller theoretical picture of the possibilities of fusion.

Generally, one needs to enlarge the perspective and branch out to study the hydrogen-hungry materials, those with high hydrogen affinity, and those with large diffusivity in particular. Are there other materials, such as alloys of the various hydrides, that have the potential to give interesting results?

Problems of surface physics need serious theoretical attack, to characterize and understand the microstructure, and other properties of hydride surfaces. What lives on surfaces? What is the effect of lithium, for example?

The theorists identified a list of problems in the category of dynamic processes, which need both theoretical and experimental attack. How do the isotopes of hydrogen diffuse in materials of high hydrogen affinity, as well as in the corresponding hydrides? Because diffusion involves very low-mass particles, the process is not simply classical but has a considerable quantum component via tunneling, with simultaneous dissipation. What are the effects of stresses and strains on these systems? How, for example, does deuterium interact with strain fields? The issue here is not simply a question of statics, but one should also concentrate on time-dependent effects, including determining the responses to finite frequency stresses, and finite frequency electric and even magnetic fields. Theorists should be on the lookout for threshold phenomena in dynamical processes.

Another area requiring further work is the physics associated with cracks and voids. What, in particular, is the theoretical basis of acceleration across cracks, the role of external electric fields, and the requisite timescales, compared to those for diffusion and electrical conduction.

The above questions are, by and large, conventional materials issues; however they

are ones which the present community has considerable impetus to study in much greater detail.

Turning now to questions of nuclear reactions, one immediate issue is whether one should have confidence in the present understanding of low-energy reaction cross sections at energies down to a few electron volts? Can there be unusual mechanisms that can take place? Do there exist relevant many-body effects in nuclear reactions, e.g., the suggestion we have heard of Coulomb interactions stimulated by nearby bodies exerting electric fields in the nuclear channels? Theoretical, as well as experimental, searchs ought not be limited simply to hydrogenic fusions, but should include reaction mechanisms involving other elements: palladium, lithium, uranium, beryllium, etc.

One interesting possibility is that of exotic neutron-transfer mechanisms, processes involving hypothetical new particles, "champs" or "misshuggetrons," for instance. Such processes would have to occur at sufficiently low probabilities not to be seen readily in accelerator experiments. Important here is to determine limits on masses and interaction strengths of such particles. High-energy physicists and cosmologists have much experience with the problem of placing such constraints on particles. For example, comparison of primordial nucleosynthesis with observed light element abundances indicated rather early that there can exist at most three species of neutrino, a result recently verified in measurements of the width of the Z^0. A further example are the useful constraints that have been placed on hypothesized new particle masses from study of supernovae.

Generally, any exotic reaction would have to be consistent with what we already know about low-energy systems, information gathered both theoretically and experimentally in over a half-century of low energy nuclear physics; they would also have to be consistent with our experience with conventional fission reactors and thermonuclear explosions, as well as astrophysical systems. As Edward Teller correctly pointed out, one must not postulate things that one would have noticed in the normal procedures of nuclear physics. A further caveat in invoking such exotic mechanisms is to understand why matter is stable in the presence of the mechanism. Why, for example, should heavy water be stable, given that its density of deuterons is quite comparable to that in highly-loaded Pd. Eventually one should also ask whether the present data on nuclear products is sufficiently compelling to search fully for such mechanisms?

One possible reaction mechanism certainly calling for further study is a chain reaction, triggered, for example, by a cosmic ray entering the system. Cosmic rays are not easily avoided, even underground. Very helpful would be to know the results of experiments with cosmic-ray detectors providing coincidence data with other activity in an electrolytic cell. A very nice example of such a study has been the search in superfluid liquid ^{3}He

at millikelvin temperatures, to see if the transition from the superfluid A to B phase – which, when thermodynamically preferred, requires a cooperative nucleation involving many particles – is triggered by a cosmic ray producing local heating and subsequent nucleation of the thermodynamically favorable phase.

Theorists must, should the present experiments resist theoretical explanation within the framework of conventional chemistry and solid-state physics, remain open to the possibilities of chemistry revealing new nuclear physics. I was pleased to learn recently that the first chemical element discovered in America (of atomic number 61), was discovered in 1926 by chemists at my university, from which it took its original name, "Illinium."

The following points were raised in the discussion following the summary:

It was stressed that when looking for new or exotic phenomenon, there may be strange induction periods. If one postulates something not usual, there may be an indication that it was not there at the inception; it may be produced in the apparatus before the main effects are visible. Another point stressed was that where tritium has been seen in a reaction which appears to be favored over the other branches, the energetics should be checked. One may have an indication of the participation of another particle which can carry away energy from the system. All such additional facts deduced from the observations should be taken into account, thus limiting the choice of the exotic effects which should be considered. However, the experimentalist should not ignore puzzling results or coincidences, for they may have real meaning to a theoretician.

It was mentioned that palladium deuteride and palladium hydride have peculiar superconducting properties. Palladium is not superconducting, but palladium hydride begins to be, when the H/Pd ratio rises above 0.6, an effect presumably connected with the β phase. The general rule is that the heavier isotope has the lower transition temperature. An exception is palladium hydride, where palladium deuteride has the higher T_c, with palladium tritide having an even higher value, perhaps 10 or 20 % different. This is a sizable effect. An explanation for this is in itself challenging, and it may well give details about the behavior of palladium hydride in its normal state, and thus about the boundary conditions for calculations. For instance, there is the question whether there can be more than one hydrogen in one octahedral site. The answers to questions of this kind are not full explanations, but they can influence the approach to explanations. Superconductivity indicates changes in band structure or mobility, and in general, about association of electrons, not of hydrogen nuclei. However, association of electrons can then lead to

conclusions about the distribution of the hydrogen nuclei, which is of more direct interest. Do the superconducting anomalies correlate with similar anomalies in diffusivity axnd in other phenomena?

However, it was then pointed out that the inverse isotope effect is known for a number of materials other than palladium, and is explained for these systems as the result of Coulomb potential changes. A T_c difference of one or two kelvin is well understood. It can be analyzed and understood in terms of different couplings to local optical modes for deuteride vibration at the octahedral site and has nothing to do with multiple occupancy.

Finally, the issue of the band structure of the deuterides themselves, viewed as ionic entities, was raised. This question has interplay with diffusivity and may also correlate with ionically-mediated superconductivity.

DISCUSSION (BAYM)

Hoffman: Did you state that helium is lost from palladium? Its diffusion in palladium is very slow.

Mansour: Helium certainly stays within palladium. Even after heat treatment, some still remains behind.

Baym: There is no evidence of any unusual binding between helium and palladium.

Kim: How did you calculate the nuclear matrix?

Baym: I am assuming that those are the experimentally measured values.

Chubb: How do you include phonon-deuteron interactions? You appear not to be doing so exactly, since you are treating them as individual fluctuations at a site.

Teller: If I understand the reasoning correctly, you use two steps to estimate the reaction probability. You use a theorem which is not exact, but it gives the upper limit to the rate, taking into account the Gamow tunneling factor.

Baym: It is more complex, but it is effectively as you say.

Teller: You then take the matrix element which contains assumptions independent of the Gamow factor. The two nuclei are now in contact, but the history of how they reached that position is no longer relevant. The estimated Gamow tunneling factor has been considered. The experimentally determined matrix element for the two particles in contact is now used to estimate the reaction rate. I agree entirely with this approach.

Baym: Thank you. I assume standard laboratory nuclear physics, and then I ask what effect the presence of the solid lattice can have.

Chubb: How does the Coulomb barrier enter into the expression?

Baym: I do not want to spend time over all the mathematical details, but the trick is to take a sequence of trial many-bodied wave functions which give bounds on the exact expression.

Chubb: Do the many-bodied wave functions contain the electron structure of the metal, for example, Bloch functions?

Baym: I have not considered the detailed wave function. I have used the Born-Oppenheimer approximation to give the bounds on the exact potential.

Teller: Thus, you consider a one-sided limit.

Baym: The other side would be too cumbersome to determine.

Chubb: You said that you have used an effective Gamow barrier height of 1.78 eV?

Baym: That value should be approximately correct.

Mansour: Your calculations for the reaction probability are based on a special case of r close to zero. What is your feeling about the corresponding probability for a separation distance of 0.5 angstroms, which would be more practical when referring to a crystal lattice?

Baym: For such reaction distances, I would suggest the use of the classical turning point in reaction space.

Chubb: I believe that the squares of the energy nuclear expressions which you use are incorrect in these circumstances. This analysis is not valid for the well-screened environment in which species are ionically bounded in a periodic lattice structure.

Baym: I would disagree with you.

Chubb: Do the pair-correlation functions which you use possess the appropriate periodicity?

Baym: Of course.

Chubb: If you are using the correct periodicity, and if you consider the different particle sites correctly, you should then proceed to the calculations of the transition matrix. In my view, the distances involved are far apart, perhaps 12 lattice vector distances. You should not be concerned with $r = 0$. The expression should be $r = r_n$ or $r = r_n + d$. In addition, you are considering a periodic environment in which you are attempting to calculate a matrix element. The events which you are considering are scattering processes over a periodic environment, which would require periodic density correlation functions, i.e., Green's functions which possess Bloch symmetry.

Baym: I am considering the nuclear forces in the matrix.

Chubb: The nuclear forces depend upon the overlap of the nuclear part of the interaction with other forces. I would also like to point out that for particles which possess small zero-point energies, the use of the Born-Oppenheimer approximation is valid.

Baym: I believe that the use of Born-Oppenheimer assumption is reasonable, although I certainly cannot prove it.

Rafelski: Because the nuclear reaction produces a charged particle in the space where fusion has occurred, any coherence which was present at the start of the process will break down.

Baym: My point is that a coherence mechanism of this kind would not work, and I do not propose to use such a mechanism.

Danos: I have a comment which is relevant to Dr. Baym's presentation. One has Coulomb forces between two charged particles. They collide as deuterons, but a type of Born-Oppenheimer transition occurs involving the neutron in a preassociation of the type described in the Oppenheimer-Phillips paper. The

neutrons have no barrier to penetrate, but low and higher order configurational correction terms are required to estimate the probability. Two photons are formed. The expressions are shown in the figures. One takes the terms to generate the series of states, and then the higher configurations are mixed in using the Coulomb forces. It happens that the mixing of the higher configurations is highly probable, as the calculations show. The figures refer to the D-D process, but the mechanism is generalized and would apply to other postulated processes. For D-D, the matrix element is equal to 10^{17} per second. To obtain the overall rate, one squares the matrix element and multiplies it with the appropriate preexponential factor. The rates obtained are of the correct order of magnitude, i.e., between 10^{-7} and 10^{-25} or 10^{-30} per second.

Baym: The energy which you use for the intermediate state is large, which implies that dissociation will occur. How do you obtain enhanced rates by mixing with a state with a large energy denominator?

Danos: I do not believe that dissociation will occur, since the energies in the higher order process are not large.

Section 26

NUCLEAR THEORY HYPOTHESES FOR "COLD FUSION"

Yeong E. Kim

Department of Physics

Purdue University

Nuclear Theory Hypotheses for "Cold Fusion"*

Yeong E. Kim
Department of Physics, Purdue University
West Lafayette, IN 47907

ABSTRACT

Based on nuclear theory hypotheses, a consistent and plausible explanation is described for tritium production and excess heat generation above that due to the electrode reaction recently reported by Fleischman, Pons, and Hawkins (FPH) and others in their electrolysis experiments. A surface reaction mechanism is proposed for electrolysis experiments in which deuterium-deuterium (D-D) fusion takes place in the surface zone of Pd cathode where whiskers of metal deuterides are formed in the electrolysis experiments. Conventional theoretical estimates of the D-D fusion rate at room temperature are critically re-examined and are shown to be inadequate. Other nuclear theory hypotheses involving neutron-induced reaction processes, which may occur subsequent to and concurrent with the D-D fusion, are also discussed. Experimental tests of the proposed mechanism and new improved devices for the cold fusion are suggested.

Introduction

Tritium production and excess heat generation above that due to the electrode reaction observed by Fleischman, Pons, and Hawkins (FPH) [1] and others [2-5] in their electrolysis experiments with a palladium cathode immersed in heavy water (with 0.1M LiOD) can not be explained by conventional theoretical estimates for deuterium-deuterium (D-D) fusion, since the estimated D-D fusion cross-sections and rates are too small at room temperature. However, the conventional theoretical estimates of the cold D-D fusion rate and branching ratio are arbitrary and may not be valid since they are based on an extrapolation of the reaction cross-sections at higher energies ($\gtrsim 3keV$) to lower energies where no direction measurements exist, except the indirect measurements of FPH and others. Recent experimental results indicate that the extrapolation method is not valid at low energies. Plausible nuclear theory explanations are discussed. Experimental measurements of the D-D fusion cross-sections and branching ratios at very low energies are suggested. In order to explain the FPH effect, a surface reaction mechanism is proposed for the cold D-D fusion with electrolysis. Experimental tests of the proposed mechanism and new improved electrolysis devices for cold fusion are discussed. A dynamical cold D-D fusion theory should be formulated in terms of a four-nucleon scattering problem in which both Coulomb interaction and nuclear forces are included and also both elastic and inelastic channels are treated on an equal basis.

Theoretical Estimates for Cold D-D Fusion

Because of the complexity of the four-nucleon system, no rigorous theoretical calculations of the D-D fusion rates and branching ratios have been carried out. Recent estimates [6, 7-9] for the D-D fusion rate of D atoms bound in metals at room temperature are mainly based on a formulation of the D-D fusion rate for the D_2 molecule. The fusion rate, $\Lambda(sec^{-1}$ per D-D pair), of

the D_2 molecule $(E < 0)$ is expressed as

$$\Lambda = A|\Psi_{D_2}(r_N)|^2,$$

with the total intrinsic nuclear reaction rate given by

$$A = \frac{S(E = 0)}{M_D c^2} \frac{c}{\pi \alpha} \approx 1.5 \times 10^{-16} cm^3 sec^{-1}$$

where the S-factor, $S(E = 0) = 0.1$ MeV barn [10], is extrapolated from the experimental values of the S-factor, $S(E)$ with $E \gtrsim 3keV$ [24]. The probability density of finding two D's within $r_N \lesssim 8F$ is found to be [6, 7-9],
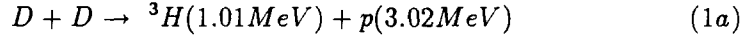
$$|\Psi_{D_2}(r_N)|^2 \sim (10^{-31} cm^{-3} \sim 10^{-58} cm^{-3}),$$

which is obtained from solutions of the Schroedinger equation with a diatomic potential for the D_2 molecule or D atoms imbedded in Pd. With the above values of A and $|\Psi_{D_2}(r_N)|^2$, the fusion rate per D-D pair is estimated to be [6, 7-9],
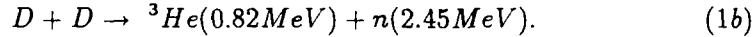
$$\Lambda = A|\Psi_{D_2}(r_N)|^2 \sim (10^{-47} sec^{-1} \sim 10^{-74} sec^{-1}),$$

which is at least thirty-seven orders of magnitude smaller than the observed rate $(10^{-10} sec^{-1})$ inferred from excess heat generation [1, 2, 4] and tritium production [3, 5].

With $E \gtrsim 0$ appropriate for a surface reaction mechanism described later for the electrolysis experiments [1-5], two dominant channels for the D-D fusion are

$$D + D \rightarrow {}^3H(1.01MeV) + p(3.02MeV) \tag{1a}$$

and

$$D + D \rightarrow {}^3He(0.82MeV) + n(2.45MeV). \tag{1b}$$

Reaction (1a) is not a "real" fusion but a neutron-transfer reaction, while reaction (1b) is a fusion reaction in which two protons are fused to form a ${}^3He$ nucleus. The reaction rate, R_{DD}, for (1a) or (1b) is given by [10]

$$R_{DD} = n_D \Lambda(E_o) = \frac{n_D n_D}{2} < \sigma v > (cm^3 sec^{-1})$$

with

$$< \sigma v > = \frac{(8/\pi)^{1/2}}{M^{1/2}(E_o)^{3/2}} \int \sigma(E) E e^{-E/E_o} \, dE$$

where E_o is the "average" kinetic energy and the cross-section, $\sigma(E)$, is parameterized as (E is in the c.m.)

$$\sigma(E) = \frac{S(E)}{E} e^{-(E_G/E)^{1/2}} \tag{2}$$

in the conventional estimates assuming that non-resonant charged particle reactions for reactions (1a) and (1b). E_G is the "Gamow energy" given by $E_G = (2\pi\alpha Z_D Z_D)^2 Mc^2/2$ or $E_G^{1/2} \approx 31.28(keV)^{1/2}$ with the reduced mass $M \approx M_D/2$. The extrapolated values (S(E $\approx$ 0) $\approx$ 55keV - barns) of the S-factors for both reactions (1a) and (1b) are nearly equal at $E \approx 0$, although S(E) for reaction (1b) is slightly larger than S(E) for reaction (1a) for $E \gtrsim 20keV$ [11].

If there is no resonance behavior for $\sigma(E \lesssim 3keV)$ and the above relation (2) between $\sigma(E)$ and S(E) turns out to be valid for $0 < E \lesssim 3keV$, then a minimum value of the "average" kinetic energy (c.m), $E_o \approx 75eV$, is required to obtain the claimed value of $\Lambda \approx 10^{-10} sec^{-1}$ [1, 3] for reaction (1a), since $R_{DD} = (n_D^2/2) < \sigma v > \approx 1.8 \times 10^{14} cm^{-3} sec^{-1}$ (or $\Lambda \approx 0.3 \times 10^{-10} sec^{-1}$ per D-D pair) with $< \sigma v > \approx 10^{-31} cm^3 sec^{-1}$ and $n_D \approx 6 \times 10^{22} cm^{-3}$ in the Pd cathode or in heavy water [1, 3]. However, there are currently no known mechanisms which enable deuterium atoms to gain average kinetic energies of $\gtrsim 75eV$ and at the same time suppress reaction (1b) in the electrolysis experiments with the Pd cathode [1, 3, 5]. For the claimed value of $\Lambda \approx 10^{-23} sec^{-1}$ [12] for reaction (1b), deuteron "average" kinetic energy (c.m.) of $E_o \approx 15eV$ is required.

Eq. (2) is valid only for the case of one charged particle scattering off another like charge. For scattering problems involving many nucleons such as reactions (1a) and (1b), eq. (2) is to be modified [13]. $S(E \approx 0) \approx 394keV - barn$ has been used to fit the experimental values of the cross-sections for reaction (1a) at deuteron kinetic energies (lab.) of $E \approx 4, 6, 8, 10$, and 12 keV [14]. Rigorous tests of eq. (2) at $E \lesssim 3keV$ are yet to be carried out

by future experimental measurements. Justification of eq. (2) has not been demonstrated by theoretical calculations based on a dynamical four-nucleon theory for reactions (1a) and (1b).

Conventional theoretical estimates of the cold D-D fusion rate and branching ratio are arbitrary and may not be valid since they are based on an extrapolation of the reaction cross-sections at higher energies ($\gtrsim 4keV$) to lower energies where no direct measurements exist, except the indirect measurements of FPH and others. Recent experimental results of Beuhler, Friedlander and Friedman [15] at $\sim 0.3keV$ show that both the fusion rate and the branching ratio for ($^3H - p$) channel are extremely large as in the case of the FPH effect compared to the conventional estimates, thus indicating that the extrapolation method is not valid at low energies. For E = 0.15 keV in the c.m. (corresponding the case of Beuhler et al. [15] with 0.3 keV in the laboratory system), the use of eq. (2) gives $\sigma_{calc}(E \approx 0.15keV) \approx 3 \times 10^{-57}cm^2$ for both reactions (1a) and (1b). For the case of $(D_2O)_{100}$ clusters accelerated to 300 keV (corresponding to deuteron C.M. energy of ~ 0.15 keV), deuteron flux, Φ, is approximately $\sim 1.25 \times 10^{12}cm^{-2}sec^{-1}$ in their experimental setup [15, 16]. The observed reaction rate of R ≈ 0.05 sec^{-1} for reaction (1a) is related to the cross-section, $\sigma(E)$, by

$$R = n\sigma(E)\Phi t A,$$

where n is the deuteron density in the target TiD, t is the target thickness and A is the surface area (~ 1 cm^2) of the target. For an effective interaction thickness of t $= 10^{-5}cm$, the above relation leads to $\sigma_{exp}(E \approx 0.15keV) \approx 0.67 \times 10^{-31}cm^2$ which is 25 orders of magnitude larger than $\sigma_{calc}(e \approx 0.15keV) \approx 3 \times 10^{-57}cm^2$ obtained from eq. (2) [16].

The results of $\sigma_{exp}(E \approx 0.15keV) \approx 0.67 \times 10^{-31}cm^2$ extracted from the experiment by Beuhler et al. [15] can be regarded as the first direct measurement of $\sigma_{exp}(E)$ at $E \approx 0.15keV$ for reaction (1a), and also as an experimental test invalidating the conventional extrapolation method based on eq. (2) at low energies. It also supports the recent results of enhanced D-D fusion rates observed in electrolysis experiments by Fleischmann et al. [1] and others [3,

5, 12].

Another significance of the experimental results of Beuhler et al. [15] is that the reaction rate for (1b) appears to be substantially suppressed compared with that of reaction (1a) in their experiment, contrary to the conventional assumption of nearly equal rates for both (1a) and (1b). The suppression of reaction (1b) and enhancement of reaction (1a) at low energies have also been observed in the recent electrolysis experiments by Wolf et al.[3], Iyengar [5], and others. One possible explanation is that there may be a broad resonance behavior in $\sigma(E)$ for reaction (1a) but not in $\sigma(E)$ for reaction (1b), which is plausible since the final state Coulomb interaction is present in reaction (1a) but not in reaction (1b). If $\sigma(E)$ happens to have resonance behavior near $E \approx 0$, the extrapolation may yield erroneous values of $\sigma(E \approx 0)$ or $S(E \approx 0)$, since the non-resonant relation (2) is not applicable to resonance reactions. Therefore, it is very important to investigate the possibility of resonance behavior for $\sigma(E)$ near $E \approx 0$ theoretically, and also to measure $\sigma(E \approx 0)$ directly with precision experiments.

Recent observation of neutron bursts at $-30°C$ at a rate of $\Lambda \approx 10^{-23} sec^{-1}$ reported by Menlove et al. [17] may be interpreted as the existence of a sharp resonance in the reaction channel (1b).

At present, there are no direct experimental measurements and theoretical calculations of the branching ratios for reactions (1a) and (1b) below $E \lesssim 3kev$. One would expect the branching ratio of reaction (1a) to be larger than that of reaction (1b), since reaction (1b) involves a fusion of two protons to form ^3He while reaction (1a) does not fuse two protons but merely transfers a neutron from one deuteron to another to form ^3H (known as the "deuteron stripping reaction" in nuclear physics). Theoretical calculations of the reaction cross-sections and branching ratios of reactions (1a) and (1b) are being carried out based on four-nucleon scattering theory [18] using nucleon-nucleon forces and the Coulomb interaction.

Direct experimental tests of the above interpretation of the results of the electrolysis experiments [1-5] and Beuhler et al. [15] can be carried out by measuring $\sigma(E)$ for both reactions (1a) and (1b) at the energy range of $0 \lesssim$

$E \lesssim 0.3keV$, using the inverse reactions, $p(^3H, D)D$ and $^3H(p, D)D$ for (1a) and $^3He(n, D)D$ for (1b) in addition to using the direct reactions (1a) and (1b).

Surface Reaction Mechanism for Cold D-D Fusion

If the experimental result of Beuhler et al., $\sigma_{exp}(0.15keV) \approx 10^{-7}b$, is conclusively confirmed in future experiments, smaller average deuterium kinetic energies of $E_D \approx 1 \sim 10eV$ are needed to obtain the reaction rates of $\Lambda \approx 10^{-10} \sim 10^{-23}sec^{-1}$ for reactions (1a) and (1b). There are no known mechanisms which can provide $E_D \approx 1 \sim 10eV$ for deuterium atoms imbedded in Pd lattice sites in the electrolysis experiments. However, it is possible to generate the average kinetic energies of $E_D \approx 1 \sim 10eV$ in the surface zone outside the Pd cathode as described below.

It is known that whiskers of Pd deuteride and/or LiD form on the cathode surface in electrolysis experiments in which the Pd cathode is immersed in D_2O with 0.1 M $LiOD$ electrolyte. These whiskers are known to occupy the surface zone of $\gtrsim 10\mu m$ thickness, where most of D_2 gas bubbles are formed from the dissociation of D_2O. Depending on electrolysis conditions, many spherical and hemispherical D_2 gas bubbles of varying sizes (radii ranging from few μm to few mm) will be produced continuously in the surface whisker zone and will stay there for certain time durations before they move out of the electrolysis cell. Most of these D_2 gas bubbles in the surface whisker zone will have whiskers protruding into the bubbles creating field emission potentials around the tips of whiskers. The average potential in each D_2 bubble is expected to be approximately that of the applied potential of the electrolysis cell, but the electric field near the whisker tips can be several orders of magnitude larger than the average field, as is well known from field emission studies. Due to this electric field, D^+ ions in the bubble will gain kinetic energies with a statistical distribution which depends on the bubble size and values of the

varying electric field inside the bubble. The average kinetic energy of the D^+ ions in each bubble is expected to be $1 \sim 10eV$, when the applied potential is $1 \sim 10V$.

The surface reaction mechanism described above is consistent with the recent observation reported by Appleby et al. [2] that the use of NaOD does not produce excess heat during electrolysis, since whiskers may not form with NaOD electrolyte (without Li) during electrolysis.

The surface reaction mechanism for cold D-D fusion can be tested by measuring the production rates of fusion products of reactions (1a) and (1b) from field emission experiments in which metal deuteride tips (Pd deuteride, Ti deuteride, etc.) are surrounded by D_2 gas at different pressures in a container with different values $(1 \sim 10V)$ of applied electric potential.

Cold Fusion Devices with AC Field

If the surface reaction mechanism turns out to be a correct mechanism for cold D-D fusion, new improved devices can be designed based on the same mechanism. One of the promising designs is to use both DC and AC fields as described below.
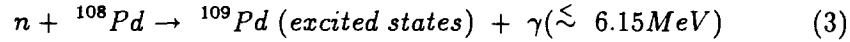
One particular design with AC field is shown in Figs. 1(a) and 1(b). The sample is a metal sheet which can be deuterated to a high degree (such as Pd, Ti, NiLa, etc.) and which can form whiskers on its surface with a high density and large depth. Pt electrodes on both sides of the sample sheet are also sheets or flat wire meshes. Initially the electrolysis is carried out with DC voltage $(1 \sim 10V)$ using the sample as a cathode and Pt as anodes, as shown in Fig. 1(a). After deuteriums are loaded into the sample maximally and whiskers have grown on both sides of the sample, the DC voltage is switched to AC voltage as shown in Fig. 1(a) or Fig. 1(b). For both cases of Fig. 1(a) and Fig. 1(b), a small negative voltage bias can be applied to the sample in order to retain deuterium atoms in the sample.

There are two important advantages for the use of AC field. The first advantage is that a much higher value (up to 10^3V) of the AC voltage can be used without dissociating D_2O too rapidly. With a higher voltage, the

D-D fusion rates can be scaled up substantially. The second advantage is that the size and stability of D_2 gas bubbles in the surface reaction zone can be controlled by adjusting the modulating frequencies ($100 \sim 40,000 cps$) of the AC field, which can be used to maximize D^+ flux in D_2 gas bubbles and to increase the D-D fusion rates for reactions (1a) and (1b).

Neutron-Induced Chain-Reaction Hypotheses

A neutron-induced chain reaction hypothesis [19] has been proposed, which involves radiative neutron capture in the Pd cathode,

$$n + {}^{108}Pd \rightarrow {}^{109}Pd \ (excited\ states) \ + \ \gamma(\stackrel{<}{\sim} 6.15 MeV) \qquad (3)$$

with the resultant γ-rays ($\stackrel{<}{\sim} 6.15 MeV$) breaking up deuterium in Pd and heavy water by photodisintegration,

$$\gamma(\stackrel{<}{\sim} 6.15 MeV) + D \rightarrow p + n - 2.225 MeV \qquad (4)$$
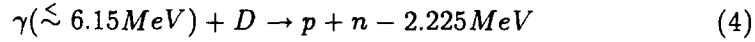
which generates neutrons with kinetic energies $\stackrel{<}{\sim} 2 MeV$. The cross-section for reaction (3) is large at thermal energies $\sigma = (8.3 \pm 0.5)b$ [20]. The reaction rate (cross-section times velocity, σv) for reaction (3) is also large, $\sigma_{nPd} v_n \approx 2.64 \times 10^{18} cm^3 sec^{-3}$. The cross-section for (4) has a maximum value of $\sigma \approx 2.5 mb$ at $E_\gamma \approx 4 MeV$, and a value of $\sigma \approx 2 mb$ at $E_\gamma \approx 6 MeV$ [21]. Hence the reaction rate is $(\sigma c) \sim 7 \times 10^{-17} cm^3 sec^{-1}$. These neutrons can then feed back into reaction (3) thereby establishing a chain reaction which is designated as (3) $\rightarrow$ (4). The chain reaction, (3) $\rightarrow$ (4), may be initiated by reaction (3) with neutrons generated from reaction (1b).

In addition to reaction (3), there are other possible radiative neutron-capture reactions such as

$$n + {}^{105}Pd \rightarrow {}^{106}Pd (excited\ states) + \gamma \qquad (3b)$$
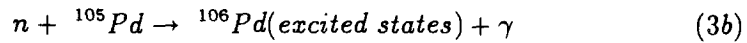
which has a sizable cross-section ($20.0 \pm 3.0b$) at thermal energies [20]. There are additional radiative neutron capture processes by other Pd isotopes but their cross-sections are much smaller than those of reaction (3) and (3b): $\sigma_{n\gamma} \approx$

$3.4 \pm 0.3b$ for $^{102}Pd(n,\gamma)$, $\sigma_{n,\gamma} \approx 0.6 \pm 0.3b$ for $^{104}Pd(n,\gamma)$, $\sigma_{n,\gamma} \approx 0.293 \pm 0.029b$ for $^{106}Pd(n,\gamma)$ ^{107}Pd (g.s., $6.5 \times 10^6 yr$ half-life), $\sigma_{n,\gamma} \approx 1.8 \pm 0.2b$ for $^{107}Pd(n,\gamma)$, $\sigma_{n,\gamma} \approx 0.190 \pm 0.030b$ for $^{110}Pd(n,\gamma)$ ^{111}Pd (g.s., 23.4 *min* half-life)[20]. The natural abundances of Pd are 1.02% ^{102}Pd, 11.14% ^{104}Pd, 22.33% ^{105}Pd, 27.33% ^{106}Pd, 26.46% ^{108}Pd, and 11.72% ^{110}Pd [20].

Another neutron-induced chain-reaction hypothesis is that of neutron induced fission-fusion process [22-24]. The first stage of the fission-fusion process is ignited by neutrons from reaction (1b) and/or reaction (4), which produces tritium (^3H or T) via the following fission reaction,

$$n + \, ^6Li \rightarrow \, ^4He(2.05MeV) + T(2.73MeV), \tag{5}$$
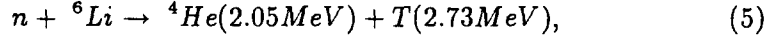
with kinetic energies indicated in parentheses. The cross-section for reaction (5) is very large at thermal energies ($949 \times 10^{-24} cm^2$) [25]. The reaction rate (cross-section times velocity, σv) for reaction (5) is also very large, $\sigma_{nLi} v_n = (2.1 - 1.3) \times 10^{-16} cm^3 s^{-1}$, for a range of neutron energies up to 14 MeV [26]. The natural abundances of Li are 7.5% ^6Li and 92.5% ^7Li.
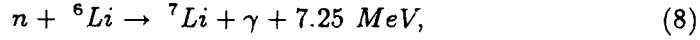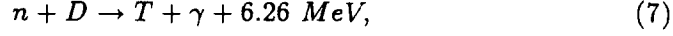
The second stage of the process is T-D fusion with T(2.73 MeV) generated from the first stage (5) and/or from reaction (1a),

$$T + D \rightarrow \, ^4He(3.52MeV) + n(14.07MeV). \tag{6}$$
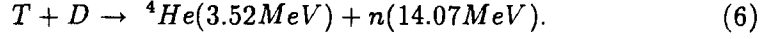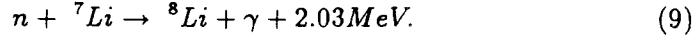
The T-D fusion cross-section is maximum ($\sim 10^{-23} cm^2$) at a T kinetic energy of ~ 100 keV and is nearly three orders of magnitude larger than the D-D fusion cross-section for the same D kinetic energy. The T-D fusion reaction rate for reaction (6) is large [27], $\sigma v \gtrsim 10^{-16} cm^3 s^{-1}$, for T(10 keV $\sim$ 10 MeV).

Both chain-reaction hypotheses (3) $\rightarrow$ (4) and (5) $\rightarrow$ (6) for the FPH effect lead to a set of predictions which can be tested experimentally. However, very low reported values [3, 28-30] of the neutron production rate ($\lesssim 10^{-23} sec^{-1}$ per D-D pair) compared with the reported rates of tritium production (~ 6 hour burst, $10^{-10} sec^{-1}$) [3] and excess heat generation ($\sim$ days to weeks, with an inferred D-D fusion rate of $10^{-10} sec^{-1}$) [1, 2, 4] are inconsistent with the chain-reaction hypotheses, (3) $\rightarrow$ (4) *or* (5) $\rightarrow$ (6) at present.

The reaction rates for reactions (4) and (6) may be comparable with neutron-induced reactions (3), (3a), and (5) which may occur using neutrons produced from reaction (1b), concurrent with reactions (1a) and (1b). Other neutron induced reactions, which may contribute to produce nuclear products, are

$$n + D \rightarrow T + \gamma + 6.26 \ MeV, \tag{7}$$

$$n + {}^6Li \rightarrow {}^7Li + \gamma + 7.25 \ MeV, \tag{8}$$

and

$$n + {}^7Li \rightarrow {}^8Li + \gamma + 2.03 MeV. \tag{9}$$
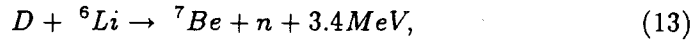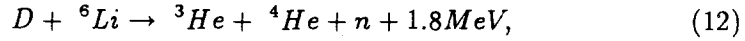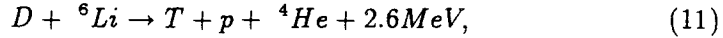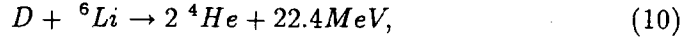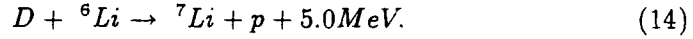
The cross-sections for reactions (7),(8), and (9) are 0.519 ± 0.007 mb, 0.0385 ± 0.0030b and 0.0454 ± 0.003b, respectively, at thermal neutron energies [20]. Reaction (5) is expected to proceed much faster than reactions (8) or (9), because of its larger cross-section.
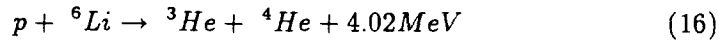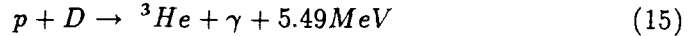
Possible reactions involving ${}^6Li$ and D are:

$$D + {}^6Li \rightarrow 2 \ {}^4He + 22.4 MeV, \tag{10}$$

$$D + {}^6Li \rightarrow T + p + {}^4He + 2.6 MeV, \tag{11}$$

$$D + {}^6Li \rightarrow {}^3He + {}^4He + n + 1.8 MeV, \tag{12}$$

$$D + {}^6Li \rightarrow {}^7Be + n + 3.4 MeV, \tag{13}$$

and

$$D + {}^6Li \rightarrow {}^7Li + p + 5.0 MeV. \tag{14}$$
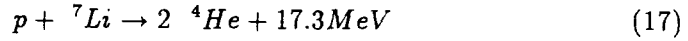
Possible reactions invoiving p from reaction (1a) are:

$$p + D \rightarrow {}^3He + \gamma + 5.49 MeV \tag{15}$$

$$p + {}^6Li \rightarrow {}^3He + {}^4He + 4.02 MeV \tag{16}$$

and

$$p + {}^7Li \rightarrow 2 \ {}^4He + 17.3 MeV \tag{17}$$

All of reactions (5), (8) - (14), (16) and (17) involving Li are expected to occur preferentially in the surface zone of Pd cathode, since the Li density is higher there.

Monte Carlo simulation calculations of all of reactions, (3) $\rightarrow$ (17), will be needed for specific geometries of each electrolysis experiments in order to choose and discriminate these reactions when conclusive experimental data for nuclear products become available in the future.

Summary

Recent experiments [1-5, 12, 15] have demonstrated that (i) reaction (1b) is suppressed while reaction (1a) is enhanced at low energies $E \lesssim 0.15 keV$, (ii) the conventional extrapolation estimates of the D-D fusion rates at low energies are at least 20 orders of magnitude smaller than the low energy experimental results [1-5, 12, 15] and hence are invalid, and (iii) the FPH effect is a nuclear fusion phenomenon because of the experimental observations of tritium production reported previously by Wolf et al.[3] and Iyengar [5], and also reported by others at this workshop.

For the purpose of establishing conclusively that the FPH effect is due to the D-D fusion (1a), it is important and urgent to measure the D-D fusion cross-sections at low energies, $0 \lesssim E \lesssim 0.3 keV$, using the inverse reactions, $p(^3H, D)D$ and $^3H(p, D)D$ for reaction (1a) and $^3He(n, D)D$ for reaction (1b) as well as the direct reactions (1a) and (1b), in addition to improving the electrolysis experiments using new devices with AC voltage. The proposed surface reaction mechanism for the cold D-D fusion should be tested with the use of the new devices and with the proposed field emission experiments.

Contrary to many highly publicized claims, there are no reliable theoretical calculations of the D-D fusion cross-sections at near zero positive energies. Rigorous theoretical calculations based on four-nucleon scattering theory are yet to be carried out for the D-D fusion at low energies.

REFERENCES

1. M. Fleischmann, S. Pons, and M. Hawkins, Journal of Electroanalytic Chemistry, **261**, 301 (1989); and errata, **263**, 187 (1989).

2. A. J. Appleby, S. Srinivasan, Y. J. Kim, O. J. Murphy, and C. R. Martin, "Evidence for excess heat generation rates during electrolysis of D_2O in LiOD using a palladium cathode - a microcalorimetric study", a talk presented by Appleby at Workshop on Cold fusion Phenomena, May 23-25, 1989, Santa Fe, New Mexico; "Anomalous calorimetric results during long-term evolution of deuterium on palladium from lithium deuteroxide electrolyte" submitted to Nature; A. J. Appleby, Y. J. Kim, O. J. Murphy, and S. Srinavasan, "Specific effect of lithium ion on anomalous calorimetric results during long-term evolution of deuterium on palladium electrodes", submitted to Nature.

3. K. L. Wolf, N. J. C. Packham, D. R. Lawson, J. Shoemaker, F. Cheng, and J. C. Wass, "Neutron emission and the tritium content associated with deuterium loaded palladium and titanium metals", in the Proceedings of Workshop on Cold Fusion Phenomena, May 23-25, 1989, Santa Fe, New Mexico, to be published in J. Fusion Energy.

4. A. Belzner, U. Bischler, G. Crouch-Baker, T. M. Gur, G. Lucier, M. Schreiber, and R. Huggins "Two fast mixed-conductor systems: deuterium and hydrogen in palladium-thermal measurements and experimental considerations", presented by R. A. Huggins, in the Proceedings of Workshop on Cold Fusion Phenomena, May 23-25, 1989, Santa Fe, New Mexico, to be published in J. Fusion Energy.

5. P. K. Iyengar, "Cold Fusion Results in BARC Experiment", in the Proceedings of the 5th International Conference on Emerging Nuclear Energy Systems (ICENES V), Karlsruhe, West Germany, July 3-6, 1989.

6. C. D. Van Siclen, and S. E. Jones, J. Phys. G; Nucl. Phys. **12**, 213 (1986).

7. A. J. Leggett and G. Baym, "Exact upper bound on barrier penetration probabilities in many-body system: application to cold fusion", Phys. Rev. Lett. **63**, 191 (1989).

8. S. E. Koonin and M. Nauenberg, "Calculated fusion rates in isotopic hydrogen molecules", Nature **339**, 690 (29 June 1989).

9. K. Langanke, H. J. Assenbaum, and C. Rolfs "Screening corrections in cold deuterium fusion rates", Z. Phys. A - Atomic Nuclei **333**, 317 (1989).

10. W. A. Fowler, G. R. Caughlan, and B. A. Zimmermann, Ann. Rev. Astr. Astrophys. **5**, 525-570 (1967).

11. N. Jarmie and N. E. Brown, Nucl. Inst. Method **B10/11**, 405-410 (1985); A. Krauss, H. W. Becker, H. P. Trautvetter, and C. Rolfs, Nucl. Phys. A **465**, 150 (1987).

12. S. E. Jones et al., Nature **338**, 737 (27 April 1989).

13. H. A. Bethe, Rev. Mod. Phys. **9**, 166 (1937).

14. A. von Engel and C. C. Goodyear, Proc. Roy. Soc. A **264**, 445 (1961).

15. R. J. Beuhler, G. Friedlander, and L. Friedman, Phys. Rev. Lett. **63**, 1292 (1989).

16. Y. E. Kim, "Comment on Cluster-Impact Fusion", PNTG-89-11 (October 1989).

17. H. O. Menlove et al., "The measurements of neutron emissions from Ti plus D_2 gas", in the Proceedings of Workshop on Cold Fusion Phenomena, May 23-25, 1989, Santa Fe, New Mexico, to be published in J. Fusion Energy.

18. O. A. Yakubovsky, Yad. Fiz. **5**, 1312 (1967) [Sov. J. Nucl. Phys. **5**, 937 (1967)]; P. Grassberger and W. Sandhas, Nucl. Phys. **B2**, 181 (1967); E. O. Alt, P. Grassberger and W. Sandhas, J.I.N.R. Report No. E4-6688 (1972).

19. Y. E. Kim, "Neutron-induced photonuclear chain-reaction process in palladium deuteride", PNTG-89-7 (July 1989).

20. S. F. Mughabghab et al. *Neutron Cross Sections*, Vol. 1, Academic Press, N.Y. (1981).

21. E. Segre, *Nuclei and Particles*, W. A. Benjamin, Inc. New York (1965) p. 422.

22. Y. E. Kim, "New cold nuclear fusion theory and experimental tests", an extended summary of a talk presented at Workshop on Cold Fusion Phenomena, May 23-25, 1989, Santa Fe, New Mexico, to be published in J. Fusion Energy.

23. Y. E. Kim, "Hybrid inertial confinement fission-fusion for large scale power generation", Purdue Nuclear Theory Group Report PNTG-89-10 (September 1989).

24. Y. E. Kim, "Neutron-induced tritium-deuterium fusion in metal hydrides", Purdue Nuclear Theory Group Report PNTG-89-4 (April 14, 1989); "Fission-induced tritium-deuterium in metal deuterides", PNTG-89-5 (June, 1989).

25. T. Lauritsen, and F. Ajzenberg-Selove, Nucl. Phys. **78**, 39 (1966).

26. H. Goldstein, and M. H. Kalos, "An Index to the Literature on Microscopic Neutron Data", NDL-SP-10, Nuclear Defense Laboratory, Edgewood Arsenal, MD (1964); Nuclear Data Tables.

27. D. L. Book, "NRL Plasma Formulary", Naval Research Laboratory Publication 0084-4040 (Revised 1987).

28. R. D. Petrasso, et al., Nature **339**, 183 (1989); and erratum, **339**, 264 (1989).

29. M. Fleischmann, S. Pons, and R. J. Hoffmann, Nature **339**, 667 (1989).
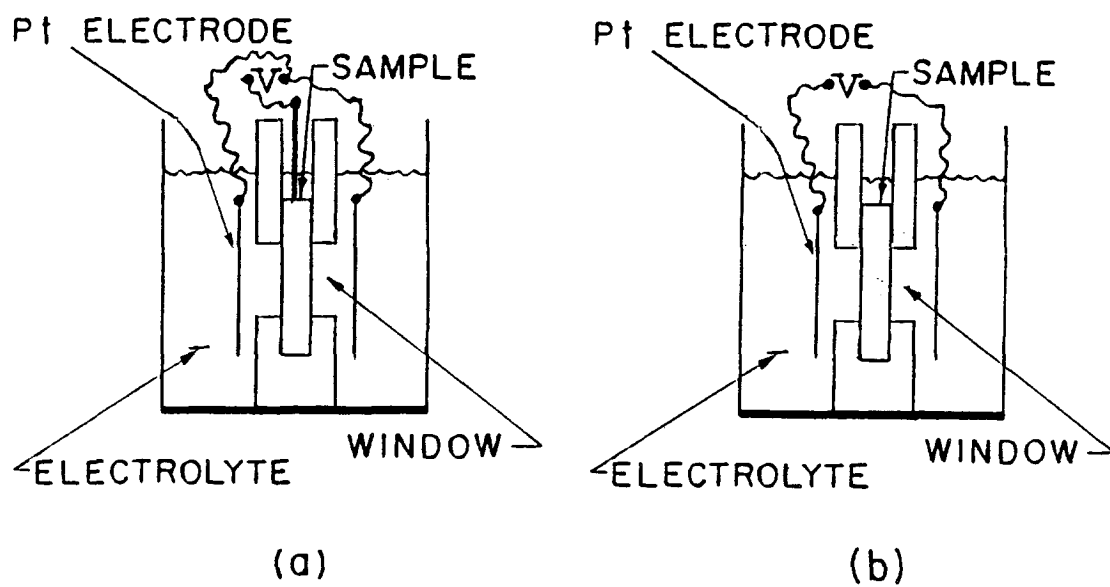
30. R. D. Petrasso, et al., Nature **339**, 667 (1989).

Fig. 1　A new device with AC field for cold D-D fusion

DISCUSSION (KIM)

Rafelski: You appear to be using standard astrophysical expressions in your theory.

Kim: That is correct.

Rafelski: Since this is textbook theory, the answer could have been given without the derivations.

Kim: I intended this as a tutorial for the chemists, who are not familiar with the background.

Chubb: There are also solid-state physicists here, and I certainly appreciate it.

Baym: What temperatures do you assume to obtain the rates reported by Dr. Jones?

Rafelski: On the order of 15 eV, but the kinetic energy at which fusion occurs is a hundred times greater. The reasoning corresponds to that in the 1936 Gamow-Teller formula.

Baym: After you remove the Gamow tunneling term from your data, you obtain a straight-line relationship. For DD fusion, the two channels are not identical because of the imposed forces. You extrapolate your results to zero energy, and I would question that. If a resonance energy exists, such an extrapolation is not possible. Your assumptions will then be invalid. Concerning the Brookhaven data shown in your figure, Dr. Bond indicates that the He-3 energy spectrum could not be detected because of X-ray interference, yet the amount was still consistent with the normal ratio in the two fusion product channels.

Kim: On the other hand, if you interpret the data as a cross section for monoenergetic deuteron, the rate is at least 10 orders of magnitude larger than that predicted from the standard Gamow tunneling calculation. The extrapolation is done to show this discrepancy. If the Brookhaven data can be accepted as correct, Dr. Jones's results will not require deuterons with an energy of 15 eV. Based on this assumption, their energy could be much less than 15 eV. The calculations should be treated as a scattering problem with a deuteron velocity distribution, not as a bound-state problem.

Appleby: If we suppose that Dr. Jones's data refer to the same process, how does that relate to the situation for palladium under electrolysis conditions? What deuteron energies would be required to account for the rate probabilities?

Kim: About 100 eV without a velocity distribution.

Appleby: For the gas-phase experiment, the highest deuteron energy would be expected to be equal to some multiple of kT, so that a very small fraction would

have an energy of, say, 1 eV. The average energy of the discharging deuteron in the electrolysis experiments might be about 1 eV. This would be many times higher than that in the gas-phase experiments. Would that energy difference account for the increased rate?

Kim: It may be sufficient.

Baym: I believe that you are misrepresenting the problem. You state that the treatment should not involve a bound-state problem, but a scattering problem, since you suppose that the deuterons in the many-bodied system are in motion until they reach a classical turning point at a distance of a fraction of an angstrom. However, a close look shows that the physics is in fact the same.

Kim: I disagree. The scattering treatment with a velocity distribution is appropriate for a surface reaction mechanism and can give very different results from a bound-state treatment.

Rafelski: The orders of magnitude used here must be established properly because they are confusing. I have already mentioned the Gamow-Teller equation. This would indicate that at an equivalent temperature of 5 eV, the maximum reaction rate occurs at around 200 eV. In other words, at a temperature 5 eV, the reaction occurs at 200 eV. Thus, at a given temperature the reaction occurs at a much higher energy, which seems to be impossible in a solid. If one computes the rates for a realistic 0.25 angstrom screening length, at 10 eV temperature, with reaction occurring at 200 eV, one can reach close to the supposed reaction rates. The D-D reaction rate dominates, but just barely.

Kim: I disagree. It may be possible in deuterium gas bubbles on the Pd surface.

Wolf: I have a standard question for the nuclear theoreticians concerning a well-documented physical problem. How effectively do your models describe the neutron-scattering length for slow neutrons in ortho- and para-hydrogen? This situation includes many of the ingredients of our present problem, including the wave functions and the nuclear spins of the hydrogen over about the same dimensions.

Rafelski: Since muon hydrogen is like a neutron, one can carry out this calculation. We have numerically solved the complex wave functions for the system. As a result of these calculations, I am confident that we understand the fusion processes.

Miley: Could you explain the difference between your and Dr. Kim's approaches?

Rafelski: He showed only the equations to be solved, whereas I showed the computed results.

Kim: The difference was the fact that I used standard equations involving a deuteron velocity distribution, whereas Dr. Rafelski used his own expressions for monoenergetic deuterons. I maintain that for low-energy nuclear reactions, the calculation must be done under dynamic conditions as a four-nucleon scattering

problem, including both nuclear and Coulomb forces. We are only just starting to do that.

Miley: Concerning Dr. Baym's earlier question, why do you think one can violate the limit?

Baym: Dr. Kim is not violating the limit. Instead of using the average system energy, one assumes that the system is at some higher temperature.

Jones: After Dr. Wolf's challenge, have you applied the calculation to the published Brookhaven experiment? There seems to be a discrepancy between theory and experiment for the low-energy case.

Baym: I tried to fit the data, and I believe that the results indicate that fusion is possible in the 200 keV energy range. However, I would question whether the experiment was carried out correctly, and that the real energy was as they indicate.

Section 27

BOSON DYNAMICS OF DEUTERIUM IN METALS

K.B. Whaley

Department of Chemistry

University of California, Berkeley

Boson Dynamics of Deuterium in Metals

K.B. Whaley
Department of Chemistry
University of California, Berkeley
Berkeley, CA 94720

Abstract

The effects of coherent many-particle dynamics in providing local site density fluctuations at finite temperatures for hydrogen isotopes in metals, are analyzed with tight binding calculations based on a Hubbard hamiltonian. Boson species show marked enhancements, which increase with temperature, concentration and magnitude of the site-to-site tunneling amplitude. The effects of such fluctuations on deuterium dynamics at high concentrations are evaluated within a self-consistent formulation of the deuteron-deuteron interaction. Application to the nuclear regime yields estimates of finite temperature bosonic collective enhancements of nuclear reaction rates between deuterons in palladium deuterides.

The dynamics of hydrogen isotopes in metals is dominated by quantum transport. Phonon-assisted tunneling is believed to provide the primary mechanism for mobility below about 700 K [1]. There has been considerable theoretical work on the tunneling dynamics of isolated interstitial hydrogenic species in metals, but very little is understood about the high concentration behavior. In this regime, strong interactions between the interstitial species render the usual small polaron quantum treatment invalid, while the tunneling mechanism is inadequately described by classical hopping theories and simulations. Anomalies in the isotope dependence of diffusion coefficients for hydrogenic species near 1:1 interstitial:host concentration ratios [2] have led us to a model for tunneling dynamics at high concentrations which contains nuclear statistical effects. We use this model to demonstrate below that d + d fusion rates are enhanced by finite temperature Bose collective effects in the metallic environment.

The theory we outline here is based on a generalized Hubbard Hamiltonian for the dynamics of interstitial hydrogen isotopes in metals, which will act on particles of spin 1/2 (fermions) for hydrogen and tritium, and on spin 1 particles (bosons) for deuterium. The Hamiltonian is given by

$$\mathcal{H} = (-t)\sum_{\substack{\langle ij \rangle \\ \sigma}} c_{i\sigma}^{+} c_{j\sigma} + \frac{1}{2} U \sum_{\substack{i \\ \sigma\sigma'}} c_{i\sigma}^{+} c_{i\sigma'}^{+} c_{i\sigma'} c_{i\sigma} \tag{1}$$

where t is the single particle inter-site tunneling term between nearest neighbor sites ij, and U the two-particle intra-site repulsion. These two terms constitute the most important physics for hydrogen dynamics at high concentrations. The choice of statistics corresponds to the ionized form of the interstitial, as suggested by experimental dynamical studies [3]. Although the Hamiltonian is identical for fermions and bosons, its effect on many-body states is very different [4]. Previous calculations of the extent of delocalization of eigenstates in small periodic clusters, showed that the difference between statistics, rather than the magnitude of the spin is important [4], so we restrict ourselves here to the computationally simpler case of spin 0 for deuterium. We can solve this Hamiltonian exactly with a periodic cluster technique, obtaining the exact many-body eigenstates and energies for small clusters, either with or without periodic boundary conditions [4].

For application to the D/Pd system, we consider N=2 clusters without periodic boundary conditions, and N=4 clusters with periodic boundary conditions, as being representative of minimal and maximal ranges of coherent motion. The N=4 cluster could represent four inter-connected octahedral sites in the Pd fcc lattice, and the N=2 either two octahedral sites, or two tetrahedral sites. Generalization to clusters containing inequivalent sites is straightforward, but will require more detailed knowledge of the single particle tunneling amplitude t_{ij} than is currently available, in addition to the single site energies (omitted from eq.(1) since they provide only a constant term). The experimental isotope dependence of hydrogenic mobilities in Pd has been interpreted as implying coherent propagation in a band of excited vibrational states extending over an octahedral-tetrahedral-octahedral tunneling path [5]. The values of t in excited states will be larger than for ground vibrational states, and a detailed calculation for such a tunneling pathway will require specific knowledge of t between each pair of connected sites, for each band of vibrational states accessible at room temperatures. We shall consider, in what follows, a range of possible values of t for excited states.

These tight binding calculations are used to evaluate the thermally averaged local site density fluctuation operator

$$\left\langle (\delta n)^2 \right\rangle = \left\langle \overline{n_i^2} \right\rangle - \left\langle \overline{n_i} \right\rangle^2 \tag{2}$$

where

$$\overline{n_i} = \frac{1}{N} \sum_i n_i, \qquad \overline{n_i^2} = \frac{1}{N} \sum_i n_i^2 \tag{3}$$

and < > denotes a thermal average. Once the eigenstates of H have been determined for n particles on an N-site cluster, $<(\delta n)^2>$ is evaluated within the canonical ensemble at temperature T. $<(\delta n)^2>$ thus contains both a thermal average over the many-body states, and a site average over all sites i in the cluster of N interstitial sites. It is a measure of the temperature dependent density susceptibility within the cluster, i.e., of the local density fluctuations possible on each site, within the constraint of a constant cluster occupancy of n particles on N sites.

We evaluate this local susceptibility for a range of parameters U, t and kT, for both bosons and fermions on clusters of N=2 and N=4 sites, over a range of concentrations n/N. Figures 1 and 2 show the behavior of $<(\delta n)^2>$ as a function of n, for spin 1/2 fermions and spin 0 bosons, at various ratios of U/t on the 4-site cluster, with periodic boundary conditions. We find that the fluctuations are considerably greater for bosonic than for fermionic species under all conditions, and at all temperatures. At double site occupancy, i.e. n=2N, the fermionic fluctuations are zero as a consequence of Pauli exclusion, while the boson fluctuations continue to increase with density. Although this effect is most marked for U=0, even in this limit the increase of $<(\delta n)^2>$ with n is considerably suppressed relative to a free, ideal Bose-Einstein gas [6], reflecting the tight-binding nature of the motion. As temperature decreases, relative to U, the magnitude of the fluctuations decreases, even leading to a local minimum for bosons at single-site occupancy, n=N. The general conclusion is that as long as t is finite, small non-zero site density fluctuations are possible at full coverage, and are significantly greater than the corresponding fluctuations allowed in the atomic limit. Furthermore, these fluctuations increase with temperature, and for bosons, with concentration, n/N. For a given set of parameters U, t and kT, the absolute magnitude of $<(\delta n)^2>$ is decreased for the N=2 cluster without periodic boundary conditions, reflecting the reduced contribution of coherent single particle motion to enabling local site density fluctuations.

A conservative estimate of $<(\delta n)^2>$ for deuterium in Pd may now be obtained by adapting typical values of the Hubbard U and t parameters for interstitial hydrogen in metals, to Pd. Estimates of t range from $\sim 10^{-6}$ to ~ 1 meV in ground vibrational states of H, and up to 30 meV in excited states [1]. Since at room temperature the relevant values of t will be for excited states, as discussed above, an initial estimate of t~1 meV for D in Pd is reasonable. Estimation of U is not so straightforward, since for interstitial hydrogenic species, the repulsion U is a complex parameter expressing the overall repulsive energy between the nuclei and their associated electron distributions in the metal environment. U is thus essentially a screened Hubbard U, and will in general also be dependent on the vibrational level. Recent binding energy calculations allow us to obtain an approximate estimate of U~3 eV for the energy to take two hydrogen interstitials from adjacent octahedral sites and put them on the same site [7]. We expect however that U may actually vary from 1-10 eV, and a full ab initio calculation would very useful.

27-4

Table 1 summarizes $<(\delta n)^2>$ for D (bosons) in Pd, with $U/t=10^2$, 10^3, 10^4 and kT=1-25t. Both single site occupancy, n=N (PdD), and double site occupancy, n=2N (PdD$_2$) values are shown. Entries in rows 1,4 and 5 correspond to t=1 meV, kT=25 meV (room temperature) and U varying from 0.1-1.0 eV. Row 2 corresponds to parameters U=0.25 eV, t=2.5 meV, kT=25 meV, and row 3 to U=2.5 eV, t=25 meV, kT=25 meV. For comparison, rows 6 to 8 show the corresponding values at T=0, i.e. in the ground state.

The results shown in Figures 1-2 and Table 1 clearly show enhancement of local site density fluctuations for bosonic interstitial species. The magnitude of these fluctuations increases with the range of coherent motion, i.e. both by increasing N and also by employing periodic boundary conditions. These are equilibrium fluctuations, which exist at room temperature despite an unfavorable on-site repulsion energy U, because of the small but non-negligible contribution from coherent tunneling motion. Thus a large apparent repulsive energy between two deuterium species in one site does not necessarily mean that such configurations are impossible at room temperatures.

The effects of these enhanced boson density fluctuations on the deuteron-deuteron interaction is now evaluated within self-consistent linear response theory. In the Hubbard description, coulombic interactions of d+ with d+ are subsumed into U, and the collective motion of the d+ species is given by the Hubbard tight-binding dynamics. Treating the response of the metal electrons and the Hubbard screened d+ species independently, linear response yields an effective potential due to a charge Q,

$$V_{eff}(r) = \frac{Q}{r} - \iint dr' dr'' \frac{e}{|r - r'|} \chi_e(r'r'') V_{eff}(r'')$$

$$- \iint dr' dr'' \frac{e}{|r - r'|} \chi_d(r'r'') V_{eff}(r'')$$

(4)

27-5

for the effective potential at r due to a charge Q at the origin. Here χ_e and χ_d are the density-density susceptibilities of the electrons and of the Hubbard d+ species respectively. Note that eq.(4) could in principle be used to self-consistently determine the quantities χ_d and $V_{eff}(r)$, provided the electronic interactions were also well characterized. Within the present aims of understanding the maximal effects of $<(\delta n)^2>$, we neglect this interdependence, and consider U and χ_d as independent variables determining $V_{eff}(r)$. Fourier transforming, we obtain

$$\hat{V}_{eff}(k) = \frac{4\pi Q}{k^2 \varepsilon(k)}$$ (5)

$$\varepsilon(k) = \left[1 + 4\pi \frac{e^2}{k^2} (\hat{\chi}_e(k) + \hat{\chi}_d(k)) \right]$$ (6)

with

$$\hat{\chi}(k) = \beta \left\langle n_{-\underline{k}}; n_{+\underline{k}} \right\rangle$$ (7)

The behavior of the electronic contribution to $V_{eff}(r)$ is well known, consisting of a short-range screening charge distribution which can to first order be described at the Thomas-Fermi level, and a long-range oscillatory part deriving from the singularities of $\varepsilon(k)$[8]. To obtain order-of-magnitude estimates of tunneling through the Coulomb barrier, it suffices to consider only the short-range repulsive part of $V_{eff}(r)$. We can obtain an upper estimate of the screening of this by combining the Thomas-Fermi electronic screening contribution with the k-independent approximation to $\hat{\chi}_d(k)$, obtained from the Hubbard calculations

$$\hat{\chi}(k) = \beta \left\langle n_{-\underline{k}}; n_{+\underline{k}} \right\rangle \approx \beta \left\langle (\delta n)^2 \right\rangle$$ (8)

This yields a total screened Coulomb potential between two deuterons which contains a new 'boson screening' term, in addition to the usual electronic screening provided by the metal environment:

$$V_{eff}(r) = \frac{e^2}{r} e^{-K_s r} \tag{9}$$

with

$$K_s^2 = 4\pi e^2 N(\varepsilon_F) + 4\pi e^2 \beta \langle (\delta n)^2 \rangle = K_e^2 + K_d^2 \tag{10}$$

The boson screening arises from the ability of the mobile deuterons to respond collectively to local displacements of inter-deuteron separations. The procedure outlined above amounts to replacing χ_d by its value at an intermediate length scale, and also includes some degree of polarization of the electronic environment by the deuterons, by virtue of the screened Hubbard U parameter. Thus although its use down to the nuclear region is an extrapolation, it does not imply a completely uniform background, and so does not obviously violate the Born-Oppenheimer approximation.

Small values of $<(\delta n)^2>$ are sufficient to cause appreciable enhancement of the total screening. For example, $K_s = 2.76 \text{Å}^{-1}$ and 16.41Å^{-1} with $<(\delta n)^2> = 0.2 \times 10^{-3}$ and 0.29×10^{-1} respectively (Figure 3). These values of $<(\delta n)^2>$ correspond to stoichiometric PdD with coherent motion in the N=4 site cluster, with a) t~1 meV, U~1 eV, kT=25 meV, or b) t~25 meV, U~2.5 eV, kT=25 meV. In comparison, electronic screening alone yields $K_s = 2.40 \text{Å}^{-1}$ (with $N(\varepsilon_F) = 0.47$ states/eV/Pd for PdH [9]).

This boson screened coulomb potential is then used to estimate fusion rates for the reaction

$$d + d \rightarrow He^3 + n \tag{11}$$

The thermally averaged fusion rate is given by

$$\Lambda = \frac{1}{a^3} \langle A 2\pi\eta e^{-B} \rangle \tag{12}$$

where $A = 2 \times 10^{-16} \text{ cm}^3 \text{ s}^{-1}$ is the nuclear reaction rate constant, $\eta = e^2/\hbar v$ and B is the semiclassical WKB tunneling integral for the screened Coulomb potential:

$$B(E) = \frac{2}{\hbar} \sqrt{2\mu_{dd}} \int_{r_0}^{r_1} \sqrt{V_{eff}(r) - E} \ dr \qquad (13)$$

Eq. (12) contains a thermal average over different vibrational bands of states, in each of which both the relative kinetic energy E, and the screened potential $V_{eff}(r)$ will generally differ. For order of magnitude estimates it suffices to replace the full thermally averaged fusion rate by the room temperature contribution from a single band of vibrational states of D in Pd,

$$\Lambda = \frac{A 2\pi\eta}{a^3} e^{-B} \qquad (14)$$

We set E=298K, and v=2 x 10^5 cm s^{-1} (the velocity of a deuterium species in the ground vibrational state of an octahedral Pd site). The volume a^3 is the volume of an octahedral interstice, 0.774Å^3.

The boson screened fusion rates resulting from the range of values of $<(\delta n)^2>$ in Table 1, are shown in Figure 4, where they are seen to be strongly dependent on the magnitude of the density fluctuations. Two lower limits are of interest here. Firstly, the limit when $<(\delta n)^2>=0$, i.e. no boson screening. A fusion rate of $\Lambda = 4 \times 10^{-99}$ s^{-1} is obtained using the density of electronic states appropriate to stoichiometric PdD. This value, which is consistent with other recent calculations [10], is considerably less than that predicted for fusion in gas phase D$_2$ molecules [11]. This is a consequence of the low electron density in PdD, rather than of the delocalized nature of the metallic electrons. Secondly, the T=0 limit. The T=0 results obtained for both PdD and PdD$_2$ with ratios U/t > 10^3 lie below the upper bound of $\Lambda \sim 10^{-47}$ s^{-1} obtained by Leggett and Baym, assuming a deuterium affinity of Pd equal to that at low concentrations [12]. For U/t=10^2, the N=2 cluster results also lie below this, while the N=4 cluster rates lie above this bound. This implies that U/t>10^2 in the ground vibrational state, as expected (see above).

Analysis of the finite temperature fusion rates in PdD and PdD$_2$ can now be made subject to the aforementioned T=0 restrictions on parameter ratios U/t. Finite temperature rate enhancements can derive from population of excited vibrational states with a smaller ratio of U/t. We consider a realistic range of possible values of the Hubbard parameters U and t in excited

vibrational states to be given by $t\sim 1\text{-}25$ meV, $U\sim 0.1\text{-}10$ eV. Figure 4 shows that fusion rates of 10^{-25} s^{-1} and greater require $\langle(\delta n)^2\rangle$ to be greater than 6×10^{-2}. Analysis of the U,t,kT and N dependence of Λ leads to the following conclusions:

i) At room temperature, $kT\sim 25$ meV, fusion rates greater than $\Lambda\sim 10^{-25}$ s^{-1} are not possible if the range of coherent motion extends only to $N=2$ clusters. This holds for both PdD and PdD$_2$.

ii) Fusion rates are considerably enhanced by increasing the range of coherence to $N=4$ interstitial clusters. Now there exists a critical range of the ratio U/t between 10^2 and 10^3, over which room temperature fusion rates vary from negligibly small to detectable values. Thus for a) $t\sim 25$ meV and $U\sim 25$ eV, $\Lambda\sim 10^{-93}$ s^{-1}, while with b) $t\sim 25$ meV and $U\sim 2.5$ eV, $\Lambda\sim 10^{-31}$ s^{-1}, for PdD with $N=4$ site clusters ($kT=25$ meV). A similar U/t ratio with a larger kT/t ratio, c) $t\sim 1$ meV, $U\sim 0.1$ eV, $kT=25$ meV, yields $\Lambda\sim 10^{-19}$ s^{-1}. These three values refer to stoichiometric PdD. Recent experimental rates reported by some groups for reaction (11) are 10^{-23} s^{-1} [13]. These comparisons lead us to conclude that, given what is currently known about the energetics and dynamics of D in Pd, such fusion rates of 10^{-23} s^{-1} are unlikely in PdD since they require an unusually low value of U. (see above discussion)

iii) In this same regime however, the concentration dependence is dramatic. For example, with the previous set of parameters b), the rate increases to $\Lambda\sim 10^{-20}$ s^{-1} when PdD is replaced by PdD$_2$. Thus, although for stoichiometric PdD it therefore appears impossible to achieve rates of order $\Lambda\sim 10^{-23}$ with realistic values of U/t, it may well be possible with PdD$_2$.

We conclude that boson screening induced by finite temperature coherent dynamics of deuterons can induce huge enhancements over the d+d fusion rates in gas phase molecular D$_2$, and also over the corresponding T=0 rates in metallic Pd. This additional screening mechanism is significant, even for very small amounts of finite temperature boson fluctuations. It is very sensitive to both deuteron concentrations, and to the relative magnitudes of the Hubbard parameters U and t.

Several implications for experimental studies follow from this analysis of boson screening. Firstly, the estimates made here based on realistic values of U/t indicate that at least local ratios of

D:Pd greater than 1:1 are required to obtain rates comparable to those reported by Jones et al. [13]. Such locally high concentrations may obtain near the surface or associated with defects. More detailed knowledge of the D distribution at high concentrations would be useful. Secondly, given a high enough deuterium concentration, the boson screening mechanism described here would also be correspondingly effective in enhancing the rates of other fusion reactions in the metal. Several difficult theoretical issues are also raised. Our analysis of bosonic collective effects has assumed i) an approximate Hamiltonian, ii) linear response for the effective interaction, and iii) a k-independent dielectric constant. Each of these approximations must be critically examined and possibly superseded, to obtain more accurate estimates of finite temperature rates. More precise calculations of the Hubbard parameters, and of the effective dielectric constant, eq.(8), will be especially useful. The latter requires investigation of the dynamical interaction between the highly mobile and strongly interacting deuterons, and the electrons, at high concentrations. Nevertheless, despite the approximations made here, the magnitude of the fusion rate enhancements obtained with realistic parameters suggest that further exploration of environments favoring collective coherent motion will be extremely interesting.

References

1.   Y. Fukai and H. Sugimoto, Adv. in Phys. 34, 263 (1985); extensive references to recent theoretical and experimental studies are given here.

2.   S.C. Wang and R. Gomer, J. Chem. Phys. 83, 4193 (1985); R. DiFoggio and R. Gomer, Phys. Rev. B 25, 3490 (1982).

3.   H. Wipf, Ch. 7 in "Hydrogen in Metals II", ed. G. Alefeld and J. Volkl, Springer-Verlag 1978.

4.   K. B. Whaley and L.M. Falicov, J. Chem. Phys. 87, 7160 (1987).

5.   G. Sicking, Ber. Buns. Ges. Phys. Chem. 76, 790 (1972).

6.   E.M. Lifshitz and L.P. Pitaevskii, "Statistical Physics I", Pergamon Press 1980.

7.   O.B. Christensen, P.D. Ditlevsen, K.W. Jacobsen, P. Stoltze, O.H. Nielsen and J.K. Norskov, Phys. Rev. B 40, 1993 (1989).

8.   S. Dietrich and H. Wagner, Z. Phys. B 36, 121 (1979); H. Horner and H. Wagner, J. Phys. C 7, 3505 (1974); V.G. Vaks, N.E. Zein, V.G. Orlov and V.I. Zinenko, J. Less Comm. Met. 101, 493 (1984); K.H. Lau and W. Kohn, Surf. Sci. 75, 69 (1978).

9.   C.T. Chan and S.G. Louie, Phys. Rev. B 27, 3325 (1983); D.A. Papaconstantopoulos, B.M. Klein, J.S. Faulkner and L.L. Boyer, Phys. Rev. B 18, 2784 (1978); A.C. Switendick, Ber. Buns. Ges. Phys. Chem. 76, 535 (1972).

10.   A. Burrows, Phys. Rev. B 40, 3405 (1989).

11.   C.D. Van Siclen and S.E. Jones, J. Phys. G 12, 213 (1986); S.E. Koonin and M. Nauenberg, Nature 339, 690 (1984) (the values obtained here by more accurate calculations, predict $\Lambda \sim 10^{-64} s^{-1}$).

12.   A.J. Leggett and G. Baym, Phys. Rev. Lett. 63, 191 (1989).

13.   S.E. Jones, E.P. Palmer, J.B. Czirr, D.L. Decker, G.L. Jensen, J.M. Thorne, S.F. Taylor and J. Rafelski, Nature (London) 338, 737 (1989).

Table 1 $\langle(\delta n)^2\rangle$ for d+ in Pd, evaluated for a) N=4 site clusters with periodic boundary conditions, and b) N=2 site clusters without periodic boundary conditions. Integers in brackets refer to the power of 10.

U/t	kT/t	N=2		N=4	
		n=2	n=4	n=4	n=8
10^2	25	0.33(-1)	0.36(-1)	0.11	0.16
10^2	10	0.59(-3)	0.18(-2)	0.30(-1)	0.10
10^2	1	0.40(-3)	0.12(-2)	0.29(-1)	0.10
10^3	25	0.40(-5)	0.12(-4)	0.20(-3)	0.62(-3)
10^4	25	0.00	0.00	0.20(-5)	0.60(-5)
10^2	0	0.40(-3)	0.12(-2)	0.29(-1)	0.10
10^3	0	0.40(-5)	0.12(-4)	0.20(-3)	0.62(-3)
10^4	0	0.00	0.00	0.20(-5)	0.60(-5)

<u>Figure Captions</u>

Figure 1. $\langle(\delta n)^2\rangle$ for bosons (————) and fermions (••••••) in the N=4 site cluster with periodic boundary conditions, for the parameter ratio U/t=36, at temperatures a) kT=1000t, b) kT=10t, c) kT=t.

Figure 2. $\langle(\delta n)^2\rangle$ for bosons (————) and fermions (••••••) in the N=4 site cluster with periodic boundary conditions, with a) U=0, t=1, kT=10t, and b) t=0, U=36, kT=10.

Figure 3. V_{eff} (r) given by electronic and boson screening according to eqs.(9) and (10). i) Electronic screening alone, with $K_e = 2.40\text{Å}^{-1}$, corresponding to a Fermi surface density of states $N(\varepsilon_F) = 0.47$ states/eV/Pd for PdH [9] (————). ii) Electron and boson screening, with $K_s = 2.76\text{Å}^{-1}$, corresponding to $\langle(\delta n)^2\rangle = 0.2\times10^{-3}$ (– – – –). iii) Electron and boson screening, with $K_s = 16.41\text{Å}^{-1}$, corresponding to $\langle(\delta n)^2\rangle = 0.29\times10^{-1}$ (••••••) (Table 1).

Figure 4. $Log_{10}\,\Lambda$ as a function of log $\langle(\delta n)^2\rangle$ for the reaction d + d → ^{3}He + n. Λ is evaluated with eqs. (9-10) and (13-14). Circles indicate the points obtained with the values in Table 1. (An additional point for $\langle(\delta n)^2\rangle$=1.0 is shown for reference.)

U/t=36, kT=1000

Figure 1a

U/t=36, kT=10

Figure 1b

U/t=36, kT=1

Figure 1c

U=0, t=1, kT=10
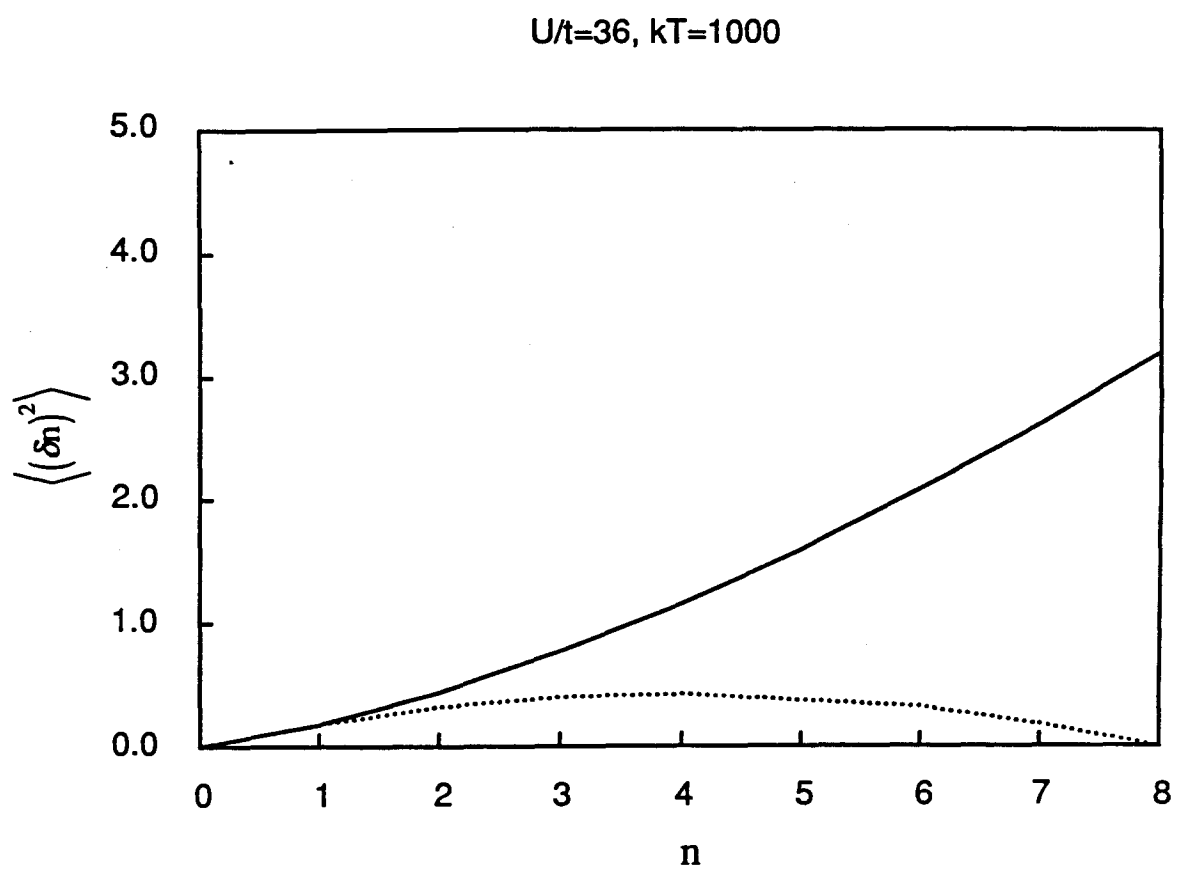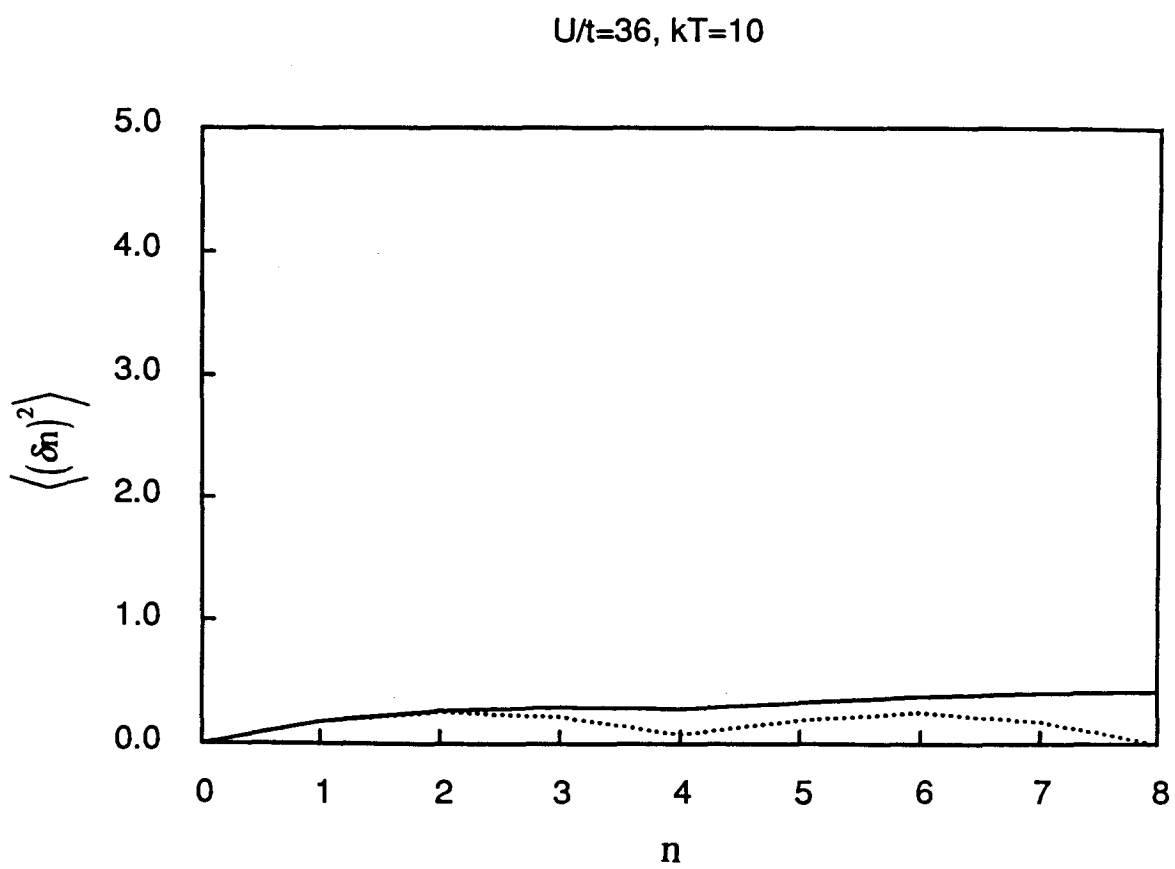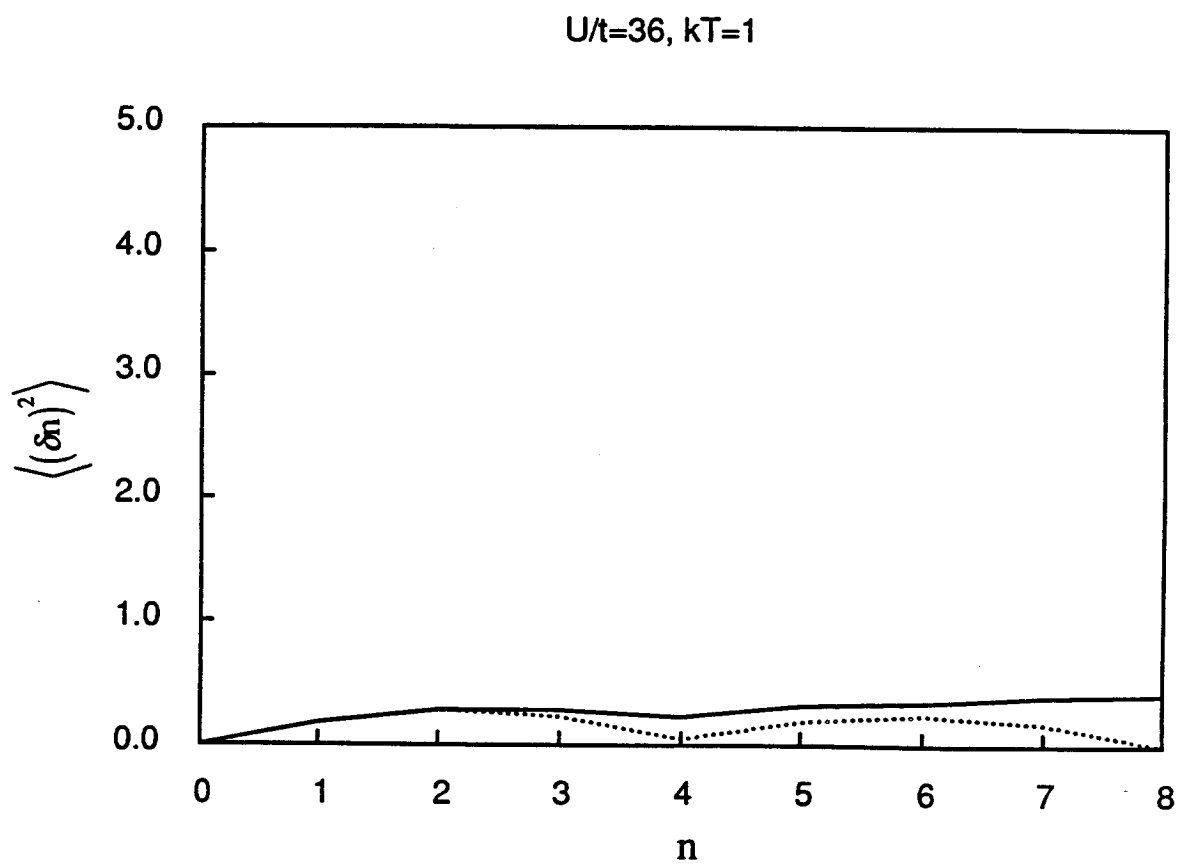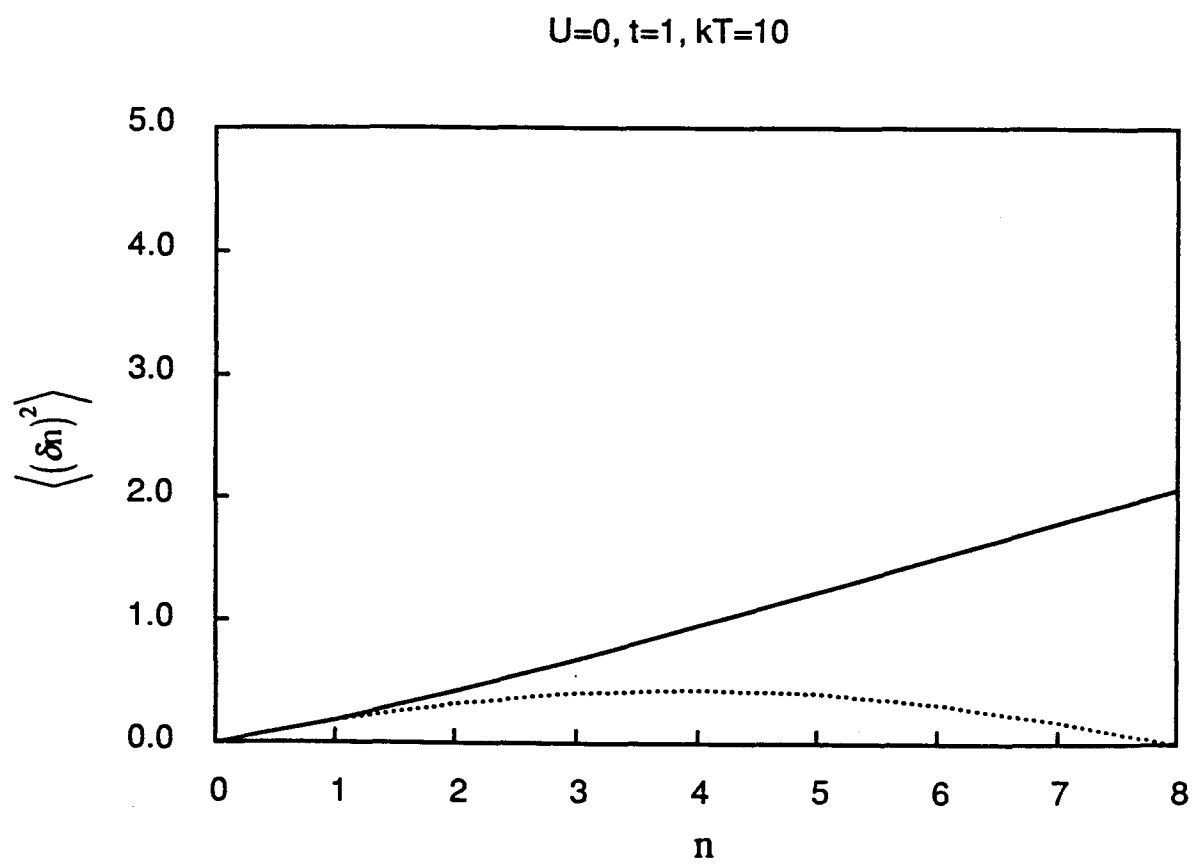
Figure 2a

U=36, t=0, kT=10
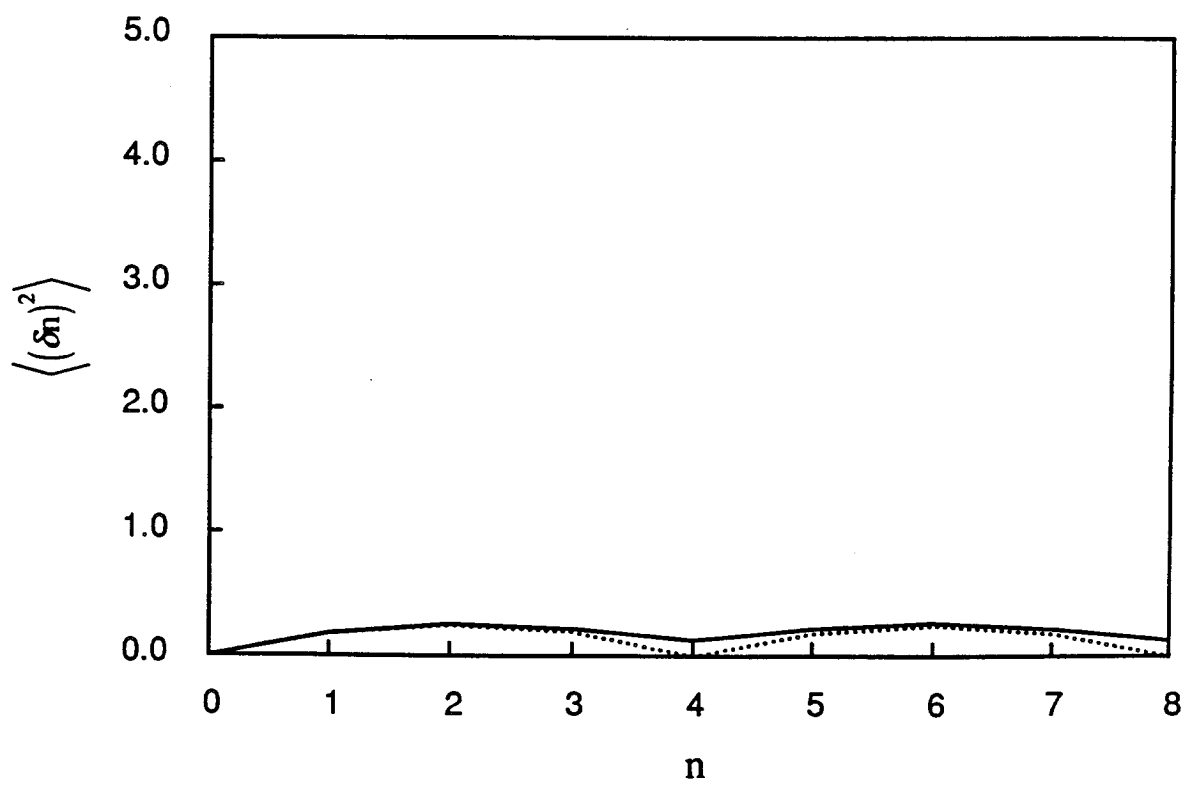
Figure 2b
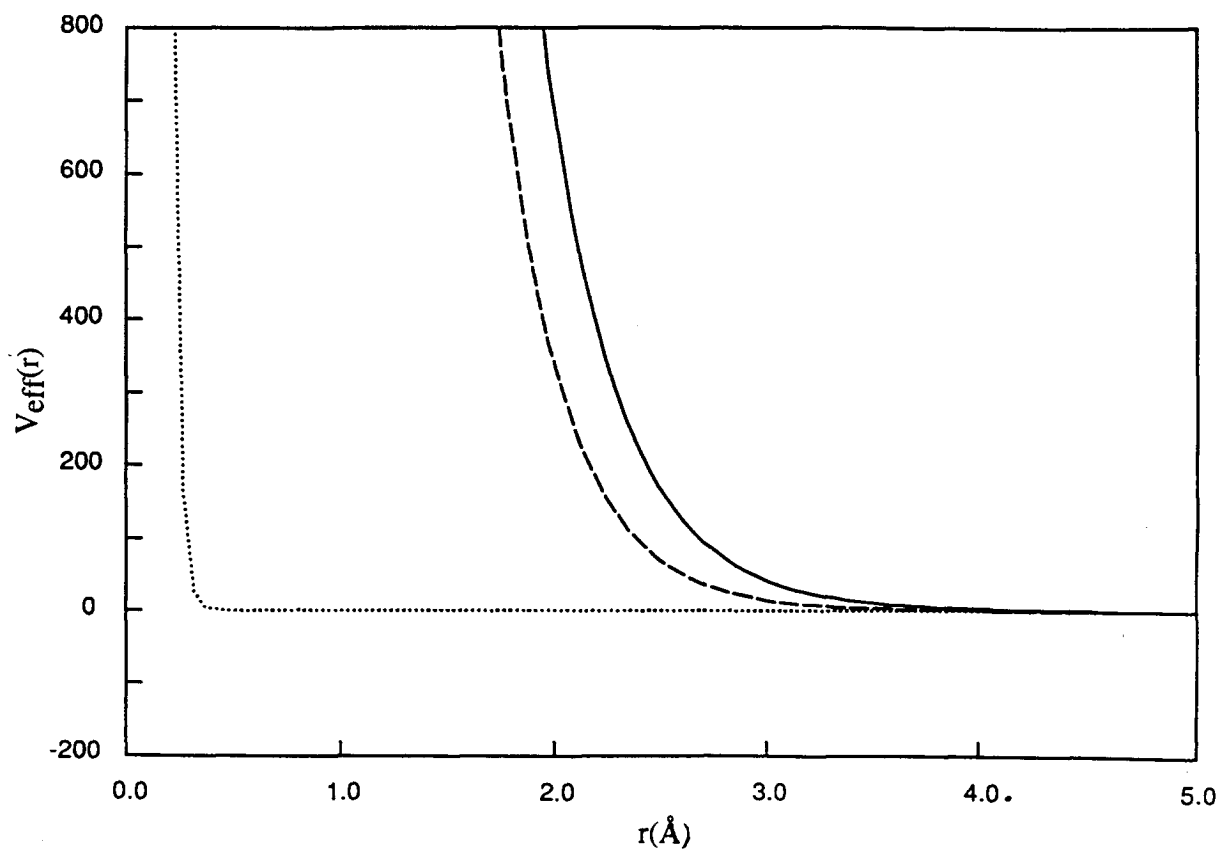
Figure 3
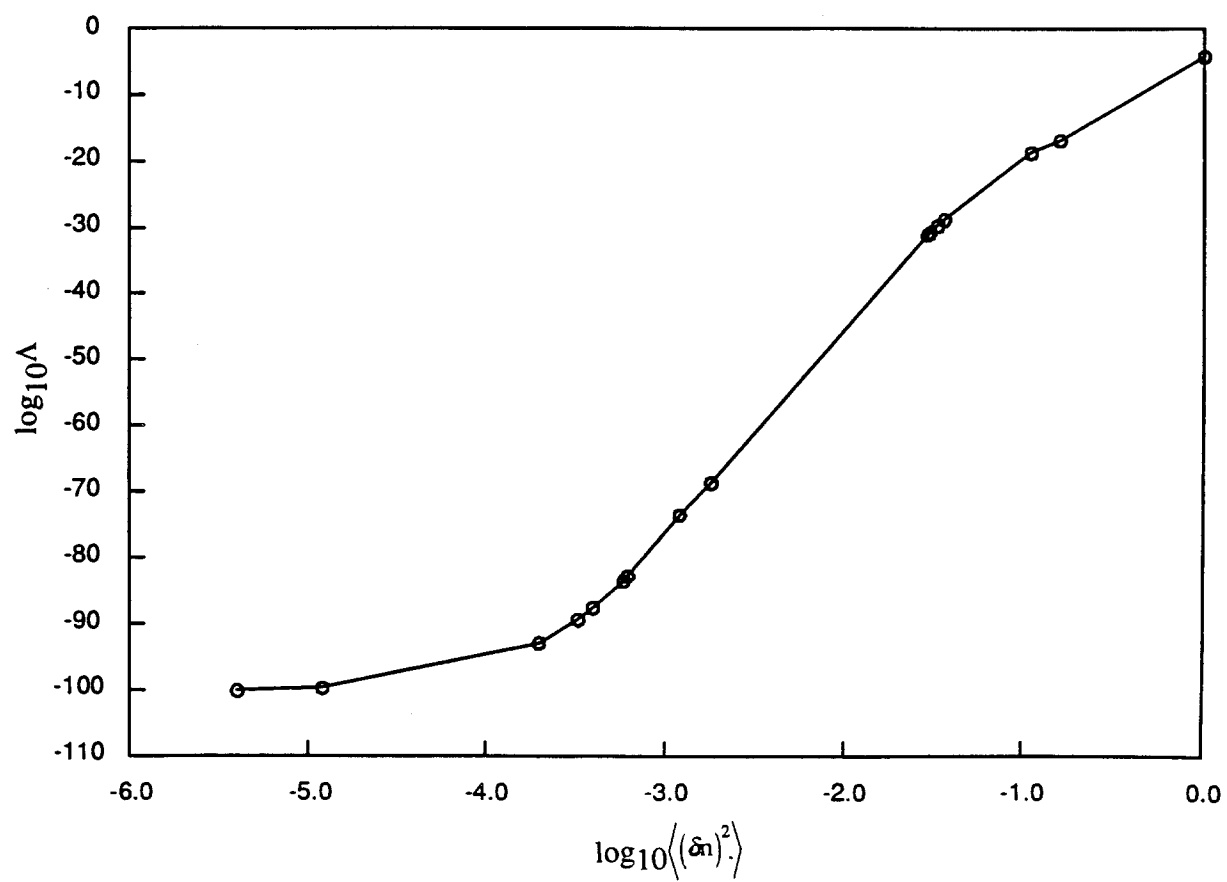
Figure 4

Section 28

POSSIBLE MECHANISMS FOR FUSION IN A SOLID LATTICE

Mario Rabinowitz and David H. Worledge

Electric Power Research Institute

Possible Mechanisms for Fusion in a Solid Lattice

MARIO RABINOWITZ and DAVID H. WORLEDGE

Electric Power Research Institute

Palo Alto, CA 94303

ABSTRACT

A crystalline solid may present a potentially rich environment for enhancing the fusion rate of hydrogen isotopes. We hypothesize and examine contributions to the fusion rate from deuteron effective mass, electron screening, and deuteron proximity which lead to significant predictions and testable results. These bulk mechanisms can account for reported cold fusion rates because of an exponential increase in the tunneling coefficient. In addition the lattice may provide preferential pathways of motion which provide nearly one-dimensional collisions, increase the collision frequency, the center-of-mass energy, and make it more likely that the nuclei will collide and fuse. Cluster-impact fusion experiments appear to have features in common with cold-fusion.

I. Introduction

Although much further experimental data are needed to establish the claimed cold fusion results as scientific fact, these claims have nevertheless focussed attention on the possibilities of fusion in a crystal lattice which deserve to be scrutinized carefully by the scientific community. If these data prove to be correct, there are many important experimental and theoretical questions which need to be answered. Based upon conventional mechanisms, quite general arguments could be made that cold fusion cannot occur, but this view does not address the available data (1,2,3,4,5,6,7,8). To do so, we will explore the sensitivity of the

fusion rate to various parameters to shed light on their respective roles and to hopefully provide guidance to future experiments. If fusion were to occur at the reported levels, it appears that hitherto unconsidered physical mechanisms must be present in the host solid at high d loading that are otherwise not present.

There are four essential ingredients or processes for sustained controlled nuclear fusion of either the hot or the cold variety: tunneling probability, collision frequency, fusion probability, and sustaining the reaction. The fusion rate is proportional to the product of the first three processes. The fusion probability is dependent on processes that occur inside the nuclear well and which determine the reaction products. The fourth process involves prevention of poisoning the reactions and replenishment of the deuterium and tritium fuel. The ability to achieve fusion at low temperature appears to be related most strongly to unexpected increases in tunneling probability.

2. Cold Fusion

The fusion rate is extremely sensitive to the tunneling probability. Even small variations in the relevant variables can substantially change this coefficient, which in practical terms is a measure of how easily the two nuclei can overcome the barrier of their electrical mutual repulsion. Once this barrier is overcome, the attractive nuclear force dominates. Tunneling is considered to be a quantum mechanical phenomenon in which a particle whose energy is less than the potential energy of a barrier can nevertheless be found on the other side of the barrier. Classical tunneling as demonstrated to be analogous to quantum tunneling by Cohn and Rabinowitz (9) can provide an insight into the physical process.

Recent publications have postulated effective mass concepts for the electrons in a solid as an analog to muon catalyzed fusion, as well as other mechanisms to account for increased tunneling (10,11,12,13,14,15). Even if the electron concepts are not applicable for a bound system to enhance the fusion rate, our fusing particle (d) effective mass concept appears valid (16,17) as it is applied outside the barrier where the inertia of the unbound deuterons (d) is determined by the lattice. Subsequent to this workshop, we learned that Alicki(18) also considers the d effective mass.

The cross-section, σ_r, for a nuclear reaction between charged particles can be expressed as a product of four factors:

$$\sigma_r = \sigma_c \, G \, T \, \rho \tag{1}$$

where σ_c is the cross-section for collision, G is the coulomb tunneling coefficient, T is the ratio of net flux of particles transmitted into the nuclear potential well compared to that penetrating the coulomb barrier and ρ is a function of the strong interaction leading to a given fusion reaction (exit channel).

For nuclei at low energy whose reduced de Broglie wavelength, λ , is therefore large compared to nuclear dimensions, $\sigma_c = \pi \lambda^2 \, (L+1)$ for interactions by partial waves with orbital angular momentum $L\hbar$. For s-waves (no angular momentum) this is just $\pi \lambda^2 = \pi h^2/\mu^{*2} v^2$.

A very important effect of the solid is to bring d's much closer together than they could otherwise be at ambient temperature. Although the average separation of the d's is about 1.4A in heavily loaded Pd, the d's can

be in equilibrium *locally* at a separation as close as 0.94A (19,20,21). Closer separation is possible in non-equilibrium processes. Various models for the screening potential of the free electrons in the solid lead to roughly similar results. The differences in the models may be important when better experimental data are available and a close correlation between experiment and theory is sought. At this stage a model of a spherical shell of radius R of negative charge surrounding each d will suffice even though other models such as a uniform cloud of electrons give significantly higher tunneling and fusion rates. This model leads both to an analytical solution, and to fusion rates which can account for the present experimental results. The potential energy as a function of radius r, outside the nuclear well is

$$V = (e^2/4\pi\varepsilon_0)[(1/r)-(1/R)] \qquad r_1 \leq r \leq R, \qquad (2)$$

where e is the deuteron charge, r_1 is the nuclear well radius. V= 0 for r > R. V= V_n (the square well nuclear potential) for $0 \leq r \leq r_1$.

The periodic potential in which d's move in Pd and their interaction with the ionic lattice and its constituents is similar to that of electrons, and the effective mass concept applies to both. A d in such a crystal is subject to forces from the crystal lattice as well as the Coulomb force from another d. The Hamiltonian of two d's contains contributions from the periodic potential of the lattice, electrons, and from interaction of the two d's. Simplification to the two-body (two d) Hamiltonian may be accomplished by using the effective mass for r>a, the lattice spacing.

Experiments involving r>a and time t>a/c, which consider only external forces, will infer an inertia for the charged particle equal to the effective mass. As nuclear distances ($\sim 10^{-15}$ m) are approached, the interaction between the two d's dominates over the lattice contribution, and the free mass is appropriate. Thus we assume the d's have a reduced effective mass μ^* for r>R. In the nuclear well the d's have a reduced mass μ = their free reduced mass (d mass/2). Inside the barrier (classically forbidden region), their mass varies continuously from the reduced effective mass outside the barrier to the reduced free (true) mass inside the nuclear well, as a two-body approximation of the many body problem. (In the many body approach, the reduced free mass would apply everywhere.) To obtain an analytic solution, we have μ at r_1 to μ^* at r_2 the classical turning point: $\mu_B \stackrel{=}{=} (\mu - \mu^*)(r_1/r) + \mu^*$ for $r_2 >> r_1$.

Solution of the Schroedinger eq. yields the tunneling coefficient

$G = A \exp\{-2g(r_1)\}$, where ... (3)

$g(r_1) = (\pi/2\hbar)[(2e^2/4\pi\varepsilon_0)\mu^* r_2]^{1/2}$ . ... (4)

Finally, the barrier transmission flux coefficient, T , is given by :

$T = [4 k/K]$, $K >> k$ . ... (5)

k is the wave number for the asymptotic region (outside the Coulomb barrier) : $k = m v /\hbar$ and, $K = (2 m V_n)^{1/2}/\hbar$. Thus

$\sigma_r = (2h/\mu^* vK)A\rho \exp\{-2g(r_1)\}$ ... (6)

ρ depends on the specific reaction. Cross sections for d-d fusion have not been measured below ~ 10 keV. Resonances might exist at lower

energies like the ^{5}He resonance for d-t fusion and where there is no inhibition of the nuclear events e.g. by requiring a radiative transition as in d-p fusion. It would then be possible for ρ to be much larger than for ordinary d-d fusion. We assume the dominant nuclear events to be the normal isobaric analogues : $d + d = p + t$ and $d + d = n + ^3$He, with some branching ratio . The measured value (13,14) of the astrophysical function,S, for d-d fusion is between 53 and 108 keV-barn $= 1.73 \times 10^{-42}$ J-m^2 which can be combined with Eq. 6 to yield

$$\sigma_r = (S/E) \exp\{-2g(r_1)\}. \qquad (7)$$

The number of d-d fusion reactions/cm^3/sec is :

$$N = (1/2)n^2\sigma_r v \qquad (8)$$

where n is the d number density, and v is the mean thermal velocity. Thus

$$N = (1/2)[2n^2S/(2\mu^*E)^{1/2}] \exp\{-2g(r_1)\} \text{ where,} \qquad (9)$$

E is the energy in the center-of-mass (CM) system.

We now proceed to examine the effects upon this relationship of the crystalline environment. These effects address the d effective mass. To our knowledge we were the first to apply these concepts to the fusing particles as a possible explanation for cold fusion.(16,17)

In a region of periodic potential perturbations, charged particles behave dynamically as if they possess an effective mass, m* (less or greater than the free mass) , given by :

$$m^* = \hbar^2 /[d^2E/dk^2]. \qquad (10)$$

Just as the electrons see an attractive periodic potential, the d's see a repulsive potential at each of the metal ions with further periodic

potential peaks at the positions of the octahedral interstitial sites when essentially all are occupied by d as in the β-phase PdD_x with x ≥ 0.75. Although we do not attempt a band calculation for the d effective mass m*, the magnitude to be expected can be estimated from the simple Kronig-Penney model for a unit charge moving with periodicity, a :

$$m^* \sim \hbar^2/2a^2E \tag{11}$$

where E are the eigenstate energies for d moving between the interstitial sites. Eq.(11) properly estimates the effective mass of electrons in terms of the Fermi energy ~ eV. For d (bosons of spin 1), even though their energies are low,being distributed around thermal, equation (11) gives m_e~.01 times the free d mass as a lower limit. A decreased mass can profoundly increase the G factor. A triton(t) should have an even smaller effective mass than a d because it is a Fermi particle and hence has higher E. Because of this, a prediction of this model is that heavy loading of the lattice with t and d should give even higher fusion rates.The difference in zero-point amplitude of d, t, and p in Pd may also be significant.

The effects of d effective mass are calculated in Table 1 where the number of d-d fusions/cm^3/sec is calculated for PdD_x for x≥0.75. The fusion rate is calculated for a series of values of effective mass for CM energies 0.025eV, 0.15 eV, and 1 eV, as could be found in the high energy tail of the thermal energy distribution.

$E_{Lab} = E_{CM}$ corresponds to symmetric collisions of d in transit between interstitial sites, which may be more likely in a lattice which provides preferential pathways of motion, than in a high temperature plasma. This

28-7

is another mechanism which can increase the fusion rate by many orders of magnitude. As Table 1 shows, fusion rates $>10^{10}/cm^3/sec$ may be obtained by these mechanisms which can account for the reported excess power and radiation attributed to cold fusion.

Table 1. d-d fusion rate in powers of 10 per cm^3/sec of PdD_x.

E_{CM} (eV)	(μ_e/μ) for R=0.5A				(μ_e/μ) for R=2.7A			
	1	0.1	0.05	0.02	1	0.1	0.05	0.02
0.025	-45	+11	+19	+25	-156	-27	-8	+7
0.15	-44	+11	+19	+26	-152	-25	-7	+8
1.0	-43	+12	+20	+26	-139	-22	-4	+11

In addition to accounting for reported fusion rates (1,2,3,4,5,6,7), this theory further predicts two generic (i.e. for $\mu^*= \mu$) properties of cold fusion in the bulk of a solid: 1) There is an extremely strong dependence on d concentration. 2)There is not a strong temperature dependence of the fusion rate right up to the melting point. For Pd this is 1828K, corresponding to E = 0.152eV. In free space, a large increase in fusion rate would be expected with increased temperature. With a decreased solubility of d in Pd, and hence decreased density as indicated by the large differences between the R=2.7A and R=0.5A cases, one may expect a decrease in the fusion rate with increased temperature. These predictions could be tested by externally increasing the temperature of an active fusion cell, and by adjusting the d concentration.

As stated earlier, the fusion rate is also proportional to the collision frequency of the deuterons. In three dimensions, the collision frequency

per particle is $F_3 = n\sigma_c v$, where n is the number density, σ_c is the collision cross section, and v is the mean thermal velocity. We expect this number to be roughly the same in the liquid state and in ordinary solid solution as found in Pd.

There may be preferential pathways that decrease the degrees of freedom in the solid so that the fusing particle is confined essentially to two- or one- dimensional motion in the solid-- that is, the particles may be able to move only in certain planes or channels. Decreasing the dimensionality or degrees of freedom decreases the number of ways potentially colliding particles can miss each other.

For the purposes of numerically illustrating that a significant increase in collision frequency may be achieved in such cases, let us consider some very simple equations as crude approximations of the real situation. In two dimensions the collision frequency is $F_2 = n^{2/3} \sigma_c^{1/2} v$. In one dimension the collision frequency is $F_1 = n^{1/3} v$. Depending on the particular values of n and σ_c when the particles are confined to planar or channel motion in the solid, F_2 can be orders of magnitude larger than F_3, and F_1 can be many orders of magnitude larger than F_3. Similarities to superconductivity are interesting to note (22). Thus by increasing the collision frequency and the center-of-mass energy, channeling greatly increases tunneling and hence the fusion rate.(16,17) Channeling increases the probability of a nearly one-dimensional collision, with essentially the absence of angular momentum in the final state. This may permit low energy resonances which greatly increase the fusion cross section.

These effects, in conjunction with an effective d mass of only 0.1 x the free d mass can account for the known positive experimental observations. The strong exponential dependence of the fusion rate upon the concentration and effective mass is evident from Table 1. This may in part explain the wide spread in positive and negative experimental results of different investigators. (23)

3. Cluster-Impact Fusion

Small singly ionized D_2O ice crystals containing clusters of 25 to 1300 D_2O molecules were used to bombard TiD targets, producing high one-dimensional compression and high fusion rates. (24)   Even though the ~ 100 eV/d energies of the latter are significantly higher than the ~ 0.03 eV of cold fusion, they share much in common.   In particular, they both represent anomalously high fusion rates based upon conventional wisdom. This is obvious with respect to cold fusion, but much less so for cluster fusion and may be a factor that contributed to the relative ease by which it was accepted.   If "cold fusion" is a proper term for   ambient temperature fusion, then the term "lukewarm fusion" is both convenient and appropriate for fusion at ~ 100eV.

In demonstrating d-d fusion rates of 10^{-1}/d-sec at incident deuteron energies of only ~ 100 eV Beuhler, Friedlander, and Friedman (BFF) have made a most significant contribution in their cluster-impact fusion experiments. (24) They note that their experimentally obtained fusion cross section is "more than 10 orders of magnitude larger" than their computed value. Actually, their experimental fusion cross section is 25 orders of magnitude larger than their theoretical value. Significantly,

Rabinowitz and Worledge (25) have shown that even when both compression and electron shielding effects are included, the experimental cross section is still 15 orders of magnitude larger than the theoretical cross section.

4. Acknowledgment

We gratefully acknowledge A. W. Overhauser's valuable criticisms and F. Culler's encouragement.

5. References

1. M. Fleischmann, S. Pons, and M. Hawkins, *J. Electroanal. Chem.* *261*,301(1989).

2. S.E. Jones et al *Nature* **338,** 737 (1989).

3. P.K. Iyengar,*5th Intl. Conf. Emer. Nuc. Energy Sys.* Karlsruhe,GER.(1989).

4. K.S.V. Santhanam et al, *Indian J. Tech.* **27**, 175 (1989).

5. S.K. Rangarajan, *Current Science 58*, 598 (1989).

6. W. Hively, *American Scientist* **77**, 327 (1989).

7. A.J. Appleby et al, *Workshop on Cold Fusion Phen.* Sante Fe,NM (1989).

8. R.Taniguchi,T.Yamamota,and S.Irie, *Jap. J. Appl. Phys.* **28**,659 (1989).

9. A. Cohn and M. Rabinowitz, *Intl. J. Theo. Phys.* **29**, No.3 (1990), in press.

10. C. Walling and J. Simons, *J. Phys. Chem.* **93**, 4693 (1989).

11. R.E. Brown, and N. Jarmie, *Phys. Rev. C.* in press (1989).

12. J. Rafelski, M. Gajda,and D. Harley (Univ.Arizona preprint AZPH-TH/89).

13. K. Szalewicz, J.D. Morgan III, and Monkhurst (preprint 4-29-89).

14. S.E. Koonen, M. Nauenberg, *Nature* **339**, 690 (1989).

15. J. Gittus and J.O. Bockris, *Nature* **339**, 105 (1989).

16. M. Rabinowitz and D.H. Worledge, *EPRI Journal* July/Aug., 42 (1989); and *IEEE POWER Engr. Review* **9**, No.11, 8 (1989).

17. M. Rabinowitz, *Respons. Energy Tech. Symp. and Intl. Expos.* June (1989).

18. R. Alicki, *Preprint 89-0381 Gdansk* and *Preprint 31827 CERN* June (1989).

19. F. Liu, B. K. Rao, and P. Jena, *Solid State Commun.* in press (1989).

20. Z. Sun and D. Tomanek, *Phys. Rev. Lett.* **63**, 59 (1989).

21. L. L. Lohr, *J. Phys. Chem.* **93**, 4697 (1989).

22. M. Rabinowitz, *Intl. J. Theoretical Phys.* **28**, 137 (1989).

23. M. Rabinowitz, *IEEE Power Engr. Review* **10**, No.2 (1990) in press.

24. R.J. Beuhler, G. Friedlander, and L. Friedman, *Phys. Rev. Lett.* **63** (1989) 1292.

25. M. Rabinowitz and D. H. Worledge, "An Analysis of Cold and Lukewarm Fusion," *Fusion Technology* **17** (1990), in press.

DISCUSSION (WORLEDGE)

Carrero: What cluster size do you assume to obtain your probabilities?

Worledge: The calculation which I present is for energy on the order of 150 eV. If one assumes the possibility of enhanced screening effects, perhaps consisting of a shell of negative charge giving you a shifted Coulomb potential, then reaction rates can be calculated which are of the required order of magnitude.

Mansour: How do you account for the deuterium loading factor in your calculations?

Worledge: It is included in the density term.

Chubb: Both Coulomb and nuclear forces are involved. Which force do you assume to be acting on the effective mass? Do you assume that it is the one relative to the strong interaction, since the electrostatic mass effects are small?

Worledge: A calculation of the effective mass is not used. The expression simply shows the effect of a reduced effective mass.

Whaley: To clarify the issues, the expression Dr. Worledge uses is basically a 3-particle approximation, which is valid for electrons. At the bottom of the band the dispersion function is quadratic, and the energy would be the level above zero for the band. This is the energy determining the Coulombic effective mass. For heavy particles such as hydrogen and deuterium, the dispersion of the band is much, much narrower. At the bottom of the band, a quadratic approximation can still be used. For tunneling in the eV barrier energy range, heavier effective masses are the rule, which for electrons are normally an order of magnitude larger than the rest mass.

Chubb: The energy used in the expression is a measured unit. It should be measured relative to the chemical potential of the system, which changes as electrical potential, concentration, and other factors change.

Worledge: I would still like to point out that the energy expression which you refer to is not used to derive any of the reaction rate probabilities. I have simply calculated the rates assuming that the rest mass applies, or effective masses smaller than the rest mass apply. If the effective mass increases, the tunneling rates would no longer be of interest. If the effective mass goes in the other direction, then the rates can increase markedly.

Miley: Does this give us any information about branching ratios?

Worledge: At zero particle separation we can say nothing about branching ratio. I assume that the process is dominated by the strong interaction.

Carrero: The formula used for the effective mass tends to the rest mass at high energy, not to zero.

Worledge: The expression which I used may not be the only description of the effective mass. I believe that we should explore other possibilities, since a lower effective mass would be one approach to explaining the results.

Jones: I think that conducting a parametric study such as this one is useful.

Worledge: The expression for rate is a product of the Gamow tunneling factor and the S function. The S function has not been measured down to low energies, and our assumptions concerning it are more suspect. Perhaps, we are measuring rates under these conditions now. Nevertheless, it is also worthwhile to look at the Gamow factors under these conditions.

Section 29

FUSION WITHIN A SOLID THROUGH SOLID STATE EFFECTS: THE GRAND IDENTITY CRISIS

Scott R. Chubb

Space Sensing Branch and Space Applications Branch

Space Systems Technology Department

Talbot A. Chubb

Bendix Field Engineering Corp.

Space Systems Development Department

Naval Center for Space Technology

Naval Research Laboratory

FUSION WITHIN A SOLID THROUGH SOLID STATE EFFECTS:
THE GRAND IDENTITY CRISIS

Scott R. Chubb

Space Sensing Branch and Space Applications Branch

Space Systems Technology Department

Talbot A. Chubb

Bendix Field Engineering Corp.

Space Systems Development Department

Naval Center for Space Technology

Naval Research Laboratory

I Introduction

It has been suggested by various participants of this workshop that there is a need to postulate "new physics" in order to explain the phenomena associated with "cold fusion". In fact, "new physics" is not required. "Cold fusion" can be explained in terms of known quantum mechanical effects that become physically realizable in a well-defined limit within a solid[1]. Furthermore, the extaordinary circumstances associated with the prolonged overcharging of Pd electrodes by Fleischmann and Pons[2] suggest that in fact this well-defined limit may very well have been obtained during the experiments[2].

The relevant limit should accompany slight overcharging of an electrolytically induced stoichiometric Pd-D compound within a periodic Pd host. This limit has relevance to potentially new forms of fusion because further charging of the electrode favors the formation of cooperative ionic fluctuations in which small, though equal, indistinguishable amounts of charge are distributed uniformly to different unit cells throughout the lattice. The evolution of these ionic fluctuations becomes favorable because of the large energy costs associated with lattice strain at individual lattice sites that occur when more than one deuteron attempts to occupy the same unit cell. The periodicity of the lattice

provides a means, through quantum mechanics, to eliminate these strains through the occupation of quantum mechanical "Bloch" (or energy band) states.

The occupation of these solid state matter states and the resulting behavior of the wave function provide a means for an entirely new form of nuclear interaction. The result is that nucleons that are separated by macroscopic distances in a classical sense may interact in a nuclear fashion quantum mechanically, thereby modifying significantly the conventional problem associated with nuclear fusion (of two nuclei colliding at nuclear separations at an isolated site) and the related coulomb barrier tunnelling requirement.

Because the resulting nuclear interaction is initiated in a low energy environment in which the reactants are predominantly electrostatically stable proton-neutron pairs, nuclear fusion of deuterons may occur in a manner in which unfamiliar products are released, governed by a new selection rule associated with the requirement that the initial and final states in the primary reactions involve nuclear particles that are derived from integer numbers of proton-neutron pairs. Also, the presence of the periodic solid significantly alters the ionicity and effective electrostatic volume of each deuteron in a manner that runs contrary to conventional thinking.

Because of the origin and spatial location and cooperative nature of these ionic fluctuations, their physical impact on nuclear behavior can only be described appropriately when the dynamics and time evolution are treated in a fully quantum mechanical manner that incorporates the presence of the lattice, the possibility of many-body fluctuations at all lattice sites, the correct volume dependence of each deuterium nucleus that results from interaction with the lattice, and the cooperative nature of a state composed of indistinguishable bosons. These requirements have been largely ignored until now because the physical situation, involving a cooperative fluctuation whose electrostatic interaction must be treated quantum mechanically, is very different than the situation of fusion in free space (which provides the conventional intuition associated with fusion), where the process may be described by nuclear-sized

particles that first move in a classical manner, then interact electrostatically where they experience strong repulsion, and finally "tunnel" into each other in a semi-classical manner (derived within the WKB approximation) through the associated coulombic barrier.

This paper provides the quantum mechanical theory of such ionic fluctuations and the selection rules for the resulting nuclear interactions. Because these fluctuations become energetically favorable during the overcharging of Pd electrodes associated with the prolonged electrolysis of LiOD, 1) they probably are responsible for the associated heating[2], and 2) this heating[2] is probably the result of a new form of nuclear interaction.

Because these fluctuations result from overcharging of the electrode, their creation leads to an overpotential condition, in which the potential difference between electrode and electrolyte opposes the potential that is applied across the cell. It is important to note that a strong correlation between such an overpotential condition and the anomalous heating has been observed by numerous participants of this workshop.

II Misconceptions, Preconceptions and All That

The major reason that it is difficult to understand within the framework of conventional thinking (about the fusion problem) how "cold fusion" can occur is the result of three premises that, until now, have been almost universally believed to hold within a solid:

1) Fusionable reactants *must* be located near one another.

2) The ionic deuteron cores inside a solid are "point-like" particles that have characteristic sizes comparable to those of $^2D^+$ ions in free space.

3) The products of condensed matter fusion somehow *must* "resemble" those of "conventional" fusion, associated with fusion in free space, and that it is appropriate to view condensed matter fusion as a "cooler" version of "hot fusion".

In fact, within a periodic Pd-D electrode, quantum mechanical effects, associated with the electrostatic interaction during *slight* over-charging through the injection of additional deuterium ions, invalidate each of these of premises. The need for close proximity of reactants, as required in free space, is replaced by the requirement that reactants and the associated condensed matter host form a periodic lattice in which reactants "see" on the average a periodic, single particle potential. The premise that deuterons are "point-like" is altered dramatically as a consequence of electrostatic interaction with the lattice, which effectively enlarges the volume of the electrostatic "density" of each D^+ ion by as much as a factor of 10^{13} relative to the comparable volume in free space. The requirement that "cold fusion" mimicks "hot fusion" in the sense that similar fusion products should be expected is altered by the collective nature of the interaction and the stability of the proton-neutron pair with respect to electrostatic interaction of D^+ ions in the range of initial energies from which "cold fusion" is initiated.

As a consequence, "cold fusion" is different from any previous known form of fusion. As discussed below, in the primary reactions "cold fusion" provides a conservation rule: in each reaction, when the initial state is formed from "bosons" composed of proton-neutron pairs, the final state will consist of "bosons" composed of proton-neutron pairs. Thus, reactants and products predominantly obey Bose Einstein statistics on the length scales associated with electrostatic interactions. There are no free fermions as a consequence, such as free neutrons, protons, $^3He^{++}$, or $^3H^+$, in the primary reaction channels. Condensed matter fusion proceeds through collective phenomena in which the concept of collision may be replaced by an entirely new idea, *the breaking of periodic order*.

III The Grand Identity Crisis

The associated theory of condensed matter fusion[1] requires only that the electrostatic potential be periodic and that some macroscopic number of deuterons become indistinguishable for a sufficiently long period of time. When this occurs, depending upon the relative magnitude of the bonding between lattice and ions, it may become possible for deuterons, which on the average are located in different unit cells, to interact in a nuclear fashion with each other, through "self-interaction" (the process in which an ion sees its own potential and readjusts its motion and spatial distribution, thereby modifying its own potential).

The starting point for interaction occurs near the D-concentration (one D per Pd) at which stoichiometric D-Pd forms. Then, a large percentage of each of the additional D that are subsequently injected interacts with an electrostatic potential that is predominantly periodic. Within this environment, to eliminate the possibility of large coulomb repulsion between D ions that results when two distinguishable D nuclei "attempt" to occupy the same lattice site, it becomes favorable once the stoichiometric compound is formed, for each additional D to occupy an "energy band" state. These states are defined by the requirement that 1) each wave function obey Bloch's theorem,

$$\psi_i(r+R_n) = \exp(i\underline{k}\cdot R_n)\ \psi_i(r) \qquad (1),$$

2) the wave function satisfy a periodic, single-particle Schroedinger (or other Hamiltonian based) equation, and 3) that the density $\rho(r)$ of indistinguishable D^+ ions is given by

$$\rho(r) = \Sigma_{i,\alpha}\ \psi_{i,\alpha}^{*}(r)\ \psi_{i,\alpha}(r)\ n_{\alpha,i} \qquad (2).$$

Here, R_n is a Bravais lattice vector, and the two indices i and α are used to

denote the eigenvalue $\epsilon_{i,\alpha} = \epsilon^{\alpha}(k)|_{ki}$, where ϵ^{α} is the αth energy band, k_i is the ith value of the wave-vector k. Each eigenstate $\psi_{i,\alpha}$ has been normalized to the volume of the crystal. Also, $n_{\alpha,i}$ is the band occupation factor; $n_{\alpha,i} = (e^{(\epsilon\alpha(ki)-\mu)/kT} \pm 1)^{-1}$, where the positive or negative sign is used, respectively, for the case of fermions or bosons, μ is the chemical potential, k is the Boltzmann constant, and T is the temperature.

In the physical case associated with modest overcharging of stoichiometric Pd-D, (as calculated below) $\rho(r)$ corresponds to a very small number, and, as a consequence of the dynamics of the electrostatic potential associated with Pd-D, is expected to be appreciable within the region where the density of D is appreciable prior to overcharging. This means that $\rho(r)$ should be viewed as a small density of ionic charge, associated with the overcharging, that provides an effective "dressing" of the ionicity of each deuteron core, leading to a very slight ($\sim 10^{-7}$ e) total positive increase in the charge of each of these cores. Again, as a consequence of the local electrostatic environment, it follows that the spatial extent of $\rho(r)$ must be greater than or equal to the spatial extent of the physical charge density of D in Pd-D.

Within this framework, the process of fusion within a solid may be understood in terms of a very different picture than is present in free space. This process involves the emergence of a new form of nuclear interaction, based upon collective self-interaction that becomes possible after many distinguishable deuterons "lose" their identities. We have named the emergence of this form of collective interaction "*the grand identity crisis*".

The grand identity crisis proceeds as follows: 1) D^+ ions become indistinguishable in order to alleviate lattice strain associated with injection beyond the point of perfect Pd-D stoichiometry. 2) This additional charge enters the lattice through the occupation of band states, leading to minimal deuteron-

deuteron electrostatic repulsion and maximal screening of coulombic repulsion through interaction with electrons, through fractional occupation (on the average) of each lattice site by additional deuterons. 3) In this environment, each additional D^+ contributes fractional charge at an individual lattice site, is bound weakly to the lattice (about some average position) through an approximately periodic coulomb potential, and, with increasing D, the spatial deviation (zero-point-motion) of each D from its average position increases. 4) Because of Bloch's theorem (Eq. 1), through self-interaction from this initial state, an entirely new identity may emerge in which multiple particle fluctuations at individual lattice sites occur, which may lead to fusion.

We have named this new collective state, from which fusion may emerge, "Bose Bloch Condensate" (BBC). The formation of the BBC and its properties are dictated by the lattice dependent interplay of the symmetries associated with periodicity and the properites of the boson wavefunction.

IV Properties and Formation of the Bose Bloch Condensate (BBC)

The formation of a D^+ BBC is a requirement for condensed matter fusion. Its properties are dictated by the interplay between the Bloch symmetry (implied by Eq. 1) of the single particle wave functions and the properties of the many-body boson wave function. A requirement for the formation of such a BBC state is that Bloch's theorem be valid and that each particle be indistinguishable from the others for a sufficiently long period of time.

For Bloch's theorem to be valid, 1) sufficient periodicity must be present, and 2) each particle must interact with approximately the same, single-particle, periodic potential. These criteria are satisfied when a macroscopic number of bosons (involving some subset of deuterons within the crystal) interact

electrostatically with each other and the lattice in a well-screened environment by itinerant electrons in which the overlap between electrons and deuterons occurs in a sufficiently ionic manner so that each of the subset of deuterons satisfies a single particle Schroedinger equation.

The large deuterium zero-point-motion (~0.2 Å) for stoichiometric Pd-D that has been measured in neutron scattering experiments[3] and small heat of solution at slightly lower D-concentrations reveals that the each D^+ is relatively weakly bound to the lattice. (Each D possesses a zero-point energy of 10's of meV.) This indicates that the associated bonding between deuteron cores and lattice may be viewed as ionic for time-scales that are less than $\sim 10^{-14}$ s. Similarly, the lattice may be viewed as periodic over a comparable time scale. The fact that for values of x>0.4 in Pd-D_x , the electrons that are injected with the D during electrolysis predominantly occupy Pd s-like states[3], which remain predominantly near the Pd cores but have itinerant character, provides further evidence that the bonding of D to the lattice may be viewed as ionic.

On thermodynamic grounds, we anticipate that the injected D should remain well-screened by itinerant electrons. Evidence of this phenomenon is provided by sensitivity of the energies and spatial orientation of the comparable electronic states with respect to H-concentration for the case of H-injection into Pd (as revealed through photoemission experiments[4] and electronic structure calculations[5]). It follows (by inference) that for Pd-D, near x=1 in PdD_x, similar screening by electrons occurs.

The total BBC injected charge is small. Also, the associated BBC density $\rho(r)$ should possess greater spatial extent and, hence, greater zero-point-motion (as a consequence of the coulombic repulsion, as discussed in the last section) than the D already present within the lattice. The combination of these factors; the ionic character of the bonding, large zero-point motion, and small binding

energy; imply that a single particle potential, on the time scale ($\sim 10^{-14}$ s.) associated with D zero-point-motion in the stoichiometric compound, should adequately describe the dynamics of the ionic D^+ that is injected after Pd-D has formed. Because stoichiometric Pd-D provides a periodic potential, it also follows then that Bloch's theorem may be used to characterize the single particle wave functions of the additional injected D^+ ions.

As discussed in the last section, during the *grand identity crisis*, to alleviate lattice strain, it becomes favorable for the injected D^+ to occupy band states. Because these band states are all derived from the same, approximately periodic potential, it follows that once these states begin to be occupied, the associated charge is derived from indistinguishable particles. The time-scale associated with this indistinguishability ($\sim 10^{-14}$ s.) is determined by the time-scale of the lattice, which is also suitably approximated using the period of oscillation associated with the zero-point-energies of the deuterons and Pd atoms that are already within the electrode prior to the point of overcharging.

The properties of the BBC follow from the properties of the many body wave function $\Psi(\epsilon_p, r)$ associated with the occupation by bosons of N_B band states (denoted by eigenvalues ϵ_p) possessing N_B coordinate dependencies r, which is given by

$$\Psi(\epsilon_p, r) = (1/N_B!)^{1/2} \sum_{\{r_m\}} \prod_{m=1}^{N_B} \psi_{Bloch}(k_p, r_m) \qquad . (3)$$

Here the sum over $\{r_m\}$ includes interchange of each coordinate r_m with the remaining N_B-1 coordinates, ensuring that Ψ is suitably Bose symmetric.

As a consequence of Eq. 1, when the single particle wave function centered about any lattice site is evaluated at the identical location relative to any other (Bravais equivalent) lattice site, its value only differs by a phase factor (of unit magnitude). Because of this fact, it follows that within any Fermi

Golden Rule, or comparable quantum mechanical rate expression, *the (electrostatic) wave functions associated with* densities of deuteron charge, which *may be* separated by macroscopic distances in a time-averaged (classical) sense, have appreciable overlap. Collectively, within this time-independent, Bloch picture (which applies rigorously to the idealization of a perfectly periodic, time independent lattice), 1) it follows that the identities of the individual indistinguishable deuterons have been lost, and 2) each component of the ionic density associated with these indistinguishable band states must be viewed as a collective entity, derived from all of the occupied N_B bosonic band states.

In the physical situation, fluctuations in energy and periodicity associated with the electrostatic interaction and perturbations of the electrostatic interaction provide both 1) the limiting effects associated with the adequacy of the Bloch picture, and 2) in fact, lead to the possibility of fusion. The relevant fluctuations associated with the fusion problem arise from non-number conserving perturbations (associated with deuteron occupation) of the nuclear and electrostatic potentials.

Because these fluctuations in deuteron number, as fusion proceeds, result in a depletion of the BBC density and lattice periodicity, and increase the entropy of the lattice, their behavior and characteristics are governed in a delicate manner by the thermodynamics and size of the lattice, and by externally applied forces. At sufficiently low temperatures, because of increases in entropy that result when these fluctuations are located near each other, the relevant limit involves the case of perturbations that violate deuteron number conservation at isolated lattice sites, located far apart from each other.

In the next section, we will examine how it becomes possible for such fluctuations to result in "self-induced" fusion (i.e., through a fusion process

driven by self-interaction) from a BBC initial state. With this end in mind, and to better understand the implications of the many-body band state wave function given in Eq. 3, it is both convenient and important to rewrite this many-body wave function in a time-dependent manner in which the possibility for fluctuation in particle number at an individual site is made transparent. The relevant expression follows from rewriting each Bloch state in terms of time dependent Wannier states, ϕ_s

$$\psi_{Bloch}(k,r) \exp(-\epsilon(k)t/\hbar) = (1/N_L)^{1/2} \sum_{s=1}^{N_L} \phi_s(r,t) \exp(ik\cdot R_s) \ . \quad (4)$$

Here R_s is a Bravais lattice vector, $\hbar=h/2\pi$, where h is Planck's constant, $\epsilon(k)$ is the band energy of ψ_{Bloch}, and k is the crystal momentum. In the harmonic approximation, each ϕ_s is suitably approximated at t=0 by the ground state wave function of a parabolic well,

$$\phi_s(r) = (2/\pi r_{zp}^2)^{3/4} \exp(- r_s^2/r_{zp}^2) \qquad , \quad (5)$$

where $r_s = r-R_s$, and r_{zp} (= the zero-point-motion radius ~0.2 A for Pd-D) is theclassical turning point of the well. Substituting Eq. 4 into Eq. 3, we find

$$\Psi(\epsilon_p,r) = (1/N_B!)^{1/2} \sum_{\{r_m\}} (1/N_L)^{N_B/2} \{ \prod_{m=1}^{N_B} \sum_{s=1}^{N_L} \phi_s(r_m) \exp(ik_p\cdot R_s) \} \ . \quad (6)$$

The possiblity for many-particle fluctuations appears through the bracketed product of summed terms in Eq. 6. In these terms, there exist subsets of terms containing multiple values of m contributing to fixed site s Wannier functions $\phi_s(r_m)$. All terms for which n values of m contribute to any of the $\phi_s(r_m)$ correspond to n-fold occupation of the lattice site s. Within a Fermi Golden Rule expression for the fusion rate (for example) for large N_B, small c, and small occupation number n, in the evaluation of the square of the matrix

element, there exist $(N_L)^{N_B} c^n/n!$ terms corresponding to n-fold occupations by distinguishable bosons. For indistinguishable bosons, these terms become n!-degenerate due to the equivalence of n! permutations of the coordinate dependencies in each of these terms. As a consequence,
there are $(N_L)^{N_B} c^n$ terms corresponding to n-fold ocupations by indistinguishable bosons.

It is important to recognize that the multiple occupation (associated with the product of any number [$\leq N_B$] of Wannier states) of a specific site by deuterons is a direct result of the indistinguishability of D^+ particles that compose the BBC. Because this result reflects a property of the wave function and not the density, it is possible for a macroscopic number of deuterons to interact with each other collectively through fluctuations in the number of deuterons at an individual site, while preserving a charge distribution which on the average involves deuterons that are separated by macroscopic distances, with each unit cell contributing a total number of (chemically bonded and BBC) deuterons that is very slightly greater than unity.

Thus, the BBC resembles a quantum fluid, such as HeII, in being composed of indistinguishable particles. Unlike HeII, however, the BBC requires a host lattice. Also, it can exist at very low boson concentration $\underline{c}$. Also, it does not form exclusively through the ground state but possesses many forms (or phases) associated with the occupation of different quasi-continuous energy bands. At low temperatures, collectively all of the constituents of the D^+ BBC will occupy the lowest k=0 energy band, and a "true" Bose condensate will form, which will exhibit ionically mediated superconductivity and a highly anisotropic Meissner effect. The BBC is a distinct matter state, differing in important ways from quantum fluids such HeII or ^3He. The BBC possesses properties similar to

well-known bosonic quasi-particles associated with the presence of a lattice, such as phonons, magnons and excitons.

V The Field Theory of Nucleons on a Lattice

From the limit in which the BBC forms, fusion becomes possible through three quantum mechanical effects: 1) the indistinguishability of the D^+ ions from which the BBC is formed, and 2) overlap between the single particle wave function associated with each BBC D^+ ion with the others, that results as a consequence the periodic structure of the lattice, and 3) the broadening of each D^+ ion wave function that results from interaction with the lattice. The importance of these quantum mechanical effects in the resulting fusion rate is revealed by examining the possibility of self-induced fusion. In much of the discussion, we use the Bloch state representation instead of Wannier states. Near room temperature, it follows that self-induced fusion occurs only at isolated lattice sites that are far from each other. As a consequence, in the actual calculation of the fusion rate given in the next section, we use the Wannier state representation. The appropriate starting point involves a Fermi Golden rule (or more general) expression for the rate at which BBC D^+ ions fuse through the multi-particle interactions associated with self-interaction. Within this context, because the identity of each D^+ ion is lost with respect to the others and periodic order leads to important overlap between single particle D^+ wave functions centered about different sites, the time-scales associated with such multi-particle interactions become significantly different than for cases involving isolated collisions between free space D^+ ions.

Before demonstrating explicitly how these differences enter into the calculation of a fusion rate that incorporates these very important distinctions, it is necessary to present various points associated with the interactions of

nucleons on an ordered lattice. In particular, it is important to examine the relationship of the purely bosonic, many-body wave function (associated with BBC formation on the scale of electrostatic interactions) presented in Eqs. 3-6 to the many-body initial state wave function associated with the various nucleons that comprise the individual deuterons of the BBC. This problem is associated with separability between nuclear and electrostatic interactions that results from the electrostatically-induced broadening of each D^+ wave function that accompanies deuteron interaction with the host lattice. It is also necessary to examine the impact of periodicity and wave function broadening on the possibility of inter-lattice-site nucleon-nucleon many-body interactions and fluctuations in deuteron particle number at a specific lattice site.

In this section, we address these points by providing some detail concerning the possibility of multiple-particle interactions at a specific site and the required constraints associated with the resulting nuclear interactions. In particular, first, we show that Quantum Mechanics, in a natural way, through Bloch's theorem, allows for the possibility of inter-lattice site nucleon-nucleon interaction. We do this first by examining the implications of extending Bloch's theorem to nuclear dimensions. We find that because of Bloch symmetry, alone, there are possibilities for inter-site nucleon interaction that are reflected in all many-body interactions since the associated thermal Greens function is constructed from Bloch symmetric wave functions. We then examine the more relevant limit in which periodicity is only required on the length scale of electrostatic interaction. Here, we observe that the large zero-point-motion of each deuteron that is present within Pd-D implies that near the limit in which a deuteron BBC may form, the single deuteron nuclear and electrostatic potentials are separable. We use this separability of potentials as an initial condition for introducing the possibility that nuclear and electrostatic interactions may

become approximately separable over a finite period of time. Again, the resulting thermal Greens function automatically allows for inter-site nucleon-nucleon interaction, subject to the constraint that the single particle electrostatic potential alone (and not the nuclear potential) be periodic. In this derivation, we present the necessary and sufficient conditions that guarantee that this form of separability is obeyed by all successive perturbations associated with multiple deuteron interaction that is made possible by a field theory based on the associated, initial thermal Greens function. In this manner, we provide the necessary and sufficient conditions that guarantee the existence of a suitable "inter-action potential" associated with self-interaction between nucleons at each order in perturbation theory that is consistent with the initial requirement that nuclear and electrostatic interactions remain separable. Because these conditions are derived based on the assumption that initially the electrostatic and nuclear potentials are separable, these conditions guarantee that the associated many-body interaction potentials are appropriate when each single particle D^+ wave function initially obeys Born-Oppenheimer separability. (This fact justifies our using symmetrized products of Bloch functions [as well as the other wave functional representations discussed in the last section] to construct the initial BBC many-body wave function.) The necessary and sufficient conditions for separability of nuclear and electrostatic many-body interactions also lead to an important selection rule: in each reaction, when the initial state is formed from "bosons" composed of proton-neutron pairs, the final state will consist of "bosons" composed of proton-neutron pairs. Thus, reactants and products predominantly obey Bose Einstein statistics on the length scales associated with electrostatic interactions. There are no free fermions as a consequence, such as free neutrons, protons, $^3He^{++}$, or $^3H^+$, in the primary reaction channels. In the next

section, we estimate the relevant self-interaction energies associated with multiple deuteron interaction at a site and find that to first order in the relevant perturbation, the criteria for separability are satisfied. This result enables us to examine the possibility of a variety of possible nuclear interactions and justifies our use of the Fermi Golden Rule to estimate the associated fusion rate.

It is important to recognize that though the name Bose Bloch Condensate places special emphasis on the bosonic character of the D^+ ion, the Bose behavior of this particular "condensate" is only significant on the length and time scales associated with the electrostatic interaction. Also, our use of terminology that involves "Bose" and "condensate" should not be confused with the more commonly used term "Bose Condensate". A Bose Bloch Condensate only resembles a "Bose Condensate" at low temperatures and only then on length scales that are much larger than nuclear dimension. The condensate aspect of a Bose Bloch condensate is present at all temperatures in which each deuteron may be viewed as an independent particle that has become indistinguishable from a macroscopic number of other deuterons.

Though the Bose character of the BBC only exists over length and time scales associated with the electrostatic interaction, it is possible that (e.g. in crystalized neutron star matter) the Bloch character of the condensate potentially *may* have consequence on length and time scales that are associated with nuclear behavior. This fact follows because of the extremely short range of the strong force and because when periodicity is extended to the dimensions associated with the strong interactions between protons and neutrons within each deuteron (a limit that *may be* appropriate for deuterons but that does not apply to most solids because most solids are not isotopically pure), Bloch's theorem *may be extended* so that the single particle wave function of each proton and

neutron may be selected separately to be a Bloch state. (In this case, as a function of a single coordinate r', each function $\psi_{elect}(r')$ and $\psi_{nuc}(r')$ is separately a Bloch state.) Within this context, each proton and neutron separately obeys a Schroedinger (or Dirac) equation, in which the electrostatic and strong interactions are represented approximately using one single particle, periodic potential.

The implications and limitations of the possibility that periodicity may extend to nuclear dimensions become more transparent when we recast the associated quantum mechanical problem in terms of the (four component) thermally averaged, single particle, nucleon Greens functions $G(r,r',t,\beta)$,

$$G(r,r',t,\beta)_{ij} = -i\text{Tr}\{ e^{(-\beta H_o)}{}_\tau \left[\psi^{op+}_i(r',0)\ \psi^{op}_j(r,t)\right] \}/\text{Tr}\{e^{-\beta H_o}\} \qquad .(7)$$

Here, ψ^{op}_j denotes the second quantized nucleon field operator possessing ispin ($=\pm 1/2$) and magnetic spin ($=\pm 1/2$), both denoted by j. H_o is the second quantized form of the single particle periodic Hamiltonian,

$$H_o = \Sigma_{i,k,m}\ \epsilon_i\ a^+(\epsilon_i)_m\ a(\epsilon_i)_m.$$

Here $a^+(\epsilon_i)_m$ and $a(\epsilon_i)_m$, respectively, are the creation and annihilation operators of the nucleon possessing band energy $\epsilon_i = \epsilon_i(k)$, wave-vector k (i and k are both included within the summation) and ispin value m. These may be represented in terms of the field operators $\psi^{op}_j(r)$ and the eigenstate, Bloch functions $\psi^{nucleon}_j(\epsilon_i,r)$ of the single particle Schroedinger (or Dirac) equation from which the band energies $\epsilon_i(k)$ are derived:

$$a^+(\epsilon_i)_m = \int d^3r'\ \psi^{nucleon}_m(\epsilon_i,r')\ \psi^{op+}_m(r',0),$$

and

$$a(\epsilon_i)_m = \int d^3r'\ \psi^{*nucleon}_m(\epsilon_i,r)\psi^{op}_m(r,0).$$

Also, in Eq. 7, $\beta = 1/(k_B T)$, T is the temperature, and τ is the standard time ordering operator, defined by

$\tau(A(t),B(t'))= \theta(t-t')A(t)B(t') \pm \theta(t'-t) B(t')A(t),$

where the terms are added [subtracted] when A and B are boson [fermion] operators and θ is a step function defined by

$\theta(x) = 1,$ $x>0$

       $= 0$ $x \leq 0.$

When periodicity extends to nuclear dimensions, H_o is measured relative to the Fermi energy associated with the occupation of $2*N_B$ ($=N_B$ proton + N_B neutron) energy band states (each of which is measured relative to the initial rest energy of the solid).

In principle, on some time scale, if sufficient periodicity is present, Bloch's theorem would apply even to sub-nuclear particles, such as the gluons and pions that bind together each deuteron, and a representative field theory could be constructed based on the two particle Greens functions associated with any of these entities, using the assumption of periodicity. When this is done, because of Bloch's theorem, site-site interaction becomes possible in the associated field theory in a manner that is entirely different than when periodicity is not present.

To understand the possibility of such site-site interaction, it is sufficient to note that for any particle whose time evolution *may be adequately described* in terms of a single particle, periodic Hamiltonian, the associated two particle Greens function $G^{rep}(r,r',t,\beta)$ may be written using a spectral decomposition in terms of representative Bloch functions $\Psi^{rep}(\epsilon_i,r')$. For example, in the low temperature limit, for any of these representative particles (boson or fermion),

$$G^{rep}((r,r',t,\infty)) = \int \frac{dw}{2\pi} \Sigma_{i,k} \frac{\Psi^{rep}(\epsilon_i,r)}{} \frac{e^{-iwt}}{(w-\epsilon_i(1-i\delta))} \Psi^{*rep}(\epsilon_i,r') \ ,$$

where the summation is over all (occupied and unoccupied) states (all of which are band states because the potential is periodic). Here, δ is the standard infinitesimal increment associated with the time ordering operator that insures that in any scattering process, for positive temperatures, each Greens Function is associated with the creation of a positive energy "hole state" (associated with excitation) at times in the future and the annihilation of an excited state particle through the occupation of a negative energy "occupied state" at times in the past. Also, each $\Psi^{rep}(\epsilon_i,r')$ satisfies Eq. 1.

However, the applicability of an approach based upon a band theory of "sub-nuclear" particles, or even of a band theory of separate fermionic nucleons, to the problem of nuclear interaction within a conventional solid is impossible because 1) periodicity does not extend in a meaningful way to the length and time scales associated with nucleonic dimensions, and 2) even if such periodicity does exist (because of the very different length and time scales associated with the electrostatic and strong interactions), it is not clear that there exists a single particle potential that governs the eigenvalue spectrum of the associated particles over a meaningful period of time. Such a band theory of individual sub-nuclear or isolated nucleon particles appears to have little physical relevance. Because the individual fermions that constitute each deuteron statistically behave very differently (either as Fermions or as a bound boson) over the length scales associated with the electrostatic and nuclear interactions, it is apparent that over intermediate length scales, considerable interplay (and correlation) between electrostatic and strong interaction potentials takes place. As a consequence, the existence of such a single particle, periodic potential is questionable.

In the limit in which the BBC forms, periodicity is maintained through the

electrostatic interaction over length and time scales that are much greater (by a factor of 10^5 and more) than the comparable length and time scales of nuclear interaction. As a consequence, the energy (~ 1 eV and less) associated with the binding of the center of mass of each D^+ ion to its average position is as much as a factor of 10^6 less than the binding energy (~ 2 MeV) between each proton and neutron. This means that regardless of whether or not periodicity exists on the scale of nuclear interaction or at intermediate scales between nuclear and electrostatic dimensions, for the case in which a single, predominantly neutral, D is located near lattice site s, the wave function of each nucleon (proton or neutron) $\Phi^{nucleon}$ is well described by a Born-Oppenheimer separable form

$$\Phi^{nucleon}(r, r_{cm,s}) = \psi^{nucleon}(r - r_{cm,s}) \, \psi^{elect}(r_{cm,s}) \qquad (8).$$

Here, $r_{cm,s} = (r_n + r_p)/2 - R_s$ (r_n and r_p are the coordinates of the neutron and proton) is the center of mass of a deuteron located within a zero-point-motion radius r_{zp} of the site at R_s. (The coordinate r is r_n when the nucleon is a neutron and equals r_p otherwise.) In Eq. 8, the nuclear behavior and the associated proton-neutron binding are governed by a highly localized nuclear function $\psi^{nucleon}$, which vanishes when $r - r_{cm,s}$ becomes greater than the effective nuclear radius ($\sim 10^{-13}$ cm) of a deuteron R_{deut}, while ψ^{elect} is a slowly varying function which varies (in the neighborhood of the lattice site) over the known length scale r_{zp} associated with the electrostatic motion of the center of mass r_{cm} of each deuteron. Similarly, the wave function for the proton-neutron pair about site s may be written in the form,

$$\Phi^{Deuteron}(r_n, r_p) = \psi^{nuc}(r_n - r_p) \, \psi^{elect}(r_{cm,s}) \qquad (9),$$

which is consistent with our use of the Born-Oppenheimer separability condition, and where the electrostatic function ψ^{elect} is the same in Eqs. 8 and 9. When the electrostatic potential is periodic, as in the case of stoichiometric Pd-D,

provided Eq. (8) holds, each ψ^{elect} may be approximated by one of the single particle BBC deuteron Bloch functions $\psi_{Bloch}(k,r)$ discussed in the last section. Then it follows that the associated many-body, initial state wave function given by Eqs. 3 and 6 may be used with the understanding that each of the N_B Bloch functions is multiplied by a nuclear function ψ^{nuc}, where the functional form of ψ^{nuc} does not depend on the absolute position of any of the deuterons and does not interact with the electrostatic potential.

It should be emphasized that these forms (Eqs. 8 and 9) are only suitable for the case in which Born-Oppenheimer separability applies. Because the fusion problem deals with a situation in which the effects of multiple-particle fluctuations at an individual lattice site occur, it is important to examine the impact of these effects on the functional forms given in Eqs. (8) and (9). These forms are rigorously suitable in the limit in which the energy scales associated with the nuclear potential of the initial state and (in order to apply the Fermi Golden Rule) of perturbations (associated with the application of the Fermi Golden Rule) to this nuclear potential are very different from the scales associated with the comparable electrostatic potential and perturbations of the electrostatic potential.

We will demonstrate in this section that it is possible to construct a self-consistent, field theory in which each field operator is constrained so that the electrostatic and nuclear interactions remain separable. The effect of this constraint is to eliminate all processes associated with transitions to states in which the characteristic length and time scales fall in an intermediate range between the characteristic length and time scales of the electrostatic and nuclear interactions that are present in a particular subset of many-body interactions associated with a particular perturbation at a particular order of the perturbation in the perturbation expansion.

This approximation neglects a large number of possible processes. In any particular order of the perturbation expansion, however, as the difference in nuclear and electrostatic characteristic length scales of the initial state becomes sufficiently large, the overlap between the initial state and perturbations associated with intermediate range processes becomes considerably smaller than the overlap of the initial state with the perturbation associated with the subset of many-body processes in which the difference between electrostatic and nuclear length scales is large. As a consequence, in low temperature environments, after the BBC forms, provided the electrostatic time scale of a particular process is sufficiently long relative to a particular nuclear process, both processes may be approximated within a self-consistent field theory, in which non-separable nuclear-electrostatic interactions are prohibited. (As we will see, this form of field theory automatically leads to the selection rule of cold fusion nuclear physics: "Bosons in and Bosons out", where it is understood that each boson is composed of proton-neutron pairs.) Because the zero-point-motion of the center of mass of each deuteron is quite large[3], first order self-interaction perturbations that involve fluctuations in deuteron number at a site and the associated electrostatic self-interaction are many orders of magnitude less than the comparable perturbations associated with nuclear self-interaction. As a consequence, the approximation of nuclear and electrostatic separability (as well as Born-Oppenheimer separability of the wave function) applies rigorously both to the initial BBC state and to self-induced perturbations involving deuteron particle number fluctuation in which deuterons coalesce over a common volume.

In principle, the self-consistent BBC field theory in which nuclear and electrostatic interactions remain separable for a specified interval of time should be based on the necessary and sufficient condition that guarantees that

Eq. 8 remain valid for all times t within the specified interval. However, there are ambiguities associated with applying this condition to Eq. 8 (as discussed below) that result from the Fermi statistics associated with the individual nucleons that are eliminated when the condition is applied to Eq. 9. It is important to recognize that these ambiguities reflect more the nature of field quantization than Fermi vs Bose statistics. As a consequence, in the quantization of the field, by choosing Born-Oppenheimer separability as an initial condition and requiring it to remain valid for a finite period of time, we have imposed constraints on the field theory that can only be done unambiguously by quantizing the fields associated with Eq. 9 in a suitable manner, in which both fields are composed of bosons. In the context of a more complete theory in which separability is not required, the constrained fields of the self-consistent BBC case result from the limit of the complete theory in which in all many-body interactions, all processes are discarded in which separability is violated during any physical or virtual transition. By requiring separability, we unambiguously find an approximate form of the more complete field theory. The fact that this separability constraint leads to the situation that both the nuclear and electrostatic fields are composed of bosons means that in any of the diagramatic expansions of either theory in which strict separability between nuclear and electrostatic interactions is required, the "Bosons in and Bosons out" selection rule is obeyed. We will return to the explicit derivation of this rule later in this section.

The necessary and sufficient condition that guarantees separability of the classical nuclear fields ψ^n (either the fields from Eq. 8, $\psi^{nucleon}(r-r_{cm},t)$ and $\psi^{+nucleon}(r-r_{cm},t)$, or the fields from Eq. 9, $\psi^{nuc}(r,t)$ and $\psi^{+nuc}(r,t)$) from the electrostatic functions $\psi^{elec}(r',0)$ for all times t within a finite interval of time is that during the interval ψ^n and ψ^{+n}, each, evolve in a manner that is

independent of the evolution of either ψ^{elec} or ψ^{+elec}. This condition is satisfied when at time t, the functional derivatives of the various functions in Eq. 8 (and their complex conjugates) with respect to each other all vanish:

$$\frac{\delta\psi^{n}(r,t)}{\delta\psi^{elec}(r',0)} = \frac{\delta\psi^{elec}(r,t)}{\delta\psi^{n}(r',0)} = \frac{\delta\psi^{*elec}(r,t)}{\delta\psi^{n}(r',0)} = \frac{\delta\psi^{*elec}(r,t)}{\delta\psi^{*n}(r',0)}$$

$$= \frac{\delta\psi^{*n}(r,t)}{\delta\psi^{*elec}(r',0)} = \frac{\delta\psi^{elec}(r,t)}{\delta\psi^{*n}(r',0)} = 0$$

Because each Schroedinger (or Dirac) equation is first order in time, ψ^{elec} and $i\psi^{*elec}$ are canonical, conjugate fields. Similarly, ψ^{n} and $i\psi^{*n}$ are canonical conjugate fields. As a consequence, the vanishing of each of these functional derivatives can be related to the vanishing of all of the Poisson bracket relationships between the two sets of classical fields at all times within the interval. The canonical quantization of the associated fields (in which the Poisson bracket is equated with the product of $-i\hbar$ and the commutator [anti-commutator] of the boson [fermion] field variable) can be used unambiguously as a means of imposing these separability constraints between the nuclear and electrostatic fields only when the nuclear fields associated with Eq. 9 and not Eq. 8 are used.

The reason these constraints can not be applied unambiguously to the fields associated with Eq. 8 is because with respect to the electrostatic interaction, each deuteron must obey Bose statistics (so that after quantization, ψ^{elec} and ψ^{+elec} become boson operators), while $\psi^{nucleon}$ and $\psi^{+nucleon}$ are fermion fields. In the case of Eq. 9, on the other hand, the nuclear functions ψ^{nuc} and ψ^{+nuc} provide the probability distribution associated with finding a proton-neutron pair within a specific volume surrounding the proton-neutron center of mass. This probability distribution describes a tightly bound configuration of nuclear matter that in the second quantized form may be thought of as a boson derived from pairs of fermions. Thus, when the classical nuclear and electrostatic fields from Eq. 9

are quantized, the vanishing of the various functional derivatives that is required by separability can be unambiguously interpreted as the vanishing of associated commutators since both sets of fields are treated as bosons. The comparable canonical quantization procedure can not be applied to Eq. 8 unambiguously because, when, for example, the nuclear fields are associated with fermions, the vanishing of the functional derivative $\delta\psi^{nucleon}(r,0)/\delta\psi^{elec}(r',t)$ (associated with the classical field Poisson bracket $[\psi^{nucleon}(r,0),\psi^{+elec}(r',t)]$) leads to the result (through canonical quantization of the electrostatic field) that $\psi^{nucleon}$ and ψ^{+elec} commute. The quantization of the nucleon field requires that the vanishing of the functional derivative $\delta\psi^{+elec}(r,0)/\delta\psi^{+nuc}(r',t)$ leads to the result that $\psi^{nucleon}$ and ψ^{+elec} anti-commute. As a consequence, the choice of anti-commutability or commutability has bearing on the separability constraint. When both forms of quantization are imposed (as is rigorously necessary when the fields of Eq. 8 are constrained to be separable), the null result, in which one or both fields vanish identically at all times, is the only allowable solution.

The required constraints associated with length scale that are needed as an initial condition for the separability may be incorporated in each Greens function in Eq. 7 by first replacing the idealized single particle Hamiltonian H_o (which had been assumed to be periodic for both the nuclear and electrostatic length scales), with a more realistic form in which the electrostatic potential is periodic, but the nuclear potential need not be periodic. It is also required that the two potentials are separable. In second quantized form, the appropriate Hamiltonian is

$$H_o = \Sigma_{i,k,m} \epsilon_i \, D^+(\epsilon_i) \, D(\epsilon_i) + N_B \sum_{\epsilon_{nuc},b} \epsilon_{nuc} \, A^+(\epsilon_{nuc})_b \, A(\epsilon_{nuc})_b.$$

Here, $D^+(\epsilon_i)$ is the boson creation operator associated with the occupation of the deuteron energy band $\epsilon_i(k)$, measured relative to the electrostatic chemical potential μ_{elec}. (The value of μ_{elec} is fixed by the requirement that N_B

deuterons be electrostatically bound to the solid). In the second term, the sum, in principle, should be taken over the precise eigenvalue spectrum, using operators with the spectrum of a Hamiltonian involving N_B different strong potentials, separated by large (on the scale of nuclear dimension) distances. (In this case the factor of N_B would be omitted.) For simplicity, in this term, we have used approximate boson creation and annihilation operators, $A^+(\epsilon_{nuc})_b$ and $A(\epsilon_{nuc})_b$, associated with the proton-neutron pairs of nuclear dimension (b signifies magnetic spin), and approximate eigenvalues ϵ_{nuc}, associated with a different single particle problem in which the various strong potentials are averaged at a common location. Consistent with this "average potential" solution to the problem of N_B disordered strong potentials separated by large distances, we must introduce a nuclear chemical potential μ_{n-p} to conserve proton-neutron pairs (required both for total fermion conservation within the initial state and for separability of nuclear and electrostatic interactions). Here, the value of μ_{n-p} is fixed by the constraint that there is one bound proton-neutron pair state (occupied by two fermions) per occupied deuteron state. As a consequence, each occupied proton-neutron pair is bound, a factor of N_B appears as a prefactor of the sum in the second term, and the energy ϵ_{nuc} of each proton-neutron pair state is measured relative to μ_{n-p} . The approximate eigenvalues may be constructed using:

$$\left(\frac{-\hbar^2}{2\mu_{nuc}} \nabla^2 + U_{nuc,eff}(r_{n-p}) \right)\psi^{nuc}(\epsilon_{nuc};r_{n-p},t) = \epsilon_{nuc}\ \psi^{nuc}(\epsilon_{nuc};r_{n-p},t),$$

μ_{nuc} is the reduced mass ($= M_D/4$, where M_D equals the mass of a deuteron), r_{n-p} ($= r_n - r_p$) is the separation between proton and neutron in each proton-neutron pair, each proton-neutron pair wave function $\psi^{nuc}(\epsilon_{nuc};r_{n-p},t)$ is represented in four component column vector form, possessing components $\psi^{nuc}_j(\epsilon_{nuc};r_{n-p},t)$, where j denotes values of the spin (the triplet spin=1 and singlet spin=0 values are allowed), and U (also represented as a matrix) is

derived from the average of the different strong potentials

$$U_{nuc,eff}(r) = \frac{1}{N_B} \Sigma_{c=1}^{N_B} U_c(r).$$

Then, in the expression for H_0, the proton-neutron pair operators obey the standard boson commutation relationships with respect to each other and commute with the electrostatic boson operators. The procedure for evaluating the Greens function consists of using this alternate form for H_0 in Eq. 7 and replacing each nucleon field operator $\psi^{op}_j(r)$ and the adjoint operator ψ^{op+}_j, using alternative operators $\psi^{op}_j{}'$ and $\psi^{op+}_j{}'$, where

$$\psi^{op}_j{}'(\pm r_{n-p}/2 + r_{cm}, t) = \psi^{nuc}_j(\pm r_{n-p}/2, t) \, \psi^{elec}(r_{cm}, t), \qquad (10a)$$

In eq. 10a, the positive (negative) value of $r_{n-p}/2$ on the right side and in the value of the field coordinate, r_f,

$$r_f = \pm r_{n-p}/2 + r_{cm} \qquad\qquad , \qquad (10b)$$

of $\psi^{op}_j{}'$, corresponds to the position of the neutron (proton). The adjoint $\psi^{op+}_j{}'$ is defined by replacing $\psi^{nuc}_j(r_{n-p}, t)$ and $\psi^{elec}(r_{cm}, t)$ with their adjoints. Here, $\psi^{nuc}_j(r_{n-p}, t)$ is the proton-neutron pair field operator associated approximately with the function $\psi^{nuc}_j(r_{n-p}, t)$ of Eq. 9, while $\psi^{elec}(r_{cm}, t)$ is the boson field operator associated with $\psi^{elec}(r_{cm}, t)$:

$$\psi^{nuc}_j(r_{n-p}, t) = \underset{\epsilon_{nuc}}{\Sigma} A(\epsilon_{nuc})_j \psi^{nuc}_j(\epsilon_{nuc}; r_{n-p}, t) \qquad (11a)$$

and

$$\psi^{elec}(r_{cm}, t) = \Sigma_{i,k} \, D(\epsilon_i) \, \psi_{Bloch}(\epsilon_i(k), r_{cm}) \qquad (11b).$$

In Eq. 11b, the sum is over all deuteron energy bands.

Having made these substitutions into Eq. 7, because the proton-neutron pair creation and annihilation operators all commute with the remaining electrostatic

boson operators (as required by the separability condition), and H_o involves only the separable single particle Hamiltonians, we may explicitly evaluate the trace. Because this approximation is only applicable in cases in which the nuclear interaction is considerably stronger than the electrostatic interaction, in the resulting proton-neutron pair contributions to the single particle Greens function, we may also pass to the T=0, $\beta = \infty$ limit. Specifically, when Born-Oppenheimer separability applies, we may use

$$G(r_f, r_f', t, \beta)_{ij} = G^{BBC}(r_{cm}, r_{cm}', t, \beta)$$
$$\times \rho^{nuc} (\pm r_{n-p}/2, \pm r'_{n-p}/2, t)_{i,j} \qquad . \quad (12)$$

Here, and throughout, the field coordinates r_f and r_f' are evaluated as in Eq. 10b. Also, consistent with the use of separable functions, each integration over the field variable r_f or r_f' associated with any many-body process requires integration over both the associated center of mass variable (r_{cm} or r_{cm}') and proton-neutron pair separation coordinate. Also, in Eq. 12, $\rho^{nuc}(r_{n-p}/2, r'_{n-p}/2, t)_{ij}$ is the nucleon (neutron-pair) density matrix defined by,

$$\rho^{nuc}(r, r', t)_{ij} = \int \frac{dw}{(2\pi)} \Sigma_{\epsilon nuc} \psi^{nuc}_i(\epsilon_{nuc}; r, 0) \, e^{-iwt} \, \delta(W - \epsilon_{nuc}) \, \psi^{*nuc}_j(\epsilon_{nuc}, r', 0), \quad (13a)$$

which vanishes unless

$$|r_{n-p}| \sim R_{deut} \qquad , \quad (13b)$$

and

$$|r'_{n-p}| \sim R_{deut} \qquad . \quad (13c)$$

Also, as a consequence of evaluating the trace in Eq. 7, in Eq. 10, we use

$$G^{BBC}(r,r',t,\beta) = \int \frac{dw}{2\pi} \Sigma_{i,k} \Psi(\epsilon_i,r)e^{-iwt} \quad \Psi^*(\epsilon_i,r')$$

$$X \quad \left\{ \frac{1}{(w-(\epsilon_i-i\delta))(1-e^{((-\beta)w)})} + \frac{1}{(w-(\epsilon_i+i\delta))(1-e^{((\beta)w)})} \right\} \quad ,(14)$$

with $\epsilon_i = \epsilon_i(k)$. Eqs. 12-14 imply

$$[i\partial_t - H^{nuc,eff}(\pm r_{n-p}/2) - H_o^{elec}(r_{cm})]G(r_f,r_f',t,\beta) = \delta(t)\delta(r_{cm}-r_{cm}') \delta((r_{n-p}-r_{n-p}')/2),$$

where the positive or negative sign is used consistently with the choice of sign associated with the field point (as in Eq. (10b)). Also,

$$H_o^{elec} = (-\hbar^2\nabla^2/(2M_D) + U_{elec}(r)),$$

and

$$H^{nuc,eff} = (-\nabla^2/2\mu_{unc} + U_{nuc,eff}(r)).$$

Here $U_{nuc,eff}(r)$ and μ_{nuc} are defined by the average, single particle proton-neutron pair problem discussed above, and U_{elec} is the single particle electrostatic potential provided by the lattice.

In Eq. 14, each $\Psi(\epsilon_i,r')$ is a single particle deuteron Bloch function (as in Eq. 6). Since each of these functions has appreciable value only within a zero-point-volume of one of the lattice sites, it follows that although any intermediate integrations over the field coordinates r_f (which includes separate integrations over both the (center of mass) electrostatic (r_{cm}) and nuclear separation (r_{n-p}) coordinates, each of which extends throughout the crystal), contributions to the integral occur only from the regions where each BBC deuteron wave function has non-negligible value. Of greater significance, because of the separability of nuclear and electrostatic interactions, we have been able to

write the entire Greens function as the product of a nuclear quantity $\rho^{nuc}(r,r',t)_{ij}$ (whose coordinates only depend on the possible nuclear distance separations between proton and neutron in each deuteron) multiplied by a much more slowly varying electrostatic Greens function $G^{BBC}(r_{cm},r_{cm}',\beta,t)$ whose coordinates correspond to the center of mass of a deuteron. Of special importance to the cold fusion problem is that periodicity of the electrostatic potential provided by the lattice and Bloch's theorem imply that it is appropriate to express G^{BBC} in terms of the eigenstates of the electrostatic potential, the Bloch functions $\Psi(\epsilon_i,r')$. As a consequence, in any integral over the center of mass coordinates in Eq. 12, comparable terms in the expression for $G^{BBC}(r_{cm},r_{cm}',t,\beta)$ (Eq. 14) evaluated at Bravais equivalent positions of r_{cm} and r_{cm}' provide contributions to the integrand that differ by a simple phase factor (of unit magnitude). Thus, despite the fact that the proton-neutron separations $|r_{n-p}|$ and $|r_{n-p}'|$ in the nuclear part of the Greens function (provided by ρ^{nuc}) both must be less than $-R_{deut}$ (since the nuclear wave functions $\psi^{nuc}_i(\epsilon_{nuc};r,0)$ in Eq. 13a are solutions to a Schroedinger equation based on a real strong potential), when Born-Oppenheimer separability is applicable and Bloch's theorem applies, regions in which the center of mass variables r_{cm} and r_{cm}' are far apart (in particular, when these variables are centered on different lattice sites) provide significant contributions to any integrand involving G. This means that $G(r+R_n,r',t,\beta)_{ij}$ and $G(r,r',t,\beta)_{ij}$ have comparable value.

Thus, provided Born-Oppenheimer separability applies initially, a second quantized form of the theory applies where site-site interaction is implied in all integrations of the internal variables r and r' of the two particle Greens function $G(r,r',t,\beta)_{ij}$. This means that it is possible for nucleons separated by macroscopic distances, in a classical sense, (in particular, nucleons located at different lattice sites) to interact collectively with each other quantum

mechanically as if they are located within a nuclear distance of each other. In particular, any "self-interaction" corrections, (which all may be represented [at least schematically] in terms of suitable integrals involving $G(r,r',t,\beta)_{ij}$) due to modifications of the binding of a proton to a neutron at one site through modification of its own self-generated pion field have comparable magnitude to the associated corrections that result from changes in the pion field that are induced by changes of nucleon binding at a different site. This means that in any diagramatic calculation based on integration of the field variables r_f and r_f' of $G(r_f,r_f',t,\beta)$, all contributions to self-interaction corrections that enter when r_{cm} and r_{cm}' are displaced relative to each other by a Bravais lattice vector have comparable magnitude. Each of these contributions is comparable to the contribution from the term in which r_{cm} and r_{cm}' are not displaced relative to each other, i.e., to the contribution which is associated with deuterons coincident over a common zero-point volume centered about a specific site. (It is quite important to recognize that this last limit of deuterons coalescent over a zero-point volume is quite different from the case of "point" deuterons [whose electrostatic dimensions are $\sim R_{deut}$] coalescing over a nuclear volume because of the very large [on the scale of nuclear dimensions] zero-point-volume that each deuteron occupies within the lattice.) As a consequence, within a BBC, contributions to multiple deuteron interaction from deuterons that are located on different sites enter with the same magnitude as do comparable contributions associated with a free space Greens function in which multiple numbers of deuterons coalesce over a common electrostatic volume of comparable (i.e. zero-point-motion) size. Since all self-interaction corrections, associated with short-distance (ultraviolet) contributions to the self-energy that arise in conventional field theory associated with multiple nucleon occupation of a common volume, are expressible (using standard many-body techniques) in terms of a Wick

expansion of the associated perturbation using the two particle Greens function, it follows that commencing from the BBC, subject to the constraints associated with separability, these corrections take on an entirely different form within a solid. In particular, the role of Coulomb repulsion as it appears in any (free space) many-body interaction associated with multiple occupation of free space deuterons at a common location (bubble diagrams), is entirely different, and because site-site *nuclear* contributions are present, the traditional role of the "Coulombic Barrier" is very different. In the next section, we will estimate explicitly the coulombic and nuclear self-interactions associated with four deuterons interacting at a common location.

Finally, the BBC field theory corresponds to a limit of a more complete theory. Within the BBC limit, there are important, implicit selection rules that result from the requirement of separability between nuclear and electrostatic interactions. Thus, to obtain the BBC limit from the more complete theory, it is necessary to impose these selection rules on the more complete theory. The rules are implied by the fact that all BBC many-body reactions evolve from $\psi^{op}_j{}'(r,t)$ (as defined by Eq. 10), by the assumption that each function $\psi^{nuc}(r_{n-p})$ has appreciable value only when $|r_{n-p}| \sim R_{deut}$, and the requirement that each deuteron-boson (electrostatic) field operator $\psi^{elec}(r_{cm},t)$ (and its adjoint) commutes with each of the proton-neutron pair boson field operators $\psi^{nuc}(r_{n-p},0)$. The BBC limit may be obtained by removing from the complete theory all many-body processes, real or virtual, in which separability between nuclear and electrostatic interactions is violated. Though this procedure omits many processes, when the BBC becomes occupied, the dominant interactions with which the BBC has overlap have separability built into them provided the length and time scales associated with the nuclear and electrostatic interactions remain sufficiently different. A necessary condition associated with this prescription

is to require that, beginning from the more complete theory, all contractions between different (fermion) nucleons only occur when at all times, each proton (neutron) associated with the contraction is located within a nuclear dimension of a second neutron (proton) prior to the interaction. This means that from the various hierarchies of many-body potentials that are present in an unconstrained field theory (in which the nucleon and electromagnetic wave functions are not constrained to be separable), the BBC limit is only consistent with those in which the proton-neutron pair provides the stable particle from which the field theory evolves. As a consequence, the only allowable interaction potentials that can be constructed from the BBC field theory (and in the limit in which the more complete theory reduces to the BBC theory) are derived from proton-neutron pairs. Then if the initial state involves primarily deuterons (i.e., when there are no free fermions at an isolated lattice site), it follows that the final state must contain equal numbers of protons and neutrons, in which each proton is "paired" to at least one neutron located within "close" (i.e., nuclear) proximity of it. As a consequence, except in regions where periodicity breaks down (for example, near surfaces or interfaces), or impurities are present, the allowable self-interaction perturbations are constructed only from Greens functions that obey Eqs. 10 and 11 throughout the bulk solid. (Such perturbations always are constructed from Feynman diagrams that begin and end within a zero-point-volume of a lattice site.) Thus, the prerequisite conditions that allow for the formation of the BBC, which lead to separability of the nuclear and electrostatic interactions also lead to the selection rule: "Bosons in and Bosons out", where it is understood that each boson is formed from pairs of protons and neutrons. As a consequence, tritium release and $^3\text{He}^{++}$ production should not appear as primary fusion products!

As we have emphasized, the limiting effect that governs whether or not

fusion occurs is the applicability of Born-Oppenheimer separability. The suitability of this approximation is dictated by an uncoupling of nuclear coordinate motion associated with variations in the proton-neutron separation $r_{n-p} = r_n - r_p$ from the motion of the center of mass coordinate $r_{cm} = (r_n + r_p)/2$. This uncoupling becomes possible when the zero-point-motion of each deuteron is large enough. We will examine this effect in the next section.

VI Self-Interaction, and Self-Induced Fusion

In this section, we estimate the relevant self-interaction energies associated with multiple deuteron interaction at a site and find that to first order in the relevant perturbation, the criteria for separability are satisfied. The large difference in energies allows us to conclude that the prerequisite conditions for separability are justified through leading order in perturbations associated with the ultraviolet behavior of the field theory, allowing us to estimate the resulting rate for self-induced fusion. This result enables us to examine the possibility of a variety of possible nuclear interactions associated with multiple deuteron occupation of a common zero-point-volume about a specific lattice site for a finite period of time, based on the "Bosons in and Bosons out" selection rule required by BBC reactions, using the Fermi Golden Rule. We then consider the limit in which heat production is dominated by one particular reaction, associated with direct ^{4}He production from a perturbation (as required by separability) that involves only the strong interaction through the virtual coalescence of four D^+ nuclei over a common electrostatic volume. Because this calculation applies to the low temperature limit, the nuclear perturbation occurs at an isolated location. As a consequence, in this calculation, we find the Wannier representation of the BBC to be useful. Using this result we are able to calculate a suitable lower bound on the concentration c of BBC deuterons that

are required to obtain the observed heating rate[2]. Because the value of $\underline{c}$ is very low, we are able to justify our conclusion that the cooperative ionic fluctuations associated with BBC formation become energetically favorable as a means of reducing lattice strain.

In the previous sections, we have defined the relevant Greens function and initial state associated with BBC formation and its time evolution away from the quasi-equilibrium state from which it forms. Both of these quantities become applicable near the overcharging condition that occurs as the physical D concentration becomes slightly greater than one D per Pd. Then, as discussed in sections III-V, it becomes energetically favorable, as additional small concentrations of D are injected, for the injected D to occupy energy band states. In this limit, each D "sees" an approximately periodic, single particle, coulomb potential. Also, the single particle wave function of each injected D is well described by a Born-Oppenheimer separable form because of the very large difference in energy between the electrostatic binding of the D to the lattice and the binding of each proton to neutron within each D. The relative stability of this quasi-equilibrium BBC initial state and the possibility for nuclear self-interaction from this state are governed by the properties of the state and its time evolution in the presence of the "true" many-body potential. The second quantized form of this many-body potential V is given by the sum of the second quantized form of the two-body coulombic $V^{elec}(t)$ and strong interaction $V^{nuc}(t)$ potentials. Near the BBC limit, the single particle potential $U^{elec}(r)$ from which the band energies of the BBC deuterons are derived is assumed to be a good approximation of the functional derivative of V^{elec} with respect to the field variable $\psi^{elec}(r_{cm},t)$:

$$U^{elec}(r_{cm},t)\psi^{elec}(r_{cm},t) \sim \delta V^{elec}(t)/\delta\psi^{elec}(r_{cm},t) \qquad ,(15a)$$

where the "classical" field variable ψ^{elec} (as opposed to the second quantized

operator) functional form is used both on the right side of the equation and in the expression for V^{elec}. Here, U^{elec} is the single particle potential of the band problem,

$$(\frac{-\hbar^2}{2M_D} \nabla^2 + U^{elec})\psi_{Bloch}(\epsilon_i(k),r_{cm}) = \epsilon_i(k)\psi_{Bloch}(\epsilon_i(k),r_{cm}) \quad , \text{(15b)}$$

and $\psi^{elec}(r_{cm},t)$ is an arbitrary linear combination of the Bloch state functions. $\psi_{Bloch}(\epsilon_i(k),r_{cm})$. Similarly, each of the N_B single particle nuclear potentials $U^{nuc}(r)$ from which the proton-neutron pair energies ϵ_{nuc} are derived is assumed to be a good approximation of the functional derivative of V^{nuc} with respect to the classical field variable $\psi^{nuc}(r_{cm},t)$

$$U^{nuc}(r,t)\psi^{nuc}(r,t) \sim \delta V^{nuc}/\delta\psi^{nuc}(r,t) \qquad \text{,(15c)}$$

$$(\frac{-\hbar^2}{2\mu_{nuc}} \nabla^2 + U^{nuc})\psi^{nuc}(\epsilon_{nuc};r,t) = \epsilon_{nuc}\psi^{nuc}(\epsilon_{nuc};r,t) \qquad \text{.(15d)}$$

The classical field variable $\psi^{nuc}(r_{cm},t)$ is an arbitrary linear combination of the eigenstates $\psi^{nuc}(\epsilon_{nuc};r,t)$. Perturbation theory associated with many-body fluctuations about the BBC mean field theory consists of including within the time (and thermal) evolution of the dynamical variable of interest, the terms that result from incorporating the "classical" expectation values (i.e., the thermal expectation values as in Eq. 15a and 15c) of the higher order functional derivatives of V^{nuc} and V^{elec}, evaluated using the thermal and functional forms associated with the BBC limit. (The second quantized form is used merely as a convenient method for evaluating the associated functional differentiations.)

In the Greens function language, presented here and discussed in various text books[6], the relevant dynamical variable is nucleon density, provided by the difference between the exact nucleon Greens function $G^{exact}(r,r',t)$ and the $G(r,r',t,\beta)_{ij}$ of Eq. 12 (and functional derivatives of this difference with respect to the instantaneous nucleon fields) evaluated in the limit in which r → r' as a function of time. The time derivative of the integral of the absolute

square of this quantity in the limit that $t \to 0^-$ is the total rate of change of BBC occupation. The self-energy matrix Σ (as it is referred to in the Dyson Equation) is defined order by order in the expansion in terms of functional derivatives by

$$\Sigma \, G^{exact} = G^{-1} \, G^{exact} - 1,$$

where a matrix sum over position, time and all spin indices is implied, 1 is the four dimensional δ-function, and

$$G^{-1}(r_f, t; r_f', t') = [i\partial_t - H^{nuc,eff}(\pm r_{n-p}/2) - H_o^{elec}(r_{cm})]\delta(t-t')\delta((r_{n-p} - r_{n-p}')/2)$$

$$X \qquad \delta((r_{cm} - r_{cm}'))$$

Using these two relations, it is easy to show that the approximation for Σ given by

$$\Sigma(r, t; r', t')_{i,j} = [-i\partial_{t'} - H^{nuc,eff} - H_o^{elec}]\{ -i\theta(t-t')\underline{\delta \qquad [<\delta V^{nuc}(t)>]} \atop \delta\psi_j(r', t')\delta\psi^{+i}(r, t)$$
$$-i\theta(t-t') \, \underline{\delta[<\delta V^{nuc}(t)/\delta\psi^{+i}(r, t)>]} \} \atop \delta\psi(r', t')_j$$

provides the leading order, many-body correction to the time evolution operator associated with deviations of the precise field variables $\delta\psi(r, t)$ from their BBC values. We have used the symbol "<..>" to denote thermal averaging with respect to H_o (the total single particle potential), and the subscripts i and j designate the spin value.

The total "effective field mass" M of the field theory is provided by the integral over space of $\pm i Tr(\Sigma G)$ (the negative or positive sign, respectively is used for fermions or bosons) at a common spatial point. Thus, the quantity

$$M = \int \lim_{\delta \to 0} \Sigma_{i,j} \, i\Sigma(r, \delta; r, -\delta)_{i,j} G(r, r, -\delta, \beta)_{ij},$$

establishes the stability criterian of the expansion in terms of functional

derivatives. If M > 0, the expansion is stable; when M < 0, the expansion is unstable. (Here, the integration over r includes integrations of both the center of mass and nuclear coordinates at a common field point r_f.) In the current case, where separability is required, all of the various functional derivatives of the electronic field variables with respect to the nuclear field variables must vanish and vice versa. A sufficient condition to guarantee that this is the case is that the energy and momentum scales associated with nuclear and electrostatic contributions to M be very different everywhere so that the expansion is either strongly stable (M << 0) or unstable (M>>0). Also, because of the short range of the strong interaction, it follows from Dysons equation that, in the low temperature limit, the only non-negligible many-body contributions associated with the possibility of fusion can arise near $\lim_{r \to r'}$, $\Sigma(r',t';r,t)_{i,j}$.

Thus, not surprisingly, both the possibility of fusion and the question of whether or not nuclear and electrostatic interactions remain separable in the limit in which fusion may occur are governed by the ultraviolet (short wave length) limit of the associated many-body physics. When the electrostatic and nuclear interactions are separable, it follows that the quantity $\Sigma(r,t;r,t')_{i,j}$ and the functional derivatives of $\Sigma(r,t;r,t')_{i,j}$ may be used to establish a hierarchy, of effective many-body interaction potentials associated with successively higher order corrections in the functional expansion of the time evolution operator. Provided M remains sufficiently negative as these corrections are included, the resulting effective potential may be used as the interaction perturbation in the Fermi Golden Rule expression for the transition rate via strong interaction to any of the allowable nuclear final states. In the case of the strong potential contribution, provided M is strongly negative, for the purpose of establishing an upper bound on the fusion rate, the relevant

matrix elements can be evaluated using a simplified description based on a single particle problem involving a reasonable approximation of the strong interaction contribution to the quantity $\Sigma(r,\delta;r,-\delta)_{i,j}$.

Near the quasi-equilibrium environment associated with the BBC state, $\Sigma(r,\delta;r,-\delta)_{i,j}$ may be evaluated using the BBC Greens function $G(r,r',-\delta,\beta)_{ij}$ (Eq. 12)

$$\Sigma(r,\delta;r,-\delta)_{i,j} = \Sigma_{i',j'} \int d^3r' \lim_{\delta \to 0} \quad S(r,r')_{ij} G^*(r,r,+\delta,\beta)_{ji}$$

$$+ \quad \int \frac{d^3r' \ e^2 \ G^*(r',r',-\delta,\beta)_{i'j'}}{|r-r'|} \ \delta_{i,j}\delta_{i',j'} \tag{16}$$

Here, $\delta_{n,m}$ is the Kronecker delta tensor ($=1$ if $n=m$ and vanishes otherwise), the r' coordinate in the second integration is over the center of mass and the proton position relative to the center of mass ($-r_{n-p}/2$), with $r' = r_f = -r_{n-p}/2-r_{cm}$, and $S(r,r')_{ij}$ is the short-ranged strong potential. This potential also includes the exchange term (associated with replacing (r,r) with (r,r') and (r',r') with (r',r) in each Greens function in the second term). The exchange term (which is normally considered to be of electrostatic origin) should be included with the strong interaction because it is considerably shorter in range and provides an important source of magnetic correlation, which is known to be of consequence on nuclear length scales since each ground state deuteron possesses a total magnetic spin quantum number of unity. The second term is associated with the familiar direct, coulombic self-interaction, which in the case of free space nuclear physics provides the barrier to fusion, where it precludes the phenomenon except at high temperatures.

Renormalization (regularization) of any field theory is defined by the behavior of the right side of Eq. 16 in both the $r \to 0$ (ultraviolet) and $r \to \infty$

(infra-red) limits. To understand the possibility of fusion, it is sufficient to define $\Sigma(r,\delta;r,-\delta)_{i,j}$ to be the effective interaction potential for each nucleon, and to define all higher order, fluctuations in the associated many-body expansion in terms of functional derivatives of $\Sigma(r,\delta;r,-\delta)_{i,j}$. In doing so, because the field points where Σ is applied are coincident, by definition, we have chosen any of the associated perturbations automatically to be the result of self-interaction. Then the regularization of the theory, as well as the possibility of fusion are defined primarily by $S(r,r')$, since this term plays a critical role in the $r{\rightarrow}r'$ limit. In priniciple, S could be constructed from a first-principles nuclear field theory, using Yukawa potentials, for example. In practice, it is simpler to model S in a suitable manner that provides a realistic estimate of its magnitude and spatial distribution.

Because the second term becomes quite small as the value of r_{zp} approaches its value in stoichiometric Pd-D (~0.2 A as shown in ref. 3), detailed information concerning S is not required other than the fact that it is very short-ranged (~by a factor of 10^5 smaller) in radial extent and large in magnitude compared to the second term. As a consequence, a refined estimate of S is not required to obtain a meaningful upper bound on the fusion rate, provided separability applies. To demonstrate that separability does apply, it is sufficient (through the first order corrections in the self-interaction perturbation), to demonstrate that M is very negative (and dominated by the strong interaction). We may estimate the value of the electrostatic contribution to the mass, M^{elec} using the form for the Greens function derived in the last section.

$$M^{elec} = \sum_{j,j'} \int d^3r' d^3r \; e^2 \; \frac{G^*(r',r',\delta,\beta)_{j',j'} \; G(r,r,-\delta,\beta)_{j,j}}{|r-r''|} \qquad (17)$$

Using Eq. (12), we find

$$M^{elec} = \sum_{j,j} \int \int d^3r_{n-p}{}'/2 \, d^3r_{n-p}/2 \int \int d^3r_{cm}{}'d^3r_{cm} \{ \rho_{nuc}(r'_{n-p}/2, r'_{n-p}/2, \delta, \beta)_{j,j} \quad .(18)$$

$$x \qquad \rho_{nuc}(r_{n-p}/2, r_{n-p}/2, -\delta, \beta)_{j,j} \}$$

$$x \qquad \frac{e^2}{|-r_{n-p}/2 + r_{cm} + r_{n-p}{}'/2 - r_{cm}{}'|}$$

$$x \quad G^{*BBC}(r_{cm}, r_{cm}, \delta, \beta) \; G^{BBC}(r_{cm}{}', r_{cm}{}', -\delta, \beta)$$

Because the nuclear variables have appreciable weight only in the nuclear region, we may use

$$\frac{1}{|-r_{n-p}/2 + r_{cm} + r_{n-p}{}'/2 - r_{cm}{}'|} = \frac{1}{|r_{cm} - r_{cm}{}'|} + O(10^{-5}),$$

and neglect the dependence of r_{n-p} and $r_{n-p}{}'$ within the integrand except within the nuclear density factors $\rho_{nuc}(r_{n-p}, r_{n-p}{}', \delta, \beta)$ found in the bracketed term on the first two lines of Eq. (18). As a consequence, the integrations over the nuclear coordinates r_{n-p} and $r_{n-p}{}'$ contribute unity, and we are left with

$$M^{elec} = \int \int d^3r_{cm}{}'d^3r_{cm} \frac{G^{*BBC}(r_{cm}, r_{cm}, \delta, \beta)}{} \frac{e^2}{|r_{cm} - r_{cm}{}'|} \frac{G^{BBC}(r_{cm}{}', r_{cm}{}', -\delta, \beta)}{} \qquad (19)$$

Using Eqs. 4 and 5 to rewrite each G^{BBC} in terms of Bloch functions, $\psi_{Bloch}(\epsilon_i(k), r_{cm})$, in Eq. 19, we find after taking the $\delta \to 0$ limit that M^{elect} reduces to the correct electrostatic limit,

$$M^{elec} = \int \int d^3r_{cm}{}'d^3r_{cm} \frac{\rho(r_{cm}, \beta)}{} \frac{e^2}{|r - r'|} \frac{\rho(r_{cm}, \beta)}{} \qquad (21)$$

where

$$\rho(r_{cm}) = \sum_{i,k} \frac{\psi^*_{Bloch}(\epsilon_i(k), r_{cm}) \psi_{Bloch}(\epsilon_i(k), r_{cm})}{(e^{\beta \epsilon_i(k)} - 1)} \qquad (22)$$

To estimate M^{elec}, we take the low temperature, $\beta = \infty$ limit of Eqs. 21 and 22, in which only the lowest k=0 energy state contributes to the sum. Then using Eq.

4, we find that

$$\rho(r_{cm}) = 1/N_L \, \Sigma_s \, \phi_s^*(r_{cm}) \, \Sigma_m \, \phi_m(r_{cm}) \qquad\qquad ,(23)$$

where $\phi_s(r_{cm})$ and $\phi_m(r_{cm})$, respectively, are the Wannier states for the sites s and m in the lowest energy band. Using Eq. 5, and the value $r_{zp} = 0.5$ Bohr ~ 0.26 A, to estimate each Wannier state wave function $\phi_m(r_{cm})$, and substituting it into Eq. 23, we find that in the double sum, a single contribution (from the diagonal contribution s=m) dominates the other contributions to the density (by ~ 15 orders of magnitude), and provides a single dominant contribution for each density at each lattice site. Defining each of the site diagonal contributions to the double sum from the nth site by ρ_n, with

$$\rho_n = \phi_n^*(r_{cm}) \, \phi_n(r_{cm})/N_L = (2/\pi r_{zp}^2)^{3/2} \, \frac{\exp(-2r_n^2/r_{zp}^2)}{N_L},$$

where $r_n = r - R_n$, with negligible error, we may approximate $\rho(r_{cm})$, using

$$\rho(r_{cm}) = \Sigma_n \, \rho_n(r_{cm}) = (2/\pi r_{zp}^2)^{3/2} \, \Sigma_n \, \frac{\exp(-2r_n^2/r_{zp}^2)}{N_L} \qquad .(23a)$$

Substituting Eq. 23a into Eq. 21, we find,

$$M^{elec} = \int \int d^3r_{cm}' d^3r_{cm} \, \frac{\rho(r_{cm},\beta) \, e^2 \, \rho(r_{cm}',\beta)}{|r_{cm}-r_{cm}'|} \qquad\qquad (24)$$

$$= \Sigma_{n,m} \int \int d^3r_{cm}' d^3r_{cm} \, \frac{\rho_m(r_{cm},\beta) \, e^2 \, \rho_n(r_{cm}',\beta)}{N_L^2 \, |r_{cm}-r_{cm}'|}$$

$$< \int \int d^3r_{cm}' d^3r_{cm} \, \frac{\rho_0(r_{cm},\beta) \, e^2 \, \rho_0(r_{cm}',\beta)}{|r_{cm}-r_{cm}'|}$$

$$= 54.4 \text{ eV}$$

This value should be compared with the comparable value of M^{elec} (~ 10's of MeV) that results when the zero-point-radius of each deuteron is reduced to nuclear dimensions, and to the approximate values for M^{nuc}, where

$$M^{nuc} = \int \int d^3r \, d^3r \, \Sigma_{i,j,i',j'} \, S(r,r')_{ij,i'j'} \, G^*(r,r',\delta,\beta)_{ji} \, G(r,r,-\delta,\beta)_{j',i'}.$$

The translational invariance of the binding of each proton to each neutron with respect to translations of the center of mass implies that to an excellent approximation, when separability between electrostatic and nuclear interactions holds, $S(r,r')$ is translationally invariant with respect to displacements of both of its coordinates. The magnitude of M^{nuc}, then, could become unbounded since

$$G(r'+R_n, r'+R_n), -\delta, \beta)_{j',i'} = G(r', r', -\delta, \beta)_{j',i'}.$$

The possibility of this unphysical bound, however, is due to the infrared divergence of the theory.
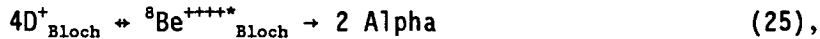
Near $T=0$, we may obtain a more realistic bound by observing that increases in entropy necessarily result when a set of fluctuations in nuclear self-interaction energy (associated with M^{nuc}) are allowed to occur at lattice sites located near each other as a consequence of coupling to processes whose length scales fall intermediate in range between the nuclear and electrostatic interaction length scales. Thus, at sufficiently low temperature these fluctuations can only occur at isolated lattice sites, located far apart from each other. To establish a meaningful bound, then, for M^{nuc}, we may consider this limit in which an isolated fluctuation in self-interaction energy occurs at a specific site. In this case, a lower bound for the magnitude of M^{nuc} is several MeV (since the binding energy of each deuteron ~ 2MeV), while a reasonable upper bound is provided by the average energy per deuteron pair ~ 11.9 MeV that results from $D + D \rightarrow {}^4He$, in which 23.8 MeV is released. Thus, $M^{nuc} \sim 10^5 \times M^{elec}$. As a consequence, $M = -|M|^{nuc} + M^{elec}$ is in fact extremely negative, even in the limit of low temperature, meaning that Born-Oppenheimer separability is valid both for the initial state and in the presence of the perturbation.

The same argument demonstrates that when four deuterons coalesce over a nuclear volume, the associated electrostatic self-interaction mass repulsion M^{elec} is on the order of several hundreds of eV compared with a nuclear attractive self-interaction of mass $M^{nuc} = 47.6$ MeV. These estimates of the four deuteron per lattice site occupation do not include higher order bubble diagram corrections to the self-interaction. However, each of these higher order corrections enters with additional powers of the electrostatic overlap and nuclear overlap of wave functions at a common lattice site in a manner in which greater electrostatic repulsion favors reduction in electrostatic overlap (and increased zero-point-motion), while enhanced nuclear attraction favors greater nuclear overlap. As a consequence, it is to be expected that if these higher order corrections are included, they would further increase the disparity between M^{nuc} and M^{elec}. This would further improve the validity of the separability condition.
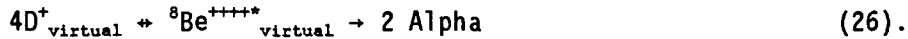
Since Born-Oppenheimer separability applies equally well for the initial state and in the presence of a self-interaction perturbation, it is valid to estimate fusion rates from the initial state using the self-interaction potential, based on the Fermi Golden rule. Though the associated perturbation expansion is asymptotic, at best (since both the electrostatic and nuclear interaction corrections are an order of magnitude greater than the initial state nuclear and electrostatic single particle potentials), provided Born-Oppenheimer continues to apply, higher order corrections from the expansion, in which separability also applies, should improve the accuracy associated with the initial estimate. If these higher order corrections reduce the overlap of the electrostatic wave function (and Greens function) with the nuclear region, it is to be expected that further improvement of the separability should apply, meaning that further nuclear interaction will further improve the representation,

provided that Bloch symmetry is maintained. In this manner, it can be seen that an infinite number of diagramatic contributions can be constructed, each of which further reduces the overlap of corrections associated with electrostatic repulsion relative to those associated with nuclear attraction, there-by improving the initial approximation based on separable wave functions.

We now consider the fusion problem. The most probable reaction appears to be the pure bosonic, momentum balanced reaction

$$4D^+_{Bloch} \leftrightarrow {}^8Be^{++++*}_{Bloch} \rightarrow 2 \text{ Alpha} \tag{25},$$
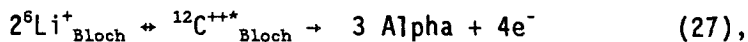
or its Wannier state equivalent,

$$4D^+_{virtual} \leftrightarrow {}^8Be^{++++*}_{virtual} \rightarrow 2 \text{ Alpha} \tag{26}.$$

In Eqs. 25 and 26, $4D^+$ refers to the 4-fold occupancy state or quad-deuteron (associated with the coalescence of four deuteron electrostatic functions over a common zero-point-volume), and ${}^8Be^{++++*}$ stands for a compact configuration at nuclear density which possesses the symmetries and internal quantum numbers associated with the initial four deuterons. This intermediate state has the same total energy as the initial four deuterons, but nucleons within the "nuclear force bag" have high kinetic energies. The final state requires rearrangement of nucleons so as to produce two spin=0 Alpha's each containing 23.8 MeV relative to the center of mass.   The full reaction is in principle reversible and satisfies the "bosons in and bosons out" selection rule (all components can exist as BBC states involving integer numbers of proton-neutron pairs).

We also consider the possibility of two other reactions, suggested by the apparent requirement that LiOD (as opposed to NaOD) be electrolyzed to produce anomalous heat in a Pd electrode. With overvoltage electrolysis some Li can be expected to enter the host lattice. Although the effect of interstitial Li is likely an electronic structure effect, there could be possible nuclear reactions:

$$2{}^6Li^+_{Bloch} \leftrightarrow {}^{12}C^{++*}_{Bloch} \rightarrow 3 \text{ Alpha} + 4e^- \tag{27},$$

and

$$D^+_{Bloch} + \, ^6Li^+_{impurity} \leftrightarrow \, ^8Be^{+++}_{impurity} \rightarrow 2 \, Alpha + 2e^- \quad (28).$$
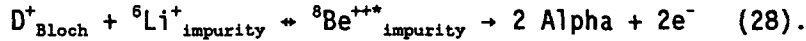
In Eq. 27, 2^6Li^+ is a double occupancy $^6Li^+$ Bloch state. In Eq. 28, $^6Li^+_{impurity}$ is a real interstitial Li^+ ion which is assumed to react with the D^+ BBC initial state. Eq. 28 would reflect an apparently different type of BBC reaction. However, since the final Alpha particle states can be considered impurity states, the difference may be more apparent than real. We will not further consider either Li reaction.

Let us now consider whether the formation of a D^+ BBC can lead to the observed heat release in Pd by fusion reaction 25. Details of our analysis are sketched below. A more complete derivation is given elsewhere[1]. Using the observed[2] value of the power density $P_{fusion} \sim 10$ W/cm^3 (4 MJ / 120 hours), we set an approximate lower bound ($\underline{c}^{lower}$) for the concentration ($\underline{c}$) of injected D^+ ions, required to obtain the observed[2] heating. Our estimate of $\underline{c}^{lower}$ follows from an estimate of the fusion rate, Γ_{fusion}, based on the Fermi Golden rule, and the interaction potential $\Sigma(r,\delta;r,-\delta)_{i,j}$, based on Eq. 16, using a model strong interaction for S, based on the known decay of the excited $^8Be^*$ nucleus to two alpha particles. Also, the low temperature limit in which multiple nucleon interactions associated with S occur at an isolated site, it is appropriate to consider the initial state to be formed exclusively from electrostatic Bloch functions from the lowest energy, k=0 band state.

Because the self-induced perturbation, S, associated with Eq. 25 is short-ranged and involves interactions between eight nucleons at an isolated location, two consequences follow from Eq. 1. 1) Large contributions to the associated perturbation matrix element result from the product between any four single particle D^+ Bloch states throughout the lattice in the initial state and the

product of the highly localized perturbation with the final state ψ_f functions associated with the recoiling alpha particles. 2) All contributions to the matrix element are negligible except for those associated with the integrations over regions near the site where interaction takes place. Then, the number of distinct contributions that arise from the overlap of each of the N_B ($\gg 1$) single particle Bloch states associated with the initial state (in which there is at most 1 D^+ wave function centered at each site, and each state is normalized over the crystal) with the product of S and the 4 D^+-double-alpha particle final state wave functions near the location R_{fusion} of the perturbation is $N_b(N_b-1)(N_b-2)(N_b-3) \approx N_b^4$. Hence, given an approximate value for the energy release per fusion, Q_{fusion}, for fixed values of $P_{fusion} = \Gamma_{fusion} \, Q_{fusion}$, it follows that $P_{fusion} \propto \underline{c}^4 \, \Gamma_{nuc}$, where Γ_{nuc} is the reaction rate of a highly localized nuclear reaction at the single site R_{fusion}.

To evaluate $\underline{c}^{lower}$ we determine an upper bound for Γ_{nuc} using a simplified reaction model for Eq. 25. This simplified model provides a higher reaction rate than is expected. We replace the eight nucleon problem of the reaction by an independent particle nucleon model[7] in which the fusion process is modelled through a square well perturbation of the nucleonic potential. This square well is defined by a suitable upward shift in the kinetic energy T_o of each D^+ ion over a characteristic nuclear dimension within the vicinity of R_{fusion}. This is equivalent to requiring in the reverse of reaction 25, an immediate dissipation of the energy of both alpha particles (which may be viewed as a short-lived virtual state) in the immediate region in which the nuclear reaction takes place. The height of the square well is $Q_{fusion} = 47.6$ MeV (calculated from the decrease in rest mass[8]), which is inferred from the assumption that the wave function overlap associated with the quadruple deuteron (associated with the coalescence of four deuteron Wannier states over a common lattice site) may be viewed as

an excited state of a $^8Be^{++++}$ nucleus.

Explicitly, using a suitable set of minimal uncertainty gaussian wave packets in which the initial state is defined with a characteristic electrostatic dimension r_{zp} = 0.26 A and volume $V_{z.p.}$ = 4/3 π r_{zp}^3, while the final state is confined to the nuclear volume, V_{nuc} = 4/3 π R_{Be}^3, defined by the Be^{++++} nuclear radius R_{Be} = 9.108 x 10^{-13} cm, we find that

$$\Gamma_{fusion} = 2\pi/\hbar \; [2 \; M_D \; R_{Be}^2/(3\hbar^2)] \; (16/3)^{3/2} \; [V_{nuc}/V_{z.p.}]Q_{fusion}^2 \; x \; (\underline{c}^{lower})^4 \quad (29),$$

Using P_{fusion} = 10 W/cm^3 = $N_{site} \; Q_{fusion} \; \Gamma_{fusion}$, where N_{site} ($\cong$ 4.81 x 10^{22} cm^{-3}) is the density of Pd, and Eq 9, we find that $\underline{c}^{lower}$ equals 2.8 x 10^{-7}. Though Eq. 29 was derived for an isolated perturbation, which applies to low temperature, the identical argument can be generalized to the case of higher temperature by performing a suitable averaging over initial state band energies in the Fermi Golden rule. In this case, it is still true that $P_{fusion} \propto \underline{c}^4 \; \Gamma_{nuc}$. However, Γ_{nuc} and $\underline{c}^4$ may both become strongly dependent on temperature due to disruption of Bloch symmetry by the fusion process. This feature could prove valuable for controlling the process.

VII Predictions

The BBC D^+ fusion picture requires a suitable host lattice. One critical feature enabling condensed matter fusion is the establishment of conditions in which some D resides in the lattice in ionic form screened by itinerant electrons. A second requirement is that energies of the reactant single particle band be close to that of chemically bonded D so that it is possible to populate BBC states at realizable temperature. A third requirement is that the lattice provide adequate regularity and size to maintain approximate Bloch symmetry. A large r_{zp} appears favorable and reflects a low interstitial D^+ binding energy,

important for reducing electrostatic self-interaction. A large r_{zp} favors high diffusivity. It is interesting that Pd provides a diffusivity[3] for D that is greater than for H, contrary to expectation, suggesting that the bosonic character of D^+ may contribute substantially to the diffusivity. This line of reasoning suggests that a Pd-V host, which provides the most enhanced H-diffusion of any substitutional Pd alloy (as pointed out by Whalely[9] during this workshop), could be favorable for fusion reactions.

The key observable of BBC fusion by Eq. 25 would appear to be intense Alpha emission. However, Eq. 25 may not be the dominant mode of BBC energy release. A mode in which the BBC undergoes scattering with chemically bonded D, potentially, could involve heat release without intense alpha particle production. Additional coupling of the energy associated with this kind of scattering also should occur. For the 4-deuteron reaction (Eq. 25), the Alpha particles have a range in Ilford emulsion of more than 240 microns[7]. Strong M- and N- shell x-ray line emission at ~0.68 and ~0.094 keV should be present. Neutrons are not predicted except as a result of Alpha bombardment of host impurities or of the surrounding electrolysis medium. Ionic superconductivity at sufficiently low temperature is expected. The anomalous superconducting behavior associated with increased critical temperature[3] T_c (from 9.5 °K to 11.5 °K) that accompanies H for D substitution in Pd-H, which runs contrary to expectations based on conventional thinking about isotopic substitutions, could be accounted for by the presence of a small ionic component to the superconducting charge density. It is important to recognize that both the anomalous increase in T_c and the enhanced D-diffusivity provide important evidence that bosonic effects (on the scale of electrostatic interaction) may be present in charge transport phenomena in deuterated Pd.

Finally, it is appropriate to note some additional experimental results

associated with our theory and to provide some further comments concerning the generation of tritium and other secondary products. Secondary products either from the primary alpha particle emission, or through secondary interactions that become favorable where Bloch symmetry is disrupted or partially removed (such as at surfaces and interfaces) should occur. Also, the tentative observations of Rolison and O'Grady[10] could be the result of BBC nuclear scattering interactions near the cathode surface, possibly a consequence of reduced or lost Bloch symmetry.

The tritium production results due to Storms and Talcott[11] and Wolf[12] all appear to have involved cases in which surface area and interfacial effects are important, suggesting that the breakdown of Bloch symmetry in these environments is playing an important role in the observed phenomena. Alternatively, it is also possible that this secondary tritium production may result from secondary scattering of moderately energetic D or ^{4}He (possessing energies of ~ 100's of eV) with chemically bonded D after the onset of BBC fusion. This secondary scattering may lead to tritium production through still an alternative form of fusion, recently hypothesized by us, "not-so-cold" fusion. This alternative form of fusion (which explains the "cluster impact fusion" experiments of Beuhler et al[13]) is the result of the collisions between modestly energetic (~100's of eV) deuterons with chemically bonded D (or other light ions or atoms) near the surface. The possibility of nuclear interaction, which to our knowledge has not been explained before, based on a quantum mechanical treatment of the electrostatic interaction, at these energies can be quantified through an application of the ideas of zero-point-motion broadening of charge, as presented in this paper. In particular, chemically bonded D in the surface region, for example, has a zero-point-radius of ~0.2 A. An incident particle possessing an energy of 100's of eV has a characteristic deBroglie wave length λ_{inc} of several

hundredths of an angstrom. We may use an electrostatic wave function ϕ^{target} for the chemically bonded D (assumed to be bound within a harmonic well of zero-point radius r_{zp}), analogous to our choice of Wannier states (Eq. 5).

$$\phi^{target}(r) = (2/\pi r_{zp}^2)^{3/4} \exp(- r^2/r_{zp}^2)$$

We may approximate the incident particle wave function by

$$\phi^{incident}(r) = (2/\pi \lambda_{inc}^2)^{3/4} \exp(- r^2/\lambda_{inc}^2).$$

Then we may demonstrate explicitly that the electrostatic repulsion is reduced by 5 orders of magnitude by calculating the first order energy shift $M^{(1)}$ in the incident particle's energy (the analogue of the electrostatic contribution to the total "effective field mass" M^{elec})

$$M^{(1)} = \int \int d^3r' d^3r \frac{|\phi^{*incident}(r)|^2 e^2 |\phi^{target}(r')|^2}{|r-r'|} .$$

We find that M equals $e^2(2/(\pi(r_{zp}^2 + \lambda_{inc}^2)))^{1/2} \sim 40$ eV. This value again is roughly a factor of 10^6 less than the comparable value associated with the free space case. As a consequence, as in the case of cold fusion, in "not-so-cold" fusion, the electrostatic repulsion between deuterons is many orders of magnitude less than the strong interaction perturbation, and Born-Oppenheimer separability applies. Appreciable transition rates for fusion then become possible at dramatically reduced incident energies, as compared with those that are required in the absence of the zero-point-motion induced broadening.

Most importantly, to lend credence to our view that alpha production should be important, it should be pointed out that Chambers et al[14] have in fact observed high energy, charged particles (presumably alpha particles) in the energy range (at ~ 21 MeV) predicted by our theory, during D^+ ion implantation experiments in a 130 A thick Pd film. Possible detector failure may have been responsible for the the signals observed. However, the fact that no signal was seen at other, unpredicted energies is then difficult to explain. These extraordinary observations should be repeated, using a reliable detector.

Acknowledgment

References

[1] Chubb, S.R. and T.A. Chubb, "Distributed Bosonic States and Condensed Matter Fusion", *NRL memorandum report 6600*, Documents, code 2627, Naval Research Laboratory, Washington, D. C. 20375-5000, in press; also submitted to Nature, (1989). Chubb, T.A. and Chubb, S.R., "Nuclear Fusion in a Solid via a Bose Bloch Condensate", *NRL memorandum report* (unnumbered), Documents, code 2627, Naval Research Laboratory, Washington, D. C. 20375-5000, in press; also, submitted to *Phys. Rev. Lett.* (1989).

[2] Fleischmann, M. & Pons, S. *J. Electroanalytical Chem.* **261**, 301 (1989).

[3] Wicke, E. and Brodowsky, H., in *Hydrogen in Metals II* (eds Alefeld, G. and Völkl, J.) 73 (Springer, Berlin, 1978).

[4] Eberhardt, W., Greuter, F. and E. W. Plummer, *Phys. Rev. Lett.* **46**, 1085 (1981).

[5] Chubb, S. R. and J. W. Davenport, *Phys. Rev. B* **31**, 3278 (1985). Chubb, S. R., "Studies of Surface Electronic Structure Based on the Layer KKR Method", Ph D. dissertation, State University of New York at Stony Brook, Stony Brook, New York 11794. Switendick, A. C. in *Hydrogen in Metals*, (eds Alefeld, G. and Völkl, J.), p 101 (Springer, Berlin, 1978); Z. Phys. Chem. neue Folge, 117, Suppl. 89 (1979).

[6] cf Abrikosov, A. A., Gor'kov, L. P. and I. Ye. Dzyaloshinskii, *Quantum Field Theoretical Methods in Statistical Physics, Second Edition*, chapter V (Pergamon

Press, Oxford, 1965); or, Fetter, A. L. and J. D. Walecka, *Quantum Theory of Many-Particle Systems*, 601 p. (McGraw-Hill, San Francisco, 1971).

[7]cf DeBenedetti, S. *Nuclear Interactions* 70-97 (John Wiley & Sons, New York 1964).

[8] Gray,D.E. *American Institude of Physics Handbook, First Edition* p. 8-32 (McGraw-Hill, New York, 1957).

[9]Whaley, K. B., in this Proceedings, and private communication.

[10]Deborah Rolison and William O'Grady, in this Proceedings.

[11]Edmund Storms and Carol Talcott, in this Proceedings.

[12]Wolf, K. in this Proceedings.

[13]Beuhler, R. J., Friedlander, G. and L. Friedman, *Phys. Rev. Lett.* **63**, 1292 (1989).

[14]Chambers, G. P., Eridon, J. E. Grabowski, K. S., Sartwell, B. D. and D. B. Chrisey, Journal of Fusion Energy: Proceedings of the Utah Conference on Cold Fusion (May 23-25, 1989), in press.

DISCUSSION (CHUBB)

Mansour: Dr. Whaley's paper also assumed periodic conditions. How does your approach differ from hers?

Chubb: She was discussing it in terms of a periodic density function.

Mansour: Whereas you use Bloch functions?

Chubb: Both approaches are closely related. However, there is an important distinction. In Dr. Whaley's approach, fusion processes are modeled using the Gamow tunneling formula. In this case, implicitly, the final tunneling process is the result of wave function overlap derived from functions which at large separation asymptotically obey the boundary conditions of free-space, unbound particles. In our approach, the final tunneling process is the result of wave function overlap derived from Bloch functions which obey the boundary conditions of particles that are bound to a periodic solid. This distinction is significant because as a consequence, in the relevant electrostatic tunneling probability calculation, our model prohibits the deuteron from occupying large regions of space that are far from the location where nuclear interaction occurs, while in Dr. Whaley's model, only near the location of nuclear interaction does the probability of overlap become small. This means that in our model, the set of nuclearly active states are implicitly prepared in a manner consistent with a case in which the individual particles are bound to a solid with low binding energy. This leads to enhanced probability at low energy for quantum mechanical interaction relative to the case in which nuclear interaction is presumed to occur from particles which are initially unbound.

Mansour: How large are the energy fluctuations which you consider?

Chubb: They are dictated by correlation effects of self-interaction.

Baym: If we suppose your particles were distinguishable, with the same mass and the same interactions, they would possess the same wave function, identical to that for indistinguishable protons. When they are distinguishable, it makes no difference whatsoever.

Chubb: It does in considering self-interaction effects.

Baym: The consequences should be the same. In addition, the points of changing local potential which you show in the lattice are very far separated.

Chubb: They can be, since they represent ionic fluctuations.

Baym: You seem to be assuming a superconducting material.

Chubb: Potentially, it could be superconducting.

Baym: In my view, it would be a superconductor.

Chubb: The particles can be in different K states.

Baym: If the Green's function for the system has a non-zero charge separation, then it is a superconductor.

Chubb: At finite temperature, the behavior of the Bose Bloch condensate Green's function is the same as the Green's function associated with other charged particles in a solid, such as electrons, except that it is derived from particles which obey Bose statistics. As non-vanishing wave-vector states become thermally occupied, implied momentum transfer to finite-temperature processes is required, leading to a breakdown of the superconducting behavior associated with the zero-temperature state.

Whaley: What in your view is a true Bose condensate?

Chubb: One in which all the particles are condensed and in the same energy state.

Whaley: I have estimated whether or not long-range order can be expected in tight binding situations. Basically, the same conditions hold as in the fluid, i.e., macroscopic fluctuations on a single site must occur. These will not take place under your conditions, or at extremely low temperatures.

Chubb: That is a subject for further discussion. Our present model is certainly not at zero temperature.

Baym: I still maintain that if a Bose condensation occurs, then the material is a superconductor.

Chubb: I disagree. At finite temperature, it is not a superconductor. Even in the idealization of the zero-temperature limit, in which the BBC presumably would exhibit superconductivity, it is possible, because the timescale associated with nuclear self-interaction is considerably shorter than the timescale of any electrostatic process, that fusion would occur more rapidly than the equilibration time required for superconductivity and that superconductivity would never be observed. It is also important to recognize that, in any realistic experiment, the formation of Bose Bloch condensate requires the presence of an applied electric field, as well as the attainment of an over-potential condition, and that the associated Bose Bloch condensate chemical potential, as a consequence, has a complicated dependence on applied electric field, which could eliminate the possibility of the formation of a true, zero-temperature Bose condensate. Finally, it is also important to recognize that the Bose Bloch condensate deuterons can and do constitute only a small fraction of the total deuteronic charge. This is required since the band picture from which BBC deuterons are derived is only meaningful when the participants in the BBC population are well-screened from each other by itinerant (Pd-like) electrons. As a result, only a very, very small ($\sim 10^{-7}$) concentration of deuterons would be superconducting, and

the impact of this component on the superconductivity would be small. It is possible that the anomalous behavior of the superconducting temperature of PdD relative to PdH (PdD has a superconducting temperature two degrees greater than PdH, contrary to conventional expectation) could be partly the result of BBC occupation, though this conclusion may not be justified for the reasons I have just given.

Baym: The model situation would indicate room-temperature superconductivity.

Miley: Is there a specific experiment that could be carried out to verify this hypothesis?

Chubb: An experiment would attempt to detect α-particles using good single crystals of material. Other points requiring investigations are the fact that the diffusivity of D in palladium is twice that of H. If α-particles are produced, and He-4 is detected, with Pd-106 it would be possible to produce Ag-107 and tritium. The α-particles would have large energies, but they could, in principle, become Bloch states and be trapped as exitons inside the lattice. Thus, the palladium, as well as the off-gas, should be assayed for helium.

Baym: Can long-range interaction occur via nuclear rotational states?

Chubb: No. For the case of a Tokamak and free-particle boundary conditions, the boundary conditions and energy ranges are quite different than in cold fusion, and the rotational nuclear states will not provide a means for obtaining long-range interaction. The potentials of relevance inside the solid are small. By using the appropriate boundary conditions associated with boundary particles, one preferentially prepares the system in a correct manner that is very, very different than a Tokamak. This fact provides the underlying reason that the long-range interaction, through periodicity, becomes possible.

Whaley: I sense that a great deal of confusion is occurring concerning single-particle states and many-bodied states. When a single particle has a particular K value, that does not mean that the identical particles have the same value. One must allow for the interactions between the particles which occur in tight-binding situations.

Chubb: I agree. When these interactions are included, nuclear processes become possible.

Section 30

NUCLEAR FISSION GENERATED BY A HIGH POWER NEUTRON BEAM SHOT THROUGH
A CYLINDRICAL PALLADIUM LATTICE PACKED DENSELY WITH DEUTERON FUEL

Harold Szu

Naval Surface Warfare Center

Nuclear Fission Generated by a High Power Neutron Beam Shot through a Cylindrical Palladium Lattice Packed Densely with Deuteron Fuel

Harold Szu
Naval Research Laboratory, Washington D.C. 20375-5000
Current Address: Naval Surface Warfare Center Dalhgren Division, Code R44,
Silver Spring/White Oak, MD 20903-5000

ABSTRACT

A lot can be learned from an alleged cold fusion experiment. For example, it points out the missing knowledge of the macroscopic quantum medium characterized by dense Bosons at an intermediate scale length which is shorter than the atomic scale length, Angstrom, and longer than the nuclear scale length, Fermi. To create a dense medium for engineer exploitations is a recent trend of molecular engineering, the high temperature superconductivity and the low temperature fusion are two notable examples, other than the genetic engineering in biomedical sciences. Thus, what seem to be most useful out of the attempt of cold fusion are twofold: experimentally the molecular pressure technology of how to pack deuteron fuel densely within a palladium lattice, and theoretically the macroscopic quantum theory of a densely packed Bosons in a metallic lattice medium. That such a dense medium of overlapping deuteron nuclear wavefunctions acting like a macroscopic Boson state is indeed useful will be exemplified by a collective deuteron fission, stimulated by a high power neutron beam shot through the cylindrical package of dense deuteron-palladium medium, which can produce a collimated nuclear radiation with a gain, namely a possible nuclear laser with a collimated particle beam.

Key Words: Collimated Beam Nuclear Laser, Gammar Laser, Macroscopic Quantum

1. Dense Packaging of Deuteron Fuel in a Palladium Medium

A high power nuclear radiation beam that shot through a dense cylindrical package of deuteron fuel inside a palladium lattice acting like a macroscopic (quantum) state can generate a collimated nuclear radiation powered by the stimulated fission mechanism, rather than the spontaneous fusion. This is theoretically possible because the inverted population concept is valid for the Free Neutron Laser (FNL), described in Sect. 2, and the palladium metal caging effect [17] has help the extraordinarily dense fuel package, described in this section. The impinging nuclear radiation can be a neutron beam, the gamma ray, or a charged particle beam. Each choice has a different challenge to be overcome with a different potential barrier described in Sect. 3. Then, we call for the experimental and

theoretical investigations about the physics of the intermediate atomic and nuclear region in Sect. 4.

The difficulty in generating a short wavelength coherent radiation, such as the X-ray Laser, lies in the fact that the prospective source of radiation is not dense enough when compared with the radiation wavelength. Thus it is crucial for a coherent scheme to create a dense packing, as demonstrated by the cold fusion setup. Although the fission system is sufficiently dense, but may not be dense enough for a strictly coherent amplification. Thus, we are only talking about the gain coefficient of a collimated (rather than a strictly coherent) nuclear radiation. For coherent amplification an exponential-folding length must be greater than the spacing among successive contributing sources, but in an incoherent periodical deuteron sources it can be made to be an integer subdivision spacing of the palladium lattice (face-centered-cubic lattice at edge lengths: 3.879Ax2.743Ax1.6797A) caged with deuterons which are Bosons with overlapping wave functions at about 0.15 °A apart.

Such a package is compressed by the molecular pressure so that the distance becomes much less than the atomic separation in the D_2 molecule. This is possible because the quadruple lattice pressure at the molecular level and the external electric field are simultaneously applied to squeeze the molecular deuterium (D) in loading into the palladium lattice, in order to form a densely packed nuclear deuteron (d) fuel.

Fusion research followed the understanding of our solar fusion mechanism verified by the experimental test of hydrogen bomb under a tremendous pressurization. Recently, an efficient molecular pressure was employed in the experiment of Stanley Pons and Martin Fleischmann [2], and Jones et al. [3] supported later in Japan by indirect measurements of charged particles emitted [20]. Although the idea of portable fusion by molecular pressure may prove to be inadequate by Williams et al. [18], the attempt is nevertheless inspirational in creating an alternative approach to the externally macroscopic pressure fusion. It gives rise for example to a cluster-impact fusion at Brookhaven Lab [19]. It led us to suspect that a weaker fusion cross section might intuitively mean a stronger fission cross section in the compressed medium. In that sense it can serve a constructive purpose.

The trend of material engineering is to work at the molecular level directly. For example, replacing the high pressure used in a traditional methodology for raising the superconductivity transition temperature, Paul Chu and his student M.K. Wu et al. have succeeded to do away the macroscopic pressure with a molecular pressure (clamp upon the the unit crystal cell and buckled the minor axes plan) by using the the Yttrium atom being smaller in size and located in the same column of Lanthanum in the Periodic Table of the Elements (used first by A. Muller, G. Bednorz, IBM Zurich group), in order to build the 1,2,3 compound (Yttrium, Barium, Copper, Oxide). As a matter of fact, the superconductivity is anisotropic, meaning only along the minor axes, a buckled plan by the molecular pressure, but not along the major crystal c-axis, without the molecular pressure. This insight of molecular pressure created the celebrated superconducting in a new family of layered Copper Oxides at the liquid nitrogen temperature ($77^{o}K$) by Cava et al. at AT &T [21] in 1988, and a new technology of bulk production by Chu et al. [22] in 1990.

Although molecular solutions of material science problems have been implicitly emphasized by the high temperature superconductivity and the low temperature fusion, the molecular pressure becomes the obvious key concept, when pondering over the commonality in these two endeavors. Thus far, the most significance contribution is (not so much whether the cold fusion, or the FNL concept works or not works, but rather) the way scientists think. We begin to tap the molecular technology to achieve the wonder. (Besides the well known biomedical engineering at the molecular DNA genetic cloning level, we have elaborated the molecular pressure in both the high temperature superconductivity and the low temperature fusion.) Thus, Chu and Wu, Pos and Fleischmann have changed the way of thinking. We begin to respect the power and the efficiency of dealing directly at the molecular engineering level.

2. Can a Collimated Nuclear Radiation be generated by a High Power Neutron Beam shot through a dense Deuteron-Palladium fuel?

Early speculations of nuclear lasers were based on dilute and ordinary media [5-8]. The present scheme of passing a high power of nuclear beam through a densely packed macroscopic quantum medium whose lattice spacing of deuterons is about $0.15\ ^{o}A$ apart inside a palladium lattice.

The possible nuclear laser, Graser, requires the concept of an inverted population needed for the coherence and gain effect. The present scheme is similar to Meady's Free Electron Laser (FEL) [9-12], which in the present context becomes 'Free Neutron Laser (FNL)'. Let a neutron beam satisfy a Maxwellian-like distribution with an averaged beam velocity U with respect to the rest frame of the condensed medium. Then, by definition, the central peak of a Maxwellian-like distribution has more neutrons/gamma ray/deuterons populated at a higher energy with respect to the trailing edge of the Maxwellian distribution which has lower population as well.

Since the shortest path traversed by the fission particles through the cylindrical fuel package follows the input neutron beam direction, together the net beam can generate more fission particles in a shortest possible time along the straight cylindrical path. Thus, it has the largest possible energy to simulate more fission products along the way. Such a positive feedback enhancement yields a collimated beam by the available cylindrical kinematic phase space, which has furthermore a possible gain. We are not so much interested in the coherence, rather in the concentration power along the collimated direction.

The major difference between FEL and FNL is the nuclear interaction occurred in the macroscopic quantum medium, rather than the Compton scattering of FEL in a free space. What is the most significant in FNL is the compact geometry that Deutrons have been lined up in a close package under the sub-Angstrom spacing. The relative gain contribution between such a kinematics effect and the dynamic interaction needs to be investigated. Particularly, the relativistic 'focusing' effect by the forward propagation cone might be similar to the relativistic effect of electron cyclotron radiation [13-14].

Such a stimulated beam-deuteron fission might produce a collimated beam of nuclear radiation that may have coherent or incoherent gain. Even without a gain, the scheme is nevertheless interesting because it is a portable source inspired by the portable fusion. If the output were collimated, it could be exceedingly useful (for medical or military applications).

The typical analysis about the coherent multiple scattering may be borrowed from that dimensional analysis given by Rayleigh and verified later by the quantum mechanical calculation by Rutherford, namely the coherent scattering amplitude must be proportional to ($\approx$)the coherent volume, V, weighted by the inverse distance, L, and then the square of the wavelength, λ, as follows.

$$E \approx V/L\,\lambda^2$$

In the short wavelength limit, the formula might not be valid, it should behave like a geometric ray optics. Some qualitative analysis may be possible if the important ratio between the wavelength and the internuclear distance can be taken as the perturbation expansion scale factor.

A slow neutron and a gama ray acts like a catalyst for a stimulated nuclear fission reaction. The possibility of stimulated nuclear reaction in a dense media at the length scale between the nuclear Fermi unit and the atomic Angstrom unit is a relatively unknown territory.

3. Nuclear Fission of Deuterons

A deuteron has a proton and a neutron. Since each has a spin quantum number 1/2, together a deutron has an integer spin quantum number. Therefore, a deuteron is a Boson, according to Bose-Einstein statistics, while a hydrogen is a Fermion, according to Fermi-Dirac statistics. Since bosons allow to occupy a identical quantum mechanical state, a dense overlapping of deuterons may create a macroscopic state. The quantum superfuidity behavior of bosons has been observed at a low temperature.

There are three kinds of fission: the instantaneous (charge number $Z^2 > 52\,A$, mass number), the finite life-time ($Z^2 > 17.7\,A$), and the quantum mechanical tunnelling. The last kind of fission can be stimulated if molecular engineering can manipulate the overlapping Boson wave functions in a solid state metalic lattice environment for a favorable disintegration stimulated by a high power neutron beam. There three possible fission-stimulating beams, charged particle, neutron, and Gamma ray, and each has a different challenges. Data relevant to deuteron and fission is recapitulated as follows.

• size: At the low energy, the short range potential of deuteron is local and everywhere attractive within 3 fm(one fermi is one femtometer: 1 fm=10^{-15} m).

• Coulomb barrier: the electrostatic Coulomb potential e^2/r at the nuclear diameter is about 600 KeV

•electric quadrupole moment, mixture of S and D states: The ground state of deuteron has an electric quadrupole moment , + 0.00282 barns (1 barn = 10^{-24} cm^2), a prolate spheroid contributed only by the proton, indicating a non-spherically symmetric wave function and non-constant orbital angular momentum, but a tensor or non-central force. (For the high energy case, the Case and Pais non-local potential, such as the spin-orbit coupling potential, must be used.)

•magnetic moment, non-zero orbital angular moment: The magnetic moment of deuteron is smaller than the sum of the magnetic moment of proton and that of neutron

$$\mu_d (= 0.8574) \quad < \quad \mu_p (= 2.7927) \quad + \quad \mu_n(= -1.9131)$$

that means in the ground state of the deuteron the proton and the neutron must for a small part of the time be in a state of non-zero orbit angular momentum. The total spin of the deuteron is 1 that is contributed by spin quantum number of the proton 1/2 and the neutron 1/2

•Tunnel Effect: The binding energy of deuteron is 2.22 MeV, while the binding energies of ^{3}He is about 7.72 MeV, and that of ^{4}He is 28.3 MeV.

The well known binding energy ratio discrepancy : 1:3.5:12.7 is due to the tunnel effect that <u>the nucleons in the deuteron will spend about half their time outside the range of each other short range forces.</u>

4. The Interaction Region between the sub-atomic scale and the super-nuclear scale

In the last several decades, our knowledge in both the atomic physics and the nuclear physics has been matural to a great deal by physicists and chemists working almost independent of each other since the the advent of quantum mechanics. Thus, there has created relative void in our knowledge about the intermediate interaction scale in a densely packed condensed medium. The void exists within the sub-atomic length (sub-Angstrom distance) and the sup-nuclear length (super-Fermi distance) which falls short within these two fundamental interaction scale lengths. It so happens that the prospective of cold fusion occurs at the knowledge void. The spacing of deuterons is about 0.15 ^{o}A which is much less than the atomic separation in the D$_2$ molecule. The interatomic spacing between two nucleons in a

deutron is 0.74 °A. On the other hand, the conventional fusion reaction of deuteron(denoted as d) must happen at the the interaction length about the Fermi distance. Thus, a macroscopic quantum medium happens about the palladium medium, that individual deuterons are no longer localized particles. The palladium, denoted as Pd, is a rare metallic element of the platinum group, but lighter easily fusible than platinum, silver-white, ductile, malleable. at. no. 46, at. wt. 106.7. The dense package of deuterons that do not spend all the time binding inside the nuclei create the collective interaction between deuterons and palladium lattice. Clearly, theory just begins to elucidate the dense medium effect of unstable nuclei.

The experimental setup of fission can be essentially identical to those provided by the cold fusion experiment. If an identical setup were used for beam-deuteron fission, this externally radiation beam stimulated fission process might be thought of as the inverse process used by Fleischmann, Pon and Hawkins for their signal radiation of thermalized neutron capture. Such a stimulated fission process takes the advantage of the molecular porous architecture of palladium [1], that can electrochemically be applied to the electrolysis of heavy water in order to line up all ducks, nickname for the deuterium with a quadruple moment, via a 0.1 M LiOD/D_2O electrolyte, in the porous channel cubic cells. These ducks are unstable that their outward-spilling wave functions are electrically forced to approaching one other at the separation less than the atomic distance of 1 Angstrom (1 °A). In other words, the line-up ducks by the clever molecular engineering will be shoot at by a powerful beam of nuclear radiation are used as the fission fuel sources of neutrons and gama ray emission, rather than used as a fusion unit for the helium. The input is a powerful but Maxwellian-like and thermally distributed radiation beam, and the output will be collimated and cold nuclear radiation beam with or without gain. The cold fusion can yield helium and produce neutron beam at the rate of about 4×10^4 neutrons per second, suggested by the Utah group [2], (with a factor of 50 smaller according to MIT fusion group Parker et al. [4])

$$d + d \longrightarrow n \ (2.45 \ \text{MeV}) \ + \ ^3\text{He} \ (0.82 \ \text{MeV}) \qquad (1)$$
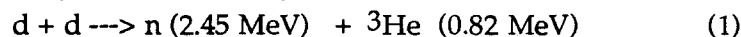
and then the neutron capture produces the γ-ray signal radiation of the 2.22 MeV (by [4] a terrestrial artefact such as Radon gas may be observed with possible linewidth inconsistency by a factor 2 using identical NaI(Ti) 3x3 inches crystal spectrometer detector system)

$$n + p \longrightarrow d \ + \ \gamma \ (2.22 \ \text{MeV}) \qquad (2)$$

The present viewpoint departs from neuclear fusion physicists and cold fusion chemists [3]. We admit our ignorance in this sub-atomic and super-neuclear region that calls for more experimentation and collaboration. Because of the obviously bio-medical and military payoff, the fission speculation calls for research about the important intermediate region of the sub-atomic condensed medium.

5. Conclusions

Since the molecular engineering technique involving packing of deuteron fuel into the palladium lattice has been developed, it can be employed, instead of cold fusion, to generate a collimated nuclear radiation through a stimulated fission process.

The possibility of a collimated and powerful coherent nuclear radiation is always exciting, because of biomedical and military applications. Such a device begins with a non-radioactive portable source and charged by a wall-plug-in electricity in order to pack deutron fuel into the palladium, and then the collective fission is triggered by an external neutron beam. This protocal is almost unreal. To make either fission or fusion possible, further studies in the compressed and condensed quantum medium between the sub-Angstrom and the super-Fermi scale lengths is much needed both theoretically and experimentally.

References

1. Fritz Paneth, Kurt Peters, "The Transmutation of Hydrogen into Helium," Naturwissenschaften, Vol.14, pp. 956-962, 1926;
 Fritz Paneth, "The Transmutation of Hydrogen into Helium, " Nature, Vol.119, pp.706-707, 1927
2. Martin Fleischmann, Stanley Pons, "Electrochemically Induced Nuclear Fusion of Deuterium,"J. Electroanal. Chem. , Vol.261, pp. 301-308, 1989
3. S. E. Jones, E. P. Palmer, J. B. Czirr, D.L. Decker, G.L. Jensen, J.M. Thorne, S.F. Taylor, J. Rafelski, "Observation of Cold Nuclear Fusion in Condensed Matter," Nature, Vol.338, 27 April 1989, pp. 737-740
4. R. D. Petrasso, X. Chen, K. W. Wenzel, R.R. Parker, C.K. Li, C. Fiore, "Problems with the g-ray Spectrum in the Fleischmann et al. Experiments," Nature, Vol.339, pp. 183-185, 18 May 1989

5. Z. Gy. Horvath, N. Kroo, "X-ray and Gama Lasers," Fiz. Sz. (Hungary), Vol. 24, No.6, pp. 167-176, June 1974

6. D. Dialetis, "Generation of Coherent X rays by a Relativistic Charged Particle Traveling Through a Crystal, " Phy. Rev. A 17, No.3, pp. 1113-1122, March 1978

7. A. G. Molchanov, "Lasers in the Vacuum Ultraviolet and in the X-ray Regions of the Spectrum," Soviet Physics USPEKHI Vol.15, No.1, pp.124-129, Julu-Aug. 1972

8. G. Kepros, " Theoretical Model Explaining Some Aspects of the Utah X-ray Laser Experiment," Applied Optics, Vol.13, No.4, pp.695-696, April 1974

9. H. Szu, "Laser Backscattering off an Electron Beam-Plasma System," IEEE J. Quantum Electronics, Vol. QE-19, No.3, pp. 379-388, March 1983

10. H. Szu, P. Sprangle, V.Granatstein, "Powerful X-ray from Laser Backscatter off an Intense Relativistic Electrin Beam," Am. Phys. Soc. Bulletin, Vol. 20, PP 1339-1340, 1975

11. A. Hasegawa, K. Mima, P. Sprangle, H. Szu, V. Granatstein, " Limitation in Growth Time of Stimulated Compton Scattering in X-ray Regime," Applied Phys. Letters, Vol. 29, No. 9, pp. 542-544, Nov. 1976

12. H. Szu, "Synergistic Quasi-Free Electron Laser," U.S. Patent 4,538,278, August 1986

13. H. Szu, "A Football Coil, a Device to Produce Absolute Minimum Magnetic Field and Isochronous Cyclotron for Heavy Ions," IEEE Trans. Nuclear Science, Vol.NS-24, No. 3, pp. 1-7, Jun. 1977

14. H. Szu, "Isochronous Cyclotron,"U.S. Patent 4,197,510, Apr. 8, 1980

15. V.R. Nargundkar, M. Srinivasan, O. P. Joneja, "A comparative study of thermal neutron fusion blanket arrangements," Fusion Technology, Vol.13, pp. 153-156, Jan. 1988

16. J. R. McNally, Jr. "(ultra-)Cold Fusion (^{9}beryllium + ^{3}hellium--> ^{8}beryllium + ^{4}hellium without the Coulomb barrier and at liquid helium temperature) and Graser Prospects," Fusion Technology, Vol.7, pp. 331-333, May 1985

17. R. H. Parmenter and W.E. Lamb,Jr.,"Cold Fusion in Metal," Proc. Natl. Acad.Sci.,USA, Vol.86, pp.8614-8616, Nov. 1989

18. D.E. Williams, D.J.S. Findley, D.H. Craston, M.R. Sene, M. Bailey, S. Croft, B.W. Hooton, C.P. Jones, A.R.J. Kucernak, J.A. Mason, & R.I. Taylor, "Upper Bounds on Cold Fusion in Electrolytic Cells," Nature, Vol.342, pp.375-384, 23 Nov. 1989

19. R.J. Beuhler, G. Friedlander, and L. Friedman, "Cluster-Impact Fusion," Phys. Rev. Lett., Vol.63, pp.1292-1295, 18 Sept. 1989

20. R.Tankrichi, T. Yamamoto, S. Irie,"Detection of Charged Particles Emitted by Electrolytically Induced Cold Nuclear Fusion, Jap. J. of Appl. Phys., Vol.38, pp. 659-661, Nov. 1989.

21. R.J. Cava, B. Batlogg, J.J. Krajewski, L.W. Rupp, L.F. Schneemeyer, T. Siegrist, R.B. vanDover, P. Marsh, W.F. Peck, Jr., P.K. Gallagher, S.H. Glarum, J.H. Marshall, R.C. Farrow, J.V. Waszczak, R. Hull & P. Trevor, "Superconductivity near 70 K in a New Family of Layered Copper Oxides,"Nature, Vol.336,pp.211-214,17 Nov. 1988.

22. R. L. Meng, C. Kinalidis, Y. Y. Sun, L. Gao, Y. K. Tso, P.H. Hor, & C. W. Chu, "Manufacture of Bulk Superconducting YBCuO by Continuous Process." Nature, Vol. 345, pp. 326-328, May 24, 1990 (A. Muller, G. Bednorz, Z. fur Physik 1986, April.; M-K Wu, et al, C.W. Chu, Phys. Rev. Lett., March 1987).

Part 5

SUMMARY DISCUSSIONS

Three panels were convened (Excess Heat, Nuclear Products, and Theory) which met separately. The panels then dispersed, and three discussions followed. Edited summaries for each of the three discussion sessions, as well as ensuing comments, are given in the following sections.

Section 31

EXCESS HEAT

E. Yeager

Excess Heat (Topical Discussant: Ernest Yeager)

The first recommendation of the Excess Heat Panel had to do with the design and construction of reliable calorimeters for electrochemical studies. These problems should be approached using several types of calorimetry, which have individual advantages for different types of measurements. Furthermore, it is important to run blanks in all calorimetric experiments. A large number of measurements are required, and in general, the calorimetric instrument should be kept simple. There is a general preference for measurements on closed systems from the standpoint of thermodynamic simplicity, in that any thermodynamic corrections due to solvent additions or losses are avoided. This can be an annoying problem in open systems, since it is difficult to determine the errors in the corrections, which may exceed any excess enthalpy detected.

There was a strong recommendation for joint studies between groups observing excess heat and those not observing such. Different types of calorimeters may optimize for steady state, nonsteady state, or heat bursts. In general, the calorimeters used are relatively ineffective for accurate measurement of transients. Thus, calorimeters are required which will operate with a time resolution better than currently available. It is quite evident from the results presented at the meeting that heat bursts are observed, and it would be desirable to have data with higher resolution.

There was considerable discussion regarding a "standard" supply of palladium with a high probability of yielding "excess heat." Not all of the group believed that the excess heat apparently observed is sufficient to require a nuclear hypothesis as to its origin. The present state of affairs is that the physical factors concerning palladium which are important in the generation of excess heat in the hands of those who observe it have yet to be pinned down. However, there are cases where three, four, or more experiments performed on the same lot of palladium have all given positive results. The probability then is that a certain type of palladium will give positive results in a more general sense. If this is so not just for one worker or workers, the probability that other groups entering the field with their special expertise will be able to observe the effect is greatly increased. At present, a characteristic situation has been that many workers go for weeks, if not months, through very large numbers of palladium samples without observing heat. If one can improve the probability of finding appropriate experimental conditions which do favor excess heat, then the acquisition of data of value will have been greatly helped. The Bureau of Standards or a

similar type of group might create a library of appropriate palladium samples, and effort should be intensified to determine why palladium of that particular sample seems to assure higher probability of success.

The difficulty is that this phenomenon depends on a large number of factors, which are not well identified in the statistics for observing the effect. For example, it has been said that the statistics for observing excess heat may be excellent for certain deuterated palladium samples but are insufficient in respect to the number of samples run in blank experiments. Since blanks do not provide very exciting data, typically only one or two blank samples have been run by any given group. However, the same statistics apply to blanks as to samples which produce excess heat. In other words, if one works hard enough, one may see excess heat of perhaps a less appreciated type in a "blank" experiment.

The identification of the factors leading to positive results is crucial. The electrolyte factors are particularly, though not uniquely, important. These include the effect of "poisons." Several statements were made about the fact that such "poisons" can have beneficial effects. In order to confirm this, one must prepare a system which is not poisoned, i.e., where the palladium is not contaminated with platinum, silica, iron, and a long list of other possible impurities. Such experiments are possible. Electrochemical laboratories can list many cases where electrolytes have been purified and have stayed clean for long periods of time. However, the effort to purify systems to this extent is not trivial. Impurities must be preabsorbed from the system, under conditions where they literally have to be "tricked" to come out of adsorption surfaces of high area. Similarly, one has to be scrupulously careful regarding the materials from which the cells are made: it is more than a simple matter of changing to Teflon or other more optimal materials of construction.

Surface conditions are generally important and need to be further characterized; for example, dentrites may play a role. A simple way is required for measuring the bulk properties of the palladium, particularly the deuterium loading. While the deuterium can be stripped out, that will, however, perturb the systems. Experiments must be coupled: the generation of tritium and radiation effects should be simultaneously measured in cells generating excess heat, so that correlations, if any, can be established. Such correlations are not at all well-documented at present.

A further suggestion was to deliberately dope the palladium surface by ion implantation or by alloying with metals such as beryllium, uranium, or lithium, which possess special nuclear properties. This may open up an approach to the electrochemical generation of excess heat at unusual temperatures, for example, either an extremely low or high temperatures, using non-aqueous solutions. There is no reason why the phenomenon should be unique to an aqueous solution, and one possibility may involve a fused hydrate melt. There was also the suggestion of the use of a hydride at an anode, as well as discussion of the use of superacids which show extremely high thermodynamic activity for deuterons, compared to those, for example, for the hydrogen ion in sulfuric acid.

Regarding recommendations for future experiments, two sets of conditions were suggested. The first would address the question of how to sufficiently understand the phenomenon to make it reproducible and well-accepted. Second, once that is established, a whole list of variations may arise, whose effects would not be eliminated unless surface conditions are carefully controlled.

DISCUSSION (YEAGER SUMMARY)

Hoffman: One missing area in your suggestions for future work is to deliberately dope the cathode surface by ion implantation or by alloying with elements such as lithium, beryllium, or uranium. This may allow us to see if excess electrochemical heat may be obtained, either under high temperature conditions or at extremely low temperatures, by not using aqueous electrolytes. Did you consider that and then reject it as not appropriate?

Yeager: The effect of temperature was briefly discussed. There is no reason why the electrolytic phenomenon should be unique to an aqueous solution, and one possibility would be the use of a fused deuterate melt. Hopefully, for future energy generation, it will be necessary to go to higher temperatures.

Appleby: One might also use a hydride (deuteride) melt, with an anode consisting of palladium or other metal forming a hydride.

Yeager: That is an interesting suggestion. We also considered the use of the superacids, which have extremely high activities for deuterons. These may be 10^{16} times higher than those in, e.g., the deuterons in sulfuric acid at the same concentration.

Hoffman: Is surface modification also not a worthwhile area to explore?

Yeager: Yes, it is. General changes in surface conditions should include dendrite formation and composition.

Mansour: For the sake of completeness, I would like to ask the same question that emerged from the theory session, which I have not seen addressed so far. If tritium is indeed formed, where does its formation and storage occur? According to different hypotheses, it could be in the solid, in the liquid, or in the gas. Did you address this question in your session?

Yeager: At least in part, it was addressed earlier this morning in the course of the discussion about the tritium enhancement in aqueous electrolytes. It was pointed out that it could be dissolved as a gas in the electrolyte, and not necessarily exchanged with the liquid phase.

Mansour: It could also be in the liquid phase.

Yeager: Many of us who have seen tritium have assumed that it is present as DTO, but it could also be in the form of DT or TT.

Chu: We do not seem to be addressing the question of excess heat.

Yeager: You are correct, the question of tritium is really outside of our territory.

Hoffman: Is ion implantation a worthwhile technique to explore concerning surface modification, or did your group think that it is not worthwhile?

Appleby: I think that it is a good idea.

Yeager: I also think so. One can introduce very interesting species into the surface in this way.

Bard: I think that there is a problem in trying to make recommendations about future experiments. We seem to have tried to suggest two separate sets. The first addresses the question of understanding enough to make this a reproducible and well-accepted phenomenon, which I think should be our focus, since it seems to be the primary problem. After this has been established, the second question involves the list of experimental variations which should then be examined. I believe that it would be a mistake to randomly ion implant palladium without knowing the important variables before the work takes place.

Yeager: All of us have intuitive ideas which we would like to try rapidly and see the results. A systematic large-scale study should be more disciplined.

Teller: For the sake of systematics, I have been impressed by both the variability of the results, by some correlation of this variability with the state of palladium cathode, and many suggestions about the condition of the palladium surface. I believe that there is a 50 percent probability that the variability would not be eliminated unless the surface conditions are carefully controlled. There, I would be opposed to the separation of these two problems.

Schneider: I would like to add an additional point. I believe that some of the conclusions from the next two reports also affect the recommendations in the chemistry area. As has been stated, if neutron absorption occurs, one must address the nature of the reactions taking place at the palladium cathode surface. One normally does not consider such transformations in ordinary chemical posttest analysis. In this case, analysis to detect isotopic changes will be appropriate.

Teller: May I make a supplementary statement? Livermore has conducted a group of experiments which have only been incompletely reported. They were carried out rapidly, and because of this I was unaware of many aspects of the work. Last night Dr. Lowell Wood summarized the results by telephone, while I reported to him on the NRL palladium experiments. In particular, he reported a result of which I was unaware. He has analyzed the lithium isotope content in a palladium cathode to a depth of 3 microns. In the first 1-micron layer, strong depletion of Li-6 was observed, whereas below that, the isotopic ratio was normal. I must warn you that this must not yet be accepted as fact, since mistakes in measurement can be made. Nevertheless, the presence of dendrites on different palladium samples, their surface composition, consisting of a wide range of chemical elements, and the possible isotopic changes all suggest that complete surface analytical results

should be systematically reported. People may make unusual observations of this type, without paying attention to them. However, such an observation may open up a new field.

Yeager: I believe that those points are all very important. The surface conditions usually control the electrochemical phenomema. For example, where the interfacial properties of single crystal have been studied, the differences between different crystal faces of a metal such as platinum, gold, or palladium are as great as they are between different bulk metals. Surface topography and faceting should be part of the systematic surface studies.

Section 32

NUCLEAR PRODUCTS

George H. Miley

Nuclear Products (Topical Discussant: George Miley)

A primary conclusion from the discussion is that the observed tritium measurements appear to be so far above background that they are difficult to dispute. However, the measurements are very puzzling in that they are incomplete in terms of time-history correlation and also in terms of any energy balances which should be applicable, assuming known fusion reactions. The first priority should be to continue attempts to refine tritium detection and combine it to a maximum extent with other variables which can be measured. This is difficult, because of the wide dispersion of appropriate people, diagnostics, and operating cells across the country. Collaboration to a maximum extent is clearly required to move ahead rapidly in this area.

There was strong agreement that helium (^{4}He) should be one of the essential products of the type of nuclear reactions which are thought to be occurring. This has already been recognized by workers in the area. Consequently, some analyses for ^{4}He have been attempted, but the data is inconclusive. Clearly, a concerted effort is required for its resolution. For example, one point which emerged is that for a large (e.g., 50-megajoule) heat burst, the helium product would amount to a few cubic centimeters at standard temperature and pressure. It is not known at present if the helium is produced in the volume of the electrode or on the surface layer, where it may be lost. Thus, it is necessary to examine both the electrode and gas escaping and dissolved in the electrolyte for a meaningful helium detection.

There is a strong likelihood that any helium created would be either at the surface or in the near-surface layer. Unfortunately, it appears that all of the most productive electrodes have been wiped to remove electrolyte after electrolysis, disturbing the surface and removing any dendrites that were formed. Thus, in retrospect, one should be careful about any surface treatment after electrolysis prior to gas analysis. There was also a strong recommendation that the gas produced should be continually analyzed, to clarify the correlation of ^{4}He production and other products, heating, etc. In addition to the analysis of ^{4}He, new methods for the determination of both ^{3}He and ^{4}He should be attempted. As far as tritium is concerned, the time history of its production is extremely important relative to our understanding of the phenomena involved. Later, the correlation of neutrons and other

reaction products can be performed, but presently it is most important to establish the time history of tritium production. Clearly, there is a delay time between tritium production and its detection, so a fast time response is not possible. However, a moderate response time can be achieved using on-line instrumentation with flow-through liquid scintillators, etc. Unfortunately, this instrumentation is quite expensive, and it must be integrated with an operating cell. Alternatively, one can produce good time-integrated his-tories, over blocks of time, using closed cells. In any case, care should be taken to analyze gas and liquid phases carefully.

Another observation concerns neutrons or neutron bursts, which also require time and energy resolution. There seems to be some optimism that the detectors which are now being brought to bear on the problem in several laboratories may be capable of this. However, a complete determination may still be difficult, since there is still debate about the problem of neutron energy resolution, much less time resolution.

The neutron energy spectrum brings up the question of 14-MeV neutrons and whether or not these should serve as a fingerprint of secondary tritium reactions. Some unsuccessful attempts to measure 14-MeV neutrons have been reported. However, it is not clear if the number of neutrons from secondary reactions would have been expected to be large enough to detect with the cells employed. It has also been suggested that D-T experiments might be useful for future studies. To take one extreme argument, if the reactions apparently taking place are induced by micro hot-fusion cracking or by dendrites, under accelerator target conditions, then the D-T reaction should occur very copiously and enhance the ability to make measurements of 14-MeV neutrons which have less background interference than the 2.5 MeV D-D neutrons. Thus, it should be very instructive to make such measurements in order to eliminate some of the current background issues. While there is good logic to consider such an experiment, it would be hazardous from the radiation viewpoint. Probably, it should be a National Lab experiment, especially in view of the significant amount of tritium which would be involved.

In addition to detecting neutrons, it is very important to attempt to correlate neutron emission rate with the production of other products. One obvious effect to focus on in this respect would be to look carefully, in as many laboratories as possible, for the 20-kV, k-shell X Rays from palladium.

Groups using high-pressure cells should consider how to obtain diagnostic access to them, to allow such measurements. Thus, to build up a complete history of neutron production, their time and energy dependence, as well as their correlation with X-rays, are required.

Palladium isotope examination should be undertaken by the community as soon as possible. Preliminary results reported at this meeting for the first time indicate that mass-resolution can be reasonably well defined. These results suggest that a transmutation of the palladium may have occurred. However, the atomic number must be clearly identified to confirm that isotopic changes are involved. Also, contributions from contaminates must be shown to be negligible. Thus, a complete analysis requires specialized high resolution equipment that is only available at a few laboratories. There was general agreement that mass-spectrometer analysis should be a high-priority diagnostic for everyone capable of performing it.

For future measurements, it was suggested that some labs should be concerned with the use of materials for electrodes other than palladium. This topic brought up a discussion of the use of other materials such as uranium or beryllium. This use of such materials would be classed as "new" exploratory experiments, whereas the use of other electrode materials such as titanium would represent more "conventional" experiments. The "new" experiments would explore such things as possible neutron-induced fission in uranium and neutron capture reactions in the loosely bound beryllium.

There was also some discussion that detection of surface electrical barriers might help in resolving the dendrite issue. The question is: what can be done to initiate dendrite growth? Apart from dendrites, is there some other method of initiating arcing, e.g., via lasers, and how can this be studied?

Detection of alpha particles, protons, and tritons was also mentioned, as well as of γ-rays. Detection of gammas is difficult, since if one considers cascading γ-rays, a clear resolution of lines may be obscured by the background. Detection of charged particles requires access to the source region that avoids absorbing materials in front of the detector. This is especially difficult to achieve in electrolytic cells but is more feasible in gas cells where space is freer.

Another conclusion of the discussion was that radiography should be routinely performed, using photographic film around the electrodes after experiments. This would help to determine if "hot spots" occur. Similarly, the Utah metallurgy experiment found differences in hardness in certain surface areas. A question for study is whether these spots correspond to those that have shown up in film exposures at the Bombay Laboratory in India.

Regarding palladium isotopes, interesting (perhaps, arc-initiated) experiments might be performed with enriched electrodes containing one or more selected isotopes. Such experiments might fit in with the Claytor experiment at Los Alamos, which focuses on defects produced in junction diode configurations under high D_2 gas pressure. This type of defect might also be studied with an electrolytic cell, perhaps by attempting to run a cell in a high radiation field to initiate certain reactions.

The recommendations from this discussion are summarized in the following outline taken from a slide developed during the discussion.

Nuclear Products Discussion Group
Dr. George Miley, Chairman

Recommendations

Near Term

The evidence for nuclear products, especially tritium, seems convincing but puzzling.

- Continue attempts to improve nuclear product detection and heat production while working to improve reproductibility; (implies) collaboration of teams which have "operating" cells with teams capable of detailed nuclear diagnostics (especially, on-line tritium detection).

Further Work

- The helium ash issue is critical. Experiments have reported bursts up to 50 megajoules of heat. Assuming conventional nuclear reactions, this is roughly 2cc (STP) of He. Thus, workers should look for He, both in the palladium electrode and in gas evolving from cells and in electrolyte. The "secondary" possible use of ^{3}He spin resonance diagnostics should be considered.

- On-line T, P measurement/flow through liquid scintillation (also closed system gas/liquid).

- Time/energy resolution of neutron bursts should be feasible with next-generation detectors. Also, 14-MeV neutrons from D-T reactions should be studied carefully.

- Correlation of neutrons with second-product particles (e.g., K X-Rays at 20-keV from Pd) (use window in pressure cell).

- Pd isotope transmutations should be studied with high-resolution measurements of nuclear mass and charge (M,Z) using a precision mass spectrometer. Other electrode metals should also be examined.

- The use of other materials for electrodes is encouraged, including:

  - Uranium
  - Be
  - Titanium
  - Also, Pd-V and Nb

- U and Be experiments represent a "new" direction to explore neutron-induced fission and neutron capture reactions under unique conditions.

- Detection of charged particles (protons and alphas): use surface bainer detectors, especially in gas cell experiments (this should also address concept of acceleration of charged particles or ions in dendrite-enhanced electric fields).

- Autoradiography experiments (spots on film) are recommended as a routine measurement. This should identify hot spots as well as variations in surface hardness.

- Gamma measurements are important but difficult due to the overlap of cascaded and background. This diagnostic should be attempted in laboratories with appropriate equipment. Collaboration with groups having "operating cells" is, however, essential.

- A prime overall objective should be to closely tie experiments to theory and continue efforts to pull all available information together into a coherent picture.

- "New" experiments which should be considered include:

  - Beryllium/uranium electrodes
  - Palladium isotope electrodes
  - Arc initiation
  - Irradiated palladium electrodes
  - Irradiated electrode cells

DISCUSSION (MILEY SUMMARY)

Bard: To my knowledge, there was an agreed format for the double-blind analysis of palladium from different laboratories, including samples of helium-implanted material. You seem to be recommending experiments that are already being conducted.

Miley: The question concerns reproducibility in operating cells. These experiments need to be attempted again after exposure of samples to reproducible operating conditions.

Bard: The agreement, as I recall, was that the results of helium analysis for the double-blind experiment would be announced on October 8. I would like to know the results, since there are clearly people here who are familiar with them.

Miley: That topic was not discussed in our session. Does anyone have the answer to this question?

Hoffman: I was involved in the analyses, and we do have some of the answers. There was an agreement that the University of Utah should be able to analyze the results for three weeks before a public announcement was made. The results were given to Utah on October 5. Dr. Pons and Dr. John Murray met for discussions on October 9, and we obtained the complete results last Friday, October 13.

Miley: I would assume that independent of the results from the double-blind tests, we would not change our recommendations, which are to reanalyze under more carefully controlled conditions.

Hoffman: As long as we are on this subject, I would like to raise one important point. All of the active specimens had been wiped after electrolysis.

Bard: What do you mean by "wiped"?

Hoffman: The slimy surface dendrite film was removed by wiping with a tissue, to reveal the palladium surface. I have personally examined the surfaces of many electrodes after removal from the electrolyte. Iron and other metals are invariably present. The surface of the cathodes examined for helium consisted of pure palladium, without even any platinum. Since we now feel that there is a strong likelihood that any helium created would be in the near-surface area, we are now urging people to be very careful about the way in which they treat the surface after electrolysis.

Bard: Was the gas phase analyzed, since helium formed near the surface would be expected there?

Hoffman: We only analyzed for He-3 and He-4 inside the bulk palladium.

Miley: We recommend analysis of the gas phase, since helium may be present in the gas if surface reactions occur.

Chubb: Do you recommend attempting to detect highly energetic α-particles?

Miley: Yes, they are on our list.

Jones: The problem will be the short range of α-particles.

Chubb: Our calculations show that they may be detected if they are produced near the surface.

Miley: We are recommending the use, wherever possible, of surface barrier detectors. Although we intended these for measurement of energetic protons, they might also detect α-particles. We also need triton detection. Among other things, film can be placed around the electrodes, as was done in the BARC experiments.

Chubb: That should also be done in titanium gas-phase experiments.

Miley: May I ask a question concerning the helium analysis? Can you explain the procedure which was followed?

Hoffman: The University of Utah sent specimens via Battelle Northwest to five different laboratories for He-3 and He-4 analysis. As I stated, the analyses were given by Battelle Northwest to Utah early in October. All of the laboratories who participated in the analyses agreed not to say anything publicly until at least three weeks after Utah had been given the information. This precludes me from saying anything other than the fact that the results obtained were ambiguous.

Miley: The cathodes examined had presumably produced anomalous effects.

Hoffman: At least one had not. Some had been artificially ion-implanted with helium to check the analytical capabilities of the laboratories for trace amounts of helium. A specimen was included which was untreated.

Miley: Would such a service be available to other groups who may wish to send in electrodes for analysis?

Hoffman: I work at Atomics International, Division of Rockwell Corporation, at the Department of Energy Laboratory which analyzes around 1500 to 2000 specimens per year for He-3 and He-4 in solid materials. The solids are evaporated in special equipment, and the helium isotopes are determined by mass spectrometer. A small number of other laboratories around the country have the same capability. They would be delighted to have the commercial business.

Bard: Do you know when the results are going to be announced by Dr. Rossi?

Rossi: In approximately three weeks. The timing will depend on further discussions between Dr. Pons and Dr. John Murray, which will take place next week.

Section 33

THEORY

Gordon Baym

<u>Theory (Topical Discussant: Gordon Baym)</u>

"Cold fusion," as it has come to be known is obviously a new field, in which theory must be supported by consistent and systematic data. The subject is in its very early stages. As is usual when dealing with "almost-phenomena," it is an experimentally-driven, not a theoretically-driven, field. Two classes of phenomena invoke the major theory issues. One uses equilibrium-versus-nonequilibrium phenomena, involving conventional physics as we know it. The second concerns the question as to whether some kind of exotic nuclear physics, or yet other new physics, is required, e.g., the possibility that there is a breakdown of elementary quantum mechanics for very small probability events. This certainly has never been tested in a laboratory. However, there was general consensus that it is necessary to stay as close as possible to conventional physics for as long as is required. Three sets of issues were suggested for future directions: materials, nuclear physics, and reaction mechanisms.

Regarding the materials issue, they may be divided into static versus dynamic, though this is a somewhat artificial distinction. By static, we really mean problems concerning equilibria, but there is a large overlap between the two. Good systematic studies of the various materials in question are needed, with those for possible variations of the materials, i.e., band-structure calculations. Following are some questions to be answered. What are the energetics involved in these materials? What is the electron structure? Where, for example, can the various types of hydrogen be found in the lattice? Where is tritium to be found in palladium, for example? Is it in molecular, atomic, or ionic form? Are there special sites (which may be due to impurities) where tritium and the other hydrogen isotopes can be found? How strong is helium binding to palladium? There is a paucity of data in regard to the above, for which very simple measurements are required.

Better understanding of the elementary properties of these materials is needed. This will involve understanding of the screening effects via fundamental calculations. Studies of alloys of the various hydrides are required. More generally, the perspective should be enlarged to study the materials with high hydrogen affinity, of which there are various systems with large diffusivity. Are there other materials which may also give interesting results? What are the special properties of deuterium in systems such as palladium at large concentrations?

Are there clustering phenomena? Are there phase transitions beyond the available data, outside the critical loading? Will phase transitions occur to a state with large numbers of clusters? Intensive studies are required to provide data on highly loaded materials, using neutrons, X-rays, and other methods. Problems concerning surface physics need examination from a theoretical viewpoint. What is the effect of lithium, for example? What are the general properties of hydride surfaces? An additional area requiring attention is that of characterizing and understanding the microstructure of these materials.

A similar list of problems may be identified in the category of dynamic processes. For example, how does hydrogen diffuse in hydrogen, deuterium, and tritium environments? How does it diffuse in the corresponding hydrides? Another problem concerns very low-mass particles in which the diffusion is not simply classical but has large quantum aspects via tunneling. What are the effects of stresses and strains on the systems? For example, how does deuterium interact with potential fields? These need theoretical and experimental attack. What are the finite frequency responses of systems involving electrolyte fields and stresses? It is not just the question of examining statics, but also finite frequency events. Another area is that of understanding the physics associated with cracks and voids. In particular, what is the role of electric fields here?

For example, there is the issue of whether acceleration causes cracks. Quantum-mechanical tunneling returns to the fundamental question of diffusion. All these are intimately related. What are the dynamics associated with clusters, if there is any cluster formation? Another question that theorists should consider is that of threshold phenomena. There is evidence that there are critical current densities where one begins to get anomalous phenomena.

Regarding nuclear reactions, doubts were expressed about our understanding of their physics. Are low-energy reaction cross-sections really understood down to a few electron volts? Are there unusual mechanisms which may take place? Can there be exotic reactions which are consistent with what is already known in low-energy systems, such as conventional fusion reactors as well as thermal-nuclear explosions? Are there interesting many-body effects, e.g., concerning nuclear reaction cross-sections, when coulomb interactions are stimulated by other nearby bodies exerting electric fields on the nuclear channels? One certainly needs to study reaction mechanisms involving elements other than palladium, lithium, uranium, beryllium, etc.

There is the possibility that theorists should be concerned about exotic neutron-transfer mechanisms, involving effects which are not readily seen in an accelerator experiment, because they occur at low probabilities. For conceivable new particles, one caveat in trying to understand any such exotic mechanisms is to be concerned about why stability occurs. Why, for example, is deuterium or heavy water stable?

It was proposed that one should not postulate things which would occur according to the normal procedures of cosmological nuclear physics. The high-energy physicists and cosmologists have much experience with the problem of placing constraints on nucleosynthesis issues. For example, this led rather early to the constraint of the existence of three species of neutrino.

Another area which certainly requires more study is that of possible chain reactions in such systems. These might be triggered, for example, by cosmic rays, which are not easily avoided at ground level. It would be very helpful to have experiments where one has a cosmic-ray counter on top of a "cold fusion" cell. For instance, a good example which has been studied is the $\alpha-\beta$ phase transition in liquid helium at very low temperatures in the milli-Kelvin range, where it is triggered by cosmic rays.

There was a question of specificity of palladium in "cold-fusion" phenomena. Other atomic species should also be examined, particularly metals of high hydrogen diffusivity. In this respect, there are the anomalies associated with superconducting behavior of such materials. For example, why does palladium deuteride have a higher T_c than palladium hydride? How do these anomalies correlate with similar anomalies in diffusivity and in other phenomena?

It was stressed that when looking for a new or exotic phenomenon, there may be unusual induction periods. If one postulates something not usual, there may be an indication that it was not there at the inception. It may be produced in the apparatus before the main effects are visible. Another point stressed was that where tritium has been seen in a reaction which appears to be favored over the other branching ratios, the energetics should be checked. One may have an indication of the participation of another particle which can carry away energy from the system. All these additional facts which already seem to agree with the observations should be taken into account, thus limiting the choice of the exotic effects which should be considered. However, the experimentalist should not

ignore puzzling results or coincidences, for they may have real meaning to a theoretician.

It was mentioned above that palladium deuteride and palladium hydride have peculiar superconducting properties. Palladium is not superconducting, but palladium hydride begins to be, when the H/Pd ratio rises above 0.6. This is presumably connected with the β phase. The rule is that the heavier isotope always has the lower transition temperature. An exception is palladium hydride, since the palladium deuteride has the higher T_c, with palladium tritide having an even higher value, perhaps 10 or 20 percent different. This is a sizable effect. An explanation for this is in itself challenging, and it may well give details about the behavior of palladium hydride in its normal state, and thus about the boundary conditions for calculations. For instance, there is the question whether there can be more than one hydrogen in one octahedral site. The answers to questions of this kind are not full explanations, but they can influence the approach to explanations. Superconductivity indicates changes in band structure or mobility, and in general, about association of electrons, not of hydrogen nuclei. However, association of electrons can then lead to conclusions about the distribution of the hydrogen nuclei, which is of more direct interest.

There is the issue of whether the study of isotopes is significant. The converse isotope effect is known for a number of materials other than palladium, and it is explained for these systems as being the result of the coulomb potential changes. The new star in the formulas for changes in T_c in these materials must show how the inverse isotope effect arises. This is well explained for a number of systems, such as palladium hydride and deuteride. A T_c difference of one or two Kelvins is well understood. It can be analyzed and understood in terms of different couplings to local optical modes for deuteride vibration at the octahedral site and has nothing to do with the multiple occupancy.

Finally, there is the issue of the band structure of the deuterides themselves. They are viewed as ionic entities. This has interplay with diffusivity and may also correlate with ionically mediated superconductivity.

DISCUSSION (BAYM SUMMARY)

Worledge: While the evidence may be fairly reliable concerning a threshold current density for excess heat, whether there is a threshold for tritium production is more doubtful. The majority of the tritium production cells at Texas A&M seem to have been exposed at one time or another to a high-current episode, but it is difficult to make a firm conclusion.

Jones: Would you call the approximate -30°C correlation for neutron bursts in the gas-phase experiments involving titanium a threshold?

Baym: I do not know.

Teller: I would like to caution that the broader questions of the origin of the universe go beyond our topic today. However, when exotic reactions are being considered, a limitation must be imposed. One must not postulate processes that would be considered if normal procedures of nuclear physics are used. This is a very useful restriction, when one is looking for new effects.

Baym: Absolutely. High-energy physicists and cosmologists have a great deal of experience with the problems of placing constraints resulting from issues in nuclear synthesis. For example, this led rather early on to the constraint of the existence of three species of neutrino. In addition, constraints on the possible masses of particles and other physical phenomena in supernovae have been established. Concerning the question of exotic nuclear physics, this would not be the first time that chemistry has revealed new nuclear physics. I should remind you that the first new chemical element reported in America was discovered at the University of Illinois in 1926. It was promethium, atomic number 61. Another area requiring more study is that of possible chain reactions, triggered, for example, by cosmic rays. Experiments should be set up with cosmic-ray counters on the top of the cells. A well-known example of such a phenomenon is the liquid-helium phase transition in the millikelvin range, which requires multiparticle cooperative phenomena triggered by cosmic rays.

Miley: We took the opposite view, namely, if this is a triggered process, then a higher intensity trigger should be supplied to increase the rate.

Baym: The issue is understanding the triggering events. Does anyone among the theorists, indeed, anyone else, want to make additions to this list?

Whaley: There is the question of the specificity of palladium. Work is required to determine whether there is something specific about palladium or other metals which have the capability of absorbing hydrogen. What are the characteristics

required to show these anomalous effects? Experiments should not just be restricted to palladium, but other metals of high deuteron diffusivity should be examined.

Miley: What would you recommend as prime candidates?

Whaley: Palladium and palladium alloys.

Chubb: The anomalies associated with superconducting behavior require attention, particularly why palladium deuteride has a higher superconducting temperature than palladium hydride.

Teller: I would like to remind you of a further aspect of these observations. You did not mention specifically the strange induction periods which appear to occur for these apparently new or exotic phenomena. One should not simply attempt to explain the main peculiarity but also why the effect does not start immediately. If one postulates an unusual process with an induction period, perhaps it was not there at the beginning of the experiment. Alternatively, it was occurring all the time, but earlier the main effects were not visible. A more important point is that when tritium production appears to be favored over the other branching ratios, after all the energetics have been checked, it is an indication of the participation of another particle, i.e., something that can carry away energy. When the observations are shown to be reproducible, then an explanation for all these additional pieces of information must be considered in the choice of exotic effects which might provide an explanation.

Hoffman: I have a comment concerning Dr. Teller's remarks about Dr. Lowell Wood's experiment. Apparently, they saw an isotopic anomaly, which they first ignored because it did not seem to be of significance. Combined with other observations, it would take on added meaning. Perhaps, many of us have observed something similar in our experiments, where there was a result or coincidence which was so puzzling that we deliberately ignored it. Such a result may mean a great deal to a theoretician. Dr. Baym mentioned events triggered by cosmic rays. One of our experiments at Leadville showed results whenever a solar 10-MeV proton event was detected by the GEOS satellite. I ignored the coincidence, because I believed that there could not be a relationship between the two events. All of us may have seen analogous effects. It is important that if you find some such anomaly or something unusual, discuss it with other people who might be interested.

Voice: This leads me to think that we should look seriously at possible triggering mechanisms.

Chubb: I entirely agree.

Miley: I would like to make a point on this topic. As editor of "Fusion Technology," I have often been criticized for instructing reviewers that they should accept technical notes in which negative results have been obtained,

provided that the results were such that they might inform other workers about what to do or not to do in the future. I believe that learning from the negative results of other groups will be valuable.

Teller: I have been reminded that I ought to make one more comment. As has been stated, it is well established that palladium deuteride and palladium hydride have unusual superconducting properties. Palladium metal is not a superconductor, and the phenomenon begins to appear as hydrogen is dissolved in the palladium at an atomic ratio above 0.6. The indications therefore are that the superconductivity is connected with the β-phase. Since superconductivity is by now an almost generally observed peculiarity, this is not remarkable in itself. An isotope effect is sometimes observed in superconductivity, with the rule being that the heavier isotope has the lower transition temperature. Well-known exceptions to this rule, which may or may not be general, are the palladium hydride isotopes. Palladium deuteride has a higher T_c than the hydride, and the value for palladium tritide is higher still. The effect is sizeable, not microscopic. Whether this effect is directly related to the phenomena discussed here is debatable. However, the explanation of the superconducting isotope effect is a challenge. It may well produce details concerning the behavior of palladium hydride and deuterides in their normal states, and therefore, about the starting point for calculations. As an example, we have asked whether one octahedral site can contain more than one hydrogen. My impression would be no, but since the superconducting effect is peculiar, then it is perhaps not out of the question. Theoretical studies of this kind will be helpful. In themselves, they will not provide the explanations, but they could assist in approaching them.

Baym: My question is, what does the superconductivity effect tell us about band structure and mobility?

Teller: The superconductivity can tell you something about band structure and mobility, and generally, about the association of the mobile particles. These would be the electrons, not the isotopic hydrogen nuclei. However, the association of the electrons can provide conclusions concerning the distribution of the hydrogen nuclei, which would be of direct interest.

Bray: The superconducting phenomenon may unfortunately be a red herring. The converse isotope effect is known for a number of other materials, not just palladium, and it may be explained as resulting from Coulomb potential changes. The frequency term in the formula for T_c changes in the correct way to give the inverse isotope effect, which is well understood in a number of other isotope systems. I do not know of work which uses this specific approach for the palladium hydrogen isotope family. For palladium hydride and deuteride the T_c difference of 1-2 K has been well analyzed in terms of different coupling to local

optical deuteron vibrational modes at the octahedral site. It has nothing to do with the multiple occupancy. However, I am not sure about the palladium-tritium system.

Chubb: We have been talking about the electron band structure. We also should examine the ionic energy bands of the deuterons themselves, which near the stoichiometric compound PdD should become occupied, provided that deuterons which are injected beyond the stoichiometric concentration, one D per Pd, remain sufficiently ionic. These band-state deuterons, which may have importance for fusion, may be important as well at lower D concentrations where their occupation would have an impact on diffusivity effects, and if there is a correlation, with an ionically mediated (low temperature) superconductivity.

Mansour: I have a final, perhaps extremely optimistic, proposal. Do you think that an outcome of this meeting should be the formation of a Task Team in each of the three areas, which would be charged with examining or at least coordinating the efforts which we have discussed?

Hoffman: It is my personal opinion that networking among the researchers working in the same area will be one of the best ways to ensure that the science moves rapidly. You all have each other's names, telephone, and fax numbers, and I hope that you will interact together for a continual interchange of information.

Appendix A

LIST OF INVITEES

NSF/EPRI WORKSHOP ON ANOMALOUS EFFECTS IN DEUTERATED MATERIALS

National Science Foundation
1800 G Street NW, Room 543
Washington, DC

October 16–18, 1989
Invitees List

Dr. John Appleby
238 Wisenbaker Engineering Research Center
Texas Engineering Experiment Station
The Texas A&M University System
College Station TX 77843-3577

Dr. A. J. Bard
Department of Chemistry
Welch 4218
University of Texas at Austin
Austin TX 78712

Dr. Gordon Baym
Department of Physics
University of Illinois-Champaign
1110 West Green Street
Urbana IL 61801

Dr. John O'M. Bockris
Texas A&M University
Department of Chemistry
College Station TX 77843

Dr. Peter Bond
Physics Department 510A
Brookhaven National Lab
20 Pennsylvania Street
Upton NY 11973

Dr. James Bray
Building K-1 Room 1C25
General Electric Research Dev. Center
River Road
Schenectady NY 12301

Dr. Carlo Carraro
Division of Physics
Department of Mathematics and Astronomy
California Institute of Technology
Mail Stop 106-38
Pasadena CA 91125

Dr. Tarun K. Chaki
Department of Mechanical &
Aerospace Engineering
State University of New York
Buffalo NY 14260

Mr. Bendi Chexal
Nuclear Power Division
Electric Power Research Institute
3412 Hillview Avenue
P.O. Box 10412
Palo Alto CA 94303

Dr. Paul C. W. Chu
Texas Center for Superconductivity
University of Houston
Houston TX 77204-5506

Dr. Scott Chubb
Naval Research Laboratory
4555 Overlook Avenue
Code 8310
Washington DC 20375

Dr. Ted B. Flanagan
Program in Materials Science
Department of Chemistry
University of Vermont, Cook Building
Burlington VT 05405

Dr. Martin Fleischmann
University of Utah
2420 Henry Eyring Building
Salt Lake City UT 84112

Dr. Moshe Gai
Department of Physics
Yale University
P. O. Box 6666
New Haven CT 06511

Dr. Ryszard Gajewski
Basic Energy Sciences
US Department of Energy
ER-16, GTN
Washington DC 20545

Dr. Richard Goldstein
Electric Power Research Institute
3412 Hillview Avenue
P. O. Box 10412
Palo Alto CA 94303

Dr. Peter Grimes
Exxon Chemical Co.
P.O. Box 536
Linden NJ 07036

Dr. Nathan Hoffman
Energy Technology Engineering Center (ETEC)
Rockwell International Corporation
P. O. Box 1449
Canoga Park CA 93104

Dr. Frank Huband
Division of Electrical and Communication System
National Science Foundation
1800 G Street NW, Room 1151
Washington DC 20550

Dr. Robert Huggins
Department of Material Science
Stanford University
Building 550, Room 550I
Stanford CA 94305

Dr. Donald P. Hutchinson
Physics Division 372
Martin Marietta Energy Systems
Oak Ridge National Laboratory
Oak Ridge TN 37831-8070

Dr. Robert Jaffee
Electric Power Research Institute
3412 Hillview Avenue
P. O. Box 10412
Palo Alto CA 94303

Dr. Steve Jones
Department of Physics and Astronomy
Brigham Young University
176 ESC
Provo UT 84602

Dr. Joseph Jordan
Department of Chemistry
Pennsylvania State University
University Park PA 16802

Dr. Yeong E. Kim
Department of Physics
Purdue University
West Lafayette IN 47907

Dr. Steve Koonin
Division of Physics
Department of Math & Astronomy
California Institute of Technology
Mail Stop 106-38
Pasadena CA 91125

Dr. Nathan Lewis
Department of Chemistry
California Institute of Technology
Mail Stop 127-72
Pasadena CA 91125

Dr. Khalid Mansour
Savannah River Site
Westinghouse Savannah River Company
773-42A, Room 1611
Aiken SC 29808

Dr. Mike McKubre
SRI International
333 Ravenswood Avenue
Menlo Park CA 94025

Dr. Howard O. Menlove
Los Alamos National Laboratory
Los Alamos NM 87544

Dr. George H. Miley
Fusion Studies Laboratory
University of Illinois
103 South Goodwin Avenue
Urbana IL 61801

Dr. Walter E. Myerhof
Physics Department
Stanford University
Stanford CA 94305-4060

Dr. Kevin (Mike) Myles
Electrochemistry Technology Program
Argonne National Laboratory
9700 South Cass Building 205
Argonne IL 60439

Dr. William E. O'Grady
Naval Research Laboratory
4555 Overlook Ave.
Code 6171
Washington DC 20375-5000

Dr. Richard Oriani
Chemical Engineering and Materials Science
University of Minnesota
151 Amundson Hall
Minneapolis MN 55455

Dr. Richard Petrasso
Plasma Fusion Center
Massachussetts Institute of Technology
167 Albany Street
Mail Stop NW16132
Cambridge MA 02139

Dr. Stanley Pons
University of Utah
2420 Henry Eyring Building
Salt Lake City UT 84112

Dr. Johann Rafelski
Department of Physics
University of Arizona
Tucson AZ 85721

Dr. Debra R. Rolison
Naval Research Laboratory
Code 6171
Washington DC 20375-5000

Dr. Hugo Rossi
National Cold Fusion Institute
390 Wakara Way
Salt Lake City UT 84108-1214

Dr. Michael Saltmarsh
Oak Ridge National Laboratory
P.O. Box 2009
Oak Ridge TN 37831-8070

Dr. Joe Santucci
Nuclear Power Division
Electric Power Research Institute
3412 Hillview Avenue
P.O. Box 10412
Palo Alto CA 94303

Dr. Thomas Schneider
Electric Power Research Institute
3412 Hillview Avenue
P. O. Box 10412
Palo Alto CA 94303

Dr. Glen Schoessow
Department of Nuclear Engineering Sciences
202 Nuclear Science Center
University of Florida
Gainsville FL 32611

Dr. Chaucey Starr
Electric Power Research Institute
3412 Hillview Avenue
P. O. Box 10412
Palo Alto CA 94303

Dr. Edmund Storms
Los Alamos National Laboratory
Mail Stop C348
Los Alamos NM 87545

Dr. Harold Szu
Naval Surface Warfare Center
White Oak Information Processing Group
10901 New Hampshire Avenue
Code R-44
Silver Spring MD 20903-5000

Dr. Carol Talcott
Los Alamos National Laboratory
Mail Stop C348
Los Alamos NM 87544

Dr. EdwardTeller
Lawrence Livermore National Laboratory
7000 East Avenue
P.O. Box 808
Livermore CA 94550

Dr. David Thompson
Johnson-Matthey Technical Center
Blount's Court
Sonning Commen
Reading RG-49 N11
United Kingdom

Dr. Milton Wadsworth
Dean of College of Mines and Earth Science
University of Utah
209 Browning Building
Salt Lake City UT 84112

Dr. Robert D. Weaver
Electric Power Research Institute
3412 Hillview Avenue
PO Box 10412
Palo Alto CA 94303

Dr. Paul Werbos
Division of Electrical and Communication Systems
National Science Foundation
1800 G Street NW, Room 1151
Washington DC 20050

Dr. John Werth
Engelhard Corporation
Menlon Park
Edison NJ 08818

Dr. K. B. Whaley
Department of Chemistry
University of California at Berkeley
Berkeley CA 94720

Ms. Kathy Williams
Westover Consultants
500 E St. S.W. Suite 910
Washington DC 20024

Dr. Kevin Wolf
Cyclotron Institute
Department of Chemistry
Texas A&M University
College Station TX 77843

Dr. David Worledge
Electric Power Research Institute
3412 Hillview Ave.
P.O. Box 10412
Palo Alto CA 94303

Dr. Mark S. Wrighton
Department of Chemistry
Massachusetts Institute of Technology
77 Massachusetts Ave, Room 6-335
Cambridge MA 02139

Dr. Ernest Yeager
Department of Chemistry
Case Western Reserve University
Morley Blvd., Room 108
Cleveland OH 44106

Appendix B

LIST OF ATTENDEES

NSF/EPRI WORKSHOP ON ANOMALOUS EFFECTS IN DEUTERATED MATERIALS

National Science Foundation
1800 G Street NW, Room 543
Washington, DC

October 16–18, 1989
Attendees List

Dr. John Appleby
238 Wisenbaker Engineering Research Center
Texas Engineering Experiment Station
The Texas A&M University System
College Station TX 77843-3577

Dr. A. J. Bard
Department of Chemistry
Welch 4218
University of Texas at Austin
Austin TX 78712

Dr. Gordon Baym
Department of Physics
University of Illinois-Champaign
1110 West Green Street
Urbana IL 61801

Dr. John O'M. Bockris
Texas A&M University
Department of Chemistry
College Station TX 77843

Dr. Peter Bond
Physics Department 510A
Brookhaven National Lab
20 Pennsylvania Street
Upton NY 11973

Dr. James Bray
Building K-1 Room 1C25
General Electric Research Dev. Center
River Road
Schenectady NY 12301

Dr. Carlo Carraro
Division of Physics
Department of Mathematics and Astronomy
California Institute of Technology
Mail Stop 106-38
Pasadena CA 91125

Dr. Tarun K. Chaki
Department of Mechanical &
Aerospace Engineering
State University of New York
Buffalo NY 14260

Mr. Bendi Chexal
Nuclear Power Division
Electric Power Research Institute
3412 Hillview Avenue
P.O. Box 10412
Palo Alto CA 94303

Dr. Paul C. W. Chu
Texas Center for Superconductivity
University of Houston
Houston TX 77204-5506

Dr. Scott Chubb
Naval Research Laboratory
4555 Overlook Avenue
Code 8310
Washington DC 20375

Dr. Ted B. Flanagan
Program in Materials Science
Department of Chemistry
University of Vermont, Cook Building
Burlington VT 05405

Dr. Martin Fleischmann
University of Utah
2420 Henry Eyring Building
Salt Lake City UT 84112

Dr. Ryszard Gajewski
Basic Energy Sciences
US Department of Energy
ER-16, GTN
Washington DC 20545

Dr. Richard Goldstein
Electric Power Research Institute
3412 Hillview Avenue
P. O. Box 10412
Palo Alto CA 94303

Dr. Peter Grimes
Exxon Chemical Co.
P.O. Box 536
Linden NJ 07036

Dr. Nathan Hoffman
Energy Technology Engineering Center (ETEC)
Rockwell International Corporation
P. O. Box 1449
Canoga Park CA 93104

Dr. Frank Huband
Division of Electrical and Communication System
National Science Foundation
1800 G Street NW, Room 1151
Washington DC 20550

Dr. Robert Huggins
Department of Material Science
Stanford University
Building 550, Room 550I
Stanford CA 94305

Dr. Donald P. Hutchinson
Physics Division 372
Martin Marietta Energy Systems
Oak Ridge National Laboratory
Oak Ridge TN 37831-8070

Dr. Steve Jones
Department of Physics and Astronomy
Brigham Young University
176 ESC
Provo UT 84602

Dr. Joseph Jordan
Department of Chemistry
Pennsylvania State University
University Park PA 16802

Dr. Yeong E. Kim
Department of Physics
Purdue University
West Lafayette IN 47907

Dr. Nathan Lewis
Department of Chemistry
California Institute of Technology
Mail Stop 127-72
Pasadena CA 91125

Dr. Khalid Mansour
Savannah River Site
Westinghouse Savannah River Company
773-42A, Room 1611
Aiken SC 29808

Dr. Mike McKubre
SRI International
333 Ravenswood Avenue
Menlo Park CA 94025

Dr. Howard O. Menlove
Los Alamos National Laboratory
Los Alamos NM 87544

Dr. George H. Miley
Fusion Studies Laboratory
University of Illinois
103 South Goodwin Avenue
Urbana IL 61801

Dr. Kevin (Mike) Myles
Electrochemistry Technology Program
Argonne National Laboratory
9700 South Cass Building 205
Argonne IL 60439

Dr. William E. O'Grady
Naval Research Laboratory
4555 Overlook Ave.
Code 6171
Washington DC 20375-5000

Dr. Richard Oriani
Chemical Engineering and Materials Science
University of Minnesota
151 Amundson Hall
Minneapolis MN 55455

Dr. Richard Petrasso
Plasma Fusion Center
Massachussetts Institute of Technology
167 Albany Street
Mail Stop NW16132
Cambridge MA 02139

Dr. Stanley Pons
University of Utah
2420 Henry Eyring Building
Salt Lake City UT 84112

Dr. Johann Rafelski
Department of Physics
University of Arizona
Tucson AZ 85721

Dr. Hugo Rossi
National Cold Fusion Institute
390 Wakara Way
Salt Lake City UT 84108-1214

Dr. Joe Santucci
Nuclear Power Division
Electric Power Research Institute
3412 Hillview Avenue
P.O. Box 10412
Palo Alto CA 94303

Dr. Thomas Schneider
Electric Power Research Institute
3412 Hillview Avenue
P. O. Box 10412
Palo Alto CA 94303

Dr. Edmund Storms
Los Alamos National Laboratory
Mail Stop C348
Los Alamos NM 87545

Dr. Harold Szu
Naval Surface Warfare Center
White Oak Information Processing Group
10901 New Hampshire Avenue
Code R-44
Silver Spring MD 20903-5000

Dr. Carol Talcott
Los Alamos National Laboratory
Mail Stop C348
Los Alamos NM 87544

Dr. EdwardTeller
Lawrence Livermore National Laboratory
7000 East Avenue
P.O. Box 808
Livermore CA 94550

Dr. David Thompson
Johnson-Matthey Technical Center
Blount's Court
Sonning Commen
Reading RG-49 N11
United Kingdom

Dr. Milton Wadsworth
Dean of College of Mines and Earth Science
University of Utah
209 Browning Building
Salt Lake City UT 84112

Dr. Robert D. Weaver
Electric Power Research Institute
3412 Hillview Avenue
PO Box 10412
Palo Alto CA 94303

Dr. Paul Werbos
Division of Electrical and Communication Systems
National Science Foundation
1800 G Street NW, Room 1151
Washington DC 20050

Dr. John Werth
Engelhard Corporation
Menlon Park
Edison NJ 08818

Dr. K. B. Whaley
Department of Chemistry
University of California at Berkeley
Berkeley CA 94720

Dr. Kevin Wolf
Cyclotron Institute
Department of Chemistry
Texas A&M University
College Station TX 77843

Dr. David Worledge
Electric Power Research Institute
3412 Hillview Ave.
P.O. Box 10412
Palo Alto CA 94303

Dr. Ernest Yeager
Department of Chemistry
Case Western Reserve University
Morley Blvd., Room 108
Cleveland OH 44106

Appendix C

AGENDA

NSF/EPRI WORKSHOP ON ANOMALOUS EFFECTS IN DEUTERATED METALS

Washington, DC — October 16 - 18, 1989

AGENDA

MONDAY, OCTOBER 16, 1989
Morning Session (8:00 - 12:00) Chairman: Paul Chu

8:00 - 8:45	**Continental Breakfast**
8:45 - 9:00	*Introduction: Welcome and Charges* Frank Huband, Paul Werbos, and Tom Schneider
9:00 - 9:40	Keynote Nuclear Physics Review Edward Teller
9:40 - 10:20	Keynote Electrochemistry Review Martin Fleischmann
10:20 - 10:30	**Break**
10:30 - 11:10	Relevant Electrochemical Values in the 0.10 Normal LiOD/Pd System Nate Lewis
11:10 - 11:50	Relevant Material Issues (Pd/D system) Ted Flanagan
12:00 - 1:00	**Lunch**

Afternoon Session (1:00 - 6:30) Chairman: David Worledge

1:00 - 4:20	Recent Post-Santa Fe Results: Nuclear Products
1:00 - 1:50	Ed Storms: Presentation and Discussion
1:50 - 2:40	Steve Jones: Presentation and Discussion
2:40 - 3:30	Howard Menlove: Presentation and Discussion
3:30 - 4:20	Kevin Wolf: Presentation and Discussion
4:20 - 4:30	**Break**
4:30 - 5:10	Possible Criteria for the Detection of Nuclear Products George Miley

| 5:10 - 5:50 | Possible Sources of Error in the Quantitative Analysis of Nuclear Products |
| | Nate Hoffman |

5:10 - 5:50   Possible Sources of Error in the Quantitative Analysis of Nuclear Products
        Nate Hoffman

5:50 - 6:30   Tritium Detection Considerations
        Carol Talcott

7:00 - 8:00   *Dinner*

Evening Session (8:30 - 9:30) Chairman: Paul Werbos

8:30 - 9:30   Review: Pre-Santa Fe Experimental Status
        Allan Bard

TUESDAY, OCTOBER 17, 1989
Morning Session (8:30 - 12:10) Chairman: Tom Schneider

8:00 - 8:30   **Continental Breakfast**

8:30 - 12:10   Recent Post-Santa Fe Results: Excess Heat
    8:30 - 9:05 Martin Fleischmann/Stanley Pons
    8:05 - 9:40 Richard Oriani
    9:40 - 10:15 Milton Wadsworth

    10:15 - 10:25   **Break**

    10:25 - 11:00 John Appleby
    11:00 - 11:35 John Bockris
    11:35 - 12:10 Robert Huggins

12:20 - 1:20   *Lunch*

Afternoon Session (1:30 - 5:00) Chairman: John Appleby

1:30 - 3:00   Possible Criteria for the Detection of Excess Heat
        Material and Measurement Techniques
3:00 - 3:10   **Break**

3:10 - 5:00   Topical Discussions on Excess Heat
    3:10 - 3:40 Assessment of Experimental Status of Excess Heat
    3:40 - 4:10 Identification of Issues Related to Excess Heat
    4:10 - 5:00 Possible Future Research Related to Excess Heat

5:15 - 6:15   *Dinner*

Evening Session (6:45 - 10:00) Chairman: George Miley

6:30 - 8:10   *Causal Hypotheses*
      6:30 - 6:45 *Gordon Baym*
      6:45 - 7:05 *Yeong Kim*
      7:05 - 7:20 *K.B. Whaley*
      7:20 - 7:35 *David Worledge*
      7:35 - 8:10 *Johann Rafelski*

8:10 - 10:00   *Topical Discussion on Nuclear Products*
      8:10 - 8:40 *Assessment of Experimental Status of Nuclear Products*
      8:40 - 9:10 *Identification of Issues Related to Nuclear Products*
      9:10 - 10:00 *Possible Future Research Related to Nuclear Products*

WEDNESDAY, OCTOBER 18, 1989
Morning Session (8:30 - 11:45) Chairman: Nate Hoffman

8:30 - 9:00   **Continental Breakfast**

9:00 - 9:50   *Summary Statement Preparations*
      Excess Heat - Chairman: Ernest Yeager
      Nuclear Products - Chairman: George Miley
      Causal Hypotheses - Chairman: Gordon Baym

9:50 - 10:00   **Break**

10:45 - 11:45   *Summary Statements*
      10:00 - 10:35 *Excess Heat*
      10:35 - 11:10 *Nuclear Products*
      11:10 - 11:45 *Causal Hypotheses*

Co-Chairmen:

John Appleby, Texas A&M University   *Paul Chu, University of Houston*

Agency Coordinators:

Tom Schneider, EPRI ·   *Paul Werbos, National Science Foundation*

Workshop Secretaries:

Harold Szu, Naval Research Lab.   *Nate Hoffman, ETEC*

Meeting Arrangements:

Kathy Williams, Westover Consultants

ADDENDUM

Monday Afternoon Session

4:20 - 4:30 **Break** *William Ogrady/Debra Rolison*
Presentation and Discussion